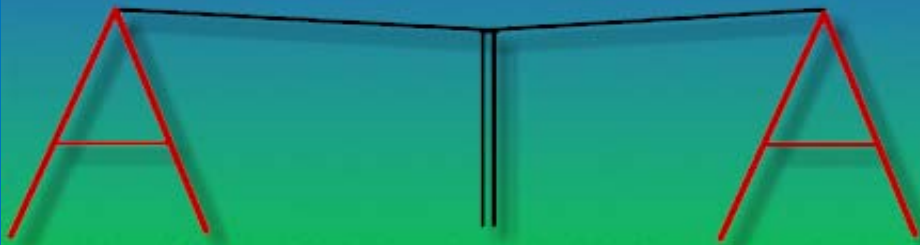


# **Antennas**

## **Made of Wires**

### **Volume 3**

***Simple & Effective***



**A Collection from the Works  
of L.B. Cebik, W4RNL**

---

# **Antennas Made of Wires Volume 3**

---

---

*Published by*  
***antenneX Online Magazine***  
<http://www.antennex.com/>  
POB 271229  
Corpus Christi, Texas 78427-1229 USA

---

---

Copyright © 2010 by Publisher ***antenneX Online Magazine***. All rights reserved. No part of this book may be reproduced or transmitted in any form, by any means (electronic, photocopying, recording, or otherwise) without the prior written permission of the publisher.

---

ISBN: 1-877992-87-9

---

## About the Author

L. B. Cebik, W4RNL, passed away in April 2008. He had written extensively about antennas and antenna modeling (as well as other electronics subjects) in most of the U.S. ham journals, including QST, CQ, Communications Quarterly, QEX, Ham Radio, 73, QRP Quarterly, Radio-Electronics, and QRPP. Besides the continuing series of antenna modeling columns he does for *antenneX* (*continues through 2010*), he also wrote a column for 10-10 News (An-Ten-Ten-nas) and another for Low Down (Antennas from the Ground Up). A life member of ARRL, he served as both Technical and Educational Advisor. Several years ago, LB joined the position as Technical Editor for *antenneX*.



L. B. has published over two dozen books, with works on antennas for both the beginner and the advanced student. Among his books are a basic and intermediate tutorial in the use of NEC antenna modeling software and compilations of his many shorter pieces. Some 30 of these books have been published by *antenneX* and listed in the Bookshelf at our website.

He was a ham since 1954 and also a life member of QCWA and of 10-10 International. He also maintained a web site (<http://www.cevik.com>) on which he has placed a large collection of entries from his notebooks and publications sponsored by *antenneX*. A PhD and a teacher for over 30 years, he retired as professor emeritus of philosophy at the University of Tennessee, Knoxville. *antenneX* is/was very fortunate, indeed, to have had LB as a member of its writing team and Tech Editor for some 12 years.

I for one, lament daily at the tragic loss of one of my closest friends. I think of him often to this day. — November 2010

— Jack L. Stone, Publisher

## PREFACE

***"it's not just wires anymore, it's an antenna!"***

**W**hile numerous articles and books have described various wire antenna designs, but here is a series of new books from the works of antenna master, L.B. Cebik, W4RNL (SK). He is known the world over for his unique ideas about new ways to "bend wires" to get the most out of them. With LB's guidance, your success is practically guaranteed. It would be a rare occasion indeed that any design recommended by this author will not work as described. One can proceed with that confidence in mind.

This book is dedicated to the design, construction and use of antennas of various types of wire. The reader can save a lot of time and effort by reading these books. Then, experiment to your heart's content with an aim toward the goal of achieving the best signal for your unique environment.

With wire, antennas are very simple and easy to build at a very lowest of cost to achieve one's goal. This book will demonstrate a number of designs from conventional antenna wisdom. How satisfying is it to twist and bend wires together and make connections only to suddenly discover, ***"it's not just wires anymore, it's an antenna!"***

One book is not enough to describe all of the best-known and LB's unique designs, but we continue with this third Volume picking up where Volume 1 and 2 left off and progress toward the more complex designs.

Along with some recommended wires, a pair of gloves and simple hand tools, wonders will sprout from your efforts quickly. And, with wires, such designs can be made to fit within the closest of environments. Many tips are suggested about how to make cramped spaces an asset rather than a liability—and keep your neighbors friendly as well.

We know the reader, newbie or advanced, will enjoy this book, Volume 3 of a 3-book series, by one of the masters and have fun in the process!

## Table of Contents

### BROADBAND COVERAGE OF 80/75-METERS WITH AWG #12 WIRE

Chapter 51: Coverage of the 80/75-Meter Band with AWG #12 Copper Wire-----7

Chapter 52: Fine-Tune Broadband Antennas for 80/75 Meters-----38

### SOME LONG WIRE

Chapter 53: Center- & End-Fed Unterminated Long-Wire-----60

Chapter 54: Terminated End-Fed Long-Wire Directional Antennas-----91

Chapter 55: V Arrays and Beams-----116

Chapter 56: Rhombic Arrays and Beams-----146

Chapter 57: Multi-Band, Multi-Wire & Multi-Element Rhombics-----174

### THE RHOMBOIDS

Chapter 58: The Dual Rhomboid for 1296 MHz-----204

Chapter 59: The Dual Rhomboid, a True Laport Version-----222

Chapter 60: The Dual Rhomboid, Some Comparison Standards-----237

### MORE ON WIRE BEAMS

Chapter 61: Folded X, Hex, Square & Moxon Rectangle Beams-----254

Chapter 62: The EDZ Beams-----283

Chapter 63: Feeding the EDZ-----300

### NVIS

Chapter 64: NVIS: Some Background-----307

Chapter 65: NVIS: Some Basic Antennas Used-----330

Chapter 66: NVIS: Antennas with Reflectors-----385

Chapter 67: NVIS Dipoles, Inverted-Vs, 1- $\lambda$  Loops & Doublets-----434

Chapter 68: Fixed 3-Band NVIS Antennas-----477

Chapter 69: NVIS Antennas for Special Needs-----505

### WIRE LOOPS

Chapter 70: All-Band Horizontal-Plane Loops-----553

Chapter 71: A 40-Meter Star-Shape Loop-----563

Chapter 72: Horizontally Oriented & Polarized Big Wire Loops-----576

Chapter 73: Configuring Horizontal Wire Loops-----653

Chapter 74: Closed & Interrupted Loops for 40 Meters-----676

Chapter 75: The IL-ZX Loop for 40 Meters-----686

### OTHERS

Chapter 76: Experimental Omni-Directional Antennas for 6M-----704

Chapter 77: Modeling the T2FD-----741

Chapter 78: Wire Linear-Resonator Dipoles -----759

Other Publications-----789

## Chapter 51: Coverage of the 80/75-Meter Band with AWG #12 Copper Wire

The chapter in *The ARRL Antenna Book* (9 in the 20<sup>th</sup> edition) is an excellent introduction to techniques for obtain full coverage of the 3.5-4.0-MHz amateur band, a 13% bandwidth as such things are reckoned. It is also a tribute to long years of work, analysis, and measurement by Frank Witt, AI1H, the chapter's author. Nevertheless, the subject is not completely closed.

The premise for these notes is that we have an endless supply of AWG #12 copper wire. As well, we can support an 80-75-meter dipole at 90° above average ground. Besides a little preliminary modeling in free space, we shall use these values as constants. Our goal is to create a dipole antenna that covers the entire band with an SWR of less than 2:1, using a reference impedance value that is appropriate for each situation that we examine. We shall look at ribbons, cages, parasitic drivers, and transmission lines. We shall omit the various broadband antennas that involve using coaxial sections as part of the construction simply because we cannot effectively model coaxially arranged wires. As we proceed, we shall recall a pair of matching techniques that employ combinations of transmission lines, including the system that Witt calls the transmission-line resonator or TLR. Toward the end, we shall do something that seems to have eluded authors to this point: we shall combine techniques for improved radiation and SWR performance. But first, we shall wrap ourselves in wire.

### *Some Ribbon and Cage Basics*

We may create virtual fat wires by combining thinner wires in certain arrangements. The most popular forms are the ribbon and the

cage. **Fig. 1** outlines some of the basic shapes and some of the critical dimensions. We shall consider ribbons with 2 and 4 wires. As well, we shall look at cages consisting of 4 and 6 wires. Our first task will be to see what dimensions for each shape coincide with which single-wire diameters. We may do this within the boundaries of NEC modeling if we observe a few precautions.

The ends of ribbons and cages often come to a point at both the center feedpoint gap and at the outer ends to which we normally attach support ropes. Both angular geometries tend to yield AGT values that are not ideal (1.000 in free space), and these variations can distort comparisons. We can avoid the variable AGT values by two simple modeling techniques. At the outer ends of cages and ribbons, we can use a simple set of perimeter wires to join longitudinal ends. At the feedpoint, we may run the wires in straight parallel lines. To create a common feedpoint, we next select one wire as the source wire. We then connect from this wire to each other wire in the group a near-zero length of lossless transmission line. The characteristic impedance is not critical, since the length is almost zero ( $1e10^{-5}$  or shorter) and virtually no impedance transformation can occur. These models tend to yield more accurate results relative to physical ribbon and cage antennas than do models that try to replicate the details of the many angular junctions. For example, the current values along wire that are directly fed and fed via the lengthless lines are identical. As well, the scheme yields rather precise feedpoint impedance values that coincide with physical antennas.

Some Basic Shapes for  
"Fat" Wire Simulation  
with Thin Wires

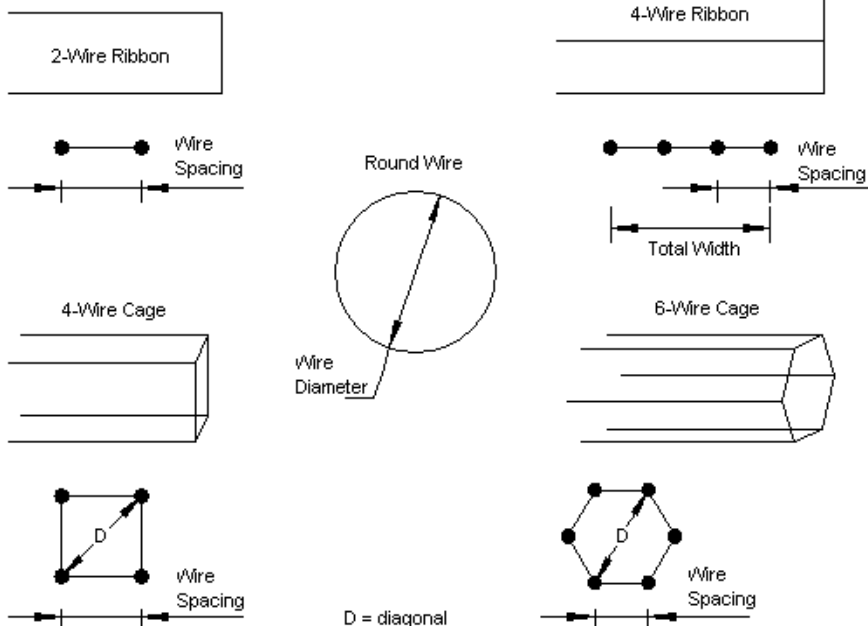


Fig. 1

Preliminary modeling consisted of checking the correlation between multi-wire dipole ribbons and cages with roughly equivalent round-wire dipoles. The test begins with a simple 1-wire dipole. Then it proceeds to various multi-wire dipoles. In each case, the maximum dimension is 1' (12"). So for ribbon elements, the outer wires are 1' apart. There is a 2-wire ribbon and also a 4-wire ribbon with the wires 0.3333"

(4") apart. The 4-wire cage is 0.707' per side for a diagonal dimension of 1'. The 6-wire cage has wires 0.5' apart for a diagonal of 1'.

In each case, I adjusted the length of the dipole to resonance  $+/-j1\Omega$  reactance at 3.6 MHz in free space. The resistive component in each case is 72 Ohms  $+/-1\Omega$ . For each resonant length, I then created a single-wire dipole of the same length and adjusted the wire diameter for resonance. A comparison of the “fat” single wire dipole gain values with the gain for ribbon or cage dipole elements gives a comparative measure to the relative losses of equally resonant structures. All models showed an AGT score of 1.000, eliminating the need for any gain value adjustments. No intermediate current-equalizing shorting wires are used, although they are common in actual practice.

**Table 1** provides the results of the initial runs for a resonant frequency of 3.6 MHz. From the data, we may draw a few initial conclusions.

1. The minor drop in gain for each multi-wire element relative to its associated fat-single-wire element shows the small but numerically noticeable difference in losses. In each case, the fat-wire element also has a slightly wider 2:1 72- $\Omega$  SWR span than the associated multi-wire element.

Table 1. Multi-wire dipoles and the equivalent single fat-wire dipoles

Antenna	Length	Gain dBi	72-Ohm SWR Span
Single wire	133.07	2.04	3.50 to 3.71 MHz
2-wire ribbon	130.90	2.09	3.45 to 3.76
Fat 2.5" wire	130.90	2.13	3.40 to 3.78
4-wire ribbon	130.30	2.11	3.43 to 3.79
Fat 4" wire	130.30	2.13	3.43 to 3.80
4-wire cage	129.40	2.11	3.43 to 3.80
Fat 7" wire	129.40	2.13	3.41 to 3.80
6-wire cage	129.10	2.12	3.42 to 3.80
Fat 8" wire	129.10	2.13	3.41 to 3.83

2. The added two wires in the 4-wire ribbon element are inside the outer wires that are 1' apart. The current levels on the inner wires are about 0.75 the values on the outer wires: lower but still very significant, as indicated by the shorter resonant length of the 4-wire ribbon relative to the 2-wire ribbon.

3. The differences across the range of multi-wire models are too small to be operationally noticeable. Even the SWR variation is only 0.07 MHz.

The slight differences in losses between each multi-wire dipole and its single fat-wire equivalent is not as important a result as the progression of increases in equivalent single-wire diameters as we increase the complexity of the multi-wire dipole. If we wish to obtain less than 2:1 SWR across the entire 3.5-4.0-MHz span, we can expect to use much wider wire spacing. However, as we move from simple wire ribbons to cages, we can also expect a decrease in spacing between wires. At this stage in our efforts, we may expect some spacing values

that would place the dipole structure outside the range of practicality. Nevertheless, we shall explore almost all of the initial options. The one exception is the 2-wire ribbon. This structure did not achieve the desired goal even with a spacing of 9', so I eliminated it from the list of samples.

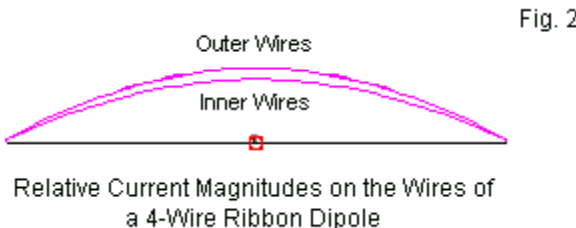
**Table 2** lists the remaining candidates for full-band 80-75-meter coverage, beginning with a 16"-diameter single-wire dipole. All antennas are 90' above average ground, and the multi-wire structures are composed of AWG #12 copper wire. The antenna specifications list the wire spacing and the total or the diagonal spacing, as appropriate. See **Fig. 1** to identify the indicated dimensions relative to the structure. The new table also replaces the data on the SWR span (which is at least 3.5 to 4.0 MHz) with the resonant frequency and the impedance at resonance. Because these values are all about  $72\ \Omega$ , the SWR values are referenced to that value.

The table has a few minor surprises. Although the spacing between wires shows the progression established in the preliminary tests, the antenna lengths do not all grow shorter as we increase the complexity of the structure. The 6-wire cage is somewhat longer than the 4-wire cage. The table also omits gain values for the 90'-high dipoles, since we shall address the question of gain across the band once we add a few other broadband AWG #12 wire antennas to our collection.

Table 2. Multi-wire dipoles for full coverage of 3.5-4.0 MHz

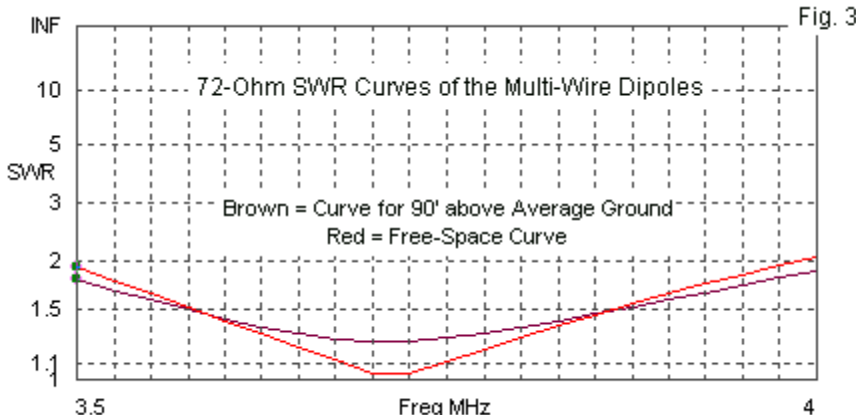
Antenna	Length	Res. Fq.	Impedance
Single wire 16" diameter	123.6'	3.72 MHz	71.6 - j0.4 Ω (free space) 89.1 - j4.8 Ω (90')
4-wire ribbon Wire spacing 2' Total width 6'	123.4'	3.72 MHz	72.4 + j0.4 Ω (free space) 89.3 - j4.1 Ω (90')
4-wire cage Wire spacing 3' Diagonal 4.24'	121.8'	3.71 MHz	72.1 - j0.5 Ω (free space) 88.3 - j6.0 Ω (90')
6-wire cage Wire spacing 1.5' Diagonal 3'	122.2'	3.73 MHz	72.1 - j0.7 Ω (free space) 88.6 - j5.9 Ω (90')

4-wire ribbon structures are subject to some overgeneralization to the effect that most of the current lies in the outer wires (with the presumption that little current is along the two inner wires. As shown in **Fig. 2**, the differential is only about 15%. (Since the antenna view is in the plane of the wires, only two current curves appear, with overlapping outer-wire and overlapping inner-wire values.) The ratio of maximum current on the inner wires to the maximum current on the outer wires increases as the spacing between wires increases. The ratio for the 4-wire ribbon with a wire-to-wire spacing pf 0.333' is about 75% in contrast to the 85% value for the widely space wires of the full-band 80-75-meter 4-wire ribbon element.



The models used in developing the data in **Table 2** initially used a free-space environment. The goal in each case was to achieve a  $72\Omega$  SWR curve. When placed at 90' above average ground, the values change, as shown in the table for the free-space resonant frequencies. However,  $72\Omega$  SWR curve actually becomes shallower, as shown by **Fig. 3**. One desirable consequence is the fact that there is enough “play” to allow for variations in ground quality and potential interactions with other objects in the near field of the antenna with minimal need for field adjustment of the antenna. In addition, the use of a coaxial cable feedline of any length will further increase the SWR bandwidth, but with the usual losses associated with coaxial cables.

The SWR curves in **Fig. 2** are based upon the impedance values at the actual antenna feedpoint. Before we close these notes, we shall have occasion to add a feedline to the system. However, it will not be the sort of single-cable installation that we usually think of in connection with dipole antennas.



Except for the 16"-diameter single-wire dipole, all of the antennas modeled are feasible constructs for a serious 80-75-meter installation. The 4- and 6-wire cages may be the most compact in terms of the cross section, but require special attention to the set of wire spacers along the length of the antenna. The 6' total width of the 4-wire boon version requires, in contrast, only linear spacing bars at periodic positions along the element. In all cases, the construction of both the element and the necessary supports represents a serious antenna installation project.

### Parasitic Driver Basics

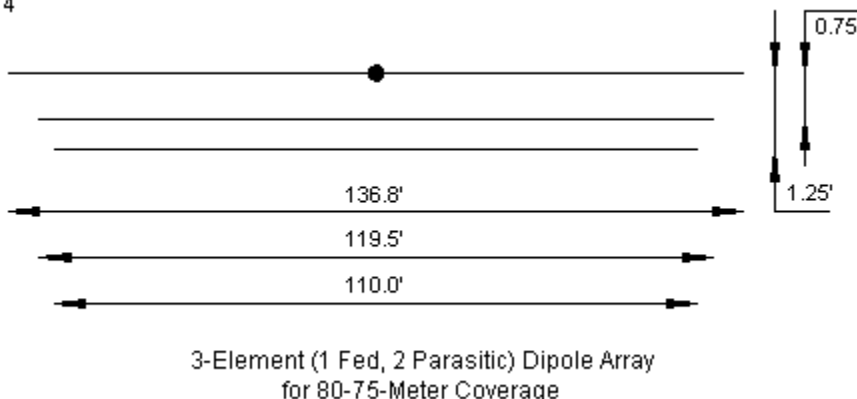
The cage and ribbon elements share some common features. All have very significant cross section dimensions. As well, all show a typical single-element dipole SWR curve with a single minimum at a frequency just below the arithmetic mid-band point. If we can give up the shape of the SWR curve, we may achieve full-band 80-75-meter coverage with

other antenna designs, some of which are more compact with respect to the cross section dimensions.

The use of open-sleeve or coupled resonator dipoles (and monopoles) has been around for a considerable length of time. Chapter 7 of *The ARRL Antenna Book* contains a good introduction to the practice, although mostly in a multi-band context. The principle is simple to state, but more difficult to implement, either in models or in physical antennas. Essentially, we directly feed an element for the lowest desired frequency in a set of frequencies. By selecting proper spacing and length values, we may add a series of parasitically coupled elements and achieve resonance on one or more higher frequencies as determined by the measured impedance at the feedpoint of the fed element. The goal is not simply to achieve any resonant condition whatever, but to show an impedance similar to that of the fed element along. This condition allows us to use a single transmission-line characteristic impedance to provide a matched impedance system for all frequencies covered by the multi-element antenna.

The most common applications of the use of coupled resonators include collections of monopoles with a common radial system and Yagi-type directional antennas. In most cases, the goal is to cover 2 or more amateur bands with a single directly fed element. However, we may also apply the same technique to expand the SWR coverage of a single antenna with multiple horizontal wires to cover a very wide band, such as 3.5-4.0 MHz. Slaved or secondary driver elements tend to have a narrower SWR bandwidth than the directly fed driver. Hence, a single parasitic element will not normally suffice to spread the coverage of an AWG #12 copper wire to handle the entire band. We may need more than one slaved element.

Fig. 4

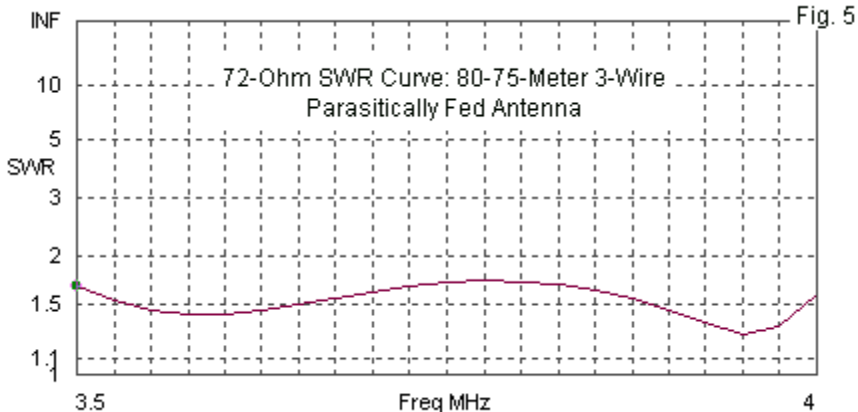


3-Element (1 Fed, 2 Parasitic) Dipole Array  
for 80-75-Meter Coverage

**Fig. 4** shows one version of a 3-wire broadband dipole array for 80 and 75 meters. The elements are AWG #12 copper wire, and the dimensions apply to that diameter element. Only the longest element has a direct connection to the feedline, although all three elements contribute to the ability of the antenna to provide satisfactory SWR coverage from 3.5 to 4.0 MHz. The elements shown are arrayed below the fed element running from the longest to the shortest. Equally possible is a version of the antenna with one parasitic element on each side of the directly fed element, although such an arrangement might well require adjustments to the length and spacing values used. In the version shown, note that the spacing between the two slaved elements is less than the spacing between the fed element and the first parasitic element.

The 3-wire system shown requires a cross-section width of only 1.25', considerably less than required by any of the multi-wire dipoles shown in the previous section of these notes. Moreover, the SWR pattern shown at the driven element feedpoint does not have a single minimum

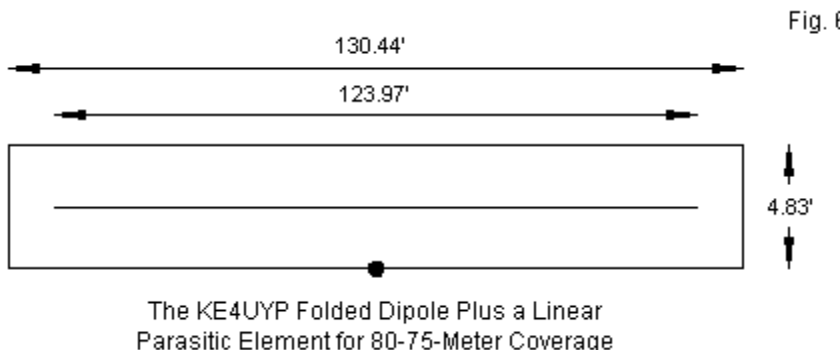
value with slowly rising values above and below the resonant frequency. Instead, as shown in **Fig. 5**, the SWR show multiple minimum. The values are well below 2:1 across the band, but often higher than 1.5:1, a value at which some high-power amplifiers for amateur service set their fold-back circuit cut-off points. However, like the ribbon and the cage dipoles, the SWR curve for the 3-wire parasitic system does not include the losses of reasonable lengths of coaxial cables in the 70-75- $\Omega$  range.



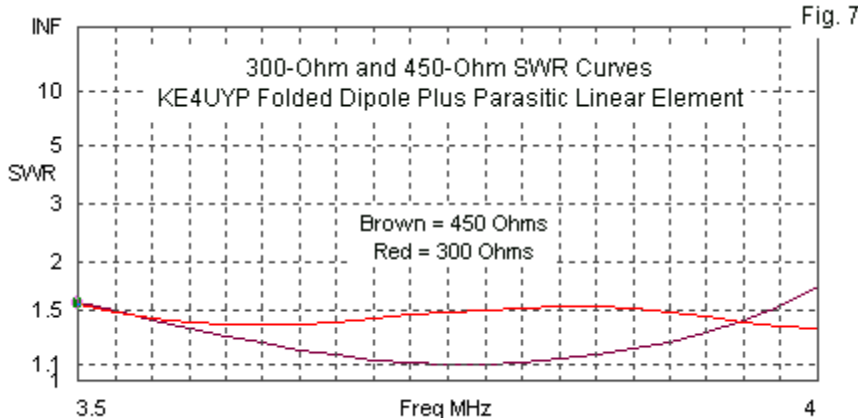
The design shown, although generated just for these notes, is not unlike coupled resonator antennas that have appeared in amateur journals, such as *QST*. Construction may be simpler than for any of the other antennas examined so far, and it does not require any further matching relative to current equipment input/output impedance standards.

An alternative method of achieving a similar goal is to use a folded dipole structure in which we place a linear parasitic element in the center. Lou Rummel, KE4UYP, developed such a design for AWG #12 copper

wire, and the outline and dimensions appear in **Fig. 6**. The wire arrangement is one possibility within a continuum of dimensions that yield a multi-minimum SWR pattern.



The width of the folded structure is less than 5'. This width is in a frontier zone between the folded structure acting like a folded dipole and the structure acting like simply a highly elongated loop. The loop alone is resonant at about 3.52 MHz, with the linear element having a self-resonant point at about 4.05 MHz if it were not subject to very high interaction with the loop. In turn, the parasitic linear element raises the self-resonant point of the loop to produce the 300- $\Omega$  SWR curve in **Fig. 7**. The curve for 450  $\Omega$  shows that the antenna would be equally at home with a higher-impedance parallel line, such as common window line. The latter has about half the loss per unit length as even transmitting versions of 300- $\Omega$  ribbon or tubular line.



The folded-dipole-linear-parasitic element version of the coupled-resonator 80-75-meter antenna is the logical counterpart of the 3-wire version for those who prefer to feed antennas with parallel transmission line. Since advantages or disadvantages would lie mainly in the preferred feeding system, we may bypass them for this discussion.

#### *Transmission-Line Broad-Banding*

Back in 1997, Dave Leeson, W6NL, brought to my attention an interesting technique for achieving wide-band operation on the lower HF bands, especially the 80/75-meter band. The technique derived from mentions in texts and from references in ARRL publications by Frank Witt, AI1H, a noted experimenter and evaluator of low-HF broad-banding methods.

The broad-banding method begins by selecting the geometric mean between the two desired frequencies (that is, the square root of the product of the two frequencies). Suppose that we cut a dipole to be

resonant at this frequency. Next, for the dipoles design frequency, we should cut a length of  $50\text{-}\Omega$  coax that is a multiple of a half wavelength so that its length is perhaps from  $0.5\text{-}\lambda$  to  $2.0\text{ }\lambda$ . Of course, the physical length will be the line's velocity factor times the electrical wavelength at the design frequency. To the shack or source end of this line, we connect a  $1/4\text{-}\lambda$   $75\text{-}\Omega$  transformer line section, again multiplying the electrical length by the line's velocity factor to arrive at a physical length. The result is a well-established broadening of the operating SWR-bandwidth.

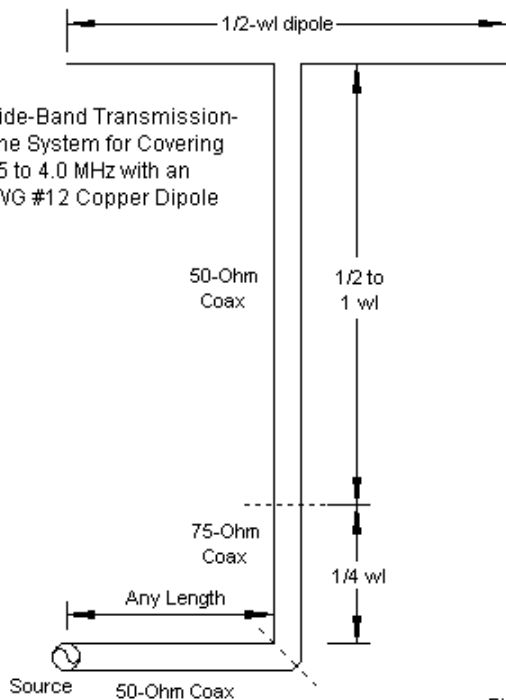
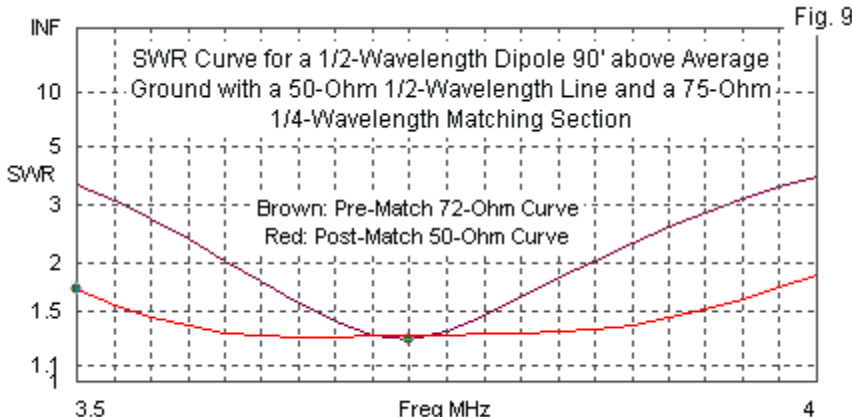


Fig. 9

**Fig. 8** shows the general outline of one recommended system consisting of a  $0.5\lambda$  length of  $50\Omega$  cable, followed by a  $0.25\lambda$  section of  $75\Omega$  cable. Essentially, the  $50\Omega$  cable replicates the antenna feedpoint impedance at resonance, but off resonance, the line is no longer  $\frac{1}{2}\lambda$  and the impedance is either capacitively or inductively reactive, according to whether we move below or above the resonant frequency. Once we further transform these initially transformed impedance values with the  $75\Omega$  matching section, we obtain a usable  $50\Omega$  impedance across the band.

The results of the technique can be modeled in a misleading way if we only use the lossless transmission lines available within NEC. However, recent implementations of the NEC have introduced methods of including line losses and arriving at a more accurate picture of the results. To provide a clearer view of how well the system works, I used the following lines to model the matching system with the dipole at 90' above average ground:  $50\Omega$ : RG-213, VF 0.66, loss 0.6 dB/100' @ 10 MHz;  $75\Omega$ : RG-216, VF 0.66, loss 0.7 dB/100' @ 10 MHz. These cables easily handle the upper limits of amateur power levels. The sum of the two lines, accounting for the velocity factors involved, is 129.83' of cable that is both part of the matching system and part of the main feed system, since the elements are in series. (This line length will become significant shortly.) The total line length is not unreasonable as nearly a minimum value for a dipole that is 90' above ground and somewhat offset from the station equipment.



**Fig. 9** shows the 72- $\Omega$  SWR curve for the dipole without the matching system in place and the 50- $\Omega$  curve at the junction of the matching section and the main feedline. The system easily covers the entire band, although the SWR values exceed 1.5:1 near the ends of the band. Theoretically, we can use any multiple of  $\frac{1}{2}\lambda$  for the 50- $\Omega$  section of the line. Longer lines will show the double-dip SWR curve that is not fully visible with a single half-wavelength section. However, for real lines with losses, the band-edge SWR performance will deteriorate.

In 1995, Frank Witt, AI1H, presented an alternative to the 50-75- $\Omega$  transmission-line broadband matching system. He called the system the Transmission-Line Resonator (TLR). It consisted of three lengths of 50- $\Omega$  cable. We shall continue to use RG-213 with a velocity factor of 0.66 and a loss factor of 0.6 dB/100' as our implementation, which coincides with Witt's own version. A length of cable connects the antenna terminals to the source, which can be the station equipment or a further length of 50- $\Omega$  cable that reaches the equipment. At the antenna terminals, he connects

an open stub across the terminals, effectively adding a shunt capacitance (more correctly, a capacitive reactance) to the antenna terminal impedance. At the source end of what Witt calls the "link" line, he adds a shorted stub across the line, effectively adding a shunt inductance (or inductive reactance). With the proper proportions, shown for the 80/75-meter band in **Fig. 10**, the combination yields a broadband 50- $\Omega$  match for the dipole. The dimensions used in the model vary slightly from Witt's original, but fit the dipole length and cables used in the model. Any implementation of the matching system would require a bit of field adjustment to arrive at the final lengths of the two stubs and the linking line. (For detailed information on and calculations for the TLR matching system see chapter 9 of the current (20<sup>th</sup>) edition of *The ARRL Antenna Book* and Witt's original article.

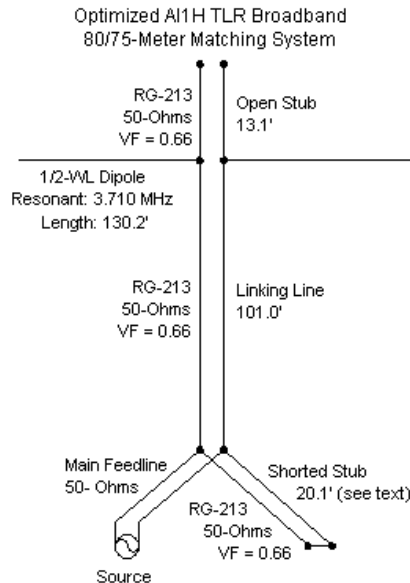
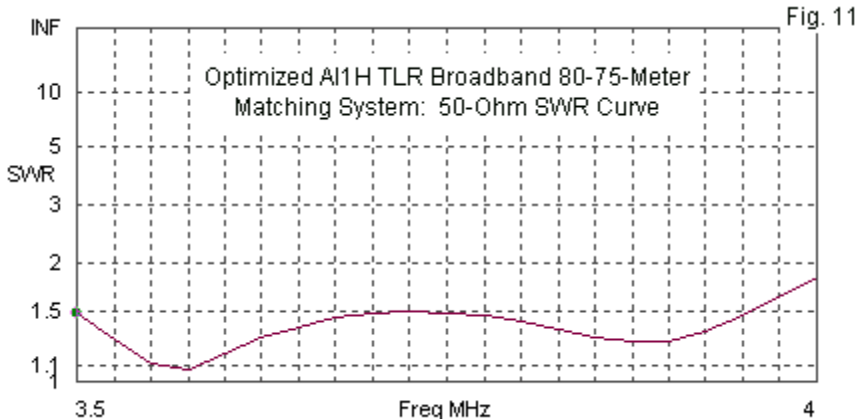


Fig. 10

We can view the Witt system as a version of the “match line and stub” matching system, after suitable adjustment of the feedpoint impedance values with the top open stub. The calculated values required for each of the three lines provides for broad-band service by opposing the natural trends in impedance transformation at key points in the system. The result is the double-dip 50- $\Omega$  SWR curve shown in Fig. 11.



Of the systems that we have examined, only the two transmission-line matching systems and the 3-wire coupled resonator array arrived at 50- $\Omega$  impedances. The ribbon and cage systems use 72- $\Omega$  reference impedances to achieve full band coverage, while the folded-dipole and linear parasitic element array uses a high impedance value suited to parallel transmission lines. 50- $\Omega$  coaxial cable remains the preferred feedline based on the nearly universal standard of a 50- $\Omega$  input and output impedance value of current amateur equipment.

## *Efficiency*

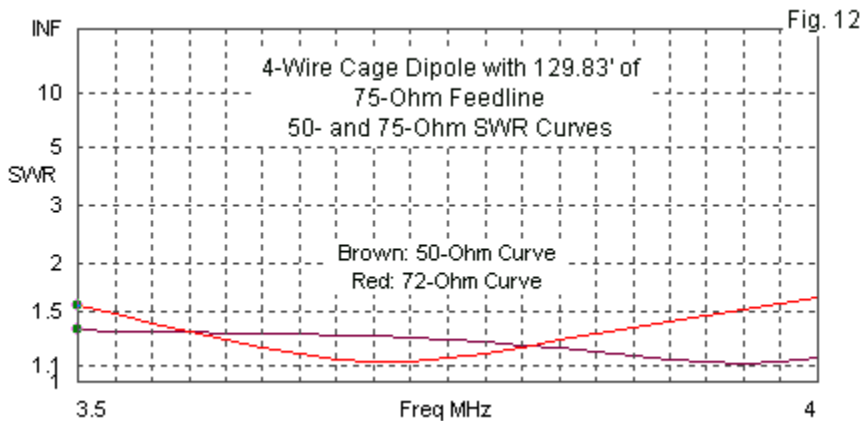
When we combine any antenna with a transmission line in broadband service, we incur losses at one or both ends of the band relative to potential performance of the dipole alone. None of our systems is immune to this condition. Even a system that is well matched at the resonant frequency is subject to increased feedline losses as we move away from the resonant frequency and add the SWR multiplier to basic matched line losses.

Arriving at a reasonably fair comparison of system losses is difficult at best when we consider that two of the systems require certain lengths of coaxial cable as part of the matching system. The maximum line length involved in matching for our 80-75-meter samples is 129.83'. Therefore, to equalize the playing field, I added to each sample antenna a cable of this length, using RG-213 for the 50- $\Omega$  runs and RG-216 for the 75- $\Omega$  lines. The ribbon and cage antennas required a single cable, while the TLR system requires the addition of a short section of 50- $\Omega$  cable to arrive at the total cable length. Rather than calculating losses in dB, I simply obtained gain values for each entire system, including antenna wire and cable losses. The resulting pattern of gain values will reveal—by comparison with an uncabled AWG #12 copper dipole—not only the level of loss, but as well the pattern of where in the band those losses are likely to occur. **Table 3** summarizes the loss picture with sample gain values at 3.5, 3.75, and 4.0 MHz.

Table 3. Comparative gain values of broadband 80-75-meter antennas and matching systems at 90' above average ground with 129.83' of feedline

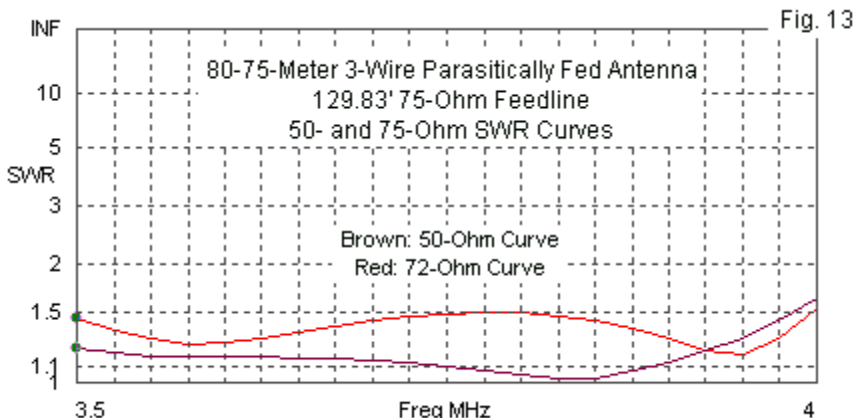
Antenna	Gain in dBi at 3.5 MHz	3.75 MHz	4.0 MHz
Bare antenna with no feedline	6.10	6.24	6.44
"W6NL" $\frac{1}{2}$ - $\lambda$ + $\frac{1}{4}$ - $\lambda$ matching system	5.07	5.68	5.36
AI1H TLR matching system	5.07	5.68	5.36
16" dia reference dipole /75- $\Omega$ line	5.52	5.75	5.86
4-wire cage dipole /75- $\Omega$ line	5.51	5.76	5.88
3-wire coupled-resonator/75- $\Omega$ line	5.58	5.74	5.69

Except at mid-band, the two matching systems show about 0.5-dB lower gain than the wire antenna samples. Besides showing a higher band-edge gain, the addition of 129.83' of 75- $\Omega$  transmission line provides improved SWR bandwidth at the source end of the line by forming a  $3/4 - \lambda$  transformer. **Fig. 12** exemplifies the altered SWR curve by showing 50- $\Omega$  and 75- $\Omega$  curves for the 4-wire cage. All of the ribbon and cage dipoles would show similar curves.



The SWR curves are satisfactory for virtually all applications. Perhaps only users of high power amplifiers with very sensitive fold-back

circuits might find a shortcoming: the 72- $\Omega$  SWR exceeds 1.5:1 at the band edges, although the 50- $\Omega$  curves is quite well tamed. A similar concern might strike the user of a 3-wire coupled resonator system with an equal length of 75- $\Omega$  cable, as shown in **Fig. 13**.



The final question is whether we can further tame the SWR curves without adversely harming dipole efficiency.

### Combining Techniques

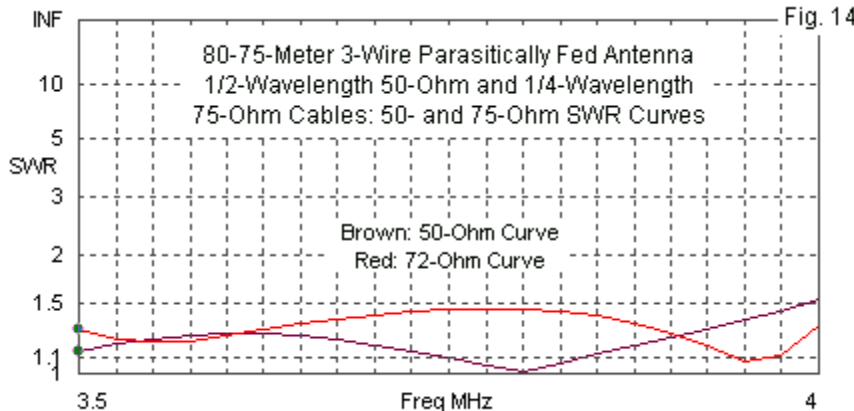
A simple AWG #12 copper wire dipole responds to either the W6NL or the AI1H transmission-line based matching systems with an SWR curve that yields a 50- $\Omega$  SWR less than 2:1 across the 80-75-meter band. Equipping the ribbon and the cage dipoles with a 75- $\Omega$  cable of the specified length (129.83') produces even lower SWR values using a 50- $\Omega$  reference. The final question, applicable only to those who use

equipment sensitive to 50- $\Omega$  SWR values above 1.5:1, is whether we can lower the SWR curve even further. To a limited extent, we can.

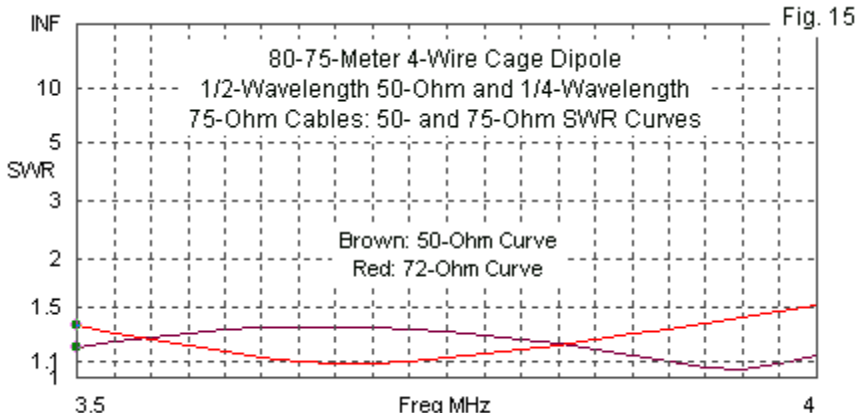
Although I am aware of no actual attempt to do so, there is no rule against combining a wide-band dipole with the W6NL matching system. Like the thin-wire dipole, all of the cages and ribbons have resonant impedances close to 72  $\Omega$ . Therefore the mid-band SWR values for the original design and when applied to a ribbon or cage will be quite similar. The differences will appear as we move away from the resonant frequency. The thin-wire dipole shows a rising SWR based on a slow change in the resistive component and a faster change in the reactance.

The 3-wire coupled resonator system shows a relatively flat SWR relative to 72  $\Omega$  across the band. At the band edges, we find no significant increase in the reactance, but instead a small fluctuation. As a consequence, the band-edge values should not depart radically from the mid-band SWR value.

In fact, as revealed by the SWR curves in **Fig. 14**, we do obtain a small amount of improvement, but it applies in the main to the 72- $\Omega$  SWR curve. The 50- $\Omega$  curve average value is not quite as good as when we use a simple run of 75- $\Omega$  cable, but the value at 4.0 MHz is marginally better. (In either case, we might shorten the second parasitic driver slightly and stretch the SWR curve to give us a value of less than 1.5:1.) Modeling simplifies the calculation of both the antenna impedance and the line losses at each frequency in the 3.5-4.0-MHz span so that we can obtain a relatively reliable assessment of our design options.



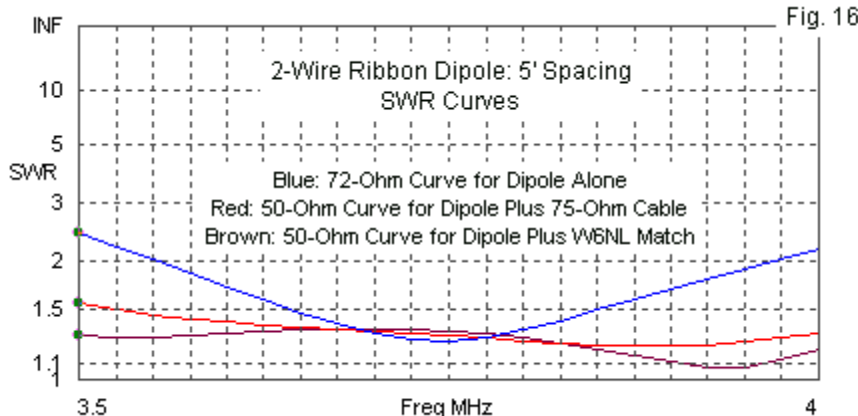
We can apply the same technique to any one of the wide-band ribbon or cage dipoles and assess its performance against the use of a 75- $\Omega$  cable alone. **Fig. 15** provides the 50- $\Omega$  and 72- $\Omega$  SWR curves for the 4-wire cage version. Once more, the improvement accrues to the 72- $\Omega$  curve rather than to the 50- $\Omega$  curve.



Perhaps the best application of combined broad-banding methods involves dipole designs that do not quite reach the desired goal of an SWR curve with maximum values of less than 2:1, but that are improvements upon the simple thin wire (AWG #12) dipole. Early on, we rejected the use of a 2-wire ribbon dipole for this very reason. Suppose that we construct such a dipole with a 5' wire spacing. The 72- $\Omega$  SWR curve in **Fig. 16** shows why we omitted the design. The SWR rises above 2:1 well before we arrive at either band edge, although the curve is certainly an improvement upon the thin-wire dipole shown as one of the curves in **Fig. 9**.

If we add our standard 129.83' length of 75- $\Omega$  cable, we obtain a 50- $\Omega$  curve with a maximum SWR value of about 1.6:1. However, if we instead employ a  $\frac{1}{2}\lambda$  50- $\Omega$  cable plus a  $\frac{1}{4}\lambda$  75- $\Omega$  matching section, we obtain a curve with a maximum 50- $\Omega$  SWR of about 1.3:1. This final curve would satisfy the requirements of even the most sensitive fold-back

circuit. Similar results would emerge with undersized versions of most of the ribbon and cage dipoles.



Whether we lose anything by using the matching system rather than the simple cable run appears in **Table 4**. The data compares antenna-only gain values with values that emerge from the use of a simple 75- $\Omega$  cable and from the more complex matching system.

**Table 3.** Comparative gain values of a 2-wire ribbon dipole for 80-75-meter at 90' above average ground alone, with 129.83' of feedline, and with a 129.83' matching system

Antenna	Gain in dBi at 3.5 MHz	3.75 MHz	4.0 MHz
2-wire ribbon ant with no feedline	6.13	6.26	6.45
2-wire ribbon/75- $\Omega$ line	5.33	5.70	5.77
2-wire ribbon/ "W6NL" match	5.36	5.70	5.73

As we might expect, the 2-wire ribbon dipole with either feedline shows better gain values than a thin-wire dipole equipped with either the AI1H TLR match or what we have labeled for convenience as the W6NL match. The similarity of gain values between the single-cable feedline and the matching system shows that there is essentially no difference in feedline efficiencies, since the SWR values at the antenna feedpoint do not rise to very high values but instead only to inconveniently high values. One way to minimize losses from a matching system and to arrive at a more nearly perfect SWR curve is to begin with a reasonably wide-band dipole design (even if not perfect) and to apply the matching system to it rather than to a thin-wire dipole.

### *Conclusion*

We have examined numerous, but by no means all, of the broadbanding techniques. We progressed from complex wire dipoles to multi-wire coupled resonator arrays and finally to transmission-line-based matching systems. We required no lumped components or coaxial antenna sections to achieve exceptionally broadband results. Our only presumption was that we would need a feedline about 1.4 times the height of the antenna above ground for the 90' height used in the samples.

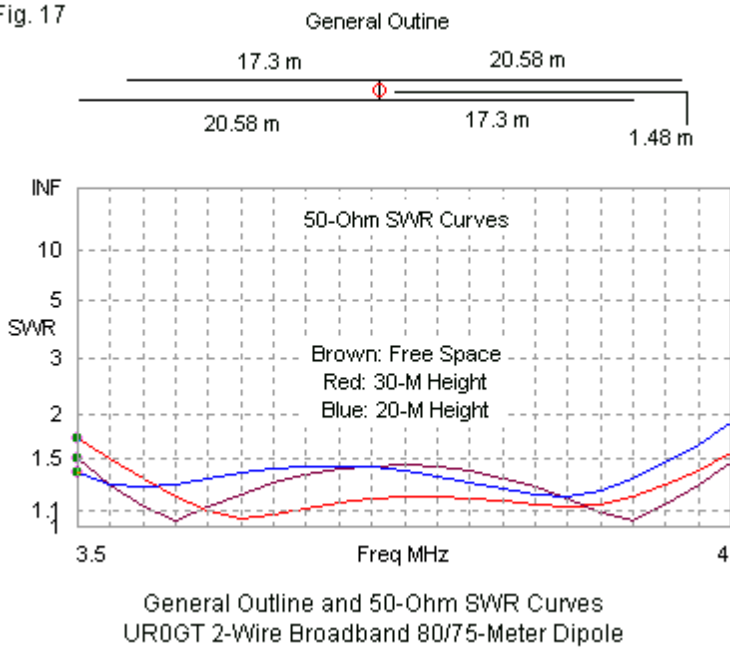
The best results occurred with broadband dipoles and either  $75\Omega$  cable or one of the transmission-line-based matching systems. Although the samples used the W6NL system, the AI1H system would have returned equivalent results. Each case showed that if we opt for a coaxial cable feedline, a certain reduction in gain is a cost of the option, however we arrange the cable. However, the broader the bandwidths of the initial dipoles, the lower were the losses at the band edges. Moreover, by combining physical methods of creating broadband dipoles with

appropriate matching methods, we could reduce the required structural size of the dipole and still obtain a  $50\text{-}\Omega$  SWR curve that never reach a value of 1.5:1. Hence, the initial broadband ribbon and cage dipoles can have smaller cross sections and still arrive at a very desirable SWR curve without further sacrificing gain at either band edge.

### *Appendix: The UR0GT Broadband 80-75-Meter Dipole*

Recently, I uncovered an interesting dual-wire broadband antenna for 80 and 75 meters from Russia, a design by UR0GT. In metric terms, it consists of two 2-mm diameter copper wires, each 37.88 m long. However, as shown in **Fig. 17**, the wires are offset relative to the center point. The shorter wire is (in my NEC-4 model) 17.3 m long, while the longer wire is 20.58 m. The spacing is 1.48 m, although this dimension is not critical within several centimeters, but it does set the mid-band relative phase angles of the element currents. At the center point, between the two wires, we run a single wire and feed it in the middle.

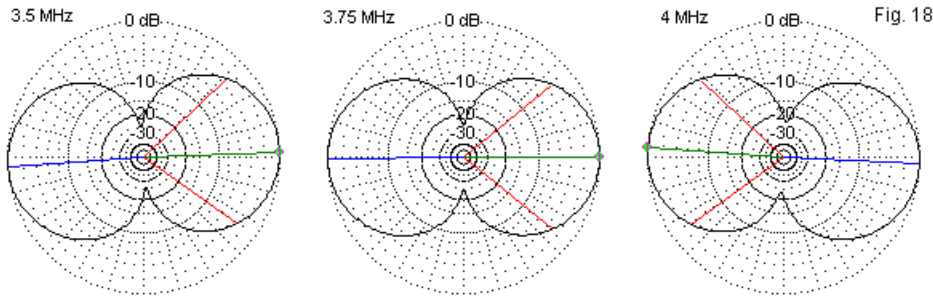
Fig. 17



The 50- $\Omega$  SWR curves show distinct higher and lower frequency resonance points. To move each resonant frequency, one may adjust the length of either the longer wire or the shorter wire. Although the frequencies of the resonant points are relatively independent, their positions determine both the band-edge and the mid-band SWR values. Note from the SWR curves that, like all broadband 80/75-meter antennas, the SWR curves will be somewhat height-sensitive, since on average, antennas for the band are less than  $\frac{1}{2}\lambda$  above ground. Therefore, anyone who wishes to replicate the antenna—and it is worthy of

replication—should model the exact dimensions for the planned installation height.

The offset wires of the antenna produce some patterns—at the band edges—that are also offset from a true broadside to the wires. **Fig. 18** provides 3 E-plane free-space patterns to show the effect. In general, the pattern offset is only about 3° relative to a true broadside in the extreme cases. Therefore, with a beamwidth approaching 80°, an operator could not detect the pattern offset during use, even when switching from the low end of the CW band to the top end of the phone allocation.



Free-Space E-Plane Patterns of the UR0GT 2-Wire 80/75-Meter Antenna

One key to the operation of the UR0GT wide-band antenna is the fact that on each side of center, the two wires are 90° apart in current phase angle at 3.75 MHz. The relative current magnitudes on the short and the long sections vary with frequency within the overall passband, yielding a low 50-Ω SWR across the entire band. Note in **Fig. 19** the dominance of either the long wire or the short wire at the lower and upper band edges. (The last line in the data in the figure shows the ratio of higher to lower

current and also the phase-angle difference [ $\Delta$ ] between the wires at each sampled frequency.)

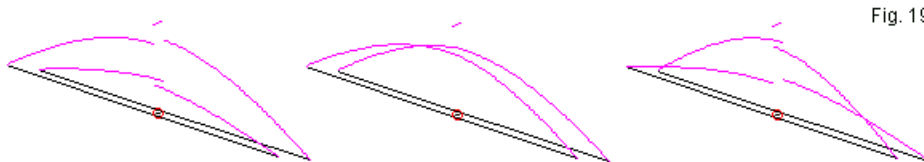


Fig. 19

Frequency	3.50 MHz		3.75 MHz		4.00 MHz	
Current	Mag.	Phase	Mag.	Phase	Mag.	Phase
Short Wire	0.335	44.05°	0.703	44.27°	0.783	19.34°
Long Wire	0.792	162.72°	0.700	134.84°	0.369	134.61°
Ratio/Delta	2.36:1	18.67°	1:1	90.57°	2.12:1	115.27°

Current Distribution of the UR0GT 2-Wire 80/75-Meter Antenna

The relative simplicity of the UR0GT antenna recommends it for consideration among the array of broadband options for the 80/75-meter band. With the usually lengths of coaxial cable necessary to connect the antenna to the station, the SWR curves at the equipment end of the line should be even flatter than those shown. However, as with all antenna designs, successful replication lies in the details of the installation.

## Chapter 52: Fine-Tune Broadband Antennas for 80-75 Meters

In Chapter 51: “Coverage of the 80/75-Meter Band with AWG #12 Copper Wire”, I explored some of the methods for obtaining full coverage across the 3.5 to 4.0 MHz span with a single antenna. I re-examined some further options in a QEX column that opened some additional possibilities offered by combining broadbanding techniques. Some of the methods of matching via combinations of transmission line proved robust enough to allow the use of ribbon or cage constructs with relative small proportions, instead of the very large dimensions required for direct full coverage by the antenna alone. In fact, we were able to obtain 50- $\Omega$  SWR curves with values less than the 1.5:1, thus meeting the most rigorous requirements of amateur amplifiers having the most sensitive fold-back circuits.

Near the end of the QEX piece, I cautioned that the dimensions shown in the samples applied only to antennas in the 70' to 100' height range over average ground. Outside that range, the antenna builder will have to make a considerable number of experimental adjustments to assure performance, and at some heights, the arrangement may not work at all. Because most amateurs under-appreciate the effects of height on the resonant frequency and feedpoint impedance of dipoles less than 1  $\lambda$  above ground, we might well re-visit the question. Along the way, we shall discover why certain matching schemes have application only at certain heights for 80-75-meter antennas. As well, we can investigate how we might tailor the dipole length and the lengths of cables forming the matching system to optimize performance at heights within the usable range.

## Some Fundamentals

The restrictions and the goals for our project remain unchanged relative to earlier investigations. The antenna material is AWG #12 copper wire. I use the following transmission lines to model the matching system with the dipole at 90' above average ground:  $50\ \Omega$ : RG-213, VF 0.66, loss 0.6 dB/100' @ 10 MHz;  $75\ \Omega$ : RG-216, VF 0.66, loss 0.7 dB/100' @ 10 MHz. These lines easily handle amateur power limits on 80 and 75 meters. The goal is to achieve with reasonable efficiency a  $50\text{-}\Omega$  SWR curve from 3.5 to 4.0 MHz with no SWR value exceeding 1.5:1.

**Fig. 1** reviews the most common options for obtain wide-band performance directly from the antenna structure. A single wire that is 16" in diameter will just cover the band with a  $72\text{-}\Omega$  SWR of 2:1 or less. Such a wire is impractical in amateur (or any other) service, so we tend to create simulations composed of several wires (AWG #12 by our specification). One popular choice is a ribbon element composed of 2 or more wires in a common plane. An alternative is the 4-wire or 6-wire cage of wires.

Models of these structures use end structures similar to those shown in the sketches rather than creating junctions of wires forming a point. At the center feedpoint, the models use linear wires and create a parallel feedpoint by running near-zero length transmission lines from the designated source wire to the center segment of each other wire. These measures result in uniformly ideal average gain test values that facilitate comparisons. In these notes, we shall be interested almost solely in matters relating to the feedpoint impedance and the SWR curves across the 3.5-4.0-MHz band.

Some Basic Shapes for  
"Fat" Wire Simulation  
with Thin Wires

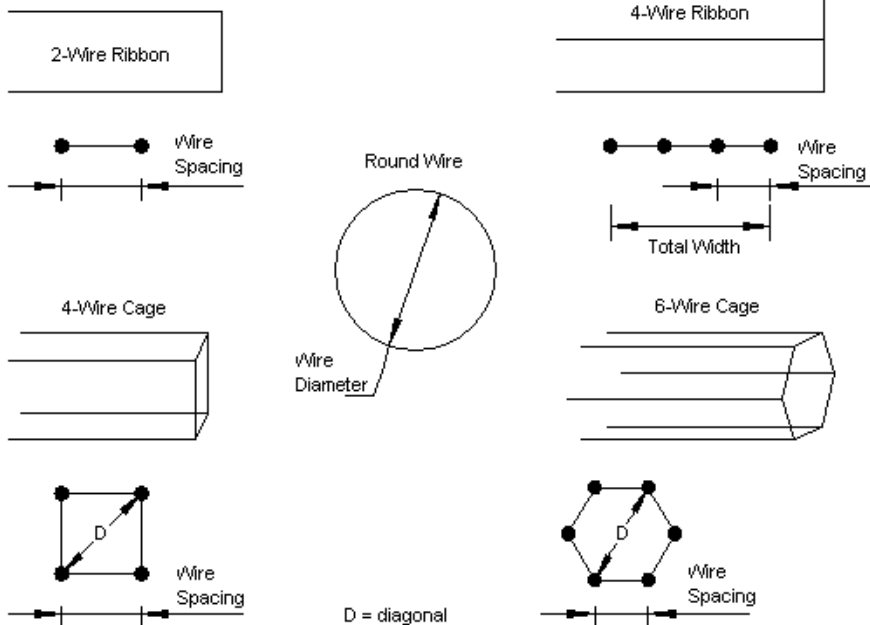


Fig. 1

**Table 1** provides the required dimensions for full-size dipoles using each type of structure displayed in **Fig. 1**. The 2-wire ribbon antenna is missing because there is no practical size that will cover the entire band.

**Table 1.** Dimensions of dipoles with virtually identical full-band coverage of 80-75 meters with less than a 2:1 72- $\Omega$  SWR value

Antenna	Length	Res.	Frequency	Impedance
Single wire 16" diameter	123.6'	3.72 MHz		71.6 - j0.4 $\Omega$ (free space) 89.1 - j4.8 $\Omega$ (90')
4-wire ribbon Wire spacing 2' Total width 6'	123.4'	3.72 MHz		72.4 + j0.4 $\Omega$ (free space) 89.3 - j4.1 $\Omega$ (90')
4-wire cage Wire spacing 3' Diagonal 4.24'	121.8'	3.71 MHz		72.1 - j0.5 $\Omega$ (free space) 88.3 - j6.0 $\Omega$ (90')
6-wire cage Wire spacing 1.5' Diagonal 3'	122.2'	3.73 MHz		72.1 - j0.7 $\Omega$ (free space) 88.6 - j5.9 $\Omega$ (90')

Since our goal is to combine the simulated fat dipole with a second broadbanding technique, we do not need to achieve full band coverage. Instead, we may opt for more reasonable cross-section dimensions for the multi-wire dipoles. **Table 2** provides very usable dimensions of dipoles having virtually identical properties. Note that the band-edge 72- $\Omega$  SWR values are just about the same in each case. The cross section dimensions fall within the shop capabilities of most serious 80-75-meter antenna users. Despite the smaller dimensions, the ribbons and cages achieve a fair amount on initial broadbanding when compared to the reference single AWG #12 wire dipole at the bottom of the list.

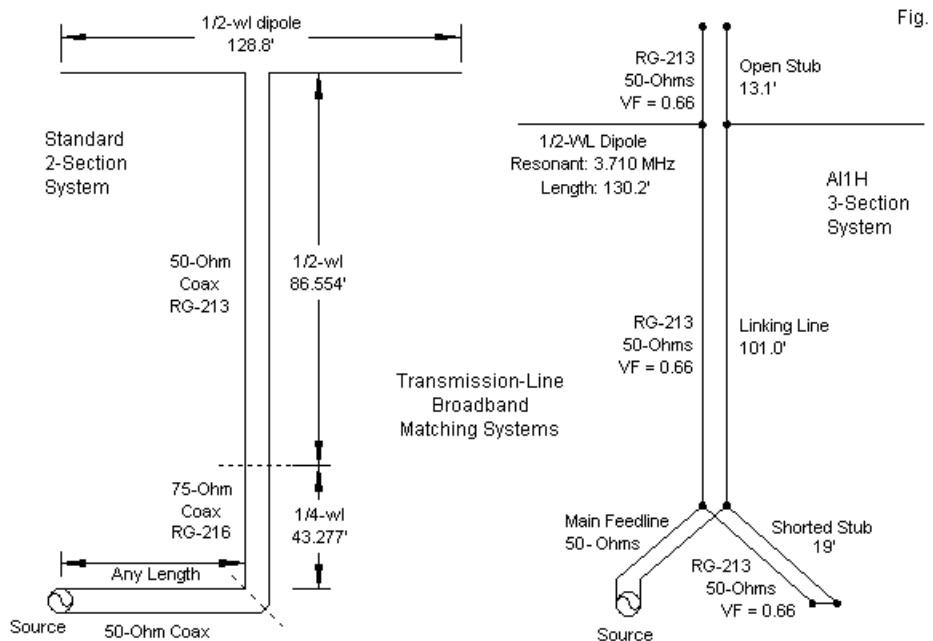
Table 2. Dimensions of dipoles at 90' above average ground with virtually identical coverage of 80-75 meters

Antenna	Length	72- $\Omega$ SWR at	
		3.5 MHz	4.0 MHz
2-wire ribbon Wire spacing 5' (60")	122.4'	2.42	2.17
4-wire ribbon Wire spacing 0.3' (3.6") Total width 0.9' (10.8")	125.3'	2.41	2.15
4-wire cage Wire spacing 0.4' (4.8") Diagonal 0.57' (6.79")	125.2'	2.41	2.16
6-wire cage Wire spacing 0.2' (2.4") Diagonal 0.4' (4.8")	125.4'	2.39	2.16
Single #12 wire (reference)	128.8'	3.54	3.78

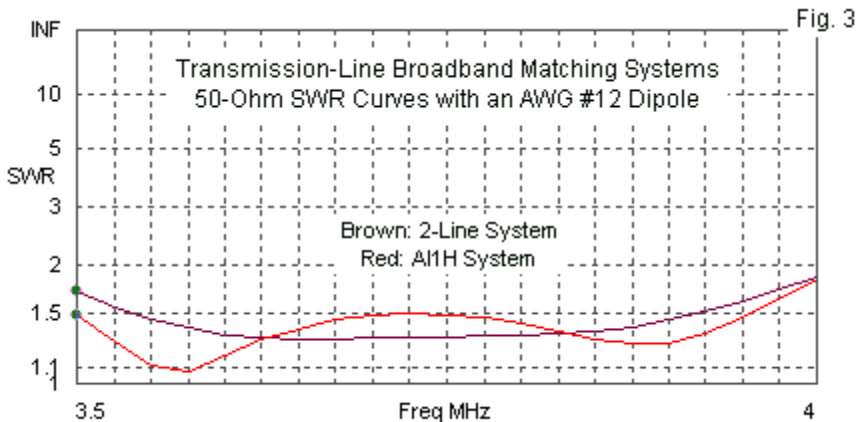
We do not need to use a 2:1 limiting value of SWR because the transmission-line matching systems we shall employ are capable of achieving that value with a single AWG #12 wire dipole. Instead, we need sufficient broadbanding from the antenna structure alone so that when we apply the transmission-line matching schemes, the maximum 50- $\Omega$  SWR value will be less than 1.5:1.

There are two general matching methods in use, and both appear in **Fig. 2**. The two-line system uses a  $\frac{1}{2}\lambda$  section of 50- $\Omega$  cable followed by a  $\frac{1}{4}\lambda$  section of 75- $\Omega$  cable. At 90', the dipole impedance is close to 90  $\Omega$  at resonance. If we cut the  $\frac{1}{2}\lambda$  section of 50- $\Omega$  cable for the geometric mean frequency of the passband (about 3.742 MHz), the feedpoint impedance will repeat itself at that frequency. On either side of this frequency, the cable length will no longer be precisely  $\frac{1}{2}\lambda$ . Hence,

the impedance at the source end will be a transformed value. When we pass the range of transformed impedance values through a  $\frac{1}{4}\lambda$  75- $\Omega$  matching section, the new impedance values will be very close to 50  $\Omega$  across the entire band. Adjusting the cables for the 0.66 velocity factor that applies to both lines, we obtain a combination of 86.55' and 43.28' for a total length close to 130'. For an antenna that is 90' above ground and offset from the operating position, the line length is reasonable as a minimum needed to reach from the equipment to the antenna. Any additional cable length would use 50- $\Omega$  cable.



The right side of **Fig. 2** shows the three-line system developed by Frank Witt, AI1H, in 1995. One can view the system equally as a single line with the antenna tapped down from the open top and the main  $50\Omega$  feedline tapped upward from the shorted bottom. For full-band coverage with a simple AWG #12 dipole, Witt discovered that the SWR bandwidth improved if he moved the self-resonant dipole frequency downward from the geometric mean frequency to the indicated value of 3.710 MHz. Since we shall make comparisons and since the line length of this all- $50\Omega$  system between the antenna and the main feedline does not quite equal 130', I added 30' of RG-213 between the shorted-stub junction and the model source.



As the 50- $\Omega$  SWR sweeps in **Fig. 3** show, both matching systems are capable of matching a single-wire AWG #12 copper dipole to values less than 2:1 across the entire 80/75-meter band. In the test model, the total transmission-line length is 130'. Moreover, the antenna is at a fixed 90' height above average ground. Our requirement is more severe: 50- $\Omega$

SWR values of less than 1.5:1 across the band. In pursuit of that goal, we shall have to adopt a dipole with an initial SWR bandwidth that is wider than the value we may obtain from a single #12 wire. Moreover, we may wish to vary the antenna height and the soil quality. Each of these variations from the original problem confronts us with limitations of the matching systems.

Both matching systems rely on the fact that at about 90' the dipole impedance at resonance is approximately  $90\ \Omega$ . An impedance value in this vicinity provides the correct conditions for the main  $50\text{-}\Omega$  line in either system to transform off-resonance impedance values within the passband to values that, when further transformed by the  $\frac{1}{4}\text{-}\lambda$  series section or compensated for by the open and shorted stubs, provide near- $50\text{-}\Omega$  impedance values across the band. At other heights, the dipole resonant impedance may not be optimal.

To sample what happens to a dipole with changes in antenna height, let's select one of the semi-fat multi-wire constructs. Since they all have the same resonance impedance and SWR bandwidth, any of the constructs will do the job. Therefore, I selected the 4-wire cage as our representative from the group in **Table 2**. I then surveyed the results of varying the height in 10' increments from 30' to 150'. **Table 3** provides data from this series.

Table 3. The effects of antenna height above average ground on the impedance properties of a semi-fat 4-wire cage dipole 0.4' (4.8") per cross-section side dimension

Height Feet	$\lambda$	Impedance (Ω) at 3.745 MHz	72-Ω SWR		Resonant Frequency MHz
			3.5 MHz	4.0 MHz	
30	0.114	51.1 + j14.6	2.68	3.81	3.675
40	0.152	61.2 + j17.6	2.27	3.54	3.650
50	0.190	71.9 + j16.4	2.05	3.21	3.650
60	0.228	80.8 + j11.3	2.00	2.90	3.675
70	0.266	86.5 + j3.8	2.07	2.61	3.700
80	0.304	88.4 - j4.7	2.22	2.36	3.725
90	0.342	86.9 - j12.5	2.41	2.16	3.750
100	0.380	82.6 - j18.4	2.62	2.03	3.775
110	0.418	76.8 - j21.7	2.83	1.99	3.800
120	0.457	70.6 - j22.3	3.03	2.07	3.800
130	0.496	65.2 - j20.3	3.18	2.24	3.775
140	0.533	61.3 - j16.5	3.26	2.45	3.775
150	0.571	59.6 - j11.6	3.25	2.64	3.750
(Free Space		72.4 + j0.6	2.73	2.41	3.745)

Notes: 1. Dipole length: 125.2'. 2. Height in  $\lambda$  at 3.745 MHz.  
 3. Resonant frequency to nearest 0.025-MHz increment.

The table reveals that the impedance at the geometric mean frequency of the 80-75-meter band varies both the resistive and reactive components, but the cycles are offset from each other. There are two significant consequences of the variation. First, the impedance value is only optimal for broadband transformation in a fairly narrow range of heights above ground, perhaps in the 70' to 110' range for the low maximum value of permitted 50-Ω SWR. Second, the shifting reactive component strongly suggests that the dipole length itself may become one of the variables as we attempt to optimize the matching system for different heights above ground.

### Adjusting the 2-Line Matching System with a 4-Wire Cage Dipole

As shown in **Fig. 2** on the left, the 2-line matching system consists of a  $\frac{1}{2}\lambda$  50- $\Omega$  line that functions to pre-transform dipole feedpoint impedance values in preparation for the final transformation in the  $\frac{1}{4}\lambda$  75- $\lambda$  line section. The initial system used lines calculated for a height of 90' above average ground and for the geometric mean frequency in the passband. The SWR curve in **Fig. 4** shows that the result meets the initial specifications. The character of the curve differs somewhat from the curve for the same matching system applied to the single-wire dipole. Rather than having SWR peak values only at the band edges, we also find a mid-band peak value. We shall use this peak value in conjunction with the band edge values as we characterize the performance of the system at various heights above ground.

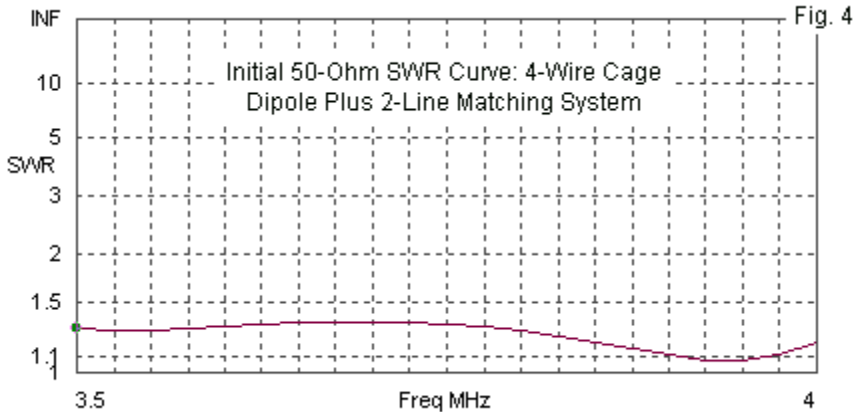


**Table 4.** The effects of antenna height above average ground on the impedance properties of a semi-fat 4-wire cage dipole plus a 2-line matching section

Height Feet	$\lambda$	Impedance ( $\Omega$ )		50- $\Omega$ SWR		Resonant Frequency MHz	
		at 3.745 MHz	3.5 MHz	Mid-Band	4.0 MHz	Frequency MHz	
30	0.114	88.0 - j39.1	1.94	2.27	1.86	3.650	
40	0.152	76.2 - j31.9	1.70	1.97	1.74	3.650	
50	0.190	69.5 - j23.9	1.48	1.72	1.61	3.625	
60	0.228	66.0 - j16.6	1.33	1.52	1.49	3.650	
70	0.266	64.6 - j10.3	1.24	1.40	1.38	3.650	
80	0.304	64.7 - j4.6	1.24	1.33	1.28	3.700	
90	0.342	66.1 + j0.4	1.29	1.33	1.18	3.745	
100	0.380	68.7 + j4.8	1.37	1.40	1.10	3.775	
110	0.418	72.6 + j8.2	1.47	1.50	1.09	3.800	
120	0.457	77.7 + j10.1	1.56	1.61	1.16	3.800	
130	0.496	84.1 + j9.5	1.65	1.72	1.26	3.775	
140	0.533	89.6 + j5.7	1.72	1.81	1.34	3.750	
150	0.571	92.1 - j0.8	1.75	1.87	1.40	3.750	

Notes: 1. Dipole length: 125.2'. 2. Height in  $\lambda$  at 3.745 MHz.  
3. Resonant frequency to nearest 0.025-MHz increment.

**Table 4** provides data on what happens as we change the antenna height with the standard matching system. The italicized entries show the range of acceptable SWR curves to meet the stringent 1.5:1 50- $\Omega$  SWR limit. As the changing difference in the band-edge SWR values with different heights suggests, the mid-band peak value may vary its frequency. In most instances, the mid-band peak SWR value is the limiting factor in meeting specifications. Still, we may note that for all heights except the lowest, the semi-fat cage plus the matching system meets the usual 2:1 SWR limit that may apply to less critical systems.

There are no rules against adjusting the dipole and the transmission line lengths to better optimize the system. The standard calculation of the  $\frac{1}{2}\lambda$  50- $\Omega$  line section yields a length of 86.5', while the 75- $\Omega$  transformer section is half that length—when we adjust the lengths for the velocity factor of 0.66. The standard calculation uses the

geometric mean frequency of about 3.742 MHz. We may alter any one or more of the three variables to seek a better curve. We may define a better curve as one in which all peak SWR values are the lowest possible with relatively equal values for all three peaks (band-edge and mid-band). We shall eventually modify this definition slightly.

As samples of what the adjustment process may yield by way of different lengths for the dipole and the two transmission lines, let's arbitrarily select dipole heights of 70', 90', and 110'. In this way, we can compare the results with the initial table that used standard calculated length for the transmission lines. In general, changing the dipole length has no significant effect on the mid-band peak. However, it does allow one to equalize as best possible the band-edge peak values of SWR. Changing the line length affects the impedance transformations and may raise or lower all three peaks. **Table 5** provides the key dimensions and SWR results from optimizing the system for each of the three heights.

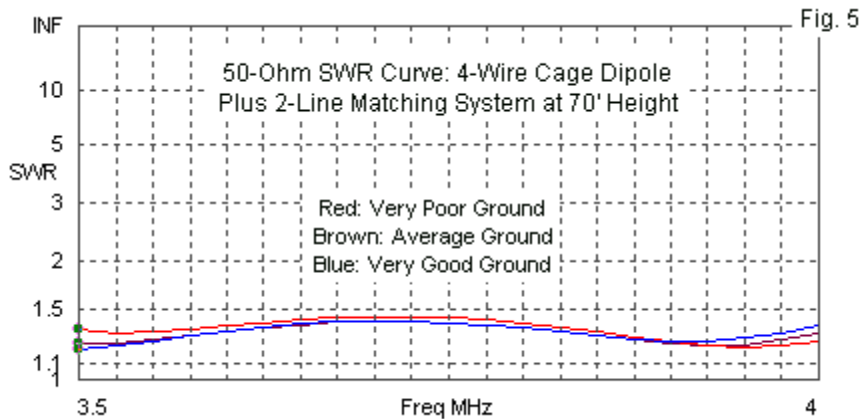
**Table 5. Optimized dimension and 50- $\Omega$  SWR results for 70', 90', and 110' high 4-wire cages dipoles with a 2-line matching system**

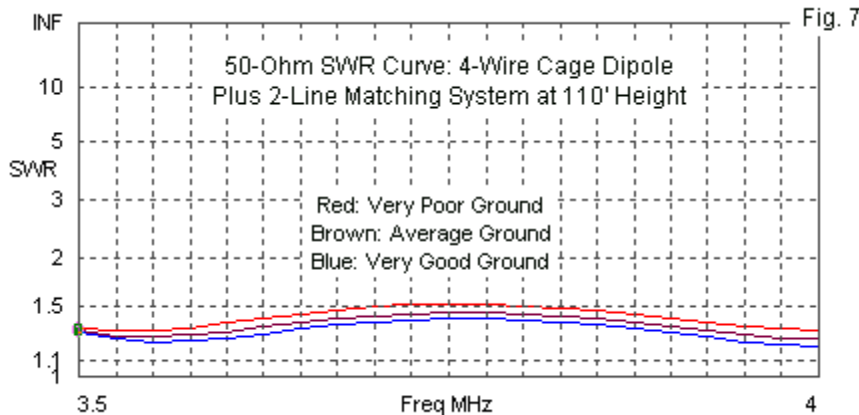
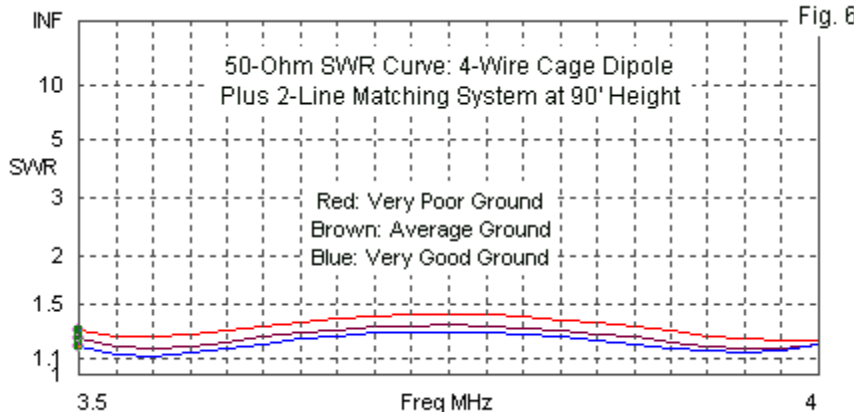
Dipole Height	Dipole Length	$\frac{1}{2}\lambda$ Line Length	$\frac{1}{4}\lambda$ Line Length	50- $\Omega$ SWR		
				3.5 MHz	Mid-band	4.0 MHz
70'	124.4'	85.5'	43.75'	1.23	1.39	1.30
90'	125.2'	86.0'	41.25'	1.22	1.32	1.19
110'	126.0'	85.5'	42.25'	1.33	1.44	1.24

The changes in line lengths for a 90' dipole height are largely cosmetic, compared to using the standard calculations. However, at both 70' and 110', the changes in all three variables yield superior SWR curves compared to making no changes at all. The required dipole length increases with height. However, for both new heights, the  $\frac{1}{2}\lambda$  50- $\Omega$  line is slightly shorter than for 90'. In contrast, in both cases, the  $\frac{1}{4}\lambda$  75- $\Omega$  transformer section is longer. The precise changes are functions of the

fact that as we change the antenna height, the resistive and reactive components of the impedance do not change in step with each other.

Although we have altered the dimensions to improve the SWR curves over average soil at the three test heights, we have yet to see how the curves change as we change the soil quality. To test this aspect of the broadbanding question, I created SWR curves for each variation of the original system for three soil types: very good (cond. 0.0303 S/m, perm. 20), average (cond. 0.005 S/m, perm. 13), and very poor (cond. 0.001 S/m, perm. 5). **Fig. 5, 6, and 7** show the family of curves for each antenna height. The results may provide us with clues as to further refinements we might make to the adjustments.





In conjunction with the data in **Table 5**, the three SWR plot collections tell us a bit of a story. Over average ground, the dipole at 90'

provides the best SWR pattern across the passband. We must note that soil improvement also yields SWR improvement—however small it might be—while soil degradation provides a less optimal plot. As we reduce the antenna height, with a resulting change in the dipole length to keep the curve centered, we find slightly lesser values over average ground than we found at 90', but the three curves for different soil types are more tightly grouped with far less difference related to soil quality. In contrast, the family of patterns at 110' results in patterns with a higher set of mid-band peak values. In fact, the SWR curve for very poor soil yields a mid-band peak value just slightly above our 1.5:1 limit. The variations that we see inform us of a basic system limitation.

The 2-line matching system limits the degree of variation that we can put into the antenna and feedlines in terms of adjusting the impedances that the lines transform. As a result, the basic curves for heights that depart from the most optimal value (90' in this example) are less optimal (although quite acceptable). A superior matching system would be one that would allow us to match at 70' and at 110' the basic curves displayed at 90'. Such a system would not necessarily be able to fully compensate for the antenna impedance changes for all mounting heights, especially when the impedance approaches  $50\ \Omega$ . However, it would allow us to carry the compensation for height changes a good bit further.

### *Adjusting the AI1H Matching System with a 4-Wire Cage Dipole*

If we use the same 4-wire cage construction for our dipole and then employ the AI1H matching system, as outlined on the right in **Fig. 2**, we add a fourth variable to the adjustment list. We may change the length of the dipole itself, which will be longer than the dipole for the 2-line system. In addition, we can change the lengths of the main linking line,

the open stub at the dipole end, and the shorted stub at the junction with the main feedline. Before we explore these changes, let's create a set of data on the changes created by simple height changes with the standard set-up relatively optimized for a height of 90'. **Table 6** provides the necessary information.

**Table 6.** The effects of antenna height above average ground on the impedance properties of a semi-fat 4-wire cage dipole plus the AI1H matching system

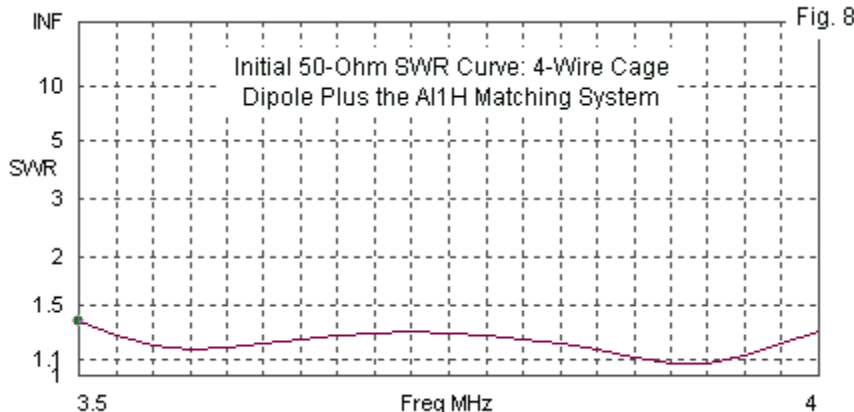
Height Feet	$\lambda$	Impedance ( $\Omega$ )		50- $\Omega$ SWR			Resonant Frequencies MHz
		at 3.745 MHz	3.5 MHz	Mid-Band	4.0 MHz		
30	0.114	103.4 - j27.4	1.28	2.26	1.79	3.650, 4.000	
40	0.152	87.8 - j28.7	1.22	2.02	1.72	3.625, 4.000	
50	0.190	76.5 - j25.0	1.21	1.79	1.64	3.525, 3.975	
60	0.228	70.1 - j20.1	1.24	1.60	1.55	3.550, 3.950	
70	0.266	65.9 - j15.0	1.28	1.46	1.47	3.575, 3.950	
80	0.304	63.6 - j10.1	1.32	1.34	1.38	3.600, 3.925	
90	0.342	62.6 - j5.4	1.36	1.28	1.29	3.650, 3.925	
100	0.380	62.9 - j0.9	1.38	1.28	1.20	3.625, 3.950	
110	0.418	64.4 + j3.4	1.40	1.35	1.12	3.600, 3.975	
120	0.457	67.4 + j7.0	1.39	1.45	1.11	3.575, 4.000	
130	0.496	71.9 + j9.4	1.38	1.56	1.18	3.550, 4.000	
140	0.533	77.4 + j9.5	1.34	1.65	1.27	3.525, 4.000	
150	0.571	82.6 + j6.6	1.29	1.72	1.35	3.525, 4.000	

Notes: 1. Dipole length: 125.2'. 2. Height in  $\lambda$  at 3.745 MHz.

3. Resonant frequency to nearest 0.025-MHz increment.

For reference, **Fig. 8** shows the 50- $\Omega$  SWR sweep for the initial system at 90' above average ground. The curve is similar to the one for the 2-line system (in **Fig. 4**) in having not only band-edge peak values, but also a distinct mid-band peak SWR value. Essentially, when we place an antenna analyzer at the junction of the main feedline and the matching system, we shall find two near-resonant frequencies, as reflected in the tabular data. We may note in passing that the two frequencies are closest together at the height at which we obtain the most optimal results.

As we move away from that height, either upward or downward, the two frequencies grow farther apart.



The height range for basically acceptable results extends from about 70' to 120' over average ground, using the unmodified matching system. In fact, performance tilts toward higher elevations using a 2:1 standard, with usable values all of the way to 150' and beyond. However, at lower height (30' and 40'), the curves exceed even a 2:1 50- $\Omega$  SWR limit.

Adjusting all four of the variables to optimize the curves for various heights requires patience, and even so, there are other combinations that can produce virtually the same results. **Table 7** shows the results of optimizing the 50- $\Omega$  SWR curves for 70', 90', and 110' above average ground. Once more, the dipole length increases as we increase the antenna height over the span of the samples. However, the other length values do not appear to follow a clearly regular pattern because the

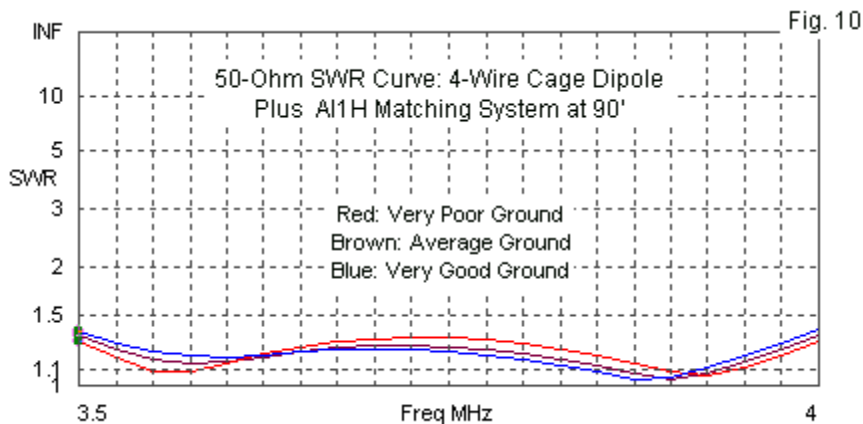
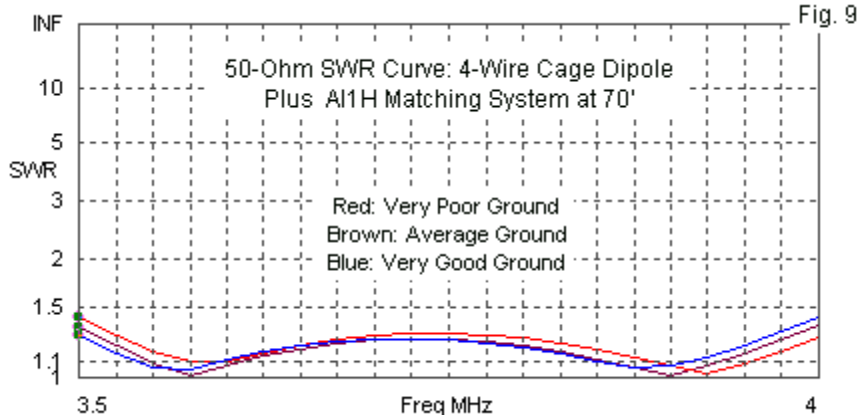
antenna feedpoint impedance value changes with both the height above ground and the length of the dipole. Since the resonant points are widely separated, resonating the dipole at a particular frequency does not provide ready guidance.

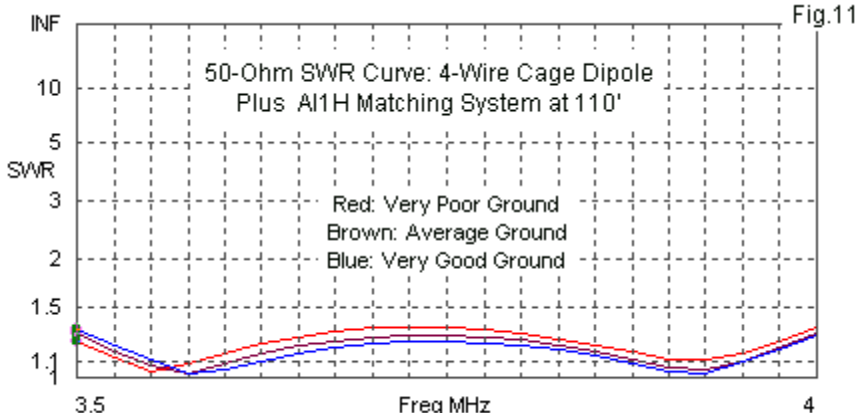
**Table 7. Optimized dimension and 50- $\Omega$  SWR results for 70', 90', and 110' high 4-wire cages dipoles with a 2-line matching system**

Dipole Height	Dipole Length	Open St. Length	Shorted St. Length	Link Line Length	50- $\Omega$ SWR		
					3.5 MHz	Mid-band	4.0 MHz
70'	124.4'	13.5'	21.5'	99.0'	1.33	1.25	1.35
90'	127.0'	13.5'	21.0'	99.0'	1.33	1.25	1.33
110'	127.8'	13.1'	22.0'	99.5'	1.28	1.27	1.28

The goal of the optimizing exercise was to produce roughly equal band-edge SWR values accompanied by the lowest possible mid-band peak SWR value. The process does yield curves for each height that are very close to coincident, unlike our results with the 2-line system. In none of the curves does the SWR value exceed 1.35:1.

As we did for the 2-line system, we shall compare the SWR curves with the optimized settings for very good, average, and very poor soil. **Fig. 9, 10, and 11** provide the visual comparisons among the soil types for each of the 3 heights. Because the availability of 4 variables allows the basic curves at each height to reach similarly low levels, none of the soil variations pushes any curve close to the 1.5:1 50- $\Omega$  limit.





The curves share a common trait: as the soil quality increases, the frequency differential between resonant points decreases. In fact, the frequency spacing between SWR minimum points follows the same pattern with the 2-line matching system, but those curves are too shallow to detect it easily. The poorest soil yields the highest mid-band SWR peak values, regardless of antenna height (within the sampling range), but the spread of the SWR minimum points often accompanies these peaks with lower band-edge SWR values. In the end, construction and installation site variables would likely obscure the fine shades of difference in the plots.

Nevertheless, the similarity in SWR plot families is a function of adjusting the variables in the antenna and its matching system, and the differences show up as measurable differences in the dimensions used. Whatever the matching system, modeling and optimizing the system in advance of installation yields two beneficial results, even in the presence of unmodeled site objects. First, it normally leads to first tests that are

closer to final adjustments. Second, the modeling process gives some insight into what adjustments are necessary to move the system's SWR curves in the desired direction.

### *Conclusion*

Of the two transmission-line matching system, the AI1H version offers more flexibility in bringing SWR curves under the most stringent control over a greater range of dipole heights, if we presume the use of a semi-fat wire simulation, such as the 4-wire cage used in these exercise. Similar results would accrue to the other equivalent dipoles in ribbon or cage form. The variability of a dipole's impedance with height changes in the region below  $1\lambda$  limits any matching system, but for covering the full 80-75-meter band with a single antenna that requires no tuning and that is at heights normal to serious amateur operation, The AI1H matching system has a few distinct advantages compared to the simpler two line system

The more complex matching system also has one disadvantage: a slight deficiency in efficiency relative to the 2-line system. **Table 8** compares the maximum gain of each system to a 4-wire cage dipole fed directly at its source (with no transmission line at all). The difference is small and perhaps not operationally noticeable. But it exists and is worth noting.

Table 8. Comparative performance of the composite solutions to broadbanding antennas for 80-75-meters using 4-wire cage dipoles at 90° above average ground plus a transmission-line matching system

System	Gain at		
	3.5 MHz	3.75 MHz	4.0 MHz
4-wire cage fed at feedpoint	6.16	6.29	6.48
With 2-line system	5.41	5.75	5.78
(Gain loss)	(0.75)	(0.54)	(0.70)
With AI1H system	5.18	5.56	5.52
(Gain loss)	(0.98)	(0.73)	(0.96)

Whichever system one uses, the combination of a semi-fat dipole and a transmission-line match, assuming that the antenna height is within the range of the matching system, does allow a degree of adjustment that is worth exploration if the goal is to produce the lowest 50-Ω SWR over the widest possible 80-75-meter bandwidth.

## Chapter 53: Center- & End-Fed Unterminated Long-Wire

**A**mong the oldest directional antennas are the ones labeled "long-wire" antennas. Dating to the late 1920s and early 1930s, we still find some of these antennas in active use--not only in amateur circles, but as well in government and military service. Classic names, such as Beverage and Bruce attach to early developments of long-wire antennas. In the group, we include bi-directional antennas such as the long center-fed doublet and end-fed wire, along with more directional arrays such as the terminated long-wire, the terminated V-beam, and the rhombic.

The theory of long-wire antennas appears early on in most college antenna texts. Once noted, along with the obligatory collection of basic equations that describe some long-wire properties, most authors pass on, never to touch the long-wire group again.

Amateurs come upon one or more representatives of the group and wonder what they do and how they do it. Few have access to the seminal articles out of which long-wire technology arose or even to classic books in the field, such as Harper's *Rhombic Antenna Design* or Walter's *Traveling Wave Antennas*. Today, some of the terminology surrounding long-wire antennas seems strange. For example, how long is a long-wire antenna? Some folks see a 135' doublet (or even a 135' end-fed wire) and think of it as a long-wire antenna. On 80 meters, where the wire is about 1/2-wavelength, it is not a long-wire. However, on 10 meters, the wire is 4 wavelengths and is entering into the realm of long-wire aerials. There is no definite boundary that marks the entry point to long-wire antennas. However, when we examine the properties of long wires

to see what performance properties that we want to derive from them, then we shall quickly learn that "long-wire" means for practical purposes "many wavelengths long."

The ready availability of a vast literature on long-wire antennas seemingly makes these notes superfluous. The end of each episode in this series has a short list of basic references. However, I receive numerous questions about the properties of long-wire, enough to suggest that a review of long-wire technology might be in order. We shall have occasion in these notes to touch upon a few of the equations defining long-wire antennas, but we shall mostly try to develop a more visually intuitive understanding of their basic properties. Antenna modeling software has the ability to provide polar plots of antenna patterns and other important data that will assist us in this process. As well, by the judicious use of the software, we shall discover that some of the more complex equations that define some of the equally complex forms of long-wire antennas will become unnecessary: we can design optimized long-wire arrays wholly within the software.

Along the way, we, we shall encounter some traditional terms, such as rhombic "tilt angle" and "traveling-wave" antenna. Many college texts are gradually replacing the term "traveling-wave" with "non-resonant" or "terminated." As we shall discover, a terminated antenna is one that ends with a resistance. Since the resistance will dominate the feedpoint impedance, the antenna becomes non-resonant over a fairly wide operating bandwidth. How these two ideas relate to the term "traveling-wave" we shall learn at the proper place along our path?

Everything begins with the wire antenna, plain and simple. So our journey will start with the center-fed doublet that is familiar in its shorter forms. We shall also look at longer forms of the doublet, as well as at long end-fed wires. Virtually everything in long-wire technology depends on how lobes develop as we increase the length of a wire. Most important will be the direction in which the strongest or main lobes point relative both to the broadside direction (that is, the direction for the lobes of a half-wavelength dipole) and to the axis of the wire itself.

Understanding lobe development is a major part, but only one part of our foundation in understanding long-wire antennas. In Part 2, we shall introduce a second critical element to the creation of long-wire beams, a resistor to terminate the end-fed wire and create a directional long-wire antenna. Along the way, we shall look at a number of interesting questions involving antenna height, wire losses, and ground quality as they bear upon long-wire antennas. These factors introduce both physical antenna issues and modeling issues. Therefore, we shall have to reserve the final steps of our meanderings for the later episodes. There, we shall encounter the V-beam and the rhombic. Both classic arrays have terminated and unterminated forms, as well as a few complexities. The V antennas will occupy the whole of Part 3, while the rhombic will occupy us for Parts 4 and 5.

Before we can fully appreciate the early work that developed the V-beam and the rhombic, we must begin our trek in more familiar territory. Since--as noted--everything begins with the doublet that is the place to take the first step.

## The Center-Fed Doublet

We shall want to examine what happens to a center-fed wire doublet as we change its length in 1-wavelength increments from 1 to 11 wavelengths. We might extend the exercise further, but the rate of change decreases as the antenna becomes longer, and the limit set here is long enough for us to get hold of all of the fundamental ideas. One key to understanding long-wire antennas is to shift our thinking about antenna size. Instead of thinking in physical lengths, such as X meters or Y feet, we shall think wholly in terms of wavelengths. Hence, as we increase the frequency, the physical length of a wave becomes shorter. So a 10-wavelength antenna at 80 meters is physically 8 times longer than a 10-wavelength antenna at 10 meters.

*The Model:* If we are to make fair comparisons among antennas--even in modeled form--we must set up some parameters that will remain unchanged from model to model. Obviously, the antenna length from end to end will always be variable in every exercise. For simplicity, I shall use the physical length (measured in wavelengths) rather than the actual electrical length as the increment. The electrical length of a wire antenna is always slightly more than the physical length due to end effects. The actual physical shortening required to obtain an exact electrical length varies somewhat, but many books cite a general value of about 0.95 as the ratio for a simple 1/2-wavelength dipole. If we cut a dipole to be physically 1/2 wavelength, then it will be about 5% long electrically and show inductive reactance at the feedpoint. However, the so-called end-effect occurs for only 1 half-wavelength

of a long-wire antenna, since it has only 2 ends, no matter what its overall length may be. Therefore, the longer the antenna the less the end effect creates a difference between the physical and electrical lengths. At 1-wavelength overall, the 5% dipole difference is only 2.5%. At 10 wavelengths, the differential is only 0.25%. All antenna models will use 20 segments per wavelength.

All real wire materials have some loss that varies with frequency, but not in a linear manner. Not only does the material loss decrease the maximum gain obtainable, it also has a small affect on the feedpoint impedance. Moreover, it has a further small shortening effect--like the end effect itself, but somewhat smaller in scale. However, material loss shortening of the physical wire acts all along the antenna and not just at the ends. To eliminate this factor, our models will use lossless or perfect wire.

We need a test environment. I shall place all long-wire models 1 wavelength above average ground (conductivity 0.005 S/m, permittivity 13). In theory, the main elevation lobe of a horizontal antenna is tightly connected to the height of the antenna above ground. Texts on long-wire antennas usually give an equation for selecting the height of a proposed antenna in terms of the desired elevation angle required for a communications link.

$$H_{wl} = 1 / (4 \sin a)$$

where H is the height in wavelengths and a (usually given as alpha) is the elevation angle. Since a good bit of science now prefers to count angles from the zenith (overhead) downward as a theta

angle,  $\alpha$  or alpha is simply  $90 - \theta$ , and vice versa. We may estimate the elevation angle of our antennas initially by reversing the equation:

$$\alpha = \arcsin 1 / (4 H_{wl})$$

You may see  $\arcsin$  written also as  $\sin^{-1}$ . Theoretically, our 1-wavelength height should produce elevation angles that are consistently 14.48 degrees. We shall set the software to increment patterns in 1-degree intervals. Since the calculated angle is almost directly between increments, we shall be satisfied if the angles appear as either 14 or 15 degrees.

The effects of ground are not constant for all frequencies. Even for a horizontal wire 1-wavelength above ground, the ground losses change, increasing as we raise the frequency. To sample the degree of change, let's set the wire diameter for all models at the test frequency of 3.5 MHz. We shall use 0.16" diameter wire, approximately AWG #6. If we perfectly scale our antenna for other frequencies, then the wire size changes as well. At 7 MHz, it is 0.08" (AWG #12). At 14 MHz, it is 0.04" (AWG #18). At 28 MHz, the size drops to 0.02" (AWG #24). Next, let's use a 1-wavelength wire at 1 wavelength height and scale it over the set of frequencies to sample the maximum gain values.

**Maximum Gain Values: 1 WL Wire at 1 WL Above Average Ground**

Frequency MHz	Wire Dia. inches	Maximum Gain dBi
3.5	0.16	9.83
7.0	0.08	9.67
14.0	0.04	9.54
28.0	0.02	9.47

**Gain differential 3.5 vs. 28 MHz: 0.36 dBi**

Although the differential is small, it is numerically evident. Hence, we should conduct all modeling tests using as consistent a set of values for all possible aspects of the antenna and modeling environment. Our choice of the ground quality also has an effect upon gain values. Indeed, the effect of changing the ground quality is more pronounced than the effect of changing the test frequency. Let's take our 1-wavelength antenna at its 1-wavelength height and check it using 3 different levels of soil quality.

**Maximum Gain Values: 1 WL Wire at 1 WL above Various Grounds**

Ground Label	Conductivity S/m	Relative Permittivity	Maximum Gain dBi @ 3.5 MHz	Maximum Gain dBi @ 28.0 MHz
Very Poor	0.001	5	9.41	9.01
Average	0.005	13	9.83	9.47
Very Good	0.0303	20	10.02	9.75
<b>Gain differential: VP to VG Soil</b>			<b>0.61</b>	<b>0.74</b>

Although the differentials between very good (VG) soil and very poor (VP) soil are similar, it is clear that ground effects on antenna losses are not completely linear. Nevertheless, the effects do not change enough to invalidate the general trends in center-fed doublet patterns if we select any other HF frequency to replace the 3.5-MHz test frequency for our investigation.

One way to eliminate the effects of all loss sources is to model all antennas in free space using perfect or lossless wire. These conditions allow us to scale an antenna with no change in performance values. Scaling, of course, means proportionately adjusting for frequency or wavelength the length of elements, the spacing between elements in a multi-element array, and the diameter of the elements. However, to make the comparisons among long-wire antennas reasonably realistic, we shall employ a given height (1 wavelength) and a specific ground quality (called "average") and omit only the smallest loss sources, such as wire material and frequency.

*The Center-Fed Doublet and Its Patterns:* We are now ready to show the results of setting up long-wire center-fed doublets ranging from 1 wavelength to 11 wavelengths in 1-wavelength increments. For each increment, we shall be very interested in 3 key data items. First is the maximum gain of the strongest lobe or lobes in the doublet radiation pattern. We shall call this value simply the maximum gain. Second, we shall note the elevation angle of maximum gain for the main lobe or lobes, also called the TO or take-off angle. The number should--by theory--always be 14 degrees. Finally, we shall note the azimuth angle of one of the main lobes relative to the antenna wire. If the main lobe is perfectly broadside to the wire, the angle will be 0 degrees. We shall count in a consistent direction away from broadside toward one end of the antenna wire if the main lobe departs from the broadside direction. The larger the number for the azimuth angle, the closer the main lobe comes to aligning with the wire end. A value of 90 degrees will indicate that the main lobe is directly off of and aligned with the

antenna wire from end to end. Since our investigation is confined to pattern properties, we shall not list the feedpoint impedance or other data that models might give us. The following table gives us the results of our examination.

**Center-Fed Doublet Data**

Total Length WL	Maximum Gain dBi	Elevation Angle deg	Azimuth Angle of Main Lobe deg
1	9.83	14	0
2	9.36	14	33
3	10.16	14	45
4	10.93	14	52
5	11.47	14	57
6	11.85	14	61
7	12.14	14	63
8	12.43	13	65
9	12.65	13	67
10	12.82	13	68
11	13.01	13	70

The chart shows the growing gain of the main lobes of the center-fed doublet, once the number of lobes reaches 4 (at the 2-wavelength mark). The increased strength of the main lobe is accompanied by a decreasing beamwidth. As well, the angle moves steadily toward the ends of the wire, but never reaches that point. In fact, at 11 wavelengths, the main lobes are still 20 degrees shy of a true end-orientation. Also note that the elevation angle of the strongest lobe drops slightly as the antenna length passes the 7-wavelength point. The angle would show a smoother curve if the increment between sampling points had been smaller than 1

degree. However, the drop is real and may be more dramatic with other types of long-wire antennas.

What the chart cannot show is the growth in the number of lobes and their relative strengths as we increase the length of the antenna. **Fig. 1** provides a gallery of sample elevation and azimuth plots to illustrate the growth of lobes in both directions. You may gauge the shrinking beamwidth from the red line marking the half-power points on the main lobes. The elevation patterns are taken along a line using the azimuth angle in the table. The azimuth patterns are taken at the listed elevation angles.

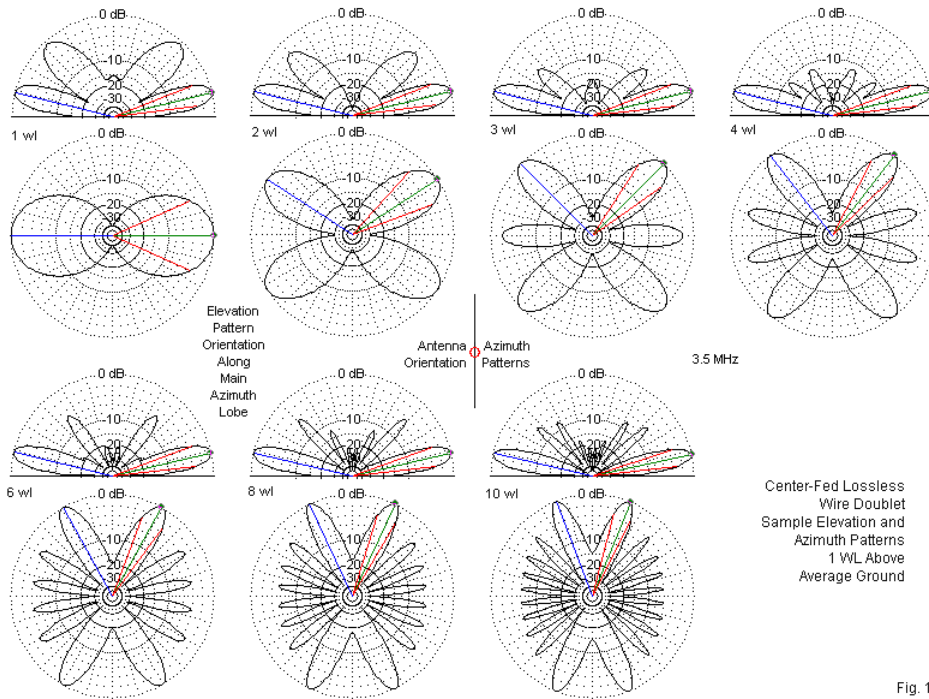


Fig. 1

The pattern selections are closer together for shorter versions of the doublet, since the azimuth angle of the main lobes changes more rapidly. As the antenna grows longer, the rate of azimuth-angle change decreases. However, of considerable note is the total number of lobes in each pattern. For antennas that are very close to integral numbers of wavelengths long, we can express the total number of lobes in a simple equation.

$$N_{\text{dbl}} = 2 L_{\text{wl}}$$

where  $N_{\text{dbl}}$  is the number of identifiable lobes and  $L$  is the doublet length in wavelengths. Lobes do not suddenly appear, but rather emerge, grow, peak, diminish, and finally disappear. The cycle occurs for every progression from one integral wavelength to the next. At the midpoint between integral lengths,  $L.5$  wavelengths, the number of doublet lobes becomes considerable larger. The antenna pattern shows the growing lobes of the next integral length plus the diminishing lobes of the preceding integral length. So the equation becomes somewhat messier.

$$N_{\text{dbl}} = 2 (L_{\text{wl}} + L^{+1}_{\text{wl}})$$

where  $L$  is the preceding integral wavelength value and  $L^{+1}$  is the next integral wavelength value. Since a 2-wavelength doublet has 4 lobes and a 3-wavelength doublet has 6 lobes, a 2.5-wavelength doublet has 10 total lobes. The main lobes are still those furthest from the broadside angle to the wire. The existence of 10 lobes forces the azimuth angle of the main or outer lobes to be further from broadside than for either of the two integral lengths (2 and 3 wavelengths) used in the sample calculation.

## The End-Fed Long-Wire Antenna

Understanding the pattern evolution of the center-fed doublet gives us a baseline against which to measure succeeding steps in the development of long-wire antennas, and eventually directional long-wire antennas. The doublet patterns were all very symmetrical as a

consequence of feeding the antenna at the center. However, most practical long-wire antennas feed the antenna at one end. In terms of models, we may simply move the feedpoint to the last segment. The segmentation remains the same: 20 segments per wavelength. The test frequency remains 3.5 MHz, and the lossless wire is still 0.16" in diameter. The antennas are 1 wavelength above average ground.

Therefore, we may proceed directly to the table of results that tells us the maximum gain, the elevation angle, and the azimuth angle of the main lobe(s) of the end-fed wires. Note that we here avoid any use of terms like "end-fed Zepp" and similar informal names for the antenna. They are all end-fed wires. As well, we by-pass any discussion of antenna installation practicalities, such as the imbalance of current magnitudes and phases on the parallel feedline normally used with such antennas.

However, we shall expand the table of gathered data by reducing the increment of length between antennas in the list. Instead of proceeding in 1-wavelength increments, we shall step along in 0.5-wavelength intervals.

#### End-Fed Wire Antenna Data

WL	Total Length	Maximum Gain dBi	Elevation Angle deg	Azimuth Angle of Main Lobe deg
1		8.44	14	37
1.5		9.45	14	49
2		10.27	13	56
2.5		10.86	13	60
3		11.32	13	63

3.5	11.68	13	65
4	11.99	13	67
4.5	12.26	13	69
5	12.48	13	70
5.5	12.71	12	71
6	12.90	12	72
6.5	13.08	12	73
7	13.24	12	74
7.5	13.38	12	75
8	13.50	12	76
8.5	13.64	11	76
9	13.72	11	77
9.5	13.87	11	77
10	13.96	11	77
10.5	14.07	11	78
11	14.15	11	78

The end-fed wire antenna begins at 1 wavelength by showing a small gain deficit relative to the center-fed doublet. However, the end-fed wire quickly catches up and shows more gain in the main lobe than the corresponding doublet. In fact, by the 11-wavelength version, the end-fed wire has over a 1.1-dB gain advantage. The added maximum gain accompanies a larger decrease in the elevation angle of maximum radiation as the antenna grows longer. The third column adds further information to digest: the azimuth angles are much larger for any given total end-fed antenna length than for doublets of the same length. In fact, the 1-wavelength version shows an azimuth angle that is greater than zero, suggesting that it has more than 2 lobes. **Fig. 2** can go a long way toward clearing up the differences between doublet and end-fed wire patterns when both have the same length.

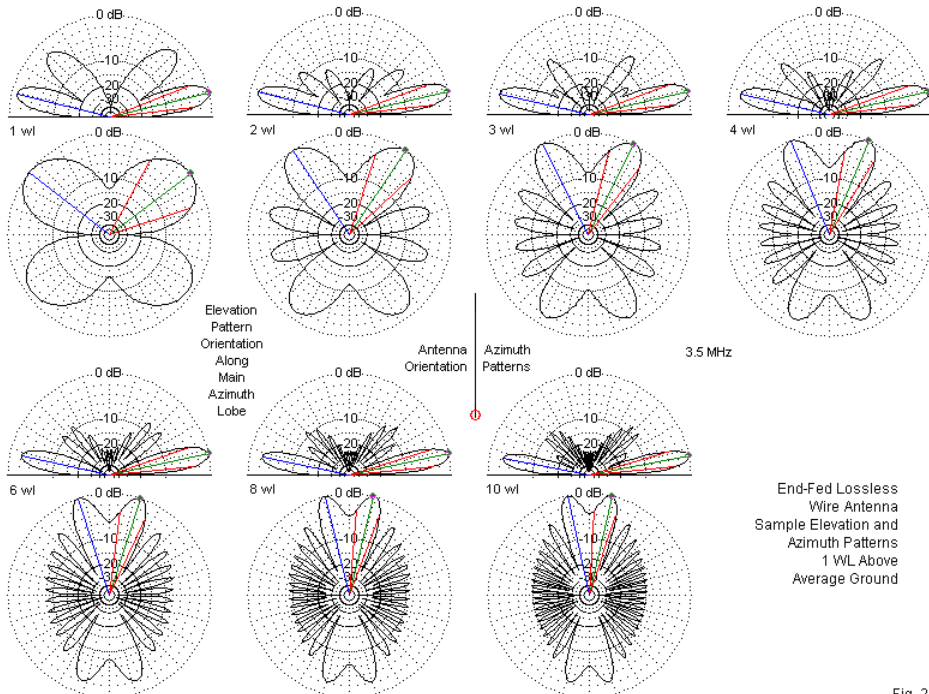


Fig. 2

The increased maximum-gain value of the end-fed antenna over the doublet arises from the fact that even with lossless wire the end-fed azimuth pattern shows a displacement away from the feed end and toward the open end of the antenna. The difference in strength between the strongest lobes away from the feedpoint and those toward the feedpoint is just about twice the value of the improved maximum gain figure. Expressed in other terms, if the 10-wavelength antenna has a 1.1-dB advantage over the doublet in

maximum gain, then it also shows about a 2.2-dB front-to-back ratio. The lobes toward the feedpoint will be about 1.1-dB weaker than the corresponding lobes for a doublet. The end-fed wire is already directional, but not to a very significant degree.

The more obvious feature of the radiation pattern gallery is the increase in the total number of lobes for each antenna length. In fact, the end-fed wire answers to a quite different equation for calculating the number of lobes:

$$N_{\text{ef}} = 4 L_{\text{wl}}$$

where  $N_{\text{ef}}$  is the total number of identifiable end-fed wire lobes and  $L$  is the end-fed wire length in wavelengths. So the 10-wavelength end-fed wire has a total of 40 lobes. To squeeze that many lobes into the same 360-degree pattern requires that each lobe have a smaller beamwidth (that is, be narrower). As well, the main lobes have an angle farther from broadside and closer to the wire end than for a doublet of the same length. In fact, the two main lobes at each end of the antenna wire begin to fuse into a single large lobe with a deep inset. Compare these lobes with the very separate lobes of the doublet.

The data that we gather from the end-fed single long-wire unterminated antenna will play an important role in the design of more complex arrays. The data is in many ways height-specific (with additional cautions regarding the soil quality as a possible further modifier of the data). The azimuth angle of the main lobe varies with the antenna height and length. Using an increment of 1

wavelength between antenna lengths, the following table compares data for lossless long-wires 0.5-, 1-, and 2-wavelengths over average ground.

Comparative Data: Unterminated Long-Wire Antennas at 0.5- 1-, and 2-Wavelengths Above Average Ground.											
Length WL	Height = 0.5 Wavelength			Height = 1.0 Wavelength			Height = 2.0 Wavelength			Elevation Angle deg	Azimuth Angle deg
	Maximum Gain dBi	Elevation Angle deg	Azimuth Angle deg	Maximum Gain dBi	Elevation Angle deg	Azimuth Angle deg	Maximum Gain dBi	Elevation Angle deg	Azimuth Angle deg		
1	7.99	27	40	8.44	14	37	8.75	7	37		
2	9.11	25	61	10.27	13	56	10.75	7	54		
3	9.85	24	70	11.32	13	63	11.72	7	61		
4	10.33	22	74	11.99	13	67	12.62	7	66		
5	10.68	21	78	12.48	13	70	13.23	7	68		
6	10.95	20	81	12.90	12	72	13.75	7	70		
7	11.19	19	83	13.24	12	74	14.22	7	72		
8	11.40	18	84	13.50	12	76	14.62	7	73		
9	11.60	17	85	13.72	12	77	14.97	7	74		
10	11.79	16	85	13.96	11	77	15.28	6	75		
11	11.97	15	85	14.15	11	78	15.57	6	76		

**Fig. 3** compares the maximum gain of the end-fed wire antenna at each height and length. These curves are completely unexceptional, but may be useful as a reference.

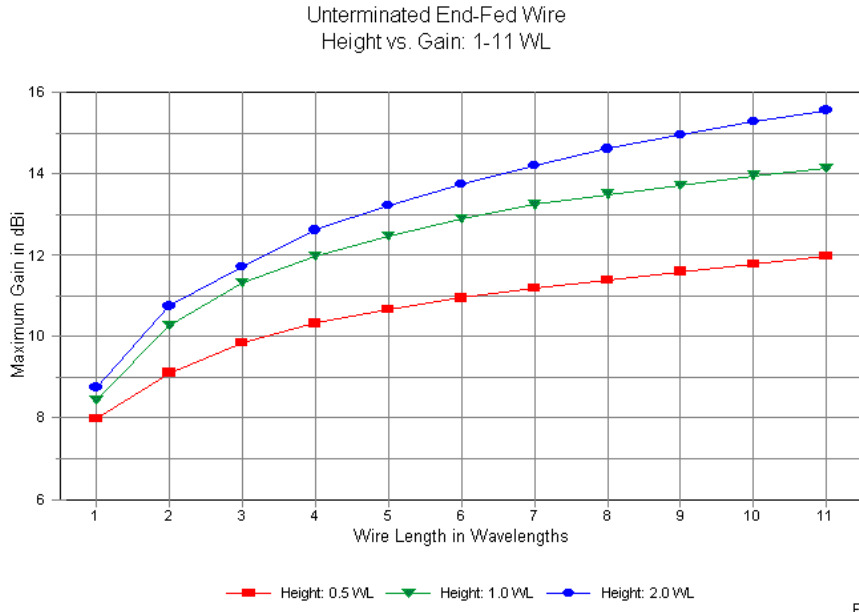
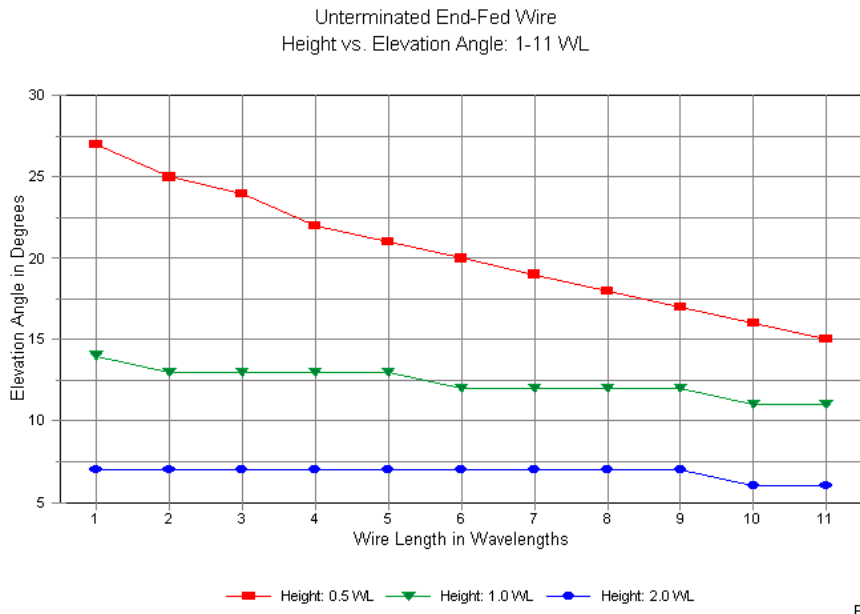


Fig. 3

Although we may be tempted to focus upon the gain data, those numbers may not be the most important for the long-term use of the information. The elevation angle columns tells us that the lower we place a single unterminated long-wire antenna, the faster the elevation angle of maximum radiation decreases as we increase the long-wire antenna length. **Fig. 4** converts the numbers in curves. The stair-stepping results from the fact that elevation angles use a 1-degree increment.



Still more significant for designing more complex long-wire arrays is the azimuth angle of the strongest lobe relative to the broadside direction (in these models). For any given antenna length, the azimuth angle of the strongest lobes changes with antenna height. **Fig. 5** shows the amount of change with height for each sampled antenna length. Once more, the 1-degree radiation pattern increment limits the smoothness of the curves. However, we may clearly see that the lower the antenna height for any given antenna length, the closer that the main lobes approach the axis of the wire and the closer they grow to each other on each side of the wire.

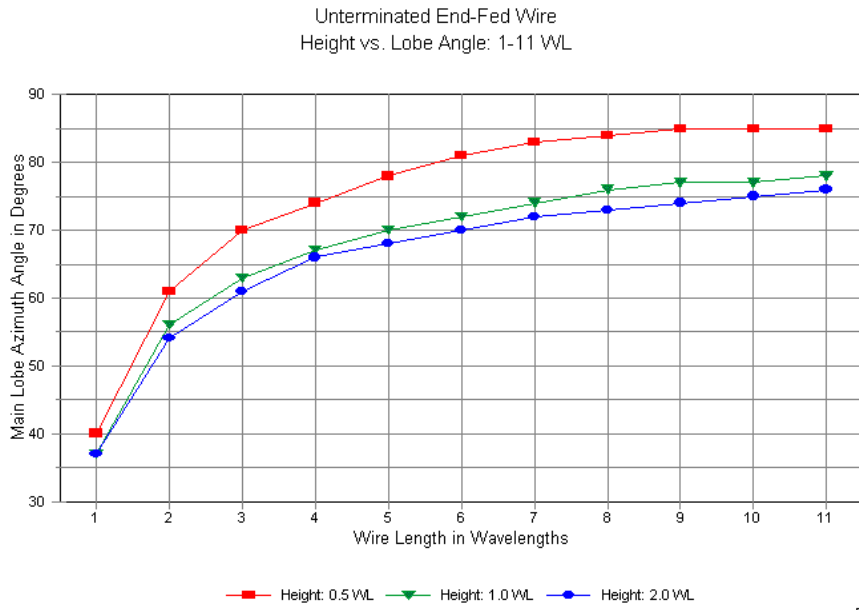
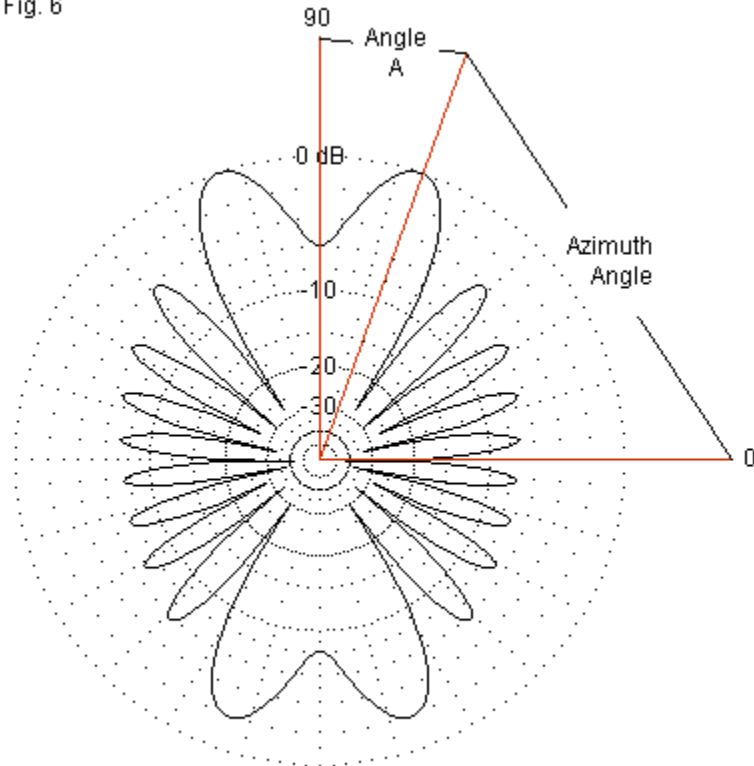


Fig. 5

The azimuth angle has been a very convenient measure for our initial examination of both center-fed and end-fed long wire antennas. It has shown us by how much the main or strongest lobes of the antenna pattern move from the broadside or zero-degree position as we make the wire longer, as counted in wavelengths. In other applications, for example, the discussion of V and rhombic arrays to come in future parts of this series we shall view the same angle from a different perspective. We shall be interested in the amount by which the main lobe is displaced from the axis of the wire, defined as a line drawn along and beyond the

antenna wire. In literature about long-wire arrays, the off-axis angle is usually designated as "alpha," although we shall use the letter "A" as a designation in these notes. **Fig. 6** shows the relationship of the 2 angles.

Fig. 6

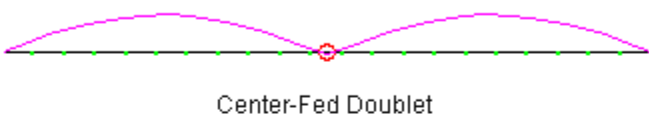


Azimuth and Off-Axis (A) Angles  
for an Unterminated Long-Wire Antenna

We shall eventually convert the azimuth-angle values to angle-A values with respect to the wire. The relationship is simply this: Angle A = 90 - (Az Ang) degrees. We need not do the arithmetic now. However, these angles and their derivatives will come in handy in later parts of this series.

Since most of our experience is with shorter antennas--say about 1/2-wavelength long--we may not fully appreciate the difference between center and end feeding for wires that are the same length. For example, a 1-wavelength doublet has only 2 lobes, while a 1-wavelength end-fed wire has 4 lobes. Both antennas show 2 complete excursions of current magnitude, showing 2 maximum current points at approximately 1/4 and 3/4 wavelength along the wire. The only other significant variable is the phase of the currents in each excursion. **Fig. 7** shows us the difference in this parameter.

Fig. 7



Center-Fed Doublet

End-Fed Wire



Relative Current Magnitude and Phase on 1-WL Wire Antennas  
Center-Fed-Doublet and End-Fed Wire at 1 WL above Ground

The center-fed doublet graph shows that the currents have the same phase in each half of the overall antenna length. Hence, the radiation pattern has only two lobes with contributions from each half of the total wire length. Not until the antenna reaches a significantly greater length (2 wavelengths is the next step in our pattern development sequence) will each half of the doublet show a current phase reversal. Therefore, we do not find 4 lobes until we reach the 2-wavelength mark. (Of course, a 1.5-wavelength antenna will show 6 lobes as the initial 2 diminish and the next 4 emerge and grow.) With the end-fed wire, the currents in each half of the initial 1-wavelength wire are 180-degrees out of phase relative to each other. Hence, we see 4 lobes at this shorter length.

Unlike the center-fed doublet, the end-fed wire shows only a single progression of the number of lobes in the azimuth pattern.

Therefore, the single equation for calculating the number of lobes applies not only to wire lengths that are at or near integral wavelengths; as well, it applies to wire lengths at are at or near N.5 wavelengths.

Indeed, the way in which lobes appear and grow differs markedly between center-fed and end-fed antennas that are the same length.

**Fig. 8** provides a glimpse of the process by tracking the lobe structure of the two types of antennas from 2 wavelengths to 3 wavelengths, in 0.25-wavelength increments. I chose this set of lengths so that the lobes are clear and countable--even when they are very small. However, similar graphs are possible between any 2 length markers.

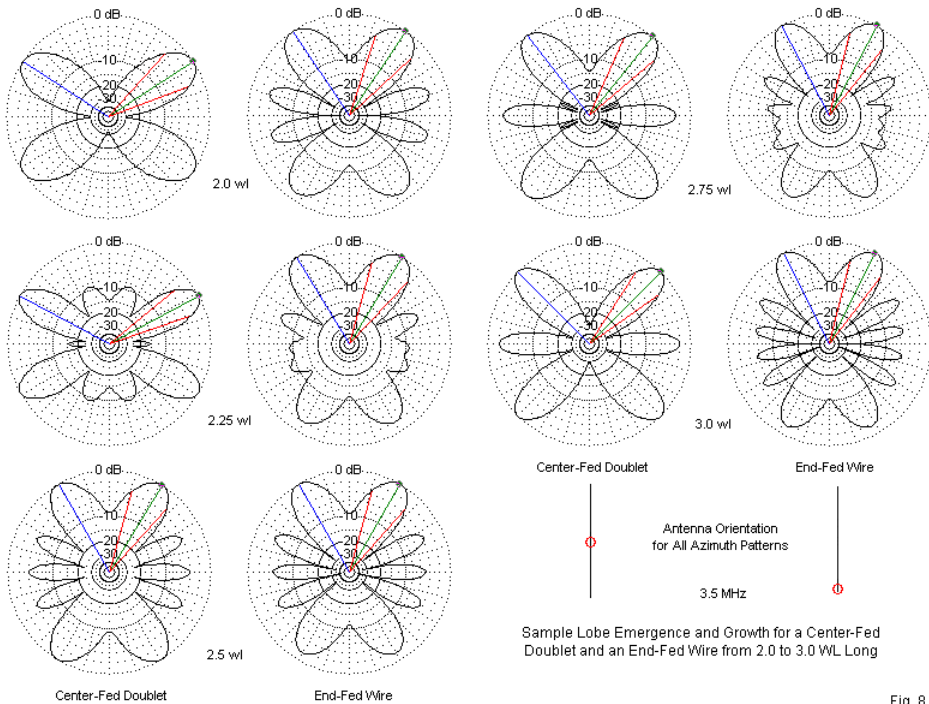


Fig. 8

At 2.5 wavelengths, the two patterns are almost identical differing only in the end-fed wire's small front-to-back ratio resulting from a slight forward tilt to the pattern. The center-fed antenna shows its new lobes at angles outside the existing set of 4 lobes, and in between any pair of existing lobes. The presence of the new outermost lobes forces the existing lobes toward a more broadside direction. At 2.25 wavelengths, the old lobes are still the strongest, but show a more broadside angle than when they were alone at 2

wavelengths. Beyond 2.5 wavelengths, the new lobes dominate and the old ones shrink. At 2.75 wavelengths, the old lobes are barely visible. By 3 wavelengths, we find only 6 lobes at their familiar positions. The following table tracks the progression.

Lobe Development in Center-Fed and End-Fed Wires Between 2 and 3 wavelengths

Antenna Length	Center-Fed		End-Fed	
	Max. Gain dBi	Main Lobe Az. Angle deg	Max. Gain dBi	Main Lobe Az. Angle deg
WL	9.36	33 deg	10.27	56 deg
2.0	10.22	28	11.37	59
2.25	10.33	59	10.86	60
2.5	10.33	51	10.91	62
2.75	10.16	45	11.32	63
3.0				

In contrast to the center-fed lobe development progression, the end-fed antenna has new lobes that emerge just to the rear of the broadside direction, where we define "rear" with respect to the general direction toward the end-fed wire's feedpoint. The 2.25-wavelength and 2.75-wavelength end-fed antennas are comparable, as each one introduces a new lobe pair. The lobe progression acquires symmetry on each side of the wire (except for the slight differential in the main lobes) only as the antenna approaches a multiple of a half-wavelength.

We should not neglect the elevation patterns in the gallery shown in **Fig. 2**. If we compare the number of elevation lobes for the doublet and for the end-fed wire, we find more lobes in each corresponding end-fed wire pattern. This feature of end-fed wire antennas will eventually play a role in our evaluation of terminated end-fed long-wire directional antennas. Just how complex the overall pattern of

an end-fed wire may become, shows up in the 3-dimensional pattern from a 10-wavelength end-fed wire in **Fig. 9**. The pattern is limited to a 5-degree increment between pattern readings, so some details are missing. However, reducing the increment to show more detail would convert the line-based sketch into a solid black blob.

3-Dimensional Radiation Pattern  
10-WL End-Fed Unterminated  
Long-Wire Antenna  
1-WL Above Average Ground

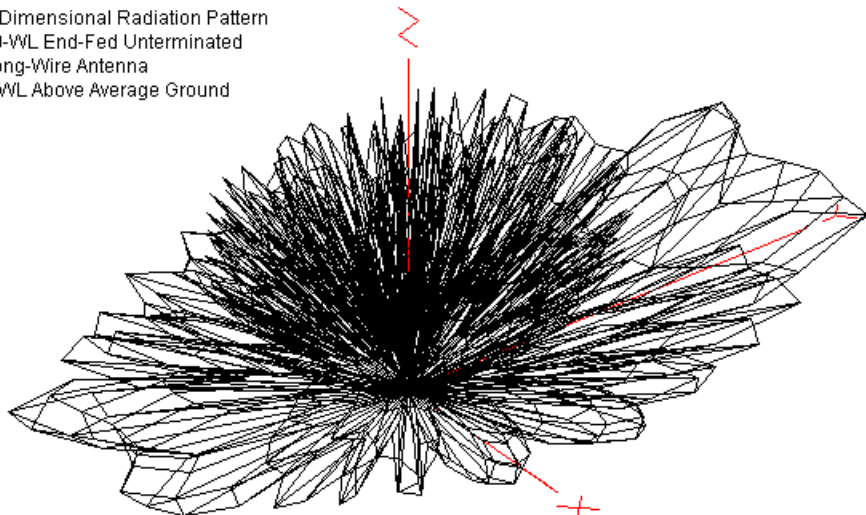


Fig. 9

Two features of the 3-dimensional pattern are especially prominent. First, the upper angles in every direction show a plethora of lobes. A free-space representation of the far-field radiation would show a tunnel with relatively smooth ridge rings for each new lobe, counting back from the tunnel entrance formed by the strongest lobes. However, our radiation pattern takes place over real (or

"lossy") ground, disturbing the ring structure as we increase the elevation angle of interest. Many of the upper-angle lobes have significant strength. Second, the forward-most lobes (along the axis labeled Y) have an interesting feature. The lowest and strongest lobe (at 10 degrees in the graphic) shows the deep null along the Y-axis between lobe peaks on either side. However, at 15 degrees elevation, the forward lobe structure displays a far-more-even front, with only a small gain depression along the Y-axis. This feature of end-fed wire patterns will become very prominent when we tackle the terminated end-fed antenna in Part 2.

Before we leave the open-ended long-wire antenna, we should briefly note that the ground plays an ever-more profound role in end-fed wire antenna performance as the wire grows longer. Let's compare the 10-wavelength end-fed wire over very good, average, and very poor grounds. In contrast to our original notes, which used a 1-wavelength doublet, we shall now be looking at a very long antenna (856.55 m or 2810' at 3.5 MHz).

Maximum Gain Values: 1 WL Wire at 1 WL above Various Grounds					
Ground Label	Conductivity S/m	Relative Permittivity	Maximum Gain dBi @ 3.5 MHz	Elevation Angle deg	Azimuth Angle of Main Lobe deg
Very Poor	0.001	5	13.55	10	77
Average	0.005	13	13.96	11	77
Very Good	0.0303	20	14.65	12	79
Gain differential: VP to VG Soil					
			1.10		

The ground quality not only changes the maximum gain attainable from the antenna, but as well changes the elevation angle of maximum radiation. The better the soil the higher the TO angle. But even over very good soil, the elevation angle of maximum radiation is significantly lower than the calculated value of 14.5 degrees.

## Conclusion

In some respects, we have not gone very far in our exploration of long-wire antennas. We have merely contrasted the behavior of center-fed doublets and end-fed wires from 1 to 11 wavelengths. Along the way, we have examined many of the variables that might alter the performance progressions in the tables. Our goal has been to become familiar with the performance parameters of long unterminated wires. The pattern galleries and tables can serve to remind us of these properties as we proceed further.

The end-fed wire, in particular, holds great importance for our future exploration. It is the foundation of all other long-wire arrays. That collection, of course, includes both complex rhombics and the simplest of the directional terminated antennas. Hopefully, from the perspective of developing reasonable expectations from end-fed wires, the foundation in these notes is sufficiently solid to make succeeding steps smoother on the trail of terminated long-wire antennas.

## A Few Basic References

Entire books exist on the subject of terminated directional long-wire antennas, with special attention to the V-beam and the rhombic. However, for a basic introduction to the subject, the following college texts, handbooks, and seminal articles might be useful.

Balanis, C. A., *Antenna Theory: Design and Analysis*, 2nd Ed., pp. 488-505: a college text.

Boswell, A. G. P., "Wideband Rhombic Antennas for HF," *Proceedings of the 5th International Conference on Antennas and Propagation (ICAP87)*, April, 1987: a source of wide-band rhombic design information.

Bruce E., "Developments in Short-Wave Directive Antennas," *Proceedings of the IRE*, August, 1931, Volume 19, Number 8: the introduction of the terminated inverted V and diamond (rhombic) antennas.

Bruce E., Beck A.C., and Lowry L.R., "Horizontal Rhombic Antennas," *Proceedings of the IRE*, January, 1935, Volume 23, Number 1: the classic treatment of rhombic design, repeated in many text books.

Carter P. S., Hansell C. W., and Lindenblad N. E., "Development of Directive Transmitting Antennas by R.C.A Communications, Inc.," *Proceedings of the IRE*, October, 1931, Volume 19, Number 10: a fundamental treatment of long-wire V antennas, along with the next entry.

Carter P. S., "Circuit Relations in Radiating Systems and Applications to Antenna Problems," *Proceedings of the IRE*, June, 1932, Volume 20, Number 6: the second of the fundamental analyses behind long-wire V antennas.

Foster, Donald, "Radiation from Rhombic Antennas," *Proceedings of the IRE*, October, 1937, Volume 25, Number 10: a more general

treatment of rhombic design, with the introduction of stereographic design aids.

Graham, R. C, "Long-Wire Directive Antennas," *QST*, May, 1937: an excellent summary of long-wire technology to the date of publication.

Harper, A. E., *Rhombic Antenna Design* (1941): a fundamental text on rhombics, based on engineering experience, with tables and nomographs as design aids..

Johnson, R. C. (Ed.), *Antenna Engineering Handbook*, 3rd. Ed., Chapter 11, "Long-Wire Antennas" by Laport: similar but not identical material to the relevant pages of Laport's own volume.

Kraus, J. D., *Antennas*, 2nd Ed., pp. 228-234; 502-509: a college text.

Laport, E. A., *Radio Antenna Engineering*, pp. 55-58, 301-339: a summary of long-wire technology up to the date of publication (1950).

Laport, E. A., "Design Data for Horizontal Rhombic Antennas," *RCA Review*, March, 1952, Volume XIII, Number 1: rhombic design data based on the use of stereographic aids developed by Foster.

Laport E. A., and Veldhuis, A. C., "Improved Antennas of the Rhombic Class," *RCA Review*, March, 1960, Volume XXI, Number 1: the introduction of the off-set dual rhombic.

Straw, D. (Ed.), *The ARRL Antenna Book*, 20th Ed., Chapter 13, "Long-Wire and Traveling-Wave Antennas." See also older versions of the volume, for example, Chapter 5 of the 1949 edition, which gives long-wire technology a more thorough treatment on its own ground, rather than in comparison to modern Yagi technology.

Stutzman, W. L., and Thiele, G. A., *Antenna Theory and Design*, 2nd Ed., pp. 225-231: a college text.

Walter, C. H., *Traveling Wave Antennas* (1965): a classic and very thorough text on traveling-wave fundamentals for all relevant types of antennas.

## Chapter 54: Terminated End-Fed Long-Wire Directional Antennas

In Chapter 53 of this Long-Wire series, we examined some fundamental properties of both center-fed and end-fed unterminated long-wire antennas. Without the kind of data that our basic investigation showed, the terminated version of the end-fed long-wire antenna might seem more odd than natural. As we move from the symmetry of an unterminated antenna, sometimes called a "standing-wave" antenna, to the asymmetry of the patterns of a terminated wire that is the same length, the assimilation of the nature and growth of both elevation and azimuth lobes will hopefully carry over to naturalize the new patterns and performance values. The mark of success in the process might be that we are able to predict in very general terms "what happens next."

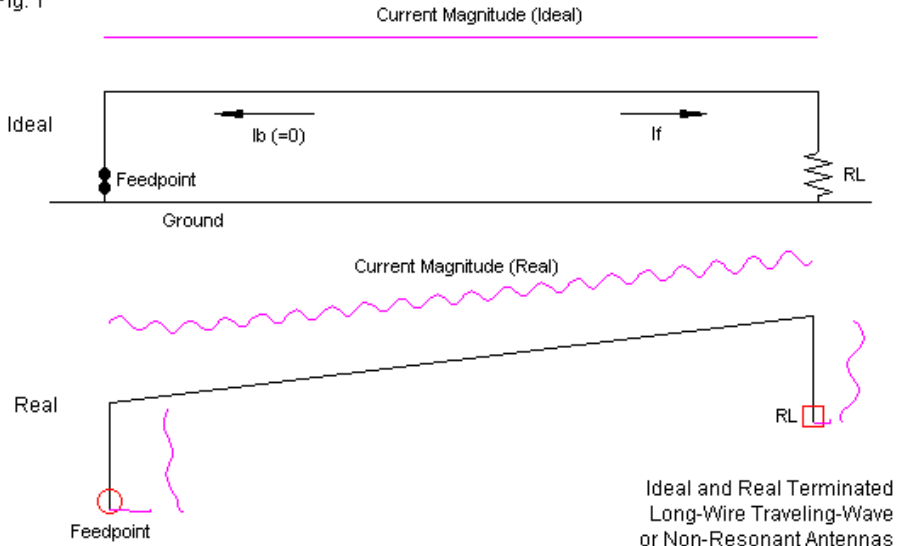
### The Terminated End-Fed Long-Wire Directional Antenna

In both of our unterminated antennas, we find an interesting picture of the current and voltage along the wire. They each form standing waves (following the accounts of Balanis and of Kraus) with peaks every half-wavelength and nulls every half-wavelength such that the peaks and nulls are 1/4-wavelength apart. The voltage peaks where the current has a null and vice versa. This portrait of voltage and current behavior forms the basis for a large part of basic antenna analysis. It derives in part from treating the antenna as an open transmission line. At the end of any transmission line, an open condition results in the complete reflection of energy toward the source. Traditionally, such antennas have received the label

"standing-wave" antennas, and the group includes most of the antennas that we commonly use.

In a long-wire antenna, we may add to the end of the wire away from the feedpoint an impedance or termination. If we select the right impedance, then the reverse or reflected energy flow is decreased ideally to zero, as suggested by the top portion of the sketch in **Fig. 1**. Under these ideal conditions, the fields or waves emerging as a consequence of the uni-directional energy flow result in radiation wholly directed toward the terminated end of the antenna wire. As well, the current at any position along the antenna wire will be the same. These conditions define the idea of a "traveling-wave" antenna.

Fig. 1



Any implementation of the terminated long-wire antenna consists not only of the wire that is parallel to the ground, but as well to 2 vertical sections. At one end of the antenna, we have a feedpoint, usually taken between the vertical leg and ground. At the other end, we find a vertical line as long as necessary to connect to the terminating impedance. The terminating impedance normally has one end directly connected to ground with the other end connected to the vertical wire. When the height of the antenna is very small relative to a wavelength, the antennas receive the label "Beverage antennas," after the individual who generated them originally. Today, such antennas--which are very long and low to the ground--find use as MF and lower HF receiving antennas. When the

antenna is an appreciable distance above ground--as in the case of our wires that are 1-wavelength high--we may simply call it a terminated end-fed long-wire directional antenna.

The idealization of our terminated long-wire antenna normally does not account for the vertical wires needed to make both feedpoint and termination connections. (See Balanis and Kraus for different approaches to the analysis of such antennas. We shall by-pass their mathematical accounts, since our goal is to make such antennas more intuitively sensible.) Ideally, we can find a loading impedance that will provide the proper conditions for achieving full traveling-wave status. The calculation is based once more on treating the wire as a transmission line, and the load impedance must equal the characteristic impedance of the line. Balanis provides the following equation to approximate the proper value of the termination.

$$R_L = 138 \log_{10} (4h/d)$$

where  $R_L$  is the value of the impedance load in Ohms,  $h$  is the height of the wire, and  $d$  is the wire diameter, when both are in the same units. Note that the impedance of the line and hence the approximate load value is independent of frequency and dependent only upon a set of physical measurements that use the same units of measurement. Our wires will be 85.655 meters above ground. The wire diameter is 0.16" or 0.004064 meters. Plugging these numbers into the Balanis equations gives us an approximate load impedance of 680 Ohms. As we shall see, values between 600 and

1000 Ohms are quite usable, although we shall eventually settle on 800 Ohms as a useful value for our initial models.

As Kraus notes, a lumped impedance may greatly reduce reflections from the termination, but it cannot provide a non-reflecting termination. In fact, the most common form of termination is a non-inductive resistor (or series/parallel combination of resistors). Under these conditions, some standing waves remain, as shown in the lower portion of the sketch in **Fig. 1**. The lower rendition of a 10-wavelength terminated long-wire antenna derives from an EZNEC model and uses its facility to generate the pattern of current magnitude along the wires. One consequence of incomplete reflection elimination is to wind up with a feedpoint impedance that is not identical to the load resistance. The feedpoint impedance for the models in this part of the investigation were 600 Ohms or below. However, this impedance value is convenient, since open ladder line commonly comes in a 600-Ohm value, and the match is good (SWR 1.25:1 or less). Hence, the user of such antennas has a wide choice of means at the operating end of the line for effecting a match to the usual 50-Ohm input/output of a transceiver.

One common misconception about terminated long-wire antennas is that the reduction or elimination of reflected energy results in half the power being dissipated by the terminating impedance (resistor). In fact, the far end load on the antennas in this exercise dissipates about 25% of the power, as calculated by NEC.

**Modeling Issues:** Modeling the terminated long-wire antenna presents a number of options and challenges, since NEC has some limitations that bear upon the models. **Fig. 2** outlines the options available.

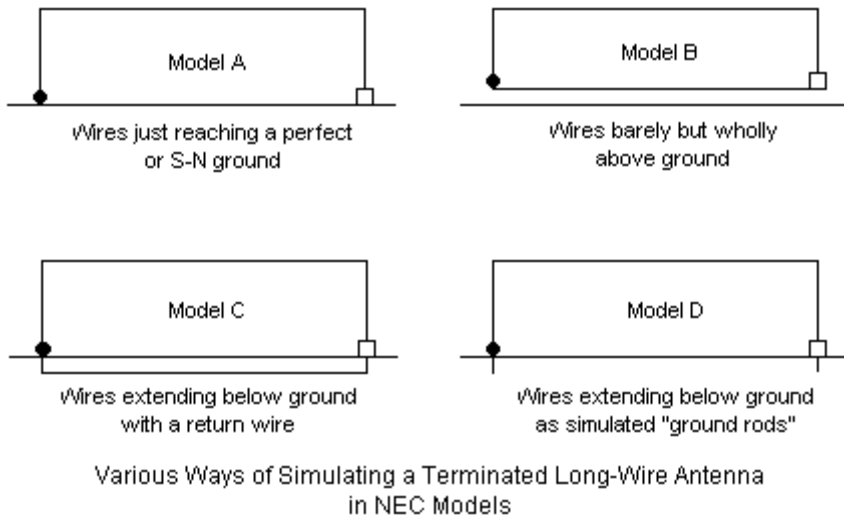


Fig. 2

Option A brings the vertical elements of the antenna down to ground. The source or feedpoint is the first segment above ground of the left wire, while the terminating load appears on the last segment above ground at the far end of the antenna. In the EZNEC Pro/4 implementation of NEC, we have at least 4 ways to model the structure: over perfect ground, with a Sommerfeld-Norton (SN)

average ground using NEC-4, with an SN average ground using NEC-2, and with a MININEC ground. Use of a perfect ground provides a reference baseline for checking the sensibleness of other models. However, neither NEC-2 nor NEC-4 recommends bringing a source wire to ground, since at a minimum, the source impedance is likely to be off the mark. The MININEC ground does not provide accurate impedance reports for the ground quality selected, since it is restricted to using the impedance report for perfect ground.

Despite the limitations, we can tabulate the results. As a test case, I shall use a 10-wavelength terminated antenna alternately using termination resistors of 600, 800, and 1000 Ohms. For each option, I shall list the maximum gain, the reported 180-degree front-to-back ratio, the elevation angle of maximum radiation, the beamwidth, the source impedance, and the 600-Ohm SWR at the test frequency.

Test Performance Values for Modeling Option A

Terminating Load Ohms	Maximum Gain dBi	Front-to-Back Ratio dB	Beamwidth degrees	Elevation Angle deg	Feedpoint Z R+/-jX Ohms	600-Ohm SWR
<b>1. Perfect Ground</b>						
600	13.98	29.04	26.4	15	439 + j 24	1.37
800	13.91	26.38	26.2	15	476 + j 43	1.28
1000	13.87	19.57	26.2	15	504 + j 59	1.23
<b>2. Average SN Ground, NEC-4</b>						
600	11.54	11.57	35.2	11	460 + j593	3.01
800	11.49	12.63	35.2	11	495 + j588	2.85
1000	11.45	12.87	35.2	11	524 + j587	2.75
<b>3. Average SN Ground, NEC-2</b>						
600	10.79	24.23	35.6	11	479 + j 14	1.26
800	10.74	21.78	35.6	11	509 + j 35	1.19
1000	10.72	18.11	35.6	11	532 + j 52	1.16
<b>3. Average MININEC Ground, NEC-4</b>						
600	11.09	23.58	35.4	11	439 + j 24	1.37
800	11.01	22.71	35.4	11	476 + j 43	1.28
1000	10.98	18.55	35.4	11	504 + j 59	1.23

Using the sequence over perfect ground as a background reference, the NEC-2 results for the SN average ground and the MININEC average ground data appear to coincide fairly well. However, the NEC-4 runs for the SN average ground appear to yield somewhat high gain values with more than anticipated inductive reactance in the source impedance.

Option B represents an adaptation of NEC-2 techniques for modeling vertical antennas with ground-plane radials. The return line between the load resistor and the source is 0.0001-wavelength above ground, about 3 times the diameter of the wire. Hence, the model violates no constraints, but as the following results for both NEC-2 and NEC-4 show, it yields a poor model of the terminated long-wire antenna.

Test Performance Values for Modeling Option B

Terminating Load Ohms	Maximum Gain dBi	Front-to-Back Ratio dB	Beamwidth degrees	Elevation Angle deg	Feedpoint Z R+/-jX Ohms	600-Ohm SWR
<b>1. Average SN Ground, NEC-4</b>						
600	7.68	16.93	35.4	11	1170 - j 97	1.97
800	7.73	14.44	35.4	11	1182 - j 80	1.98
1000	7.77	13.36	35.4	11	1192 - j 67	2.00
<b>2. Average SN Ground, NEC-2</b>						
600	7.68	16.10	35.4	11	1167 - j 99	1.96
800	7.72	14.59	35.4	11	1179 - j 82	1.98
1000	7.76	13.50	35.4	11	1188 - j 69	1.99

Although NEC-2 and NEC-4 show a very close coincidence of data, the low gain, low front-to-back ratio, and high feedpoint impedance reports combine to suggest that this model is highly inadequate. However, the beamwidth and elevation-angle reports are consistent with the other models. NEC-4 does allow the use of a subterranean return wire, shown in option C in **Fig. 2**. To test this option, I placed a return wire 0.01-wavelength below ground level, connecting it to

the above-ground vertical wires with short segments. Both the source and the load for the antenna remain above ground. Since this option is available only in NEC-4, the test-result table is quite short.

Test Performance Values for Modeling Option C

Terminating Load Ohms	Maximum Gain dBi	Front-to-Back Ratio dB	Beamwidth degrees	Elevation Angle deg	Feedpoint Z R+/-jX Ohms	600-Ohm SWR
1. Average SN Ground, NEC-4						
600	10.38	22.53	35.6	11	526 + j 87	1.23
800	10.37	19.94	35.6	11	556 + j104	1.22
1000	10.36	17.10	35.6	11	579 + j118	1.23

The results are modest, but coincide roughly with the NEC-2 results in Option A. The front-to-back reports are consistent with those for perfect ground. The difficulties with the model include the model size, since the return wire requires as many segments as its above-ground counterpart, and the return wire may actually yield slightly low gain reports by carrying more current than the ground itself. A real installation would not likely use a buried ground wire.

Therefore, I tried option D, which replaces the below-ground structure of option C with 2 simple ground rods. Each rod is a 1-segment wire about 0.05-wavelength, which is the length of the segments in the vertical wires above ground. Therefore, the source has equal length segments on each side of the feedpoint segment. 0.05-wavelength is about 4.3 meters or 14'. This length may be longer than the average ground rod, but substituting shorter segments did not change the reports by any significant amount. The results of the test appear in the following table.

Test Performance Values for Modeling Option D

Terminating Load Ohms	Maximum Gain dBi	Front-to-Back Ratio dB	Beamwidth degrees	Elevation Angle deg	Feedpoint Z R+/-jX Ohms	600-Ohm SWR
<b>1. Average SN Ground, NEC-4</b>						
600	10.49	22.94	35.6	11	513 + j 69	1.22
800	10.47	20.30	35.6	11	544 + j 87	1.20
1000	10.46	17.29	35.6	11	567 + j102	1.20

Except for the predicted very slight increase in maximum gain, all of the values correspond very well with those of the buried-return-wire model (C), but with a 45% reduction in model size. For users of NEC-4, it is likely that this style of model is about as adequate as we may get for a terminated long-wire directional antenna. In fact, for users of NEC-2, the basic model (option A) coincides well enough for general guidance. In physical reality, there will be structural variables that will inevitably limit the precision attainable by any model. For example, the models presume a flat wire horizontal to the ground, which is not likely to appear with copper wire and real supports. Even if all supports provide the same height, catenary effects will vary the actual wire height above ground along the antenna pathway.

During the model-testing procedures, I explored 2 other directions. One direction led to the variety of soil types over which one might place a terminated long-wire antenna. So I modeled the test series of 10-wavelength antennas over very good and very poor soil to see the effect upon the performance parameters.

Test Performance Values for Modeling Option D over Various Soil Qualities

Terminating Load Ohms	Maximum Gain dBi	Front-to-Back Ratio dB	Beamwidth degrees	Elevation Angle deg	Feedpoint Z R+/-jX Ohms	600-Ohm SWR
<b>1. Very Good SN Ground, NEC-4</b>						
600	11.86	25.20	33.6	12	474 + j 57	1.30
800	11.81	23.43	33.5	12	508 + j 75	1.24
1000	11.79	19.00	33.4	12	534 + j 89	1.22
<b>2. Average SN Ground, NEC-4</b>						
600	10.49	22.94	35.6	11	513 + j 69	1.22
800	10.47	20.30	35.6	11	544 + j 87	1.20
1000	10.46	17.29	35.6	11	567 + j102	1.20
<b>3. Very Poor SN Ground, NEC-4</b>						
600	9.21	21.93	33-S	10	630 - j 53	1.10
800	9.23	17.54	33-S	10	653 - j 30	1.10
1000	9.25	14.66	33-S	10	671 - j 11	1.12

As we move from better soils to worse soils, the gain decreases by about 1.3-dB per step. However, note that over very poor soil, the gain trend reverses relative to the value of the terminating resistor. The front-to-back ratio reports also decrease with worsening soil. Each soil quality yields its own consistent beamwidth and elevation angle. The annotations for very poor soil indicate that the null between maximum gain peaks is sufficient to record separate lobes with at least a 3-dB null between. Hence, the beamwidth is an estimate. The resistive portion of the feedpoint impedance shows a non-linear rise with worsening soil quality. Nevertheless, all of the 600-Ohm SWR values fall well within the usable range.

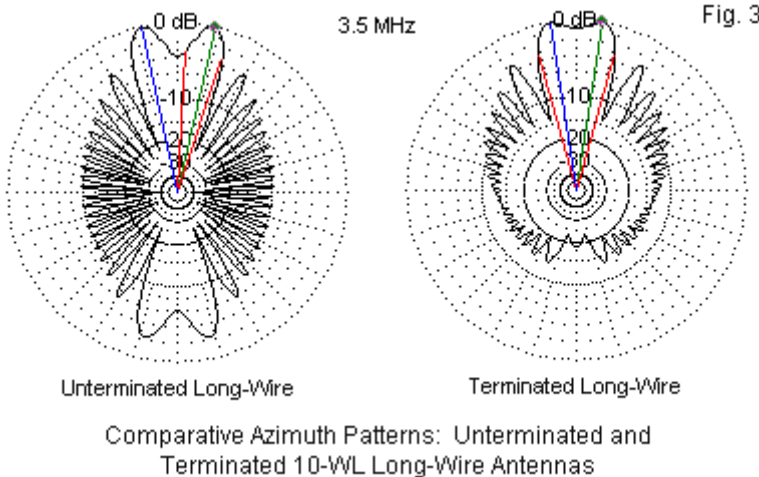
The second direction of additional modeling shows the effects of using copper wire instead of perfect wire in the 10-wavelength antenna. Both tests use average SN ground.

## Test Performance Values for Modeling Option D with Lossless and Copper Wire

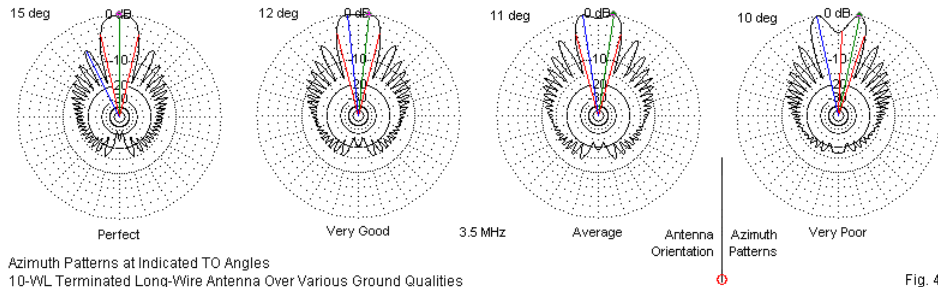
Terminating Load Ohms	Maximum Gain dBi	Front-to-Back Ratio dB	Beamwidth degrees	Elevation Angle deg	Feedpoint Z R+/-jX Ohms	600-Ohm SWR
<b>1. Average SN Ground, NEC-4, Lossless Wire</b>						
600	10.49	22.94	35.6	11	513 + j 69	1.22
800	10.47	20.30	35.6	11	544 + j 87	1.20
1000	10.46	17.29	35.6	11	567 + j102	1.20
<b>2. Average SN Ground, NEC-4, Copper Wire</b>						
600	10.28	23.06	35.5	11	518 + j 70	1.21
800	10.27	19.70	35.5	11	548 + j 85	1.19
1000	10.26	17.37	35.5	11	571 + j 97	1.19

Despite the very long length of the wire, copper losses at the test frequency only lower the gain by about 0.2 dB. All other performance values remain quite constant.

The reason that we are taking the trouble to model as adequately as feasible the terminated long-wire directional antenna is the difference that we find between its pattern and the pattern of an unterminated end-fed long-wire antenna. The differences appear in **Fig. 3** for 10-wavelength versions of both antennas. Although the terminated directional antenna is laden with sidelobes, the entire pattern provides a good front-to-rear ratio that can enhance communications by reducing rearward interference levels. Indeed, it is possible to use a remotely controlled switch to remove the load and return the antenna to an unterminated state for communications to the rear.



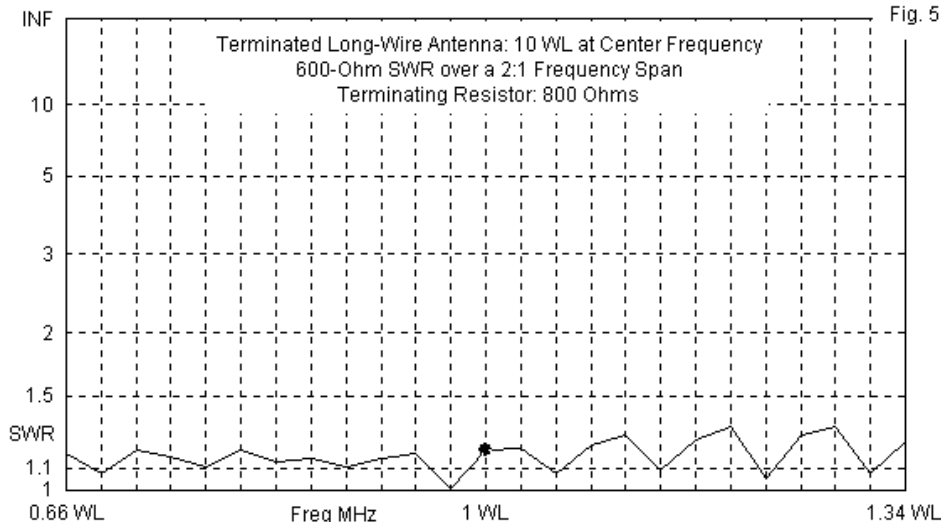
When looking over the tabulated results for various ground qualities during the modeling testing procedure, we met with split lobes over very poor soil. In order to see better the progression of the forward-most lobes of the terminated antenna, we can examine **Fig. 4**. It provides the azimuth patterns over the 3 soil qualities and over perfect ground.



The pattern over perfect ground has a single forward lobe, but all of the patterns over real ground show two peaks. As the soil quality decreases, the peaks grow farther apart, with an ever deeper depression in gain between them. Over very poor soil, the depression becomes an identifiable null, exceeding 3-dB relative to the maximum lobe strengths. Hence, the pattern identifies the peaks as separate lobes. The patterns strongly suggest that anyone who proposes to construct a terminated long-wire directional antenna should account in advance for the ground quality beneath and in the vicinity of the antenna. Depending upon the specifications of a given communications operation, the 3-dB null at the center of the 2 peaks over very poor soil might make a difference to antenna planning.

The terminated long-wire antenna has a very wide operating range in terms of the feedpoint SWR. The terminating resistor combined with the antenna height largely controls the feedpoint impedance. As a specimen test, **Fig. 5** provides the 600-Ohm SWR curve for the test antenna using an 800-Ohm terminating impedance. The curve involves no change in the antenna, although the height--in

wavelengths--varies from about 0.66 to 1.34 wavelengths above ground. It is clear that the 2:1 frequency range of the test run does not exhaust the usable SWR span for the antenna. However, it does cover one of the more usual amateur applications of a terminated wire, that is, operation from 20 through 10 meters.



*The End-Fed Terminated Long-Wire Directional Antenna and Its Patterns:* To produce a table of results for terminated long-wire antennas of various lengths and an associated gallery of patterns, I settled on an 800-Ohm termination for the models, using option D as the NEC-4 modeling foundation. The horizontal lossless wire is 1 wavelength above average ground. The total length value is the length of the horizontal span of the antenna and does not include

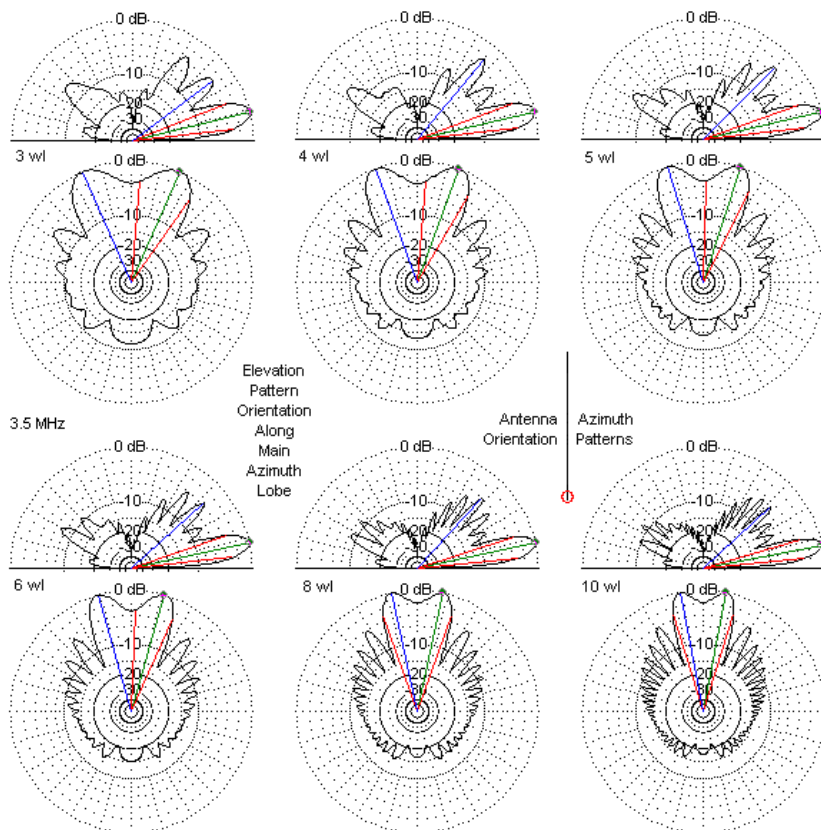
the vertical legs. As in the test data, if the main lobe is split into 2 lobes with a distinct null (>3 dB) between them, the beamwidth is an estimate with the letter "S" added to denote the split. TR Loss provides NEC's calculation of the percentage of applied power dissipated in the terminating resistor.

End-Fed Terminated Long-Wire Directional Antenna Data							
Total Length WL	Maximum Gain dBi	Front-Back Ratio dB *	Elevation Angle deg	Beamwidth degrees	Feedpoint Z R+/-jX Ohms	600-Ohm SWR	TR Loss %
3	7.11	15.32	14	69-S	537 + j92	1.22	26
4	7.99	16.48	13	59-S	539 + j90	1.21	25
5	8.65	17.91	13	51-S	541 + j89	1.21	24
6	9.15	18.30	12	46-S	543 + j89	1.20	24
7	9.57	19.30	12	43.8	543 + j88	1.20	24
8	9.92	19.51	12	40.2	544 + j88	1.20	23
9	10.20	20.12	12	37.0	544 + j88	1.20	23
10	10.47	20.30	11	35.6	544 + j87	1.20	23
11	10.70	20.58	11	33.4	544 + j87	1.20	23

The most constant data are the values for feedpoint impedance, 600-Ohm SWR, and power dissipated in the terminating resistor. The front-to-back ratio increases with antenna length. However, this value has a flag, since the value is related to the heading of peak gain, which is not the center of the pattern, that is, is not aligned directly with the wire itself. The maximum gain, the beamwidth and the elevation angle of maximum gain decrease with increasing total length.

The patterns associated with selected entries in the table appear in **Fig. 6**. Because the rate of change slows as we reach the upper length values, there are more patterns for the shorter lengths than for the longer. The azimuth patterns reflect both the tabular value entries plus the anticipated growth in the number of total sidelobes. However, because there are 2 1-wavelength vertical legs, the total number of lobes and peaks will be greater than for a corresponding

unterminated end-fed long-wire antenna. Do not neglect the elevation patterns. They show a very complex structure that will call for further comment before we conclude.



Terminated Long-Wire Antennas with Lossless Wire  
Sample Elevation and Azimuth Patterns 1 WL Above Average Ground

Fig. 6

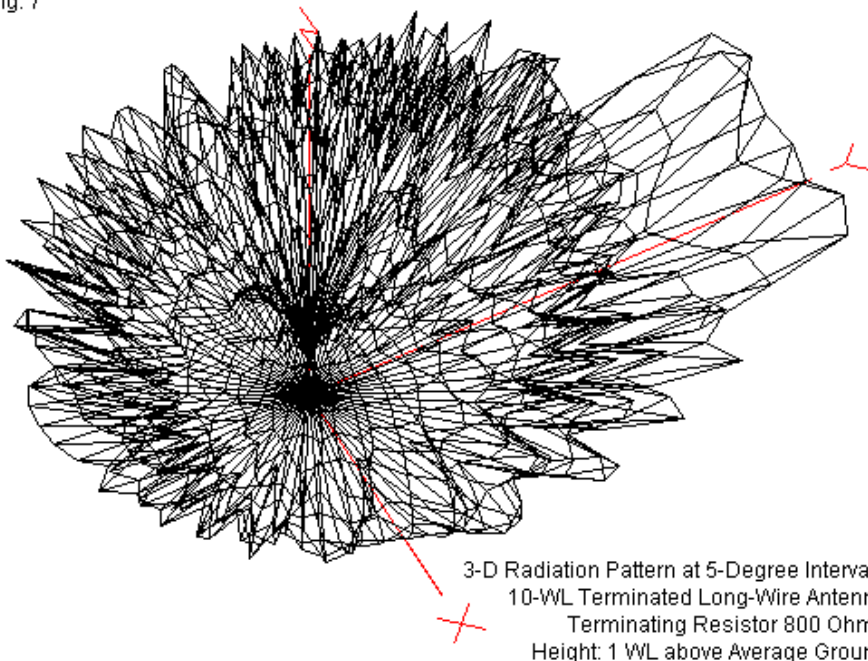
The terminated end-fed long-wire directional antenna is inexpensive and simple, assuming that one has access to the required non-inductive terminating resistor. It has 2 chief properties of merit, neither of which is raw gain. It is quite directional, although fraught with sidelobes. It is also extremely broad-banded in terms of SWR. The termination largely controls the feedpoint impedance. Large frequency excursions, of course, change not only the length of the antenna, but also the height above ground, when we measure both in terms of wavelength. However, a single antenna can cover most of the HF spectrum, if high and long enough at the lowest frequency. With increasing frequency, we obtain a narrower beamwidth and higher gain. Offsetting these variable qualities is the absence of any need for further impedance matching once we transform the average feedpoint impedance of the antenna to the value required by the transmitting and receiving equipment. Hence, the antenna is useful for directional low-angle communications that may require extreme frequency-changing agility.

The following table compares the maximum gain for terminated and unterminated end-fed long-wire antennas for lengths from 3 to 11 wavelengths. Note that the unterminated version is essentially bi-directional, although gain is slightly greater away from the feedpoint. As the antennas grow longer, the gain deficit for the directional long-wire antenna grows smaller. However, it is unlikely to become as low as 3 dB until the terminated long-wire antenna reaches wholly impractical lengths.

Gain and Elevation Angle Comparison			Unterminated Long-Wire			Gain
Terminated Long-Wire			Unterminated Long-Wire			Difference
Total Length	Maximum Gain dBi	Elevation Angle deg	Gain dBi	Elevation Angle deg	dB	
WL						
3	7.11	14	11.32	13	4.21	
4	7.99	13	11.99	13	4.00	
5	8.65	13	12.48	13	3.83	
6	9.15	12	12.90	12	3.75	
7	9.57	12	13.24	12	3.67	
8	9.92	12	13.50	12	3.58	
9	10.20	12	13.72	12	3.52	
10	10.47	11	13.96	11	3.49	
11	10.70	11	14.15	11	3.45	

One final property set needs illustration before we close the book on terminated long-wire directional antennas. We have noted the complexity of the lobe structure in both azimuth and elevation patterns. These 2-dimensional slices of the overall radiation pattern of the long-wire antenna do not do full justice to the overall radiation pattern of the antenna. To rectify this gap, at least partially, **Fig. 7** provides a 3-dimensional pattern for the 10-wavelength terminated antenna. The pattern is limited to 5-degree increments, lest finer detail turn the entire graphic into a simple opaque black-ink ball. The junction of the X, Y, and Z axes represents the antenna position relative to the pattern. Since the graphic shows a far-field pattern, the antenna itself is infinitesimally small. However, the wire extends along the Y-axis, with the terminating resistor on the +Y end (toward the field's projection of higher gain).

Fig. 7



The graphic shows us two very significant features that might be lost if we confine ourselves solely to 2-dimensional patterns. First, the overall field is littered with a morass of sidelobes in virtually every direction except downward. This facet of very long-wire antennas concerned early developers of long-wire technology. The sidelobes waste power that deserves re-direction into the main forward lobe(s). As well, the sidelobes create and receive interference. Moreover, they do nothing to secure a point-to-point

link, but instead allow reception of possibly sensitive communications to the sides of the antenna.

Second, the forward lobe structure contains an interesting oddity. Careful inspection is necessary to perceive the anomaly. At the second-lowest elevation angle (10 degrees in the graphic), we find the split lobe that marks the highest gain that the antenna can attain. At the next level (15 degrees in the graphic), the field has very nearly the same gain across the lower-level split region, but at a slightly lower gain value. Under some propagation conditions, the higher-angle smoother pattern might obscure the presence of the lower-angle split-lobe pattern. The complexity of even the forward-most lobe structure should be an important planning investigation, especially if one contemplates installing a terminated long-wire directional antenna over poor to very poor soil.

*Bending the Terminated Long-Wire Antenna:* There is a technique by which we can remove the split radiation lobe of the terminated long-wire antenna, at least when the wire is many wavelengths long. We may bend it horizontally in the middle. In effect, we create a 2-element long-wire antenna, where each element is half the total horizontal wire length. (In this sample, we shall leave the 1-wavelength vertical wire and the "ground rods" from model D just as they are.) **Fig. 8** shows the general layout.

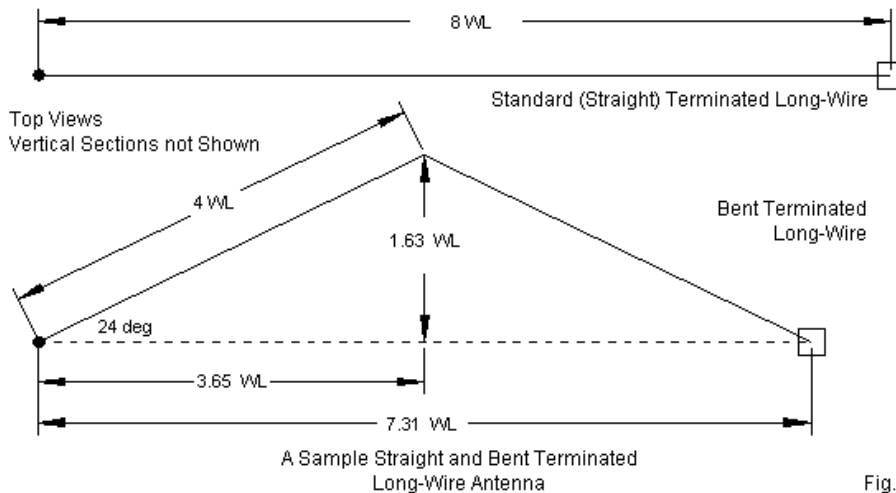


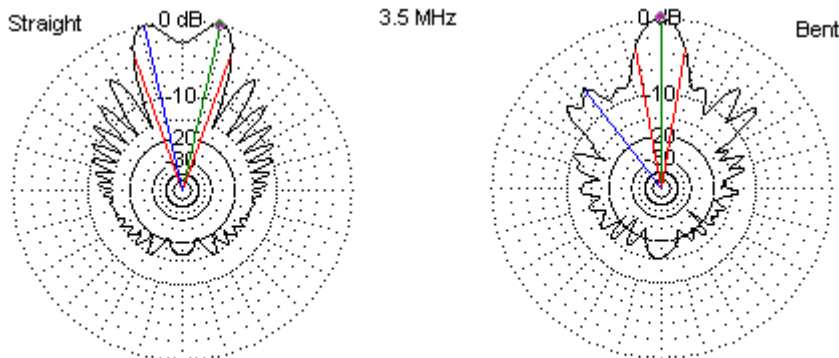
Fig. 8

One of the forward main lobes from the feedpoint-end section tends to align itself with one of the main forward lobes of the termination-end section, and the two lobes are aligned with the wire termination points. **Fig. 8** provides data for the 8-wavelength (or dual-4-wavelength) bent terminated longwire antenna. The required angle relative to the pattern centerline is 24 degrees for maximum gain. This value is a function of the antenna's 1-wavelength height, the average soil quality, and the wire length. Since the total horizontal wire length is 8 wavelengths, the angle creates a maximum antenna width of 1.63 wavelengths, but shortens the overall length to 7.31 wavelengths.

The following brief table compares the performance of the straight and bent 8-wavelength antennas. Bending the wire adds about 2.5 dB of overall gain, due to the additive effect of aligned lobes. However, the front-to-back ratio suffers by a like amount. The impedance hardly changes between the 2 antennas. The most notable change of all is the reduction in beamwidth from 40 to 20 degrees.

End-Fed Terminated Long-Wire Directional Antenna Data:						Straight and Bent 8-Wavelength Models	
Version	Maximum Gain dBi	Front-Back Ratio dB	Elevation Angle deg	Beamwidth degrees	Feedpoint Z R+/-jX Ohms	600-Ohm SWR	
Straight 8 WL	9.92	19.51	12	40.2	544 + j88	1.20	
Bent 24 deg.	12.39	15.36	13	20.3	531 + j71	1.19	

The difference in beamwidth becomes readily apparent when we examine azimuth patterns for the 2 antennas in the table. **Fig. 9** provides the patterns. The bent version has eliminated the null between peaks by creating a single forward main lobe. As well, the bent antenna's patterns shows irregular sidelobe structures that result from off-axis additions and cancellations, relative to the clean lobe structure of the straight antenna. However, most of the bent antenna sidelobes tend to be weaker than those of the straight antenna.



Azimuth Patterns at TO Angles: Straight and Bent  
8-Wavelength Terminated Long-Wire Antennas

Fig. 9

The bent terminated long-wire antenna is rarely used today. The straight terminated long-wire beam has lower gain, but it also enjoys 2 advantages: wider beamwidth and the ability to operate over a very wide frequency range at a constant impedance. The bent antenna might match the straight antenna's SWR curve, but the radiation pattern would become unusable beyond perhaps a 2:1 frequency range. The physical wire angle remains constant, but the electrical length of the wire--measured in wavelengths--changes for every change in operating frequency. The angle simply becomes incorrect to produce maximum gain in a single lobe as the operating frequency goes too high or too low. If we wish to obtain the added gain of the bent antenna's aligned main lobes, there are other designs that achieve the goal with more regular sidelobes and, in some cases, weaker sidelobes. In future episodes, we shall encounter some of those designs.

## Conclusion

So far, we have explored some of the performance properties of the simplest long-wire antennas, a single very long piece of wire placed horizontally over the ground. The notes have tried to impart a good sense of what happens as we lengthen the wire under 3 different feeding conditions: center feeding, end-feeding, and terminated end-feeding. By the use of extensive tabulated data and patterns from models of the antennas, I hope to have left reasonable expectations for the relative performance of the 3 basic types of long-wire antennas. Along the way, I have explored some of the modeling issues to reveal both my rationale for use the models involved and so that anyone else can recreate or improve them. Bending the wire at the end of the present episode in fact gives us a preview of the techniques that inform more complex long-wire arrays.

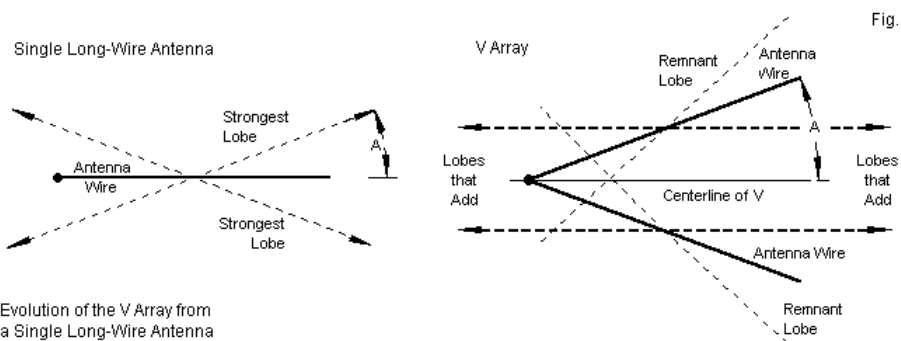
Still, we have only begun to explore long-wire technology. We have seen some of the shortcomings of the simple straight terminated long-wire directional antenna. The lobes are split. There are many side lobes. The forward gain is low. In an effort to overcome these problems, early designers ingeniously developed the V-beam and the rhombic. I have heard that Bruce would have preferred that his name be attached to the rhombic for which he was a pioneer, rather than to the planar array that bears his name in many handbooks. In Parts 3 through 5, we shall not try to change the names of antennas, but we shall try to understand better both the long-wire V-beam and the rhombic antenna using some of the same techniques employed in the notes for Parts 1 and 2.

## Chapter 55: V Arrays and Beams

In Chapters 53 and 54, we examined the simplest unterminated and terminated long-wire arrays using a single end-fed wire in both cases. Unterminated wires yield essentially bi-directional patterns in line with the wire--more in line as the wire grows longer as measured in wavelengths. There is a small residual front-to-back ratio associated with long-wire end-fed wires, with the stronger lobes toward the open or un-fed end of the wire. Adding a terminating resistor converts the bi-directional wire into a directional beam, although the gain is about 4 dB lower than the strongest lobes of the unterminated wire of the same length. At the end of Part 2, we summarized the shortcomings of the single-wire terminated end-fed wire beam: "The lobes are split. There are many side lobes. The forward gain is low." To overcome some of these problems, early antenna experimenters invented the unterminated V array and the terminated V beam. We shall look at each of these antennas in order of sequence since we have some questions that parallel those connected with the single wire terminated and unterminated antennas. For example, will the terminated V beam show the same gain deficit relative to the unterminated V array as the terminated single-wire did relative to its unterminated version? The V antennas are so intimately related to the single long-wire antennas that before we move onward to rhombics, we shall do a more detailed comparison.

## V-Array Basics

The V array derives directly from the single long-wire antenna. In fact, a V array is nothing more than two single long-wires connected at a feedpoint junction and fed in series. The V array makes use of one of the problems for a single wire: the two main lobes do not come completely together to form a single lobe. The V array turns the problem into an advantage. If we angle each leg of the V in just the right way, we can get two of the lobes--one from each leg--to point in the same direction and let their gain levels add. **Fig. 1** shows the outline of how we obtain a true bi-directional unterminated array from 2 long-wire antennas.



On the left is a representation of a single long-wire antenna (bold solid line) and the headings of its main or strongest lobes (dotted line). Note that we use the wire center as a conventional origin of the lobe indicators. Since the dotted lines represent a far field pattern, the antenna (in relation to the pattern) would have an

infinitesimal size. When thinking about the pattern, mentally shrink the antenna until it almost disappears.

In Parts 1 and 2, we represented the angle taken by the individual lobes as an angle relative to the tangent to the wire, that is, relative to a broadside direction. In this episode, we are interested in angle A (usually shown as an alpha in texts). The old angular value and A add up to 90 degrees, so conversion is easy.

If we now use 2 wires to form a V, we can set each one at angle A relative to the centerline of the V. So the total angle between wires is  $2A$ . By aligning the wires in this way, a main lobe from each wire at each end will fall into alignment and add up to a new higher gain level. As well, there will be only 1 main lobe in each direction in line with the wire. The remnant lobes become sidelobes of the array.

Note that this strategy is in principle similar to the strategy of bending a long single wire in the middle to obtain lobes that add rather than going in different directions. Indeed, the required angle for each type of design is almost the same: angle A. Indeed, for the same quantity of horizontal wire, a directional V beam and a terminated bent single wire have about the same gain. The difference is largely one of halving the total overall length (and the acreage required beneath the antenna) for a doubling of the smaller required width.

We are fortunate, since we can refer to Part 1 and find the heading of the main azimuth lobes for each test length of long wire antenna. The following table lists those headings as well as the resultant value of angle A. The table also shows several other values. The

next column lists a calculated value for angle A that we shall explain following the table. The final columns show the angles associated with corresponding long-wire terminated beams. These values will not play a role in our work. They only illustrate the fact that forming a terminated beam from the long-wire antenna does compress the angle between the maximum gain points on the beam forward pattern, in part due to the presence of the vertical wires necessary to complete a practical installation.

Long-Wire Azimuth angles of Maximum Radiation and Corresponding A-Angles					
Antenna Length WL	Unterminated Long-Wire			Terminated Long-Wire	
	Azimuth Angle degrees	Angle A degrees	Calculated Angle A degrees	Azimuth Angle degrees	Angle A degrees
2	56	34	35.4	-----	-----
3	63	27	27.6	66	24
4	67	23	23.0	70	20
5	70	20	19.8	72	18
6	72	18	17.6	74	16
7	74	16	15.8	75	15
8	76	14	14.4	77	13
9	77	13	13.2	78	12
10	77	13	12.2	78	12
11	78	12	11.3	79	11

If we did not have access to NEC-calculated values for the azimuth angles for the strongest long-wire lobes, we could have resorted to an approximation equation for calculating the value of angle A.

$$\text{Angle A} = \arccos [(N-0.5) / N] - 6$$

Angle A is in degrees, while N is the length of the long-wire legs in wavelengths. I adapted and adjusted this equation from one found in Balanis' account of long-wire antennas. Within the confines of the lengths used for our test NEC-model cases, the equation is quite adequate for forming models of V arrays. More complex angle

calculation devices exist, but they turn out to be almost spuriously precise. The gain of a V array changes very little using angle-A values that are plus or minus a full degree from the listed values. The tolerances become considerably tighter, however, if we increase the leg length well beyond the limits of the table. Hence, NEC models may be the best way to indirectly obtain the requisite values for angle A. (For much longer antennas, it may be useful to increase the resolution of the azimuth patterns from which we indirectly derive angle A. NEC is fully capable of handling 0.1-degree increments between pattern samples. In such cases, the headings for the strongest lobe will also resolve to a tenth of a degree.)

*Note:* The models in this part of our work make use of angle A as derived from our modeling of single long-wire antennas. They do not necessarily optimize that angle for maximum gain. There is a slight difference.

For basic model testing, I chose the 10-wavelength V array using 13 degrees as the value of angle A. Relative to the array centerline, shown in **Fig. 1**, the array is 9.75 wavelengths long and 4.5 wavelengths wide at the open end. Like the antennas in Parts 1 and 2, this one also uses perfect or lossless wire at 20 segments per wavelength. The main tests will place the antenna 1 wavelength above average ground (conductivity 0.005 S/m, permittivity 13). However, for initial tests on the 10-wavelength model, I placed it over very good, average, and very poor soil in order to see what differences ground quality might make to performance. The following table emerged from those tests.

10-Wavelength Unterminated V Array 1-Wavelength Above the Indicated Soil Type

Angle A = 13 degrees; Elevation angle = 10 degrees

Soil Type	Gain dBi	Front-Back Ratio dB	Beamwidth degrees
Very Good	17.21	2.55	11.0
Average	17.24	2.47	10.2
Very Poor	17.17	2.37	9.8

Unlike other antennas that we have surveyed in this collection of notes, the V array showed almost no change in its pattern, despite the wide range of soil qualities. The conductivity of the soils ran from 0.0303 S/m for very good ground down to 0.001 S/m for very poor ground. The relative permittivity range from very good to very poor was 20 down to 5. **Fig. 2** overlays the azimuth patterns for the 3 models. Except for a few distinguishable differences in nulls, the patterns almost perfectly coincide with each other. In the realm of bi-directional unterminated long-wire antennas, the V array may prove to be a good selection for use over relatively poor soils.

Azimuth Patterns of  
a 10-WL V Array  
over Very Good,  
Average, and  
Very Poor  
Ground

El. Angle: 10 deg.  
Height: 1 WL  
3.5 MHz

Ground Quality  
Black = Very Good  
Blue = Average  
Red = Very Poor

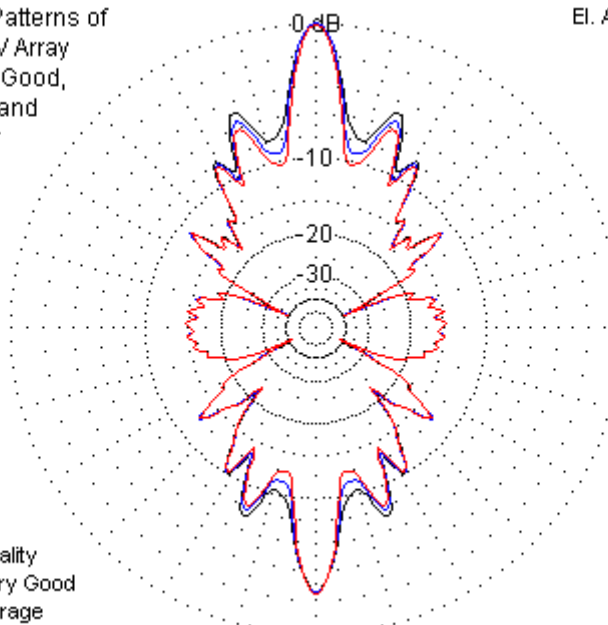


Fig. 2

In the initial tests, I also tried the 10-wavelength V array using copper wire over average ground to obtain a sense of what wire losses might be. As in past models, the wire diameter is 0.16" (AWG #6) to allow scaling of the 3.5 MHz test models to other frequencies in the amateur HF range.

## 10-Wavelength Untermminated V Array 1-Wavelength Above Average Soil

Angle A = 13 degrees; Elevation angle = 10 degrees

Wire Type	Gain dBi	Front-Back Ratio dB	Beamwidth degrees
Lossless	17.24	2.47	10.2
Copper	16.73	2.68	10.2

As the simple comparison shows, we lose about 0.5-dB relative to maximum gain by using copper wire. I would view such losses as insignificant, especially since we have no way to recover them without a 20-wavelength supply of super-conducting wire.

In order to compare the performance of a single unterminated wire to that of a V array, I constructed models of the V array using legs that ran from 2 to 11 wavelengths. The following table lists the value of angle A, the elevation angle for maximum gain, the maximum gain value, the remnant front-to-back ratio, and the beamwidth of the strongest main lobe. In addition, for easy reference, the table also lists the maximum gain of the corresponding single unterminated long-wire antenna and the gain differential between it and the V array.

## Performance of V Arrays 1-Wavelength Above Average Ground

Leg Length WL	Angle A degrees	Elevation Angle deg	Max. Gain dBi	Front-Back Ratio dB	Beamwidth degrees	Single Long-Wire Max. Gain dBi	Diff. dB
2	34	13	13.60	1.37	20.2	10.27	3.33
3	26	13	14.65	1.84	17.2	11.32	3.33
4	23	12	15.48	1.88	14.4	11.99	3.49
5	20	12	15.97	2.05	13.2	12.48	3.49
6	18	12	16.25	2.27	12.2	12.90	3.35
7	16	11	16.56	2.36	11.8	13.24	3.32
8	14	11	16.75	2.44	11.8	13.50	3.25
9	13	11	16.99	2.44	11.4	13.72	3.27
10	13	10	17.24	2.47	10.2	13.96	3.28
11	12	10	17.35	2.56	10.2	14.15	3.20

The tabulated data shows the usual progression of increasing gain and decreasing beamwidth as we lengthen the legs of the antenna. As well, length-for-length, the V array shows a maximum gain that is somewhat over 3-dB greater than the gain of a single long-wire antenna having the same length. (One might well dispute the length equivalence, arguing that the centerline of the V array is always shorter than the centerline of the corresponding single long-wire antenna. However, with 10-wavelength legs, the centerline difference is only about 1/4 wavelength due to the gradual narrowing of the angle ( $2A$ ) between the wires.)

Perhaps the most intriguing set of numbers falls in the beamwidth column. For leg lengths beyond about 3 wavelengths, the antenna requires careful alignment for the main lobe (or lobes) to hit a communications target. In fact, V arrays (and beams) found their main use as antennas having communications targets falling within a small radius. One technique used to steer the antenna's main lobe was to set multiple Vs in a physically serial arrangement that did not necessarily form a straight line. Thus, one antenna could bend the beam of the first. We should also remember that high quality copper wire in the late 1920s and through the 1930s was not as cheap as it is today, when measured against other prices. Many amateurs used less expensive phosphor-bronze wire for antennas, and government and commercial wire antenna installations were major investments. Although we today may doubt the precision that one might achieve by attaching wire to wooden telephone and telegraph poles, the engineering calculations were as precise as available techniques permitted. (Laport's *Radio Antenna Engineering* from 1952 has an interesting gallery of photos of

mainly RCA antenna installation going back as far as the 1930s. Wooden poles--some spliced to increase their height--outnumber metal masts and towers. We may also find it interesting that many installers working with hand tools wore neckties and fedora hats on the job.)

The V array is not an antenna for broad coverage of the horizon. Its wire foundation makes it immovable, and the gain comes at the expense of beamwidth. Hence, its best use is as a point-to-point antenna, where the reliability of a single communications link is more important than communications with many diverse places on the horizon. The gallery of sample elevation and azimuth patterns in **Fig. 3** will reinforce this judgment.

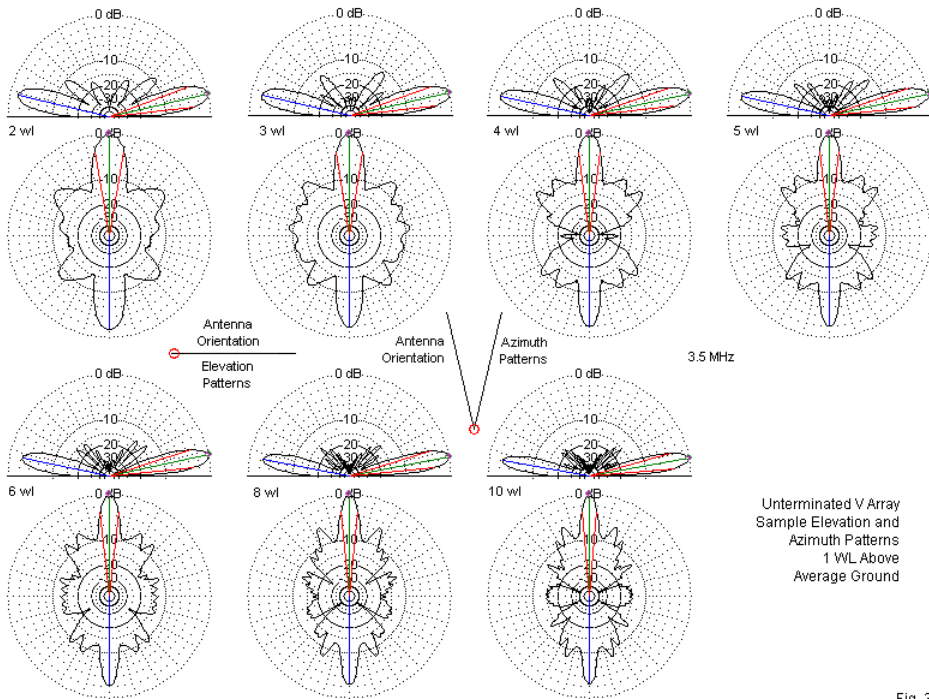


Fig. 3

Compared to the single long-wire antenna, the V array shows significantly smaller elevation lobes above the main lobes. The azimuth sidelobes, while still pronounced in the off-heading forward areas, are generally smaller than those of a single unterminated wire antenna. Many of the sidelobes from each leg tend to counter corresponding sidelobes from other legs, in part due to having different headings and in part due to the spacing between the legs. The azimuth pattern for the 4-wavelength model shows perhaps the

tightest wasp-waisted pattern. In contrast, the elevation upper lobes tend to decrease in strength in more direct proportion to the length of the legs. However, due to the interaction of the lobes from each leg and the changing included angle from one model to the next, we cannot characterize the patterns by reference to the number of lobes, as we did with the single long-wire end-fed antenna.

3-Dimensional Radiation Pattern  
5-Degree Increments  
10-WL Unterminated V Array  
1-WL Above Average Ground

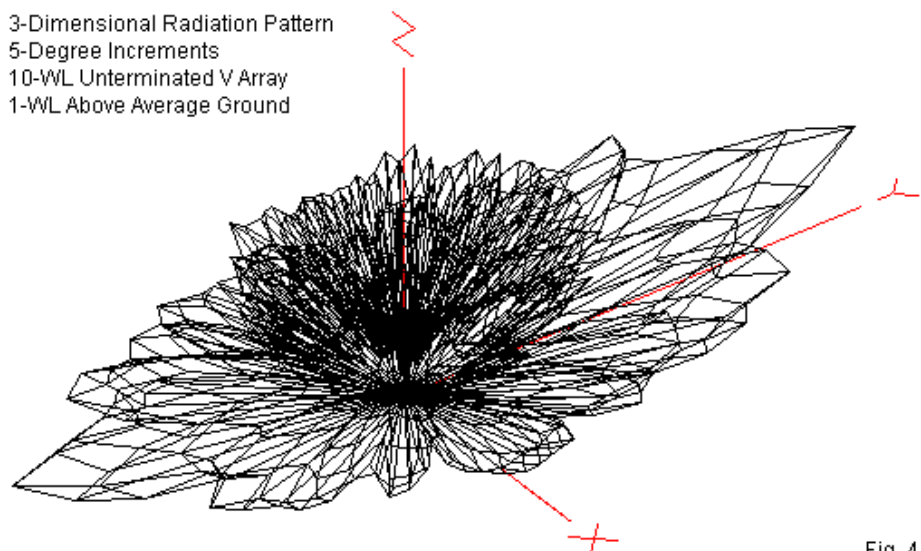


Fig. 4

The 3-dimensional radiation pattern shown in **Fig. 4** has a peculiarly crystalline appearance, given the 5-degree increment between sampling points. Nevertheless, the main lobe extremities show well. Still, one might best refer to the 2-dimensional plots before attempting to characterize the upper-angle lobes. Although

there are still many lobes--as there will be for virtually any long-wire antenna--their strength relative to the main lobes is considerably weaker than is the case for a single wire.

There is no rule that we must always optimize a V array for maximum gain. At certain values for angle A, the beamwidth will widen. Of course, the new value for A varies with the length of the legs. As well, a widening of a few degrees will actually narrow the beamwidth. However, by judicious modeling or experimentation, one can find a usable beamwidth before the pattern degenerates into peaks with a very deep null between them. For example, with 5-wavelength legs, the peak-gain angle is 20 degrees (or 40 degrees between wires). The beamwidth is 13.2 degrees. By widening angle A to 29 degrees (58 degrees between wires), the effective beamwidth becomes about 35 degrees. With a pre-planned selection of centerline headings, it is possible to cover much of the horizon in a switched set of V arrays in which each interior leg serves 2 arrays. **Fig. 5** shows the general scheme and a sample azimuth pattern. For some installations, similar schemes can be tailored to the operating site and communication needs. The 13.4-dBi gain of each V-pair still out-performs individual 5-wavelength wires.

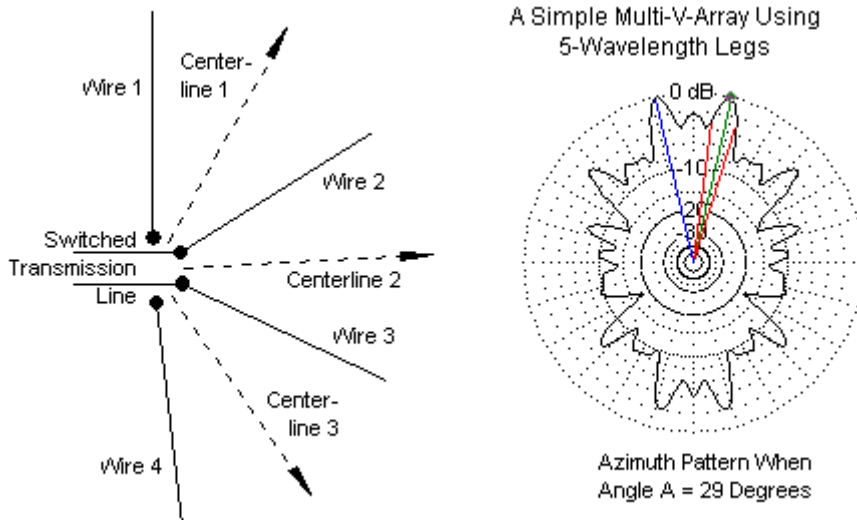


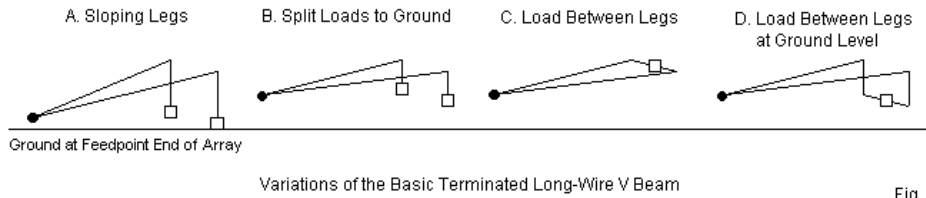
Fig. 5

The potentials for V arrays are larger than suggested by this introduction to them. However, it is time to terminate this initial discussion and the V array itself.

## V-Beam Basics

The terminated V array forms a V-beam, that is, a directional terminated V array. The technique seems simple enough. We simply place a non-inductive terminating resistor at the end of each leg. However, the resistor cannot simply float at the terminating end of the wire. One option is to bring the terminated end of the leg wire to ground. Alternatively, we may run a wire between the two

terminated wires end and place the non-inductive resistor at the center.



Variations of the Basic Terminated Long-Wire V Beam

Fig. 6

**Fig. 6** shows 4 classic implementations of the terminated V-beam. Model A places the feedpoint close to ground and slopes the legs upward to their normal (1-wavelength) height. (The opposite slope for the array is also possible. See model A1.) The terminated ends run vertically to the ground, with the terminating resistors at ground level. The model will use the same ground-rod technique used in constructing models of single terminated long-wire directional antennas. However, none of the models will use a vertical wire at the feedpoint end. The single long-wire beams could use the vertical feedpoint end with the actual feedpoint close to ground. If we apply that same technique to the V-beam, we end up with the 2 legs in parallel, which does not yield much gain or directivity. The source-ends of the legs must have the feedline across them in a series connection to yield the correct addition of peak lobes from each leg.

Selecting the correct values of the 2 terminating resistors is not so simple as it was with the single long-wire beam. As the following

trial table shows, the value is not exceptionally critical, although we may have reasons for choosing one value over another. For design purposes, the reasons may involve the best compromise among gain, front-to-back ratio, and impedance. In practical installations, the reasons generally focus on what non-inductive resistors may be available. The test table (and others to follow) uses NEC-4 models with 5-wavelength legs 1-wavelength above an average SN ground.

Test Performance Values for Modeling Option A

Terminating Load Ohms	Maximum Gain dBi	Front-to-Back Ratio dB	Beamwidth degrees	Elevation Angle deg	Feedpoint Z R+/-jX Ohms	1000-Ohm SWR
600 x2	8.89	23.15	12.2	15	988 + j184	1.20
700 x2	8.91	22.40	12.4	15	1043 + j145	1.16
800 x2	8.93	20.58	12.4	15	1091 + j109	1.14

The sloping version of the terminated V-beam shows a serious gain deficit relative to level models (options B, C, and D in **Fig. 6**). Gain is 4- to 5-dB lower than for the other versions. Therefore, we should test further V-beam designs. NEC calculates that each terminating resistor dissipates about 21% of the applied power, using the 700-Ohm resistor in each leg.

If we slope the V-beam in the other direction, with the feedpoint high and the terminations low, we do not see much change in the performance, except for a reduction in the front-to-back ratio and a reduction in the terminating resistor. Let's call the reverse slope model A1.

Test Performance Values for Modeling Option A1

Terminating Load Ohms	Maximum Gain dBi	Front-to-Back Ratio dB	Beamwidth degrees	Elevation Angle deg	Feedpoint Z R+/-jX Ohms	1000-Ohm SWR
400 x2	8.60	18.90	21.0	14	1032 + j107	1.12
500 x2	8.60	18.06	21.2	14	1096 - j 6	1.10
600 x2	8.63	15.99	21.2	14	1141 - j109	1.18

The theory behind the reverse slope is an attempt to lower the elevation angle of maximum radiation. However, the result is an antenna that is on average much lower than a model that is level at 1 wavelength. Hence, the net elevation angle, while 1 degree lower than for version A is still higher by 2 degrees than the other models (B, C, and D) in this sequence. The model A gain deficit still remains, with a gain level that is barely 1 dB higher than a 1/2-wavelength dipole at 1 wavelength above average ground.

Model B uses the same layout as Model A, but raises the feedpoint to the same height as the remainder of the antenna. Like Model A, B uses a pair of terminating resistors. The gain and elevation angle of maximum gain return to normal values, as shown in the following test table.

Test Performance Values for Modeling Option B

Terminating Load Ohms	Maximum Gain dBi	Front-to-Back Ratio dB	Beamwidth degrees	Elevation Angle deg	Feedpoint Z R+/-jX Ohms	800-Ohm SWR
600 x2	13.00	20.62	13.8	12	830 + j133	1.18
800 x2	13.02	18.41	13.8	12	926 + j190	1.30
1000 x2	13.07	16.00	13.8	12	1002 + j242	1.42

The gain level of this model changes very slowly with changes in the values of the terminating resistors. Hence, the table proceeds in 200-Ohm increments. Selecting the most optimal combination requires some decision-making based on criteria. In the absence of

practical operating goals, I chose the 600-Ohm resistors, since they yielded the highest front-to-back ratio in the group, along with having the lowest order of feedpoint reactance. The 600-Ohm resistors dissipate about 22% of the applied power--each.

Model C uses the same feedpoint treatment as model B. However, instead of bringing 2 vertical wires to ground, with 2 attached resistors, model C uses a straight connecting wire between the far ends of each leg. For the 5-wavelength legs of the test model, the crossing wire is about 3.4 wavelengths. At the center of the wire, we place a single non-inductive resistor. As the following table will show, the connecting wire is not inert, but an active part of the overall antenna.

Test Performance Values for Modeling Option C

Terminating Load Ohms	Maximum Gain dBi	Front-to-Back Ratio dB	Beamwidth degrees	Elevation Angle deg	Feedpoint Z R+/-jX Ohms	900-Ohm SWR
800	14.38	12.73	12.6	12	981 + j192	1.25
900	14.35	13.76	12.6	12	949 + j147	1.18
1000	14.34	14.73	12.6	12	919 + j110	1.13

The crossing horizontal wire between the V-leg ends contributes to the array gain in both directions. Hence, the peak forward gain is slightly higher than for model B, but the front-to-back ratio is much lower. If we select the 900-Ohm terminating resistor, NEC calculates that it will dissipate about 46% of the applied power.

Model D also uses a crossing wire with a single terminating resistor at its center. However, it brings the crossing wire much closer to ground level. In the model, the wire is 0.001-wavelength above ground; just enough for the wire to clear the ground by several wire

diameters. Each end of the V assembly runs a vertical wire down to the junction with the low crossing wire. As the table shows, this arrangement produces one of the most stable configurations relative to changes of gain with changes of the terminating resistor value.

Test Performance Values for Modeling Option D

Terminating Load Ohms	Maximum Gain dBi	Front-to-Back Ratio dB	Beamwidth degrees	Elevation Angle deg	Feedpoint Z R+/-jX Ohms	750-Ohm SWR
600	13.02	21.26	13.4	12	761 - j 49	1.07
800	13.03	20.64	13.4	12	754 - j 55	1.08
1000	13.03	20.19	13.4	12	749 - j 59	1.08
1200	13.03	19.85	13.4	12	744 - j 63	1.09

Not only is the gain stable across a 2:1 range of resistor values, but as well both the front-to-back ratio and the feedpoint impedance are equally stable. NEC calculates that in its altered position, the 1000-Ohm terminating resistor dissipates only 2.8% of the applied power, although this result stems from the proximity of the crossing wire to ground in the model. The actual dissipation may be much larger for only small increases in resistor and wire height. Nevertheless, using a very low crossing wire removes it from having a significant affect on the radiation pattern. In fact, the data for models B and D are quite similar, although model D appears to be the more stable. Further test of the V-beam using various leg lengths will employ this model and its 1000-Ohm resistor.

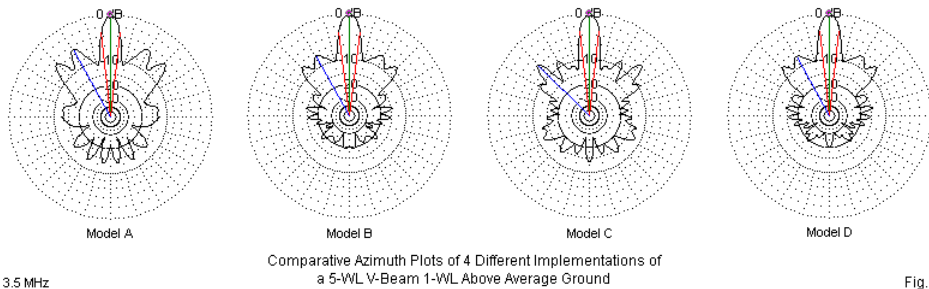
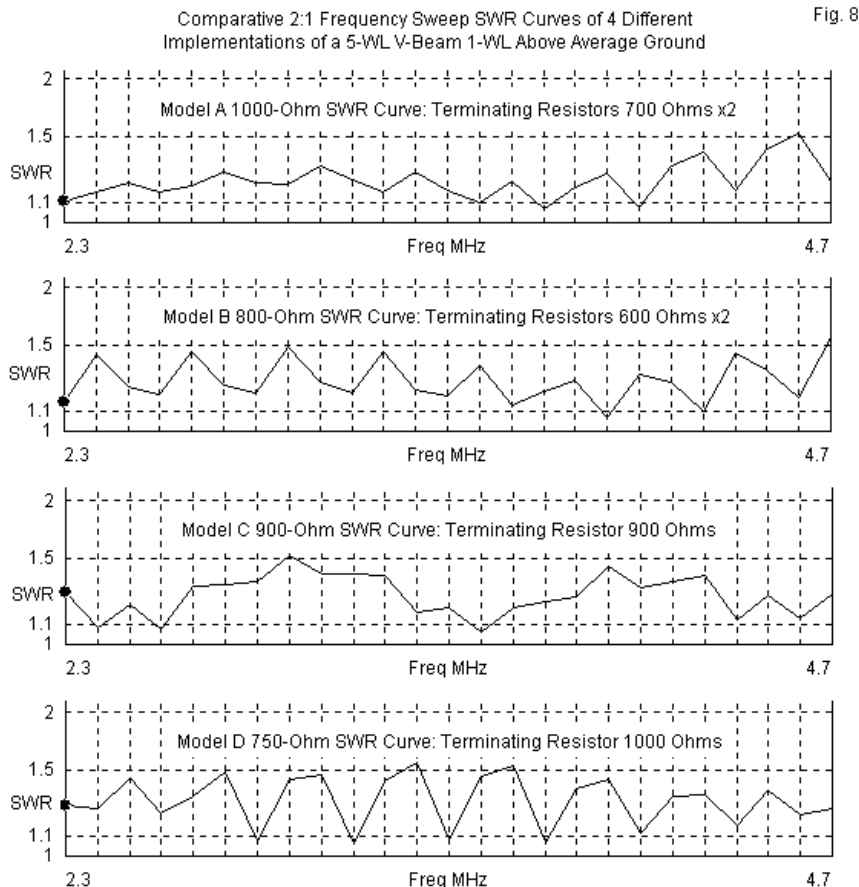


Fig. 7

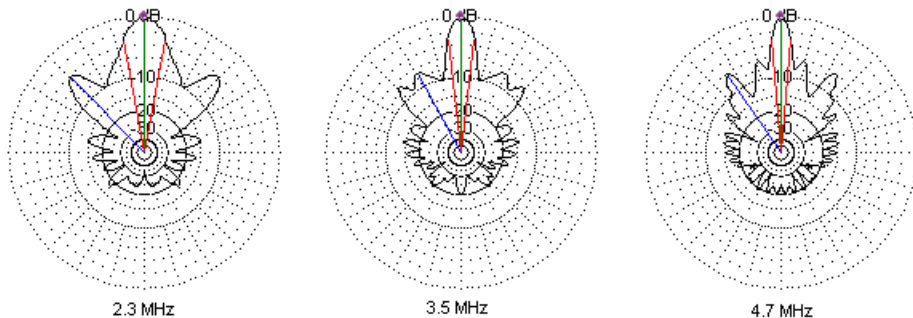
**Fig. 7** provides azimuth patterns for each of the 5-wavelength V-beam models. They show a family resemblance, especially in the forward structure of the lobes. The sidelobes of model A appear stronger because the forward gain is 4-dB or more weaker than for the other models. The data had suggested a close correlation between model B and model D, and the azimuth patterns tend to confirm the suggestion.

Although the 4 models of a V-beam use different arrangements and terminating resistor values to arrive at their patterns, all of them have the wide-band characteristic that we saw in the case of single long-wire beams. **Fig. 8** provides the SWR curves over a 2:1 frequency range using the optimal feedpoint impedance relative to the indicated values of terminating resistor or resistors. In each case, for the range tested and beyond, a single impedance-transformation device would suffice to match the antenna to most equipment. What all the SWR patterns share in common is the existence of ripples of non-harmful but noticeable proportions. These ripples are indications that the selected terminating resistor value(s) did not result in the closest equality between the

terminating resistor and the feedpoint impedance. Instead, the final component selection rested on other criteria, such as the resulting pattern, etc.



The broad SWR bandwidth of the single long-wire directional antenna is completely reliable, since the general pattern of the antenna is predictable in terms of gain and beamwidth. However, the V-beam has a more limited usable bandwidth due to restrictions created by the angle between the wires ( $2A$ ). At some frequency above and at another below the design frequency, the value of angle  $A$  will no longer be suitable to support a single forward lobe. As shown in **Fig. 9**, a 2:1 operational range is feasible for the 5-wavelength V-beam that is 1 wavelength above ground at the center frequency.



Azimuth Patterns for Model D At the Center  
and the Limits of the SWR Frequency Sweep

Fig. 9

Performance of a 5-Wavelength 3.5-MHz V-beam 1 Wavelength Above Average Ground

Model D: Terminating Resistor: 1000 Ohms

Frequency MHz	Maximum Gain dBi	Front-to-Back Ratio dB	Beamwidth degrees	Elevation Angle deg
2.3	9.84	33.30	21.8	17
3.5	13.03	20.19	13.4	12
4.7	14.42	23.77	9.8	9

When evaluating both the patterns and the tabular data, remember that at the low end of the sweep, the antenna is only 0.66-wavelength above ground, accounting for the higher elevation angle. Similarly, at the top of the sweep, the antenna is 1.34-wavelengths above ground. The changing height is an additional variable relative to the departure from an optimal value for angle A, and both contribute to the listed performance values.

Parallel to our investigation of the unterminated V array, I ran model D with a 1000-Ohm terminating resistor over several ground types. As shown in the table below, the gain changes by under 0.5 dB across the range of soils. The other values are equally stable, presenting no difficulties to using the V-beam over virtually any ground environment.

5-Wavelength Terminated V Array 1-Wavelength Above the Indicated Soil Type					
Angle A = 20 degrees; Elevation Angle = 12 degrees					
Soil Type	Gain dBi	Front-Back Ratio dB	Beamwidth degrees	Feedpoint Z R +/- jX Ohms	750-Ohm SWR
Very Good	13.18	18.89	14.4	753 - j 97	1.14
Average	13.03	20.19	13.4	749 - j 59	1.08
Very Poor	12.72	24.15	13.0	782 - j 27	1.06

Likewise, the use of a real material, such as copper wire, in place of the modeled perfect wires, offers no hindrance to the V-beam. As the following table shows, the loss due to the use of copper wire for the 5-wavelength V-beam is about 0.1-dB over average ground. All of the other performance values are completely stable.

5-Wavelength Untermminated V Array 1-Wavelength Above Average soil						
Angle A = 20 degrees; Elevation Angle = 12 degrees						
Wire Type	Gain dBi	Front-Back Ratio dB	Beamwidth degrees	Feedpoint Z R +/- jX Ohms	750-Ohm SWR	
Lossless	13.03	20.19	13.4	749 - j 59	1.08	
Copper	12.93	20.43	13.4	752 - j 52	1.07	

The full table of performance values below rests on model D, the version with a single terminating resistor centered on a wire between the V-leg end, but very close to ground level. The table does not include power dissipation values, since they likely depend on the very close proximity of the modeled resistance to the ground, as well as energy lost to ground due to the proximity. Hence, the exact dissipation values will vary with the actual height of the cross connecting wire. The table does include values for angle A, the elevation angle of maximum gain, the modeled maximum gain, the 180-degree front-to-back value, the beamwidth, the feedpoint impedance, and the 750-Ohm SWR. In addition, the table shows the maximum gain of the corresponding unterminated V array and the gain difference relative to the V-beam.

**Note:** Once again, the value of angle A is derived from our long-wire antennas and is not adjusted to achieve maximum gain.

Performance of V Beams 1-Wavelength Above Average Ground								Untermminated V Array		
Leg Length WL	Angle A degrees	Elevation Angle deg	Max. Gain dbi	Front-Back Ratio dB	Beamwidth degrees	Feedpoint Z R +/- jX Ohms	750-Ohm SWR	Max. Gain dBi	Difference dB	
2	34	13	9.88	36.86	21.0	772 + j16	1.04	13.60	3.72	
3	26	13	11.41	21.70	17.4	750 - j66	1.09	14.65	3.24	
4	23	12	12.35	22.90	14.8	772 - j38	1.06	15.48	3.13	
5	20	12	13.03	20.19	13.4	749 - j59	1.08	15.97	2.94	
6	18	11	13.50	19.97	12.4	741 - j39	1.06	16.25	2.75	
7	16	11	13.86	20.17	12.0	742 - j40	1.06	16.56	2.70	
8	14	11	14.07	19.89	12.0	731 - j42	1.06	16.75	2.68	
9	13	11	14.29	19.54	11.4	724 - j51	1.08	16.99	2.70	
10	13	10	14.59	19.32	10.4	721 - j42	1.07	17.24	2.65	
11	12	10	14.74	19.40	10.2	716 - j43	1.08	17.35	2.61	

The table shows a very normal increase in gain with leg length at the optimal angle A. Both the elevation angle and the beamwidth for the V-beam tightly correspond to comparable values for the unterminated V array, with no decrease in beamwidth as we experienced with the transition from unterminated long-wire to terminated long-wire antennas. The 180-degree front-to-back ratio holds around the 20-dB mark, and the impedance is exceptionally stable throughout the span of leg lengths. (The stability of the impedance values is an especially good marker of the adequacy of using values for angle A derived from the unterminated single long-wire models.) As a side note, compare the V-beam entry for 4-wavelength legs to the data for the bent terminated long-wire in Part 2. The gain values are virtually identical, although the V-beam improves the front-to-back ratio and reduces many of the sidelobes. Both antennas require 8 wavelengths of horizontal wire.

The V-beam, like the terminated long-wire antenna, shows a decrease in maximum forward gain relative to the unterminated version of the antenna. However, the V-beam decrease is about a dB less than for the single long-wire beam. Nevertheless, the reason for using a V-beam instead of an unterminated V array is the directivity of the pattern, with the loss of gain accepted as a fair penalty for the reduced sensitivity to the rear. If rearward pattern reduction is not a priority for a given installation, then the unterminated V array may be the better choice of antennas. **Fig. 10** provides a gallery of selected elevation and azimuth plots that show the evolution of radiation patterns with increasing leg length in the V-beam. You may wish to compare these plots directly to corresponding plots in **Fig. 3** for the unterminated V array.

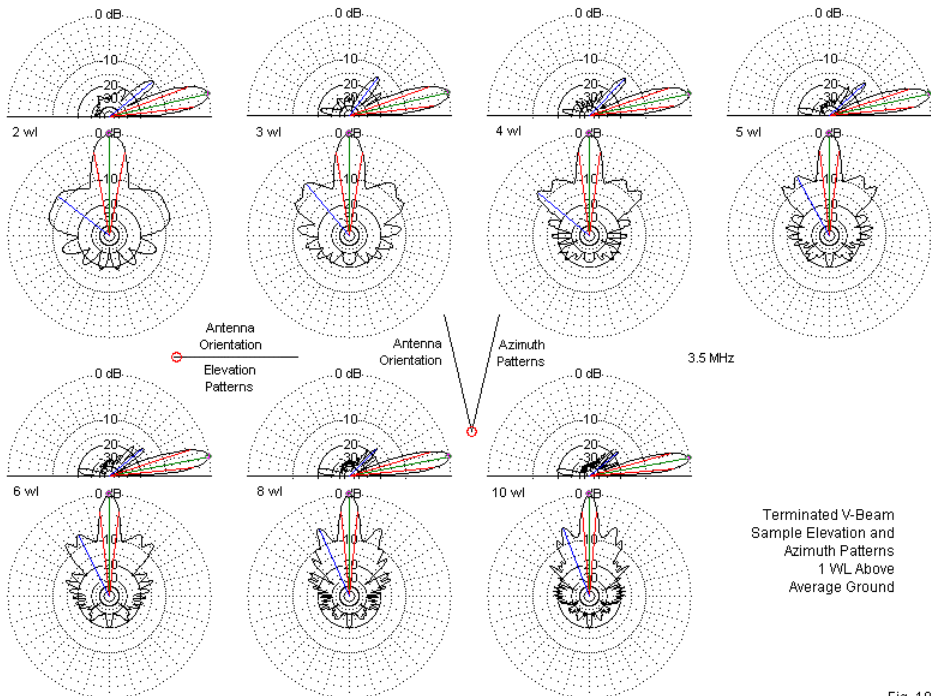
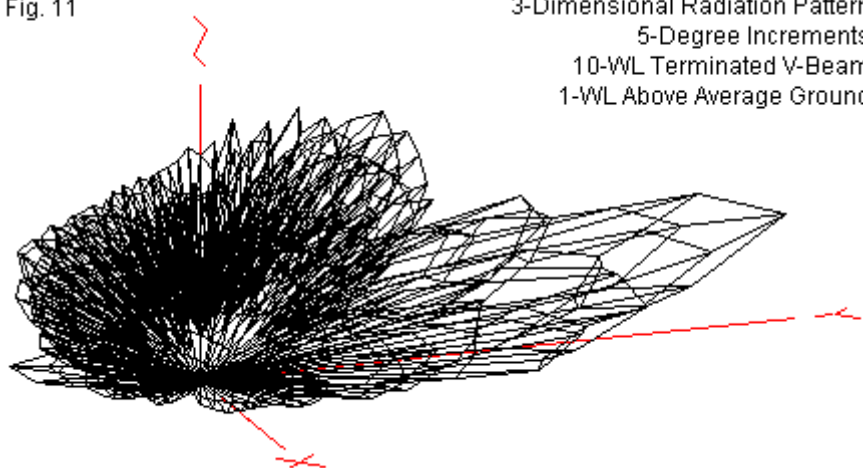


Fig. 10

The azimuth patterns have two major characteristics that we should note. First is the narrowing of the beamwidth as we make the antenna longer, a feature that also attaches to the V array. Second is the development of the secondary lobes in the 2 forward quadrants. These lobes are a function of the narrowing angle between wires and the lobes on each wire that does not add to form the strongest center lobe.

The most notable elevation-plot feature is the relative absence of strong secondary elevation lobes. Only the lobes closest to the main elevation lobe exceed the -20-dB level in strength relative to the main lobe. We may better gauge the upper-level lobe structure from a 3-dimensional radiation pattern, such as the one in **Fig. 11**. The 10-wavelength V-beam used to generate the plot clearly shows the lowest level. The apparent second level is actually a part of the main lobe. The stepped appearance is due to the 5-degree increments in pattern sampling. The next strongest level to the main lobe occurs near the 40-45-degree region and is 15-20-dB weaker than the main lobe. Although there are still many upper-level lobes in the pattern, their strength is operationally insignificant.

Fig. 11



Perhaps an appropriate way to conclude our exploration of the V-beam is by comparing it, length for length, with the corresponding single long-wire terminated beam. **Fig. 12** provides a pattern comparison, using 10-wavelength versions of both antennas. The elevation patterns show the V-beam's reduction in relatively useless upper level lobes. The azimuth pattern shows the V-beam's tighter control of sidelobes, especially in the forward quadrants. However, for some communications tasks, the terminated long-wire may have the more useful beamwidth, despite the null between forward peaks.

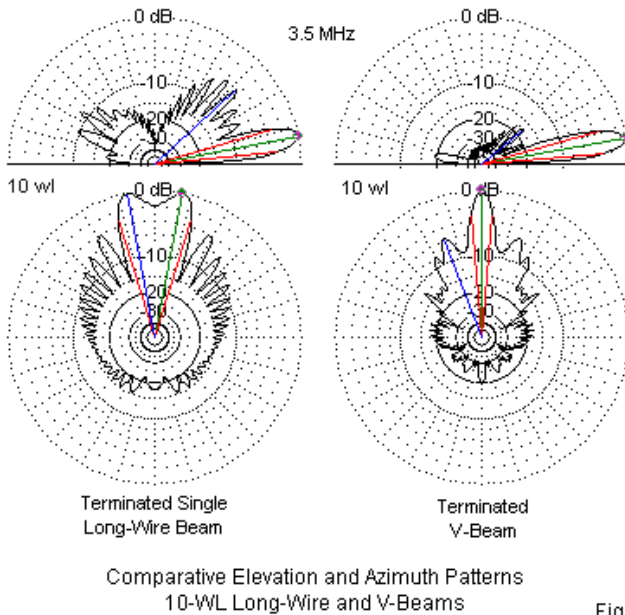


Fig. 12

The following table summarizes the gain and beamwidth differentials between the 2 terminated long-wire directional antennas.

Long-Wire and V-beam Gain and Beamwidth Values for 3- to 11-Wavelength Arrays					
Length WL	Terminated Long-Wire		Terminated V-Beam		Gain Diff. dB
	Gain dBi	Beamwidth degrees	Gain dBi	Beamwidth degrees	
3	7.11	69	11.41	17	4.30
4	7.99	59	12.35	15	4.36
5	8.65	51	13.03	13	4.38
6	9.15	46	13.50	12	4.35
7	9.57	44	13.86	12	4.29
8	9.92	40	14.07	12	4.15
9	10.20	37	14.29	11	4.09
10	10.47	36	14.59	10	4.12
11	10.70	33	14.74	10	4.04

The V-beam shows a consistent 4-dB+ gain advantage over the terminated long-wire antenna, but its beamwidth is consistently 1/3 to 1/5 the values for the long-wire. The terminated long-wire directional antenna, of course, shows a null between peaks, and for lengths from 3 to 6 wavelengths, the null is deep enough (>3dB) for modeling software to recognize two distinct forward lobes. The table does not itself make a judgment, but simply facilitates a comparison of the results in Part 2 of this series and the results obtained for this part.

## Conclusion

On this leg of our journey through the classical long-wire antennas, we have focused on the V antenna in both unterminated and terminated forms. By properly angling the legs of the V, the antenna combines a major lobe from each wire to form a single lobe in the

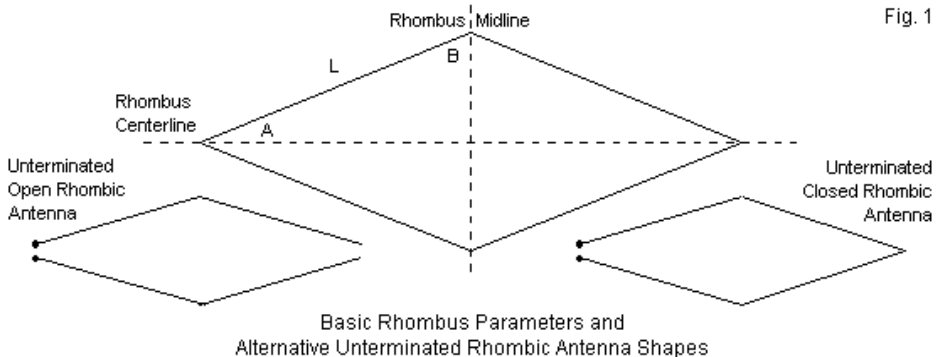
forward direction. Of course, the unterminated V array has a similar lobe to the rear and it is only slightly weaker than the lobe pointing away from the feedpoint. Terminating the legs of the Vee creates a directional antenna with superior properties to the single long-wire in terms of gain and the suppression of both elevation and azimuth sidelobes. However, the improved directional characteristics come at the expense of some of the unterminated V's gain. As well the V antennas have a very narrow beamwidth that limits the potential applications for either the terminated or unterminated versions.

Although there may be many variants on long-wire design, classical literature shows only one more major pathway to traverse: the rhombic. A Bruce development from the 1930s, the rhombic sometimes bears the title of the king of wire antennas. The antenna has had a lure that will take us 2 episodes to cover, and then only in an introductory way. One humorist has wished for his ideal antenna, and it was a very long rhombic installed on a rotatable island. Our task will be to see if there is any good sense hiding behind the humor.

## Chapter 56: Rhombic Arrays and Beams

Every step along our path through traveling-wave antennas has led us to new heights of gain per unit of wire length (as measured in wavelengths)--and to narrower beamwidths. The final steps take us to the pinnacle of long-wire development: the rhombic antenna. (We should note that there are some "fishbone" designs that may be able to achieve more gain per acre of ground than the designs with which we are working. However, these antennas use a quite different design and require at least 2 to 4 wavelengths of wire per wavelength of forward antenna dimension. We shall not cover them here. However, the *ARRL Antenna Book* chapter and the Laport volume, both cited in the short list of references, cover the basics of these designs.)

The rhombic antenna derives its name from its shape: the rhombus. In geometry, a rhombus is an equilateral parallelogram, that is, a closed 4-sided figure with all sides the same length, but with all corner angles normally using other than right angles. **Fig. 1**, at the top, shows a basic rhombus, with indications of the key dimensions.



An alternative way to look at the rhombus is to see it as 2 V antennas end-to-end. This orientation makes clear that the centerline is correctly identified, and it gives the elongated shape some sense, assuming that Part 3 of this series has had its impact. The length  $L$ , in wavelengths, defines the length of each leg, suggesting that each rhombic antenna that we examine will likely be twice as long overall as a corresponding V antenna with the same leg length.

Also apparent in the sketch is angle  $A$  (usually represented by a Greek alpha). When we examined V antennas, we used the angle of the strongest lobe of a single long-wire of length  $L$  to determine the value of angle  $A$ . We then found that angling each V wire from the centerline by the value of  $A$  produced additive lobes along the centerline. Since the far end of any rhombic antenna is a mirror image of the feedpoint end, the lobes for the far-end wires will also

be aligned with the center line. Hence, we can expect more gain from a rhombic antenna than from a corresponding V antenna.

The earliest literature, starting with the classic article by Bruce, Beck, and Lowry ("Horizontal Rhombic Antennas," *Proc. IRE*, 1935), began the practice of referring to angle B in **Fig. 1** as the tilt angle. The normal character for this angle is a Greek phi, although I have seen other characters as well. Angle B is simply 90 degrees minus angle A.

Basic rhombic calculations emerge from a situation that is usually not very realistic for the average amateur installation. The premise is that angle A represents 2 different angles in the antenna installation. First, it represents the elevation angle of maximum radiation. Hence,

$$H_{WL} = [1 / (4 \sin A)]$$

where  $H_{WL}$  is the required antenna height in wavelengths. As well, angle A represents the required V'ing angle, the same angle that we used in the V-antennas. To align the major lobe with the elevation angle, we calculate the leg-length as follows:

$$L_{WL} = [0.371 / (\sin^2 A)]$$

where  $L_{WL}$  is the leg-length in wavelengths. For maximum gain at the chosen elevation angle,

---

$$L_{WL} = [0.5 / (\sin^2 A)]$$

The difficulty faced by amateur installations is that the height is rarely a matter of open choice. As a matter of fact, neither is the length open to selection based solely on calculations. Instead, the maximum height for installations is usually prescribed by any number of limiting circumstances. All of the examples used in this Long-Wire series have set the antennas at 1 wavelength above ground on the premise that most long-wire antennas will ultimately fall in the upper HF range. 1 wavelength at 14 MHz is about 70'. Property lines usually define the absolute limits of overall array length, abetted by complexities such as the availability and feasibility of supporting very long runs of wire.

Initial and later studies in rhombic antennas provide more complex equations to calculate compromises where the elevation and the V'ing angle do not match. Some of the equations appear in nomographic form. For example, one such nomograph appears in the ARRL chapter on long-wire and traveling-wave antennas, as well as in articles and text devoted specifically to the design of rhombic antennas. (See the Harper volume in the reference list.) Such nomographs are capable of guiding the rhombic designer to excellent results, as we shall see before we close this last segment of our long-wire trek.

However, via NEC modeling, we have an easier route to designing rhombics. The process started in Part 1, with the modeling of end-fed unterminated wires, from which we obtained the values of angle A within the limits of the modeling exercise. We standardized the wire height at 1 wavelength. We might as easily develop a compendium of models using the same (or different) increments of

wire length at a number of different heights. For a practical design project, we likely would select a single height dictated by whatever constraints will govern the installation. Then, we can collect data on angle A for any set of wire lengths desired.

We may use the selected height and the associated values of angle A to design any number of rhombic antennas. In fact, we can use a simple long-wire as the starting point. NEC allows us, via the GM command, to rotate the wire by the required number of degrees dictated by the value of angle A for a given wire length. (Programs like EZNEC use a different but equally effective method of rotating wires.) Hence, we can easily create a V and find its coordinates. From those coordinates, we can complete the rhombic by doubling the overall length and bringing 2 new wires back together--or almost together. See the lower part of **Fig. 1** for 2 possible versions of an unterminated rhombic configuration.

The use of angle A assures us of lobe direction coincidence and gain addition along the centerline of the antenna. We may then let NEC calculate the gain and actual elevation angle for the selected antenna height over any selected soil. Before we close this discussion, we shall find that NEC's handling of rhombic design and at least one nomographically based design turns out to be virtually identical. Traditional methods are quite accurate, but in the present age of computerized antenna design, the modeling process is often simpler. As we have seen from our experience with single long-wire and V antennas, the modeling method also provides ready supplementary information, for example about sidelobes, feedpoint

impedances, and power dissipation in the load resistance of terminated antennas.

In our exploration of rhombic antennas, we shall simply extend our modeling methods. First, we shall leave the antenna at 1 wavelength above average ground (conductivity 0.005 S/m, permittivity 13). The test frequency will be 3.5 MHz, and the lossless wire will be 0.16" in diameter. Part 1 of the series sampled some of the variations on these choices, so you may readily extrapolate additional losses or gain from selecting different background parameters. Better yet, you may easily model most of the antennas yourself, using your own selection of parameters. Some beginning programs are limited to 500 segments. A few of the longer rhombics may require up to 900 segments if we adhere to our 20-segment per wavelength standard. However, a full 6-wavelength-per-leg rhombic comes in at under the 500 segment mark.

## Unterminated Rhombic Antennas

The lower portion of **Fig. 1** shows two ways of modeling an unterminated rhombic antenna. We may separate the far end point by a small space. This configuration is perhaps the most common understanding of an unterminated (sometimes called a resonant) rhombic. However, we may equally bring the ends together to short-circuit the gap. The options expose something of a misimpression of the rhombic antenna. If we were given to extreme (and unfortunately, contentious) modes of expression, we might

suggest that there is no such thing as an unterminated rhombic antenna.

The single long-wire unterminated antenna and the V array both make good sense of the idea of a wire without a resistive termination. Any form of termination requires extra wires and ultimately a ground connection--although there is a version of the V-beam that does not use ground at the far end of the array. The rhombic returns the 2 wires of the antenna to close proximity. In the models that we shall explore, the gap will be 0.002-wavelength. At 3.5 MHz, that distance is 170 mm, where a wavelength is over 85.6 m long. If we leave the gap open, we can treat the terminating resistance as simply indefinitely large. One modeling technique for rhombics is to use a short wire to bridge the gap. To create a terminated rhombic--as the term is generally used--we place a load resistor of a desired value on the bridge wire. To create an open circuit, we might specify the load resistance as  $1e10$  Ohms or higher. To short out the gap, we can either remove the load resistor or give it a value of 0 Ohms. Alternatively, we can remove the bridge wire and simply bring the 2 legs to the same point on the coordinate scheme.

Despite the existence of a reasonably plausible claim that all rhombics are terminated to one or another degree, we shall adhere to the common referential terms. Without a mid-range non-inductive resistor at the far end of the antenna, the rhombic will be unterminated in either the open or closed configuration. The chief difference between the open and closed versions of the unterminated rhombic antennas lies in the sidelobes, not in the

small differences in gain and inherent front-to-back ratio that is a part of all end-fed long-wire antennas. **Fig. 2** contrasts the structure of the sidelobes for open and closed unterminated rhombics. Note that the closed version shows larger sidelobes than the open version, suggesting less complete cancellation of lobes from the parallel legs.

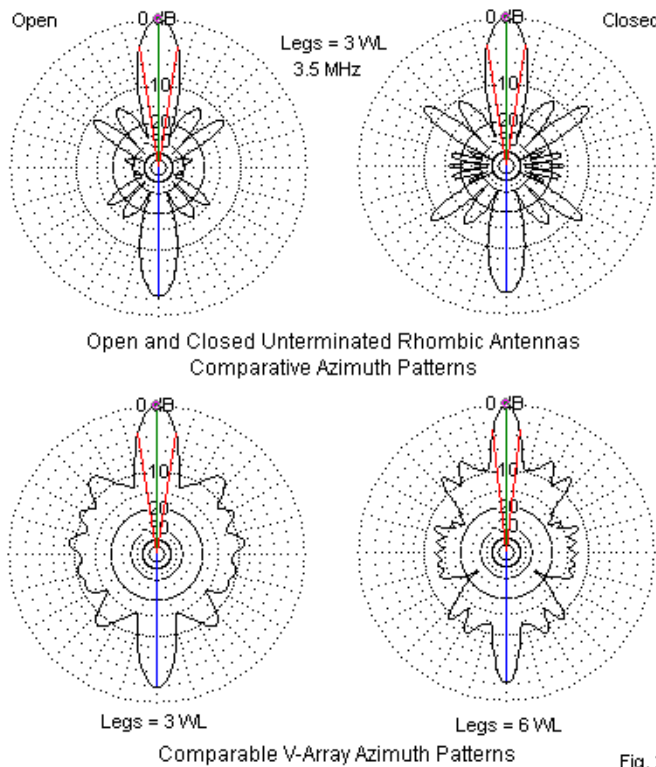


Fig. 2

For comparison and contrast, **Fig. 2** also presents two azimuth patterns from corresponding unterminated V arrays. The pattern on the lower left uses 3-wavelength legs, the same length as the legs in the rhombics. On the lower right is the pattern for a V array using 6-wavelength legs. These legs give the V array the same overall length as the rhombic with a small margin of difference due to the difference in the value of angle A. (Both rhombics are 5.39 wavelengths, while the long V is 5.71 wavelengths overall.) On the whole, the long V antenna pattern resembles in general sidelobe strength the closed rhombic pattern. However, the V patterns show the combination of many sidelobes that combine to form fewer distinct lobes and nulls. In contrast, the double-V configuration of the rhombic reduces these indefinite lobe formations down to distinct lobes and nulls. In fact, both rhombic azimuth patterns show a total of 20 lobes. The lower strength levels of the lobes at near-right-angles to the 2 main lobes for the open version of the antenna make lobe counting impossible at the scale of **Fig. 2**, but expanded renderings of the plot reveal them all. In contrast, even large renderings of the V-antennas do not permit an accurate count of the lobes and the bulges that form incipient lobes.

Clear lobe definition and numeric limitation together comprise one of the advantages of the rhombic over corresponding V antennas. The other major rhombic advantage is gain. The following table provides modeled data for both open and closed unterminated rhombics with varying leg lengths from 2 through 11 wavelengths. Remember that the overall length of the rhombic is just under twice the leg length. Like all long-wire antennas, the rhombic suffers the blight of diminishing returns as we strive to make it longer. Doubling

the leg length from 2 to 4 wavelengths provides nearly 2.5-dB more gain. However, the next doubling to 8 wavelength legs adds slightly under 2 dB of gain.

*Note:* The values of angle A derive from our earlier work with single long-wire antennas. I have not optimized those values to achieve maximum gain. There is a slight difference.

Performance of Unterminated Rhombic Antennas 1-Wavelength Above Average Ground

Type	Leg Length WL	Angle A degrees	Elevation Angle deg	Max. Gain dBi	Front-Back Ratio dB	Beamwidth degrees
Open	2	34	14	16.41	2.41	20.4
Closed	2	34	14	15.84	2.90	20.6
Open	3	26	14	17.81	2.40	17.2
Closed	3	26	14	17.50	2.66	17.2
Open	4	23	13	18.89	2.58	14.1
Closed	4	23	13	18.61	2.83	14.4
Open	5	20	13	19.57	2.57	12.8
Closed	5	20	13	19.35	2.77	12.8
Open	6	18	12	20.12	2.55	11.6
Closed	6	18	13	19.95	2.71	11.8
Open	7	16	12	20.53	2.48	11.2
Closed	7	16	12	20.39	2.60	11.2
Open	8	14	12	20.82	2.32	11.0
Closed	8	14	12	20.69	2.42	11.0
Open	9	13	12	21.17	2.27	10.4
Closed	9	13	12	21.03	2.38	10.4
Open	10	13	11	21.52	2.37	9.4
Closed	10	13	11	21.39	2.47	9.4
Open	11	12	11	21.73	2.29	9.0
Closed	11	12	11	21.61	2.38	9.0

At the top of the table, the gain differential between open and closed rhombics appears to be significant: nearly 0.6 dB. However, the differential shrinks continuously as we lengthen the legs. By the time the legs are 11 wavelengths, the gain differential is only a bit over 0.1 dB. Elevation angles, front-to-back ratios, and beamwidths

all remain very comparable for both types of unterminated rhombic antennas.

All of the closed unterminated rhombics show a modest feedpoint impedance at the integral leg lengths that appear in the table. The resistive component varies between 235 and 290 Ohms, while the reactance ranges from -j160 to -j190 Ohms. In contrast, all of the open rhombics show very high impedance levels, with resistive components running from 2900 to 3300 Ohms. The reactance seems to have a wide range--from +j130 to +j460 Ohms. However, as a fraction of the total impedance, the range is small. The differential between open and closed rhombic impedances is real, but in practical terms of designing a system, it is also illusory. The curves for changes of feedpoint resistance and reactance for the two types of unterminated rhombics are virtually identical, but displaced from each other by about 1/4 wavelength of leg length.

**Fig. 3** presents the unterminated rhombic gallery of sample elevation and azimuth plots for leg lengths of 2, 4, 6, 8, and 10 wavelengths. By comparing the plots with **Fig. 2**, you can verify that the gallery uses the open version of each rhombic.

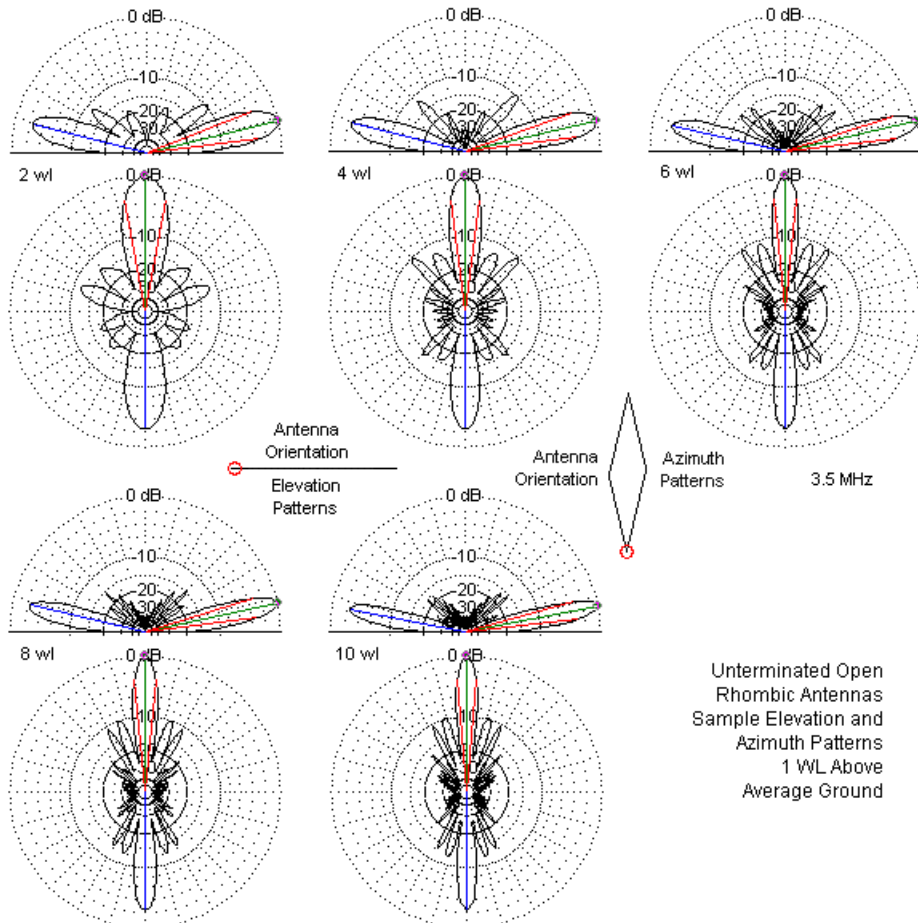


Fig. 3

The open unterminated rhombic shows excellent sidelobe control compared to the other long-wire antennas that we have surveyed.

In general, azimuth sidelobes are 10 dB of more down, with a very good front-to-side ratio for headings near or at the 90-degree mark off the main lobes. Secondary elevation lobes are 10 to 15 dB down, depending upon rhombic length. **Fig. 4** provides a 3-dimensional radiation pattern in 5-degree increments of the rhombic with 10-wavelength legs. Although the upper elevation angles still bristle with lobes, they are generally all of low strength and therefore untroublesome to antenna performance.

3-Dimensional Radiation Pattern  
5-Degree Increments  
10-WL-Leg Unterminated Rhombic  
1 WL Above Average Ground

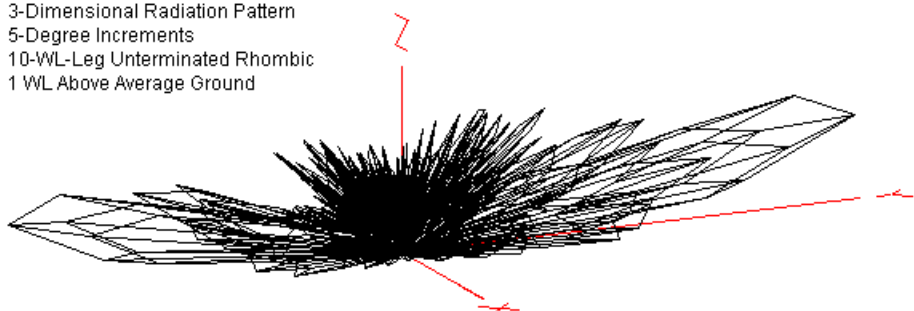


Fig. 4

As a way to summarize our meandering through various unterminated bi-directional wire antennas, the following table presents the modeled maximum gain values for each type that we have surveyed. All values are for perfect-wire antennas 1 wavelength above average ground. Remember that the center-fed and end-fed long-wire antennas show maximum gain off-axis to the wire, while the V and rhombic antennas show maximum gain in line with the antenna centerline. In addition, the rhombics overall are

twice as long as the single-wire and V antennas listed for the same leg length.

Maximum Gain of Various Types of Unterminated Long-Wire Antennas

Leg	Maximum Gain dBi				
Length	Center-Fed WL	End-Fed Doublet	V Wire	Closed Rhombic	Open Rhombic
2	9.36	10.27	13.60	15.84	16.41
3	10.16	11.32	14.65	17.50	17.81
4	10.93	11.99	15.48	18.61	18.89
5	11.47	12.48	15.97	19.35	19.57
6	11.85	12.90	16.25	19.95	20.12
7	12.14	13.24	16.56	20.39	20.53
8	12.43	13.50	16.75	20.69	20.82
9	12.65	13.72	16.99	21.03	21.17
10	12.82	13.96	17.24	21.39	21.52
11	13.01	14.15	17.35	21.61	21.73

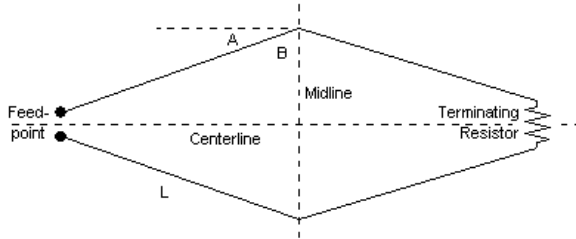
Although some of the gain increase that we see with longer and more complex long-wire antennas comes from sidelobe control, most of it emerges at the expense of beamwidth. We have noted this fact in past episodes, but it needs a reminder here. Short V and rhombic antennas (2-wavelength legs) have beamwidths just over 20 degrees. With 10-wavelength legs, the beamwidth is less than half that value. Although the high gain of long Vs and rhombics seems attractive to many, the utility of a fixed position narrow-beamwidth antenna is for point-to-point communications, not for general communications across the horizon. For comparison, a half-wavelength dipole has a beamwidth of about 80 degrees while the beamwidth of a 1.25-wavelength extended double Zepp is about 30-35 degrees. In many cases, the key design question for fixed long-wire antennas is less "With whom do I wish to

communicate?" and more "With whom am I willing not to communicate?"

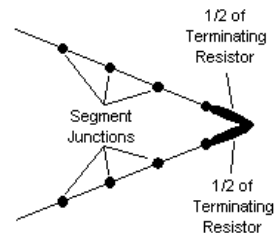
## Terminated Rhombic Antennas

The terminated version of the rhombic antenna is identical to the unterminated versions with the exception that the far junction of the wires has an intervening non-inductive resistor (or combination of resistors in series and/or parallel connection) with the desired value. **Fig. 5** shows the outline of the general arrangement. Ordinarily, the terminating resistor is somewhat arbitrarily selected in the 600-800-Ohm range. Angles A (alpha) and B (phi) play the same role in the terminated rhombic that they play in the unterminated versions. L remains the leg length measured in wavelengths, and the leg length plus the angles form unique combinations to achieve maximum gain at some prescribed antenna height.

Fig. 5



General Outline of the Terminated Rhombic Beam



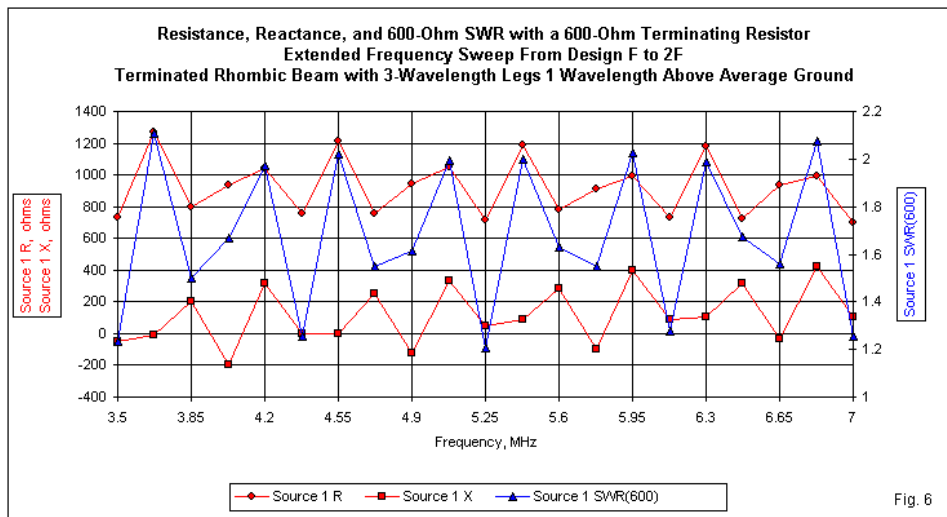
Modeling the Terminating Resistance

The models for the unterminated rhombics have used only 4 wires, one for each leg. The model source consists of a split source, that is, two sources in series. The sources go on the segments adjacent to the junction of the wires at the feedpoint end of the antenna. As the right side of **Fig. 5** reveals, I used a similar technique to place the terminating resistor. Non-reactive resistive loads go on the last segment of each far-end wire, with each resistance equaling half the total terminating resistance. These techniques of placing sources and loads preclude the need to create a short wire at each end of the rhombic structure. To preserve an equality of segment lengths, the bridge wire would have to be long enough that it would not preserve the value of angle A. Alternatively, to maintain the value of angle A, the source/load wire would be significantly shorter than adjacent leg segments, a condition on the source wire that NEC does not recommend for the most accurate calculations. Split sources and split loads preserve both the geometry of the model and the best conditions for calculation.

Like all other models in this series, the lossless 0.16"-diameters wires use 20 segments per wavelength. All terminated rhombics are 1 wavelength above average soil with a test frequency of 3.5 MHz.

Before we present a table of modeled performance values, we must select a value for the terminating resistor. Many rhombic builders rely on the tradition that the terminating resistor controls the feedpoint impedance. Since 600-Ohm ladder line is readily available or easily built, 600 Ohms has been a popular resistance for the rhombic termination. For spot frequencies in otherwise well-

designed rhombics, a 600-Ohm termination produces a low 600-Ohm SWR. However, many rhombics find use over at least a 2:1 frequency range. Therefore, I swept the version of the rhombic with 3-wavelength legs from the design frequency to twice the frequency to observe the likely undulations of resistance, reactance, and 600-Ohm SWR. **Fig. 6** shows the results.



In many ways, the resistance and reactance swings appear to be modest. Indeed, the SWR curve shows low values for 3.5, 5.25, and 7 MHz (which would correspond to 14, 21, and 28 MHz on a properly scaled version of the model). However, the SWR for 4.53 MHz (scale value: 18.118 MHz) is greater than 2:1, and the value for 6.24 MHz (scale value: 24.94 MHz) is approaching 2:1. These

values would not be troublesome for a wide-range antenna tuner between the shack end of the feedline and the transceiver. However, they may be high enough to defeat the low-loss use of a wide-range impedance transformation device, such as a transmission-line transformer balun.

Higher values of terminating resistance yield smaller resistance and reactance excursions. The result is a set of smaller SWR swings, all within an acceptable range. **Fig. 7** shows the same frequency sweep using an 850-Ohm terminating resistor, referenced at the feedpoint to 850 Ohms.

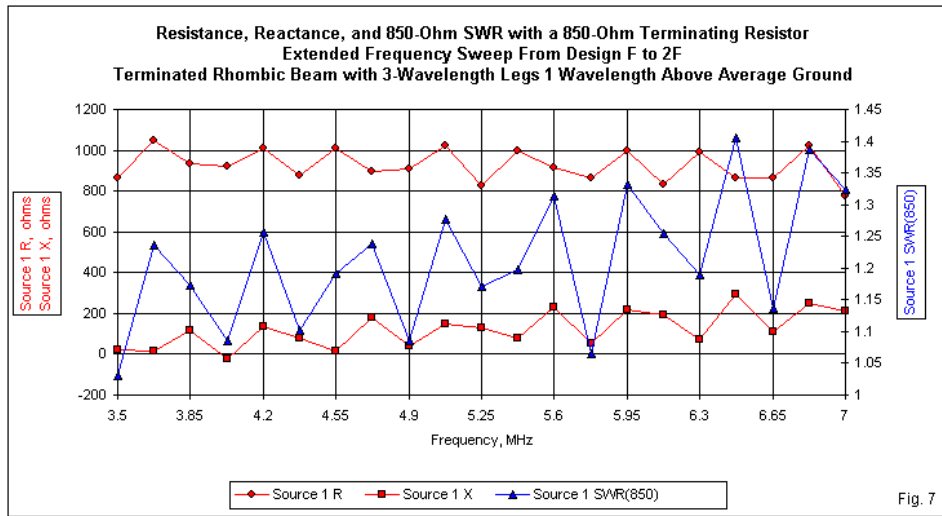
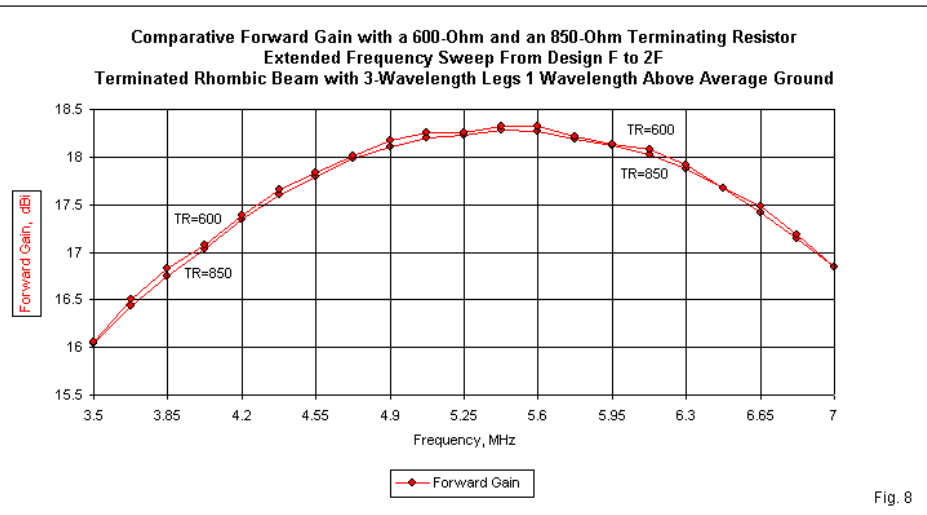


Fig. 7

Comparing the resistance and reactance lines between **Fig. 6** and **Fig. 7** reveals the smaller swings in these impedance components. The SWR (blue) line swings may appear similar in the 2 graphs. However, note the smaller limit to the Y-axis in **Fig. 7**: its highest value is 1.45:1. Although creating a wide-range impedance transformation device may be more difficult with the higher reference impedance (850 Ohms), the technique will be applicable with low losses across the 2:1 frequency range of the rhombic.

Within the usual range of terminating resistor values, the lower the terminating resistance value, the higher the array gain--but only slightly so. **Fig. 8** overlays the gain values of the rhombic beam for both the 600- and the 850-Ohm resistors. Throughout the 2:1 frequency range, the 600-Ohm version provides the higher gain, but by no more than 0.01 to 0.02 dB.



In the range of terminating resistance between 600 and 900 Ohms, certain performance parameters remain extremely stable. The elevation angle of maximum radiation and the beamwidth are two values that remain the same throughout the range of terminating resistors, at least for the sample rhombics using leg lengths that change in 1-wavelength increments between models. The impedance is also relatively stable at the test frequency for each model through the 600- to 900-Ohm resistor range. The maximum spread of resistance goes from a low of about 730 at 600 Ohms to a high of 870 at 900 Ohms, although the range is a bit smaller for any one leg-length model. The reactance swing is equally small, ranging from a -j40-Ohm value at 600 Ohms to a +j40-Ohm value at 900 Ohms.

My reason for selecting the 850-Ohm terminating resistor has as much to do with drama than with good electronics. Normal construction variables and the selection of leg lengths that are not perfect integral increments of a wavelength would likely alter the results. However, as the following performance table reveals, 850 Ohms as the termination value yields very high values of 180-degree front-to-back ratio, resulting in radiation patterns in which the main forward lobe and the sidelobes take center stage. The shortest of the rhombics has the lowest front-to-back value because the 40+-dB ratio occurs with an 800-Ohm terminating resistance. In practice, values from 750 to 900 Ohms will likely yield indistinguishable results, although the higher end of the scale will usually result in the smoothest SWR curve. However, we tend to obtain the flattest wide-range SWR curves when the terminating resistance and the feedpoint impedance are as close together as possible.

The tabular data shows the value of angle A (alpha), the elevation angle of maximum radiation, the maximum forward gain, the 180-degree front-to-back ratio, the half-power beamwidth, the modeled feedpoint impedance, and the 850-Ohm SWR. For reference, the far-right columns provide the maximum gain values for the corresponding unterminated open rhombics, along with the gain differential between the terminated and unterminated versions of the antenna.

*Note:* The values of angle A are not optimized for maximum rhombic gain, but derive from earlier work with single long-wire antennas.

Leg Length WL	Performance of Terminated Rhombic Beams (R = 850 Ohms) 1-Wavelength Above Average Ground						Unterminated Rhombics		
	Angle A degrees	Elevation Angle deg	Max. Gain dBi	Front-Back Ratio dB	Beamwidth degrees	Feedpoint Z R +/- jX Ohms	850-Ohm SWR	Max. Gain dBi	Difference dB
2	34	14	14.60	30.40	20.6	862 + j23	1.03	16.41	1.81
3	26	14	16.04	41.16	17.2	864 + j23	1.03	17.81	1.77
4	23	13	17.27	43.97	14.4	869 + j27	1.04	18.89	1.62
5	20	13	17.97	44.71	12.8	867 + j23	1.03	19.57	1.60
6	18	13	18.51	44.78	11.6	863 + j24	1.03	20.12	1.61
7	16	12	18.85	42.78	11.2	861 + j24	1.03	20.53	1.68
8	14	12	18.98	43.63	11.0	856 + j24	1.03	20.82	1.84
9	13	12	19.27	43.90	10.4	854 + j24	1.03	21.17	1.90
10	13	11	19.73	44.52	9.4	855 + j23	1.03	21.52	1.79
11	12	11	19.86	43.84	9.0	852 + j24	1.03	21.73	1.87

As we move from a single long-wire antenna to a V-beam and finally to a rhombic, the gain differential between the unterminated and the terminated versions has decreased. The differential was 3.5 to 4.5 dB for the single long-wire terminated antenna. The V-beam showed a range of 2.7 to 3.7 dB differential. In both cases, the differential decreased as the length of the legs increased. For the rhombic, the differentials range from 1.6 to 1.9 dB, a tight range for which there is no apparent correlation between gain differential and leg length.

The gallery of sample elevation and azimuth patterns of the terminated rhombic beam appear in **Fig. 9**. The gallery includes patterns for leg lengths of 2, 4, 6, 8, and 10 wavelengths. Because the arrays are twice as long overall as corresponding V-beams and single terminated long-wire antennas, the transitions in pattern shape are smaller from one increment to the next in the series. Hence, we may use fewer plots to show the evolution of rhombic radiation patterns.

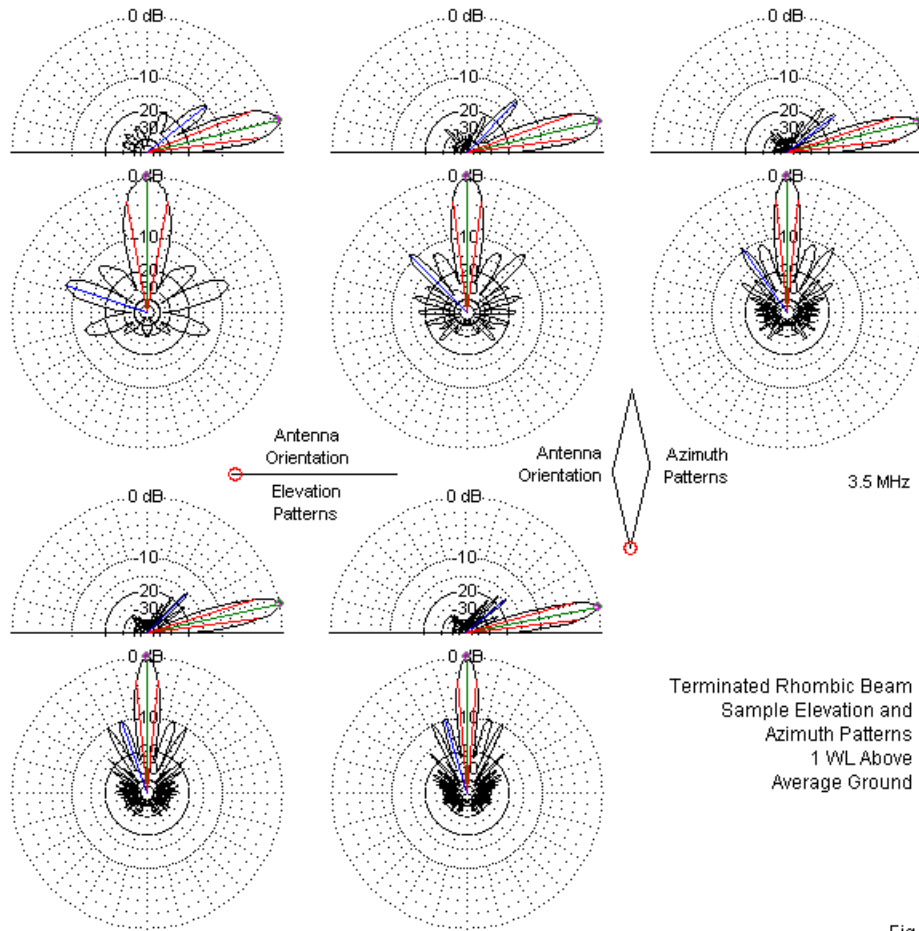


Fig. 9

Careful inspection of the sidelobe structures will show that the strength of the forward-most sidelobes--and also the strongest

sidelobes--is somewhere between the corresponding sidelobes for the open and the closed versions of the unterminated rhombics. See **Fig. 2** to estimate the limits and where between them the terminated rhombic sidelobes fall. The phenomenon suggests that there is continuity in sidelobe strength across a range of termination values ranging from an open circuit through a mid-range resistance and ending at a short circuit.

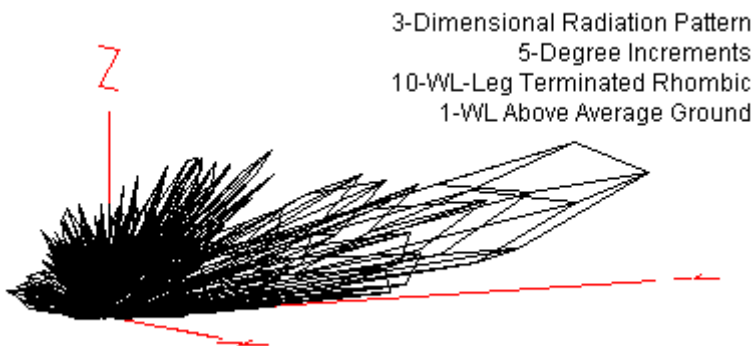


Fig. 10

**Fig. 10** provides a 3-dimensional pattern for the rhombic with 10-wavelength legs. It reveals that the terminated rhombic exerts the most control over the morass of small lobes that populate the overall radiation pattern. You may directly compare this pattern with the one in **Fig. 4** for the unterminated rhombic to correlate various lobes and their relative strengths. As well, you may compare it with corresponding patterns for other terminated long-wire arrays in earlier parts of this series.

One quick comparison that we may tabulate is the maximum gain of each of the 3 types of terminated beams that we have encountered along the long-wire pathway. Remember that the maximum gain value for the single terminated long-wire is an off-axis value, that is, not in alignment with the wire itself.

**Maximum Gain of Various Types of Terminated Long-Wire Antennas**

Leg WL	Length	Maximum Gain dBi		
		Single Long-Wire	V Beam	Rhombic
2		----	9.88	14.60
3		7.11	11.41	16.04
4		7.99	12.35	17.27
5		8.65	13.03	17.97
6		9.15	13.50	18.51
7		9.57	13.86	18.85
8		9.92	14.07	18.98
9		10.20	14.29	19.27
10		10.47	14.59	19.73
11		10.70	14.74	19.86

The gain of the single terminated long-wire would not justify its narrow-band use, since we can obtain similar gain levels from antenna ranging from dipoles to extended double Zepps at a great savings in both wire and supporting structures. The single terminated long-wire acquires its usefulness from the relative constant feedpoint impedance, allowing great frequency agility. The terminated V adds about 4-dB of gain, while maintaining a broad SWR operating bandwidth. However, any angle used as the basis for the array has frequency limits for a good pattern: outside those

limits, the forward pattern breaks into multiple lobes. As we change frequency, the antenna legs change length as measured in terms of a wavelength at the new operating frequency. Hence, the wire angles are no longer optimal to add in a forward direction.

The rhombic shares the frequency limits of the V-beam. To sense its truer gain advantage, you may wish to compare the rhombic with a given leg length to a V beam with twice the leg length. For example, a rhombic with 5-wavelength legs and nearly 18 dBi gain is roughly equivalent in overall length to a V-beam with 10-wavelength legs and a 14.6-dBi gain level. Like the V beam, the rhombic is capable of good performance over a 2:1 frequency range with good gain and a relatively constant feedpoint impedance. In fact, before we end our trek through long-wire antennas, we should take one more look at the ARRL rhombic from Chapter 13 of the 20th Edition of *The Antenna Book*; but not today.

## Conclusion

In this Chapter, we have moved beyond the V array and beam to examine what some call the highest development in long-wire antennas: the rhombic. We learned how to close the V with another V, using the same technique of aligning lobes from each wire to form a rhombus. Modeling allowed us to develop effective rhombic antennas without reference to classical equations by setting the intended height and the leg-lengths that we might use. We explored both open and closed forms of unterminated rhombic arrays, and then we turned to the most common rhombic form, the terminated beam.

By splitting both the source and load, we found a very economical way to model the terminated rhombic beam. We also uncovered some relationships between the value of the terminating resistor and the feedpoint impedance that bear on the smoothness of SWR curves that cover a 2:1 frequency range. Indeed, there is more to be said on this subject. . .

Indeed, I had planned to close the topic at this point. However, we have a significant amount of unfinished business with the rhombic.

1. *The Multi-Band Rhombic:* We have not yet evaluated the *ARRL Antenna Book* rhombic for 14-28 MHz. This design has its roots in nomographic design data from Harper's well-known book. (See the list of references at the end of each Part.) The antenna gives us a chance to compare modeling design techniques with classical methods.
2. *The Multi-Wire Rhombic:* One common method of trying to improve rhombic beam performance is to use more than 1 wire for each leg. The usual arrangement consists of 3 wires that come together at the rhombic points and spread in the middle by relatively arbitrary distances. The arrangement presents both theoretical and modeling challenges, and careless modeling of a 3-wire rhombic can lead to erroneous results.
3. *The Multi-Element Rhombic:* In the 1950s, Laport developed the multi-element rhombic beam to improve both gain and sidelobe suppression. Since the antenna has seen use on the UHF amateur

bands, the design bears at least an initial exploration to look at both design and modeling issues.

With so many outstanding rhombic ideas, I would be remiss if I did not extend the series one more episode. Even then, we shall not have examined every variation on the long-wire, V, and rhombic arrays. However, perhaps we shall have encountered enough designs along our pathway so that you may continue the trek on your own.

## Chapter 57: Multi-Band, Multi-Wire & Multi-Element Rhombics

**B**ecause the rhombic antenna, especially when terminated, offers very high gain, it has received more design attention than any of the other long-wire antennas. The straightforward basic design data sampled in Part 4 does not exhaust the significant variations on the basic configuration. One potential particularly suited to amateur service in the upper HF range is the possibility of operating a rhombic over a 2:1 frequency range, thus allowing coverage of 20 through 10 meters. We shall examine one tried and true design and try to find out the basic design premise that allows it to be successful.

When an antenna is good at what it does, we can count on efforts to make the good even better. For narrow-beamwidth point-to-point communications, the rhombic is very good. One very old technique to improve performance somewhat is the use of multiple wires in each side of the rhombic. They come together at the feedpoint and at the terminating resistor end, but spread vertically where the facing Vs are widest. Some claims about the technique will prove correct, such as the addition of a small increment of gain. However, other claims may turn out to have other foundations than the use of multiple wires.

Finally, we shall address an interesting technique for further suppressing the remnant sidelobes in the rhombic radiation pattern. Laport developed a scheme for using closely spaced rhomboid structures in parallel. The centerlines for each of the independent rhomboids fed in parallel are offset from each other. The technique

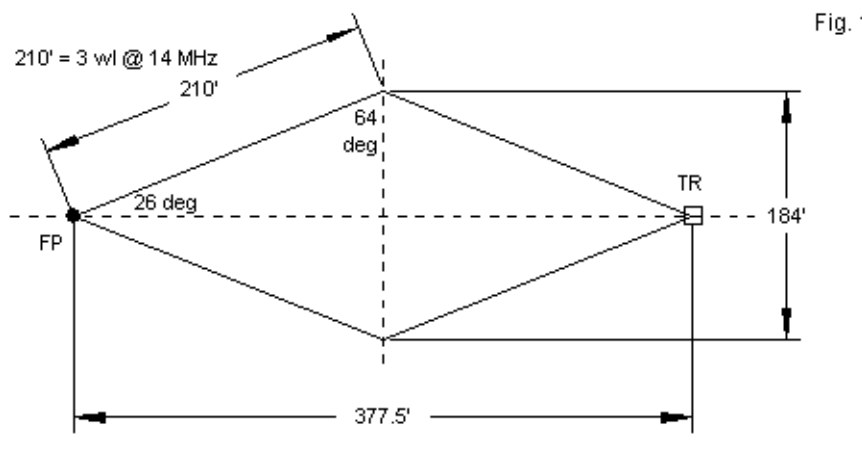
will offer a small gain advantage over the single-wire rhombic, but will reduce sidelobes by a very significant amount.

Although these developments are worth our notice here, they will not exhaust the variations on the rhombic. There is, for example, the so-called half-rhombic, consisting of one side of a rhombic played against ground. Unfortunately, lossy soil does not permit the antenna to play like a true rhombic, due to ground reflections and losses. Despite its name, the antenna operates more like a terminated, end-fed, inverted V, and highest performance occurs with only a slight elevation of the center point above ground. The antenna appears in Bruce's 1931 article and he calls it simply an inverted-V. The name "half-rhombic" came later from other builders. Other variations on the rhombic have emerged in answer to specific commercial and governmental communication needs. The result has been highly complex arrangements of wire structures well beyond the scope of these introductory notes. Nevertheless, the variations that we have selected should provide a sufficient foundation to let you examine the classical literature on advanced rhombic designs with understanding.

## Multi-Band Rhombics

Although we have briefly mentioned multi-band use of long-wire antennas, we have not paused long to investigate their performance in broadband service. We shall rectify this situation, if only briefly, by looking the ARRL rhombic intended for upper HF service from 14 through 28 MHz. The antenna first appeared in *The ARRL Antenna Book* somewhere between 1965 and 1974, and has

been a prime example in the book's treatment of traveling-wave antennas. **Fig. 1** shows the general outlines of the antenna.

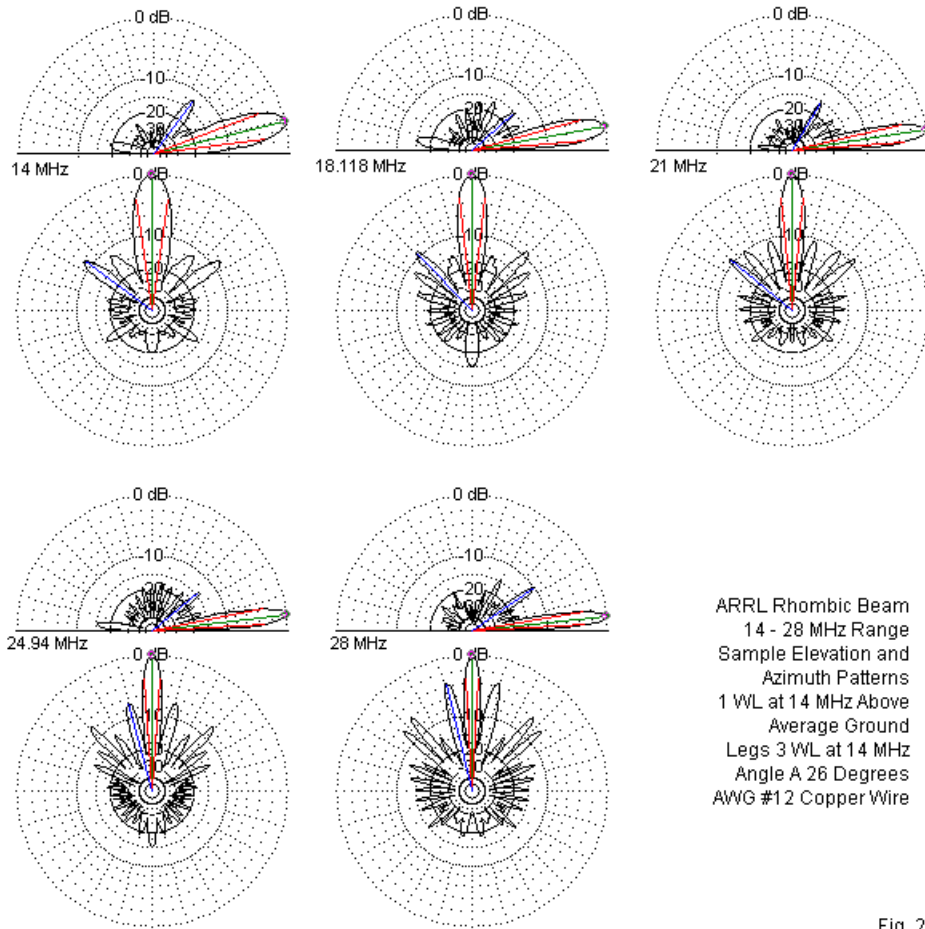


One notable feature of the antenna is that its design emerged long before modeling software became available. Hence, its outline rests directly on the original rhombic design equations, as filtered into design nomographs. The design begins with 3-wavelength legs at 14 MHz along with a height of about 70' or 1 wavelength at the lowest frequency of use. It uses a prescribed tilt angle of 64 degrees and hence an angle A value of 26 degrees. These values coincide perfectly with the values developed via computer modeling. For this model, I followed the typical amateur conventions and used a 600-Ohm termination and an SWR reference impedance of 600 Ohms. The following table lists the

modeled performance of the antenna over the 5 amateur bands between 14 and 28 MHz.

Frequency MHz	14.0	18.118	21.0	24.94	28.0
<b>Parameter</b>					
Gain dBi	16.04	17.89	18.38	18.31	17.33
El. Angle deg	14	10	9	7	6
Front-Back dB	19.93	15.28	24.68	15.27	32.12
Beamwidth deg	17.0	13.0	10.8	8.6	7.0
600-Ohm SWR	1.25	1.79	1.22	1.65	1.22

The gain values parallel almost exactly the curves in **Fig. 8** in Part 4, which is also for a rhombic with 3-wavelength legs and an angle A of 26 degrees. The three differences between the earlier model and the present one are the design frequency (3.5 vs. 14 MHz), the wire (perfect 0.16" vs. copper AWG #12 or 0.0808"), and the terminating resistor value (850 vs. 600 Ohms). **Fig. 2** shows a gallery of elevation and azimuth patterns at each of the test frequencies. Note that this gallery differs from the galleries in the earlier parts of this series because angle A is optimized in combination with the leg length only at the lowest operating frequency.



ARRL Rhombic Beam  
14 - 28 MHz Range  
Sample Elevation and  
Azimuth Patterns  
1 WL at 14 MHz Above  
Average Ground  
Legs 3 WL at 14 MHz  
Angle A 26 Degrees  
AWG #12 Copper Wire

Fig. 2

The sidelobe structure (including the rear-most lobe) of the patterns for frequencies above 14 MHz does not parallel any of the patterns

in the earlier galleries (**Fig. 9** in Part 4, for example) because angle A (and the tilt angle B) remain constant while the leg length changes as a function of the ever higher operating frequency. As a result, we find lobes that do not appear in the main gallery of optimized designs for each leg length. They result from incomplete cancellations that occur with a non-optimal combination of leg length and angle A. As well, the use of the relatively low terminating resistor value (600 Ohms) results in a set of SWR values that approximates those shown for the frequency sweep in **Fig. 6** of Part 4.

The ARRL rhombic design nevertheless shows itself to be a very competent performer over its 2:1 frequency range. It captures perhaps the key element in multi-band rhombics: optimize the design for the lowest anticipated frequency, accounting for both antenna height and anticipated leg length. As the frequency increases, the gain will rise, as indicated by 2 of the leg-length equations early in Part 4. According to those equations, peak gain would occur somewhere close to 15 meters. With a satisfactory terminating resistor, the antenna will perform quite well over a 2:1 frequency range. With a higher value than 600 Ohms, the SWR curve would smooth out more completely, if we use a reference impedance to match the termination (and hence a feedline with a higher characteristic impedance than 600 Ohms).

The general procedure has exceptions. For example, the idea of optimizing the rhombic at the lowest frequency in the 2:1 requires careful selection of the value of angle A. If we increase the angle in order to raise the gain at the lowest frequency, we shall find that we

have limited the operating frequency range upward. The gallery of azimuth patterns shows that, at 28 MHz, the innermost sidelobes are almost as strong as the main lobe. If we select a maximum gain value of angle A for 14 MHz, the 10-meter pattern will show 3 lobes, and the lobe that is on-axis with the array will no longer be the strongest. Such a condition defeats the main goal of creating a rhombic in the first place: the desire to achieve point-to-point communications on a heading in line with the two acute angles of the rhombus. If we reduce the value of angle A at 14 MHz, then the main lobe broadens with a loss of gain. For the selected height, the ARRL rhombic antenna selects a value of angle A at 14 MHz that yields roughly equal gain on both 20 and 10 meters, which is generally a good selection for amateur service. It also illustrates why much of the classical rhombic literature recommends no more than a 2:1 frequency range for the antenna, even though the range of acceptable matching is much wider.

## Multi-Wire Rhombics

Perhaps the most common variation on the single-wire rhombic beam involves the use of multiple wires running from the feedpoint to the terminating resistor on each side of the centerline. The added wires join the level wire at both the feedpoint and the terminating resistor. However, they spread above and below the level wire at the widest points in the array. In general, the wires are the same length as the level wire, theoretically resulting in the wires being further offset from any support post toward the centerline. However, the amount of differential is a very small fraction of the total wire length along each leg, and allowing the spread wires to be slightly

longer in order to align the supports will create no performance problems.

In order to model the multi-wire rhombic, using 3 wires as a sample version, we must alter the means by which we create the antenna geometry. The left side of **Fig. 3** shows the method used in Part 4. It consists of only 4 wires per rhombic, with a split source and a split load. At the source end, we simply place a source on each of the segments adjacent to the wire junction. Since they are in series, the feedpoint impedance is the sum of the source impedance values reported for each source. The split load simply creates a balance at the far end of the array by placing a load resistor on each of the wire segments adjacent to the junction. The overall terminating resistor value is simply the sum of the 2 load resistance values. To use a real example from the last episode, the 4-wavelength-leg version of the terminated rhombic used legs that are 4.00 wavelengths long. The distance from centerline to a side peak is 1.563 wavelengths, while the distance from the midline to either end junction is 3.682 wavelengths. The resulting angle A is 23.0 degrees, and the overall rhombic length is 7.364 wavelengths.

Revising the Single-Wire Rhombic Model  
In Preparation for 3-Wire Models

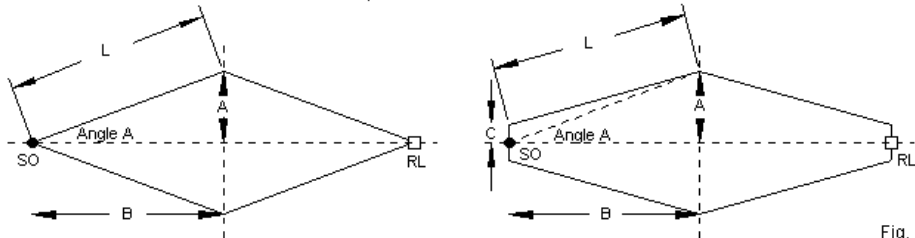


Fig. 3

The "pointy" ends of the model do not permit ready feeding for a multi-wire version of the antenna. Therefore, we must revise the modeling system to allow the wires to terminate together for a common feedpoint and for a common load resistor. The right side of **Fig. 3** shows the general technique. We create a flat or blunt end at each rhombic point. To ensure that the source segment has adjacent segments of equal length on each side, we make the blunt end-wires 3 segments long. So that the wires will have segments as close as possible in length to the segments in the long side wires, the blunt end wires are 0.14-wavelength, based on the use of 20 segments per wavelength in the side wires. Now let's set the total length of the rhombic to 7.36 wavelengths, with a 3.68-wavelength distance from either end to the midline. The distance from the centerline to the peaks will be 1.56 wavelength. The angle ( $A$ ) from the centerline to a peak will be 22.97 degrees. However, the overall wire length will not be exactly 4.0 wavelengths. Instead, the sloping portion of the side wire will be 3.97 wavelengths, added to half of the blunt end-wire (0.07 wavelength) for a total length of

4.04 wavelength. All figures are for rhombics 1 wavelength above average ground with lossless 0.16" wire at 3.5 MHz.

I have recorded seemingly insignificant variations in models because these variations do create differences in the reported performance of the antennas. The following table explores the performance of the 4-wire "pointy" version of the antenna using various terminating resistor (RL) values.

Performance of a Pointy Single Wire Rhombic with 4-Wavelength Legs and Various Terminating Resistors

Terminating Resistor (Ohms)	Maximum Gain dBi	Front-Back Ratio	Feedpoint Z $R+/-jX$ Ohms
600	17.30	18.07	737 - j 40
700	17.28	23.13	793 - j 13
800	17.27	33.22	844 + j 14
850 *	17.27	43.97	869 + j 27
900	17.28	32.75	892 + j 41
1000	17.29	24.29	936 + j 67
1100	17.30	20.40	977 + j 94
1200	17.32	17.94	1015 + j120

We should note 2 special items in this table. First, the starred item represents the version of the antenna selected for inclusion in the larger table in Part 4. There are 2 reasons for selecting this terminating resistor value. It does result in the highest front-to-back ratio, although this reason is secondary to another. Without becoming too finicky, the load resistor and the resistive component of the feedpoint impedance are most closely matched. With smaller values of terminating resistance, the resistive component of the feedpoint impedance is always higher than the load resistance. For all terminating resistors larger than the selected value, the feedpoint resistance is always lower than the terminating

resistance. Since a terminated long-wire antenna operates in a similar manner to a transmission line, matching the load resistance to the feedpoint resistance results in the widest SWR bandwidth when referenced to the load resistance value. The required value does not change with changes in the leg length so long as the angle A is selected to align the lobes for maximum gain. However, it will change with even small departures from the ideal geometry. It will also change with the height of the antenna above ground and with the quality of the ground itself, since both of these factors will change the effective impedance of the antenna when viewed as a length of transmission line.

Second, note the remnant inductive reactance in the feedpoint impedance. The reactance is inductive. One traditional reason for using multiple wires in the rhombic legs is that it introduces a compensating capacitive reactance due to interactions among the wires. A capacitive reactance represents--with respect to feedpoint impedance--a slight electrical shortening of the antenna circumference. Wire interaction is unnecessary to explain the electrical shortening of the overall rhombic loop. All closed loops of a preset total circumference become electrically shorter if we increase the wire diameter--exactly the opposite effect of fattening elements in open-ended elements. Since the 3-wire rhombics will have effectively a fatter element, even though variable in equivalent diameter along the leg lengths, the loop will become electrically shorter and thus show a more capacitive reactance at the feedpoint.

The blunt-end version of the 4-wavelength-leg rhombic makes only one change among the factors that tend to affect the optimal value of load resistance: the geometry. The shape changes are very small overall, but they do have consequences, as shown in the following table that parallels the one for the pointy version of the same rhombic.

**Performance of a Blunt Single Wire Rhombic with 4-Wavelength Legs and Various Terminating Resistors**

Terminating Resistor (Ohms)	Maximum Gain dBi	Front-Back Ratio	Feedpoint Z $R+/-jX$ Ohms
600	17.40	15.26	806 + j121
700	17.37	18.48	857 + j 81
800	17.35	22.87	903 + j 41
900	17.35	30.23	945 + j 2
975 *	17.35	38.04	973 - j 27
1000	17.35	35.88	982 - j 37
1100	17.36	26.68	1016 - j 74
1200	17.38	22.27	1046 - j110

The closest match between the terminating resistor and the feedpoint resistance occurs with a value of about 975 Ohms. The difference between the 2 models of 125 Ohms may seem significant, but it is likely that construction variables would wash out the difference in terms of trying to determine which model better captures a physical rhombic with 4-wavelength legs at a height of 1 wavelength above average ground. As well, small changes in the segmentation per wavelength will also change the reported values somewhat. Note also that the progression of inductive to capacitive reactance is the reverse of the pointy geometry. Nevertheless, the pattern of the feedpoint resistance remains: below the optimal load resistance, the feedpoint resistance is higher than the load resistor

and above the optimal load; the feedpoint resistance is less than the load resistance.

The blunt-end version of the modeled 4-wavelength-leg rhombic will become the standard against which we measure 3-wire rhombics using the same leg length. However, modeling the 3-wire rhombic presents another modeling challenge of its own. Theoretically, the wires must join on each side of both the feedpoint wire and the load resistance wire. The relevant modeling sketch of this situation appears on the left in **Fig. 4**. There is a difficulty built into this scheme. Because the wires are not widely spaced relative to their length, the segments at the junction interpenetrate for a considerable distance along the segment length. Even though the level of inter-penetration may not reach a level that raises flags within NEC, it may still be sufficient to alter the performance reports of the array, since the inter-penetration does affect NEC's current calculations.

Two Ways to Model a Three-Wire Rhombic Beam

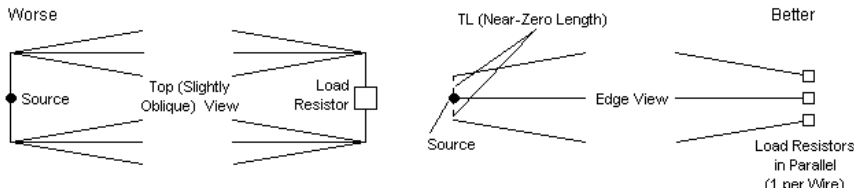


Fig. 4

To test the model, let's explore what happens as we pass the model through a number of loading resistor values. The side wire

expansion is very modest, reaching only 0.0125 wavelength at the midline. That distance amounts at 3.5 MHz to about 1.06 m or 3.49', with an antenna that is over 630 m (2068') long. Like all of the models, the 0.16"-diameter wire is lossless and the wires are 1 wavelength above average ground.

**Performance of an Angled 3-Wire Rhombic with 4-Wavelength Legs and Various Terminating Resistors**

Terminating Resistor (Ohms)	Maximum Gain dBi	Front-Back Ratio	Feedpoint Z $R+/-jX$ Ohms
600	18.92	16.76	795 + j335
700	18.92	18.57	834 + j319
800	18.92	19.64	870 + j305
900 *	18.93	19.68	902 + j291
1000	18.94	18.96	933 + j278
1100	18.95	17.93	961 + j266
1200	18.96	16.87	987 + j255

Although we are not yet positioned to evaluate the gain improvements, the impedance column should give us pause. The very large rise in inductive reactance relative to the blunt single-wire model exceeds what we might otherwise reasonably expect from adding 2 wires with fairly narrow spacing relative to the frequency. In addition, the indicated "ideal" termination resistor value (900 Ohms), does not coincide with long-standing empirical experience, which suggests a value closer to 600 Ohms.

We may reformulate the model using some techniques that have proven useful with quad loops and similar structures. The right side of **Fig. 4** outlines the techniques at each end of the antenna. At the feedpoint end, we prevent the wires from meeting, but bring them to a 0.001-wavelength spacing (about 86 mm or 3.4"). Next, we create

a bridge wire for each loop. The source excitation goes to the center (level) wire on the middle segment of the bridge wire. From the corresponding segments on the upper and lower section, run 600-Ohm transmission lines to the source segment. The impedance is not critical, because the lines will be only 0.000001-wavelength long, a number that the modeler specifies in the transmission line entry. Hence, the three wires have a common source in parallel, while preventing the inter-penetration of any wires.

The termination end of the beam uses the same modeling technique of bringing the wires close (0.001 wavelength) but not allowing them to touch. We cannot create a single parallel connection using the transmission line technique, because any load resistor would be in series with the line and hence outside it. Instead, we provide each bridge wire with a load resistance that is 3 times the desired terminating resistor value. If we run the same tests on the reformulated model, we obtain the results in the following table. Note that the actual terminating resistance values are 3 times the value in the table, but occur on 3 bridge wires.

Performance of a Separated 3-Wire Rhombic with 4-Wavelength Legs and Various Terminating Resistors

Narrow (0.0125-Wavelength) Maximum Wire Separation

Terminating Resistor (Ohms)	Maximum Gain dBi	Front-Back Ratio	Feedpoint Z $R+/-jX$ Ohms
400	18.60	17.14	586 + j 22
500	18.60	22.29	619 - j 4
600	18.60	31.34	648 - j 32
650 *	18.61	36.44	662 - j 37
700	18.61	31.37	675 - j 42
800	18.63	24.01	695 - j 73
900	18.64	20.33	714 - j 95
1000	18.66	18.02	733 - j105

The gain improvements over the single-wire model are more modest: about 1.3 dB. The rounded ideal load value comes very close to matching the feedpoint resistance and also corresponds to the highest 180-degree front-to-back ratio value. As expected, the capacitive reactance is slightly higher than for the blunt single-wire model, but only slightly so, since the average wire-diameter increase for the closed loop is not great as a function of a wavelength. Finally, the selected terminating load and feedpoint impedance tend to match reasonably with reported experience with these types of rhombic beams.

Most amateur rhombics cover the upper HF spectrum, and the spacing used at these frequencies is 3' to 4'. Therefore it seems prudent to test our 3.5 MHz model with a wider spacing than the 0.0125-wavelength used in the initial model. Using the same loop separation techniques, I increased the spacing at the midline to 0.025-wavelength (about 2.1 m or 7'). All other modeling parameters remain constant. The results appear in the following table.

**Performance of a Separated 3-Wire Rhombic with 4-Wavelength Legs and Various Terminating Resistors**

**Medium (0.025-Wavelength) Maximum Wire Separation**

Terminating Resistor (Ohms)	Maximum Gain dBi	Front-Back Ratio	Feedpoint Z $R+/-jX$ Ohms
400	18.74	17.46	597 + j 26
500	18.74	22.45	629 + j 10
600	18.74	30.19	656 + j 7
650 *	18.75	33.08	669 - j 11
700	18.75	30.20	682 - j 15
800	18.76	24.04	701 - j 55
900	18.78	20.56	721 - j 63
1000	18.79	18.30	739 - j 71

As one might expect, by enlarging the average wire diameter by a significant amount, the gain reports increase by a very small but numerically noticeable amount. More telling is the array of front-to-back values. The peak value does not reach the level attained by the narrower 3-wire array, and that value, in turn, did not reach the peak value of the single wire blunt-end rhombic beam. However, the wider 3-wire array shows a smaller fall-off in front-to-back value as we vary the terminating load across the same range as used with the narrower 3-wire version. Compare values for this antenna with 600-Ohm and with 1000-Ohm loads with the corresponding values for the narrow 3-wire rhombic.

The near-ideal load resistance remains unchanged at 650 Ohms or thereabouts. However, the capacitive reactance at that load value is not as great as with the narrow 3-wire rhombic. The important data on the reactance is not its value at the ideal load resistance so much as it is the total range of reactance across the total set of load resistors. The narrow 3-wire rhombic shows a range of 162 Ohms,

while the medium spacing (twice the narrow spacing) reduces the range to 134 Ohms--for the same set of load values.

Let's increase the maximum wire spacing at array midline one more time. We shall again double the spacing to 0.05-wavelength (about 4.3 m or 14.1'). All other parameters remain the same. Each outer leg is now about 0.0003-wavelength longer than the level center wire--about 1". With all other model parameters unchanged, we obtain the following table of modeled values.

**Performance of a Separated 3-Wire Rhombic with 4-Wavelength Legs and Various Terminating Resistors**

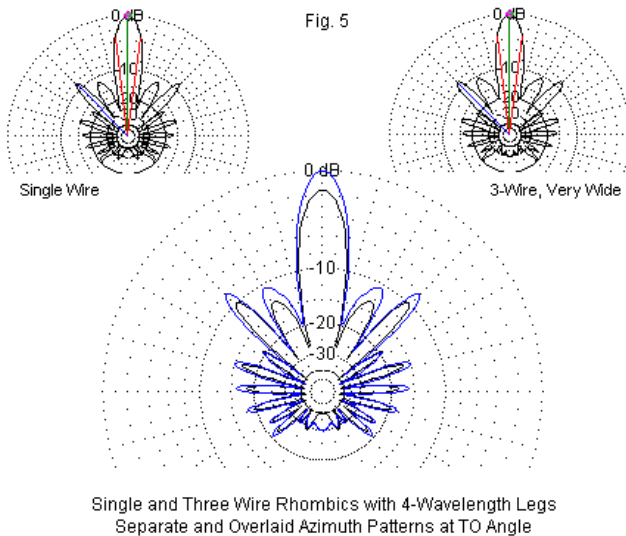
**Wide (0.05-Wavelength) Maximum Wire Separation**

Terminating Resistor (Ohms)	Maximum Gain dBi	Front-Back Ratio	Feedpoint Z $R+/-jX$ Ohms
400	18.88	17.79	607 + j 59
500	18.88	22.46	638 + j 37
600	18.89	28.31	664 + j 23
650 *	18.89	29.64	676 - j 10
700	18.90	28.16	686 - j 14
800	18.91	23.71	707 - j 9
900	18.92	20.62	724 - j 38
1000	18.93	18.50	738 - j 56

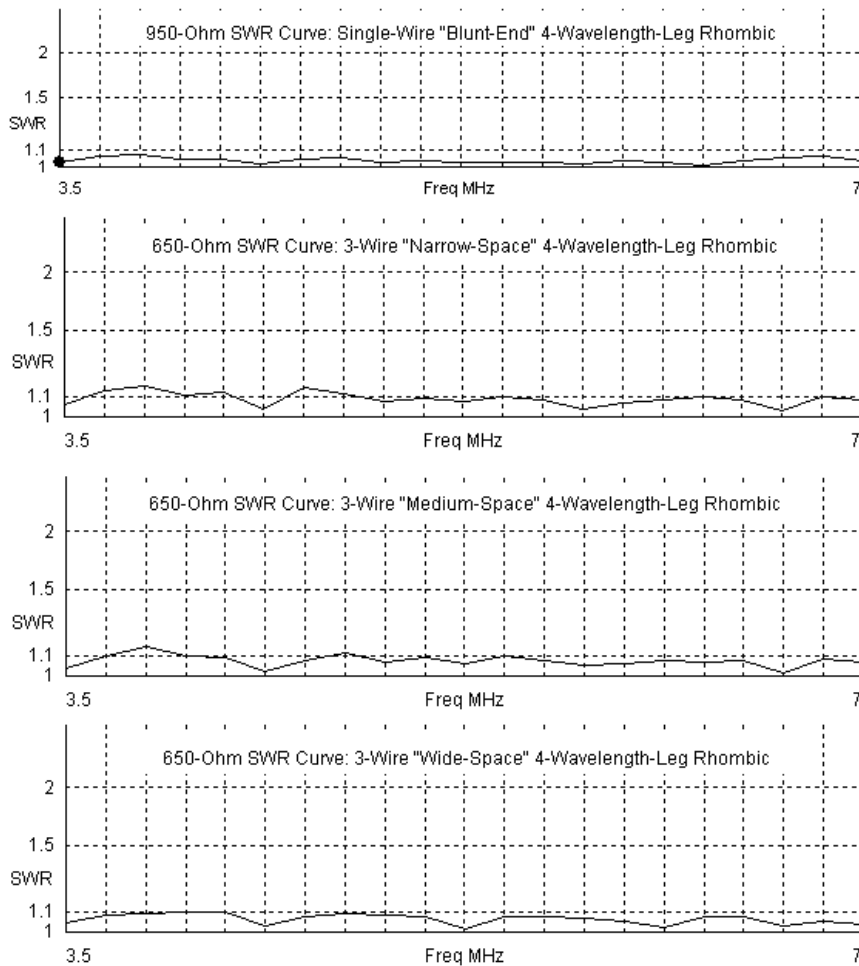
Once more, we find the small improvement in gain, which is now about 1.5-dB higher than the blunt single-wire array. The peak front-to-back ratio continues to diminish, but the values with a 400-Ohm and with a 1000-Ohm load are higher. The curve--as we might expect for increasing wire diameter--has less of a sharp peak and covers a broader range with higher values. Although I might have increased the ideal terminating resistor to 700 Ohms, continuing to use the 650-Ohm value allows us to see the other curve changes more easily. The reactance range has shrunk to 96 Ohms total. The

anomalous value for the 800-Ohm terminating resistor is accurate to what NEC reports. It may be a function of secondary effects that the other tables do not show given the 100-Ohm increment in terminating resistor values.

The use of 3-wires, whatever the spacing, does not change the essential elements of the rhombic pattern. **Fig. 5** compares the patterns for the blunt single-wire model and for the widest 3-wire model in both separate patterns and with an overlay. The overlaid patterns show the comparative raw gain of each lobe. The separate pattern establishes that there is no essential change in the relative strength of the lobes. The only exception, of course, is the 180-degree lobe.



Amateur lore on rhombic antennas suggests that the 3-wire design may be capable of a smoother SWR curve across a broad passband than a single wire model. That lore tends to neglect the need to match the terminating resistor to the feedpoint impedance--and that impedance to the characteristic impedance of the feedline. To test this way of looking at the impedance question, I ran each of the 4 main blunt models through an SWR sweep from the design frequency to twice that frequency (3.5 to 7.0 MHz). The single-wire blunt model used a 975-Ohm SWR reference impedance, while the 3 3-wire models used a 650-Ohm reference impedance. The results appear in **Fig. 6**.



SWR Curves, 2:1 Frequency Span, SWR Reference Z = Terminating Resistor  
2 Single-Wire and 3 Three-Wire 4-Wavelength-Leg Rhombic Beams

Fig. 6

In practical terms, we have no way to make a selection among the antenna models. All 4 curves remain below 1.2:1 relative to their reference impedances across the entire range. Any device capable of broadband impedance transformation at the desired ratio would operate under very low-loss conditions. The exercise, however, does show one interesting fact: none of the 3-wire models improves upon the blunt single-wire model SWR curve. The only advantage shared by the 3-wire models is that they may better use a commercial 600-Ohm parallel transmission line than the single-wire model. However, a 975-Ohm line requires more patience than skill to fabricate in one's own shop.

The 3-wire rhombic, then, has 3 advantages over a single-wire rhombic. First, the gain improvement is real, but might not be sufficient to be noticeable in practice. Second, from a practical perspective, the ideal conditions for a 3-wire rhombic--at least one that is 1 wavelength above average soil--yield a terminating resistor and feedpoint impedance that more nearly coincides with off-the-shelf components. (Note: this result applies only to the subject antenna and requires verification for any variation in height and soil condition.) Third, the "fat-wire" effect of using wider spacing gradually widens the operating curves of some operating parameters.

Besides mechanical complexity, the 3-wire rhombics have only one almost insignificant down side. The front-to-sidelobe ratio shows a very small but steady decline as we increase the effective wire diameter. Between the blunt single-wire model and the widest 3-wire model, the decline is only about 0.2 dB. However, it appears to

be a real phenomenon and runs counter to the design goals of many rhombic designers. The design goal of reducing rhombic sidelobes leads us to the third of our bits of unfinished business.

## Multi-Element Rhombics

Rhombic development persisted long after its primary period of HF service in the 1930s and 1940s. With the advent of commercial broadcast VHF television in the 1950s, followed by UHF television in the 1960s, engineers searched for wide-band antennas with high gain to satisfy consumer needs in fringe reception areas. In this period, Laport published his work on the adaptation of the rhombic for this and other services. The sidelobes for a single rhombic with an overall length of about 5 wavelengths were down less than 10 dB, a situation that made the antenna susceptible to multi-path ghosting and other forms of interference. Laport's solution to the problem was to develop a dual rhombic antenna with offset axes.

Laport's dual offset rhombic is a variant of the basic idea of using two rhombics of different sizes, each with its own terminating resistor. Only certain combinations of rhombics are eligible for such use. The main criterion is that the sidelobes of one size align closely with the side nulls of the other. The result is a significant decrease in the net sidelobe strength. The combination of a rhombic with 3.5-wavelength legs and one with 6-wavelength legs provides a prime candidate for dual rhombic service. We can shorten the overall length of the combination by combining one leg from each rhombic on each side of a pair of rhomboids. The dual offset rhombic offered higher gain and greater sidelobe

suppression. **Fig. 7** shows both the general outline and the critical dimensions.

The Laport Dual Displaced Rhombic Antenna

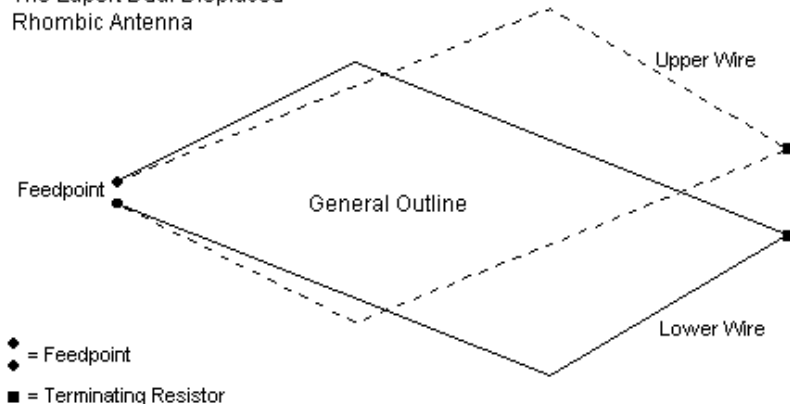
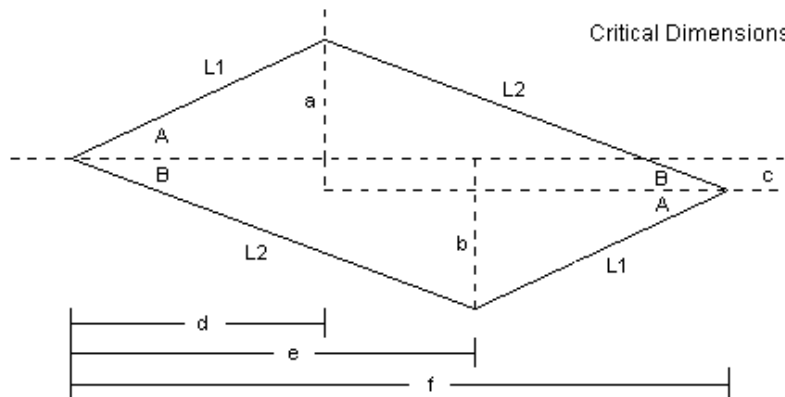


Fig. 7

Critical Dimensions



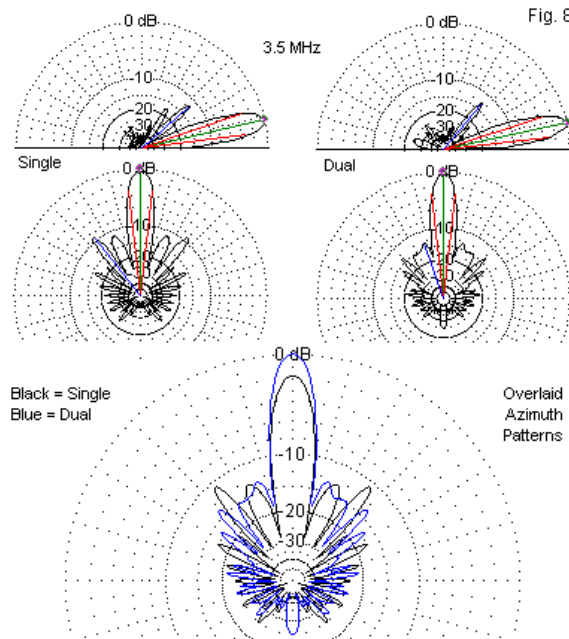
The lower half of the sketch shows the dimensions needed. If we set L1 at 3.5 wavelengths and L2 at 6.0 wavelengths, then angle A becomes 26.1 degrees and angle B is 18.85 degrees. Simple trig relations yield the physical dimensions, including the amount of offset of the far junction from the array centerline (c). To compare the dual rhombic with a single rhombic I scaled my early VHF model down to our test frequency (3.5 MHz) and set it 1 wavelength above average ground. Since the 0.16" wire diameter is much thinner at 3.5 MHz than AWG #12 is at 100 MHz, I set the spacing between wires at 0.08 wavelength and used 900-Ohm terminating resistors in each rhombic in the pair. Even so, the front-to-back ratio is only good, but not optimal. However, the combination of spacing and the terminating resistor values are adjustable in the design to improve these figures without affecting the forward gain or the sidelobe suppression.

The best single rhombic for comparison with the dual version is the model using 5-wavelength legs. It is only slightly longer overall (9.4 wavelengths vs. 8.95 wavelengths for the dual rhombic). The following table presents some of the basic performance data.

A Preliminary Comparison of Equal Length Single and Dual Rhombics						
Antenna	Leg Length WL	Elevation Angle deg	Max. Gain dBi	Front-Back Ratio dB	Beamwidth degrees	Feedpoint Z R +/- jX
Ohms						
Single	5	13	17.97	44.71	12.8	867 + j23
Dual	3.5/6.0	12	19.82	25.03	12.2	447 + j 9

The feedpoint impedance is the parallel combination of the impedances of the individual offset rhombics in the pair. At VHF and UHF, where the wire is proportionately thicker as a function of

a wavelength, dual rhombics would normally use lower values for the terminating resistors and have feedpoint impedances closer to 300 Ohms. The table shows that the dual rhombic has a 2-dB gain advantage over the single rhombic. However, the benefit of the dual design is less the added gain than the sidelobe suppression. **Fig. 8** provides elevation and azimuth patterns for the 2 antennas. It also overlays the two azimuth patterns for a more direct comparison of relative sidelobe strength.



Single and Dual-Offset Rhombics with Equal Overall Lengths  
Elevation and Azimuth Patterns: Height = 1 WL, Average Ground

The dual rhombic's strongest sidelobe is about 5-dB weaker than the strongest sidelobe of the single rhombic. We can add 2-dB to that figure when considering the sidelobe strength relative to the strength of the main forward lobe. The sidelobe strength has diminished to a level that equals the sidelobe strength of many (but not all) long-boom Yagi designs with approximately the same forward gain and front-to-back ratio values. For a further discussion of dual rhombics in VHF and UHF service, see the upcoming chapters.

## Conclusion

The study of long-wire antennas--both terminated and unterminated--is far from complete in these notes. There are numerous theoretical directions one can take to intensify one's understanding of the relationship of these antennas to fundamental mathematical concepts governing all antennas. Likewise, both historical practical applications and future possibilities leave much room for exploration, in terms of both available literature and physical experimentation. (I am, for example, unaware of any experiments using dual rhombics in the GHz range, with both rhomboids using copper strips bound to separate sides of a substrate.)

Nevertheless, this series of notes has reached its end. Beginning with all-too-often overlooked fundamentals, we explored the basics of lobe formation on both center-fed and end-fed wires ranging from 1 to 11 wavelengths. The galleries of elevation and azimuth patterns should provide a handy reference. At the same time, we

looked at the modeling issues and variables involved in portraying long-wire antennas, including changes of ground quality, changes of wire and material, and changes of height. We also saw that as we lengthen a long-wire, the elevation angle of maximum radiation gradually decreased below the traditionally calculated value. We next explored antennas that add a terminating resistor between the far end of the long-wire and ground. These end-fed terminated or traveling-wave antennas formed the simplest fixed beams, although the use of such a resistor reduced the available forward gain relative to unterminated wires of the same length. The terminating resistor largely--but not completely--controls the feedpoint impedance of the antenna, allowing the use of a terminated long-wire beam over 2 or more octaves of frequency change.

The unterminated single long-wire antennas provided us with a critical piece of information in the development of more complex long-wire arrays. The maximum gain for any long-wire antenna does not coincide with the wire end itself, but occurs at an angle that varies with the wire length. V and rhombic arrays depend on this angle to align a major lobe from each individual wire so that the lobes add to increase array gain. Long-wire V antennas are usable in both unterminated and terminated forms. In both cases, the gain is considerably higher than for a single long-wire antenna, and the strongest lobe is in line with the wire. However, the higher gain comes at the expense of beamwidth, as the main lobe becomes very narrow at longer wire lengths. Once more, the terminated V-beam has somewhat less gain than the more bi-directional unterminated V array, but the termination provides considerable bandwidth. The limiting factor for bandwidth is that the leg length

changes when measured in wavelengths as the operating frequency changes. As a result, the wire angle no longer is correct for aligning the lobes from the individual wires and the pattern breaks down.

The rhombic is perhaps the largest and most refined of the long-wire antennas, consisting of two Vs, open-end to open-end. The result is 4 wires contributing aligned lobes for higher gain and narrower beamwidth. Although the rhombic suppresses unwanted sidelobes better than the V antenna, significant sidelobes remain. The effort to further suppress the sidelobes has resulted in the development of more complex rhombic designs using multiple rhombic elements offset from each other. Although the unterminated rhombic is usable and has more gain than the terminated version, the gain differential is less than for other types of long-wire antennas. If we optimally design a terminated rhombic--by reference to the correct wire angle relative to the antenna height and leg length--we may obtain at least a 2:1 frequency ratio of high performance at a nearly constant feedpoint impedance.

Although the facts about long-wire antennas are readily available from a variety of sources, these notes have used antenna modeling software as an alternative technique in determining the correct wire angle for maximum antenna performance for any given height and leg length. Starting with the unterminated end-fed long-wire, we can determine the lobe angle and use this information in designing both V and rhombic antennas that use the same wire length for their legs. Although the models used to provide basic comparisons within each antenna type and among types employed a set height

(1 wavelength) and lossless wire of a suitable size for the test frequency, modeling software, such as NEC, allows one to vary these elements and rapidly optimize a complete design. Allied to these basic design techniques are methods of placing sources (the feedpoint) and loads (the terminating resistor) to produce accurate calculations without disturbing the basic geometry of the antenna. As the antennas grew more complex, the modeling issues became more significant, although they grew in a stepped fashion with the step-wise increase in the complexity of long-wire antenna geometry.

Long-wire technology dates back to the earliest attempts to control antenna radiation patterns and to obtain gain beyond the levels of single wires. However, the techniques may still have application today and tomorrow. At the same time, modeling design methods can shorten at least some of the calculation time needed to produce a workable long-wire antenna, whatever the type. Our trek through long-wire technology ends here, but the antennas themselves may still have far to go.

## Chapter 58: The Dual Rhomboid for 1296 MHz

In the late 1950s, Edmund Laport of RCA hand calculated a number of improved rhombic-type antennas. The improvements for a dual rhomboid consisted in the main of higher gain (with claims of 27 dB over a dipole) and lower side lobe values. The horizontal beamwidth was calculated at about 11 degrees to -3 dB points. Thus the antennas represent appropriate choices for fixed point-to-point communications or reception.

Interest in the design has periodically peaked in various parts of the overall communications field, including amateur VHF and UHF efforts and the TV reception (cable and individual) industry. For either application arena, improved rhombics offer the potential for an inexpensive antenna (some wire and wood) with high gain and relatively easy construction.

Cliff Buttschardt, K7RR, graciously provided me with some background material appearing in the October, 1976 *CATJ*, and other information has appeared in *73* and *QST*. The article's references include several *Radio-Electronics* articles between 1953 and 1960, mostly referenced to TV uses of the rhombic. As well, there are references to Laport's original papers in the *RCA Review* (March, 1952, and March, 1960). Bill Parker, W8DMR, wrote on the "Dual Rhombic for VHF-UHF" in *73* for August, 1977, and the information there was edited and relayed by Emil Pocock, W3EP, in his VHF column (p. 89) in *QST* for March, 1997. The reason for the resurgence of interest in 1997 stems from the 1296 MHz version of the dual rhomboid built by Dayton Johnson, W0OZI, which won the

1996 Central State VHF Conference antenna gain test with a measure 17.3 dBi gain value. (See *QST* for December, 1996, p. 90.)

Although Laport developed several advanced multi-element rhomboid antenna designs (hand-calculated), the most favored for its ease of implementation is the dual rhomboid. (The elements are rhomboids, but not true rhombi, since the sides are not necessarily perfectly parallel.) It is on the dual rhomboid that I shall concentrate, since it presents a number of challenges to the antenna modeler.

In this note, I shall focus on the 1296 MHz version of the antenna derived from the work of W8DMR as revised by W3EP, since that is likely the antenna design most accessible to most hams.

Apparently, W3EP scaled the antenna design from a 1255 MHz ATV version in Parker's article. Among the claims made for the antenna are the following of interest to an inveterate modeler. 1. The gain may be 20 dB better than a dipole. 2. The antenna allows for "sloppy" construction without jeopardy to success.

In all of this background material, no mention is made of the antenna's front-to-back ratio. Moreover, Laport's theoretical calculations and HF applications of the antenna suggested that terminating resistors for each section of this traveling wave design should be about 660 Ohms and yield a net feedpoint impedance of about 330 Ohms. In ham writings, this has been uncritically translated into 600 Ohm resistors and a 300-Ohm feedpoint impedance.

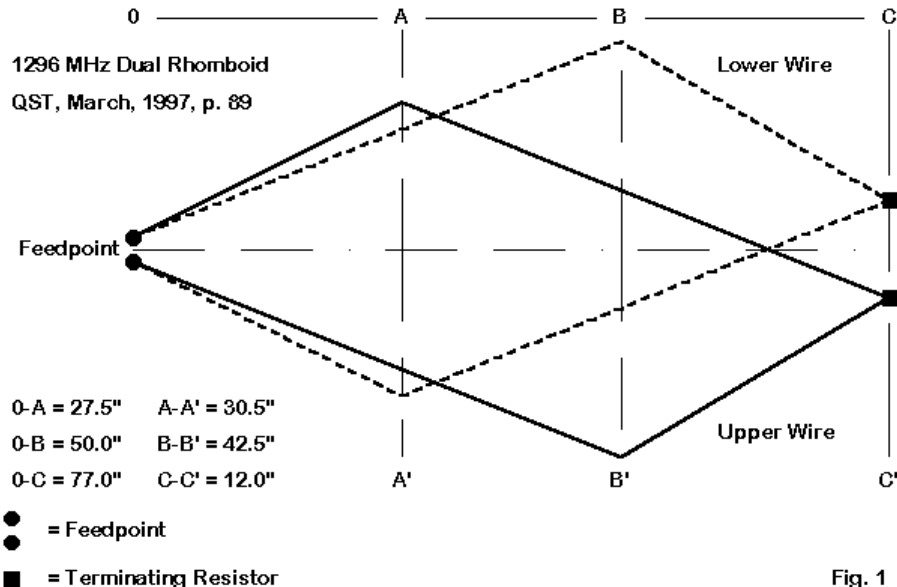


Fig. 1

To see how this works, see **Fig. 1**, a general outline--with dimensions--of the 1296 MHz version appearing in *QST*. The two rhomboids are offset from each other--left and right--by a small distance at their terminating points so that the separate patterns maximize the main forward lobe and minimize troubling side lobes that are characteristic of single rhombic designs. Both rhomboids are fed in parallel. Laport's original designs called for no separation between the "upper" and the "lower" wires, but only insulation at the crossing points. Typical ham practice has mounted the two

rhomoids on opposite sides of a frame, usually about 3/4" to 1" thick (at UHF, a minimum size for sturdiness).

At 1296 MHz, a wavelength is about 9.11" long, so the length of the antenna from feedpoint to terminating resistors is about 8.4 wl and the maximum width is about 4.7 wl. (This may account for the fact that no ham has yet constructed a rotating HF version of the antenna.) At 1296 MHz, the antenna is about 77" long and 42.5" wide--quite manageable dimensions.

There are two sets of antennas to be explored: the *QST* model and the *CATJ* versions derived directly from Laport's analysis. In this part, I shall look only at the *QST* model. One important reason for this is that modeling the antenna is tempting for anyone with a basic modeling program using NEC-2. However, creating a useful (I shall not use the term "precise") model of the Laport dual rhomboid is not so easy a task as it may seem, and I shall point to some dangers in the enterprise before seeing what the *QST* model yields.

## Modeling a Dual Rhomboid

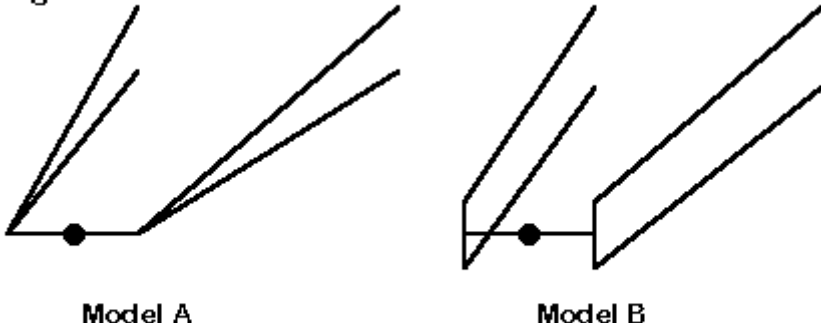
A single rhombic antenna that is 8 wl long will tax many basic NEC-2 modeling programs. The core will handle the geometry easily, but the number of segments required to achieve a relevant degree of convergence (as a test of model adequacy) may quickly approach the standard 500-segment limit attached to basic programs. If we create a dual rhomboid antenna with closely spaced wires crossing each other and sharp angles, the number of segments required for

convergence to even a reasonable degree quickly passes the 1000 mark, and some of my models approached 1600 segments before achieving an acceptable level of convergence.

Modeling a rhomboid shape with a feedpoint and two terminating resistors also requires small distortions of the ideal acutely angled points to the geometry. For the 1296 MHz model, I used 1" multi-segment wires at the points in which to place the resistors and the source. Although an inch seems small compared to a total length of 77", it is 11% of a wavelength and thus cannot be neglected as a potential error source. These wires used at least 3 segments (and some as high as 7) to ensure centering of the source and resistors and to ensure that segments adjacent to the source and load were the same length of the source and load segments.

The wires for the longer and shorter sides are equally highly segmented. I developed two models, the chief difference between them appearing in **Fig. 1A**.

Fig. 1A



#### Two Methods of Modeling the Dual Rhomboid Feed Area

Model A brings the two wires on each side of the feedpoint to a common junction. This is a somewhat dangerous modeling practice, since the wire segments closest to the junction intersect--even for small diameter wire--along an appreciable portion of the segment. This can create modeling errors. Convergence to a reasonable, but not perfect, degree required models using nearly 1600 segments.

Model B changes all of the angles to right angles, minimizing the mutual wire penetration effect. It may also reflect ham construction using a wood frame. These models converged reasonable with about 800 segments.

However, the results obtained from just the change in feedpoint area treatment differ by enough to warrant presentation of both sets of figures. For many purposes, the differences may not make a difference, but that is not something that a modeling exercise can establish from the outset. For example, the feedpoint impedance of Model A is higher than the theoretical 300 Ohms by about as much as the feedpoint impedance of model B is below that value.

In all azimuth patterns, to add to the slowness of model runs, I used a 0.1 degree resolution. The patterns of rhombics of any form are too complex for the 1-degree resolution we habitually use with Yagis.

Interestingly, in no case did I obtain anything close to the 20 to 27 dB gain over a dipole. All modeling was done in free space using copper wire losses, so a comparison with a free space dipole should reduce the reported figures by about 2.1 dB. This does not make the dual rhomboid a poor antenna, since 16 dBi free space gain from a hank of wire and a few slats of wood is still excellent performance potential.

For reference, here is the description of Model B as used below.

Dual Rhombic-QST 3-97, p89

Frequency = 1296 MHz.

Wire Loss: Copper -- Resistivity = 1.74E-08 ohm-m, Rel. Perm. = 1

----- WIRES -----

Wire Conn.--- End 1 (x,y,z : in) Conn.--- End 2 (x,y,z : in) Dia(in) Segs

1	W8E2	-0.500, 0.000, 0.000	W2E1	-0.500, 0.000, 0.500	# 12	2
2	W1E2	-0.500, 0.000, 0.500	W3E1	-15.250, 27.500, 0.500	# 12	75
3	W2E2	-15.250, 27.500, 0.500	W4E1	5.500, 77.000, 0.500	# 12	120
4	W3E2	5.500, 77.000, 0.500	W5E1	6.500, 77.000, 0.500	# 12	3
5	W4E2	6.500, 77.000, 0.500	W6E1	21.250, 50.000, 0.500	# 12	75
6	W5E2	21.250, 50.000, 0.500	W7E1	0.500, 0.000, 0.500	# 12	120
7	W6E2	0.500, 0.000, 0.500	W8E1	0.500, 0.000, 0.000	# 12	2
8	W15E2	0.500, 0.000, 0.000	W9E1	-0.500, 0.000, 0.000	# 12	3
9	W1E1	-0.500, 0.000, 0.000	W10E1	-0.500, 0.000, -0.500	# 12	2
10	W9E2	-0.500, 0.000, -0.500	W11E1	-21.250, 50.000, -0.500	# 12	120
11	W10E2	-21.250, 50.000, -0.500	W12E1	-6.500, 77.000, -0.500	# 12	75
12	W11E2	-6.500, 77.000, -0.500	W13E1	-5.500, 77.000, -0.500	# 12	3
13	W12E2	-5.500, 77.000, -0.500	W14E1	15.250, 27.500, -0.500	# 12	120
14	W13E2	15.250, 27.500, -0.500	W15E1	0.500, 0.000, -0.500	# 12	75
15	W14E2	0.500, 0.000, -0.500	W7E2	0.500, 0.000, 0.000	# 12	2

----- SOURCES -----

Source	Wire Seg.	Wire #/Pct Actual	From End 1 (Specified)	Ampl.(V, A)	Phase(Deg.)	Type
1	2	8 / 50.00	( 8 / 50.00)	1.000	0.000	I

----- LOADS -----

Load	Wire Seg.	Wire #/Pct Actual	From End 1 (Specified)	R (Ohms)	X(Ohms)
1	2	4 / 50.00	( 4 / 50.00)	600.000	0.000
2	2	12 / 50.00	( 12 / 50.00)	600.000	0.000

Ground type is Free Space

## Modeling Results

The data derived from the models will appear mostly in tabular form, with a few patterns interspersed. This is a consequence of my usual procedures of systematically exploring certain variables in the antenna design.

One question of interest is whether wire size plays any significant role in antenna performance. The easiest way to find out is to run identical antenna dimensions with various wire sizes. Here are the results for 1296 MHz, using the prescribed 600-Ohm terminating resistors. In the tables that follow, gain is the free space value in dBi, F-B is the 180-degree front-to-back ratio in dB, B/W is the -3 dB beamwidth in degrees, F/S is the ratio of the forward lobe to the most major side lobe in dB, and the Feed Z is the source impedance.

Model A (1581 segments)

AWG Size	Gain dBi	F-B dB	B/W deg	F/S dB	Feed Z $R+/-jX$
12	16.23	15.99	10.0	10.24	347 - 81
14	16.25	16.55	10.0	10.23	372 - 58
16	16.29	16.90	10.2	10.26	391 - 46
18	16.22	17.49	10.2	10.23	411 - 33
20	16.17	18.18	10.2	10.21	429 - 23

Although the gain does not change in practical terms, it does show a peak with #16 copper wire. Interestingly, the QST article suggested that #12 would be the smallest wire likely to be used. I am not certain that is a sound statement, since the #16 version of the model also showed the highest front-to-side lobe ratio. Note

also the increasing front-to-back ratio and feedpoint impedance as the wire size decreases. These phenomena are likely effects of increasing wire losses, which do not affect gain significantly.

**Model B (797 segments)**

AWG Size	Gain dBi	F-B dB	B/W deg	F/S dB	Feed Z $R+/-jX$
10	15.71	14.98	10.3	10.74	186 - 17
12	15.76	15.54	10.4	10.66	200 - 8
14	15.80	16.20	10.4	10.57	213 - 1
16	15.81	16.92	10.4	10.48	226 + 10
18	15.81	17.71	10.4	10.40	239 + 18
20	15.80	18.59	10.4	10.33	251 + 26

The antenna gain for this model is systematically about a half dB lower than for Model A, and the reported source impedance is below 300 Ohms. Interestingly, the front-to-back ratio is almost identical for each wire size between the two models. One of the reasons that I tend to trust Model B more than Model A is the smaller excursion of reactance with the changes in wire size (noting that I added #10 wire to Model B just to see what would occur). Moreover, the gain peak is less pronounced and the front-to-side ratio makes a steady progression downward as the front-to-back ratio climbs.

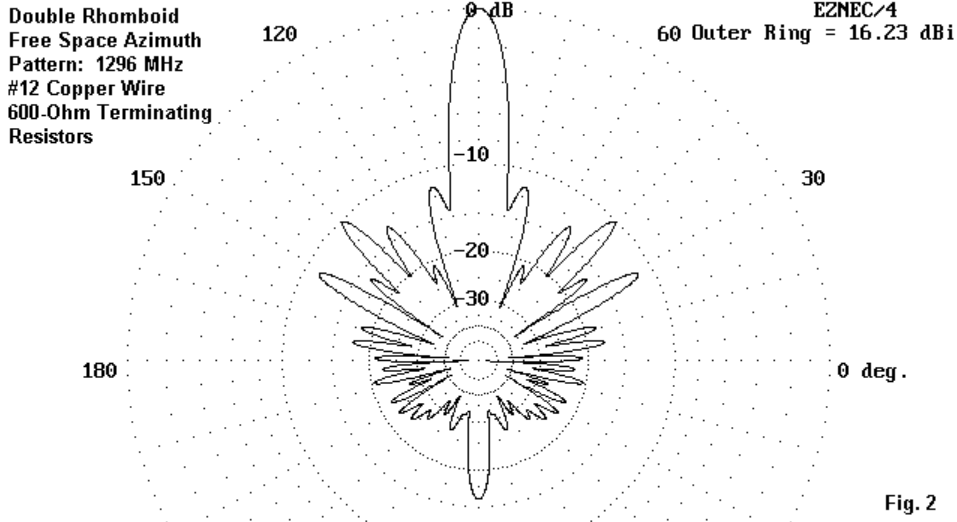


**Fig. 2** provides a free space azimuth pattern for Model A, which is virtually identical to the pattern for Model B with a slight adjustment of gain. Despite the careful calculations made by Laport, this version of his work cannot suppress the main side lobe by more than 10 dB relative to the main lobe.

Double Rhomboid  
Free Space Elevation  
Pattern: 1296 MHz  
#12 Copper Wire  
600-Ohm Terminating  
Resistors

120

EZNEC/4

60 Outer Ring = 16.23 dBi

150  
180

0 dB

-10

20

40

30

0 deg.

Fig. 3

It is interesting to compare the azimuth plot to a free space vertical (or elevation) plot for the antenna (**Fig. 3**). In this plane, we see a broadening of the main forward and rear lobes (to about 30 degrees between -3 dB points). We may also note that the largest side lobe also appears in this pattern, giving the impression that it may form a cone around the main lobe.

Fig. 4



**3-D Outline of the Dual Rhomboid  
Free Space Far Field Pattern**

A 3-D view of the pattern, shown in **Fig. 4**, can give us a better view of what is happening with the main side lobe--or side lobes. First, we must allow for the fact that the reduced resolution of the 3-D pattern converts smooth petals into crystalline points. Nonetheless, we can see that the main side lobe is actually a series of undulating lobes and nulls around the main lobe. (Those given to such things can make any sort of desired Rorschach test out of the 3-D pattern.)

To some degree, then, the dual rhomboid is sensitive to wire size in the 1296 MHz model we are examining. We may increase the front-to-back ratio by decreasing the wire size. We should also wonder what effect we might achieve by changing the values of the terminating resistors. The next data set for both models explores two versions of each model: #12 wire and #16 wire--that latter because it coincides with the gain peaks shown by the preceding data. One of the basic questions to pose is whether there is a value of terminating resistor that will maximize the front-to-back ratio. The following data set systematically reduces the terminating resistor values in 100-Ohm increments from 600 to 200 Ohms.

**Model A (#12 wire; 1581 segments)**

Res. Size	Gain dBi	F-B dB	B/W deg	F/S dB	Feed Z $R +/- jX$
600	16.23	15.99	10.0	10.24	347 - 81
500	16.21	17.77	10.0	10.17	338 - 81
400	16.17	20.23	10.0	10.07	327 - 83
300	16.14	21.97	10.0	9.95	313 - 85
200	16.09	18.31	10.0	9.77	295 - 89

**Model A (#16 wire; 1581 segments)**

Res. Size	Gain dBi	F-B dB	B/W deg	F/S dB	Feed Z $R +/- jX$
600	16.29	16.90	10.2	10.26	391 - 42
500	16.26	19.15	10.2	10.17	379 - 46
400	16.23	21.91	10.2	10.06	364 - 51
300	16.20	21.50	10.2	9.92	346 - 58
200	16.17	16.37	10.2	9.74	323 - 68

Despite differences occasioned by the smaller wire size occasioning more rapid property changes than the larger wire size, the two tables show an interesting coincidence. The maximum front-to-back ratio occurs with a load between 300 and 400 Ohms-- closer to 300 Ohms for the #12 wire and closer to 400 Ohms for the #16 version. **Fig. 5** shows the resultant azimuth pattern for the #12 version with terminating resistors of 300 Ohms.

Double Rhomboid  
Free Space Azimuth  
Pattern: 1296 MHz  
#12 Copper Wire  
300-Ohm Terminating  
Resistors

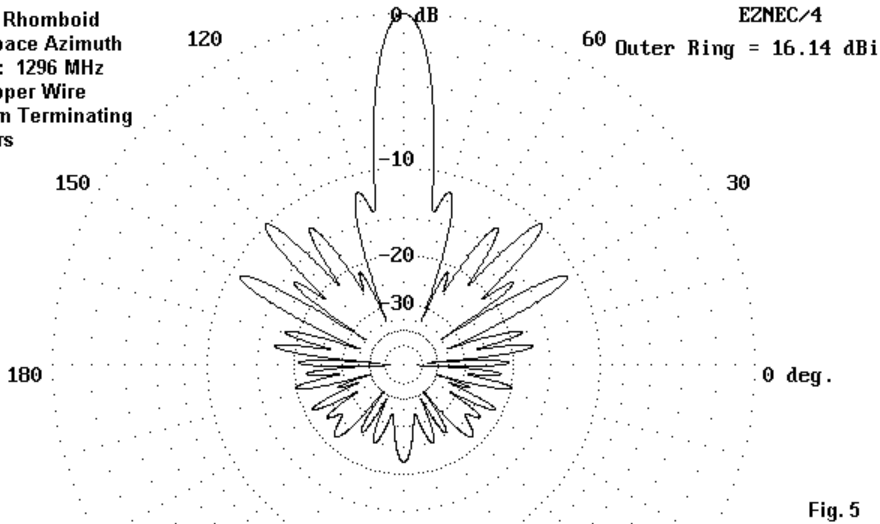


Fig. 5

**Model B (#12 wire; 797 segments)**

<b>Res.</b>	<b>Gain</b>	<b>F-B</b>	<b>B/W</b>	<b>F/S</b>	<b>Feed Z</b>
<b>Size</b>	<b>dBi</b>	<b>dB</b>	<b>deg</b>	<b>dB</b>	<b>R+/-jX</b>
600	15.76	15.54	10.4	10.66	200 - 8
500	15.74	17.64	10.4	10.55	194 - 8
400	15.72	20.92	10.4	10.42	186 - 8
300	15.69	24.15	10.4	10.23	177 - 9
200	15.67	18.91	10.4	10.00	165 - 10

**Model B (#16 wire; 797 segments)**

<b>Res.</b>	<b>Gain</b>	<b>F-B</b>	<b>B/W</b>	<b>F/S</b>	<b>Feed Z</b>
<b>Size</b>	<b>dBi</b>	<b>dB</b>	<b>deg</b>	<b>dB</b>	<b>R+/-jX</b>
600	15.81	16.92	10.4	10.48	226 + 10
500	15.79	19.64	10.4	10.37	218 + 9
400	15.77	23.64	10.4	10.23	209 + 8
300	15.75	23.11	10.4	10.06	197 + 7
200	15.74	16.59	10.4	9.83	182 + 5

As with Model A, Model B shows its maximum front-to-back ratio with terminating resistors between 300 and 400 Ohms. The consistency between the source impedance values for the two wire sizes gives me additional reason to trust Model B more than Model A, even though the primary trends coincide.

Whether the source impedances reported by Model B are accurate to a real antenna involves a number of variables. Some of those variables include limitations of the model itself, as described earlier. Other variable emerge from the construction process itself. Ideally, the support structure for the antenna should be RF-transparent at 1296 MHz. Likewise, construction practices should involve no metal

supports--not even nails--close to the wire. Even a few 1-inch brads can add up to a wavelength of nails very quickly. As a consequence, any real version of the dual rhomboid is likely to show a source impedance somewhat at variance of even the most precise model.

One final question that occurred to me resulted from the claims that the dual rhomboid forgives sloppy construction. In more precise form, one may ask to what degree the antenna may be frequency sensitive. As a partial answer to this question, I ran Model A through a few wire sizes but on the ATV frequency of 1255 MHz, about 3% lower. (Some claims for the broad-banded nature of the antenna suggested that +/- 40% of the design frequency would be usable.) The following table compares the results for Model A at 1296 and 1255 MHz for 3 wire sizes, using the standard 600-Ohm terminating resistors.

Model A (1581 segments)

Freq. MHz	AWG Size	Gain dBi	F-B dB	B/W deg	F/S dB	Feed Z R+/-jX
1296	12	16.23	15.99	10.0	10.24	347 - 81
1255	12	16.20	19.37	10.6	10.30	313 - 108
1296	16	16.29	16.90	10.2	10.26	391 - 46
1255	16	16.26	21.48	10.8	10.20	362 - 80
1296	20	16.17	18.18	10.2	10.21	429 - 23
1255	20	16.14	23.96	10.8	10.12	409 - 61

With respect to gain, no especially frequency sensitivity can be found. However, the front-to-back ratio with a given value of terminating resistor is quite frequency sensitive. At the lower

frequency, the 600-Ohm terminating resistors are close to optimal for maximizing the front-to-back ratio. Moreover, the added capacitive reactance at the source is quite evident for all of the wire sizes.

Whatever the final evaluation of the adequacy of these models, it is clear that the Laport dual rhomboid antenna is not quite the "set-and-forget" item that some sources portray it to be. Its properties vary with wire size, terminating resistor value, and frequency. Whether any of those variations are significant to a given operation can only be judged by reference to the operating specifications.

Moreover, the realizable gain from at least the QST version of the antenna is considerably less than claims derived from theory (which rarely takes into account wire losses). What I hope to squeeze time for is a look at the dimensions derived more directly from Laport's work--perhaps something in the 100 MHz range (about 8 times longer than the 1296 MHz model). When I am semi-satisfied with models of that antenna, I shall add Part 2 to this report on modeling the dual rhomboid.

## Chapter 59: The Dual Rhomboid, a True Laport Version

In looking at the *CATJ* article referenced in Chapter 58 of these notes, I was initially struck by the fact that the author tried to show as exactly as possible the dimensions of a true Laport dual rhomboid. Modeling this antenna might provide a comparison with the 1296 MHz *QST* model examined in Chapter 58.

Of course, some scaling would be necessary. The *CATJ* versions were cut for the television channels, with a 100 MHz model for reference (or for FM reception use). So we can expect in this part to find antennas over 12 times larger than the 1296 MHz model. Replacing inches with feet for the Chapter 58 model will give an idea of the size difference.

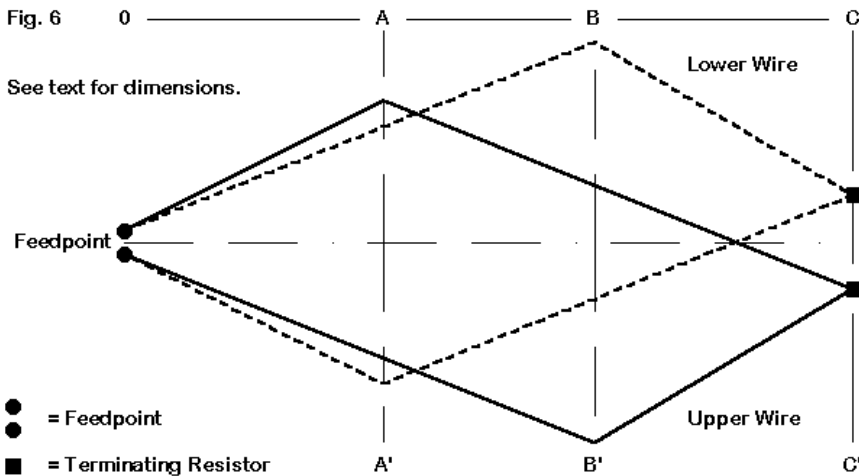


**Fig. 6** repeats the sketch in Chapter 58, but without dimensions. Just why will become immediately apparent.

Sometimes a casual reading must give way to a close reading, and in the process, what seemed clear becomes a bit muddy. The *CATJ* article provides dimensions in two ways: approximations of the distances from the feedpoint to the supporting cross members and angles between the two short legs and between the two long legs. (There is a further ambiguity because the picture of the angles refers to angles A and B but references a table where the only angles given are called X and Y.) The result was two sets of dimensions. One was based on using the prescribed leg lengths plus sines and cosines of the angles given, which resulted in what I call the narrow model. The second version was based on the approximated cross member dimensions, which yielded what I call the wide model. We shall look at a third model before we are done.

The dimensions for the narrow and wide models are as follows, using #12 AWG copper wire and the prescribed 600-Ohm loads. Refer to **Fig. 6** to place each dimension.

#### Narrow Model

0-A	31'	A-A'	30.30'
0-B	56'	B-B'	38.12'
0-C	88.5'	C-C'	7.8'

#### Wide Model

0-A	31'	A-A'	31.50'
0-B	56'	B-B'	39.35'
0-C	88.5'	C-C'	7.8'

For model construction in each case, I used the method of creating right angles among wires at the feedpoint area as perhaps yielding a more trustworthy model than bringing the wires together at a very shallow angle. The following model description table illustrates the modeling technique.

Dual Rhomboid: Laport-CATJ Frequency = 100 MHz.

Wire Loss: Copper -- Resistivity = 1.74E-08 ohm-m, Rel. Perm. = 1

----- WIRES -----

Wire Conn.--- End 1 (x,y,z : ft) Conn.--- End 2 (x,y,z : ft) Dia(in) Segs

1	W8E2	-0.100, 0.000, 0.000	W2E1	-0.100, 0.000, 0.100	# 12	1
2	W1E2	-0.100, 0.000, 0.100	W3E1	-15.750, 31.000, 0.100	# 12	75
3	W2E2	-15.750, 31.000, 0.100	W4E1	3.800, 88.500, 0.100	# 12	125
4	W3E2	3.800, 88.500, 0.100	W5E1	4.000, 88.500, 0.100	# 12	3
5	W4E2	4.000, 88.500, 0.100	W6E1	19.670, 56.000, 0.100	# 12	75
6	W5E2	19.670, 56.000, 0.100	W7E1	0.100, 0.000, 0.100	# 12	125
7	W6E2	0.100, 0.000, 0.100	W8E1	0.100, 0.000, 0.000	# 12	1
8	W15E2	0.100, 0.000, 0.000	W9E1	-0.100, 0.000, 0.000	# 12	3
9	W1E1	-0.100, 0.000, 0.000	W10E1	-0.100, 0.000, -0.100	# 12	1
10	W9E2	-0.100, 0.000, -0.100	W11E1	-19.670, 56.000, -0.100	# 12	125
11	W10E2	-19.670, 56.000, -0.100	W12E1	-4.000, 88.500, -0.100	# 12	75
12	W11E2	-4.000, 88.500, -0.100	W13E1	-3.800, 88.500, -0.100	# 12	3
13	W12E2	-3.800, 88.500, -0.100	W14E1	15.750, 31.000, -0.100	# 12	125
14	W13E2	15.750, 31.000, -0.100	W15E1	0.100, 0.000, -0.100	# 12	75
15	W14E2	0.100, 0.000, -0.100	W7E2	0.100, 0.000, 0.000	# 12	1

----- SOURCES -----

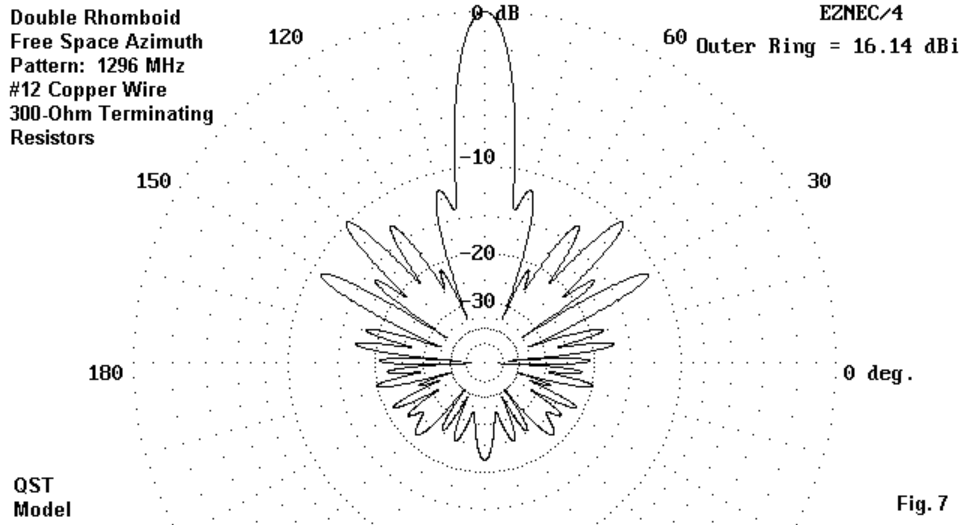
Source	Wire Seg.	Wire #/Pct Actual	From End 1 (Specified)	Ampl.(V, A)	Phase(Deg.)	Type
1	2	8 / 50.00	( 8 / 50.00)	1.000	0.000	I

----- LOADS -----

Load	Wire Seg.	Wire #/Pct Actual	From End 1 (Specified)	R (Ohms)	X(Ohms)
1	2	4 / 50.00	( 4 / 50.00)	600.000	0.000
2	2	12 / 50.00	( 12 / 50.00)	600.000	0.000

Ground type is Free Space

Before looking at the results of modeling these 100 MHz models, let's review **Fig. 7**. This is a free space azimuth pattern for one of the best 1296 MHz models, using #12 wire and 300-Ohm terminating resistors to achieve maximum front-to-back ratio. Remember that #12 wire is about 12 times fatter at 1296 MHz relative to a wavelength than it will be at our new test frequency of 100 MHz.



At 100 MHz, with 600-Ohm terminating resistors, the basic numbers given by NEC-4 for the performance of the narrow and wide models are as follows:

Model	Gain dBi	F-B dB	B/W deg	F/S dB	Feed Z $R +/- jX$
Narrow	14.96	21.94	12.2	11.56	388 - 144
Wide	15.26	24.11	11.8	11.36	364 - 148

The respective free-space azimuth patterns are shown in **Fig. 8** and **Fig. 9**.

Double Rhomboid  
Free Space Azimuth  
Pattern: 100 MHz  
#12 Copper Wire  
600-Ohm Terminating  
Resistors

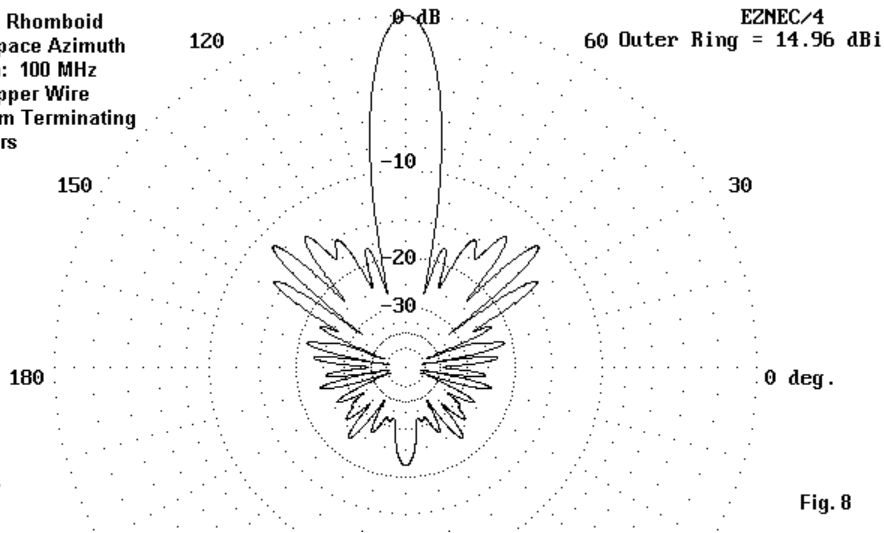


Fig. 8

**Double Rhomboid**  
**Free Space Azimuth**  
**Pattern: 100 MHz**  
**#12 Copper Wire**  
**600-Ohm Terminating**  
**Resistors**

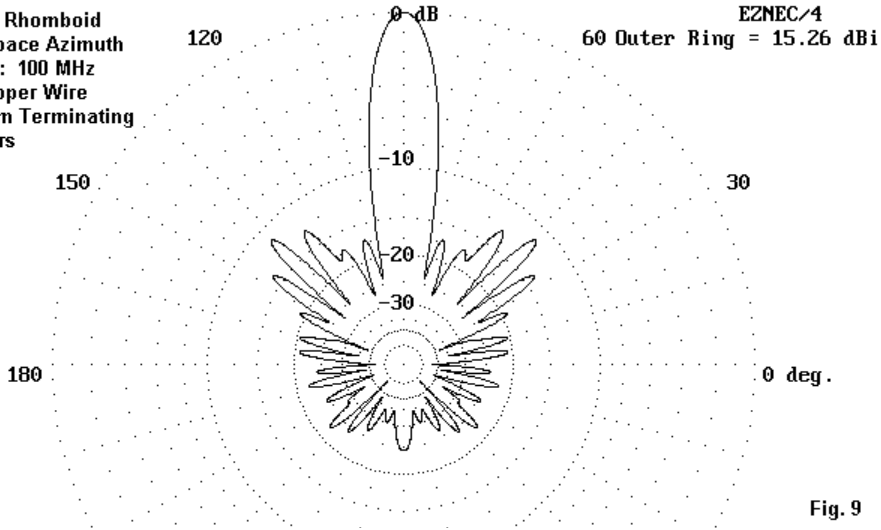


Fig. 9

Both models show less gain than the 1296 MHz model, but considerably better front-to-back ratio with the prescribed 600-Ohm terminating resistors. The beamwidth at 100 MHz is wider by a small amount, and the front-to-side lobe ratio is better, also by a small amount. Perhaps the major fact that becomes evident, especially in the narrow model, is the reduction in the amount of power overall in the rearward lobes. Every lobe past 60 degrees from the main lobe is down by at least 20 dB and mostly more. One goal of the Laport dual rhomboid design is at least partially met in these models.

To see what effect wire size might have on performance, I ran the wide model using wire sizes from #12 through 0.5" in diameter.

Throughout the exercise, the dimensions remained constant and the terminating resistors were a constant 600 Ohms.

Wire Size	Dia. In.	Gain dBi	F-B dB	B/W deg	F/S dB	Feed Z R+/-jX
12	0.0808	15.26	24.11	11.8	11.36	364 - 148
10	0.1019	15.29	25.39	11.8	11.29	345 - 147
8	0.1285	15.31	26.81	11.8	11.21	327 - 145
6	0.1620	15.33	28.27	11.8	11.13	309 - 144
4	0.2043	15.34	29.69	11.6	11.04	292 - 143
2	0.2576	15.35	31.07	11.6	10.95	275 - 141
--	0.3	15.36	31.94	11.6	10.89	264 - 140
--	0.4	15.40	33.49	11.6	10.76	242 - 136
--	0.5	15.49	33.62	11.6	10.66	222 - 131

Obviously, the performance of the dual rhomboid benefits from the use of fatter wire, whether used as a single wire or as a simulated fat wire composed of separated parallel wires. The chart does not peak within the range of values checked (nor does a similar chart for the narrow model). As we saw with the 1296 MHz model, the front-to-side lobe ratio and the feedpoint impedance both decrease with increases in the front-to-back ratio and gain.

It may be the case that using a single wire size of #6 AWG may be the most practical compromise for a 100 MHz dual rhomboid. Wire of this size or larger might best be aluminum for weight saving. Therefore, I compared the performance figures for both #12 and 0.5" wire in copper and aluminum.

Wire Size	Wire Type	Gain dBi	F-B dB	B/W deg	F/S dB	Feed Z R+/-jX
12	copper	15.26	24.11	11.8	11.36	364 - 148
12	alum.	15.24	24.10	11.8	11.39	364 - 148
0.5"	copper	15.49	33.62	11.6	10.66	222 - 131
0.5"	alum.	15.49	33.59	11.6	10.68	222 - 131

Since the performance differences between copper and aluminum wire are non-existent at the limits of the chart, any wire size within the chart will give equivalent performance, whether copper or aluminum.

As I did with the 1296 MHz model, I checked the new models to determine whether different values of terminating resistors would yield better performance than the standard 600-Ohm values. As a quick reference, here are numbers for the wide models using #12 wire and using #6 wire (copper).

#### #12 Copper Wire

Res. Size	Gain dBi	F-B dB	B/W deg	F/S dB	Feed Z R+/-jX
600	15.26	24.11	11.8	11.36	364 - 148
650	15.26	27.13	11.8	11.34	356 - 146
700	15.27	30.13	11.8	11.33	350 - 145
750	15.27	31.06	11.8	11.30	344 - 143
800	15.27	29.15	11.8	11.28	338 - 142

#### #6 Copper Wire

Res. Size	Gain dBi	F-B dB	B/W deg	F/S dB	Feed Z R+/-jX
600	15.33	28.27	11.8	11.13	309 - 144
650	15.33	31.22	11.8	11.10	304 - 142
700	15.34	31.05	11.8	11.09	299 - 141

The gain of this model (and likewise, the narrow model) rises very slowly (insignificantly so) as the value of the terminating resistors increases. However, the front-to-back ratio shows a peak that result from the interrelationship of the wire size and the terminating resistor values. The 650-Ohm value for #6 wire is close to the value recommended by Laport's original design. For reference, **Fig. 10** shows the azimuth pattern for the #6 wire wide model with the optimal terminating resistor values.

Double Rhomboid  
Free Space Azimuth  
Pattern: 100 MHz  
#6 Copper Wire  
650-Ohm Terminating  
Resistors

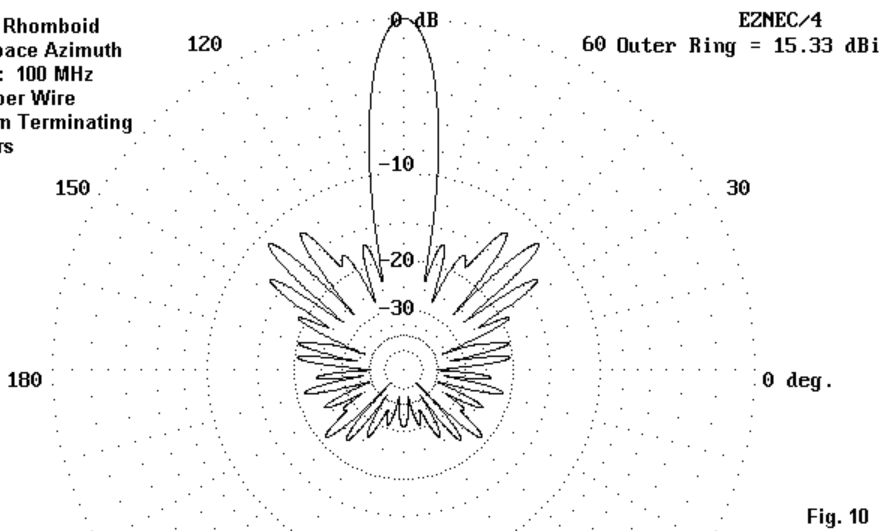


Fig. 10

## The Scaled QST Model

There remains the question of what happens if one simply scales the 1296 MHz model to 100 MHz, while retaining the #12 wire. The dimensions will be somewhat different from those of either the narrow or wide models, with a shorter overall length and somewhat wider cross supports at all positions. The scaled dimensions are these:

### Scaled QST Model

0-A	29.7'	A-A'	32.94'
0-B	54.0'	B-B'	45.90'
0-C	83.16'	C-C'	11.0'

To translate the model to 100 MHz, certain modifications were necessary. Relative to pure scaling, the spacing between rhomboids had to be reduced (to 0.2') and the spacing between feedpoint area leg junctions also had to be reduced to manageable values (0.2'). For reference, here is the model description.

Dual Rhombic-QST 3-97, p89

Frequency = 100 MHz.

Wire Loss: Copper -- Resistivity = 1.74E-08 ohm-m, Rel. Perm. = 1

### ----- WIRES -----

	Wire Conn.--- End 1 (x,y,z : ft)	Conn.--- End 2 (x,y,z : ft)	Dia(in)	Segs
1	W8E2 -0.100, 0.000, 0.000	W2E1 -0.100, 0.000, 0.100	# 12	2
2	W1E2 -0.100, 0.000, 0.100	W3E1 -16.470, 29.700, 0.100	# 12	75
3	W2E2 -16.470, 29.700, 0.100	W4E1 5.940, 83.160, 0.100	# 12	120
4	W3E2 5.940, 83.160, 0.100	W5E1 7.020, 83.160, 0.100	# 12	3
5	W4E2 7.020, 83.160, 0.100	W6E1 22.950, 54.000, 0.100	# 12	75
6	W5E2 22.950, 54.000, 0.100	W7E1 0.100, 0.000, 0.100	# 12	120
7	W6E2 0.100, 0.000, 0.100	W8E1 0.100, 0.000, 0.000	# 12	2

8	W15E2	0.100, 0.000, 0.000	W9E1	-0.100, 0.000, 0.000	# 12	1
9	W1E1	-0.100, 0.000, 0.000	W10E1	-0.100, 0.000, -0.100	# 12	2
10	W9E2	-0.100, 0.000, -0.100	W11E1	-22.950, 54.000, -0.100	# 12	120
11	W10E2	-22.950, 54.000, -0.100	W12E1	-7.020, 83.160, -0.100	# 12	75
12	W11E2	-7.020, 83.160, -0.100	W13E1	-5.940, 83.160, -0.100	# 12	3
13	W12E2	-5.940, 83.160, -0.100	W14E1	16.470, 29.700, -0.100	# 12	120
14	W13E2	16.470, 29.700, -0.100	W15E1	0.100, 0.000, -0.100	# 12	75
15	W14E2	0.100, 0.000, -0.100	W7E2	0.100, 0.000, 0.000	# 12	2

----- SOURCES -----

Source	Wire Seg.	Wire #/Pct Actual	From End 1 (Specified)	Ampl.(V, A)	Phase(Deg.)	Type
1	1	8 / 50.00	( 8 / 50.00 )	1.000	0.000	I

----- LOADS -----

Load	Wire Seg.	Wire #/Pct Actual	From End 1 (Specified)	R (Ohms)	X(Ohms)
1	2	4 / 50.00	( 4 / 50.00 )	600.000	0.000
2	2	12 / 50.00	( 12 / 50.00 )	600.000	0.000

Ground type is Free Space

Here is a small chart comparing #12 models with 600-Ohm terminating resistors for all three models:

Model	Gain dBi	F-B dB	B/W deg	F/S dB	Feed Z R+/-jX
Narrow	14.96	21.94	12.2	11.56	388 - 144
Wide	15.26	24.11	11.8	11.36	364 - 148
Scaled	15.52	32.65	10.4	10.12	293 - 96

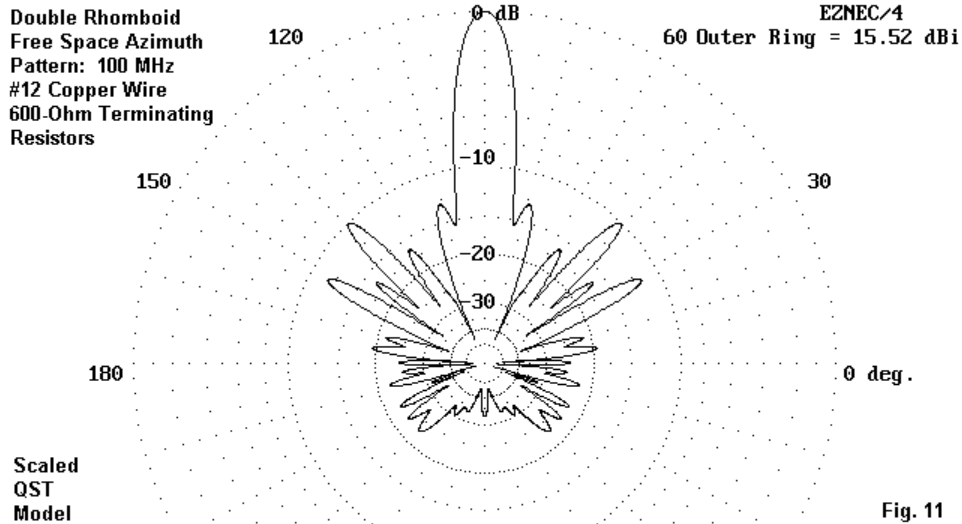


Fig. 11

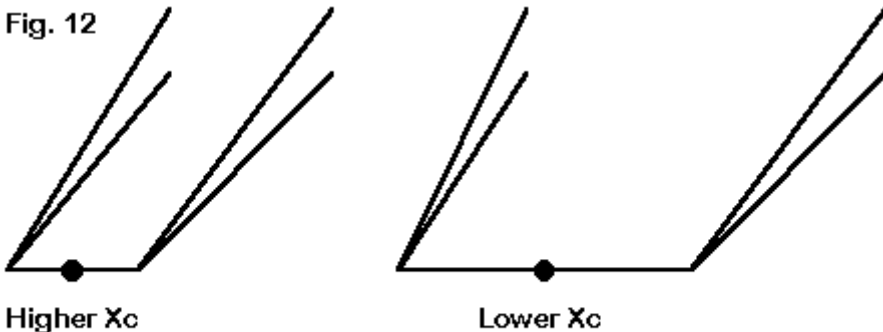
**Fig. 11** presents the free-space azimuth pattern for the scaled QST model as adjusted. Note the slightly higher gain and front-to-back ratio, but the narrower beamwidth and lower front-to-side lobe ratio. Among the more subtle features to notice when comparing patterns is the first lobe off the main lobe. In the narrow and wide CATJ models, it is a low-level distinct lobe. In the scaled QST model, the first lobe is stronger and melds with the main lobe. Whether features like these make an operational difference in most ham circumstances is dubious. However, they are interesting theoretically when considering what Laport was trying to accomplish with his design.

If the side lobes are not especially troublesome, the scaled QST 1296 MHz model may be the more advantageous design, considering the gain, front-to-back ratio, and feedpoint impedance. However, if the power to the rearward lobes is of concern for a particular operation, the CATJ version may end up as more suitable.

## A Note on Feedpoint Reactance

Virtually all of the models have shown a remnant capacitive reactance of proportions to disturb a match with 300-Ohm or similar line. Because of limitation in the models, it is not certain to what degree this reactance will appear in a real antenna. However, modeling uncovers a simple technique for changing the reactance. See **Fig. 12**.

Fig. 12



Higher Xc

Lower Xc

Adjusting Feedpoint Reactance by Spacing Wires

Where the wires of the legs join, the spacing between leg pairs can be widened or narrowed. Narrowing the spacing tends to push reactance further into the capacitive region. Widening the spacing pushed the reactance less capacitive and more toward inductive. Although the models may not predict the exact reactance value to be encountered with a dual rhomboid, the trends should be quite reliable in field adjusting the feedpoint reactance.

## Conclusion

By judiciously using the figure that emerged from the 1296 MHz model and those that emerged with these 100-MHz models, it is possible to estimate the properties of scaled versions of the dual rhomboid for 144-, 225-, and 440-MHz versions of the antenna. The key item to remember is that the "standard" #12 wire becomes effectively fatter relative to a wavelength as the frequency increases.

The dual rhomboid models produce consistent narrow beamwidth gains between 15 and 16 dBi in free space. At 100 MHz, the require length is 83-89 feet, with a 38 to 45 foot maximum width. What these numbers do not tell us is whether the antenna is worth building. So far we have produced no standards of comparison. For example, what would be the performance of a simpler single wire rhombic at 100 MHz? Does the dual rhombic have enough of a gain advantage to warrant the added construction difficulties? How large would a Yagi or equivalent gain be?

It may be useful to add one more part to this series to provide some basis for the individual to decide if the dual rhomboid is indeed the way to go.

## Chapter 60: The Dual Rhomboid, Some Comparison Standards

In thinking about building a dual rhomboid, we should carefully evaluate whether the results will be worth the effort involved. Despite its inexpensiveness at UHF, the dual rhomboid is not the simplest antenna to build.

Moreover, the dual rhomboid does not offer in modeled performance the gain theoretically claimed for it. Consistent gain figures between 15 and 16 dBi free space have emerged from the models. Even if we allow that the models have not caught the precise dimensions by which the side lobes come in for complete control, it is dubious that any constructed version of the antenna will achieve much more than 16 dBi free-space gain.

Therefore, it is reasonable to look at some other antennas in order to make some evaluative comparisons. In this note, I shall explore only two: the single-wire rhombic and a standard Yagi.

### The Single-Wire Rhombic

The *ARRL Antenna Book* has carried an HF rhombic since time immemorial. It is possible to scale this antenna to 100 MHz and to use #12 wire in order to see by how much the dual rhomboid outperforms it.

Single Rhombic: 100 MHz

Adapted and Scaled from  
ARRL Antenna Book

Fig. 13

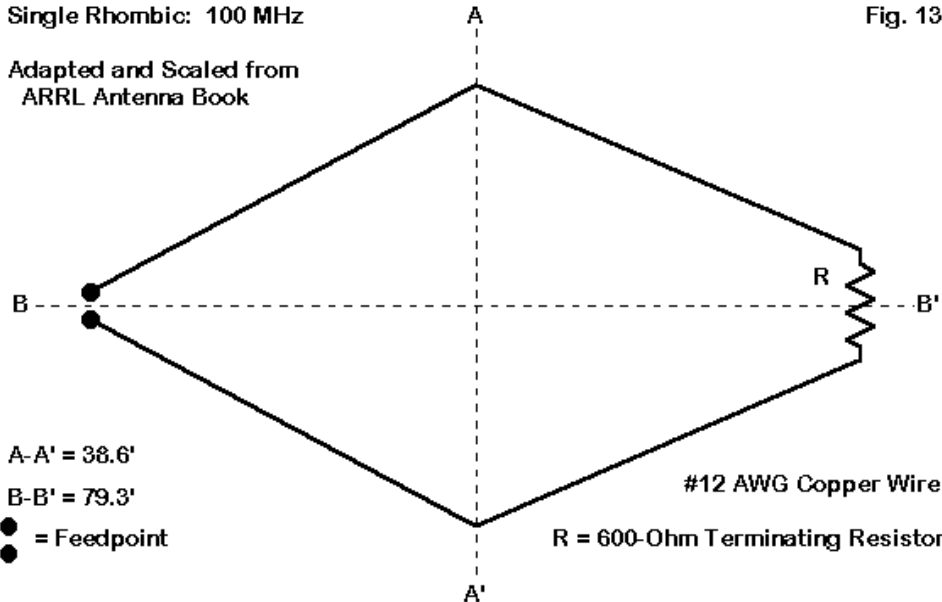


**Fig. 13** provides the essential dimensions for the 100 MHz single-wire rhombic. At 79.3' long by 38.6' wide, the antenna occupies a footprint just a tad smaller than the dual rhomboids. The model description follows.

ARRL rhombic scaled to 100 MHz

Frequency = 100 MHz.

Wire Loss: Copper -- Resistivity = 1.74E-08 ohm-m, Rel. Perm. = 1

## ----- WIRES -----

		Conn.--- End 1 (x,y,z : ft)	Conn.--- End 2 (x,y,z : ft)	Dia(in)	Segs
1	W6E2	-1.200, 0.000, 14.469	W2E1 1.200, 0.000, 14.469	# 12	7
2	W1E2	1.200, 0.000, 14.469	W3E1 19.291, 39.638, 14.469	# 12	100
3	W2E2	19.291, 39.638, 14.469	W4E1 0.344, 79.275, 14.469	# 12	100
4	W3E2	0.344, 79.275, 14.469	W5E1 -0.344, 79.275, 14.469	# 12	3
5	W4E2	-0.344, 79.275, 14.469	W6E1 -19.291, 39.638, 14.469	# 12	100
6	W5E2	-19.291, 39.638, 14.469	W1E1 -1.200, 0.000, 14.469	# 12	100

## ----- SOURCES -----

Source	Wire Seg.	Wire #/Pct Actual	From End 1 (Specified)	Ampl.(V, A)	Phase(Deg.)	Type
1	4	1 / 50.00	( 1 / 50.00 )	0.707	0.000	V

## ----- LOADS -----

Load	Wire Seg.	Wire #/Pct Actual	From End 1 (Specified)	R (Ohms)	X(Ohms)
1	2	4 / 50.00	( 4 / 50.00 )	600.000	0.000

Ground type is Free Space

The values in the Z columns are remnants of the source of this scaled model and can be replaced by zeroes for free space analysis. The wide spacing of the wires near the feedpoint represents an attempt to control some of the capacitive reactance at the feedpoint.

As I did for the *CATJ* dual rhomboid models, I ran the scaled single-wire rhombic through various wire sizes to develop a sense of the trends in performance. Note the reduction of the terminating

resistor to 600 Ohms from the HF value of 800 Ohms. Here are the results.

Wire Size	Dia. In.	Gain dBi	F-B dB	B/W deg	F/S dB	Feed Z R+/-jX
12	0.0808	13.85	45.30	11.4	8.50	625 - 96
10	0.1019	13.93	34.76	11.4	8.53	606 - 105
8	0.1285	14.01	29.84	11.4	8.56	585 - 114
6	0.1620	14.09	26.68	11.4	8.59	563 - 122
4	0.2043	14.16	24.40	11.4	8.61	540 - 130
2	0.2576	14.24	22.57	11.4	8.65	516 - 137

**Fig. 14** presents the free space azimuth pattern for the single-wire rhombic using #12 wire, where the terminating resistor has been optimized for maximum 180-degree front-to-back ratio. Obvious from the figure is the fact that a 180-degree front-to-back ratio reveals the rearward lobe behavior over only a very small portion of the rear quadrants. The number is impressive on paper only.

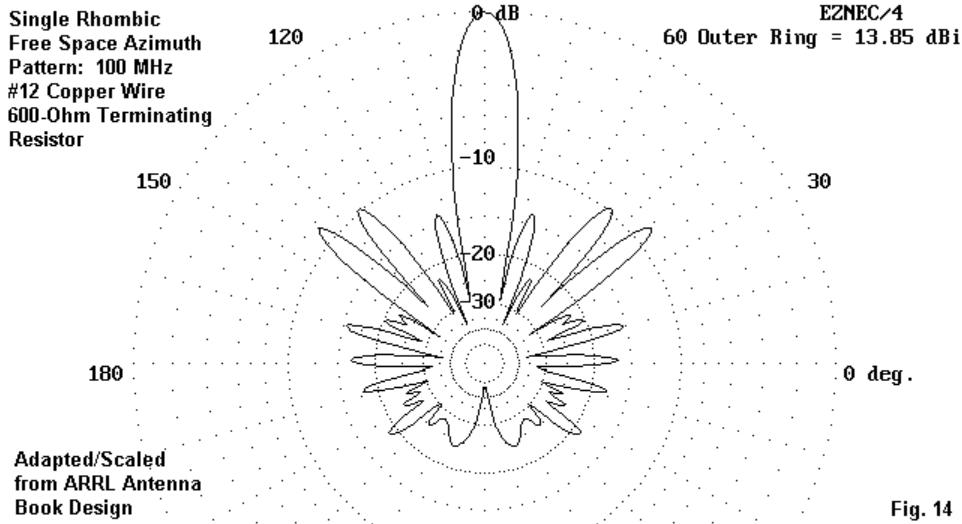


Fig. 14

Optimizing the front-to-back ratio for wire sizes other than #12 AWG will require adjustment of the terminating resistor. Larger wire versions may be preferable to the #12 model in order to increase both the antenna gain and the front-to-side lobe ratio.

The front-to-side lobe ratio numbers can be misleading if one does not also account for the strength of the main lobe. In fact, the lower front-to-side lobe numbers for the single-wire rhombic--relative to the dual rhomboid models--only indicate lobes that have about the same intrinsic strength as those of the dual rhomboids. We can see this by overlaying patterns, as in Fig. 15.

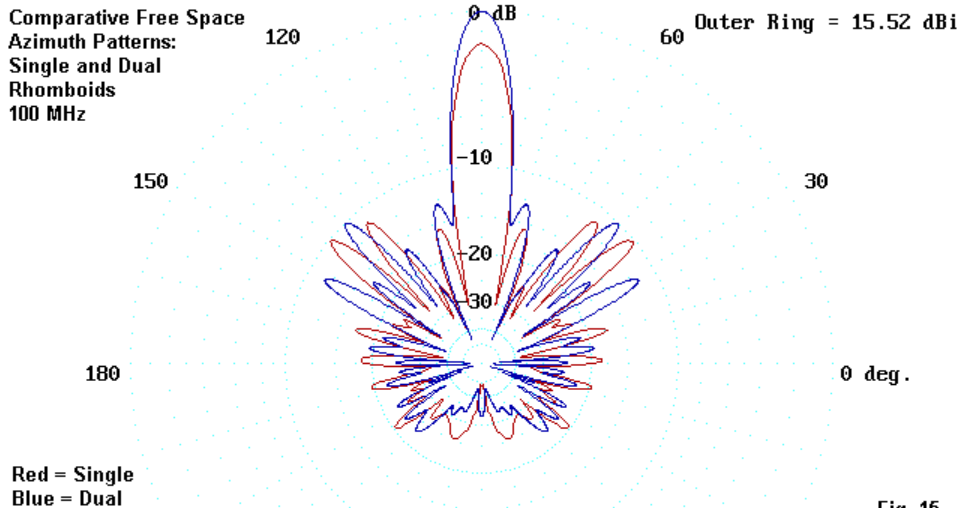


Fig. 15

The red and blue patterns in **Fig. 15** clearly show the higher gain of the dual rhomboid. However, with respect to the other lobes in the pattern, only the positions and not the strengths change from one pattern to the next. With respect to the secondary lobes, there is not much to choose between a single-wire rhombic and a dual rhomboid. Of course, this must be qualified with the recognition that the models in this collection may not have caught the precise dimensions that yield maximum lobe control. However, we have looked at enough models to suggest that if there is such a "perfect" dimension set, it is unlikely to be replicated in the home workshop.

In terms of forward gain, the difference between the best 100 MHz #12 wire dual rhomboid and the #12 wire single rhombic is less than 1.7 dB.

## A 16-Element Yagi

A second standard of comparison one might use in evaluating the dual rhomboid is a standard design Yagi of comparable gain. DL6WU designs have been around for a long time. They feature 50-Ohm feedpoint impedances and fairly broad-banded characteristics. One interesting facet of the DL6WU design is that one can cut off a longer design and still end up with good characteristics and a 50-Ohm feedpoint impedance.

For this exercise, I cut off a 26 element DL6WU design at 16 elements and then scaled the result to 100 MHz to provide a comparator for the dual rhomboid. The antenna has the appearance of **Fig. 16**.



DL6WU 16-Element Yagi: 100 MHz  
Element Dia: 5/8"; Total Length: 43.5'

Fig. 16

For reference, here is the model description.

```

DL6WU Original, 26 el 432 MHz          Frequency = 100  MHz.
Wire Loss: Aluminum -- Resistivity = 4E-08 ohm-m, Rel. Perm. = 1

----- WIRES -----

Wire Conn.--- End 1 (x,y,z : ft)   Conn.--- End 2 (x,y,z : ft)   Dia(in) Segs
1      0.000,  2.414,  0.000      0.000, -2.414,  0.000 6.80E-01 19
2      1.967,  2.339,  0.000      1.967, -2.339,  0.000 6.80E-01 19
3      2.704,  2.137,  0.000      2.704, -2.137,  0.000 6.80E-01 19
4      4.476,  2.120,  0.000      4.476, -2.120,  0.000 6.80E-01 19
5      6.591,  2.095,  0.000      6.591, -2.095,  0.000 6.80E-01 19
6      9.048,  2.071,  0.000      9.048, -2.071,  0.000 6.80E-01 19
7     11.803,  2.049,  0.000     11.803, -2.049,  0.000 6.80E-01 19
8     14.753,  2.030,  0.000     14.753, -2.030,  0.000 6.80E-01 19
9     17.851,  2.014,  0.000     17.851, -2.014,  0.000 6.80E-01 19
10    21.098,  2.000,  0.000     21.098, -2.000,  0.000 6.80E-01 19
11    24.491,  1.987,  0.000     24.491, -1.987,  0.000 6.80E-01 19
12    28.032,  1.976,  0.000     28.032, -1.976,  0.000 6.80E-01 19
13    31.720,  1.966,  0.000     31.720, -1.966,  0.000 6.80E-01 19
14    35.556,  1.956,  0.000     35.556, -1.956,  0.000 6.80E-01 19
15    39.491,  1.947,  0.000     39.491, -1.947,  0.000 6.80E-01 19
16    43.425,  1.940,  0.000     43.425, -1.940,  0.000 6.80E-01 19

----- SOURCES -----

Source  Wire      Wire #/Pct From End 1      Ampl.(V, A)  Phase(Deg.)  Type
       Seg.      Actual      (Specified)

1        10      2 / 50.00  ( 2 / 50.00)      1.000      0.000      V

Ground type is Free Space

```

This model happens to be symmetrical in the X axis. The longest element is under 5' and the element diameter for the model is a little larger than 5/8". Note that the boom length is only about 43.5' long or about half the length of a dual rhomboid.

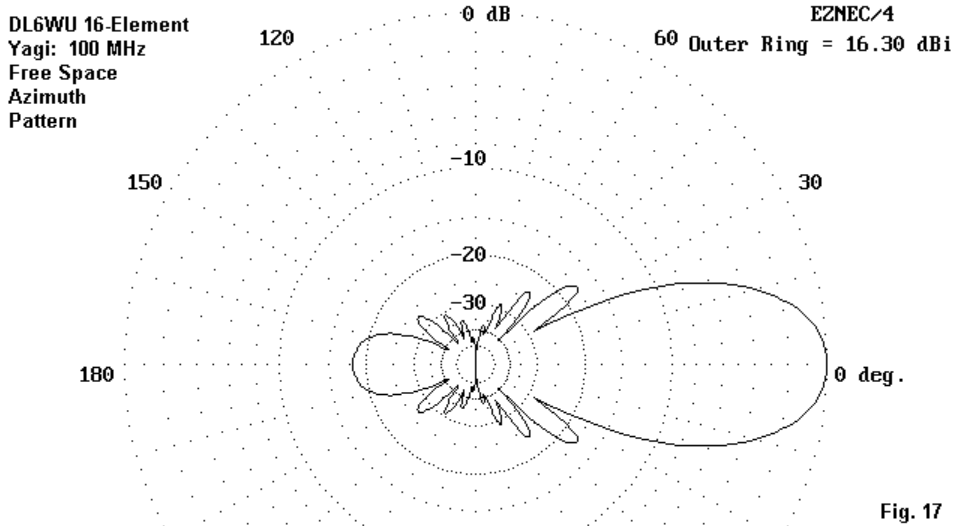


Fig. 17

**Fig. 17** presents the free space azimuth pattern for the 16-element Yagi. For comparative purposes, the modeled performance figures at 100 MHz are these.

Gain	F-B	B/W	F/S	Feed Z
dBi	dB	deg.	dB	R+/-jX
16.30	17.98	29	17.41	48 - j4

Although the front-to-back ratio of this particular model is under 20 dB, the overall power found in side lobes is much smaller than that in any of the rhomboid models. The front-to-side ratio is very good for rejection of QRM from those regions.

The beamwidth (29 degrees between -3 dB points) makes the antenna considerably easier to aim than any of the rhomboid models, whose beamwidths are only a third as wide. The Yagi's wider beamwidth can be either an advantage or a disadvantage, depending upon the operating requirements for the antenna.

The DL6WU antennas scale easily, so long as one remembers to scale the element diameter as well as the lengths and spacings. At 432 MHz, the element diameter for optimal performance is 4 mm.

## Conclusion

I have not presented the single-wire rhombic or the DL6WU Yagi either to encourage or discourage construction of a dual rhomboid. That decision belongs to the individual user. However, making that decision requires reference to relevant comparators, and the ones we have examined here seem like good choices with which to start.

## A More Precise Laport Dual Rhombic

Although the models examined in these notes will likely provide highly satisfactory dual rhomboid antennas, I have remained unsatisfied with the presentation of numbers for the builder to use. The "narrow" version of the Laport in Part 2 used a combination of lengths calculated from angles and some of the "approximations." So I decided to see what we might obtain by calculating from ground zero.

The basic information is this:

$$L_1 = 3.5 \text{ wl} = 34.425' \text{ at } 100 \text{ MHz}$$

$$L_2 = 6.0 \text{ wl} = 59.014' \text{ at } 100 \text{ MHz}$$

$$\text{Angle A (for L1)} = 26.1 \text{ degrees}$$

$$\text{Angle B (for L2)} = 18.85 \text{ degrees}$$

Let us assume that Laport used true rhombi, with parallel sides. The result is a set of calculations, sketched in **Fig. 18**.

### A More Precise Laport Dual Rhombic

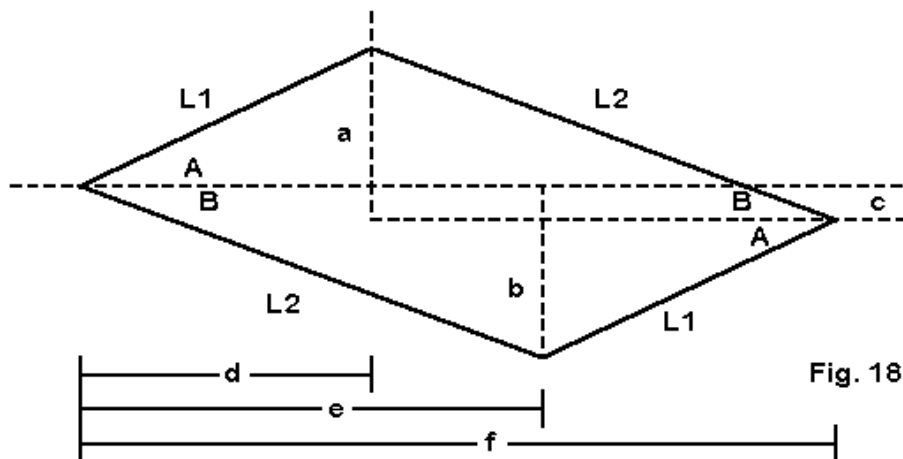


Fig. 18

The figure shows only one of the two rhombi. The horizontal line will have coordinates 0,0 at the left.

Side a, from the through horizontal line upward to the end of L1 will equal  $\sin A * L1 = 15.144'$ . Side b, from the through horizontal line downward to the end of L2 will equal  $\sin B * L2 = 19.067'$ . If the sides are parallel, the distance c will equal side b - side a = 3.923'. Distance d from the origin to the end of L1 will equal  $\cos A * L1 = 30.915'$ . Distance e from the origin to the end of L2 will equal  $\cos B * L2 = 57.031'$ . Distance f from the origin to the far peak of the rhombus will equal  $d + e = 87.946'$ .

These numbers provide us with coordinates for both rhombi of the Laport antenna. They appear in the model description below.

Dual Rhomboid: Laport-CATJ Frequency = 100 MHz.

Wire Loss: Copper -- Resistivity = 1.74E-08 ohm-m, Rel. Perm. = 1

----- WIRES -----

	Wire Conn. --- End 1 (x,y,z : ft)	Conn. --- End 2 (x,y,z : ft)	Dia(in)	Segs
1	W4E2 0.000, 0.000, 0.100	W2E1 -15.144, 30.915, 0.100	# 12	150
2	W1E2 -15.144, 30.915, 0.100	W3E1 3.923, 87.946, 0.100	# 12	257
3	W2E2 3.923, 87.946, 0.100	W4E1 19.067, 57.031, 0.100	# 12	150
4	W3E2 19.067, 57.031, 0.100	W1E1 0.000, 0.000, 0.100	# 12	257
5	W8E2 0.000, 0.000, -0.100	W6E1 -19.067, 57.031, -0.100	# 12	257
6	W5E2 -19.067, 57.031, -0.100	W7E1 -3.923, 87.946, -0.100	# 12	150
7	W6E2 -3.923, 87.946, -0.100	W8E1 15.144, 30.915, -0.100	# 12	257
8	W7E2 15.144, 30.915, -0.100	W5E1 0.000, 0.000, -0.100	# 12	150

----- SOURCES -----

Source	Wire Seg.	Wire #/Pct Actual	From End 1 (Specified)	Ampl.(V, A)	Phase(Deg.)	Type
1	1	1 / 0.00	( 1 / 0.00)	1.000	0.000	SV
2	1	5 / 0.00	( 5 / 0.00)	1.000	0.000	SV

**----- LOADS -----**

Load	Wire Seg.	Wire #/Pct Actual	From End 1 (Specified)	R (Ohms)	X(Ohms)
1	257	2 / 99.81	( 2 /100.00)	300.000	0.000
2	1	3 / 0.33	( 3 / 0.00)	300.000	0.000
3	150	6 / 99.67	( 6 /100.00)	300.000	0.000
4	1	7 / 0.19	( 7 / 0.00)	300.000	0.000

Ground type is Free Space

You may notice several alterations in this model relative to those used in preceding parts of these notes. First, two independent rhombi are used, each with its own feed and load. This move preserves the geometry of the rhombi. Second, to avoid flat wires at either end of the rhombi, split loads are used for the terminating resistors and split feed is used for each rhombus. This technique involves a compromise and a modeler's judgment of priorities. In this case, preservation of wire geometry was given priority over exact equalization of segment lengths for each fed and load segment. The model employs a high number of segments (1648), but may still not be perfectly converged. The segment lengths are equal to two decimal places, but very slight differences in segment length for split loads and feeds can prevent convergence until a very high number of segments is used in a model.

Despite these potential shortfalls of perfection, certain trends make the results close to precise. First, for all stages of convergence testing from about 800 segments upward, the same terminating resistor values produced maximum front-to-back ratio in each model tested with different wire sizes. Gain, beamwidth, and front-to-side lobe ratio remained very close during the tests, although the

higher the number of segments, the better the reported front-to-back ratio. Only the feedpoint impedance remained somewhat variable.

The following results were obtained for #12 and #6 copper wire. In the table, the given value of terminating resistor--chosen for the best front- to-back ratio--represents a series combination of two load resistors in the model description. The feedpoint impedance given is the composite parallel impedance for the two sources connected in parallel. The rhombi are vertically separated 0.2' (2.4").

Wire Size	Dia. In.	Res. Ohms	Gain dBi	F-B dB	B/W deg	F/S dB	Feed Z R+/-jX
12	.0808	600	15.01	23.38	12.4	12.10	398 - 122
6	.1620	550	15.08	23.48	12.4	11.94	348 - 130

The most interesting facet of the exercise in trying to make the Laport antenna model more precise does not appear in the tabulated numbers. Rather, it appears in the azimuth pattern of **Fig. 19.**

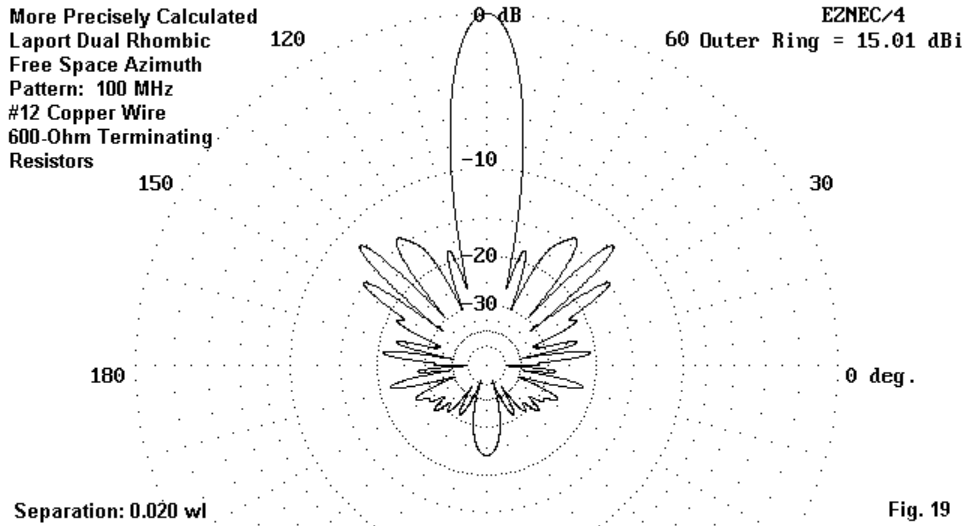


Fig. 19

The Laport antenna does indeed have potential for controlling the side lobes of the rhombic configuration. Only 3 forward side lobes rise much above -20 dB relative to the main lobe, and they are down by more than 12 dB. The reduction in rearward lobes is significantly improved relative to any of the preceding models used in these notes. Whether or not this model has succeeded in capturing the Laport dual rhombic in exact precision, it is clear that Laport was on the right track in his efforts to reduce side lobes from rhombic antennas. Perhaps the only thing not yielded by the design is the absolute maximum in gain.

Spacing between the two rhombi does make a difference in performance characteristics, including the feedpoint impedance,

which rises as the wires are brought closer together. If the spacing is increased, we obtain a lower source impedance, higher gain, high front-to-side lobe ratio, and--up to a peak value--higher front-to-back ratio. I ran a small table of ever-increasing spacing using the #12 wire, 600-Ohm terminating resistor model, and I obtained the following results.

Space Feet	Space WL	Gain dBi	F-B dB	B/W deg	F/S dB	Feed Z R+/-jX
0.2	0.020	15.01	23.38	12.4	12.10	398 - 122
0.4	0.041	15.05	29.04	12.4	12.18	342 - 105
0.6	0.061	15.07	34.27	12.4	12.23	316 - 88
0.8	0.081	15.08	35.21	12.4	12.26	303 - 77
1.0	0.102	15.10	33.13	12.4	12.30	295 - 68
1.2	0.122	15.11	31.45	12.4	12.32	290 - 62

The gain rises continuously with increasing space, although the peak cannot be far off the chart. The front-to-back ratio increases until the spacing reaches 0.8' (0.081 wl). There is no sign where the increase in front-to-side lobe ratio may peak. Given the reported impedance figures, a spacing in the region of 0.081 wl may be most optimal for a balance of operating characteristics. Why increased spacing tends to improve performance appears to be a function of the fact that the wires of the two rhombi cross at less than right angles. Thus, there is significant coupling between them. For any given geometry for the individual rhombi, there is likely a spacing that optimizes the operating characteristics. **Fig 20** provides an azimuth pattern of one of the most fully optimized Laport dual rhombic antennas obtained in this series of experiments. Even so, note the fact that, relative to the rear lobes in **Fig. 19**, some of the rear lobes in this pattern are beginning once more to grow.

More Precisely Calculated  
Laport Dual Rhombic  
Free Space Azimuth  
Pattern: 100 MHz  
#12 Copper Wire  
600-Ohm Terminating  
Resistors

150

180

120

EZNEC/4

60 Outer Ring = 15.11 dBi

30

0 deg.

Separation: 0.122 wl

Fig. 20

The Laport design deserves further study, with special reference to the designer's original papers. These notes have gone only so far as the available information will permit. Hopefully, they have indicated some useful directions for additional effort.

## Chapter 61: Folded X, Hex, Square & Moxon Rectangle Beams

**F**rom time to time, interest reemerges in some long-standing designs for compact planar (2-dimensional) beams.

Unfortunately the interest seems to focus on a single design at a time rather than on the design as a member of a family of designs. Equally unfortunately, the interest usually stems from the publication of some peak performance figures for a particular design rather than from the antenna's performance across an entire band. Consequently, misunderstandings of antenna potentials multiply endlessly.

One of the families of beams whose members rouse periodic interest is the end-coupled clan. If the ends were connected, these would all make versions of a loop. However, with the ends spaced properly, each member forms a directional beam. Another apt name for the group might refer to the semi-closed geometry of the antennas. With closed loops, these antennas share the feature of tending toward larger dimensions with significant increases of element diameter.

Under any name, the family has two branches: those whose center structures form Vees that point at each other bottom to bottom and those whose centers parallel each other. Among the features that clan members have in common is a flat structure with an area that is just over 0.6 square wavelengths--in other words, about 1/4 by 1/4 wavelength. Hence, the lure of the family is its compact size.

It may be useful to explore the main members of the family individually to seek out their potential. I have selected 20 meters as the test band. To keep comparisons fair, I have constructed all models of #12 copper wire. However, some of the family members lend themselves to self-supporting aluminum tubing construction, and I shall note the potential performance changes that may result from building a tubing version of the antenna. The use of tubing for part or all of the structure, of course, will alter the dimensions from the ones used with the #12 wire versions.

The antennas that we shall examine are these:

- 1. The folded X-beam
- 2. The hex beam
- 3. The VK2ABQ square
- 4. The Moxon rectangle

As yet, I do not have any parallelograms, pentagons, or octagons in my collection.

## The Folded X-Beam

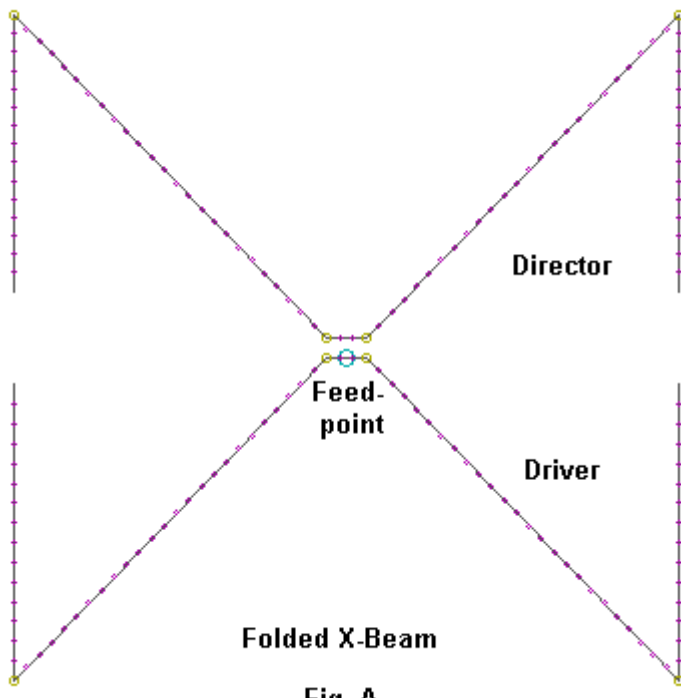


Fig. A

**Fig. A** shows the outlines of a folded X-beam. If you are interested in the history and details of the folded X-beam, see "Modeling and Understanding Small Beams: Part 1: The X-Beam," *Communications Quarterly*, 5 (Winter, 1995), 33-50. Ordinarily, the

Vee portions of the folded X-beam are constructed of tubing supported by a center hub. Then wire tails for the driver and director are run from one corner toward the other, often taped to a perimeter cord that also holds the four arms in a fixed arrangement.

Modeling the usual construction of an X-beam is not feasible with NEC, since the program has an invariant tendency to yield inaccurate results with angular junctions of wires having different diameters. So, I have fashioned a model using #12 copper wire throughout. The performance differences are these: the all-wire version has a slightly lower maximum gain (by about 0.2 dB) and a slightly narrower 2:1 SWR bandwidth (about 50 kHz narrower) than the hybrid tubing/wire version. Incidentally, the hybrid version can be directly modeled with public-domain MININEC if one uses length-tapering toward the sharp angle corners.

Folded X-beams are normally designed for driver-director arrangements, since it is difficult to obtain significant performance with a driver-reflector arrangement. In the folded configuration of **Fig. A**, the parasitic element almost "wants" to be a director. In less metaphorical terms, a modestly performing driver-reflector design, with only a slight change of reflector length will reverse its pattern and hold that reversal, even though the parasitic element is considerably longer than one might expect for a director. It is also possible to tune the director to move the peak front-to-back portion of the operating curve across the band. By lengthening the director and adding a remotely adjusted bit of capacitive reactance at the center, the peak performance region can be moved across an

amateur band. However, the model used here employs a fixed construction, as the following table shows.

X-Beam

Frequency = 14.1 MHz.

Wire Loss: Aluminum -- Resistivity = 4E-08 ohm-m, Rel. Perm. = 1

WIRES									
Wire Conn.	---	End 1 (x,y,z : in)	Conn.	---	End 2 (x,y,z : in)		Dia(in)	Segs	
1		-99.000, 17.000, 0.000	W2E1	-99.000, 99.000, 0.000		# 12	15		
2	W1E2	-99.000, 99.000, 0.000	W3E1	-6.000, 3.000, 0.000		# 12	25		
3	W2E2	-6.000, 3.000, 0.000	W4E1	6.000, 3.000, 0.000		# 12	3		
4	W3E2	6.000, 3.000, 0.000	W5E1	99.000, 99.000, 0.000		# 12	25		
5	W4E2	99.000, 99.000, 0.000		99.000, 17.000, 0.000		# 12	15		
6		-99.000,-11.000, 0.000	W7E1	-99.000,-99.000, 0.000		# 12	15		
7	W6E2	-99.000,-99.000, 0.000	W8E1	-6.000, -3.000, 0.000		# 12	25		
8	W7E2	-6.000, -3.000, 0.000	W9E1	6.000, -3.000, 0.000		# 12	3		
9	W8E2	6.000, -3.000, 0.000	W10E1	99.000,-99.000, 0.000		# 12	25		
10	W9E2	99.000,-99.000, 0.000		99.000,-11.000, 0.000		# 12	15		

SOURCES						
Source	Wire Seg.	Wire #/Pct From End 1	Ampl.(V, A)	Phase(Deg.)	Type	
	2	Actual (Specified)				
1		8 / 50.00 ( 8 / 50.00 )	1.000	0.000	V	

### Folded X-Beam (DE + Director) Free-Space Gain & Front-to-Back

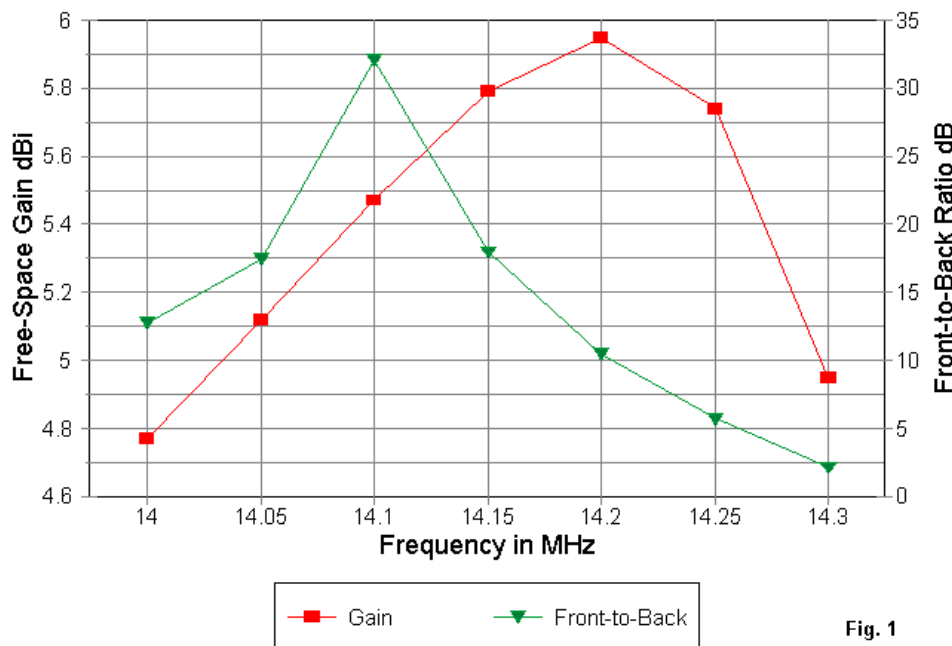


Fig. 1

In **Fig. 1**, we find both the gain and front-to-back curves of the folded X-beam. Because the direction of the beam reverses between 14.3 and 14.35 MHz, the curves are cut off at 14.3 MHz. (The reversal to a driver-reflector beam yields only poor results, never reaching a 10 dB front-to-back ratio.) One of the inherent difficulties of the folded X-beam is that the maximum gain and the

maximum front-to-back ratio are always separated in frequency. The gain at the maximum front-to-back peak is about 0.5 dB below peak. Both the gain and the front-to-back curves are quite steep, indicating a narrow operating passband, whatever the feedpoint impedance characteristics might be. In the past, the chief use of the folded X-beam has been on 10 meters as a home-brew project for those interested in the 28.3 to 28.5 MHz region of the band.

### Folded X-Beam (DE + Director) 20-Ohm VSWR

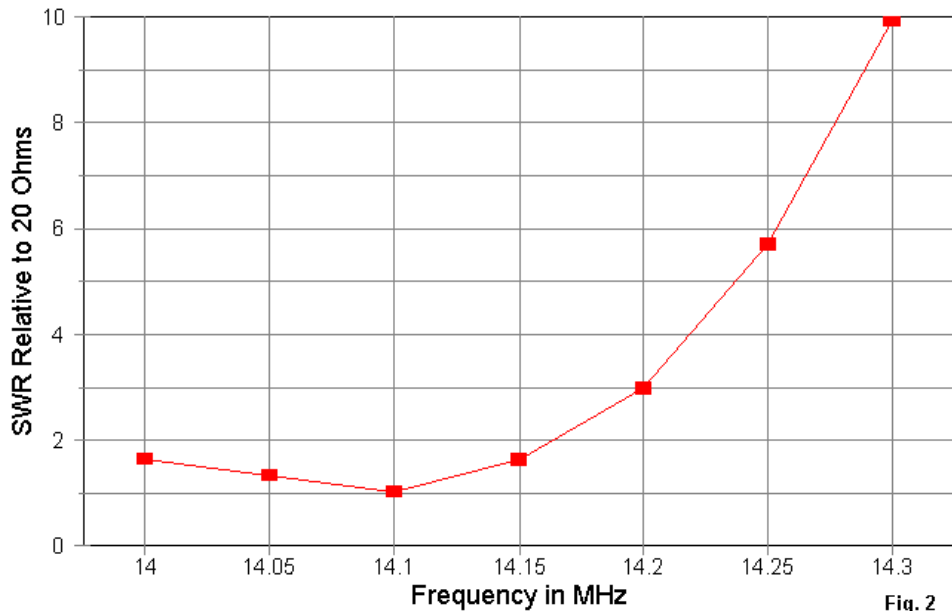
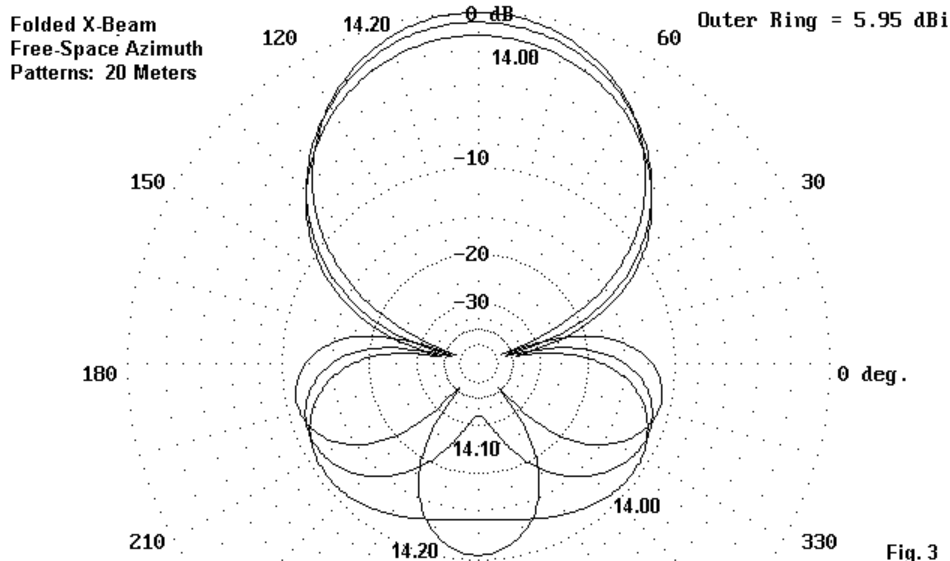


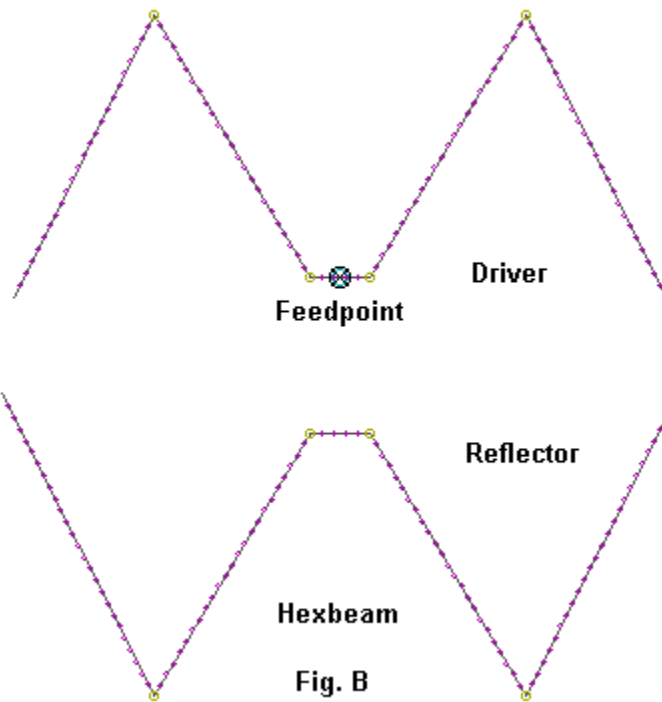
Fig. 2

The SWR curve, in **Fig. 2**, is referenced to 20 Ohms, which is approximately the impedance at the maximum front-to-back peak. Indeed, this design shows operating characteristics that are directly tied to the feedpoint impedance. A near 50-Ohm impedance is possible at the lowest frequency in the passband, with a low gain and relatively poor front-to-back ratio. Where the front-to-back ratio peaks, the impedance is from 20 to 25 Ohms, depending on the thickness of the element materials. At the maximum gain point, the feedpoint impedance drops to the 10-15-Ohm region. Wire versions of the antenna tend to show impedance values at the low end of the ranges indicated, while tubular and hybrid versions yield impedances values at the higher ends of the ranges.



The peak gain and 180-degree front-to-back ratio figures can give a misimpression. The peak gain of about 6 dBi (free space) rivals that of a 2-element Yagi whose elements take twice the space side-to-side. Likewise, the peak 180-degree front-to-back ration of over 32 dB sounds impressive. However, the patterns in **Fig. 3** tell a somewhat different tale (as do the passband graphs we have viewed). An averaged front-to-rear ratio for the entire rear area of the beam has, within the 200 kHz of prime operation, a value of between 10 and 15 dB--no better than a common 2-element driver-reflector Yagi. The Yagi would also have superior gain over X-beam at every frequency and be able to cover the entire 20-meter band. A 2-element Yagi with about 1/8 wavelength element spacing and loaded elements that are about 3/4ths full size would occupy about the same area as the X-beam with broader performance curves. Hence, the folded X-beam has fallen into relative disuse.

## The Hex Beam



If we fold the X-beam tails outward, we obtain the basic configuration of the hex(agon) beam, although true hex beams are built as closely to the hexagon geometry as the support structure will permit. **Fig. B** shows the outline of the model used to generate

performance curves. The details of the model used in this study, which is a significantly modified version of a model originally provided by N7CL, follow in the chart.

hex beam: 20 meters Frequency = 14.1 MHz.

Wire Loss: Aluminum -- Resistivity = 4E-08 ohm-m, Rel. Perm. = 1

WIRES						
Wire Conn.	---	End 1 (x,y,z : in)	Conn.	---	End 2 (x,y,z : in)	Dia(in) Segs
1		-108.00, 19.500,	0.000	W2E1	-61.800, 113.000,	0.000 # 12 22
2	W1E2	-61.800, 113.000,	0.000	W3E1	-9.950, 25.900,	0.000 # 12 26
3	W2E2	-9.950, 25.900,	0.000	W4E1	9.900, 25.900,	0.000 # 12 5
4	W3E2	9.900, 25.900,	0.000	W5E1	61.800, 113.000,	0.000 # 12 26
5	W4E2	61.800, 113.000,	0.000		108.000, 19.500,	0.000 # 12 22
6		-112.00, -12.900,	0.000	W7E1	-61.800, -113.00,	0.000 # 12 23
7	W6E2	-61.800, -113.00,	0.000	W8E1	-9.950, -25.900,	0.000 # 12 26
8	W7E2	-9.950, -25.900,	0.000	W9E1	9.950, -25.900,	0.000 # 12 5
9	W8E2	9.950, -25.900,	0.000	W10E1	61.800, -113.00,	0.000 # 12 26
10	W9E2	61.800, -113.00,	0.000		112.000, -12.900,	0.000 # 12 23

SOURCES						
Source	Wire Seg.	Wire #/Pct Actual	From End 1 (Specified)	Ampl.(V, A)	Phase(Deg.)	Type
1	3	3 / 50.00	( 3 / 50.00 )	1.000	0.000	I

TRANSMISSION LINES							
Line	Wire #/% Actual	From End 1 (Specified)	Wire #/% Actual	From End 1 (Specified)	Length	z0 Ohms	Vel Rev/ Fact Norm
1	3/50.0	( 3/50.0 )	Short ckt	( Short ck )	12.000 in	600.0	1.00

One feature of this model is the relatively wide spacing of the centers of the Vee-ed sections. This move tends to lower the feedpoint impedance to the 25-Ohm region, and the model uses a 12" stub of 600-Ohm shorted transmission line as a beta hairpin to effect a 50-Ohm match. It is possible to bring the center points of the driver and reflector closer together to obtain a direct 50-Ohm match. However, two deficits emerge with this move. First, the 50-Ohm match does not extend across the entire 20-meter band

because the sharpness of the geometry yields a corresponding tuning sharpness. In contrast, the beta-matched 25-Ohm impedance does cover the entire 20-meter band with a 50-Ohm SWR of under 2:1. Second, with the center Vee points brought closer together, array performance smoothes out across the band, but at much lower levels of gain and front-to-back ratio than we obtain from the wider-spaced center region. Therefore, I have chosen to look at the lower impedance version of the antenna with its better performance peaks.

The hex beam has a design affinity with a number of other members of the end-coupled clan that we shall not examine here. The slope of the outer sections of each end toward the other element is a property shared by several interesting antenna designs, including a 2-element reversible wire beam for 40 meters developed by AA2NN. The antenna uses a double slope, since the elements each form an inverted Vee. As well, each element end approaches the corresponding end of the other element. The result is a beam that requires only two center supports. As well, by using rope on the ends of the elements, the tie down points will also be reduced to 2. Equally related to the outer structure of the hex beam is the 3-element 40-meter reversible Yagi developed by WA3FET. It uses a linear driver and a pair of parasitic elements, each of which is sloped toward the end of the driver. One parasitic element is loaded for reflector duty. One advantage of element tips that slope toward each other rather than point directly at each other, is the greater ease of adjustment. Small changes of spacing of the tips produce less radical effects than when the tips are end-to-end.

### Hex Beam Free-Space Gain & Front-to-Back

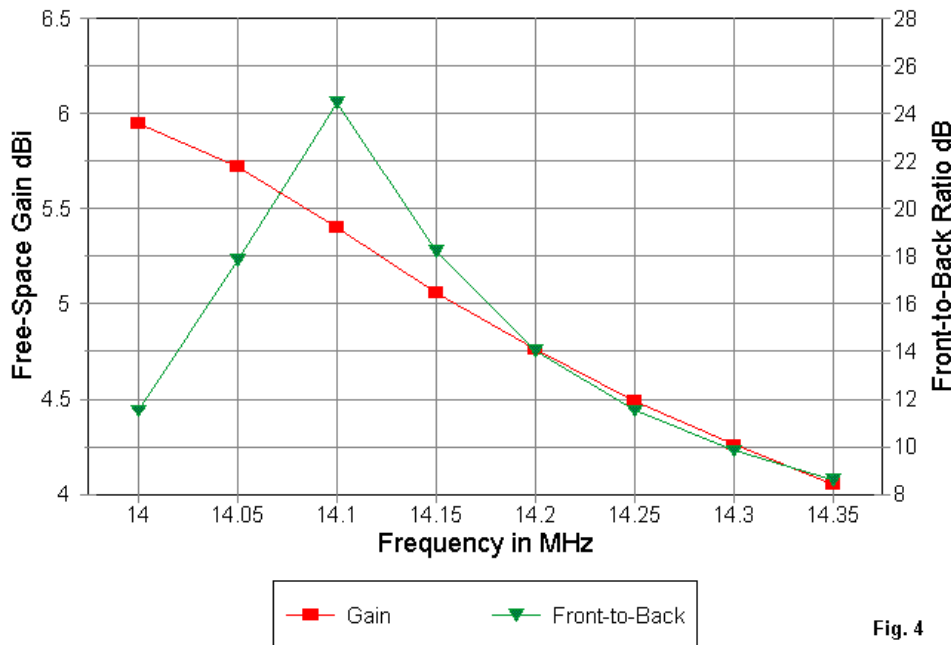


Fig. 4

**Fig. 4** presents the gain and 180-degree front-to-back ratio figures across 20 meters. The gain variation across the band is nearly 2 dB, a fairly high figure among common 2-element beam designs. The front-to-back ratio shows a very sharp peak, but decreases rapidly to band-edge values in the 8 to 12 dB range. Peak operation of this antenna has a bandwidth of 100 to 150 kHz, with the

remainder of the band showing relatively mediocre performance. Nonetheless, like all members of the semi-closed geometry family, the hex beam permits a high front-to-back peak whose decline is steeper below the peak frequency than above it.

Hex Beam  
50-Ohm VSWR

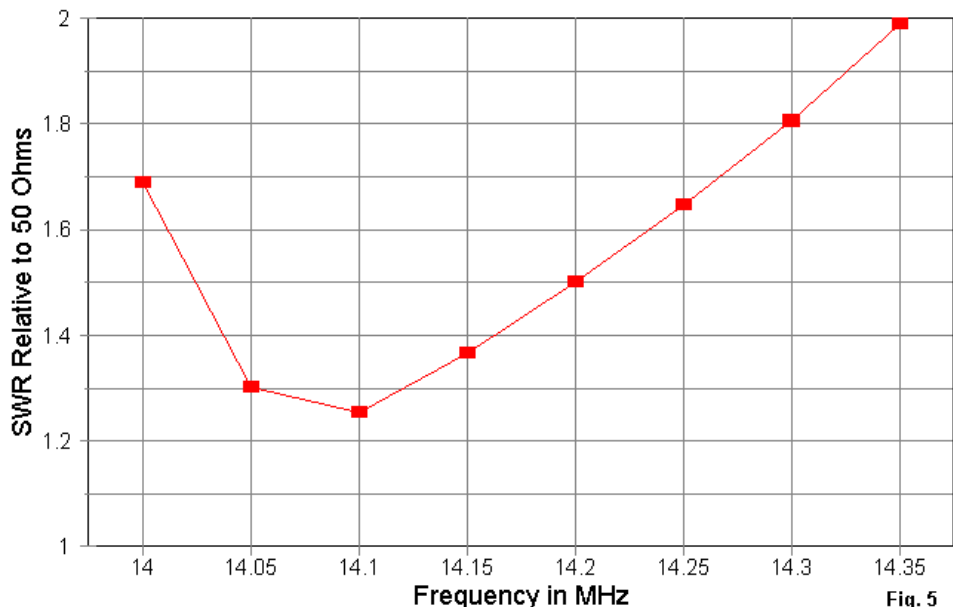
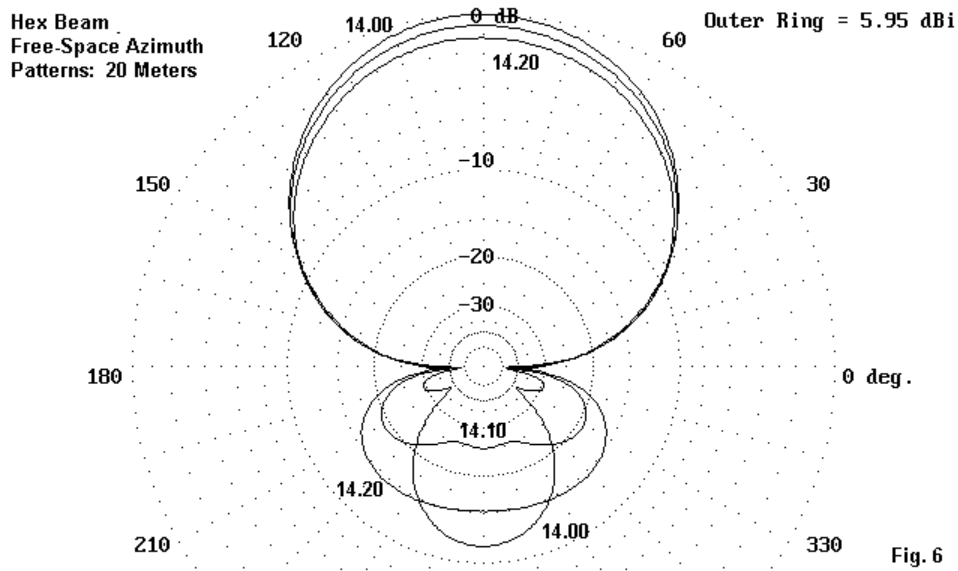


Fig. 5

**Fig. 5** illustrates one of the illusions of SWR. One could suggest that this model of the hex beam antenna has an operating bandwidth that covers the entire band, since the 50-Ohm SWR is

less than 2:1 across 20 meters. However, operating bandwidth involves more parameters than just the SWR. Evaluating the gain and front-to-back ratio is equally as important, if not more so, than the SWR. For this particular design of the hex beam, the only wide-band parameter is SWR. Gain and front-to-back ratio values are relatively narrow band properties.



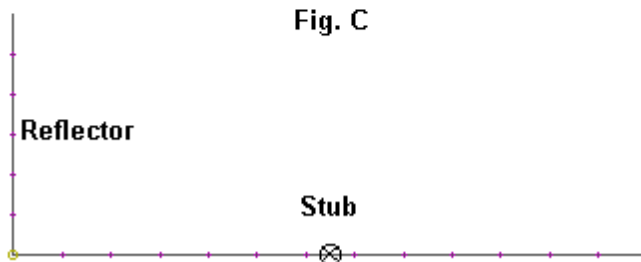
**Fig. 6** shows free-space azimuth patterns for the first 200 kHz of 20 meters. The pattern at 14.1 MHz is well controlled, but off peak, the rearward pattern spreads to average values in the 15 dB range. Beyond 14.2 MHz, the rearward pattern spreads larger and the forward gain decreases rapidly.

In general, like the X-beam and other beams based upon vee-ing the center parts of the elements, the hex beam shows a quite narrow operating bandwidth relative to gain and front-to-back ratio. The rate and total gain change across the band and the band-edge front-to-back ratio values are very important in evaluating the operating bandwidth of an antenna.

For further extensive information on home-brew hexbeams, see G3TXQ's website <http://www.karinya.net/g3txq/hexbeam/> or K4KIO's site <http://www.leoshoemaker.com/hexbeambyk4kio/general.html>

**NOTE: URLs may go stale over time.**

## The VK2ABQ Square



The VK2ABQ Square (and the Moxon Rectangle) are more fully described in "Modeling and Understanding Small Beams: Part 2: VK2ABQ Squares and The Modified Moxon Rectangle," *Communications Quarterly*, (Spring, 1995), 55-70. The origins of the square go back to the 1930s, only to disappear and re-emerge in the 1960s. **Fig. C** shows the outlines of a modified square. The modification consists of loading the reflector with a shorted

transmission line stub about 6" long to move the peak performance point without disturbing the square shape.

The original VK2ABQ square used very close-spaced element tips--only a literal coat button apart. However, very close tip spacing creates an array with narrow-band properties, and small variations in construction can yield large variations in performance. Therefore, the model below uses fairly wide spacing (34") for the element tips.

**VK2ABQ 20 Meters** Frequency = 14.15 MHz.

Wire Loss: Copper -- Resistivity = 1.74E-08 ohm-m, Rel. Perm. = 1

----- WIRES -----  
**Wire Conn. --- End 1 (x,y,z : in) Conn. --- End 2 (x,y,z : in) Dia(in) Segs**

1	-118.22, 16.889,	0.000	W2E1 -118.22,106.159,	0.000	# 12	6
2	W1E2 -118.22,106.159,	0.000	W3E1 118.222,106.159,	0.000	# 12	13
3	W2E2 118.222,106.159,	0.000	118.222, 16.889,	0.000	# 12	6
4	-118.22,-16.889,	0.000	W5E1 -118.22,-106.16,	0.000	# 12	6
5	W4E2 -118.22,-106.16,	0.000	W6E1 118.222,-106.16,	0.000	# 12	13
6	W5E2 118.222,-106.16,	0.000	118.222,-16.889,	0.000	# 12	6

----- SOURCES -----  
**Source      Wire      Wire #/Pct From End 1      Ampl.(V, A)      Phase(Deg.)      Type**

Source	Wire Seg.	Wire #/Pct From End 1	Ampl.(V, A)	Phase(Deg.)	Type
1	7	2 / 50.00    ( 2 / 50.00 )	1.000	0.000	I

----- TRANSMISSION LINES -----  
**Line      Wire #/% From End 1      Wire #/% From End 1      Length      Z0      Vel Rev/**

Line	Wire #/% From End 1	Wire #/% From End 1	Length	Z0	Vel	Rev/
1	Actual (Specified)	Actual (Specified)		Ohms	Fact	Norm
1	5/50.0 ( 5/50.0 )	Short ckt (Short ck)	5.892 in	600.0	1.00	

As the model shows, this version of the antenna is off square by about 12 inches. In this highly square (if imperfectly square) configuration, the feedpoint impedance is about 100 Ohms, making the antenna a candidate for a 2:1 balun at the feedpoint.

### VK2ABQ Square (Modified) Free-Space Gain & Front-to-Back

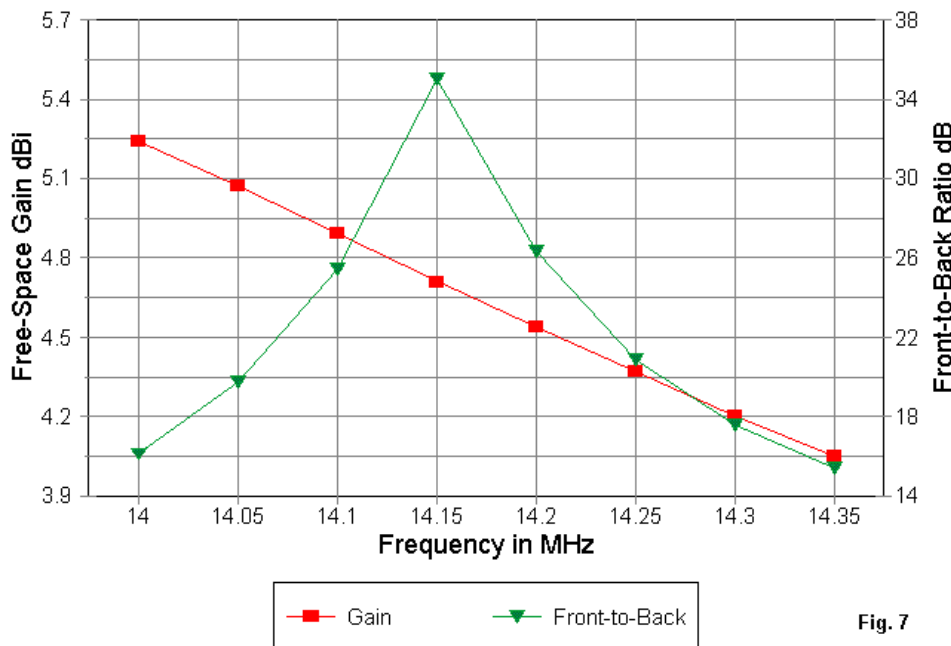


Fig. 7

As shown by Fig. 7, the VK2ABQ square is a relatively low gain beam, although the gain varies only about 1.1 dB across the band. Hence, the 4.05 dB gain at the high end of the band equals that of the hex beam. The square's 180-degree front-to-back ratio peaks above 34 dB. Although the curves are fairly steep, the band edge

values are about 15 dB--not bad for a 2-element parasitic beam that is about 1/4 wavelength on a side.

### VK2ABQ Square (Modified) 100-Ohm VSWR

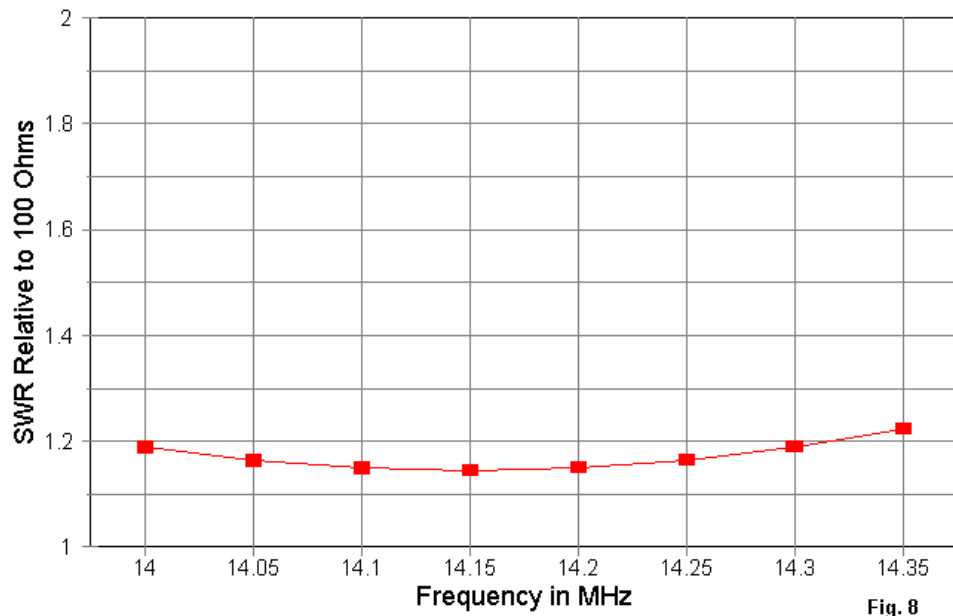


Fig. 8

As **Fig. 8** shows, the real surprise of the modified VK2ABQ square is the 100-Ohm impedance curve. Across all of 20 meters, the resistive portion of the feedpoint impedance varies by under 6 Ohms, and the reactance varies by a similar amount. Hence, the

SWR curve is very flat indeed. A 2:1 balun would permit operation across the entire 20-meter band with an exceptionally low SWR and no conditions to incur losses within the balun.

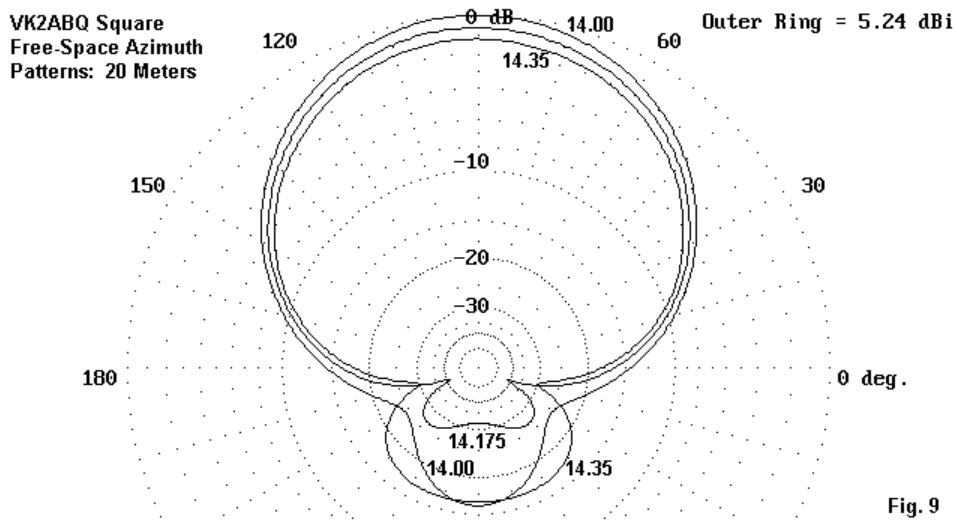


Fig. 9

The VK2ABQ was the basis for the later Moxon Rectangle. The key performance feature absorbed from the square was the excellent control of the rear portion of the radiation pattern. **Fig. 9** shows the band-edge and mid-band pattern for the square. If the square is constructed of 1" aluminum tubing, the band-edge front-to-back ratio improves to nearly 20 dB, with a small increase in array gain as well.

In all, the square is a relatively wide-band array whose characteristic remain reasonably level across the band (gain and

impedance) or hold to minimal acceptable levels (front-to-back ratio). However, the chief deficit of the square is gain. In fact, one can preserve the front-to-back performance while improving gain--and as a bonus achieve a direct 50-Ohm match. The cost is going considerably out of square.

## The Moxon Rectangle

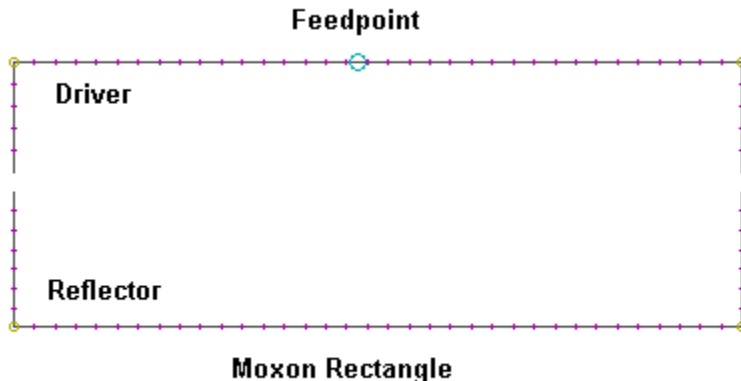


Fig. D

Because the 3 family members we have so far examined use relatively wide spacing between facing element tips, many designers have ignored the effects of this dimension. The result has been a number of fairly poor designs. The element tip spacing influences the relative proportions of every other dimension of any of the family members. Nowhere is this more apparent than with the

optimized Moxon rectangle, sketched in Fig. D. The combination of close tip coupling as well as more extended parallel element coupling allows the Moxon rectangle to recover the gain lost by the square while maintaining fairly wide-band operating characteristics. It is the longer sections of parallel elements that permit the close tip spacing to be controllable without sudden shifts in the direction of the pattern.

The #12 copper wire model for this study reveals that the side-to-side length is about 3/8 wavelength, while the front-to-back size is about 1/8 wavelength. Hence, the total area of the antenna is less than the 1/4 wavelength squares, although the turn radius is greater. The details of the model used here are as follows:

```
Moxon rectangle                               Frequency = 14.175  MHz.

Wire Loss: Copper -- Resistivity = 1.74E-08 ohm-m, Rel. Perm. = 1

----- WIRES -----
Wire Conn. --- End 1 (x,y,z : in)   Conn. --- End 2 (x,y,z : in)   Dia(in) Segs
1      -151.74, 64.188, 0.000    W2E1 -151.74,110.377, 0.000 8.08E-02  5
2      W1E2 -151.74,110.377, 0.000    W3E1 151.740,110.377, 0.000 8.08E-02  35
3      W2E2 151.740,110.377, 0.000    151.740, 64.188, 0.000 8.08E-02  5
4      -151.74, 56.433, 0.000    W5E1 -151.74, 0.000, 0.000 8.08E-02  7
5      W4E2 -151.74, 0.000, 0.000    W6E1 151.740, 0.000, 0.000 8.08E-02  35
6      W5E2 151.740, 0.000, 0.000    151.740, 56.433, 0.000 8.08E-02  7

----- SOURCES -----
Source   Wire      Wire #/Pct From End 1   Ampl.(V, A)   Phase(Deg.)   Type
          Seg.      Actual        (Specified)
1        17        2 / 47.14     ( 2 / 47.14)       0.707        0.000           V
```

As the model shows, the rectangle is about 50% longer (side-to-side) than the squares. Tip-to-tip spacing is about 8". In the August, 2000, issue of *antenneX*, I published a small program that inputs

only the design frequency and wire diameter to yield optimized dimensions for Moxon rectangles for the HF and VHF regions. The designs provide a direct 50-Ohm match, whether used for rotatable or reversible beams.

### Moxon Rectangle Free-Space Gain & Front-to-Back

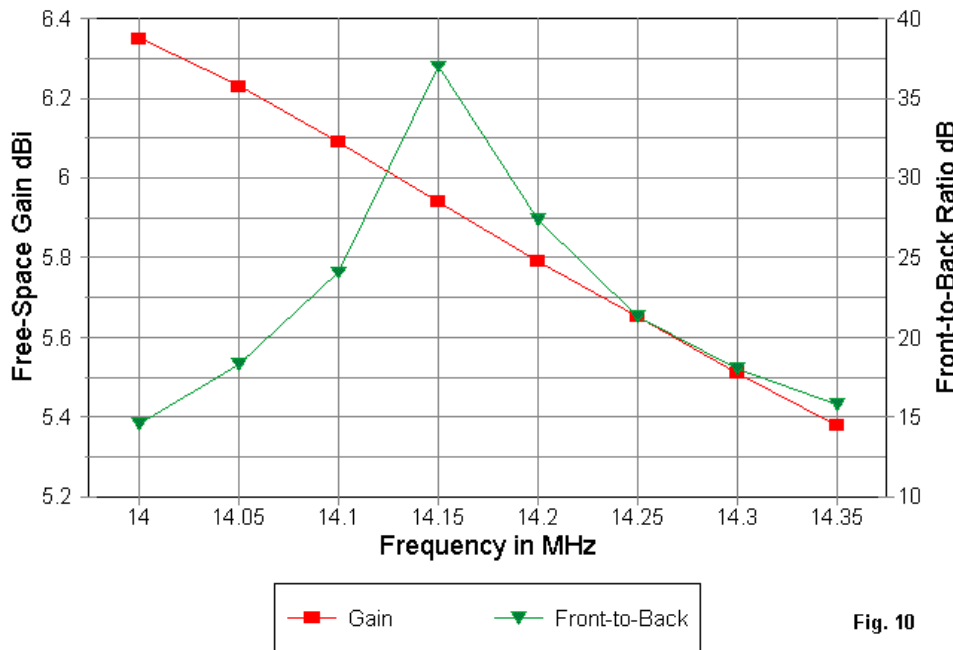


Fig. 10

The gain curve in **Fig. 10** for the Moxon is a full dB better than for the square, although the total change in gain across the band is about the same. Since the Moxon rectangle can easily be fabricated of aluminum tubing, the result will be another 0.2 dB of gain and slightly less change in the gain across the band. As well, the band-edge front-to-back ratio values will improve to nearly 20 dB from the wire values of 15 dB. As with all of the semi-closed geometry designs, the front-to-back ratio is peaked just below the center of the band in order to achieve relatively similar front-to-back values at the band edges.

Both the square and the Moxon use the combination of parallel element coupling and end-coupling to achieve a very high front-to-back ratio at a design frequency. Indeed, in both cases, the current magnitude and phasing on the parasitic element center is very close to the precise values needed for a maximum front-to-back ratio if each element were to be independently fed and phased. Only the existence of the "tails" which radiate (if only weakly), prevents the pattern from becoming the deep dimple of a perfectly phased pair of elements.

### Moxon Rectangle 50-Ohm VSWR

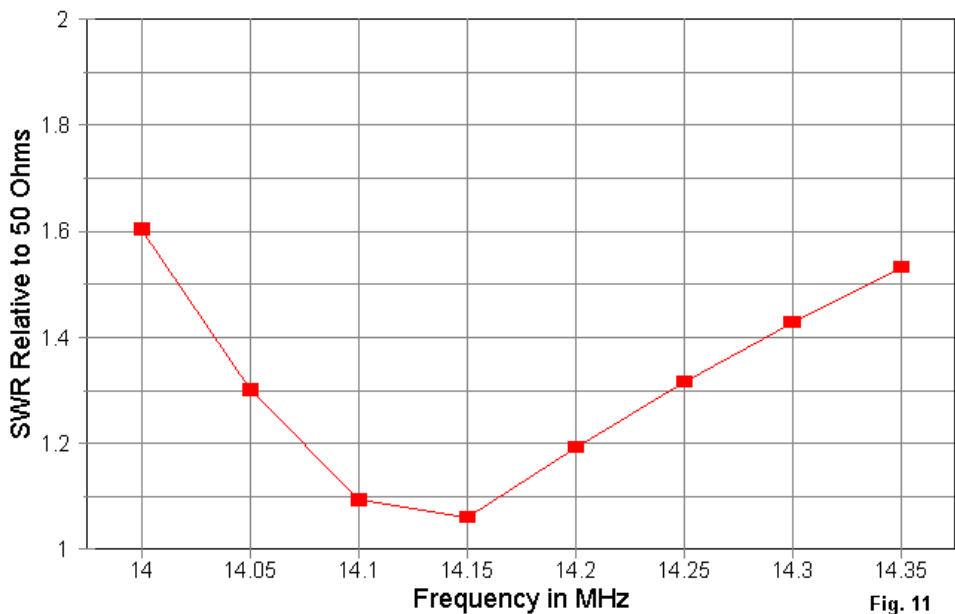


Fig. 11

The 50-Ohm SWR curve in **Fig. 11** is for a direct match to coaxial cable with no matching required (although a common-mode current suppression choke or 1:1 balun is always in order). Unlike the SWR curve for the VK2ABQ square, the Moxon SWR curve shows a definite slope, although the band edge figures are acceptable under most conditions. The curve flattens further if one uses aluminum tubing of about 1" diameter for the antenna.

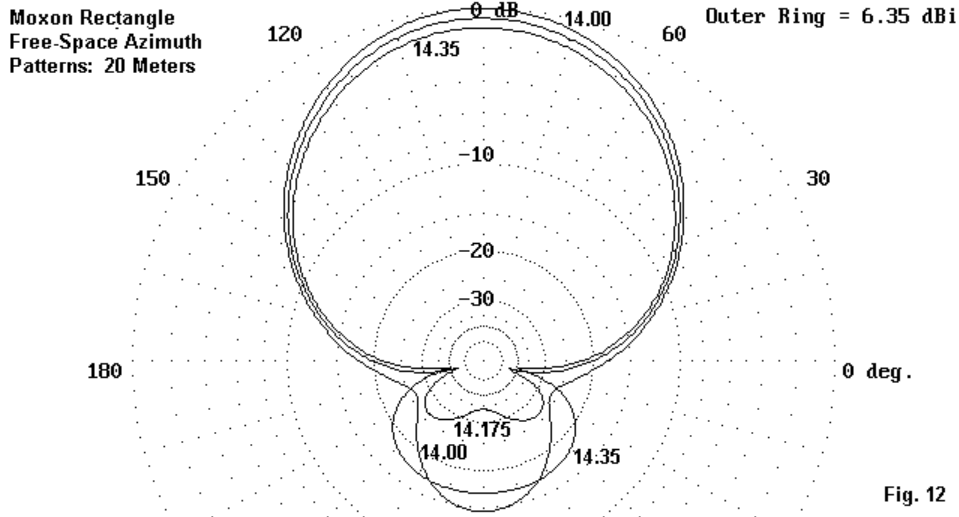


Fig. 12

The Moxon rectangle shares with the VK2ABQ square a nearly cardioidal pattern. The deepest "side" nulls do not occur at 90 degrees off the bearing of maximum gain, but somewhat further toward the rear, as is evident in **Fig. 12**. The rear lobes are well behaved, that is, they have no large quartering side lobes. The rearward lobes for the band edges shrink as the element diameter becomes larger.

### Some Tentative Conclusions

This survey of semi-closed geometry end-coupled beams should suffice to reveal the family resemblances among the members of the clan. It may be useful to summarize some of the properties that both link and separate the individual members.

1. Designs with element center regions that are parallel or only gently sloped outward toward the ends tend to show wider-band characteristics than those whose element centers are Vee-ed toward each other.
2. Element tips display two regions of coupling. Wider spacing between tips tends to produce lower gain, although small changes in spacing yield less radical effects. Closely spaced tips tend to be more critical and may be effectively usable only if most of the element length is either parallel or only gently slopes to bring the tips closer together.
3. Semi-closed beam designs tend toward loop properties, such as an increase in perimeter dimensions with an increase in element diameter. Sloping element designs are most immune to this effect and may show more typical linear element properties.
4. Designs that strive for a minimum turning radius tend either to have narrow-band characteristics or lower gain. The Moxon rectangle represents a compromise geometry that achieves as good or better gain than the other 2-element members of the clan while achieving a high front-to-back ratio and relatively broad-band characteristics. Sometimes the best square is a rectangle.
5. Both the front-to-back ratio and SWR curves tend to deteriorate much faster below the design frequency than above it. Therefore, to achieve relatively equal performance at both the lower and upper band edges, the appropriate design frequency is about 1/3 the way up the band. For 2-element driver-reflector designs, whether using

a standard Yagi configuration or one of the end-coupled designs, the gain will decrease as frequency increases.

I have over the years built and used most of the designs we have discussed here in 10-meter versions, using both wire and aluminum construction. The models employed here are variants of those antennas, as well as of published data. No commercial antennas are modeled for these notes. Their intent is simply to show both the resemblances and differences among members of the end-coupled clan of beams.

## Chapter 62: The EDZ Beams

**S**ome time back, I wrote a piece for *Communications Quarterly* on the Extended Double Zepp ("Modeling and Understanding Small Beams: Part 3: The EDZ Family of Antennas," Fall, 1995, 53-71). My hope was to improve our understanding of the EDZ and look at some of its possibilities.

The EDZ in its simplest form is a non-resonant wire antenna about 5/4 wavelengths long. Being non-resonant, exact length is non-critical. Shorter versions have smaller side lobes but higher capacitive reactance; longer versions the reverse. Feedpoint impedance ranges from 100 to 150 ohms resistive with well over 600 ohms capacitive reactance. The chief reason for using the EDZ is its 1.5+ dB gain over a dipole comparably situated.

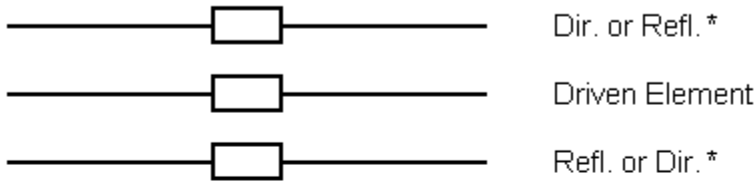
Brian Egan, ZL1LE and I had been discussing EDZ potentials since about 1991. He initially suggested a 2-element beam consisting of an EDZ driven element plus two Yagi-type reflector elements spaced a few feet behind the driven element and each pushed sideways to the wire end limits of the driven element. Modeling this configuration seemed to make a different arrangement preferable. From this arose the 2-element (driven element- reflector) beam noted in the article. The center of each element is inductively loaded, one for matching the feedline, the other for optimizing the rear element as a reflector. With 1/2 wavelength parallel lines down to near ground level, the two matching/loading units could be reversed, reversing the direction of the beam. This installation was tested for a couple of years at W4RNL and worked quite credibly.

Well, folks, as the old song says, "Everything old is new again." Bill McDowell, K4CIA, sent me a copy of an article from the June, 1938, QST, "The Extended Double-Zepp Antenna." In the back pages is a description of how to add a parasitical element to the EDZ. Author Hugo Romander, W2NB, describes a 0.2 wavelength spaced array. The driven element is stub matched to the source feedline. The other element is stub loaded inductively, but at two points: one for use as a reflector, the other for use as a director. Hence, a different system for a reversible beam--and a perfectly competent one. W2NB's system has the advantage of simplicity, while ours has the advantage of convenience. It can be fun to discover that one has reinvented the wheel. Fortunately, the information I added to the end of my article reviewing the principles of stub matching and loading would aid one to replicate the W2NB EDZ beam, so I do not feel totally disconnected from the 1938 work.

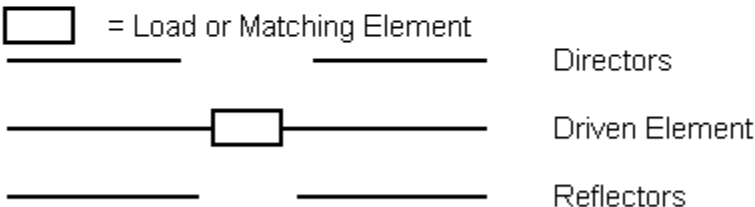
From time-to-time, folks discuss the possibilities for a 3-element EDZ beam. Henry Pollock, WB4HFL, is actually planning to build one. The idea led me to try to verify his modeling results and to compare his configuration to an alternative.

As with the 2-element EDZ, one has two main choices of configuration: 3 long elements or a long driven element with pairs of Yagi elements (directors and reflectors) at the extreme limits of the EDZ driving element.

### 3-Wire EDZ Beam



\* Depends on the values of the loading elements.



### Double-Yagi EDZ Beam

## 2 Types of Parasitical EDZ Beams

Henry has chosen the double-Yagi version, and very likely wisely so. Since he plans to put it at 60' for 10 meters, let's look at modeling results for both arrangements centered at 28.5 MHz.

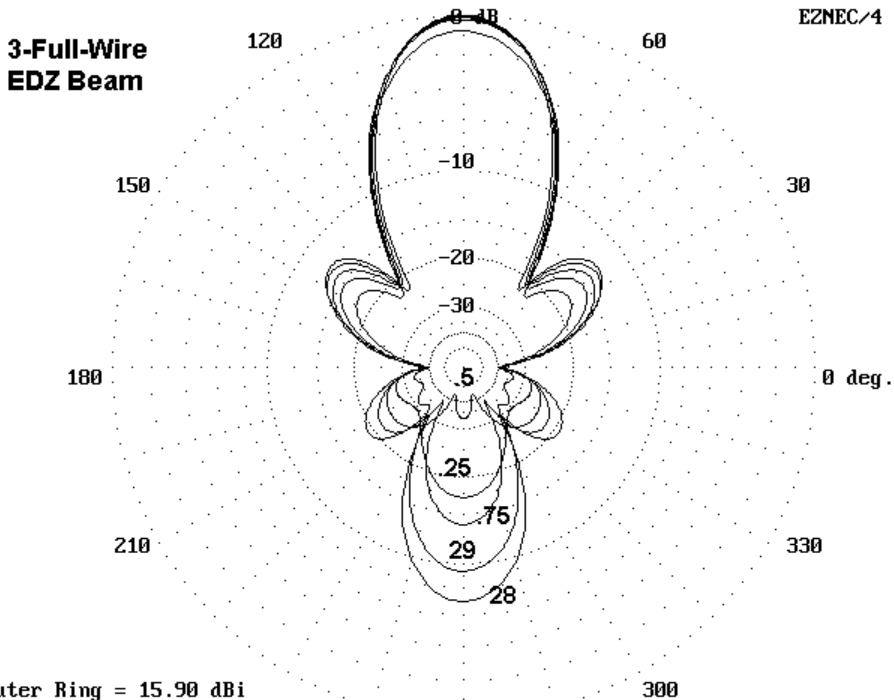
The 3-wire EDZ beam can be built from 3 41'8" lengths of #12 wire, each with a center load. The director requires about 800 ohms, the reflector 1150 ohms, and the driven element 980 ohms. The resulting antenna has a resonant feed resistance of about 90-95 ohms, just about right for a 1/4 wl matching section of 70 ohm coax

to the regular 50-ohm feedline. You can make the director and reflector inductive loads from coils or from 450-ohm parallel vinyl covered feedline stubs 5.5' and 6.25' long each. If you do not use a split coil for the driven element feed point, you may wish to design a stub matching system--or perhaps use an ATU and parallel line all the way.

The potential beam performance at 60' is quite good: 15.5 dBi gain with about 30 dB front-to-back ratio. Adding the director to our old 2-element EDZ beam really improves the front-to-back ratio more than it helps raw gain.

But here is the rub:

The 3-wire EDZ beam is quite narrow-band in pattern--and even more so in feedpoint impedance and loading. At 28 and 29 MHz, the front-to-back ratio drops to the 7-9 dB range. The feedpoint shows a 250-ohm reactance change across the band. This is a beam that needs adjustment of all 3 elements if one hopes to cover more than 100 kHz of 10 meters. (For lower band versions, narrow the bandwidth in proportion of the ratio of the desired lower frequency to 28.5 MHz.)

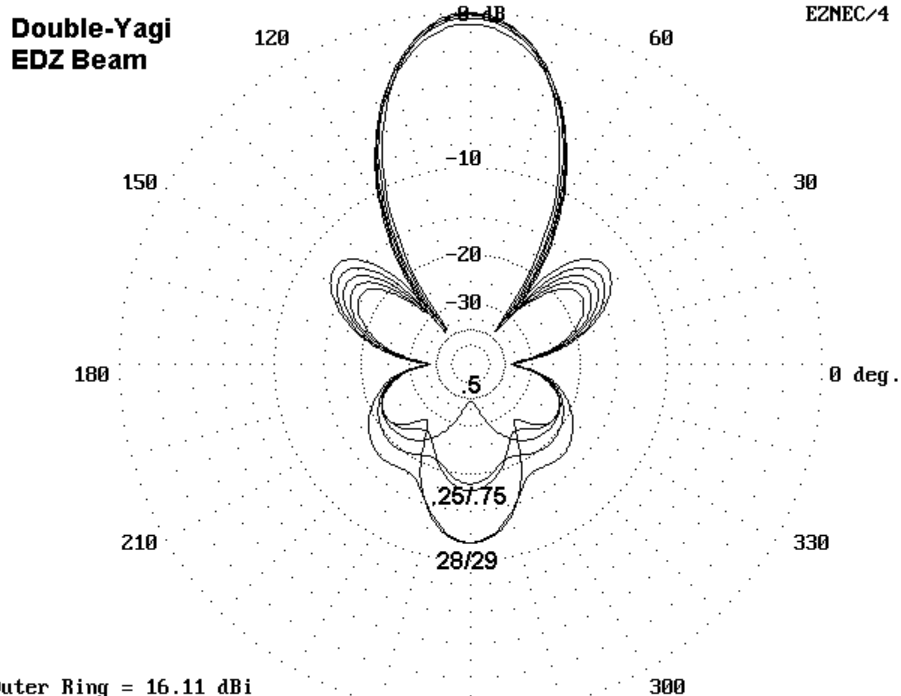


The double Yagi EDZ tells a somewhat different story. WB4HFL did not give me detailed dimensions, so I modeled my own version, with directors and reflectors spaced 5' from the driven element. Parasitical elements had outer limits in line with the end of the EDZ element (41'8"). Reflectors were 17'1" and directors were 16'0.5" long. #12 wire, of course, for consistency throughout.

The results at the design center frequency were interesting: 16.0 dBi gain with a front-to-back ratio of 38 dB at 60' height. The front-to-rear quadrants had a minimum ratio of about 21 dB. What the 3-wire gives us in a slightly better front-to-rear ratio at design center is offset by the added gain of the double-Yagi version. Feedpoint impedance of the double Yagi version is about  $90 - j1000$  ohms, calling for a stub match or an ATU feed system.

However, the WB4HFL-style design has two hidden advantages, partially revealed by a frequency sweep:

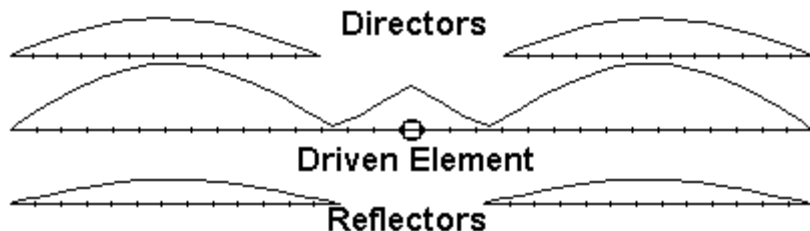
First, the double-Yagi version retains a better figure from 28 to 29 MHz, never sinking below 11 dB front-to-back ratio at those extremes. While not superlative, the ratio climbs to nearly 20 dB at the 28.25 and 28.75 marks. These numbers are far superior to the 3-wire beam.



Second, the only adjustment needed across the band is the driven element tuning. Like its counterpart, the double-Yagi version shows a 250-ohm reactance excursion across the band, along with a 75-ohm change in the resistive component. However, parallel feedline and a good ATU would take care of the problem. Because of the high reactance-to-resistance ratio, one might have to carefully select the line length in order to present the ATU with a load it can

handle most efficiently. Nonetheless, no other adjustments are necessary, a plus for the double-Yagi design.

Now why does the double-Yagi version work?



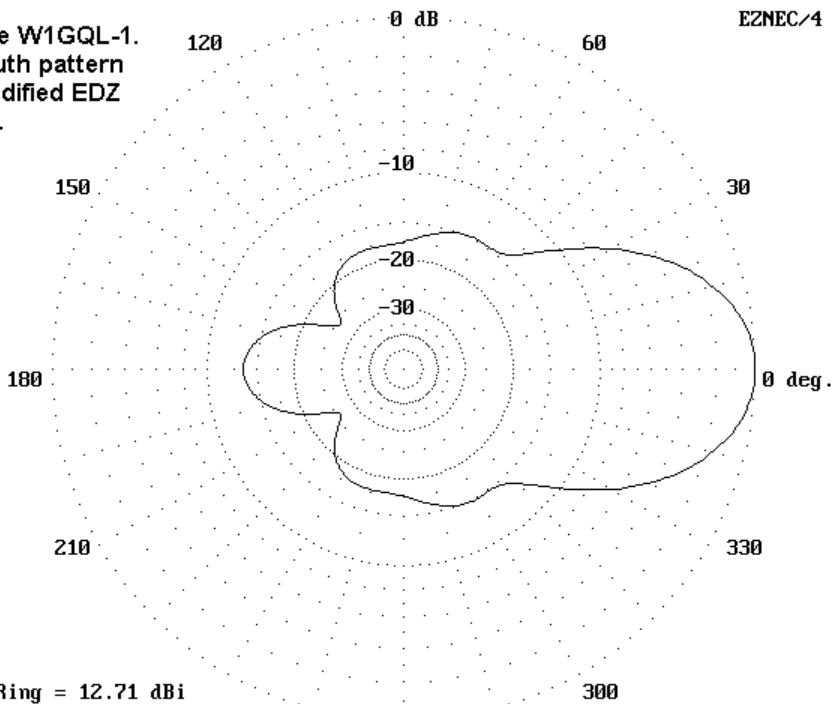
### Current patterns on the Double-Yagi EDZ Beam

If you look at the current distribution along the EDZ, it consists of a small central peak with outward dips. The outer  $1/2$  wavelength of the EDZ wire on either side is a perfect dipole current distribution pattern. Parasitical elements aligned with these peaks perform just as they would with independent in-phase separate driven elements. The 3-element double Yagi EDZ beam is actually a form of two in-phase-fed side-by-side 3-element Yagis with  $1/4$ -wavelength tip-to-tip spacing. And the performance is just about the same.

One question that often arises with EDZ beams is how do we get rid of the ears in the pattern, those quartering side lobes. W1GQL, David Billheimer, sent me a design that accomplishes just that--an

ear-less EDZ beam. Figure W1GQL-1 shows the azimuth pattern of this 20-meter 2-element wire beam.

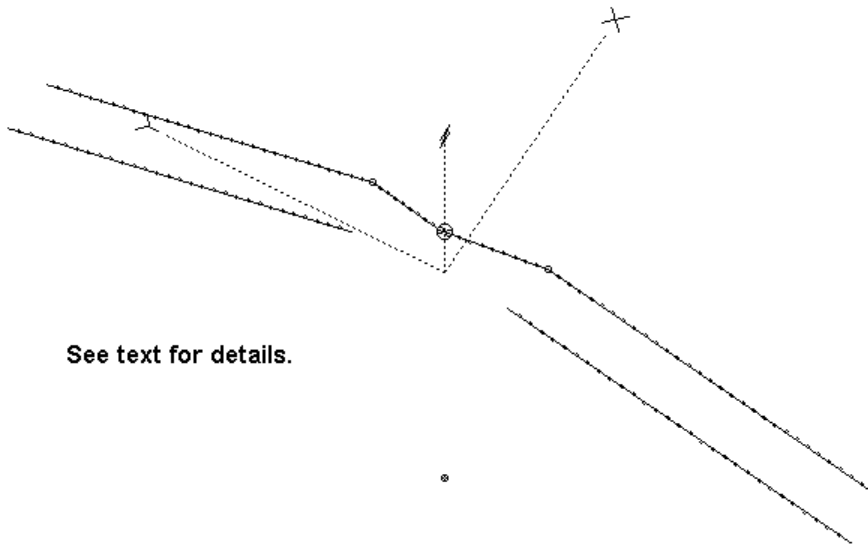
Figure W1GQL-1.  
Azimuth pattern  
of modified EDZ  
beam.



Dave's technique is to create what looks to me like a "gull-wing" design: the driven element is drawn in to midway between the 2 elements, while the parallel sections are drooped like a Vee. See Figure W1GQL-2.

EZNEC/4 2.0

Figure W1GQL-2. General outline of the "gull-wing" EDZ beam.



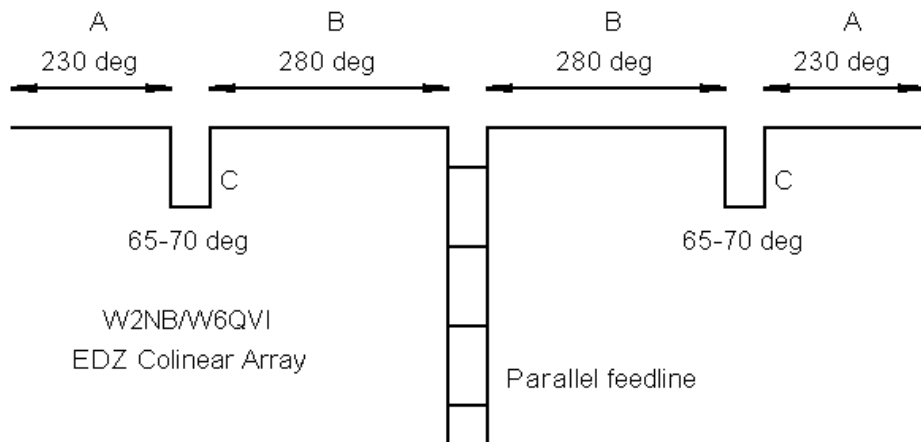
See text for details.

Dave's 20-meter CW beam has a 50' maximum height. The elements are about 5' apart. The two reflectors begin about 14.5' apart and droop to the 33.6' level at a maximum width of 39.4' each side of center. The driven element legs (beginning at center) move outward and forward to a little over 8' each side of center and then parallel the reflectors. (I have rounded the dimension numbers.)

The natural feedpoint of this ear-less EDZ beam is about 60 ohms resistive and  $-j1000$  ohms reactive. Dave uses stub-tuning to match 50-ohm coax for his narrow-band CW needs. However, the pattern of the beam holds up across 20-meters and can be fed with parallel feedline and an ATU quite effectively.

I have added Dave's beam to demonstrate that we have not yet exhausted all the possibilities with either EDZs or wire beams. Among these notes and two articles, we have look at EDZs, stacked EDZs, parasitical EDZs, bent EDZs, and phased EDZs. I must be overlooking something. . .

Of course: co-linear EDZs, George Goldstone, W8AP, sent me some correspondence he had with Hugo Romander, W2NB (W6CH in the 1960s), and Henry Pollock, WB4HFL, sent me a copy of a *Ham Radio* article by Alvan Mitchell, W6QVI. The article was an update on Hugo's co-linear EDZ array, which the *ARRL Antenna Book* of 1943 still carried. Since few folks have access to either Hugo's 1938 article or the 1943 *Antenna Book*, let's take a look at this version of the EDZ, outlined in the figure below.



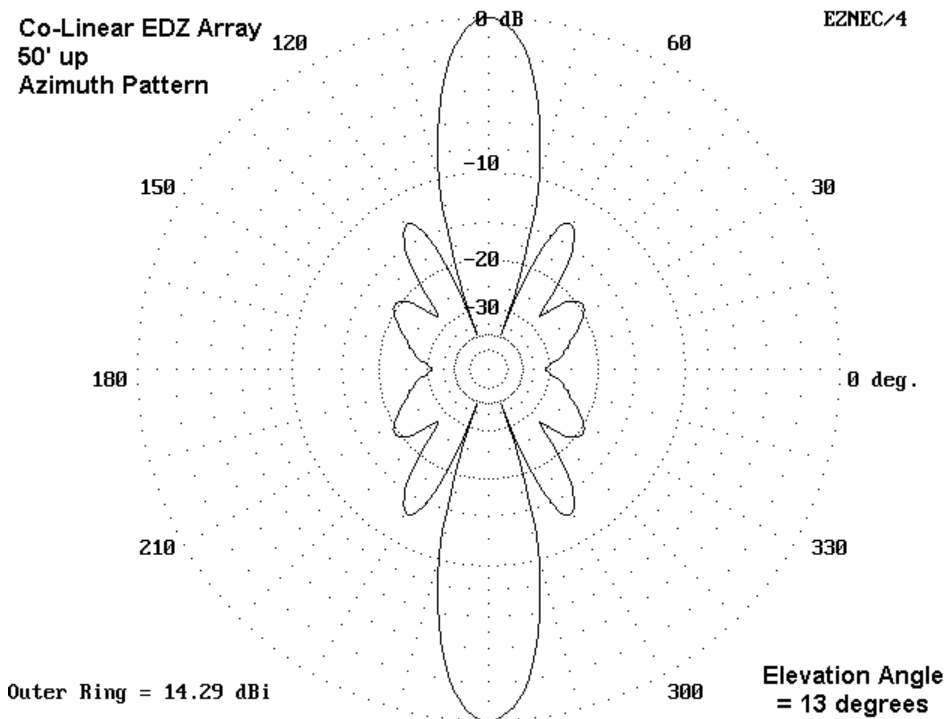
The antenna is given in terms of electrical degrees. The phasing lines are shorted parallel-line stubs. Here are Hugo's 20 meter dimensions and Alvin's 15 meter dimensions as samples: dimensions are in feet.

Band	A	B	C
14	43	53.5	11.5
21	27.5	35.5	7.7

The 15 meter version, which I modeled extensively, is 126' long, about the length of a 75-meter dipole. So what do you get for all that linear space on 15 meters?

You get almost precisely what Hugo predicted in 1938: about 7 dB gain over a dipole similarly placed in a bi-directional pattern that is

very narrow: 16°-17° between -3 dB points to be as exact as my model will permit. Modeled gain is about 14.3 dBi in a pattern like this one:



The best points for installing the parallel line stubs in the 15-meter model were actually 1.5' farther inboard than W6QVI suggests: about 29' from the ends and 34' from the antenna center. 67° proved the length required for maximum gain. The feedpoint

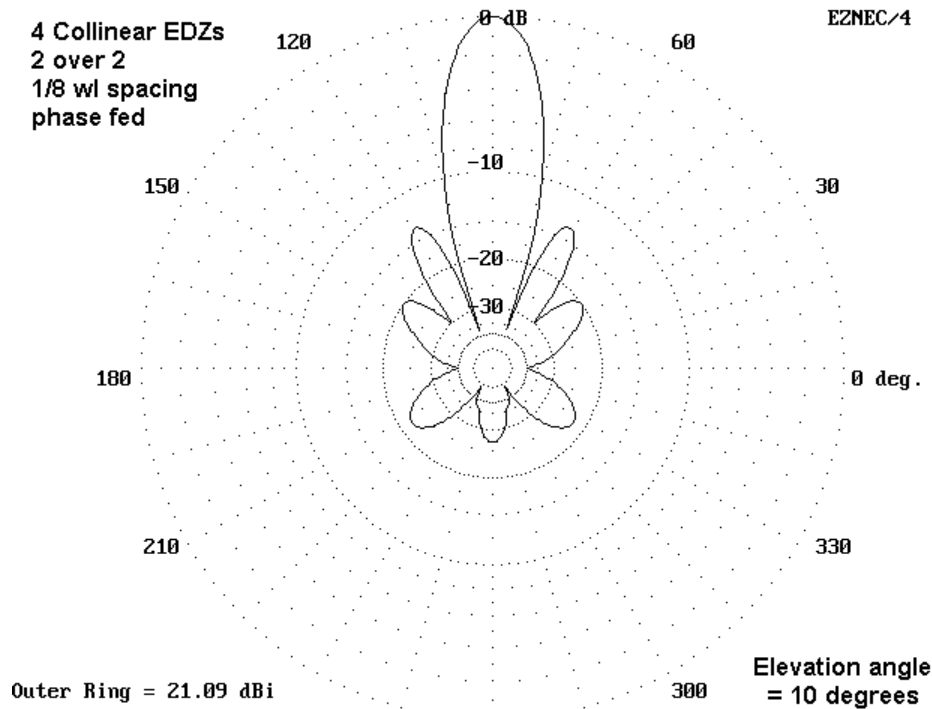
impedance is about  $170 - j740$  ohms, requiring an ATU, stub matching, or something similar.

As W2NB pointed out, careful aiming is required. (The EDZ beams earlier noted had beamwidths between 32 and 38 degrees, while a standard Yagi or quad has a beamwidth between 50 and 60 degrees, depending on the number of elements.) This is no antenna for casual worldwide DXing. Rather, it is a serious point-to-point antenna. Within that context, it is an antenna that proves that narrow beamwidths are not impossible at HF. I have expensive flashlights with wider beamwidths.

If you want a bi-directional antenna with a gain of about 18 dBi each way, while retaining the narrow ( $16\text{-}17^\circ$ ) beamwidth, try stacking two of these antennas at  $5/8$  wl separation. For the 15-meter sample, that places the two at 50' and 79' respectively. The feedpoint impedance, when fed in phase with 450-ohm line at the midpoint between the two, is about  $65 + j350$  ohms. A pair of series capacitors would cancel the reactance, providing a direct connection to 70-75-ohm cable (through a choke balun).

Let's carry the experiment one step further. To each of the vertically stacked EDZ arrays, one might arrange a series of  $1/2$  wl reflectors to achieve some further forward gain and reduce the rear lobe. Alternatively, one might place a second vertically stacked array  $1/8$  wl behind the original vertical stack. Then, feed the rear array with a current magnitude and phase to maximize forward gain and front-to-back ratio. At 21.2 MHz, the spacing would be just about 5.8'.

With proper feeding of the rear elements, we might achieve an azimuth pattern like this:



21 dBi forward gain, over 26 dB front-to-back ratio, and a 16-17° beamwidth are figures that amateur radio operators rarely see from antenna arrays whose bases are about 1 wl up and whose tops are 1.7 wl up. Of course, for most operations, such figures are contrary

to what is need for effective ham operation, but they might be useful for some specialized operations.

Antennas spaced 1/8 wl apart call for 135° phase differences in the elements on the currents: this is the received wisdom.

Unfortunately, it is wrong. Dipoles with this spacing might call for something close to this figure. However, for any two elements spaced more than a small fraction of a wavelength but less than 1/4 wl, there will be for each spacing a relative current magnitude and phase for the rear element that will yield maximum gain and maximum front-to-back ratio. With real materials, these two maxima may occur on very slightly different frequencies. For the array shown here, the maxima occurred with the rear elements fed at 0.75 the forward element current at a phase angle of 142 degrees. Slightly better performance might have been obtained if the upper and lower phased pairs had been individually optimized.

It is unlikely that standard ZL Special techniques would achieve perfect phasing. Instead, one should most likely use phasing networks to establish the operating conditions. Since the arrays are identical, one could use this method to flip the direction of the beam electronically. "But in the end, this is all hypothetical, isn't it? No one could or would build such an array." Given that all the techniques needed are standard in the field, I am not so sure of this. Some folks might engineer such an array just to say that they have an array with 21 dBi forward gain and to listen to the long-path echoes of their own signals. Hams have done far stranger things in the history of the service. I wonder what might be heard if one of these reversible arrays were aimed directly toward one of the poles.

We are still far from done with the EDZ. I am looking forward to the next step. These notes are simply the update so far. I'll add more as soon as I learn more about this interesting antenna. If I read enough old articles, I could learn more very shortly.

## Chapter 63: Feeding the EDZ

Typically, Extended Double Zepp (EDZ) users employ one of two methods in feeding this highly capacitively reactive 1.25 wl long antenna. Some users, especially those who employ the antenna as a simple center-fed long wire on bands other than the design band, simply use parallel feedline and an ATU. Others, with single-band use in mind, use a matching stub arrangement to find a 50-ohm point for a coax feedline. Of course, one can also place a split coil at the feedpoint to provide the inductive reactance necessary to cancel out the antenna's inherent capacitive reactance, although the resulting resistive impedance will still be 100 ohms or greater.

In the Summer, 1997, issue of *Communications Quarterly*, Rick Littlefield, K1BQT, presents a 2-meter EDZ that bears close examination. Besides an interesting construction method, designed to make a very durable EDZ for vertical use in hearing 2-meter repeaters, the key unique feature of Rick's design is the match and feed system that eliminates the usual center inductor to cancel out the heavy capacitive reactance at the feedpoint.

An EDZ at almost any frequency has a variable feedpoint impedance and capacitive reactance, depending on the exact length to which it is cut. However, without altering performance by more than a tenth or so of dB gain, one can cut the antenna for a feedpoint impedance in the 100-140 ohm resistive range, which gives a capacitive reactance in the 500-600 ohm range.

Rick applied a technique used with 5/8 wl vertical gap antennas: instead of an inductor, he uses a length of coax about 10.875" long, with a rod element beyond that point. Let's think of a 5/8 wl vertical and then simply place 2 of them feedpoint to feedpoint to get the final EDZ. The feed goes to the center conductor of the coax length. At the feed end, the braid is not connected to anything. At the far end, the center conductor and the braid are connected together and this junction goes to the 38" rod element. Rick calls this a delay line.

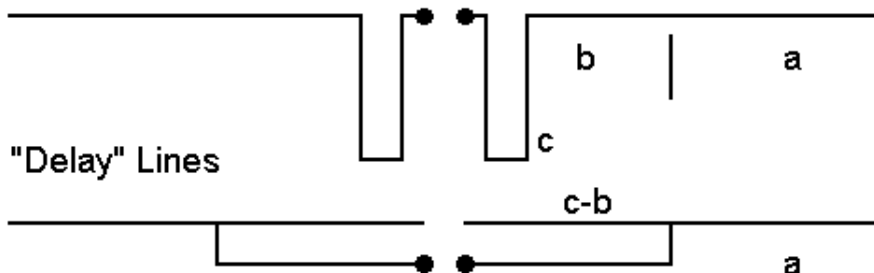
When two of these assemblies are put end to end, the coax center conductors are the two terminals making up the feedpoint. The braid ends are about an inch or two apart (and must NOT be connected together). The result is a nearly purely resistive feedpoint impedance of 100 ohms in the 2-meter model. Rick uses a 75-ohm 1/4 wl (+ 1/2 wl added) to make a combination matching section and balun for a 50-ohm coax feedline.

The delay line is interesting, because the name does not describe its function. Actually, it is a simple shorted feedline stub providing the inductive reactance necessary to cancel the antenna's capacitive reactance. Let's look at the figure to see the evolution of the arrangement.

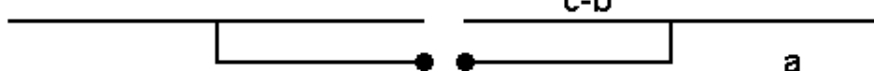
### Inductor Compensation



### Shorted-Stub Compensation



### "Delay" Lines



### The Evolution of "Delay" Lines from Inductive Compensation

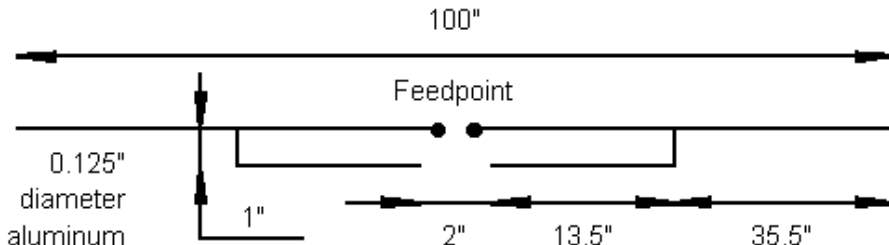
Part A shows the conventional split coil arrangement so familiar to EDZ builders (who do not use either open feedline to an ATU or a stub tuning method for a 50-ohm match). Part B replaces the inductors with a pair of shorted feedline stubs calculated to provide the same inductive reactance as the coil sections. Note that I have designated the outer part of the antenna line as "a" and the inner part as "b" in the sketch. When I substituted the parallel feedline, I designated on side of it as "c." "C" is as long as "b".

There is no rule that says you cannot sometimes make a wire do double duty. There is no incompatibility between wire "c" and wire length "b" so that we can combine them together as in Part C of the sketch. And Part C is essentially the arrangement used in Rick's coax "delay" line. Because the coax is now doing double duty, the exact length may change from simple calculations for stubs, but it is very close.

Although the final arrangement looks like a Tee match, it is not. The center must have a gap, forming at best a split-T top. The open ends of the non-feedpoint center are actually the ends of the inductive stubs away from the feedpoint and thus must be kept independent of each other by a gap.

The use of coax was possible in the original model, because the resistive portion of the feedpoint impedance was near 50 ohms on each side of center (for the 100-ohm total). Hence, the use of 50-ohm coax did not alter the feedpoint impedance.

If we use feedlines of higher impedance, two things will happen. First, the feedpoint impedance will be reduced. Second, the length of the stub will increase, placing the junction of "c-b" and "a" farther outward on each side of center. The next figure is a sketch of a model I developed while exploring this subject.



A Model 330-Ohm Matching Section for 50-Ohm Feed

To create as reliable a NEC model as possible, I used 0.125" diameter aluminum for all parts. This kept the diameter constant, thus allowing a greater reliability of the result with NEC-4. I modeled the parallel lines 1" apart, give about a 330-ohm characteristic impedance for the resultant line. With a connection point about 14.5" outward from center and a 2" gap between the open ends, the stub/line or split-T match provides about 54 ohms resistive impedance and no reactance at the feedpoint. Hence, direct 50-ohm coax feed is now possible.

The revised feed provides both capacitive reactance cancellation and resistive impedance transformation together. The length of the section is about the same as the combination of a 330-ohm shorted stub plus a length of the same line necessary to transform the overall impedance to nearly 50 ohms on its own, although treating this way of looking at the sections as a correct analysis of actions and interactions involved is far from certain at this point.

However, the model's parallel feedline section is close enough to 300 ohms to suggest that experiments may be useful with twinlead, taking into account the line's velocity factor of 0.8, of course. The technique may also be applicable using 450-ohm window line or 600 ohm ladder line, experimentally finding the correct length to use. And the technique is likely applicable at all HF and VHF frequencies at which EDZs are in use.

One advantage of the technique is that it is fairly broad-banded, giving full 2-meter coverage either in Rick's coax version or in the modified parallel line version shown here. I have not explored the consequences of this feed for use of the EDZ as a simple long wire on other HF bands--yet.

Henry Pollock, WB4HFL, took up the challenge of creating a #14 copper wire HF version of the impedance transformation "delay" line EDZ. His initial version was 42' long with 450-ohm match lines either side of center, each 66.5" long. The antenna resonated at 28.9 MHz on this first try. Modeling the exercise suggested that lengthening the antenna a bit (to 44.7') and shortening the match sections to about 65.5" (adjusted after physical modeling for velocity factor) would likely bring the antenna closer to a 28.5 MHz target. The 2:1 SWR bandwidth of the model appears to be about 600 kHz, although the use of a coax feeder will likely widen the bandwidth operationally at the shack end of the line. These figures are not unlike the bandwidth numbers for stub-tuned versions of the EDZ.

As a general rule, lengthening the antenna wire tends to reduce the resistive component of the feedpoint impedance, while lengthening and shortening the match section changes the reactance without affecting the resistance much. In general, it appears that the higher the characteristic impedance of the feedline used to effect the impedance transformation, the narrower the 2:1 SWR bandwidth of the antenna.

So here is one more experimental way to feed an EDZ. The K1BQT and WB4HFL experimental antennas prove that the principle works, yielding an EDZ with no need for stubs or ATUs: matching is built into the antenna structure itself. Have fun creating some interesting prototype EDZs for 50-ohm feeds.

## Chapter 64: NVIS: Some Background

**Near-Vertical Incidence Skywave or NVIS** propagations has proven useful, if not vital, to radio communications since at least the World War II era in the 1940s. The mode has reemerged in the 21<sup>st</sup> century as a focal point of research and practical field communications. The military, especially, has made it an essential part of its overall message-handling system. In the civilian arena, the mode has become a significant part of emergency plans.

Amateur use of NVIS propagation has grown almost exponentially over the last decade. Some amateurs use the mode for close in communications on 75 and 40 meters, with some work on the 60-meter channels and some activity on 160 meters. Hurricane Katrina proved the importance of NVIS communications when all terrestrial landline, cellular, and VHF modes fell to the fury of the storm.

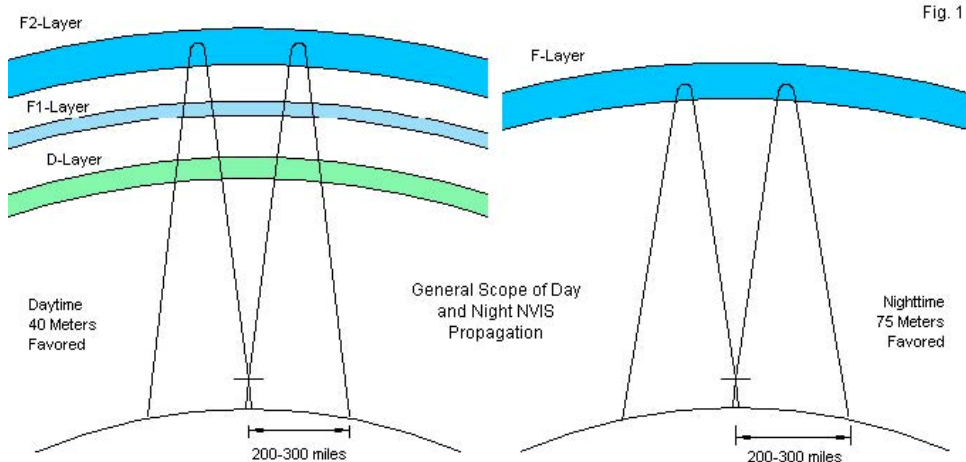
This overall collection of notes concerns the evaluation of amateur radio antennas for NVIS operation. The first section provides background on a number of matters that we must understand if we are to choose the correct antenna for NVIS work. In our initial discussions, we shall confine ourselves to antennas for the amateur bands that use NVIS and to fixed or base station permanent or long-term installations. Our goal for such antennas is not merely borderline success, but instead, optimal antenna installations that maximize the chances of successful communications.

Our first step will be to look at the ionospheric mechanisms that allow and define NVIS communications, and we shall integrate them with the typical NVIS operational situation. Together, these factors tell us what basic properties an “ideal” NVIS antenna should have in order to be effective. Although we shall not perform any evaluations of real antennas until the next episode, we can set up the conventions used to describe NVIS antenna performance, along with some good reasons to depart from the sorts of descriptions we might use with long-distance antennas. The final step in our preliminary notes will be to examine our primary tool for antenna analysis: antenna-modeling software. We shall see why only some of the available software is suitable for working with NVIS antennas.

### *NVIS Propagation and Situations*

Apart from ground-wave signals, virtually all upper MF and HF communications occurs as a result of refracting radio waves through various layers of the ionosphere. The F-layers are the most important ones, although in a negative way, the D-layer also has significance. We identify layers mostly by reference to their height above ground. The D-layer is relatively low, while the F-layers are much higher—in the vicinity of 250 miles above the earth. We used to think that we needed very low angles of incidence between the F-layers and radio signals to effect communications of any strength. However, we later discovered that we obtained returns from signals transmitted directly upward. Initially used for radiosonde work, the realities of battlefield situations showed that we could transfer information by this mode of operation.

Ionized layers of the rarified upper atmosphere form under the influence of ultra-violet radiation from the sun. Some layers exist only when there is direct sunlight (the D-layer, for instance), while others persist after dark, although they may change some of their properties between daylight and nighttime hours. **Fig. 1** shows the day and night propagation situation as it directly applies to NVIS communications.

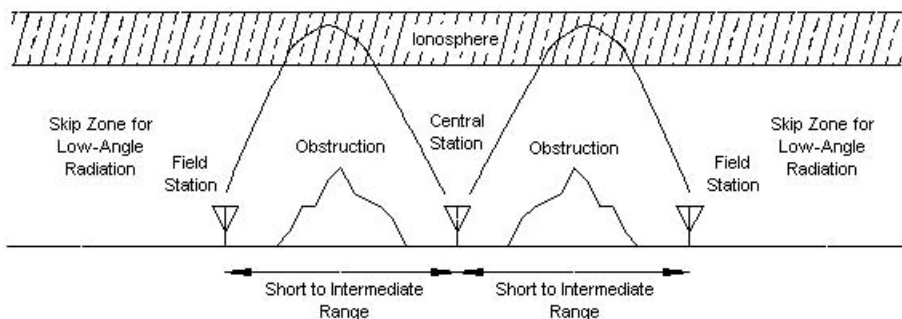


Each panel shows nearly vertical radiation from (and to) an arbitrary antenna. In daylight hours, the D-layer forms and absorbs radiation in the upper MF range and even in the lower HF range. Therefore, virtually all skip or ionospheric communications disappears from the 80-75meter band in daylight. However, 40-meter communication is generally possible via refractions from the

F2-layer (and occasionally from the F1-layer, although it is usually too weak to sustain good signal returns). After sundown, the D-layer dissipates and the two F-layers usually coalesce into a single layer that is weaker than in daylight hours. The single F-layer is capable of supporting effective communications, especially on 75 meters, with some work on 160 meters.

The sketches are not to scale, as suggested by the average range of NVIS communications compared to ionospheric layer height. In general, the NVIS range is about 200 miles from a reference station, with possible communications up to about 300 miles. The exact distance on any day depends on numerous factors. The quality of the station equipment (at both ends of the path) is critical. As well, the antenna installation design (our key interest in these notes) is a second contributor to success or failure. Although we can control these first two factors within the limits of the state of the art of radio, the third factor lies outside our control: the variables associated with the existence, strength, and height of the ionized atmospheric layers that make communications possible. These factors, as already noted, vary daily. They also vary seasonally, both in obvious ways (such as the relative length of daylight and nighttime) and in less obvious ways that stem from the changing angle of our station locations to the sun. Nevertheless, on most days and nights, we can achieve successful NVIS communications on one or another amateur band. Indeed, despite the severe power restrictions attached to the amateur channel allocations on 60 meters, the band is finding some good use during the twilight or transition hours between true daytime and true nighttime operations.

The importance of the NVIS mode of operation shows up clearly in **Fig. 2**, which portrays in very general terms the NVIS situation. For many practical—sometime vital—reasons, we need to communicate over a range that exceeds VHF and UHF line-of-sight abilities. However, the range is far shorter than we normally associate with HF skip transmissions. As well, the terrain may contain obstructions to ground-wave communications of any sort.



The NVIS Situation

Fig. 2

The NVIS communications mode allows us to leap tall mountains in a single bound, if we choose the correct frequency and if the ionosphere cooperates. Military applications are instantly clear. In fact, military research into NVIS operations is pressing the frequency limits of the mode, with investigations spreading from just above the AM BC band up to 12 to 14 MHz. Amateur applications generally focus on 75 and 40 meters, with SSB the primary method of encapsulating intelligence. However, as emergency service efforts expand, we shall find increasing use of digital message transfers and a host of other forward-looking methods.

The figure also hides an important facet of NVIS communications for our work. We shall focus initially on the antennas for the central station and presume that we have no major constraints for their installation. We shall treat the central station as having relatively unlimited power and resources with a location outside the troubles that may beset field locations. In contrast, field locations may lie within highly troubled areas—in military terms, a battlefield, and in civilian terms, a disaster area. In both cases, the field station may have limited transmitting power, limited receiving sensitivity, and somewhat primitive antennas. The field antennas may include bent-over whips, hastily erected dipoles using very low supports, and similar inefficient radiators (and receivers) of RF energy. As a consequence, a fixed position central station antenna should be—within the limits of the installation site—as efficient and effective as possible. Anything less places additional strains upon the field station, which is by definition operating under highly taxing situational stresses.

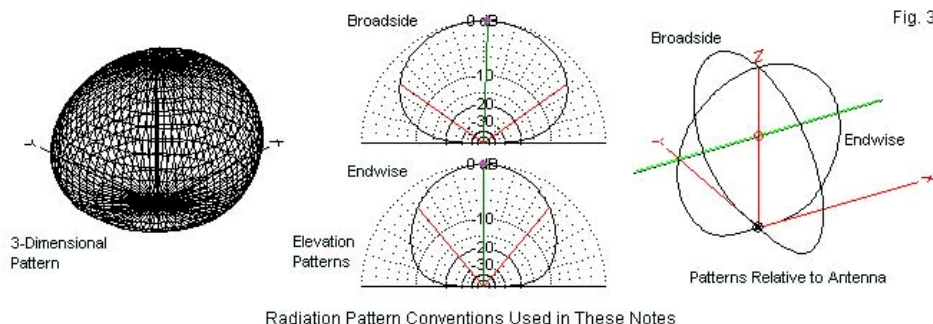
Having noted the importance of optimizing the central station antenna to the degree possible, we must also recognize that few amateur installation sites have unlimited space or other resources to erect a seemingly perfect NVIS antenna. The analysis of various antenna options for various relevant bands may help in the selection of the antenna design to implement on a given site, but the discussion will not create any automatic decisions. (The discussion will also help dispel some older misguided rules of thumb that some amateurs misapply to their NVIS antennas, thinking them to be optimal when they are not.) Equally critical to antenna decision-making is the overall mission of the NVIS station.

Some stations devote their activity solely to NVIS communications. Others may have both short and medium range communications goals and require a compromise antenna system that allows both types of operation, even if neither is truly optimal.

In the field of antennas for NVIS service, there are many options. Fortunately, most of them involve rather basic antenna designs.

### *Antenna Analysis Conventions Used in These Notes*

The analysis of NVIS antenna candidates requires that we alter some of the conventions that we use to portray information applicable to low-angle long-distance antennas. Most often, we show both the elevation and azimuth patterns of the subject antenna, especially for directional and bi-directional arrays. When our main radiation focus is straight upward, we need to change our perspective on the antenna. Fig. 3 provides a guide to the conventions that we shall employ in these notes.



On the left, we find a 3-dimensional radiation pattern for a simple NVIS antenna. The strongest radiation is upward at the zenith angle. Although the pattern is horizontally very round, it is not a perfect circle. On the right, we find a portrayal of the antenna with two nearly circular black outlines. One outline is broadside to the antenna wire—a simple dipole. The other circle aligns with the wire ends. (Virtually every NVIS antenna has a definable broadside and endwise pair of directions, even closed horizontal loops.) In the center of the sketch we find two elevation patterns, one broadside to the loop and the other endwise. We shall use these patterns—at right angles to each other—to characterize the far-field radiation patterns of all of the NVIS antennas that we consider.

In each elevation pattern we find a central line defining the direction of strongest radiation. Very often, the line may be a few (2-4) degrees off the zenith angle ( $90^\circ$ ) because in a given plane, the region of maximum gain is quite wide. We also find a pair of lines angularly equidistant from the maximum gain line. These lines define the half-power points along the pattern; the points at which gain is 3-dB lower than maximum gain. The angular distance between these lines is the conventional beamwidth of the antenna in each direction. We may define the circularity of the pattern by taking the ratio of the broadside beamwidth to the endwise beamwidth (in that order). Almost all patterns will show a larger beamwidth in the broadside orientation than in the endwise direction. Hence, most (but not absolutely all) antennas will have ratios greater than 1:1, the value for a perfectly circular pattern.

The beamwidth information will be as important to some installations as the maximum gain value associated with a given antenna. Since the beamwidth of the sample dipole is wider in the broadside direction than endwise, if a station has medium-range duties in addition to NVIS functions, orienting the wire broadside to the medium-range targets may increase communications reliability.

The analysis will bypass the azimuth patterns that we associate with long-range, low-angle radiation from the usual set of amateur antennas. Fig. 4 shows part of the reason why we do not use azimuth

Azimuth Patterns  
of a NVIS Antenna  
at Different Elevation  
Angles

Elevation Angles:  
Red: 30 degrees  
Black: 60 degrees  
Blue: 90 degrees

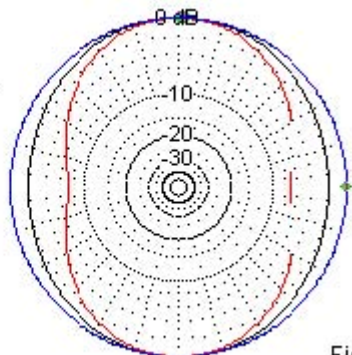
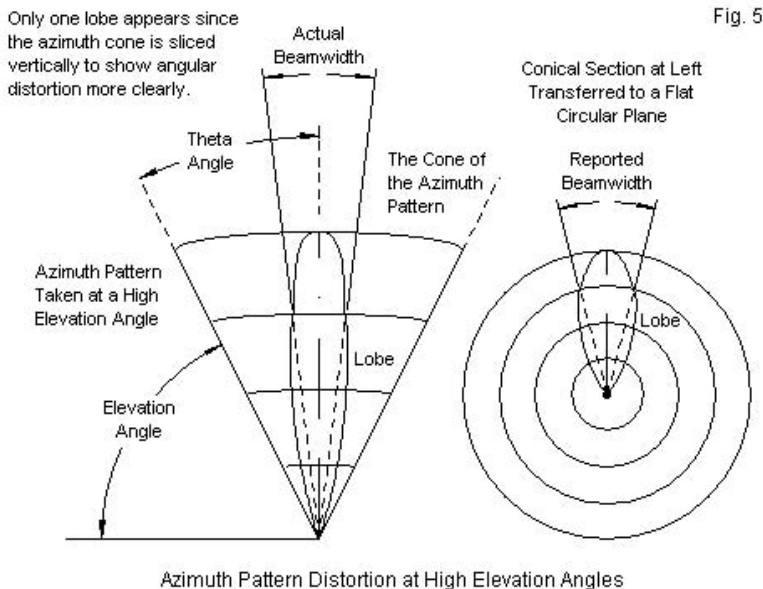


Fig. 4

patterns. The same sample dipole used to produce the elevation patterns in Fig. 3 yields the set of azimuth patterns, which vary in shape according to the elevation angle at which we take the pattern. The patterns seem to change shape as we raise the elevation angle, starting at 30° as a sharp oval, but becoming a circle at the zenith angle. The patterns show very little relationship to the 3-dimensional pattern that we viewed in conjunction with the elevation patterns.

Part of illusion fostered by the azimuth patterns arises from a systematic error that attaches to azimuth patterns as we raise the elevation angle at which we take the pattern. The higher the elevation angle for a given azimuth pattern, the greater the error that we find in the beamwidth of the azimuth pattern. The error is a function of the fact that the azimuth pattern actually forms a conical section that we then flatten into a planar azimuth pattern. At low elevation angles, the error is not sufficient to void the reported beamwidth (whether as a numerical value or as a visual impression).



As we raise the elevation angle, the error becomes very significant. **Fig. 5** shows a sample of the error. The views show only a single lobe, since the sketch slices the cone in half, eliminating one of the lobes. The flat azimuth pattern on the right shows and reports a wider beam angle than we find on the left. The differential increases as we increase the elevation angle at which we take the azimuth pattern. Let's let  $BW_a$  be the actual horizontal beamwidth on the conical section,  $BW_r$  be the NEC report of the beamwidth, while the indicated angles are the elevation or theta angle at which we take the phi/azimuth pattern. (Some NEC software employs the original notation of theta angles that count from the zenith angle downward, while most NEC implementations convert those angles to more familiar elevation angles from the horizon upward. Elevation + theta = 90°.) To correct the reported beamwidth we may perform a simple calculation.

$$BW_a = BW_r \cos(\text{elevation}) \text{ or } BW_a = BW_r \sin(\theta)$$

For example, at an elevation angle of 45°, we might have a reported horizontal beamwidth of 27.8 degrees. The cosine of 45° is 0.707. Multiplied times the reported horizontal beamwidth, we obtain 19.7° actual beamwidth. The 10° difference is significant. The cosine of an elevation angle of 60° (theta angle 30°) is 0.5, resulting in a more nearly correct beamwidth that is half the value reported on the azimuth pattern. (The correction is only approximate, since the cone itself is a curved surface.)

For low-angle azimuth patterns, the correction is not significant. For example, at an elevation angle of 20°, the cosine of the

elevation angle is about 0.94, resulting in only a very slight change in the reported beamwidth. The importance of the required correction emerges at high elevation angles, typical of those we might use to try to portray a NVIS pattern in azimuth form. For general analysis of NVIS antennas, using a pair of elevation patterns is far more revealing of the antenna's far-field radiation pattern.

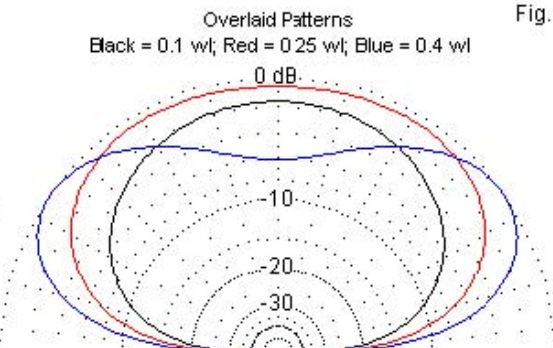
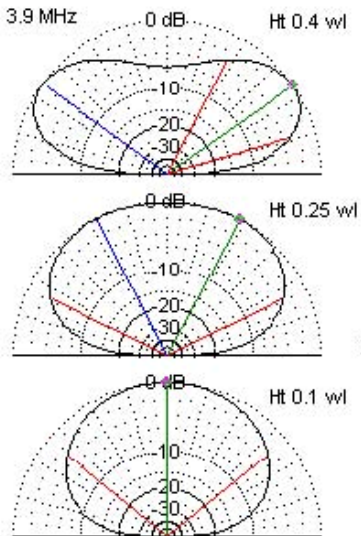
### *Modeling and Evaluating NVIS Antennas*

The broadside pattern of a proposed NVIS antenna is often a key element in its evaluation. For virtually all NVIS antennas, free-space patterns that emerge from models or basic antenna theory have little or no bearing on the antenna's NVIS performance. Instead, the critical factors that create the far-field pattern are the antenna geometry, the height above ground, and the soil quality in the region of the antenna.

Antenna geometry is an obvious factor, since we do not expect a closed  $1-\lambda$  loop to perform identically to a linear dipole or to an inverted-V dipole. Other antenna possibilities will each show performance differences from these three most basic forms in part due to their particular geometric features, that is, their shape overall and their shape relative to the position of the feedpoint in the assembly. Indeed, we may even press certain forms of beam antennas into NVIS service, not so much to create a clearly definable forward lobe as to tilt the upward NVIS pattern in a desired direction.

In the course of evaluating various candidates for NVIS service, we shall also discover that the proximity of the antenna to the ground magnifies the influence of the ground quality on various aspects of performance. The difference that ground quality makes will show up both in the maximum gain attainable from a given type of antenna and in the height above ground at which we attain the maximum gain. Moreover, when we supplement an active NVIS antenna element with additional structures in the form of reflectors—either as a single wire or as a ground screen—the degree of additional gain that we may obtain from the supplement will vary with the quality of the ground below the antenna and in the region surrounding the antenna. As is the case with all antennas, the far-field forms as a consequence not only of the ground immediately beneath the element, but as well at considerable distances from the antenna, where downward radiation intersects the ground and is reflected upward to combine with the upward incident radiation from the element.

The height above ground for a NVIS antenna is perhaps the key ingredient to the formation of the basic far-field or radiation pattern. Sometimes, individual elevation patterns (in this case, broadside patterns) can be misleading, as is the case with the patterns on the left in Fig. 6. The upper pattern, with the antenna  $0.4\lambda$  above average ground, is clearly less than optimal for NVIS work. The pattern shows a distinct null at the zenith angle.



See text for both analytical and modeling issues.

Sample of Elevation Patterns for a NVIS Dipole at Various Heights above Average Ground: Separate and Overlaid for Comparison

Lowering the antenna to  $0.25\lambda$  above the same quality of ground produces a pattern without the distinct null, but the two maximum-gain lines indicating at least a small reduction in gain at the zenith angle. Further reduction of the height to  $0.1\lambda$ , still above average ground, produces a pattern that is similar to the one shown in Fig. 3. To resolve any question about which pattern of the three is best for NVIS operation in the absence of tabular data, we may simply overlay the elevation plots. The right side of the figure shows the result. The pattern for the highest antenna level shows the highest maximum gain, but at angles that clearly depart from the desired zenith angle. The nearly circular pattern at a height of  $0.1\lambda$  shows deficiencies in gain compared to the seemingly less perfect pattern

for the antenna at  $0.25\lambda$ . The mid-level antenna placement not only yields more NVIS or zenith gain, but as well has (in the broadside direction) a wider beamwidth that might also serve for at least some medium-range communications needs.

Evaluation of NVIS antenna candidates requires close attention to the maximum gain, both overall and in the zenith direction, as well as to broadside and endwise beamwidth values. Because virtually all NVIS antennas will require heights that are less than  $\frac{1}{4}\lambda$  above ground for some or all of their horizontal structures, we are limited in the computer-based antenna modeling tools that will produce reasonable accurate views of performance potential. The key limiting factor is not the basic core itself (NEC-2, NEC-4, or MININEC).

The chief limiting factor is the ground calculation system. Only the Sommerfeld-Norton (SN) calculation system has sufficient accuracy to provide usable data on horizontal antennas closer than about  $0.2\lambda$  above ground. The SN system is a part of both the NEC-2 and NEC-4 calculating cores. One implementation of MININEC called Antenna Model has successfully grafted the SN system to its core. NEC contains an alternative ground calculation system that uses a Reflection Coefficient Approximation (RCA). The simplified calculations originally allowed faster core runs in the days of slow-speed personal and mainframe computers, but the results grow more inaccurate as any horizontal wire approaches ground level. Even less accurate is the ground calculation system that is part of the public domain version of MININEC (abbreviated here as a ground calculation system as MIN). In fact, the MIN system produces only feedpoint impedance values for perfect ground and not for the soil quality specified for the far-field pattern.

To illustrate the differences in the ground calculation systems, I used identical dipoles at identical heights above average ground to derive results for each of the ground calculation systems. Table 1 lists the outcome of the exercise, which ran the dipole in  $0.05\lambda$  increments from a maximum height of  $0.4\lambda$  down to ground level (simulated by a height of  $0.001\lambda$ ). The table lists the height in feet for each level as well as the height in wavelengths.

AWG #12 Copper Dipole Resonant at 3.9 MHz at 0.4-WL above Average Ground								Table 1					
Ground Calculation System		Sommerfeld-Norton				Reflection Coefficient Approximation				MININEC			
Height wl	Height ft	Gain dBi	TO Ang	R	X	Gain dBi	TO Ang	R	X	Gain dBi	TO Ang	R	X
0.4	100.88	6.67	35	85.2	-0.3	6.65	35	85.5	-0.4	6.30	35	92.7	-2.0
0.35	88.27	6.27	40	91.8	6.8	6.25	41	92.2	6.9	5.91	41	100.0	10.0
0.3	75.66	6.08	48	93.7	17.4	6.07	49	94.1	17.9	5.84	47	99.7	25.8
0.25	63.05	6.16	62	89.3	28.6	6.16	63	89.3	29.7	6.17	60	89.8	41.0
0.2	50.44	6.44	87	78.6	36.7	6.50	90	77.5	38.2	6.93	89	71.0	50.0
0.15	37.83	6.28	87	64.2	38.3	6.53	90	60.8	39.6	7.67	88	47.0	48.0
0.1	25.22	5.05	89	51.6	32.5	5.81	90	43.3	30.9	8.42	89	23.8	33.0
0.05	12.61	1.09	90	51.3	26.7	3.09	90	32.0	8.8	9.48	90	7.3	6.5
0.001	0.25	-9.36	88	156.6	302.7	-4.61	90	52.6	-28.9	9.29	90	1.5	-16.7

Notes: Gain dBi = maximum gain in dBi  
R = feedpoint resistance in Ohms  
TO Ang = elevation angle of maximum gain in degrees  
X = feedpoint reactance in Ohms

For each antenna height, the table reports the maximum gain and the TO (take-off) angle (the elevation angle of maximum gain) in degrees elevation. In some cases, the angle is close to but not exactly the zenith angle, because there is a range of elevation angles over which the gain does not change. The dipole is resonant in NEC-4 at 0.4- $\lambda$  above ground and does not change its dimension as the height decreases. Therefore, the columns labeled R and X show the feedpoint resistance and reactance that results from using the unadjusted dipole.

For ease of seeing the differences, **Fig. 7** plots the maximum gain values of the dipole at each height using each of the three ground calculating systems. The SN and RCA systems show good coincidence down to a height of about 0.2- $\lambda$ , below which we find a systematic departure. The RCA system somewhat overestimates the maximum gain as the antenna approaches ground level.

The MIN system begins to show a departure from the baseline SN system values at about  $0.25\lambda$  above average ground. One of the shortcomings of the MIN system, made publicly available in the 1990s in QST by Roy Lewallen, W7EL, the developer of ELNEC and EZNEC, is the radical overestimation of gain by the MIN ground calculation system for antenna at or below  $0.2\lambda$  above ground. The system provides wholly unreliable gain values for horizontal antennas close to ground. It is responsible for many misestimates of gain for 1990s 160-meter and 80meter antennas. As well, the MIN system, when only it was available to PC users, created misimpressions about very low-height NVIS antennas.

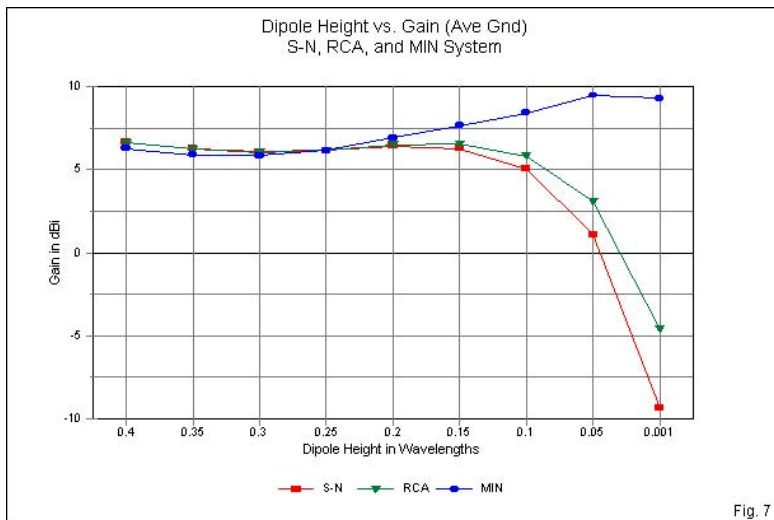


Fig. 7

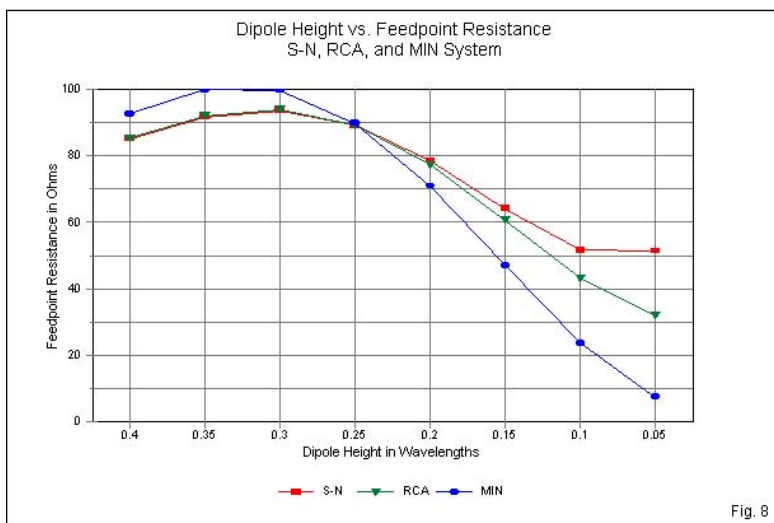


Fig. 8

**Fig. 8** shows the feedpoint resistance values reported under all three ground systems. At lower heights, the RCA system reports values below those reported with the SN system. More radically different are the values reported by the MIN system. The excessively low feedpoint resistance values accompany the excessively high gain values that the system produces for heights below about  $0.25\lambda$  for antennas with any degree of horizontal component to the radiation pattern.

The end result is that we must set aside virtually all old reports on the performance of antennas installed at NVIS heights. In fact, we must begin again with an evaluation of basic antennas using only antenna modeling software with the SN ground. In fact, these notes will employ NEC-4 throughout, with the SN ground calculation system implemented. Equally important to our effort will be a systematic exploration of basic antennas using a variety of ground quality conditions.

The following soil descriptions are commonly used in antenna modeling. Always substitute more precise values wherever known. The table represents an adaptation of values found in *The ARRL Antenna Book* (p. 3-6), which are themselves an adaptation of the table presented by Terman in *Radio Engineer's Handbook* (p. 709), taken from "Standards of Good Engineering Practice Concerning Standard Broadcast Stations," *Federal Register* (July 8, 1939), p. 2862. Terman's value for the conductivity of the worst soil listed is an order of magnitude lower than the value shown here.

<i>Soil Description</i>	<i>Conductivity in S/m <math>\sigma</math></i>	<i>Permittivity (Dielectric Constant) <math>\epsilon</math></i>	<i>Relative Quality</i>
Fresh water	0.001	80	
Salt water	5.0	81	
Pastoral, low hills, rich soil, typical from Dallas, TX, to Lincoln, NE	0.0303	20	<i>Very Good</i>
Pastoral, low hills, rich soil, typical of OH and IL	0.01	14	<i>Good</i>
Flat country, marshy, densely wooded, typical of LA near the Mississippi River	0.0075	12	
Pastoral, medium hills, and forestation, typical of MD, PA, NY (exclusive of mountains and coastline)	0.006	13	
Pastoral, medium hills, and forestation, heavy clay soils, typical of central VA	0.005	13	<i>Average</i>
Rocky soil, steep hills, typically mountainous	0.002	12 - 14	<i>Poor</i>
Sandy, dry, flat, coastal	0.002	10	
Cities, industrial areas	0.001	5	
Cities, heavy industrial areas, high buildings	0.001	3	<i>Very Poor</i> <i>Extremely Poor</i>

For our work, we shall use Very Good and Very Poor soil as extremes and Average soil as an intermediate value set between the two. Between any two of the three value sets, you can interpolate values close to reality.

NVIS antennas find applications under many circumstances for which the standard soil categories do not apply. For example, we find them in Antarctic regions placed over a mile or more of ice and snow. Therefore, as a further reference, the following table of values may have some useful data for special installations.

<i>Soil Description</i>	<i>Conductivity in S/m <math>\sigma</math></i>	<i>Permittivity (Dielectric Constant) <math>\epsilon</math></i>
Poor	0.001	4.5
Moderate	0.003	4
Average	0.005	13
Good	0.01	4
Dry, sandy, coastal	0.001	10
Pastoral hills, rich soil	0.007	17
Pastoral medium hills and forestation	0.004	13
Fertile land	0.002	10
Rich agricultural land, low hills	0.01	15
Rocky, steep hills	0.002	15
Marshy land, densely wooded	0.0075	12
Marshy, forested, flat	0.008	12
Mountainous, hilly (up to about 1000 m)	0.002	5
Highly moist ground	0.005	30
City industrial of average attenuation	0.001	5
City industrial of maximal attenuation	0.0004	3
City industrial area	0.0001	3
Fresh water	0.001	80
Fresh water @ 10° C and 100 MHz	0.001	84
Fresh water @ 20° C and 100 MHz	0.005	80
Sea water	5.0	81
Sea water @ 10° C up to 1 GHz	4.0	80
Sea water @ 20° C up to 1 GHz	4.0	73
Sea ice	0.001	4
Polar ice	0.0003	3
Polar ice cap	0.0001	1
Arctic land	0.0005	3

We generally think of signals incurring greater losses as we reduce the ground's conductivity and permittivity. However, between the worst dry-land soil (city industrial areas) and icy regions, we discover an interesting phenomenon. With conductivity values

below about  $1e10^{-4}$  and permittivity values that drop close to the minimum value of 1 (the value of a vacuum), the region beneath the antenna begins to act more like a free-space environment than like what we think of as earth. The effect has interesting consequences for practical antenna operation.

The next step is to review some very fundamental antenna types: the linear dipole, the V dipole (with a droop or slope of  $30^\circ$  from the horizontal or a  $120^\circ$  included angle between legs, and the  $1-\lambda$  closed loop. These three types of antennas are perhaps the backbone of fixed station NVIS work. We shall look at all three antennas in versions for 160 meters (1.85 MHz), 75 meters (3.9 MHz), and 40 meters (7.2 MHz). We shall try each antenna over each type of soil, seeking the best zenith-angle gain, but with an eye toward ensuring that we have an acceptable NVIS pattern throughout.

Although incidental to our work, you may wonder why I speak of “a NVIS antenna,” rather than “an NVIS antenna.” The acronym “NVIS” (at least where I come from) has acquired the pronunciation [nee'-vis], hence the article “a.” If you prefer to say [en vee eye ess], you may substitute the “an” at every suitable place.

## Chapter 65: NVIS Some Basic Antennas Used

The most fundamental NVIS antennas for fixed station operations are the linear dipole, the inverted-V dipole, and the  $1-\lambda$  closed loop. Each has its own set of mechanical advantages and disadvantages in terms of the complexity of installation. Despite the very commonness of these antennas, their properties when installed at heights appropriate to NVIS operations remain somewhat murky to many radio amateurs. Advice ranges from the idea of placing the antenna as close to the ground as possible to placing it as high as may be feasible.

There is a range of heights that optimizes the performance of each of these basic antennas in the zenith direction, that is, straight upward. The idea of straight upward in this context means a cone of radiation offset from the true zenith by enough to allow contact with stations up to 200 to 300 miles away. All HF antennas have rather broad patterns in this regard, so using the concept of zenith gain will capture the properties of the antenna within the required cone.

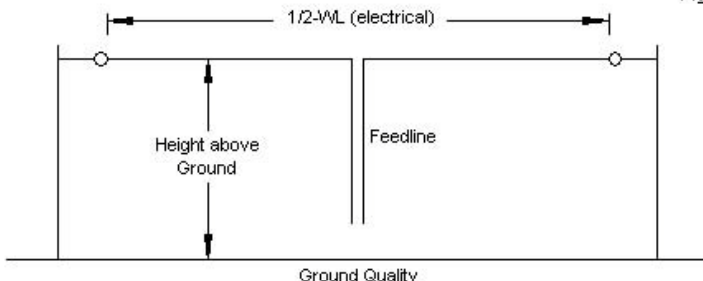
In this set of notes, we shall use the antennas alone, without supplementary wires or ground improvement screens. Our goal is to find out what we may obtain from the antenna relative to its height and the quality of the ground beneath it. Performance supplements will arise in later sets of notes. Our working tool will be NEC-4 with the SN ground calculation system. We shall examine each antenna over three of the soil quality values from standard charts. At the extremes are very good soil (conductivity 0.0303 S/m,

permittivity 20) and very poor soil (conductivity 0.001 S/m, permittivity 5), while the middle ground will be average soil (conductivity 0.005 S/m, permittivity 13). As well, we shall explore each antenna on three bands: 40 meters (7.2 MHz), 75 meters (3.9 MHz), and 160 meters (1.85 MHz) to uncover any possible differences in performance for equivalent heights above ground (as measured for each antenna in fractions of a wavelength). The results will create a considerable body of data and some fairly definite conclusions.

### *The Linear Dipole*

Of all NVIS antennas, the linear dipole is the most basic. **Fig. 1** outlines the dipole and the critical properties necessary to examine its performance at possible eights above ground. We shall start with a 40-meter dipole and then proceed to lower frequencies. We shall evaluate each dipole at heights from  $0.075\lambda$  up to  $0.255\lambda$  in  $0.01\lambda$  increments.

Fig. 1

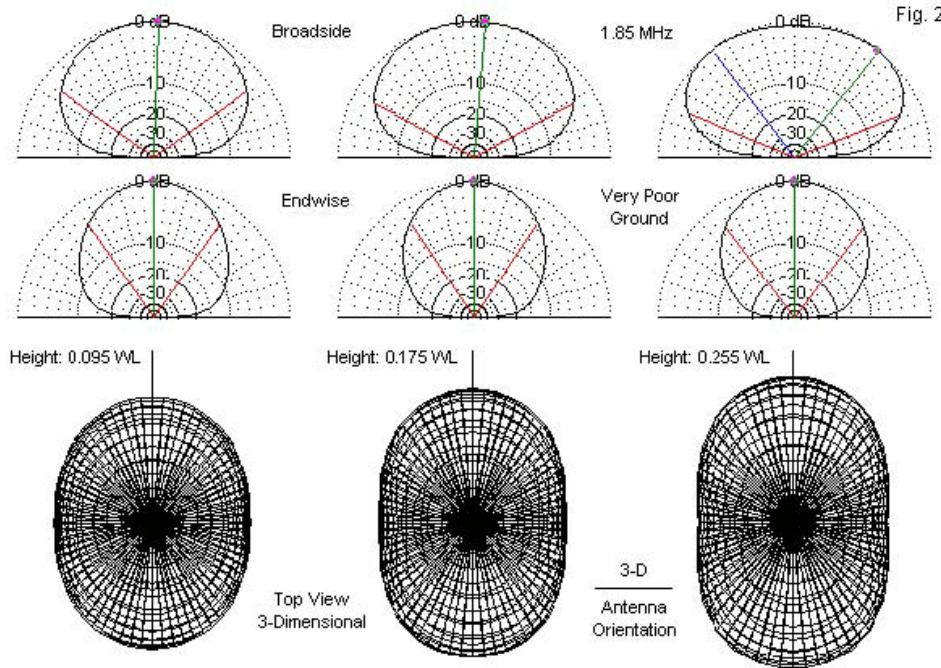


Key Properties of a Linear NVIS Dipole

The 40-meter dipole is cut for near resonance at 7.2 MHz at a height of about  $0.175\lambda$  above average ground. The length remains constant for all tests:  $0.4806\lambda$  using AWG #14 copper wire. (The length of dipoles for the lower bands will be the same. On 75 meters, we shall also use AWG #14 wire, but for 160 meters, we shall increase the diameter to AWG #12 wire.)

The basic data collected for the 40-meter dipole appears in **Table 1**. The table has separate sections for each soil quality. The left-most columns list the antenna height in wavelengths and in feet. The uppermost height used is  $0.255\lambda$ , just over  $\frac{1}{4}\lambda$ , which is only about 35' above ground. Hence, on 40, at most installation sites, the antenna height falls wholly within the operator's range of choice. On lower bands, not all heights may be feasible.

The gain columns record zenith or straight-up gain on the left. The maximum gain column only has entries where the value differs from the zenith gain value. Both values are in dBi. The need for the second column results from the standard evolution of the NVIS pattern with increasing antenna height. **Fig. 2** shows a sample set of patterns for a 160-meter NVIS dipole at several heights above very poor ground. Patterns for 75 and 40 meters and for other soil qualities will be similar, although the final step of showing different zenith and maximum gain values varies in height with different soil qualities. As the antenna height increases, the broadside beamwidth grows continuously, while the endwise beamwidth varies by slightly.



Typical NVIS Antenna Radiation Pattern Evolution with Increasing Height above Ground  
(Sample Uses a 1.85-MHz Dipole above Very Poor Soil)

At a height near the upper limit of our sampling range, the elevation pattern begins to split into broadside lobes, resulting in two maximum gain directions with a slightly depressed zenith gain value. The broadside elevation patterns and the 3-dimensional “top-down” plots provide alternative views of the phenomenon. The broadside axis line has a constant total length from the 3-D plot

center to provide a visual estimate of the growth of the broadside beamwidth with increasing dipole height.

The elevation plots contain lines showing the half-power or 3-dB beamwidth in both the broadside and endwise directions relative to the dipole. **Table 1** and subsequent tables record these values as BS BW and as EW BW. In addition, the tables contain a column recording the ratio of the broadside to the endwise beamwidths as a rough measure of the circularity of the pattern. A ratio of 1:1 would indicate a perfectly circular pattern. Values greater than 1:1 indicate an elongation of the pattern in the broadside direction. An antenna builder may productively use this information if the antenna requires an orientation favoring certain directions—and if there is available space to satisfy this need.

The final columns of the table list the feedpoint resistance and reactance at each height. Horizontal antennas close to ground undergo considerable swings of feedpoint impedance values, a fact recorded by the data in the tables. As we change the quality of the ground beneath the antenna, we also encounter some interesting variations in feedpoint impedance values for each height in the survey.



Because the tables do not allow rapid scanning of certain critical information, I have graphed two significant data items. **Fig. 3** shows the zenith gain values for the entire span of heights, with separate lines for each soil quality. The fact that better soil quality yields higher gain is self-evident. As well, it is also clear that as we reduce the soil quality, we also increase the optimal height range for maximum gain from the dipole.

40-Meter Dipole AWG #14 Copper Wire, Length = 0.4060 WL							7.2 MHz		Table 1	
Very Good Soil	Height wl	Height ft	Zen Gain	Max Gain	TO Ang	BS BW	EW BW	BW Ratio	Feed R	Feed X
	0.075	10.25	4.92		90	96.0	64.6	1.49	33.62	-2.97
	0.085	11.61	5.54		90	96.8	64.3	1.51	35.38	-0.51
	0.095	12.98	6.01		90	97.6	64.1	1.52	37.65	1.92
	0.105	14.34	6.36		90	98.6	64.0	1.54	40.32	4.19
	0.115	15.71	6.62		90	99.8	64.2	1.55	43.31	6.22
	0.125	17.08	6.82		90	101.0	64.2	1.57	45.54	7.96
	0.135	18.44	6.96		90	102.2	64.4	1.59	49.95	9.37
	0.145	19.81	7.06		90	103.8	64.8	1.60	53.47	10.42
	0.155	21.17	7.12		90	105.2	65.2	1.61	57.04	11.10
	0.165	22.54	7.15		90	107.0	65.6	1.63	60.62	11.42
	0.175	23.91	7.15		90	109.0	66.2	1.65	64.16	11.37
	0.185	25.27	7.13		90	111.0	66.8	1.66	67.61	10.96
	0.195	26.64	7.09		90	113.0	67.6	1.67	70.93	10.20
	0.205	28.00	7.04		90	115.2	68.4	1.68	74.08	9.13
	0.215	29.37	6.96		90	117.6	69.4	1.69	77.04	7.76
	0.225	30.74	6.87		90	120.0	70.4	1.70	79.77	6.13
	0.235	32.10	6.76		90	122.4	71.6	1.71	82.25	4.25
	0.245	33.47	6.63	6.67	68	124.8	72.8	1.71	84.46	2.17
	0.255	34.83	6.49	6.59	64	126.8	74.4	1.70	86.39	-0.08
Average Soil										
Average Soil	Height wl	Height ft	Zen Gain	Max Gain	TO Ang	BS BW	EW BW	BW Ratio	Feed R	Feed X
	0.075	10.25	2.78		90	101.0	67.4	1.50	51.85	-6.23
	0.085	11.61	3.50		90	102.0	66.4	1.54	51.83	-5.08
	0.095	12.98	4.09		90	103.0	65.6	1.57	52.13	-3.75
	0.105	14.34	4.58		90	104.0	65.2	1.60	53.13	-2.36
	0.115	15.71	4.97		90	105.2	64.8	1.62	54.58	-1.02
	0.125	17.08	5.28		90	106.5	64.8	1.64	56.33	0.16
	0.135	18.44	5.53		90	107.8	64.8	1.66	58.33	1.14
	0.145	19.81	5.72		90	109.5	65.0	1.68	60.50	1.89
	0.155	21.17	5.87		90	111.0	65.2	1.70	62.80	2.39
	0.165	22.54	5.97		90	113.0	65.4	1.73	65.17	2.63
	0.175	23.91	6.04		90	114.8	65.8	1.74	67.55	2.60
	0.185	25.27	6.08		90	116.8	66.4	1.76	69.91	2.30
	0.195	26.64	6.09		90	118.8	67.0	1.77	72.21	1.76
	0.205	28.00	6.07		90	121.1	67.8	1.79	74.40	0.97
	0.215	29.37	6.03		90	123.4	68.6	1.80	76.48	-0.03
	0.225	30.74	5.97	5.98	70	125.8	69.4	1.81	78.40	-1.24
	0.235	32.10	5.89	5.94	65	127.8	70.6	1.81	80.14	-2.63
	0.245	33.47	5.78	5.91	62	129.6	71.8	1.81	81.70	-4.17
	0.255	34.83	5.66	5.88	58	131.4	73.0	1.80	83.05	-5.84
Very Poor Soil										
Very Poor Soil	Height wl	Height ft	Zen Gain	Max Gain	TO Ang	BS BW	EW BW	BW Ratio	Feed R	Feed X
	0.075	10.25	1.59		90	109.8	73.0	1.50	67.33	-10.07
	0.085	11.61	2.17		90	110.8	71.2	1.56	65.88	-10.19
	0.095	12.98	2.67		90	111.8	69.8	1.60	65.10	-9.95
	0.105	14.34	3.11		90	112.8	68.6	1.64	64.79	-9.48
	0.115	15.71	3.48		90	114.0	67.8	1.68	64.90	-8.93
	0.125	17.08	3.80		90	115.2	67.2	1.71	65.32	-8.36
	0.135	18.44	4.07		90	116.6	66.8	1.75	66.00	-7.84
	0.145	19.81	4.29		90	118.2	66.6	1.77	66.89	-7.42
	0.155	21.17	4.47		90	119.8	66.6	1.80	67.92	-7.11
	0.165	22.54	4.61		90	121.4	66.6	1.82	69.04	-6.94
	0.175	23.91	4.72		90	123.2	66.6	1.85	70.24	-6.91
	0.185	25.27	4.79		90	125.2	67.0	1.87	71.46	-7.04
	0.195	26.64	4.84		90	127.2	67.4	1.89	72.70	-7.33
	0.205	28.00	4.86		90	129.0	67.8	1.90	73.90	-7.76
	0.215	29.37	4.85	4.88	64	131.0	68.6	1.91	75.05	-8.33
	0.225	30.74	4.82	4.91	63	132.6	69.2	1.92	76.13	-9.03
	0.235	32.10	4.76	4.93	59	134.2	70.2	1.91	77.12	-9.84
	0.245	33.47	4.69	4.95	55	135.6	71.0	1.91	78.01	-10.76
	0.255	34.83	4.59	4.98	53	137.0	72.2	1.90	78.78	-11.76

On 40 meters, the maximum zenith gain occurs at heights between  $0.165\lambda$  and  $0.175\lambda$  over very good soil. Reducing the soil quality to average raises the maximum gain height to about  $0.195\lambda$ . A further reduction in soil quality to the very poor level results in a maximum gain height of about  $0.205\lambda$ . As the graph lines in **Fig. 3** show, the gain goes not change very rapidly near the optimal height. For practical purposes, there is a window of heights perhaps  $0.04\lambda$  wide in which the gain changes over an operationally undetectable range (including changes in the broadside beamwidth). This range amounts to a spread of about 5.5' of height on 40 meters or  $+/-3'$  so relative to the optimal height for maximum gain. If one does not know the local ground quality, placing the antenna at the optimal height for average ground will let it fall close to the best height for other soil values.

The differences in ground quality values from very good to very poor not only affects the peak-gain antenna height, but also have perhaps even more profound effects on the feedpoint impedance. **Fig. 4** graphs the feedpoint resistance values of the dipole across the range of heights, with separate lines for each ground quality surveyed. At very low heights, the resistance values very widely for the different soils. They gradually converge so that at a height of  $0.205\lambda$ , they meet, only to separate again above that height. The convergence height coincides with the maximum gain height for very poor soil. In general, selecting an antenna height that is near the level for best gain will yield an impedance value over any soil that will produce few, if any, surprises when it comes to matching the antenna to the feedline. The convergence resistance is close to  $75\Omega$ , with up to about  $+/-j10\Omega$  reactance.

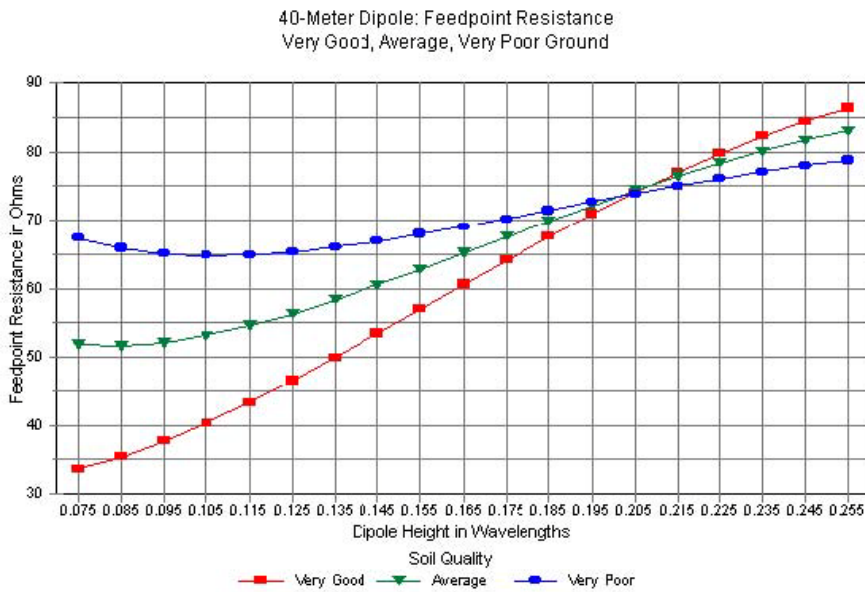


Fig. 4

The table reveals another facet of NVIS dipole behavior worth noting. If we decrease soil quality levels for any given height near the optimal range, the beamwidth ratio systematically increases. As the soil quality grows worse, the broadside beamwidth increases more rapidly relative to the slowly changing endwise beamwidth. At a height of  $0.195\lambda$ , for example, the broadside beamwidth changes by about  $14^\circ$  across the range of soils. In other terms, each half-power point is about  $7^\circ$  lower over very poor soil than over very good soil. Since antenna gain drops very rapidly beyond the half-power points, the difference may make a difference in the

performance of antennas designed for both NVIS and medium-range communications. In such cases, one may wish to place a 40-meter NVIS dipole above rather than below the maximum gain height with average or better soils. However, the height should in all cases be below the level at which the zenith gain suffers significantly.

On 75 meters, if we continue to count height in increments that are a fraction of a wavelength, we may not have the option of placing an antenna above the maximum gain height. Indeed, many sites will have difficulty raising the antenna to its best-gain height. Still, the behavior of the dipole on 75 meters over the same three soil qualities differs enough from the 40-meter properties to warrant a separate table and graph set. **Table 2** provides the parallel set of data to the 40-meter information in **Table 1**. **Fig. 5** graphs the zenith gain across the span of heights, which are, in feet, almost double those on 40 meters. At first glance, the graph lines appear to be the same as those for 40, but there are some interesting differences in the 75-meter set. Most significantly, the maximum gain values occur at lower heights:  $0.165\lambda$  for very good soil,  $0.185\lambda$  for average soil, and between  $0.195\lambda$  and  $0.205\lambda$  for very poor soil. Although the individual changes from 40 meters are small (about 1% of a wavelength), they indicate a trend that we should anticipate to continue when we examine 160-meter dipoles. In addition, the peak zenith gain values that we may obtain on 75 meters are all higher than those we can obtain on 40 meters. For horizontal antennas over ground, especially at the low NVIS heights, the ground absorption increases with rising frequency for any given soil quality. We normally notice this effect only in lower

HF surface-wave communications, but the phenomenon also affects the maximum obtainable NVIS gain.



Fig. 5

75-Meter Dipole AWG #14 Copper Wire, Length = 0.4606 WL								3.9 MHz		Table 2	
Very Good Soil		Zen Gain	Max Gain	TO Ang	BS BW	EW BW	BW Ratio	Feed R	Feed X		
0.075	18.91	5.51		90	94.8	63.8	1.49	28.92	8.11		
0.085	21.44	6.07		90	95.6	63.6	1.50	31.11	-5.48		
0.095	23.96	6.48		90	96.5	63.6	1.52	33.75	-2.36		
0.105	26.48	6.78		90	97.4	63.6	1.53	36.77	0.25		
0.115	29.00	7.01		90	98.5	63.6	1.55	40.08	2.57		
0.125	31.52	7.16		90	99.8	64.0	1.56	43.61	4.57		
0.135	34.05	7.27		90	101.0	64.3	1.57	47.30	6.20		
0.145	36.57	7.34		90	102.5	64.6	1.59	51.10	7.44		
0.155	39.09	7.38		90	104.0	65.0	1.60	54.95	8.29		
0.165	41.61	7.40		90	105.6	65.4	1.61	58.80	8.74		
0.175	44.13	7.39		90	107.4	66.1	1.62	62.60	8.80		
0.185	46.66	7.36		90	109.2	66.8	1.63	66.30	8.47		
0.195	49.18	7.31		90	111.4	67.4	1.65	69.88	7.78		
0.205	51.70	7.24		90	113.6	68.4	1.66	73.28	6.74		
0.215	54.22	7.16		90	116.0	69.2	1.68	76.48	5.39		
0.225	56.74	7.06		90	118.4	70.4	1.68	79.44	3.74		
0.235	59.27	6.95		90	120.8	71.4	1.69	82.14	1.84		
0.245	61.79	6.82	6.84	73	123.2	72.8	1.69	84.56	-0.29		
0.255	64.31	6.67	6.74	65	125.6	74.4	1.69	86.68	-2.61		
Average Soil		Zen Gain	Max Gain	TO Ang	BS BW	EW BW	BW Ratio	Feed R	Feed X		
0.075	18.91	3.51		90	99.2	66.8	1.49	46.61	-7.27		
0.085	21.44	4.19		90	100.2	66.0	1.52	47.15	-5.92		
0.095	23.96	4.74		90	101.2	65.6	1.54	48.33	-4.43		
0.105	26.48	5.18		90	102.2	65.2	1.57	49.95	-2.95		
0.115	29.00	5.53		90	103.4	65.0	1.59	51.95	-1.58		
0.125	31.52	5.80		90	104.6	65.0	1.61	54.24	-0.39		
0.135	34.05	6.01		90	106.2	65.0	1.63	56.74	0.56		
0.145	36.57	6.17		90	107.6	65.2	1.65	59.39	1.26		
0.155	39.09	6.28		90	109.2	65.6	1.66	62.12	1.67		
0.165	41.61	6.36		90	111.0	65.8	1.69	64.89	1.79		
0.175	44.13	6.40		90	113.0	66.4	1.70	67.64	1.62		
0.185	46.66	6.42		90	115.0	67.0	1.72	70.34	1.16		
0.195	49.18	6.41		90	117.2	67.6	1.73	72.94	0.43		
0.205	51.70	6.37		90	119.4	68.4	1.75	75.42	-0.55		
0.215	54.22	6.32		90	121.8	69.2	1.76	77.73	-1.78		
0.225	56.74	6.24	6.25	72	124.2	70.4	1.76	79.87	-3.22		
0.235	59.27	6.15	6.19	67	126.4	71.4	1.77	81.80	-4.84		
0.245	61.79	6.03	6.14	63	128.4	72.6	1.77	83.51	-6.63		
0.255	64.31	5.90	6.10	60	130.2	74.0	1.76	84.98	-8.56		
Very Poor Soil		Zen Gain	Max Gain	TO Ang	BS BW	EW BW	BW Ratio	Feed R	Feed X		
0.075	18.91	2.10		90	107.8	71.8	1.50	65.60	-10.75		
0.085	21.44	2.69		90	108.8	70.4	1.55	64.50	-10.82		
0.095	23.96	3.19		90	110.0	69.2	1.59	64.08	-10.58		
0.105	26.48	3.61		90	111.2	68.4	1.63	64.13	-10.13		
0.115	29.00	3.97		90	112.4	67.6	1.66	64.60	-9.65		
0.125	31.52	4.27		90	113.8	67.2	1.69	65.37	-9.17		
0.135	34.05	4.51		90	115.2	67.0	1.72	66.39	-8.79		
0.145	36.57	4.71		90	116.8	66.8	1.75	67.59	-8.52		
0.155	39.09	4.86		90	118.6	66.8	1.78	68.90	-8.39		
0.165	41.61	4.98		90	120.4	67.0	1.80	70.29	-8.42		
0.175	44.13	5.06		90	122.4	67.2	1.82	71.73	-8.62		
0.185	46.66	5.11		90	124.4	67.6	1.84	73.16	-9.00		
0.195	49.18	5.13		90	126.4	68.2	1.85	74.57	-9.53		
0.205	51.70	5.13	5.14	69	128.4	68.6	1.87	75.92	-10.22		
0.215	54.22	5.10	5.15	65	130.4	69.4	1.88	77.18	-11.06		
0.225	56.74	5.04	5.16	61	132.0	70.4	1.87	78.35	-12.02		
0.235	59.27	4.97	5.17	57	133.6	71.2	1.88	79.39	-13.11		
0.245	61.79	4.87	5.19	55	135.2	72.4	1.87	80.31	-14.28		
0.255	64.31	4.75	5.21	52	136.5	73.6	1.85	81.07	-15.54		

Apart from the difference in maximum possible gain from an un-supplemented dipole and the modeled height of occurrence, virtually every other comment on the 40-meter dipole applies equally to the 75-meter dipole. Heights in the range of 40' (for very good soil) up to about 50' (for very poor soil) yield maximum gain. If we select an arbitrary but common amateur dipole height of 35' above ground, then the gain deficit relative to maximum possible gain varies with the soil quality. It ranges from about 0.1 dB over very good soil to more than 0.6 dB over very poor soil. At 75 meters, the maximum value of the beamwidth ratio also decreases slightly relative to the values at 40 meters.

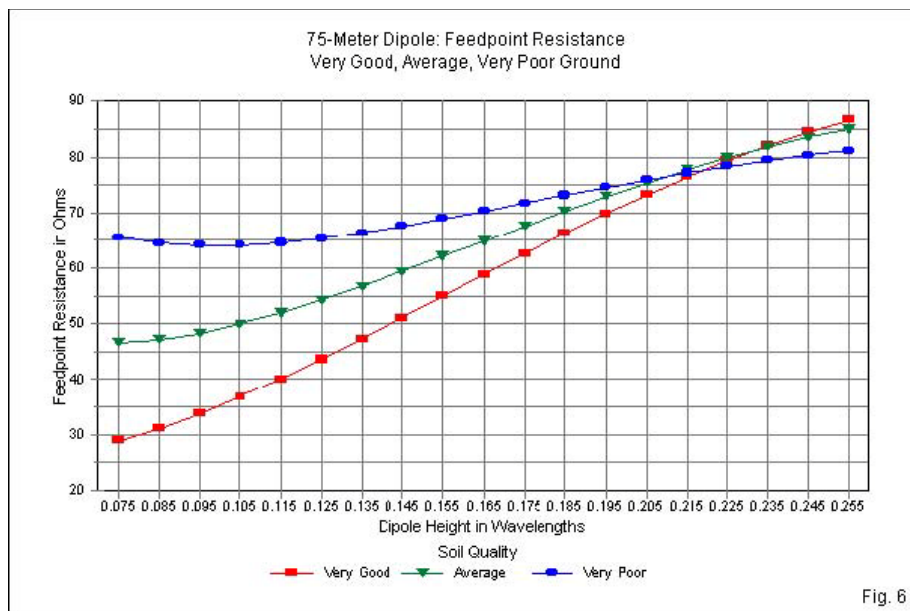


Fig. 6

The feedpoint resistance curves for 75 meters, shown in **Fig. 6**, resemble those in **Fig. 4** with a small but significant difference. The convergence region is slightly higher on 75 meters: between antenna heights of  $0.205\lambda$  and  $0.215\lambda$ . Since the optimal gain region shows lower heights on 75 meters, we can expect a wider variation in the feedpoint impedance values as we move from very good to very poor soil. In fact, if we return to the arbitrary but common amateur dipole height of 35' above ground, the impedance range runs from close to  $50\ \Omega$  over the worst soil to nearly  $70\ \Omega$  over the best.

The trends that we have noted relative to the 40-meter and 75-meter dipoles continue unabated when we examine a 160-meter dipole (set for 1.85 MHz in this sample). If the patterns hold true, we should expect higher maximum gain values, lower optimal gain heights (in wavelengths), lower maximum beamwidth ratio values, and a greater height of feedpoint resistance convergence. **Table 3** provides the numerical data to confirm each of these trends, while **Fig. 7** and **Fig. 8** supply visual references for the gain and feedpoint resistance curves. Indeed, with only a few exceptions, we may bypass extensive commentary on the 160-meter dipole's behavior, although we can hardly avoid a note on the usual amateur 160-meter horizontal antenna installation.

160-Meter Dipole AWG #12 Copper Wire: Length = 0.4806 WL							1.95 MHz		Table 3	
Very Good Soil		Zen Gain	Max Gain	TO Ang	BS BW	EW BW	BW Ratio	Feed R	Feed X	
0.075	39.87	6.10		90	94.0	63.0	1.49	24.58	13.27	
0.085	45.19	6.59		90	94.6	63.0	1.50	27.10	-9.86	
0.095	50.51	6.94		90	95.6	63.0	1.52	30.04	-6.63	
0.105	55.82	7.19		90	96.5	63.2	1.53	33.33	-3.67	
0.115	61.14	7.37		90	97.4	63.3	1.54	36.89	-1.04	
0.125	66.46	7.49		90	98.6	63.6	1.55	40.66	1.23	
0.135	71.77	7.57		90	99.8	63.9	1.56	44.58	3.11	
0.145	77.09	7.62		90	101.2	64.3	1.57	48.61	4.57	
0.155	82.41	7.63		90	102.8	64.8	1.59	52.69	5.61	
0.165	87.72	7.63		90	104.4	65.2	1.60	56.76	6.22	
0.175	93.04	7.61		90	106.2	65.8	1.61	60.79	6.42	
0.185	98.36	7.56		90	108.2	66.6	1.62	64.72	6.22	
0.195	103.67	7.51		90	110.0	67.2	1.64	68.52	5.62	
0.205	108.99	7.43		90	112.2	68.2	1.65	72.15	4.66	
0.215	114.31	7.34		90	114.6	69.2	1.66	75.57	3.35	
0.225	119.62	7.24		90	117.0	70.2	1.67	78.74	1.73	
0.235	124.94	7.13		90	119.4	71.4	1.67	81.65	-0.17	
0.245	130.26	6.84	6.99	74	122.0	72.8	1.68	84.27	-2.31	
0.255	135.57	6.85	6.89	68	124.2	74.2	1.67	86.58	-4.66	
Average Soil		Zen Gain	Max Gain	TO Ang	BS BW	EW BW	BW Ratio	Feed R	Feed X	
0.075	39.87	4.41		90	97.0	65.6	1.48	38.46	-9.76	
0.085	45.19	5.05		90	97.8	65.2	1.50	39.87	-7.85	
0.095	50.51	5.55		90	98.8	64.8	1.52	41.81	-5.88	
0.105	55.82	5.93		90	99.8	64.6	1.54	44.17	-3.99	
0.115	61.14	6.22		90	101.0	64.6	1.56	46.86	-2.29	
0.125	66.46	6.44		90	102.0	64.8	1.57	49.79	-0.83	
0.135	71.77	6.61		90	103.5	64.8	1.60	52.90	0.33	
0.145	77.09	6.72		90	105.2	65.2	1.61	56.12	1.18	
0.155	82.41	6.80		90	106.8	65.6	1.63	59.41	1.70	
0.165	87.72	6.85		90	108.4	66.0	1.64	62.70	1.88	
0.175	93.04	6.87		90	110.4	66.5	1.66	65.95	1.73	
0.185	98.36	6.88		90	112.4	67.2	1.67	69.12	1.25	
0.195	103.67	6.83		90	114.6	67.8	1.69	72.18	0.46	
0.205	108.99	6.78		90	116.8	68.6	1.70	75.07	-0.63	
0.215	114.31	6.71		90	119.1	69.6	1.71	77.79	-1.98	
0.225	119.62	6.63		90	121.5	70.6	1.72	80.29	-3.58	
0.235	124.94	6.52	6.53	69	124.0	71.8	1.73	82.55	-5.40	
0.245	130.26	6.40	6.46	67	126.0	73.0	1.73	84.56	-7.40	
0.255	135.57	6.26	6.39	61	128.2	74.4	1.72	86.30	-9.56	
Very Poor Soil		Zen Gain	Max Gain	TO Ang	BS BW	EW BW	BW Ratio	Feed R	Feed X	
0.075	39.87	2.87		90	103.8	70.2	1.48	59.18	-9.15	
0.085	45.19	3.49		90	104.8	69.0	1.52	58.87	-9.01	
0.095	50.51	3.99		90	105.8	68.2	1.55	59.22	-8.63	
0.105	55.82	4.41		90	107.0	67.6	1.58	60.05	-8.07	
0.115	61.14	4.75		90	108.4	67.2	1.61	61.24	-7.54	
0.125	66.46	5.02		90	109.8	66.8	1.64	62.72	-7.06	
0.135	71.77	5.24		90	111.4	66.8	1.67	64.41	-6.73	
0.145	77.09	5.41		90	113.0	66.8	1.69	66.26	-6.56	
0.155	82.41	5.54		90	114.8	66.8	1.72	68.19	-6.58	
0.165	87.72	5.63		90	116.6	67.2	1.74	70.16	-6.80	
0.175	93.04	5.68		90	118.8	67.6	1.76	72.12	-7.24	
0.185	98.36	5.71		90	120.8	68.2	1.77	74.05	-7.88	
0.195	103.67	5.71		90	123.0	68.6	1.79	75.91	-8.72	
0.205	108.99	5.68		90	125.2	69.4	1.80	77.66	-9.74	
0.215	114.31	5.63	5.66	68	127.4	70.2	1.81	79.29	-10.93	
0.225	119.62	5.56	5.64	63	129.4	71.2	1.82	80.77	-12.28	
0.235	124.94	5.46	5.63	60	131.0	72.2	1.81	82.07	-13.75	
0.245	130.26	5.35	5.62	56	132.6	73.4	1.81	83.20	-15.33	
0.255	135.57	5.21	5.62	54	134.2	74.8	1.79	84.14	-17.00	

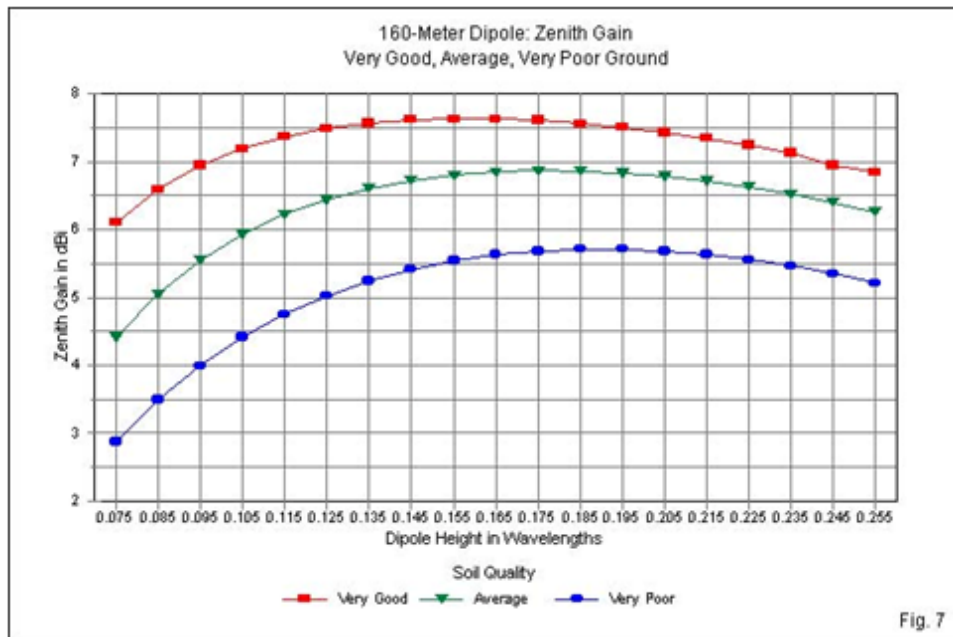


Fig. 7

For the most typical amateur installations, a height of 35' falls below the lowest height in the survey. In fact, at 35' above ground, a 160-meter dipole will lose between 1.5 dB (over very good soil) to 2.8 dB over very poor soil relative to placing the antenna at an optimal NVIS height. Since the gain of the antenna at 160 meters is higher for a given height (in wavelengths) above any given soil quality, the deficit is not quite as severe as the internal 160-meter numbers suggest, but the installation at a low height has far less performance potential than it might have. As well, at the low height,

the feedpoint impedance may range from  $25 \Omega$  up to  $50 \Omega$ , depending upon soil quality.

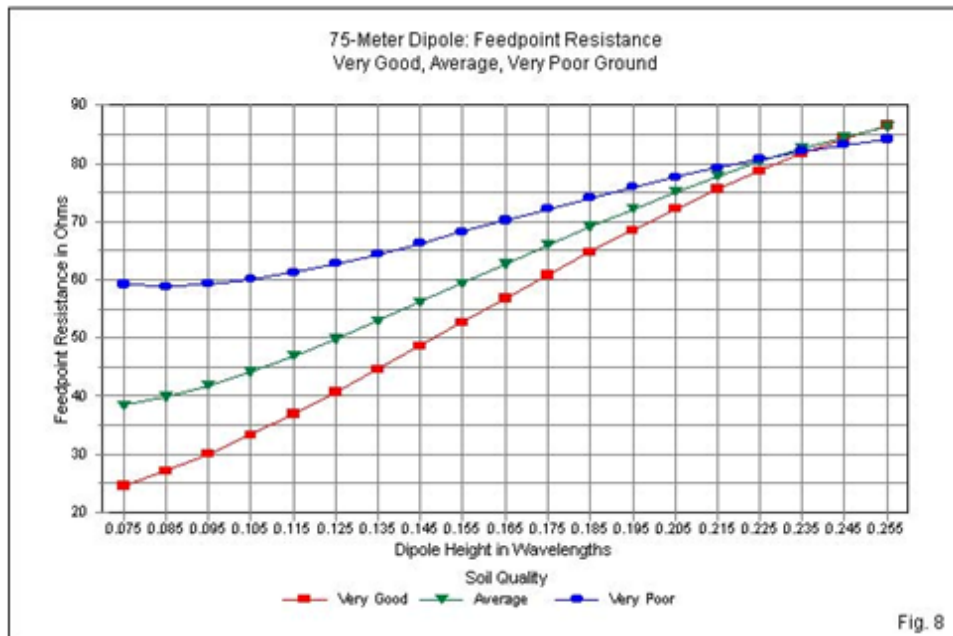


Fig. 8

We may better gauge the relative gain for the three bands covered by this survey by graphically sampling at least one set of antennas. **Fig. 9** compares the gain values over average ground for 160-, 75-, and 40-meter dipoles across the surveyed heights as measured in wavelengths. Just the change in operating frequency produces nearly a full dB difference in maximum gain when we take the values that coincide with the maximum zenith gain for each band.

As we increase the height of the antenna above ground, the differentials decrease, but remain notable even at a height greater than  $\frac{1}{4}\lambda$  above ground. Curves for other soil qualities will be similar. The idea that ground quality has very little effect on horizontal antenna performance may be true for antenna that are  $1\lambda$  up or higher, but in the range of NVIS heights in the upper MF and lower HF region, horizontal antennas show considerable effects from both height changes and from ground quality changes.

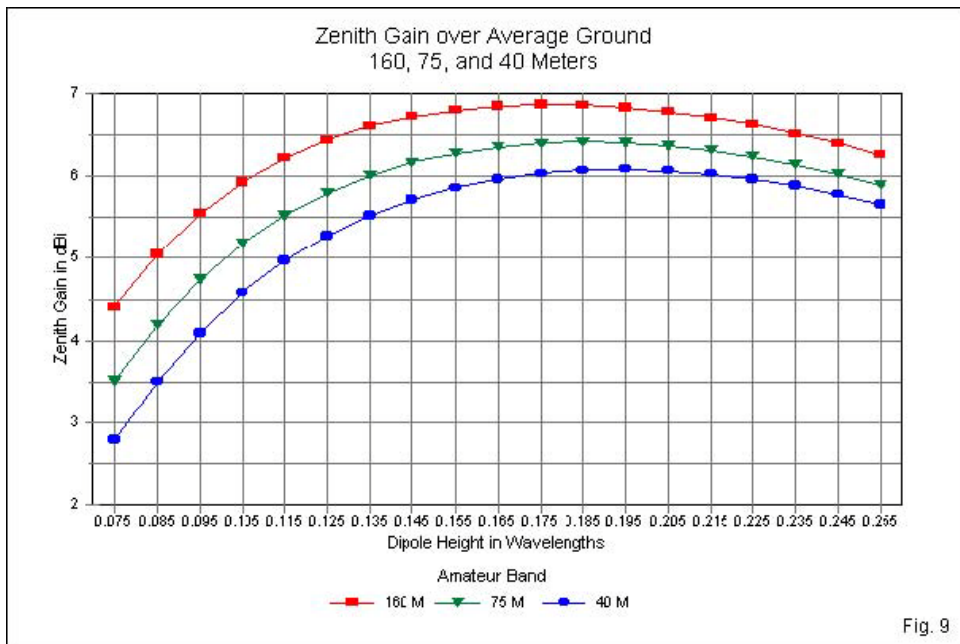


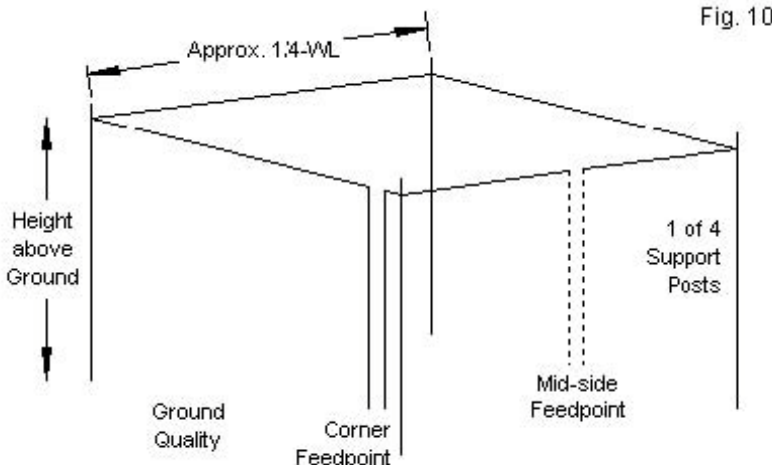
Fig. 9

We may summarize the findings—to a degree, at least—by encapsulating some of the key data from the individual data tables in a single place. **Table 4** uses a cross-matrix of the 3 bands vs. the soil quality levels. It lists the peak zenith gain for each band and the height in wavelengths at which that gain occurs. In addition, it lists the height in wavelengths at which the feedpoint resistance values converge. Wherever individual values occur at two adjacent heights, the table lists the average of the pair. Although highly incomplete, the table provides at a glance a view of some of the trends that we have noted along the way. It may also allow a fairly quick interpolation of probable values for NVIS dipoles at other frequencies, for example, 60 meters. It may also serve to make comparisons easier with other antennas in our collection.

Tri-Band Summary of Significant NVIS Dipole Values							Table 4
Ground	Very Good		Average		Very Poor		Z Cross
	Max Gain	Height	Max Gain	Height	Max Gain	Height	
Band	Zenith	WL	Zenith	WL	Zenith	WL	WL
160 m	7.63	0.160	6.87	0.175	5.71	0.190	0.240
75 m	7.40	0.165	6.42	0.185	5.13	0.200	0.210
40 m	7.15	0.170	6.09	0.195	4.86	0.205	0.205
Delta	0.48	0.010	0.78	0.020	0.85	0.015	0.035
Notes:	Max Gain Zenith = maximum zenith gain in dBi						
	Height WL = maximum zenith gain height in wavelengths						
	Z Cross WL = height at which feedpoint resistance values converge (Where 2 heights have the same value, the average appears here.)						
	Delta = maximum change between 160 and 40 meters						

### The 1- $\lambda$ Closed Loop

In basic antenna theory, the inverted-V is a dipole form and perhaps ought to come next in our survey. However, the inverted-V has some special limitations that divorce it from its close family ties to the dipole. More akin to the dipole by virtue of using a level plane for installation is the 1- $\lambda$  closed loop. In these notes, we shall deal only with a square loop, although we might in principle approximate any polygon ranging from a triangle to an almost perfect circle. Performance differences among the closed loops will be minimal.



Key Properties of a Square 1-WL Closed NVIS Loop

As shown in **Fig. 10**, we may feed the square either at mid-side or at a corner with no change in the loop dimensions, the feedpoint

impedance, or the performance. Corner feeding may be more convenient, since the post at that location can support the vertical run of feedline. We define the broadside direction of the loop as running between the feedpoint and a point directly opposite. The endwise direction is at  $90^\circ$  to this line. For modeling convenience, these notes use a mid-side feedpoint. The patterns do not differ significantly from those produced by selecting the more convenient corner feed position.

The  $1\lambda$  loop is subject to the same constraints as the dipole. The height above ground and the quality of the ground both below the antenna and in the region of far-field reflections largely determine the pattern shape and strength. Mechanically, the side dimension of the loop is about half that of a dipole, but the loop does require 4 support posts and occupies an area at the installation site. As well, the loop feedpoint impedance is higher than the impedance of a dipole, resulting in the need for a matching section if the main feedline is a standard  $50\text{-}\Omega$  coaxial cable.

At 40 meters (7.2 MHz), total circumference of the  $1\lambda$  loop is actually close to  $1.03 \lambda$  at NVIS heights. **Table 5** provides the numerical data derived from surveying the loop over the same height range as the dipole and over the three selected ground qualities. The range of reactance variation may seem striking compared to the values for the dipole. However, its affect upon the SWR relative to resonance is about the same, given the ratio of reactance to resistance at the feedpoint.

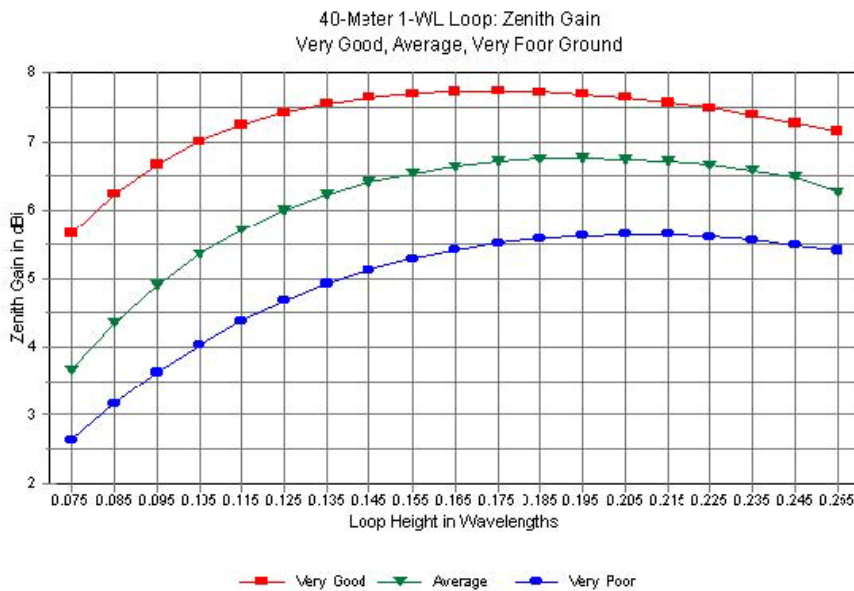


Fig. 11

The gain curves in **Fig. 11** are very similar to those for the dipole, with two major exceptions. First, the values at all heights are higher for the loop. (Whether the added gain justifies the more complex construction is a user judgment.) Second, the loop has a narrower broadside beamwidth and a very slightly wider endwise beamwidth at all heights. Hence, the column for maximum gain in the table is blank, since the broadside beamwidth never reaches a value that creates a dual line for the maximum gain direction. In essence, the loop more closely approximates the circular pattern that represents

the theoretical ideal (although that ideal may be less applicable to given installations).

40-Meter -WL Loop AWG #14 Copper Wire: Circumference = 1.0296 WL								7.2 MHz		Table 5	
Very Good Soil											
Height wl	Height ft	Zen Gain	Max Gain	TO Ang	BS BW	EW BW	BW Ratio	Feed R	Feed X		
0.075	10.25	6.66		90	77.7	68.2	1.14	63.78	38.74		
0.085	11.61	6.24		90	78.2	67.6	1.16	67.48	35.27		
0.095	12.98	6.67		90	78.9	67.6	1.17	72.11	32.93		
0.105	14.34	7.00		90	79.4	67.4	1.18	77.47	31.27		
0.115	15.71	7.24		90	80.3	67.4	1.19	83.37	29.98		
0.125	17.08	7.42		90	81.2	67.6	1.20	89.68	28.80		
0.135	18.44	7.55		90	82.1	68.0	1.21	96.25	27.56		
0.145	19.81	7.64		90	83.2	68.4	1.22	103.00	26.10		
0.155	21.17	7.70		90	84.3	68.8	1.23	109.80	24.33		
0.165	22.54	7.73		90	85.6	69.2	1.24	116.50	22.19		
0.175	23.91	7.74		90	87.0	69.8	1.25	123.10	19.63		
0.185	25.27	7.72		90	88.6	70.6	1.25	129.50	16.62		
0.195	26.64	7.69		90	90.5	71.4	1.27	135.50	13.17		
0.205	28.00	7.64		90	92.4	72.4	1.28	141.30	9.29		
0.215	29.37	7.57		90	94.5	73.4	1.29	146.60	5.00		
0.225	30.74	7.49		90	96.8	74.4	1.30	151.40	0.35		
0.235	32.10	7.39		90	99.2	75.8	1.31	155.70	-4.64		
0.245	33.47	7.27		90	101.9	77.2	1.32	159.40	-9.89		
0.255	34.83	7.15		90	104.9	78.8	1.33	162.60	-15.37		
Average Soil											
Height wl	Height ft	Zen Gain	Max Gain	TO Ang	BS BW	EW BW	BW Ratio	Feed R	Feed X		
0.075	10.25	3.67		90	80.9	71.6	1.13	94.53	25.16		
0.085	11.61	4.35		90	81.6	70.4	1.16	94.81	20.06		
0.095	12.98	4.90		90	82.3	69.4	1.19	96.37	16.41		
0.105	14.34	5.35		90	83.0	68.8	1.21	98.79	13.75		
0.115	15.71	5.71		90	83.8	68.6	1.22	101.90	11.71		
0.125	17.08	6.00		90	84.7	68.4	1.24	105.60	10.01		
0.135	18.44	6.23		90	85.9	68.4	1.26	108.60	8.41		
0.145	19.81	6.41		90	87.0	68.6	1.27	113.90	6.79		
0.155	21.17	6.54		90	88.4	68.8	1.28	118.30	5.02		
0.165	22.54	6.64		90	89.6	69.2	1.30	122.80	3.06		
0.175	23.91	6.71		90	91.4	69.6	1.31	127.30	0.84		
0.185	25.27	6.75		90	93.1	70.2	1.33	131.60	-1.68		
0.195	26.64	6.76		90	95.0	70.8	1.34	135.80	-4.48		
0.205	28.00	6.74		90	97.2	71.6	1.36	139.70	-7.58		
0.215	29.37	6.71		90	99.4	72.4	1.37	143.40	-10.96		
0.225	30.74	6.66		90	101.8	73.6	1.38	146.70	-14.60		
0.235	32.10	6.58		90	104.6	74.6	1.40	149.70	-18.46		
0.245	33.47	6.49		90	107.3	76.0	1.41	152.20	-22.51		
0.255	34.83	6.27		90	110.5	77.4	1.43	154.40	-26.71		
Height wl	Height ft	Zen Gain	Max Gain	TO Ang	BS BW	EW BW	BW Ratio	Feed R	Feed X		
0.075	10.25	2.63		90	86.5	78.6	1.10	118.00	0.91		
0.085	11.61	3.16		90	87.2	76.2	1.14	116.40	-4.00		
0.095	12.98	3.63		90	87.9	74.4	1.18	115.80	-7.57		
0.105	14.34	4.03		90	88.7	73.2	1.21	115.90	-10.17		
0.115	15.71	4.38		90	89.7	72.0	1.25	116.70	-12.18		
0.125	17.08	4.67		90	90.7	71.2	1.27	118.00	-13.79		
0.135	18.44	4.92		90	91.8	70.8	1.30	119.70	-15.19		
0.145	19.81	5.12		90	93.1	70.4	1.32	121.70	-16.51		
0.155	21.17	5.26		90	94.6	70.4	1.34	123.90	-17.65		
0.165	22.54	5.41		90	96.0	70.4	1.36	126.20	-19.22		
0.175	23.91	5.51		90	97.9	70.6	1.39	128.50	-20.72		
0.185	25.27	5.58		90	99.7	70.8	1.41	130.90	-22.38		
0.195	26.64	5.62		90	101.8	71.4	1.43	133.10	-24.20		
0.205	28.00	5.64		90	104.0	71.8	1.45	135.30	-26.20		
0.215	29.37	5.64		90	106.3	72.6	1.46	137.40	-28.36		
0.225	30.74	5.60		90	108.8	73.4	1.48	139.20	-30.67		
0.235	32.10	5.56		90	111.6	74.4	1.50	140.90	-33.12		
0.246	33.47	5.48		90	114.4	75.4	1.52	142.30	-35.68		
0.255	34.83	5.40		90	117.4	76.6	1.53	143.40	-38.34		

If you compare **Table 5** with **Table 1**, you will discover that the maximum gain occurs at the same heights over each type of ground quality for both loops and dipoles. As well, the feedpoint resistance tends to converge in the same manner as we found for the dipole, although the convergence is less complete in the case of the loop. The loop's convergence region is considerably wider as a span of heights, so we may bypass a graph. However, the tabular data will show the spread. Of special note are the beamwidth numbers, especially the ratio of broadside to endwise beamwidth. Note that the loop and the dipole both use the same wire: for 40 meters, AWG #14 copper wire.

In the case of the dipole, we found that as we lowered the operating frequency from 40 meters to 75 meters, the maximum gain value rose, while height of maximum gain decreased. These facts applied to all three ground qualities. We encounter the same phenomena in the case of the 75-meters 1- $\lambda$  loop. The numbers appear in **Table 6** (for comparison with the corresponding dipole values in **Table 2**).

**Fig. 12** compares the loop gain values for the three qualities of ground.

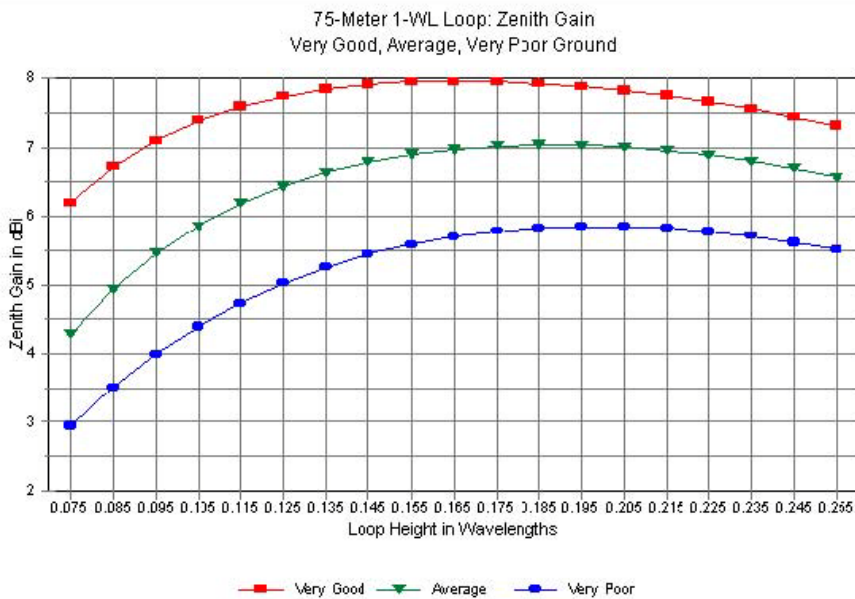


Fig. 12

As both the graphs and the tables make clear, the heights of maximum gain on 75 meters are virtually identical for both the loop and the dipole. Unlike either antenna at 40 meters, where we may easily construct the antenna at the optimal height, on 75 meters, we may need to be satisfied with a slightly lesser height. The loop is like the dipole in the fact that gain does not fall off sharply over any of the soil types as we lower the antenna by modest amounts. However, the effect may be more noticeable over the worst soils where the maximum gain height in wavelengths is greatest, while the antenna construction project may have a strict physical limit.

For example, compare the gain values at 35' (about 0.14- $\lambda$ ) with the maximum gain possible for each of the individual ground quality values.

75-Meter -WL Loop AWG #14 Copper Wire Circumference = 1.0248 WL 3.9 MHz								Table 6	
Very Good Soil		Zen Gain	Max Gain	TO Ang	BS BW	EW BW	BW Ratio	Feed R	Feed X
0.075	18.91	6.20		90	77.1	67.2	1.15	55.06	29.84
0.085	21.44	6.72		90	77.6	67.0	1.16	59.52	27.14
0.095	23.96	7.10		90	78.2	67.0	1.17	64.82	25.43
0.105	26.48	7.39		90	78.7	66.8	1.18	70.78	24.33
0.115	29.00	7.59		90	79.6	67.0	1.19	77.24	23.53
0.125	31.52	7.74		90	80.4	67.2	1.20	84.08	22.78
0.135	34.05	7.84		90	81.3	67.6	1.20	91.17	21.91
0.145	36.57	7.91		90	82.3	68.0	1.21	98.40	20.79
0.155	39.09	7.95		90	83.4	68.6	1.22	105.70	19.31
0.165	41.61	7.96		90	84.7	69.0	1.23	112.90	17.41
0.175	44.13	7.95		90	86.1	69.8	1.23	120.00	15.05
0.185	46.66	7.92		90	87.6	70.6	1.24	126.90	12.20
0.195	49.18	7.88		90	89.4	71.4	1.25	133.40	8.87
0.205	51.70	7.82		90	91.4	72.4	1.26	139.60	5.06
0.215	54.22	7.75		90	93.3	73.2	1.27	145.40	0.80
0.225	56.74	7.68		90	95.6	74.4	1.28	150.60	-3.87
0.235	59.27	7.56		90	98.0	75.8	1.29	155.40	-8.90
0.245	61.79	7.44		90	100.8	77.2	1.31	159.50	-14.25
0.255	64.31	7.31		90	103.6	79.0	1.31	163.10	-19.85
Average Soil		Zen Gain	Max Gain	TO Ang	BS BW	EW BW	BW Ratio	Feed R	Feed X
0.075	18.91	4.28		90	79.9	70.8	1.13	86.79	25.53
0.085	21.44	4.93		90	80.5	69.8	1.15	88.26	20.43
0.095	23.96	5.45		90	81.2	69.2	1.17	90.67	16.76
0.105	26.48	5.86		90	82.0	68.8	1.19	94.26	14.02
0.115	29.00	6.19		90	82.8	68.6	1.21	98.31	11.83
0.125	31.52	6.44		90	83.8	68.6	1.22	102.80	9.94
0.135	34.05	6.64		90	84.8	68.6	1.24	107.70	8.13
0.145	36.57	6.79		90	85.9	68.8	1.25	112.80	6.26
0.155	39.09	6.90		90	87.2	69.2	1.26	117.90	4.22
0.165	41.61	6.97		90	88.8	69.6	1.28	123.10	1.94
0.175	44.13	7.02		90	90.3	70.2	1.29	128.20	-0.64
0.185	46.66	7.04		90	92.0	70.8	1.30	133.10	-3.53
0.195	49.18	7.03		90	93.9	71.4	1.32	137.80	-6.75
0.205	51.70	7.00		90	96.0	72.4	1.33	142.20	-10.26
0.215	54.22	6.95		90	98.3	73.4	1.34	146.30	-14.12
0.225	56.74	6.89		90	100.8	74.4	1.35	150.00	-18.23
0.235	59.27	6.80		90	103.5	75.6	1.37	153.30	-22.58
0.245	61.79	6.70		90	106.4	77.0	1.38	156.10	-27.14
0.255	64.31	6.57		90	109.4	78.6	1.39	158.40	-31.64
Very Poor Soil		Zen Gain	Max Gain	TO Ang	BS BW	EW BW	BW Ratio	Feed R	Feed X
0.075	18.91	2.94		90	85.6	77.2	1.11	119.50	3.32
0.085	21.44	3.51		90	86.2	78.2	1.15	118.00	2.25
0.095	23.96	3.99		90	87.0	73.6	1.18	117.50	-6.42
0.105	26.48	4.39		90	88.0	72.6	1.21	118.00	-9.57
0.115	29.00	4.73		90	88.9	71.8	1.24	119.10	-12.11
0.125	31.52	5.02		90	90.0	71.2	1.26	120.80	-14.24
0.135	34.05	5.25		90	91.3	71.0	1.29	122.80	-16.17
0.145	36.57	5.44		90	92.6	70.8	1.31	125.10	-18.01
0.155	39.09	5.58		90	94.2	70.8	1.33	127.60	-19.67
0.165	41.61	5.69		90	96.7	71.0	1.35	130.20	-21.80
0.175	44.13	5.78		90	97.6	71.2	1.37	132.60	-23.87
0.185	46.66	5.83		90	99.6	71.6	1.39	135.40	-26.09
0.195	49.18	5.85		90	101.8	72.2	1.41	137.90	-28.48
0.205	51.70	5.85		90	104.1	72.8	1.43	140.20	-31.05
0.215	54.22	5.83		90	106.5	73.6	1.45	142.30	-33.77
0.225	56.74	5.77		90	109.3	74.6	1.47	144.30	-36.64
0.235	59.27	5.71		90	112.2	75.4	1.49	145.90	-39.64
0.245	61.79	5.61		90	115.2	76.8	1.50	147.30	-42.74
0.255	64.31	5.51		90	118.3	78.2	1.51	148.30	-45.90

The 75-meter loop continues the trends that we encountered with the 40-meter loop. The broadside beamwidth never reaches a value that creates a difference between the antenna's maximum gain and the zenith gain. (The exact broadside beamwidth at which the maximum gain splits into two vectors with a slight depression in the zenith gain varies from one antenna and ground quality to the next. The general region of the split is a broadside beamwidth above  $125^\circ$ , a value that the  $1-\lambda$  loop never reaches with the survey height limit of  $0.255\lambda$ .) The 75-meter beamwidth ratios parallel those for 40 meters, as do the progressions of feedpoint resistance and reactance.

If we followed the band-by-band progressions for the dipole and have digested the values for the 40-and 75-meter  $1-\lambda$  loops, we can almost predict the values that we meet for the 160-meter loop. We expect increased gain and slightly lower heights for maximum zenith gain, and the 160-meter loop does not disappoint us. **Fig. 13** graphs the gain curves to supplement the numerical information in **Table 7**.



Fig. 13

Perhaps the most limiting factor for the 160-meter loop, which also applies to the 160-meter dipole, is the physical height limit to which most horizontal antennas are subject on that band. The lowest height on the survey is almost 40' (for  $0.075\lambda$ ), which is very much below the height of maximum gain, even over the best of soil qualities. This height presents deficits of gain, as well as considerably different feedpoint resistance values. Moreover, the feedpoint resistance values (assuming one field adjusts the antenna to resonance) vary considerably with soil quality at the very low height. Almost inevitably, then, any 160-meter NVIS

installation will suffer relative to performance values that are possible for 75-meter and 40-meter NVIS antennas. However, if the antenna height may reach between 80' and 100' (depending on soil quality), the 160-meter loop is capable of excellent performance.

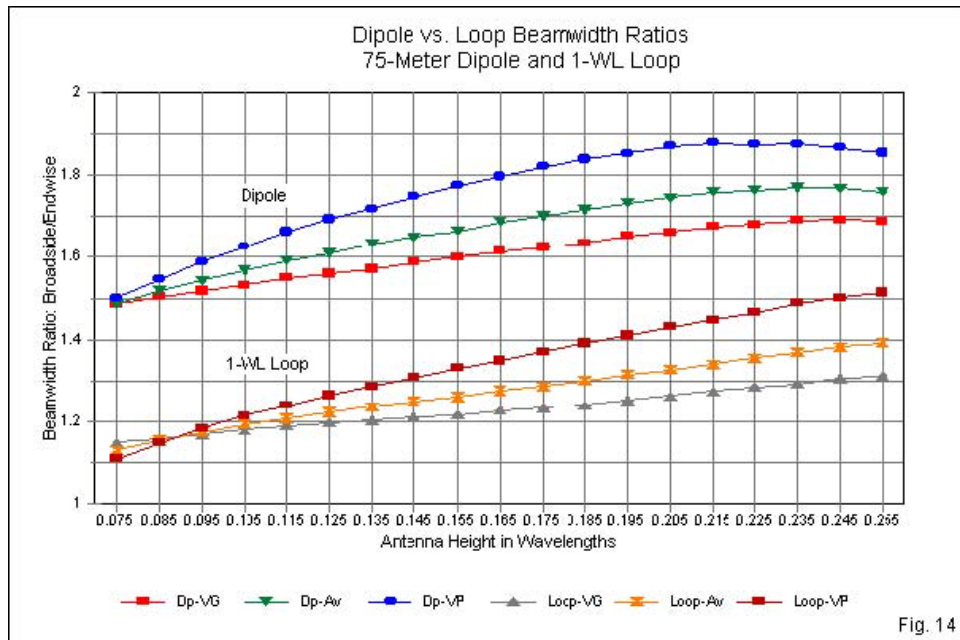
160-Meter 1-WL Loop AWG #12 Copper Wire: Circumference = 1.0212 WL 1.85 MHz								Table 7	
Very Good Soil		Zen Gain	Max Gain	TO Ang	BS BW	EW BW	BW Ratio	Feed R	Feed X
0.075	39.87	6.75		90	76.7	66.4	1.16	47.01	20.45
0.085	45.19	7.21		90	77.0	66.2	1.16	52.06	18.55
0.095	50.51	7.53		90	77.7	66.2	1.17	57.88	17.53
0.105	55.82	7.76		90	78.4	66.4	1.18	64.30	17.03
0.115	61.14	7.93		90	78.9	66.6	1.18	71.20	16.75
0.125	66.46	8.04		90	79.8	66.8	1.19	78.45	16.48
0.135	71.77	8.11		90	80.7	67.2	1.20	85.95	16.05
0.145	77.09	8.16		90	81.6	67.6	1.21	93.60	15.32
0.155	82.41	8.18		90	82.8	68.2	1.21	101.30	14.18
0.165	87.72	8.17		90	84.1	68.8	1.22	108.90	12.59
0.175	93.04	8.15		90	85.4	69.6	1.23	116.40	10.49
0.185	98.36	8.12		90	86.8	70.2	1.24	123.70	7.86
0.195	103.67	8.07		90	88.4	71.2	1.24	130.70	4.71
0.205	108.99	8.00		90	90.3	72.2	1.25	137.30	1.03
0.215	114.31	7.97		90	92.7	73.7	1.26	143.50	-3.13
0.225	119.62	7.82		90	94.4	74.4	1.27	149.20	-7.74
0.235	124.94	7.72		90	96.8	75.6	1.28	154.30	-12.76
0.245	130.26	7.60		90	99.4	77.2	1.29	158.90	-18.14
0.255	135.57	7.46		90	102.3	78.8	1.30	162.60	-23.80
Average Soil		Zen Gain	Max Gain	TO Ang	BS BW	EW BW	BW Ratio	Feed R	Feed X
0.075	39.87	5.13		90	78.5	69.2	1.13	72.39	23.33
0.085	45.19	5.73		90	79.1	68.6	1.15	75.41	18.95
0.095	50.51	6.19		90	79.8	68.4	1.17	79.40	15.87
0.105	55.82	6.55		90	80.5	68.2	1.18	84.12	13.62
0.115	61.14	6.82		90	81.3	68.2	1.19	89.40	11.83
0.125	66.46	7.03		90	82.2	68.2	1.21	95.09	10.24
0.135	71.77	7.19		90	83.2	68.4	1.22	101.00	8.66
0.145	77.09	7.30		90	84.3	68.8	1.23	107.20	6.94
0.155	82.41	7.38		90	85.5	69.2	1.24	113.30	4.97
0.165	87.72	7.42		90	87.0	69.6	1.25	119.50	2.70
0.175	93.04	7.44		90	88.4	70.2	1.26	125.50	0.06
0.185	98.36	7.44		90	90.1	70.8	1.27	131.30	-2.96
0.195	103.67	7.42		90	91.9	71.6	1.28	136.90	-6.37
0.205	108.99	7.38		90	93.9	72.6	1.29	142.10	-10.16
0.215	114.31	7.31		90	96.1	73.6	1.31	146.90	-14.31
0.225	119.62	7.24		90	98.6	74.8	1.32	151.30	-18.79
0.235	124.94	7.14		90	101.2	76.0	1.33	155.10	-23.56
0.245	130.26	7.03		90	104.0	77.4	1.34	158.50	-28.57
0.255	135.57	6.90		90	106.9	79.2	1.35	161.30	-33.77
Height wl		Zen Gain	Max Gain	TO Ang	BS BW	EW BW	BW Ratio	Feed R	Feed X
0.075	39.87	3.57		90	83.0	75.0	1.11	111.40	13.42
0.085	45.19	4.16		90	83.8	73.5	1.14	110.90	7.01
0.095	50.51	4.66		90	84.4	72.4	1.17	111.70	2.14
0.105	55.82	5.06		90	85.4	71.6	1.19	113.30	-1.65
0.115	61.14	5.39		90	86.4	71.2	1.21	115.60	-4.79
0.125	66.46	5.66		90	87.5	70.8	1.24	118.40	-7.50
0.135	71.77	5.87		90	88.8	70.8	1.25	121.50	-10.01
0.145	77.09	6.04		90	90.1	70.8	1.27	124.90	-12.46
0.155	82.41	6.17		90	91.5	70.8	1.29	126.50	-14.95
0.165	87.72	6.26		90	93.2	71.2	1.31	132.00	-17.56
0.175	93.04	6.32		90	95.0	71.6	1.33	135.50	-20.34
0.185	98.36	6.35		90	96.9	72.0	1.35	138.90	-23.31
0.195	103.67	6.36		90	99.2	72.8	1.36	142.10	-26.48
0.205	108.99	6.33		90	101.6	73.6	1.38	145.10	-29.85
0.215	114.31	6.29		90	104.1	74.4	1.40	147.80	-33.41
0.225	119.62	6.23		90	106.7	75.4	1.42	150.20	-37.14
0.235	124.94	6.14		90	109.7	76.6	1.43	152.30	-41.01
0.245	130.26	6.03		90	112.7	78.0	1.44	154.00	-44.99
0.255	135.57	5.91		90	115.8	79.4	1.46	155.30	-49.04

### Some Preliminary Dipole and Loop Comparisons

The dipole and the loop have numerous similarities in their performance curves relative to height and ground quality. They also display a number of differences worth noting. The differences are real, but their import for a given NVIS operation will vary from one installation to the next. We can here only note the differences, but the user must assign them weight in the overall decision on what sort of antenna to construct for a given fixed station system.

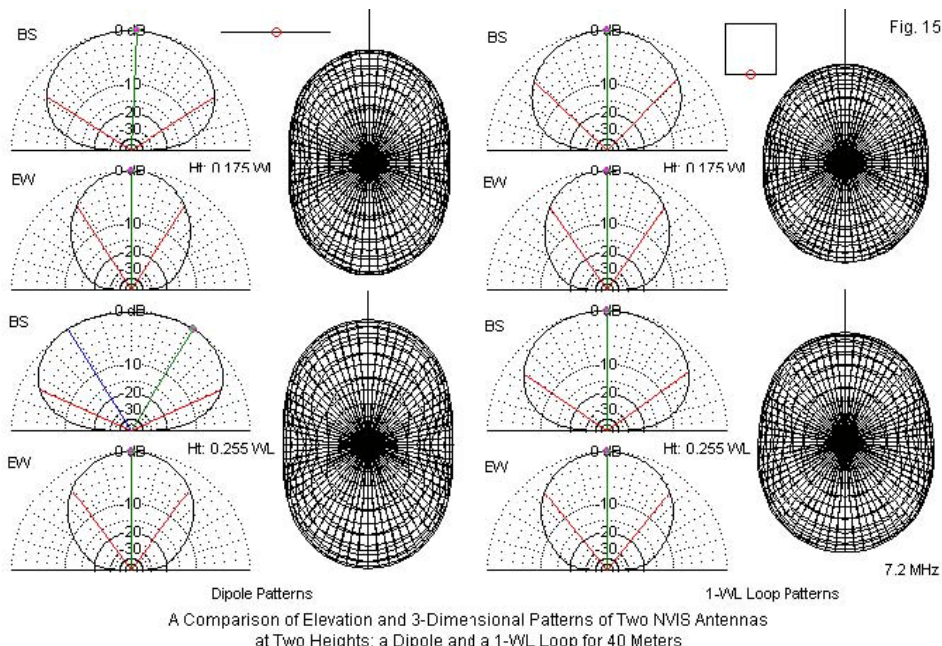
Mechanically, the dipole requires only two end-support posts (towers, trees, etc.) but the linear space is about  $\frac{1}{2}\lambda$  at the operating frequency. In contrast, the loop requires 4 supports, but at a spacing just over  $\frac{1}{4}\lambda$  per side. The dipole's feedline has only the antenna wire for support, but a corner-fed loop may use the support post to minimize feedline stress on the antenna wire.

Electrically, one of the most interesting differences between the dipole and the loop is the beamwidth ratio, that is, the broadside beamwidth divided by the endwise beamwidth. **Fig. 14** graphs the beamwidth ratios for to 75-meter dipole and loop for all ground qualities in order to clarify the difference. In the region of higher gain, the dipole values range from 1.6:1 up to nearly 1.9:1. Values increase as we lessen the quality of the soil beneath the antenna. In contrast, the loop ratios for the same region vary from 1.2:1 to 1.4:1. Again, the values increase with worse soils in the antenna region.



The significance of the numerical values shows more clearly if we present the information in the form of far-field antenna patterns.

**Fig. 15** provides a sample of elevation and 3-dimensional (top-view) patterns for the same dipole and loop. The sample uses average soil and 2 heights:  $0.175\lambda$  and  $0.255\lambda$ . The heights correspond to near-maximum zenith gain and the upper limit of the survey. For reference, the 3-dimensional patterns show the same length of broadside axis line in all cases.



At both heights, the dipole shows a greater broadside elongation of its patterns. In fact, at  $0.255\text{-}\lambda$ , the broadside elevation pattern displays the dual maximum gain lines, although the zenith gain depression is operationally insignificant. In contrast, the loop patterns are more nearly circular, even at the maximum height surveyed. (Close inspection of the 3-dimensional loop pattern at  $0.255\text{-}\lambda$  reveals a slight asymmetry or egg-shape, with the broad end at the antenna feedpoint side of the mid-side fed loop used in the sample.) In operation, either pattern may prove to be the more desirable, depending upon the mission specifications for a given

station. Nevertheless, the differences are real and may play a role in operations under difficult physical or ionospheric conditions.

We have noted in passing that the loop provides a gain improvement over the dipole. Conventionally, we tend to compare dipoles and loops in free space. In that environment, the loop has a gain advantage of about 1.1 dB over the dipole. When we place horizontal antennas close to ground, as is necessary for NVIS operations, we must set aside conventional numbers and examine the effects of the ground upon the two antennas.

**Table 8** summarizes some of the key features of the 1- $\lambda$  loop in NVIS operation. (See **Table 4** for a parallel treatment of NVIS dipoles.) Just as was the case with the dipole, lowering the operating frequency shows a greater increase in gain over very poor soil than over better soils. The table also shows the increase in the height of maximum zenith gain as we raise the operating frequency over each of the soil types.

Tri-Band Summary of Significant NVIS 1-WL Loop Values											Table 8	
Ground	Very Good		Average				Very Poor					
	Max Gain Zenith	Height WL	Gain over Dipole dB	Max Gain Zenith	Height WL	Gain over Dipole dB	Max Gain Zenith	Height WL	Gain over Dipole dB			
160 m	8.18	0.155	0.55	7.44	0.180	0.57	6.35	0.190	0.64			
75 m	7.96	0.165	0.56	7.04	0.185	0.62	5.85	0.200	0.72			
40 m	7.74	0.175	0.59	6.76	0.195	0.67	5.64	0.210	0.78			
Delta	0.44	0.020		0.68	0.015		0.71	0.02				

Notes:

- Max Gain Zenith = maximum zenith gain in dBi
- Height WL = maximum zenith gain height in wavelengths
- (Where 2 heights have the same value, the average appears here.)
- Gain over Dipole dB = gain of 1-WL loop over dipole at maximum gain; same frequency and height
- Delta = maximum loop-only change between 160 and 40 meters

The table also contains an extra set of columns showing the zenith gain advantage of the loop over the dipole when we set each antenna at the height of maximum gain (a height that is the same for each antenna type over each soil type). The gain advantage of the loop increases as we reduce the quality of the ground in the antenna region. **Fig. 16** graphs all 6 of the relevant gain curves (3 for the dipole and 3 for the loop) to shows the variation in the loop's advantage over the full spectrum of surveyed heights. The curves appear in pairs for each of the soil quality value sets. For each pair, the loop is always the higher curve. One interesting facet of comparing the curves is the more rapid drop in gain of the dipole above the height of maximum zenith gain. The loop curves are shallower above the maximum gain height. Below the height of maximum gain, the dipole and loop curves show a highly parallel shape. You may correlate this data to the beamwidth ratio information in the following way. At the maximum surveyed height, the dipole has already passed the beamwidth at which the broadside pattern begins to split into two lobes, but the loop beamwidth remains short of that value.

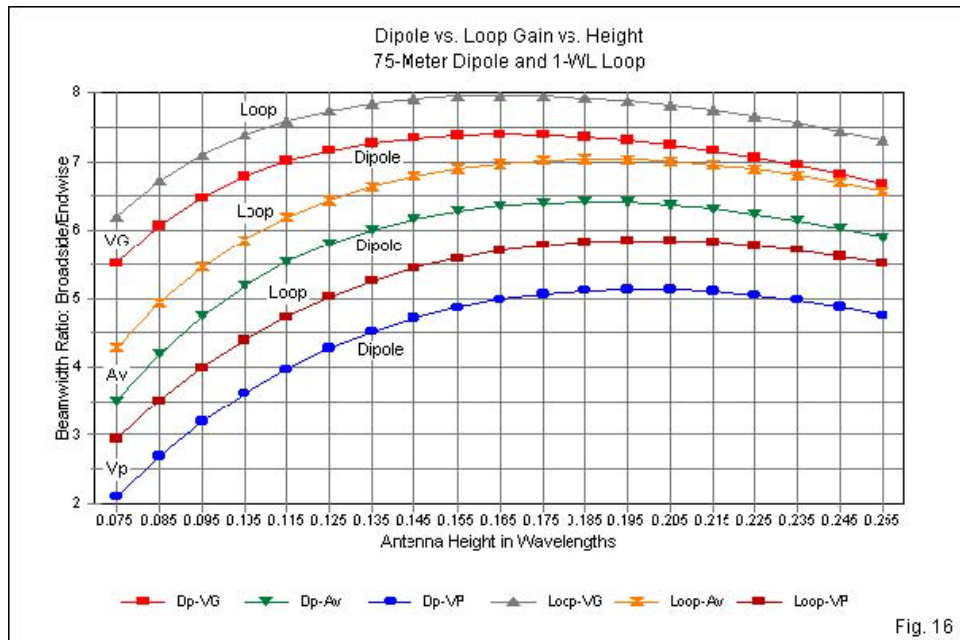
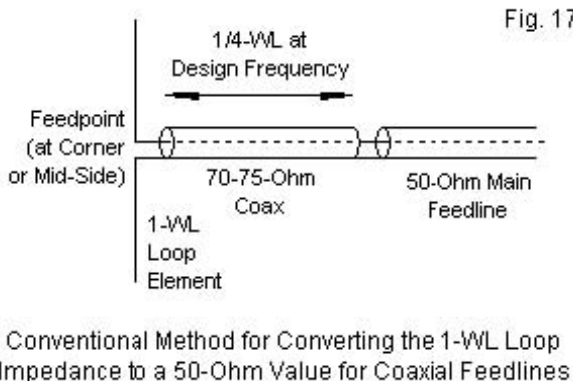


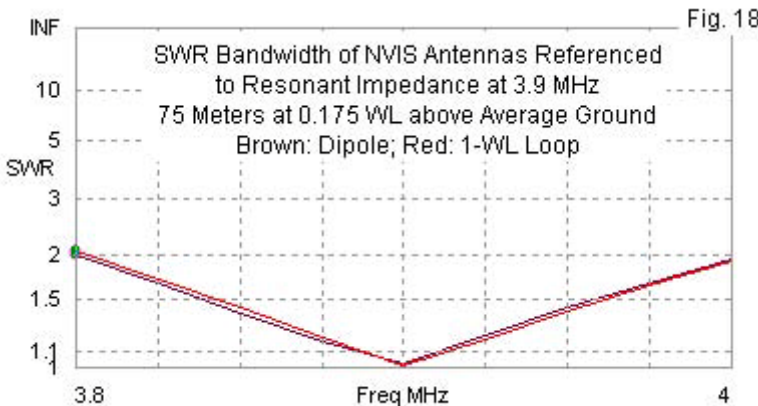
Fig. 16

The feedpoint impedance levels for NVIS dipoles are generally suitable for use with  $50\Omega$  coaxial cable feedlines, although at the heights of maximum zenith gain,  $70\Omega$  coax may yield better SWR values. Loop impedance values at the heights of maximum zenith gain range between  $100\Omega$  and  $130\Omega$ , depending upon the quality of the soil. In most cases, the simple  $\frac{1}{4}\lambda$   $70\Omega$  series matching section shown in **Fig. 17** will transform the impedance to a level compatible with a  $50\Omega$  main feedline. Since the matching-section line is in series with the main feedline and counts toward the total

feedline length from the antenna to the equipment, it does not measurably increase line losses.



Neither antenna shows an advantage with respect to the SWR bandwidth once well matched. **Fig. 18** overlays the SWR curves for both antennas, with each referenced to the resonant impedance, on 75 meters at  $0.175\lambda$  above ground over average soil. The curves are virtually indistinguishable.



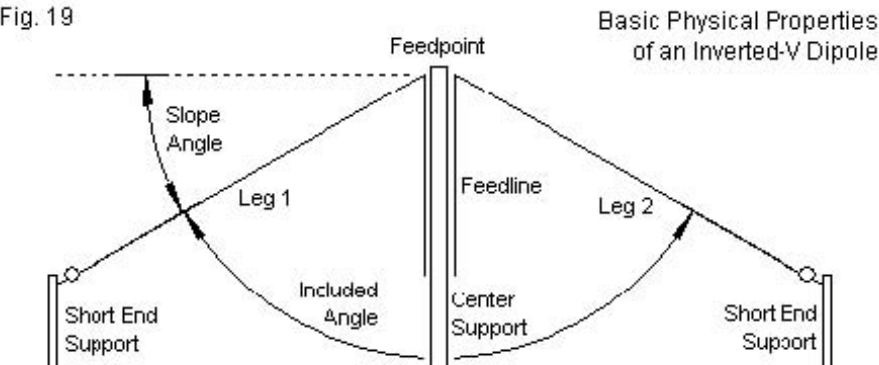
These comparative notes on the dipole and the  $1-\lambda$  loop as NVIS antennas make no decisions about which one (or which height) may be best for a given installation. That decision rests on the total span of considerations that go into planning and building an antenna with a certain set of mission specifications. The whole point of the extensive notes, graphs, and tables is to provide sufficient background information on the anticipated electrical performance of the antennas to make the decision as well informed as possible. However, among our basic antennas, we still have one more to consider. The inverted-V dipole is a form of dipole, but has a special property when placed close to ground in a NVIS environment: the V-shape.

### The Inverted-V Dipole

When we consider the inverted-V with a modest slope (or a large included angle) in a free-space environment or placed higher than  $\frac{1}{2}\lambda$  above ground, we consider it to be a slightly modified dipole with almost as much broadside gain and with a smaller gain null off the ends of the wire. In those contexts, we tend to truncate the discussion of the V and its performance. As a NVIS antenna, the inverted-V requires close attention to details of its performance.

**Fig. 19** provides some of the reasons for special focus.

Fig. 19



We ordinarily define an inverted-V in one of two ways: by reference to the slope of the line from the horizontal or by reference to the included angle between the wires. For our work, we shall select a slope angle of  $30^\circ$ , which yields an included angle of  $120^\circ$ . Larger slope angles are generally impractical for NVIS work on the lowest three amateur bands. Shallower angles will have performance

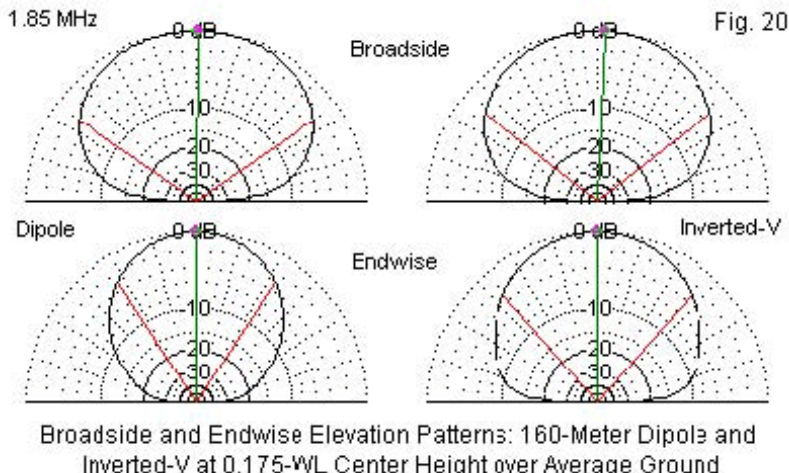
reports between the 30° V we have selected and a linear dipole, so you may interpolate the probable values.

The chief mechanical advantage of the V is that it needs only one central tall, sturdy support. The wire-end supports can be shorter and therefore lighter. In addition, the V version of the dipole has a lower feedpoint impedance value than a linear dipole. If the standard dipole has a NVIS feedpoint impedance close to  $70\ \Omega$ , then the anticipated V impedance value should approach  $50\ \Omega$ , a good match for the ubiquitous coaxial cables used in most amateur installations. Of course, we shall allow the data to eventually tell us what the most likely values are for each soil type in our survey.

The 30° inverted-V sets some limits to the lowest height at which we can set the center point. The ends must not only clear the ground, but as well leave a safety margin to prevent human or animal contact with the high-voltage end of the wires. A reasonable standard is probably about 10'. However, we shall show results for one step below this level. On 40 meters, the minimum center height will be  $0.175\lambda$ , which results in an end height of about 7.4' above ground. On 75 meters, the center minimum is  $1.55\lambda$ , for an end height of 8.7'. The 160meter center height of  $0.135\lambda$  results in an end height of 7.7' above ground. For each band, we shall use the center-height as a reference and increase that value in  $0.1\lambda$  increments to the survey limit of  $0.255\lambda$ , regardless of whether that value is practical on any particular band.

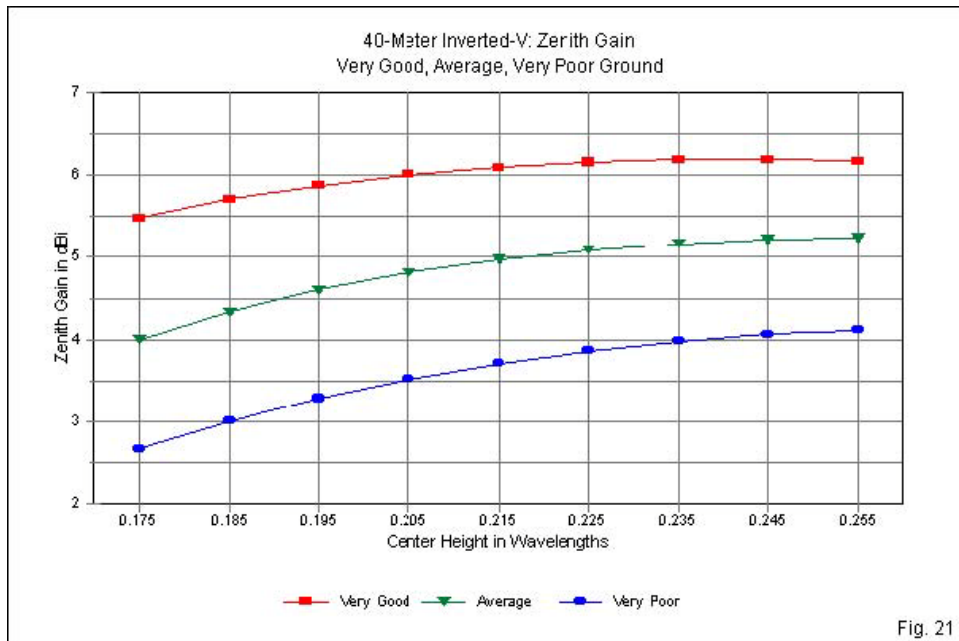
One of the most interesting aspects of the inverted-V configuration is the difference in the endwise patterns relative to either the dipole

or the  $1\lambda$  loop. **Fig. 20** compares elevation patterns for a dipole and a V for 160 meters, both with center heights of  $0.175\lambda$ . The broadside patterns show very little difference. However, the endwise patterns have quite different general shapes as well as beamwidth values. The sloping elements, even with only a  $30^\circ$  droop, show considerable radiation off the ends. The end radiation is not sufficient to dominate the pattern, but it is enough to widen the endwise beamwidth and to retain more than expected levels of radiation at lower angles. The patterns are similar on all three of our surveyed bands.



Because the V enforces a minimum height for the antenna center, our data tables will be smaller than for the other two antennas. The 40-meter V has the smallest data set of all, as evidenced by **Table**

9. However, the span of values is large enough for use to see some interesting differences in V behavior relative to the behavior of the two level antennas.



40-Meter Inverted-V AWG #14 Copper Wire: Length = 0.482 WL											Table 9
Very Good Soil											
Height wl	Height ft	Zen Gain	Max Gain	TO Ang	BS BW	EW BW	BW Ratio	Feed R	Feed X		
0.175	23.91	5.48		90	102.8	81.8	1.26	49.46	14.32		
0.185	25.27	5.71		90	104.2	80.4	1.30	51.47	11.65		
0.195	26.64	5.88		90	105.8	79.6	1.33	53.62	9.14		
0.205	28.00	6.01		90	107.5	79.0	1.36	55.85	7.42		
0.215	29.37	6.10		90	109.2	78.6	1.39	58.0	5.56		
0.225	30.74	6.16		90	111.2	78.2	1.42	60.33	3.73		
0.235	32.10	6.19		90	113.2	78.2	1.45	62.51	1.88		
0.245	33.47	6.19		90	115.4	78.4	1.47	64.59	-0.02		
0.255	34.83	6.17		90	117.6	78.8	1.49	66.54	-1.99		
Average Soil											
Height wl	Height ft	Zen Gain	Max Gain	TO Ang	BS BW	EW BW	BW Ratio	Feed R	Feed X		
0.175	23.91	4.00		90	108.4	80.2	1.35	58.61	4.12		
0.185	25.27	4.33		90	110.0	78.8	1.40	59.00	1.56		
0.195	26.64	4.60		90	111.6	77.8	1.43	59.68	-0.51		
0.205	28.00	4.81		90	113.2	77.2	1.47	60.58	-2.28		
0.215	29.37	4.97		90	115.2	76.8	1.50	61.61	-3.88		
0.225	30.74	5.09		90	117.2	76.5	1.53	62.72	-5.38		
0.235	32.10	5.17		90	119.2	76.5	1.56	63.88	-6.86		
0.245	33.47	5.22		90	121.3	76.6	1.58	65.02	-8.33		
0.255	34.83	5.24		90	123.4	76.8	1.61	66.13	-9.84		
Very Poor Soil											
Height wl	Height ft	Zen Gain	Max Gain	TO Ang	BS BW	EW BW	BW Ratio	Feed R	Feed X		
0.175	23.91	2.66		90	117.2	79.8	1.47	64.92	-8.01		
0.185	25.27	3.00		90	118.6	78.6	1.51	64.05	-10.09		
0.195	26.64	3.28		90	120.4	77.6	1.55	63.54	-11.71		
0.205	28.00	3.52		90	122.0	76.6	1.59	63.32	-13.05		
0.215	29.37	3.71		90	123.6	76.2	1.62	63.30	-14.20		
0.225	30.74	3.86		90	125.5	75.8	1.66	63.44	-15.24		
0.235	32.10	3.98		90	127.4	75.5	1.69	63.67	-16.20		
0.245	33.47	4.06		90	129.4	75.5	1.71	63.98	-17.13		
0.255	34.83	4.11	4.14	65	131.0	75.6	1.73	64.32	-18.05		

The gain tracks in **Fig. 21** show two important V idiosyncrasies.

First, the center height for maximum gain is uniformly high. Only over very good soil do we find a distinct gain maximum followed by at least one lesser value. For average and very poor soil, maximum zenith gain occurs either at or above the  $0.255\lambda$  survey-height

limitation. Ground coupling to the lower wire ends and the sloping elements combine to reduce the effective height of the V if we take the maximum gain heights of the level antennas as standards.

Second, with a center height only at the level of the dipole or loop maximum-gain heights, the V shows a much lower gain. Despite this apparent disadvantage, the anticipated lower feedpoint impedance values—close to the characteristic impedance of common coaxial cable—do show up in the data set.

The trends established by the 40-meter inverted-V reappear in the 75-meter version. As we move downward in frequency, we can add two more steps of data to the collection and maintain the minimum wire-end height. Only over very good ground does the progression of values in **Table 10** show a distinct peak zenith gain value, although the doubled value at the highest limit over average ground indicates a clear peak at that level. The required center height for peak zenith gain over very poor soil remains outside the table limits. We may also note that the inverted-V, unlike the dipole, only shows a difference between maximum gain and maximum zenith gain at the highest levels and only over very poor soil. The oddity of this phenomenon relative to the dipole and the  $1\lambda$  loop is that the differential occurs before the V over the worst ground quality has reached its peak zenith gain value.

75-Meter Inverted-V AWG #14 Copper Wire: Length = 0.482 WL										Table 10
Very Good Soil										
Height wl	Height ft	Zen Gain	Max Gain	TO Ang	BS BW	EW BW	BW Ratio	Feed R	Feed X	
0.155	39.09	5.26		90	99.2	86.2	1.15	42.01	19.02	
0.165	41.61	5.59		90	100.2	83.8	1.20	43.99	14.13	
0.175	44.13	5.85		90	101.4	82.0	1.24	46.25	11.46	
0.185	46.66	6.04		90	102.8	80.8	1.27	48.67	8.98	
0.195	49.18	6.19		90	104.4	79.8	1.31	51.20	6.90	
0.205	51.70	6.29		90	106.0	79.2	1.34	53.78	5.04	
0.215	54.22	6.36		90	107.8	78.8	1.37	56.36	3.26	
0.225	56.74	6.41		90	109.6	78.4	1.40	58.90	1.50	
0.235	59.27	6.42		90	111.6	78.5	1.42	61.36	-0.30	
0.245	61.79	6.41		90	113.8	78.6	1.45	63.71	-2.18	
0.255	64.31	6.38		90	116.1	79.0	1.47	65.91	-4.15	
Average Soil										
Height wl	Height ft	Zen Gain	Max Gain	TO Ang	BS BW	EW BW	BW Ratio	Feed R	Feed X	
0.155	39.09	3.65		90	104.0	86.0	1.21	56.52	13.17	
0.165	41.61	4.11		90	105.2	82.8	1.27	56.59	8.26	
0.175	44.13	4.47		90	106.6	81.0	1.32	57.5	4.65	
0.185	46.66	4.77		90	108.2	79.8	1.36	58.05	1.85	
0.195	49.18	5.00		90	109.8	78.8	1.39	59.19	-0.46	
0.205	51.70	5.19		90	111.4	78.0	1.43	60.49	-2.47	
0.215	54.22	5.32		90	113.4	77.8	1.46	61.88	-4.31	
0.225	56.74	5.42		90	115.4	77.4	1.49	63.32	-6.06	
0.235	59.27	5.49		90	117.4	77.2	1.52	64.76	-7.78	
0.245	61.79	5.52		90	119.6	77.4	1.55	66.15	-9.52	
0.255	64.31	5.52		90	121.9	77.8	1.57	67.48	-11.27	
Very Poor Soil										
Height wl	Height ft	Zen Gain	Max Gain	TO Ang	BS BW	EW BW	BW Ratio	Feed R	Feed X	
0.155	39.09	2.14		90	113.0	84.0	1.35	70.02	-0.87	
0.165	41.61	2.61		90	114.4	82.0	1.40	68.01	5.19	
0.175	44.13	3.01		90	115.8	80.2	1.44	66.72	-8.34	
0.185	46.66	3.34		90	117.4	79.0	1.49	65.92	-10.75	
0.195	49.18	3.62		90	119.0	77.8	1.53	65.51	-12.69	
0.205	51.70	3.84		90	120.8	77.2	1.56	65.38	-14.32	
0.215	54.22	4.01		90	122.7	76.6	1.60	65.45	-15.76	
0.225	56.74	4.14		90	124.6	76.4	1.63	65.67	-17.08	
0.235	59.27	4.24		90	126.6	76.2	1.66	65.97	-18.32	
0.245	61.79	4.30	4.32	73	128.6	76.2	1.69	66.32	-19.52	
0.255	64.31	4.33	4.38	63	130.4	76.4	1.71	66.69	-20.71	

The gain curves in Fig. 22 add two lower-level steps to the chart and thereby reveal the rapidly decreasing gain level that occurs as

the V wire ends approach ground. Even though the overall gain level for any height (in wavelengths) is higher on 75 meters than on 40 meters, the gain of a V with its ends at about the same height on both bands will be lower on the lower band. In addition, as we lower the inverted-V, the feedpoint resistance shows more parallels to the impedance of the dipole at very low levels, with a strong divergence of values as we change the quality of soil. However, in the case of the V, the divergence occurs largely as a result of the average height of the antenna, not the center height. The divergence shown by the 75meter V at its minimum height of  $0.155\lambda$  corresponds to the divergence displayed by dipoles closer to the lower survey limit of  $0.075\lambda$ .

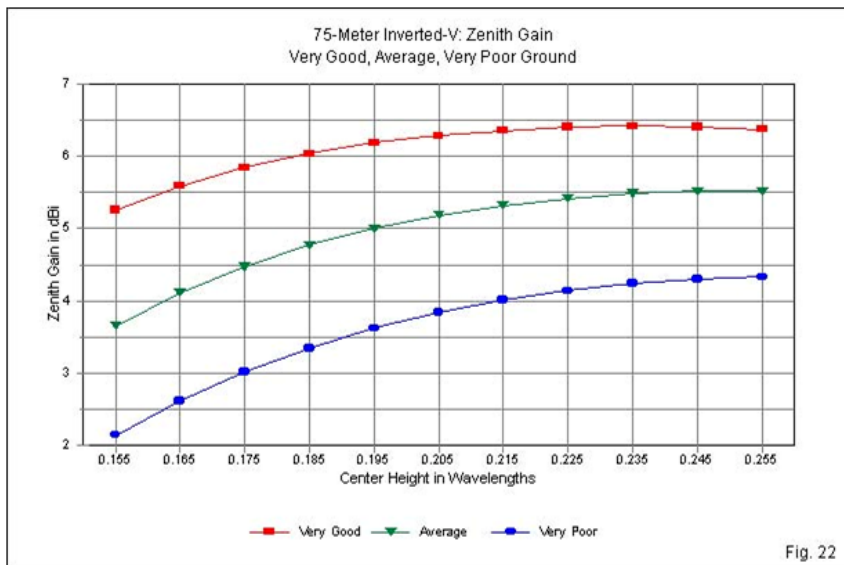


Fig. 22

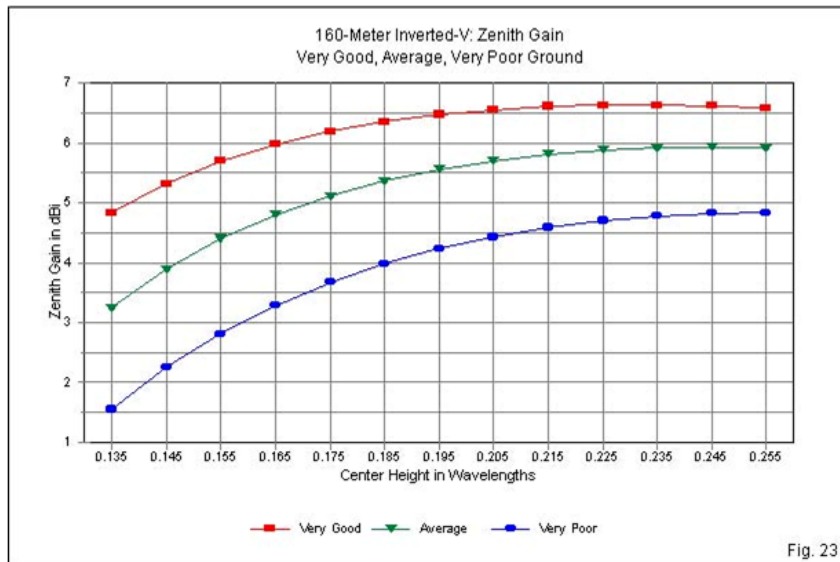
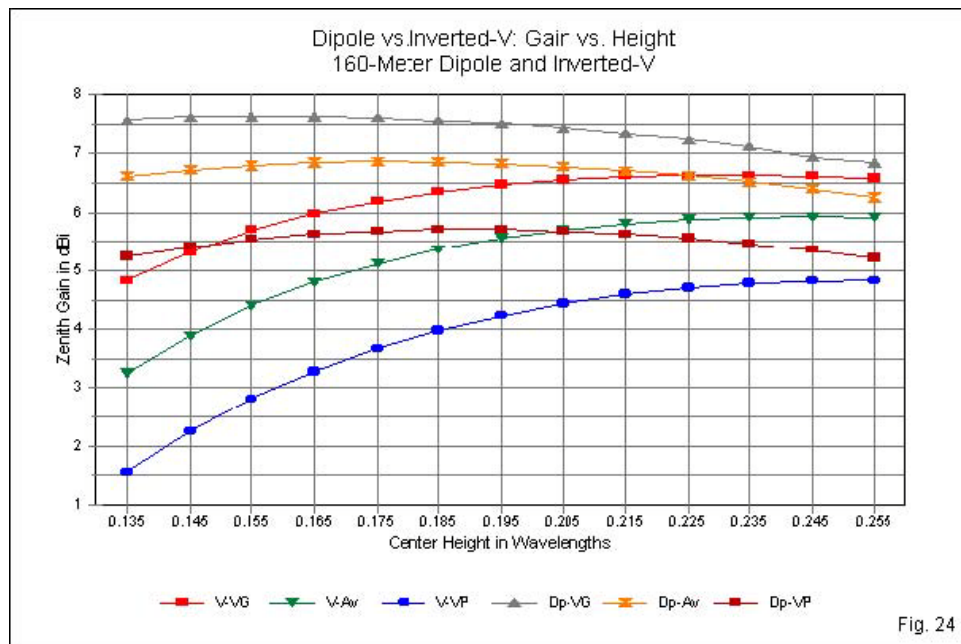


Fig. 23

160-Meter Inverted-V AWG #12 Copper Wire: Length = 0.482 WL								Table 11	
Very Good Soil									
Height wl	Height ft	Zen Gain	Max Gain	TO Ang	BS BW	EW BW	BW Ratio	Feed R	Feed X
0.135	71.77	4.83		90	96.2	94.6	1.02	34.24	31.83
0.145	77.09	5.32		90	97.0	89.6	1.08	35.88	21.64
0.155	82.41	5.70		90	98.0	86.2	1.14	38.01	15.55
0.165	87.72	5.98		90	99.0	83.6	1.18	40.44	11.50
0.175	93.04	6.19		90	100.4	82.0	1.22	43.08	8.60
0.185	98.36	6.35		90	101.8	80.8	1.26	45.85	6.35
0.195	103.67	6.47		90	103.2	79.8	1.29	48.70	4.46
0.205	108.99	6.55		90	104.8	79.2	1.32	51.58	2.75
0.215	114.31	6.61		90	106.4	78.8	1.35	54.44	1.11
0.225	119.62	6.63		90	108.4	78.6	1.38	57.24	-0.55
0.235	124.94	6.63		90	110.4	78.6	1.40	59.95	-2.28
0.245	130.26	6.62		90	112.4	78.8	1.43	62.53	-4.10
0.255	135.57	6.58		90	114.6	79.2	1.45	64.97	-6.03
Average Soil									
Height wl	Height ft	Zen Gain	Max Gain	TO Ang	BS BW	EW BW	BW Ratio	Feed R	Feed X
0.135	71.77	3.25		90	99.4	93.6	1.06	50.15	32.29
0.145	77.09	3.89		90	100.4	89.0	1.13	49.78	20.91
0.155	82.41	4.40		90	101.4	85.6	1.18	50.28	13.84
0.165	87.72	4.80		90	102.6	83.4	1.23	51.32	9.00
0.175	93.04	5.11		90	104.2	81.8	1.27	52.72	5.43
0.185	98.36	5.36		90	105.6	80.4	1.31	54.37	2.64
0.195	103.67	5.56		90	107.0	79.4	1.35	56.19	0.31
0.205	108.99	5.70		90	108.8	78.8	1.38	58.10	-1.75
0.215	114.31	5.81		90	110.6	78.4	1.41	60.06	-3.67
0.225	119.62	5.88		90	112.6	78.2	1.44	62.01	-5.53
0.235	124.94	5.92		90	114.6	78.2	1.47	63.92	-7.38
0.245	130.26	5.93		90	117.0	78.2	1.50	65.74	-9.27
0.255	135.57	5.92		90	119.2	78.6	1.52	67.46	-11.20
Very Poor Soil									
Height wl	Height ft	Zen Gain	Max Gain	TO Ang	BS BW	EW BW	BW Ratio	Feed R	Feed X
0.135	71.77	1.55		90	106.5	91.6	1.16	74.36	23.41
0.145	77.09	2.25		90	107.6	87.6	1.23	70.35	12.01
0.155	82.41	2.81		90	109.0	85.0	1.28	67.98	4.71
0.165	87.72	3.28		90	110.4	82.8	1.33	66.61	-0.41
0.175	93.04	3.67		90	111.8	81.0	1.38	65.90	-4.22
0.185	98.36	3.98		90	113.6	79.8	1.42	65.65	-7.19
0.195	103.67	4.23		90	115.2	78.8	1.46	65.74	-9.63
0.205	108.99	4.43		90	117.2	78.2	1.50	66.08	-11.74
0.215	114.31	4.59		90	119.0	77.6	1.53	66.58	-13.64
0.225	119.62	4.70		90	121.0	77.4	1.56	67.18	-15.41
0.235	124.94	4.78		90	123.2	77.2	1.60	67.82	-17.48
0.245	130.26	4.82		90	125.4	77.4	1.62	68.48	-18.72
0.255	135.57	4.83	4.86	67	127.4	77.6	1.64	69.11	-20.33

160 meters creates an additional two steps to the tabulated data and shows how low that zenith gain values may go when the V ends are close to ground. Both **Table 11** and **Fig. 23** show that lowering the operating frequency also lowers the heights of maximum zenith gain, although only slightly. Still, over very poor soil, we cannot from the existing data certify that the highest listed gain value is in fact the peak value. Once more the V over very poor ground begins to split its broadside elevation lobes prior to reaching the peak zenith gain value. The trends among all three sample inverted-V NVIS antennas are consistent with prior trends.



**Fig. 24** provides graphic evidence of how the zenith gain behavior of the inverted-V differs from corresponding behavior in a dipole (or by extension in a 1- $\lambda$  loop). In the primary span of heights within which the dipole reaches its peak gain, the inverted-V shows considerably lesser gain, since this portion of the inverted-V height span is marked by a rising gain figure. Since amateur tend to build antennas within total height limitations dictated by available materials, skills, expense, and zoning restrictions, the comparison is fair. **Table 12** provides a summary view of the gain disparity between the V and the level antennas. The table uses height values for peak zenith gain, and we have already seen that the required heights for peak inverted-V gain are considerably higher than for the other antennas. If you change the table to record a constant height—perhaps 0.175- $\lambda$  as an average of the heights of maximum gain of the level antennas over all soil types—the disparity is even greater. For example, a 75-meter dipole at 0.175- $\lambda$  above average ground has a zenith gain of 6.4 dBi, while the 75-meter loop under the same conditions shows 7.0 dBi. However, a 75-meter inverted-V with a center height of 0.175- $\lambda$  provides less than 4.5 dBi zenith gain.

Tri-Band Summary of Significant NVIS Inverted-V Values										Table 12		
Ground	Very Good				Average				Very Poor			
	Max Gain	Height	Gain vs.	Gain vs.	Max Gain	Height	Gain vs.	Gain vs.	Max Gain	Height	Gain vs.	Gain vs.
Band	Zenith	WL	Dipole dB	Loop dB	Zenith	WL	Dipole dB	Loop dB	Zenith	WL	Dipole dB	Loop dB
160 m	6.63	0.230	-1	-1.55	5.93	0.245	-0.94	-1.51	4.83	0.255	-0.88	-1.52
75 m	6.42	0.235	-0.98	-1.54	5.52	0.260	-0.9	-1.52	4.33	0.255	-0.80	-1.52
40 m	6.19	0.240	-0.96	-1.55	5.24	0.255	-0.85	-1.52	4.11	0.255	-0.75	-1.53
Delta	0.44	0.010			0.69	0.010			0.72	0		

Notes:

- Max Gain Zenith = maximum zenith gain in dBi
- Height WL = maximum zenith gain height in wavelengths
- (Where 2 heights have the same value, the average appears here.)

Gain vs. Dipole dB = maximum gain of inverted-V relative to a dipole maximum gain at same frequency

Gain vs. Loop dB: maximum gain of inverted-V relative to a 1-wl loop maximum gain at same frequency

(Heights of maximum gain are not the same for inverted-Vs and for dipoles and 1-wl loops.)

Delta = maximum inverted-V-only change between 160 and 40 meters

The behavior of an inverted-V NVIS antenna differs in further ways from the behavior of the level antenna. For example, the beamwidth ratio (broadside to endwise) increases more rapidly with increases in center height than we find in the case of dipoles of  $1-\lambda$  loops. Fig. 25 shows the phenomenon in a 160-m V in contrast to the rates for the dipole on the same band. The faster rate of increase for the V coincides, at least in part, with the V's endwise elevation pattern, and both are results of the greater radiation off the ends of the element due to its slope. (Although  $1-\lambda$  loop beamwidth ratios are smaller than those for a linear dipole, their curves are equally “flat.”)

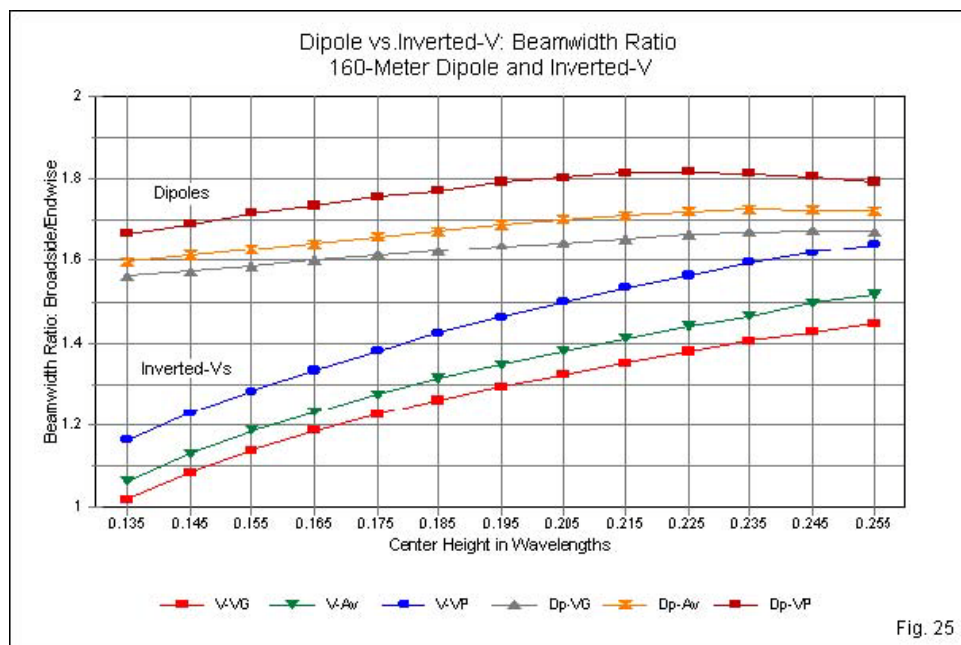


Fig. 25

As we increase the height of a dipole or a  $1\lambda$  loop, the feedpoint impedance components show particular patterns. Except for the lowest heights, the resistance tends to rise over all soil qualities, although the rate varies with the soil type. Hence, we saw the resistance values converge toward the top of the height range within the survey. In contrast, the reactance values tend to change fairly slowly. On 75 meters over average ground, the SWR curves in **Fig. 18** were equivalently wide for both level antennas, with a 2:1 SWR ratio relative to the resonant impedance (at 3.9 MHz) from 3.8 to 4.0 MHz.

If we track the feedpoint impedance in terms of the resistive and reactive components for an inverted-V, we find opposite trends. **Fig. 26** tracks the resistance and reactance of a 75-meter dipole and a 75-meter inverted-V over average ground—restricting the height coverage to the V's limited range. Although the patterns of lines may be difficult to follow, the two rising curves represent feedpoint resistance. The steeper curve belongs to the dipole, as the resistance of the V changes more slowly. Both descending curves belong to the feedpoint reactance values. The V's reactance changes more rapidly and radically than the dipole values. At the left in the graph, the V's reactance changes most rapidly when the wire ends are closest to the ground. Although the rate of change remains relatively high, it slows as the wire ends increase their height. In contrast, the dipole curve in the left part of the graph coincides with the region of highest gain, and the rate of change is very slow. The rate increases as we raise the antenna well past the region of maximum zenith gain.

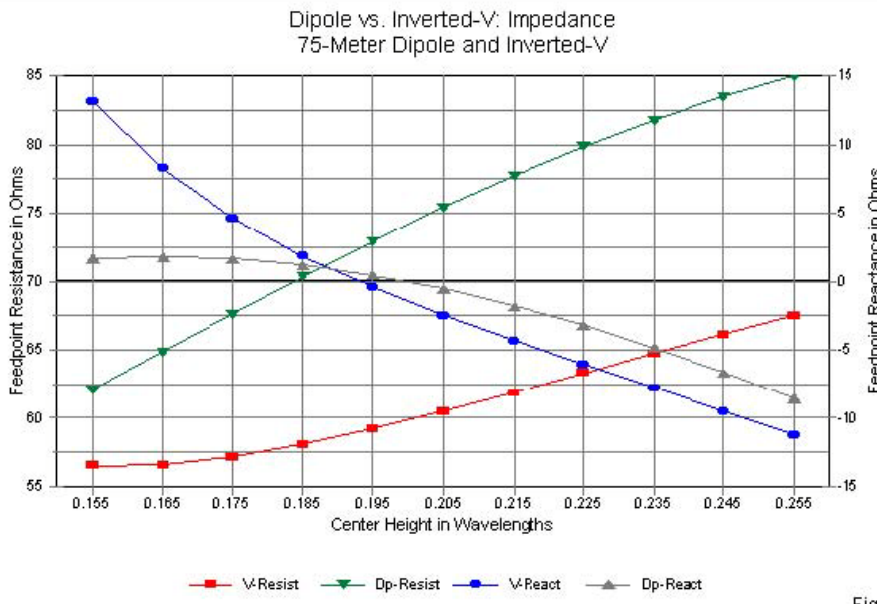
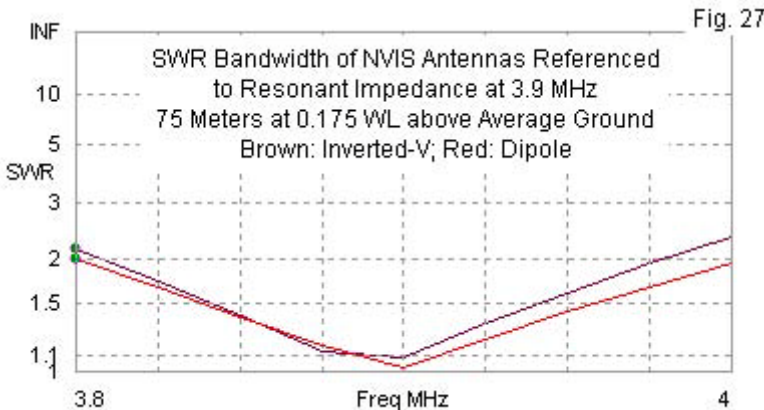


Fig. 26

The differences in the patterns of resistance and reactance change have very little effect upon the available SWR bandwidth. **Fig. 27** overlays SWR curves for a 75-meter dipole and V, both with center heights of  $0.175\lambda$  above average ground. If we judge by the endpoints of the sweeps, the V curve is not quite as broad as the dipole curve. Nevertheless, the SWR bandwidth is fully adequate to NVIS operations on the specified band. Allowing for the changes in frequency, similar curves would apply to NVIS antennas for the 40-meter and 160-meter bands.



### Conclusion

The three most basic NVIS antennas—the dipole, the  $1-\lambda$  loop, and the inverted-V configuration of the dipole—share many properties, most often as a result of the close proximity of the antenna to ground. Hence, we discovered that ground quality plays an important role in determining the maximum possible zenith gain on each of the bands surveyed. As well, it plays a role in setting the optimal height for maximum zenith gain, although for all types of antennas, precision is not necessary in order to achieve excellent results. However, we did discover that an old idea that gives very low heights a presumed gain advantage is simply false. Averaging both level antennas over all soil types, a height of approximately  $0.175\lambda$  above ground places the antenna within the expanded range of best zenith gain performance.

The inverted-V, with its wire ends close to ground and a 30° slope angle, presents a conundrum for the NVIS antenna builder.

Although easier to construct than either a linear dipole or a 1-λ loop, the inverted-V antenna shows a considerable gain deficit relative to level antennas with the same center height. The deficit may reach up to about 2.5 dB or close the half an S-unit. Although the inverted-V may be necessary for field antennas, a fixed station antenna might well enjoy the advantages of one of the level antennas.

The data compendium provided by these notes likely has surplus information. However, the extra data serves the twin goals of these notes. Not only is the information useful in making decisions about what type of antenna to create, it also aids in a better understanding of the behaviors of each antenna type. Despite the wealth of numbers and facts, these notes have only scratched the surface of even basic NVIS antennas.

## Chapter 66: NVIS Antennas with Reflectors

**A**n interesting facet of basic NVIS antennas—the dipole, the  $1-\lambda$  loop, and the inverted-V—is the suggestion that we can improve antenna gain by placing some form of wire structure below it. The possibilities are numerous, but the most common suggestion is the addition of a single-wire element. In fact, with proper consideration, the suggestion will work, but with limitations. As well, there may be better, although more complex, solutions to obtain better zenith gain from the basic NVIS antenna.

The structure that we place below the driven wire has acquired two names, one correct, the other misplaced and misleading. The correct name for the element is a reflector. If the reflector is a single-wire element optimized in size for best performance, then it is a parasitic reflector. Still, the circumstances of its use will force us to modify the expectations that we have of such elements when used with highly elevated beam antennas. If the structure below the driven element consists of a screen or a series of wires parallel to the endwise orientation of the driven element, then we have a planar reflector (sometimes called a sheet, curtain, or screen reflector). We shall eventually examine both types of reflectors for NVIS applications.

The incorrect name for the element—usually applied to the single-wire reflector—is “counterpoise.” Although widely bandied about, the term “counterpoise” actually applies only to a certain form of monopole completion structure that substitutes for buried radials. Very slightly elevated from the ground and not connected to ground

by any direct means, the counterpoise serves the monopole by capacitive coupling to the ground. Although quite effective for its function, the counterpoise has disappeared from active use, seemingly freeing the terms for other uses. Unfortunately, the terms has greatest use in lazy applications, where an investigator or writer does not take the trouble to analyze the structure's role in an application and further does not go on to optimize its physical parameters relative to the application. This situation too often applies to NVIS applications with careless element sizing and placement. Perhaps it is time to drop both the term and the associated carelessness from not only NVIS concerns, but from any antenna considerations whatsoever—except, of course, when working with the original engineering designs for monopole-counterpoise antenna systems.

In these notes, we shall treat NVIS antenna reflectors, whether parasitic or planar, as parts of an antenna system consisting of a driven element and the element or structure below it. For parasitic reflectors, we shall size them for nearly optimal performance and carefully consider their placement. We may measure placement in two ways: as their height above ground or as their separation from the driven element. For both perspectives, we shall discover that the height of the driver above ground plays a significant role in reflector placement. In addition, the ground quality also dictates the placement of a carefully designed reflector element.

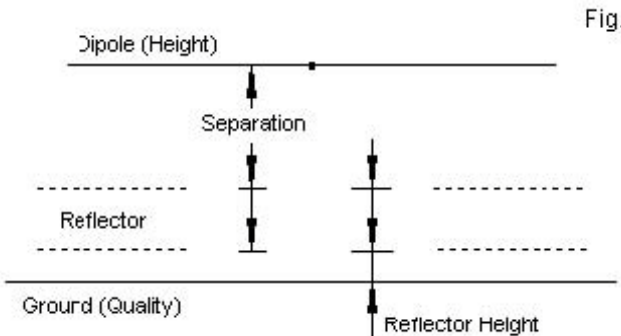
We shall also discover that dipoles and  $1-\lambda$  loops, despite the similarities of their optimal heights over various ground qualities when used alone, do not respond identically to reflector elements.

Eventually, we shall look at the inverted-V to let it reveal further oddities. Although planar reflectors improve gain most when placed close to their driven elements, practicalities dictate that we place them on or very near to the ground. Nevertheless, they will prove their merits, especially when we give proper attention to their size.

We have much to explore, even if the concept of a NVIS reflector seems simple. Let's begin with the dipole.

### *The NVIS Dipole and a Parasitic Reflector*

At its optimal height, the common linear or level dipole provides quite good NVIS performance with a range of about 5 to 7.4 dBi zenith gain, depending upon the operating frequency and the quality of the soil beneath it. Under certain conditions, we can increase the gain by adding a parasitic reflector somewhere between the dipole and the ground. Unfortunately, we cannot specify a specific place for the reflector, since numerous variables enter into the optimal placement. **Fig. 1** provides indicators of the most relevant variables.

Fig. 1  
NVIS Dipole + Reflector Variables

Like almost all parasitic reflectors, the element length must exceed the length of the resonant dipole. As well, the proper placement will vary with the dipole's height above the ground and with the quality of the ground. As shown in the sketch, we may specify the placement by two measures: the height of the dipole above ground or the separation of the dipole from the driver. Unfortunately for ease of analysis, both parameters tend to vary with the height of the dipole itself and the quality of the ground beneath.

In these notes, we shall confine ourselves to 75-meter and 40-meter dipole arrays. Rarely are 160-m dipoles high enough to sustain a reflector element. On 60 meters, one may interpolate between the 75-and 40-meter data to arrive at a reliable value, since the gain curves are not sharp enough to modify performance drastically with small variations.

Beginning with the 75-meter dipole, we shall again use AWG #14 copper wire for all elements. The main unit of measure will be the wavelength, and the dipole will be  $0.4803\lambda$  long. The reflector element will be  $0.5\lambda$  long. The reflector length theoretically will change as we move the reflector around, but not enough to disturb the trends that we find with a constant length. We shall catalog the results of modeling the dipole at three heights (to reduce the number of continuously changing variables). Heights of  $0.15\lambda$ ,  $0.175\lambda$ , and  $0.2\lambda$  will surround the optimum heights over all three of our standard ground types: very good, average, and very poor.

Tabulated results (**Table 1**) will include, for each dipole, reflector heights from  $0.005\lambda$  to  $0.06\lambda$  in  $0.005\lambda$  increments. In addition, we shall include two special heights:  $-0.001\lambda$  to cover the potential for a buried reflector element and  $0.001\lambda$  to cover the case of a reflector so low that someone might trip over it. The table shows the height in feet for every increment of reflector height. It also indicates in boldface the reflector height of maximum zenith gain and shows on the right side the indicated separation from the dipole. For each height, the tables show the zenith gain and the broadside beamwidth.

NVIS 3.9-MHz Dipole with a Single-Wire Reflector Element								Table 1	
Dipole: 0.4806-wl AWG #14 Copper Wire				Reflector: 0.5-wl AWG #14 Copper Wire					
Dipole Height		0.15 wl		37.83 feet					
		Very Good Soil		Average Soil		Very Poor Soil		Refl. Sep.	
Ref Ht wl	Ref Ht ft	Gain dBi	BS BW	Gain dBi	BS BW	Gain dBi	BS BW	wl	
No Reflector		7.37	103.2	6.23	108.4	4.79	117.8		
-0.001	-0.25	7.40	103.2	6.33	108.4	5.04	117.4		
0.001	0.25	7.46	103.2	6.50	108.2	5.39	116.8		
0.005	1.26	7.53	103.2	6.67	108.4	5.68	116.4		
0.01	2.52	7.57	103.4	6.78	108.4	5.86	116.4	Vry Gd	
0.015	3.78	7.59	103.5	6.85	108.6	5.98	116.4	0.135	
0.02	5.04	7.58	103.8	6.90	108.8	6.05	116.4		
0.025	6.30	7.55	104.2	6.91	109.2	6.11	116.6	Ave	
0.03	7.57	7.51	104.6	6.92	109.2	6.15	116.6	0.120	
0.035	8.83	7.47	105.0	6.90	109.8	6.17	116.8	Vry Pr	
0.04	10.09	7.42	105.4	6.88	110.2	6.18	117.0	0.110	
0.045	11.35	7.37	105.8	6.84	110.4	6.17	117.2		
0.05	12.61	7.31	106.4	6.80	110.8	6.16	117.4		
0.055	13.87	7.25	106.8	6.75	111.2	6.13	117.8		
0.06	15.13	7.19	107.2	6.69	111.6	6.09	118.0		
Max. Delta Gain		0.22		0.69		1.39			
Dipole Height		0.175 wl		44.13 feet					
		Very Good Soil		Average Soil		Very Poor Soil		Refl. Sep.	
Ref Ht wl	Ref Ht ft	Gain dBi	BS BW	Gain dBi	BS BW	Gain dBi	BS BW	wl	
No Reflector		7.39	107.4	6.40	113.0	5.06	122.4		
-0.001	-0.25	7.40	107.5	6.47	113.0	5.25	122.0		
0.001	0.25	7.44	107.5	6.59	112.8	5.52	121.4		
0.005	1.26	7.49	107.5	6.71	112.8	5.75	121.0	Vry Gd	
0.01	2.52	7.52	107.6	6.80	112.8	5.90	120.8	0.165	
0.015	3.78	7.52	107.8	6.85	113.0	6.00	120.8	0.160	
0.02	5.04	7.51	108.2	6.88	113.2	6.07	120.8	Ave	
0.025	6.30	7.49	108.4	6.89	113.6	6.12	120.8	0.150	
0.03	7.57	7.45	109.0	6.89	113.8	6.15	121.0	0.145	
0.035	8.83	7.42	109.2	6.88	114.2	6.18	121.0	Vry Pr	
0.04	10.09	7.38	109.8	6.86	114.4	6.19	121.2	0.135	
0.045	11.35	7.34	110.2	6.83	114.8	6.19	121.4	0.130	
0.05	12.61	7.30	110.8	6.80	115.4	6.19	121.6	0.125	
0.055	13.87	7.26	111.2	6.77	115.6	6.18	121.8		
0.06	15.13	7.21	111.6	6.73	116.2	6.17	122.0		
Max. Delta Gain		0.13		0.49		1.13			
Dipole Height		0.20 wl		50.44 feet					
		Very Good Soil		Average Soil		Very Poor Soil		Refl. Sep.	
Ref Ht wl	Ref Ht ft	Gain dBi	BS BW	Gain dBi	BS BW	Gain dBi	BS BW	wl	
No Reflector		7.28	112.4	6.39	118.4	5.14	127.4		
-0.001	-0.25	7.29	112.4	6.45	118.2	5.29	127.0		
0.001	0.25	7.32	112.4	6.53	118.1	5.51	126.4		
0.005	1.26	7.35	112.6	6.62	118.1	5.69	126.0	Vry Gd	
0.01	2.52	7.37	112.6	6.69	118.1	5.82	125.8	0.190	
0.015	3.78	7.37	112.8	6.73	118.2	5.91	125.7	0.185	
0.02	5.04	7.35	113.2	6.75	118.4	5.97	125.6	Ave	
0.025	6.30	7.33	113.6	6.76	118.6	6.02	125.6	0.175	
0.03	7.57	7.30	114.0	6.75	119.0	6.05	125.7		
0.035	8.83	7.26	114.6	6.74	119.2	6.08	125.8		
0.04	10.09	7.23	114.8	6.73	119.5	6.09	125.9		
0.045	11.35	7.19	115.4	6.71	119.8	6.10	126.0	Vry Pr	
0.05	12.61	7.16	115.8	6.68	120.3	6.11	126.0	0.150	
0.055	13.87	7.13	116.2	6.66	120.6	6.11	126.2	0.145	
0.06	15.13	7.09	116.8	6.63	121.0	6.10	126.4		
Max. Delta Gain		0.09		0.37		0.96			

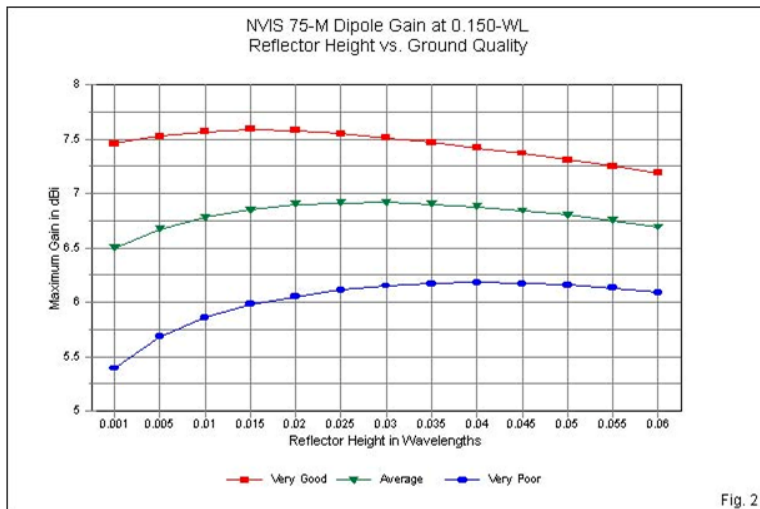


Fig. 2

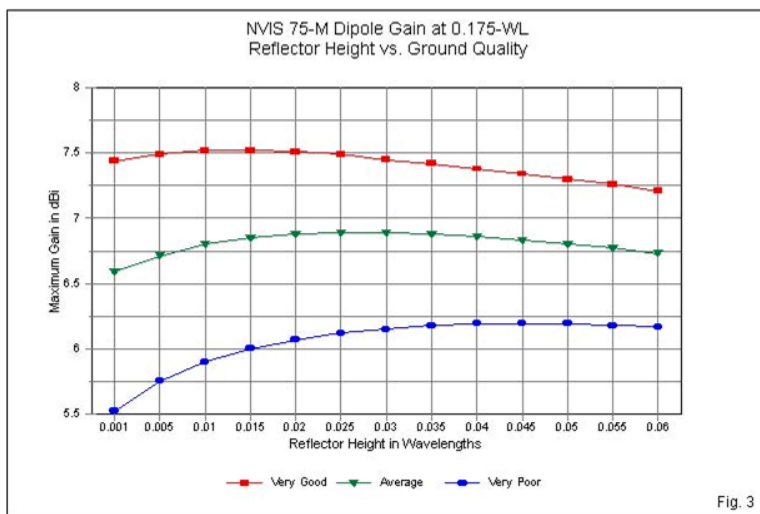


Fig. 3

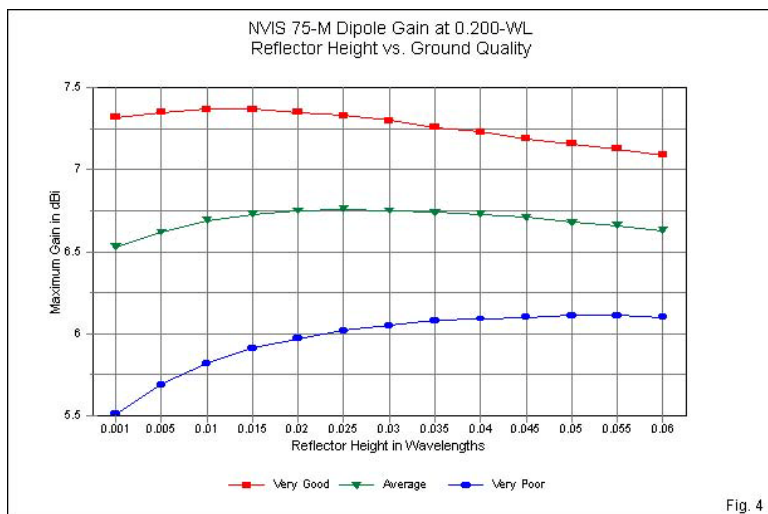


Fig. 4

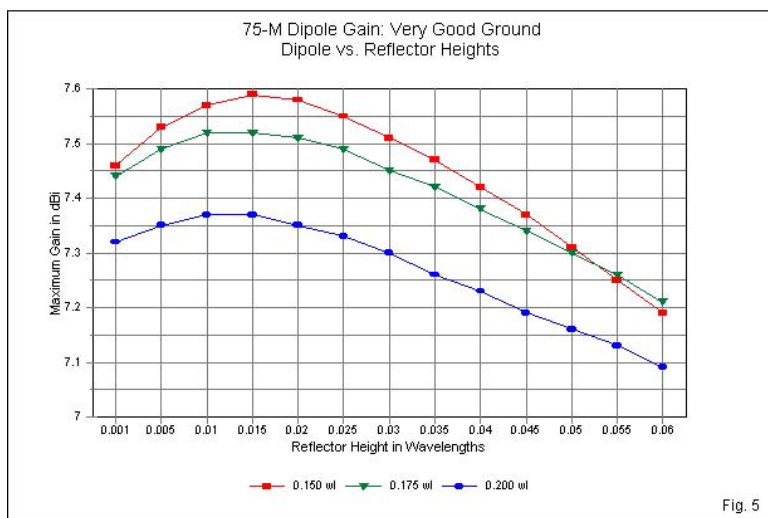
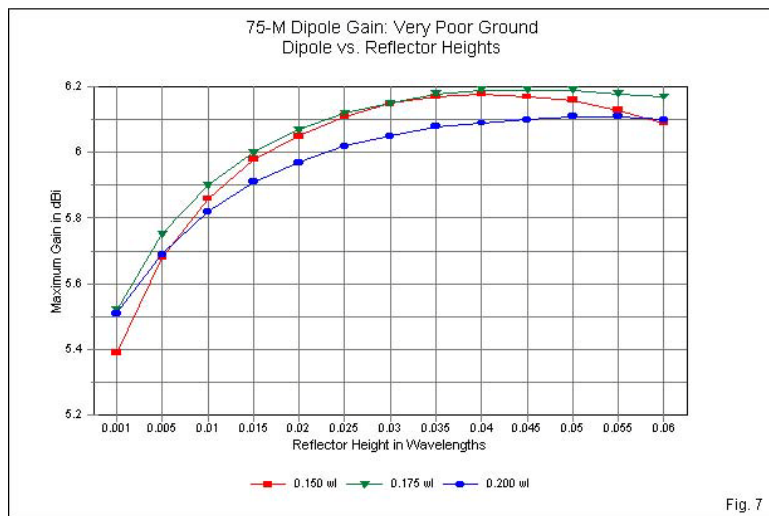
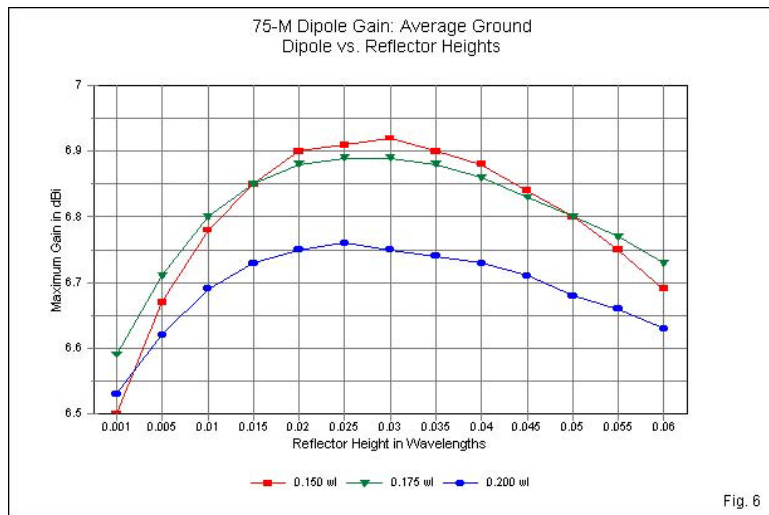


Fig. 5



As the pages following the table show (in **Fig. 2** through **Fig. 7**) we may graphically examine the data in two different ways. The easy way is to graph the gain curves for each dipole height using separate lines for each quality of soil. The first three graphs follow this plan and resemble the curves in the last set of notes for dipoles alone. They establish that the dipole-reflector over very good soil has more gain at any height than equivalent systems over lesser soil types. The three graphs vary by virtue of the dipole height since a dipole and a dipole-reflector array both reach maximum gain at lower dipole heights with very good ground than over lesser ground qualities. In contrast, the lines close up somewhat as we raise the dipole height, since the version over very good ground has passed its optimal height, while the versions over average and very poor soil reach their peak values at higher dipole altitudes.

Although the initial three graphs relate easily to past performance graphs, **Fig. 5** through **Fig. 7** may prove more revealing. In this set, each graph uses a single soil quality, with individual lines in each graph for the three selected dipole heights. With very good soil, the  $0.15\lambda$ -dipole height is clearly most nearly optimal. Over average soil, the peak values for dipole heights of  $0.15\lambda$  and  $0.175\lambda$  approach each other as most nearly optimal. Over very poor soil, the values for the two lower heights are nearly the same, while the values for a dipole at  $0.2\lambda$  above ground have nearly caught up to the other lines. These graphs are more than merely interesting; they indicate a fundamental property of all enhancements that we may bring to basic NVIS antennas. The enhancement—in this case a parasitic reflector—becomes more effective in raising zenith gain as the soil decreases in quality. In **Table 1**, compare for each major

subdivision the delta values for the three soil types. The maximum improvement for an optimized reflector over very good soil is only about 0.2 dB over very good soul. The overall performance improvement is between 0.4 and 0.7 dB over average soil, but it grows to a full dB or more over very poor soil.

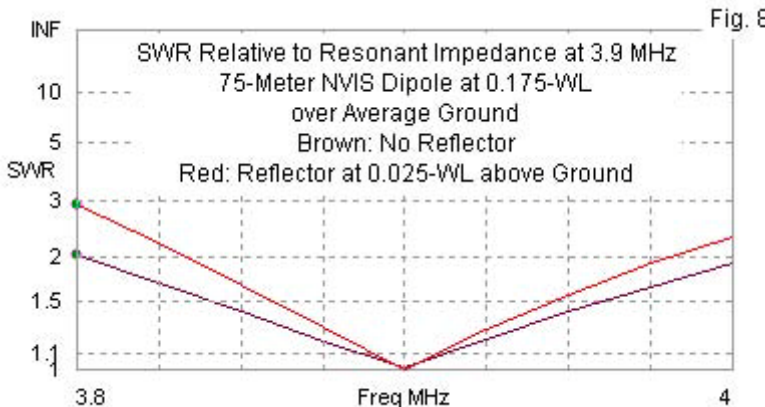
Soil quality determines in part whether adding a parasitic reflector to a given dipole is worth the effort involved for both installation and maintenance. It also tells us something very significant about parasitic reflectors in NVIS service. The added element may supplement ground reflection as the source of zenith gain, but it does not replace the ground. Note also that even though we find the greatest gain improvement over very poor ground, the total space of gain value ranges in each graph do not overlap those in another graph. Ground quality tends to dominate zenith gain, even with a parasitic reflector added to the NVIS dipole.

The table shows the antenna gain of the dipole at each height over each ground quality with no reflector. Compare the gain values to the next two entries, which show a slightly buried reflector and one just above ground. In both cases, the gain improvement is minimal to marginal, at best. The reflector does not significantly improve performance until it is well above ground. For very good soil, the reflector height is between  $0.01\text{-}\lambda$  and  $0.015\text{-}\lambda$ , regardless of the height of the dipole (within the surveyed range). Over average soil, the best reflector heights have an equally narrow range, but a different one:  $0.025\text{-}\lambda$  to  $0.03\text{-}\lambda$ . Over very poor soil, where the reflector has maximum effect in improving the dipole's zenith gain,

the ranges are split, running in the region of  $0.04\lambda$  for the lowest dipole up to about  $0.055\lambda$  for the highest.

Over very good and average soil, the reflector height remains constant, but the separation between the dipole and the reflector changes with a change in the dipole's height. The separation between the dipole and the reflector also changes for each dipole height over very poor soil, but that change combines with a change in the best height above ground to produce a more complex picture. In just the region of soil quality for which a parasitic reflector effects a worthy improvement, uniformity disappears. In fact, over poorer soils, one cannot recommend either a single height above ground or a single spacing between elements that will cover the remaining variables, such as dipole height. As soils improve, we can recommend some reasonably good reflector heights above ground, but not without also considering whether the potential improvement justifies the installation and maintenance efforts.

Because the reflectors are parasitic, the overall array is a tuned system with operating bandwidth limits. Like all parasitic systems, the SWR bandwidth (referred to the resonant impedance) is narrower than the bandwidth of the dipole alone. **Fig. 8** provides a sample comparison of dipoles at a  $0.175\lambda$  height, one with no reflector and the other with a reflector at  $0.025\lambda$  above ground. The dipole covers the 3.8-4.0-MHz spread of 75 meters completely, but the dipole-reflector array manages to cover only about  $\frac{3}{4}$  of the range.



One purpose in adding 40-meter arrays to this initial examination is to determine if the trends that we saw on 75 meters are general or idiosyncratic to the lower of the two bands. From our study of dipoles alone, we know to expect slightly lower gain values for each dipole height when measured as a fraction of a wavelength and from each soil quality. Looking at 40-meter dipole-reflector arrays can tell us if there are other variations in the trends that are frequency sensitive.

**Table 2** provides the data for 40-meter dipoles at the same three heights (measured in wavelengths. Of course, the physical heights, as shown in the table, will be only about half the 75-meter values. Otherwise, the data takes the same steps as for the longer antenna. The reflector height increments are  $0.005\lambda$  between  $0.005\lambda$  and  $0.06\lambda$ , with the addition of  $-0.001\lambda$  to simulate a buried reflector and  $0.001\lambda$  to simulate one very close to ground

level. The table also includes reference data for independent dipoles so that we can see the level of improvement created by the addition of a parasitic reflector.

The data for each entry includes the zenith gain and the broadside bandwidth. The beamwidth data has an obvious story to tell, namely, that for practical operating purposes, the beamwidth does not vary enough to be a concern over any soil quality with any dipole height. However, for both 75 and 40 meters, the beamwidth information conveys some subtle pattern changes. Over very good soil, the beamwidth continuously rises. Over average soil, the general trend is a rise in beamwidth value as we raise the reflector height, but we find in some cases an initial drop in value for the lowest reflector height. Over very poor soil, the beamwidth decreases from the initial value until we approach or reach the reflector height for maximum zenith gain, after which point, the value rises. We might also note that the rate of beamwidth value change slows or stops just before we arrive at maximum zenith gain for each soil and dipole height combination.

NVIS 7.2-MHz Dipole with a Single-Wire Reflector Element								Table 2	
Dipole: 0.4786-wl AWG #14 Copper Wire				Reflector: 0.5-wl AWG #14 Copper Wire					
Dipole Height		0.15 wl		21.48 feet					
Ref Ht wl		Very Good Soil		Average Soil		Very Poor Soil		Refl. Sep.	
No Reflector	Ref Ht ft	Gain dBi	BS BW	Gain dBi	BS BW	Gain dBi	BS BW	wl	
-0.001	-0.14	7.13	104.6	5.94	110.2	4.71	118.4		
0.001	0.14	7.22	104.5	6.15	109.8	5.13	117.6		
0.005	0.72	7.32	104.6	6.37	109.8	5.49	117.0		
0.01	1.43	7.39	104.8	6.52	110.0	5.71	116.8		
0.015	2.15	7.43	104.8	6.62	110.0	5.86	116.8	Vry Gd	
0.02	2.86	<b>7.44</b>	105.2	6.68	110.2	5.97	116.6	0.130	
0.025	3.58	7.43	105.5	6.73	110.4	6.05	116.6		
0.03	4.30	7.41	105.8	6.75	110.6	6.11	116.6	Ave	
0.035	5.01	7.38	106.2	<b>6.76</b>	110.8	6.15	116.8	0.115	
0.04	5.73	7.34	106.8	6.75	111.2	6.18	116.8	Vry Pr	
0.045	6.44	7.30	107.2	6.73	111.6	<b>6.19</b>	117.0	0.105	
0.05	7.16	7.26	107.6	6.71	111.8	<b>6.19</b>	117.2	0.100	
0.055	7.87	7.21	108.2	6.68	112.2	6.18	117.4		
0.06	8.59	7.16	108.4	6.64	112.6	6.17	117.6		
Max. Delta Gain		0.36		0.97		1.81			
Dipole Height		0.18 wl		25.05 feet					
Ref Ht wl		Very Good Soil		Average Soil		Very Poor Soil		Refl. Sep.	
No Reflector	Ref Ht ft	Gain dBi	BS BW	Gain dBi	BS BW	Gain dBi	BS BW	wl	
-0.001	-0.14	7.18	108.8	6.03	114.8	4.71	123.3		
0.001	0.14	7.23	109.0	6.14	114.6	4.97	122.6		
0.005	0.72	7.30	109.0	6.45	114.2	5.59	121.4		
0.01	1.43	7.35	109.0	6.56	114.4	5.77	121.0	Vry Gd	
0.015	2.15	<b>7.37</b>	109.2	6.63	114.4	5.90	120.8	0.160	
0.02	2.86	<b>7.37</b>	109.6	6.68	114.6	5.99	120.8	0.155	
0.025	3.58	7.36	110.0	6.72	114.6	6.06	120.8		
0.03	4.30	7.34	110.4	6.73	115.0	6.12	120.8	Ave	
0.035	5.01	7.31	110.8	<b>6.74</b>	115.2	6.16	120.8	0.140	
0.04	5.73	7.29	111.0	6.73	115.6	6.19	120.8		
0.045	6.44	7.25	111.6	6.72	115.8	6.21	121.0		
0.05	7.16	7.22	112.0	6.71	116.2	6.22	121.2	Vry Pr	
0.055	7.87	7.19	112.4	6.69	116.6	<b>6.23</b>	121.2	0.120	
0.06	8.59	7.15	113.0	6.66	117.0	<b>6.23</b>	121.4	0.115	
Max. Delta Gain		0.22		0.71		1.52			
Dipole Height		0.20 wl		28.63 feet					
Ref Ht wl		Very Good Soil		Average Soil		Very Poor Soil		Refl. Sep.	
No Reflector	Ref Ht ft	Gain dBi	BS BW	Gain dBi	BS BW	Gain dBi	BS BW	wl	
-0.001	-0.14	7.08	114.2	6.08	120.0	4.85	128.0		
0.001	0.14	7.12	114.2	6.26	119.6	5.31	126.8		
0.005	0.72	7.17	114.2	6.39	119.4	5.56	126.0		
0.01	1.43	7.21	114.2	6.48	119.4	5.72	125.7	Vry Gd	
0.015	2.15	<b>7.22</b>	114.4	6.53	119.4	5.83	125.5	0.185	
0.02	2.86	<b>7.22</b>	114.6	6.57	119.6	5.91	125.4	0.180	
0.025	3.58	7.20	115.0	6.60	119.6	5.98	125.3		
0.03	4.30	7.18	115.4	6.61	120.0	6.03	125.2	Ave	
0.035	5.01	7.16	115.8	<b>6.62</b>	120.2	6.07	125.2	0.165	
0.04	5.73	7.13	116.2	6.61	120.5	6.10	125.3		
0.045	6.44	7.10	116.6	6.60	120.8	6.13	125.3		
0.05	7.16	7.07	117.2	6.59	121.0	6.14	125.4	Vry Pr	
0.055	7.87	7.04	117.6	6.58	121.3	<b>6.16</b>	125.4	0.145	
0.06	8.59	7.01	118.0	6.56	121.6	<b>6.16</b>	125.6	0.140	
Max. Delta Gain		0.16		0.54		1.31			

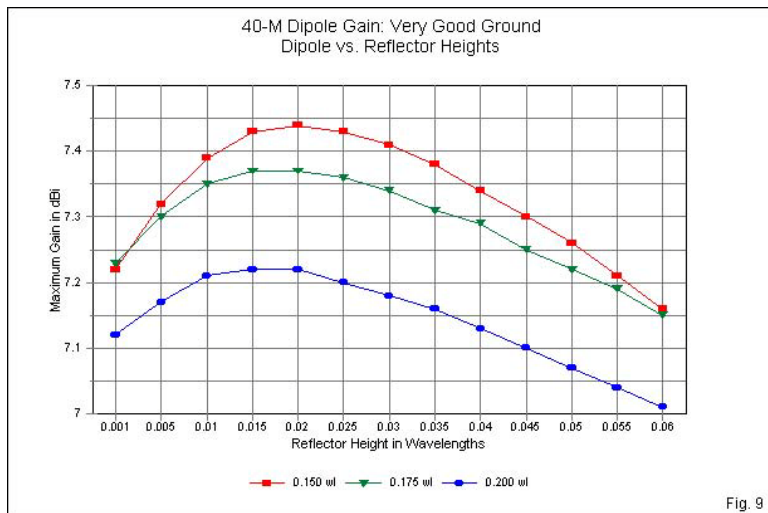


Fig. 9

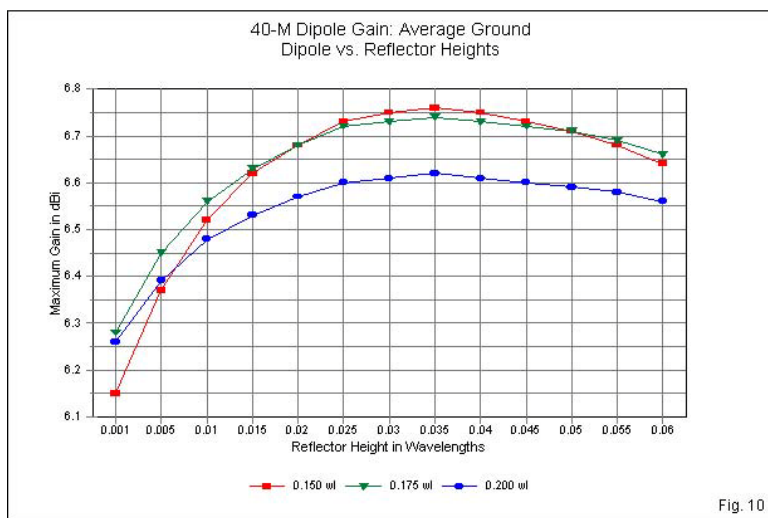


Fig. 10

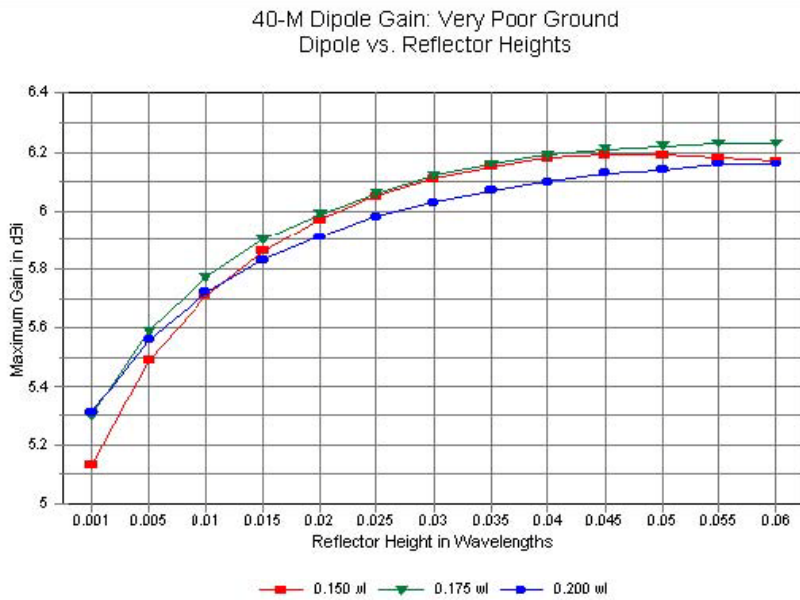


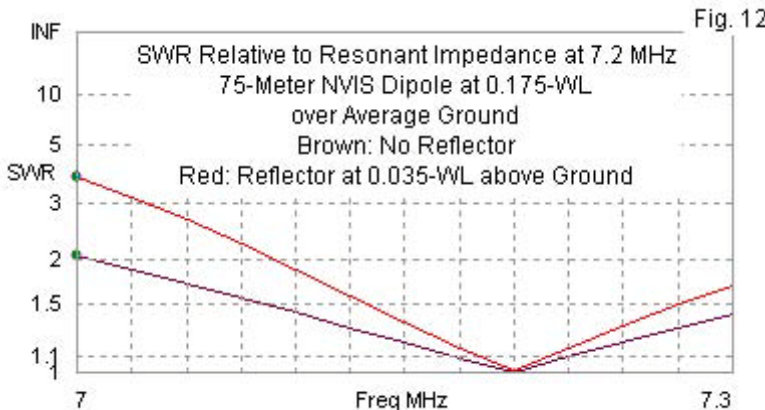
Fig. 11

The graphs in **Fig. 9** through **Fig. 11** catalog the tabular differences by separating soil types. In each graph, we have individual lines for each dipole height. Hence, we can directly compare these 40-meter graphs to those in **Fig. 5** through **Fig. 7** for 75 meters. In the main, we find the same data trends at work for each soil type, but with variations. For example, over very poor soil, the lines for each dipole height are closer together than in the corresponding 75-meter graph. Nevertheless, the overall gain ranges for each chart show no overlap from one soil quality to the next.

Like the 75-meter reflector heights that yield maximum zenith gain, the 40-meter reflector heights over very good and average soil show only a small range, regardless of the dipole height. However, on 40 meters, the ranges are slightly higher:  $0.015\lambda$  to  $0.02\lambda$  over very good soil and  $0.03\lambda$  to  $0.035\lambda$  over average soil. Over very poor soil, the ranges are also higher on 40 meters than on 75 meters, reaching  $0.06\lambda$  for dipole heights from  $0.175\lambda$  to  $0.2\lambda$ . In all cases, we find a change in the spacing from the dipole to the reflector as we change the soil quality.

One interesting, although perhaps small difference between the 75-meter and the 40-meter systems is the net improvement created by adding a reflector to the dipole over all soil qualities. The improvement is a bit better on 40 meters. This fact is consistent with the increased ground losses that we find on 40 meters relative to 75 meters. As a result, the reflector helps a bit more on the upper band. Whether the slightly higher improvement offered, for example, over average soil warrants a reflector on the upper band is a user judgment.

The 40-meter dipole-reflector arrays are just as tuned a set of systems as they are on 75 meters. Therefore, we also find a narrower operating bandwidth (measured here in terms of SWR relative to the resonant impedance of the individual antennas). **Fig. 12** provides a comparison of a solitary dipole and a dipole-reflector array. Both dipoles are at  $0.175\lambda$ , while the reflector is at  $0.03\lambda$  above ground. By a simple adjustment of the element lengths, one can better center the SWR curves within the band. However, for our purposes, the comparison of the two curves is sufficient.



At this point, we can see the relatively close parallel behavior between the two dipole-reflector arrays despite their frequency differences. In both cases, adding a reflector to a dipole over very good soil makes little sense, while adding one over very poor soil may be justified if an additional dB or more of zenith gain will enhance operations. Average soil on both bands presents a case in the margins.

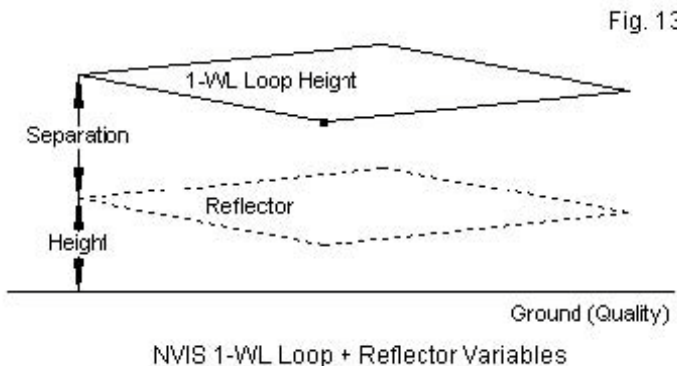
We have two directions in which we might now go. One involves the question of whether there are any reflector systems that might bring about better results than a parasitic array, considering both gain and operating bandwidth. A subsidiary question will focus on whether such systems can materially improve antenna performance over very good and average soil as well as over very poor soil.

The second direction involves our alternative level antenna, the  $1\text{-}\lambda$  loop. To what degree loops follow or depart from the trends established by the dipole arrays is a significant inquiry, since we found a close correlation between the heights of maximum zenith gain for both dipoles and loops. Because any differences might impact the investigation of alternative reflector systems, we likely should turn down the loop road first.

### *The $1\text{-}\lambda$ Loop and a Parasitic Reflector*

The  $1\text{-}\lambda$  loop inherently has more gain than a  $\frac{1}{2}\text{-}\lambda$  dipole. Its advantages for NVIS operation lie both in the gain and the greater circularity of its upward radiation patterns. As we saw in the study of the loop alone, the gain advantage of the loop tends to be about 0.6 dB (on average) over the dipole. Adding a reflector to the NVIS loop is simply a matter of creating a second loop below the first. Like the 2-element dipole parasitic array, the loop array requires a larger reflector loop circumference relative to the driven loop circumference.

The loop presents essentially the same open question as the dipole. To what degree does soil quality play a role in the final array zenith gain and in the placement and size of the reflector loop? **Fig. 13** outlines the loop situation. As with the dipole, we shall sort possible loop reflector heights from the ground upward and add special notes to show the optimal separation of the loop at its best height for each ground quality.



We may shorten the data gathering by omitting some of the improbable lower reflector heights from the survey, although we shall retain an entry for  $0.001\lambda$  above ground to reinforce the relative futility of trying to improve NVIS performance with essentially a trip wire. As well, we may reduce the number of graphs to one per band per ground quality to capture of trends in performance. As with the dipoles, we shall track data with driven loop heights of  $0.15\lambda$ ,  $0.175\lambda$ , and  $0.2\lambda$  to surround in finite steps the region of highest gain of the loop over all soil types.

**Table 3** provides the data applicable to loops with reflectors for 75 meters, again using 3.9 MHz as the test frequency. **Fig. 14** through **Fig. 16** graph the performance over very good, average, and very poor soil. Perhaps the most notable feature of adding parasitic reflectors to NVIS loops is the fact that the optimal reflector heights employ only a very small range for all ground qualities: from  $0.02\lambda$  (for very good soil) up to  $0.04\lambda$  (for very poor soil). Since the

reflector heights change very little with driven loop height, the separation values vary a lot.

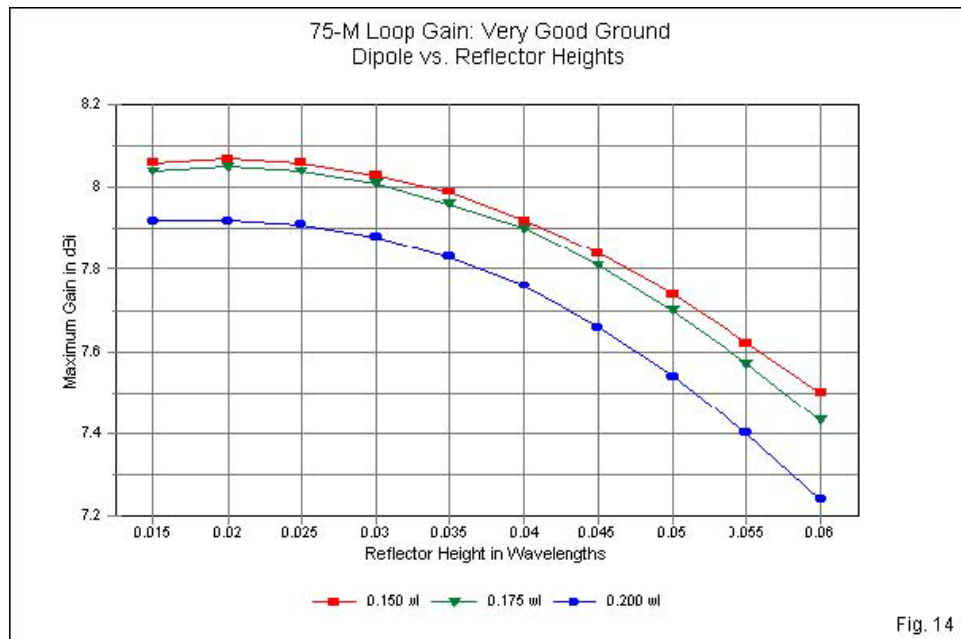
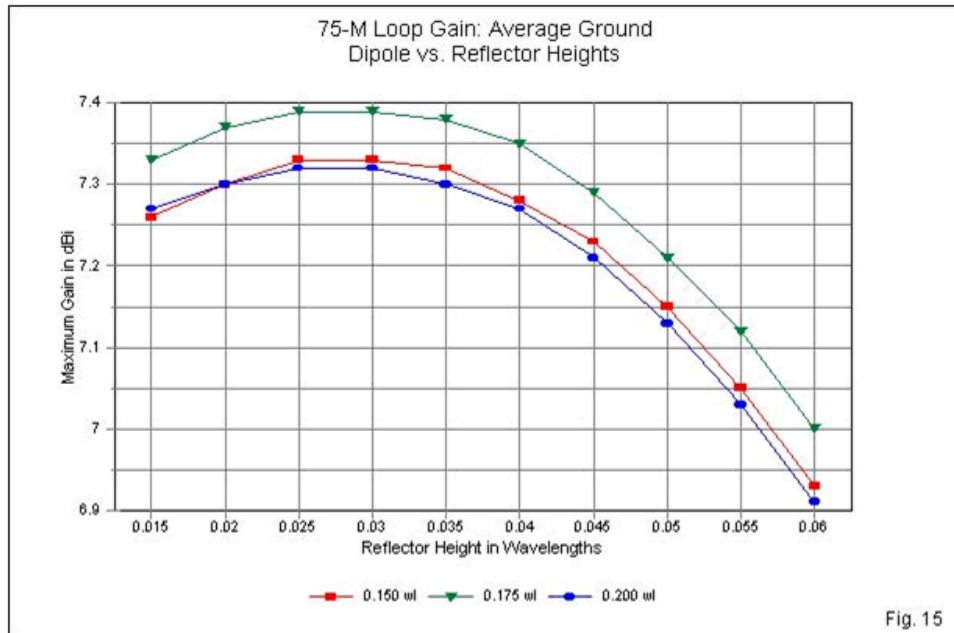


Fig. 14

NVIS 3.9-MHz 1-WL Loop with a Single-Wire Loop Reflector Element								Table 3	
Driver: 1.0176-wl AWG #14 Copper Wire				Reflector: 1.0248-wl AWG #14 Copper Wire					
Loop Height		0.15 wl	37.83 feet						
		Very Good Soil		Average Soil		Very Poor Soil		Refl. Sep.	
Ref Ht wl	Rf Ht ft	Gain dBi	BS BW	Gain dBi	BS BW	Gain dBi	BS BW	wl	
No Reflector		7.92	82.9	6.85	86.5	5.51	93.4		
0.001	0.25	7.97	83.2	7.01	86.8	5.90	92.8		
0.015	3.78	8.06	83.3	7.26	86.6	6.42	91.8		
0.02	5.04	<b>8.07</b>	83.2	7.30	86.7	6.50	91.6	0.130	Vry Gd
0.025	6.30	8.06	83.4	<b>7.33</b>	86.6	6.55	91.5	0.125	Ave
0.03	7.57	8.03	83.5	<b>7.33</b>	86.9	6.59	91.4	0.120	Ave
0.035	8.83	7.99	83.6	7.32	86.9	<b>6.60</b>	91.4	0.15	Vry Pr
0.04	10.09	7.92	83.8	7.28	87.1	6.58	91.4		
0.045	11.35	7.84	84.0	7.23	87.1	6.54	91.3		
0.05	12.61	7.74	84.0	7.15	87.2	6.49	91.2		
0.055	13.87	7.62	84.3	7.05	87.3	6.41	91.2		
0.06	15.13	7.50	84.4	6.93	87.6	6.32	91.1		
Max. Delta Gain		0.15		0.48		1.09			
Loop Height		0.175 wl		44.13 feet					
		Very Good Soil		Average Soil		Very Poor Soil		Refl. Sep.	
Ref Ht wl	Rf Ht ft	Gain dBi	BS BW	Gain dBi	BS BW	Gain dBi	BS BW	wl	
No Reflector		7.95	86.1	7.02	90.3	5.78	97.6		
0.001	0.25	7.98	86.4	7.13	90.3	6.08	97.0		
0.015	3.78	8.04	86.5	7.33	90.2	6.53	95.7		
0.02	5.04	<b>8.05</b>	86.5	7.37	90.2	6.60	95.5	0.155	Vry Gd
0.025	6.30	8.04	86.6	<b>7.39</b>	90.2	6.66	95.3	0.150	Ave
0.03	7.57	8.01	86.9	<b>7.39</b>	90.4	6.70	95.2	0.145	Ave
0.035	8.83	7.96	87.1	7.38	90.5	<b>6.71</b>	95.2	0.140	Vry Pr
0.04	10.09	7.90	87.3	7.35	90.7	6.70	95.1		
0.045	11.35	7.81	87.6	7.29	90.9	6.67	95.1		
0.05	12.61	7.70	88.0	7.21	91.2	6.62	95.1		
0.055	13.87	7.57	88.4	7.12	91.4	6.56	95.1		
0.06	15.13	7.43	88.7	7.00	91.8	6.48	95.2		
Max. Delta Gain		0.10		0.37		0.93			
Loop Height		0.2 wl		50.44 feet					
		Very Good Soil		Average Soil		Very Poor Soil		Refl. Sep.	
Ref Ht wl	Rf Ht ft	Gain dBi	BS BW	Gain dBi	BS BW	Gain dBi	BS BW	wl	
No Reflector		7.86	90.2	7.02	95.0	5.85	102.9		
0.001	0.25	7.87	90.6	7.10	95.1	6.11	102.1		
0.015	3.78	<b>7.92</b>	90.6	7.27	94.7	6.50	100.6	0.185	Vry Gd
0.02	5.04	<b>7.92</b>	90.7	7.30	94.7	6.58	100.1	0.180	Vry Gd
0.025	6.30	7.91	90.9	<b>7.32</b>	94.8	6.63	99.9	0.175	Ave
0.03	7.57	7.88	91.1	<b>7.32</b>	94.9	6.67	99.8	0.170	Ave
0.035	8.83	7.83	91.3	7.30	95.1	<b>6.68</b>	99.8	0.165	Vry Pr
0.04	10.09	7.76	91.7	7.27	95.3	<b>6.68</b>	99.5	0.160	Vry Pr
0.045	11.35	7.66	92.3	7.21	95.7	6.65	99.6		
0.05	12.61	7.54	92.8	7.13	96.0	6.60	99.7		
0.055	13.87	7.40	93.5	7.03	96.4	6.54	99.8		
0.06	15.13	7.24	94.1	6.91	97.0	6.47	100.0		
Max. Delta Gain		0.06		0.30		0.83			

The gain benefits of a reflector follow the dipole pattern: over very good soil, added gain is minimal. Even over average soil, the maximum gain addition is under a half dB. Over very poor soil, the reflector may add up to 1 dB of gain, depending upon the driven loop height.



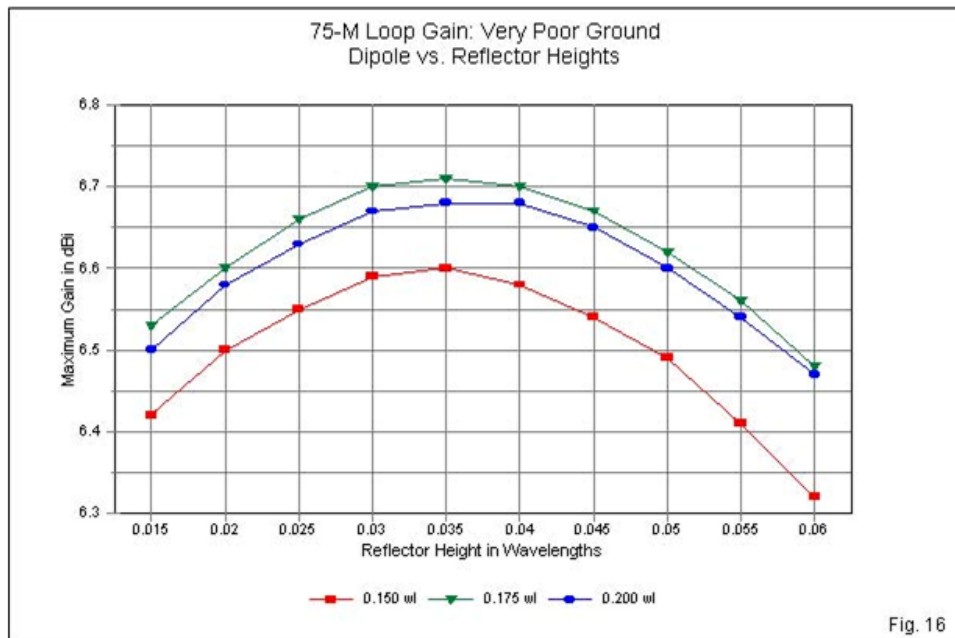
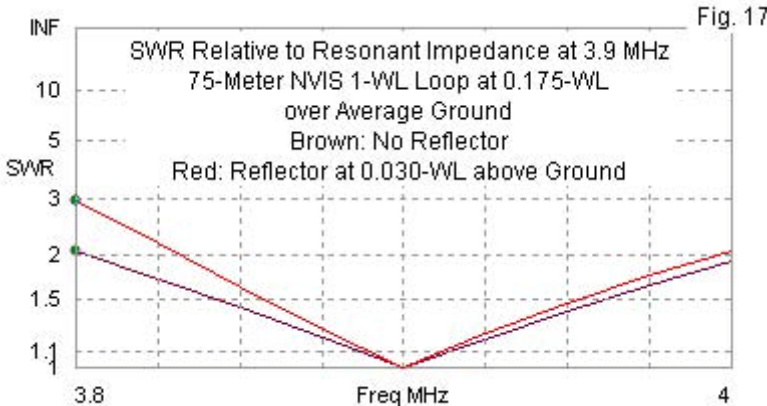


Fig. 16

Similarly to the dipole-reflector combination, the loop-reflector combination results in a narrowing of the operating bandwidth compared to a loop without supplement. **Fig. 17** overlays SWR curves relative to the resonant impedance values for a loop by itself and for a loop with a reflector when both driver loops are at  $0.175\lambda$  above ground. The sample case uses a reflector that is  $0.03\lambda$  above ground, about optimal for the antenna height over average ground.



On 40 meters, we find the same parallels with the dipole cases, as modified by the narrower range of optimal reflector heights that we found with the 75-meter loops. **Table 4** provides the numerical information. **Fig. 18** through **Fig. 20** graph the gain data for each antenna height over each of the soil qualities. The 40 meter gain values are universally slightly less than those for 75-meters. As well, we find some differences in other details of array behavior.

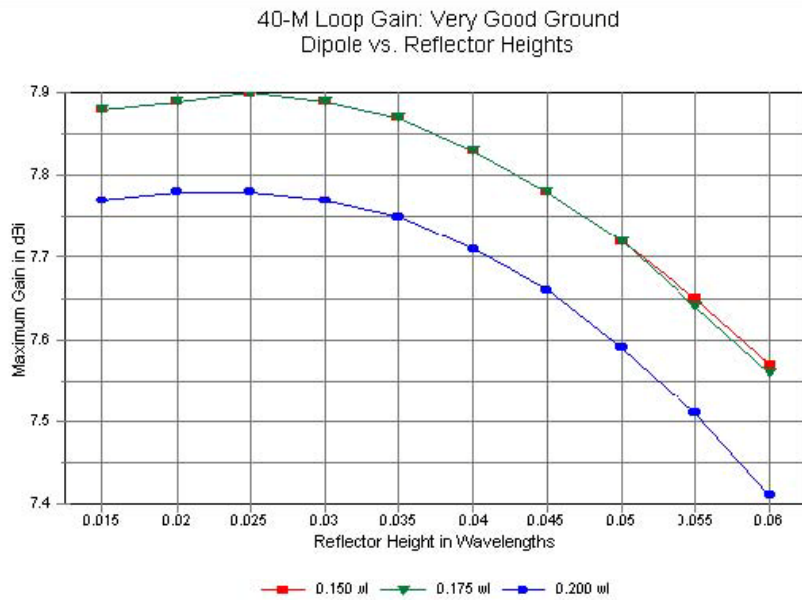


Fig. 18

NVIS 7.2-MHz 1-WL Loop with a Single-Wire Loop Reflector Element								Table 4	
Driver: 1.0184-wl AWG #14 Copper Wire				Reflector: 1.0296-wl AWG #14 Copper Wire					
Loop Height		0.15 wl		21.48 feet					
		Very Good Soil		Average Soil		Very Poor Soil		Refl. Sep.	
Ref Ht wl	Rf Ht ft	Gain dBi	BS BW	Gain dBi	BS BW	Gain dBi	BS BW	wl	
No Reflector		7.68	83.7	6.48	87.6	5.21	93.7		
0.001	0.14	7.75	84.0	6.68	87.8	5.65	93.3		
0.015	2.15	7.88	84.1	7.00	87.5	6.29	91.7		
0.02	2.86	7.89	84.2	7.06	87.4	6.41	91.4		
0.025	3.58	<b>7.90</b>	84.2	7.10	87.4	6.49	91.2	0.125	Vry Gd
0.03	4.30	7.89	84.3	<b>7.13</b>	87.4	6.56	90.9	0.120	Ave
0.035	5.01	7.87	84.3	<b>7.13</b>	87.4	6.60	90.6	0.115	Ave
0.04	5.73	7.83	84.5	7.12	87.5	<b>6.61</b>	90.6	0.110	Vry Pr
0.045	6.44	7.78	84.5	7.09	87.5	6.60	90.4		
0.05	7.16	7.72	84.7	7.05	87.5	6.57	90.3		
0.055	7.87	7.65	84.7	6.98	87.6	6.53	90.1		
0.06	8.59	7.57	84.8	6.91	87.5	6.47	89.9		
Max. Delta Gain		0.22		0.65			1.40		
Loop Height		0.175 wl		25.05 feet					
		Very Good Soil		Average Soil		Very Poor Soil		Refl. Sep.	
Ref Ht wl	Rf Ht ft	Gain dBi	BS BW	Gain dBi	BS BW	Gain dBi	BS BW	wl	
No Reflector		7.74	87.0	6.71	91.4	5.51	97.9		
0.001	0.14	7.78	87.3	6.84	91.5	5.87	97.1		
0.015	2.15	7.88	87.4	7.10	91.1	6.44	95.3		
0.02	2.86	7.89	87.6	7.16	90.9	6.55	94.8		
0.025	3.58	<b>7.90</b>	87.6	7.20	90.9	6.64	94.5	0.150	Vry Gd
0.03	4.30	7.89	87.7	7.23	90.9	6.71	94.3		
0.035	5.01	7.87	87.9	<b>7.24</b>	91.0	6.75	94.0	0.140	Ave
0.04	5.73	7.83	88.1	7.23	91.1	<b>6.77</b>	93.8	0.135	Vry Pr
0.045	6.44	7.78	88.3	7.21	91.1	<b>6.77</b>	93.7	0.130	Vry Pr
0.05	7.16	7.72	88.5	7.17	91.3	6.76	93.5		
0.055	7.87	7.64	88.7	7.11	91.4	6.73	93.5		
0.06	8.59	7.56	89.0	7.05	91.4	6.69	93.4		
Max. Delta Gain		0.16		0.53			1.26		
Loop Height		0.2 wl		28.63 feet					
		Very Good Soil		Average Soil		Very Poor Soil		Refl. Sep.	
Ref Ht wl	Rf Ht ft	Gain dBi	BS BW	Gain dBi	BS BW	Gain dBi	BS BW	wl	
No Reflector		7.67	91.3	6.75	96.1	5.64	102.8		
0.001	0.14	7.69	91.7	6.85	96.1	5.93	101.9		
0.015	2.15	7.77	91.7	7.07	95.6	6.45	99.7		
0.02	2.86	<b>7.78</b>	91.8	7.12	95.5	6.56	99.2	0.180	Vry Gd
0.025	3.58	<b>7.78</b>	91.9	7.16	95.5	6.64	98.9	0.175	Vry Gd
0.03	4.30	7.77	92.2	7.19	95.3	6.71	98.5		
0.035	5.01	7.75	92.2	<b>7.20</b>	95.4	6.75	98.2	0.165	Ave
0.04	5.73	7.71	92.6	7.19	95.4	<b>6.78</b>	97.8	0.160	Vry Pr
0.045	6.44	7.66	92.7	7.17	95.6	<b>6.78</b>	97.8	0.155	Vry Pr
0.05	7.16	7.59	93.1	7.13	95.7	6.77	97.7		
0.055	7.87	7.51	93.5	7.07	96.0	6.75	97.5		
0.06	8.59	7.41	94.0	7.00	96.3	6.71	97.4		
Max. Delta Gain		0.11		0.44			1.11		

If you compare **Fig. 14** with **Fig. 18**, you can see that over very good soil, the gain level at the two lower heights on 40 meters result in overlapping lines, rather than separate lines. Similarly, over very poor soil, the 40-meter lines for the two higher levels overlap, whereas on 75 meters, they are separate. Compare **Fig. 16** with **Fig. 20**.

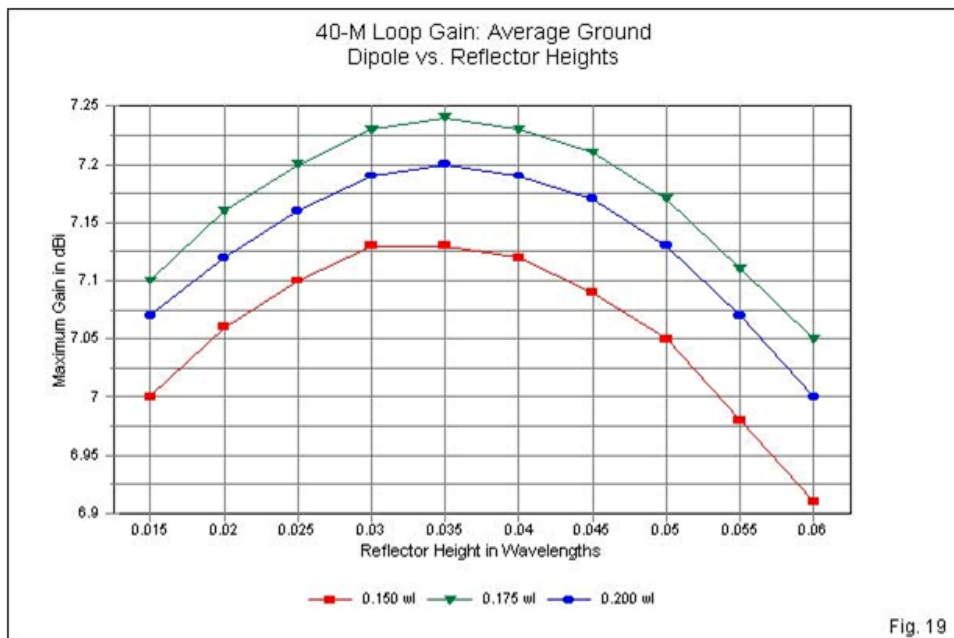
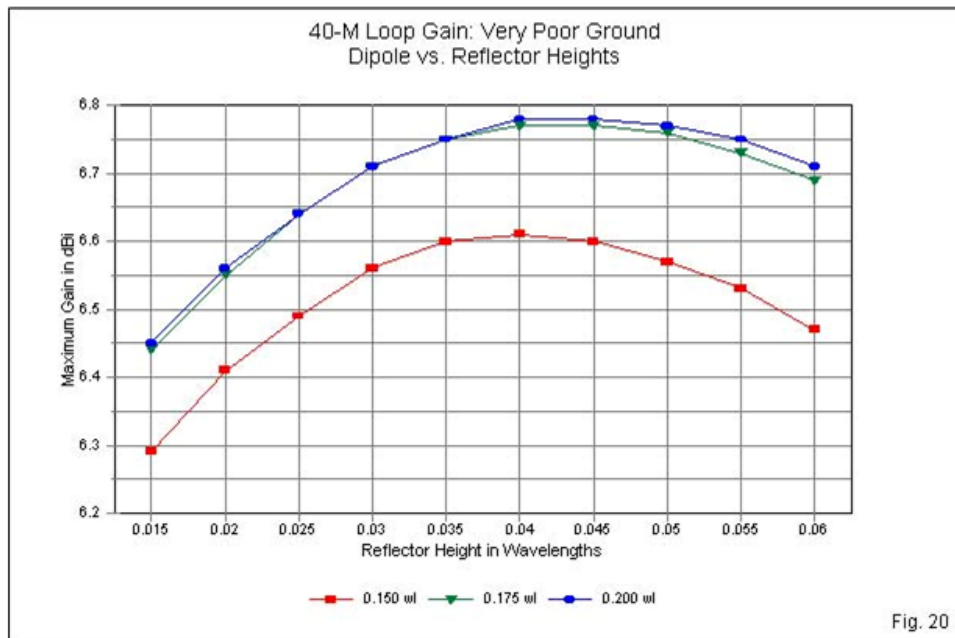
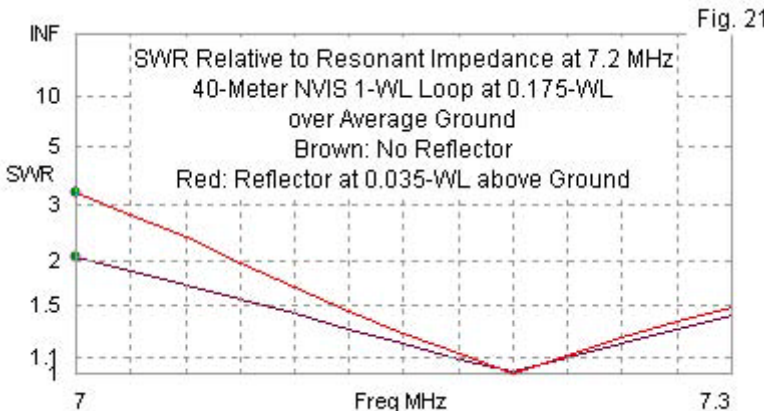


Fig. 19



Nevertheless, the loop-reflector combinations for both bands are consistent with each other and in the main are consistent with results for the dipole-reflector combinations. The consistency extends to the reduction in operating bandwidth on 40 meters, as shown in the SWR curves in **Fig. 21**. The addition of the reflector at an optimal height ( $0.035\lambda$ ) for average soil and a loop at  $0.175\lambda$  results in a significant reduction in the bandwidth. With respect to gain increase, on 40 meters, the use of a reflector is questionable over very good soil, marginal over average soil, and possibly productive over very poor soil.



As noted with respect to dipoles, the use of a parasitic reflector with a driven element creates a tuned system, although not fully isolated from ground effects. Besides limiting the operating bandwidth, the tuned system also tends to reduce the resonant impedance relative to a loop without a reflector. However, the parasitic reflector element is not the only method of improving NVIS performance.

### Dipoles, Loops, and Planar Reflectors

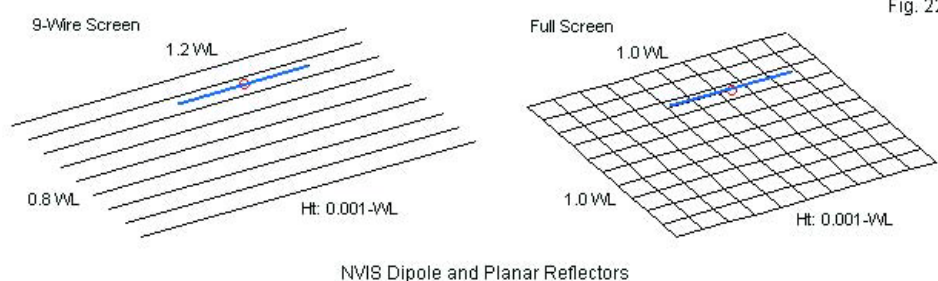
An alternative method of provide improved reflection of energy upward relative to reflections from the bare ground is the use of a planar reflector. In other applications, HF planar reflectors go under a variety of names, including screens, curtain, and billboards. A planar reflector operates according to principles largely derived from optics. In general, the reflections from an essentially flat conductive surface depend upon the size of the planar reflector and

its distance from the driven element—in this case, either a dipole or a  $1\text{-}\lambda$  loop. Although it is possible to elevate a planar reflector closer to the driven element to optimize performance, we cannot simply reduce the height of the driven element toward a ground-level reflector. The far-field gain is a function not only of the area covered by the reflector, but depends on the region several wavelengths away from the reflector. As a result, we shall only be able to obtain benefits that result from a practical ground-level reflector and an elevated driver.

As the best compromise among all possibilities, I have placed the driver at  $0.175\text{-}\lambda$  above all ground qualities. Very good soil would prefer a slightly lower height, while very poor soil prefers a slightly greater height. However, to achieve some consistency within the results of systematic modeling, a common height is best.

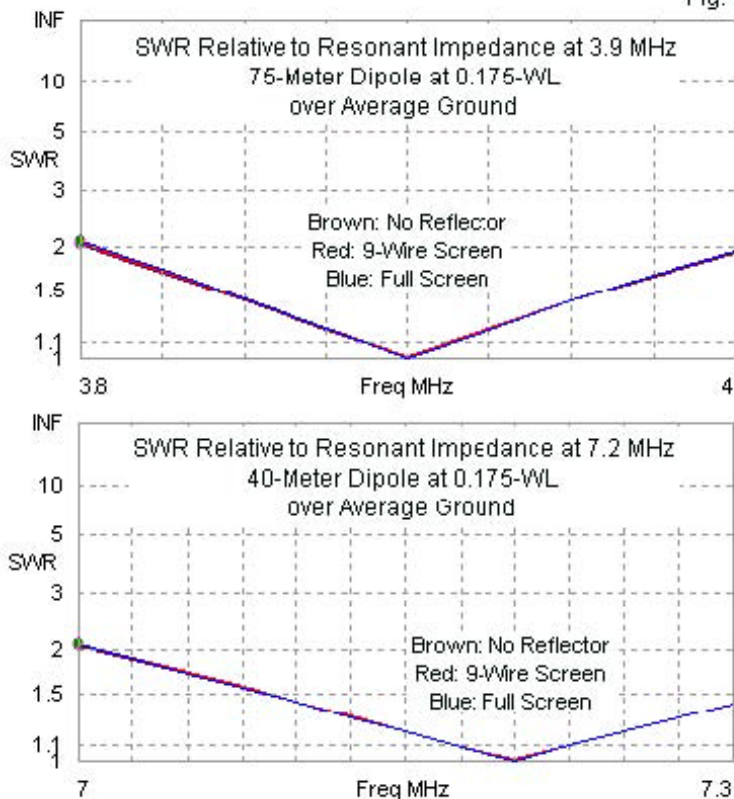
The dimensions of an optimal planar reflector vary according to the method used to construct it. In these notes, we shall consider two forms of planar reflectors, as illustrated by **Fig. 22**. The simpler reflector consists of at least 9 wires (using the same diameter wire as the driven element) spread to cover an area at least  $0.4\text{-}0.5\text{-}\lambda$  beyond each limit of the antenna.

The sample array, which yields the best performance at ground level, is  $1.2\text{-}\lambda$  in the direction of the wires and  $0.8\text{-}\lambda$  broadside to the antenna. One might add additional wires within the field.



As an alternative, one might cover the ground with conductive screening with holes smaller than  $0.05\lambda$ . In this case, a full screen that is  $1.0\lambda$  by  $1.0\lambda$  proved to be the most effective version. The modeled screen has twice as many wires as shown in the sketch, although to add them would have made it impossible to find the dipole above them.

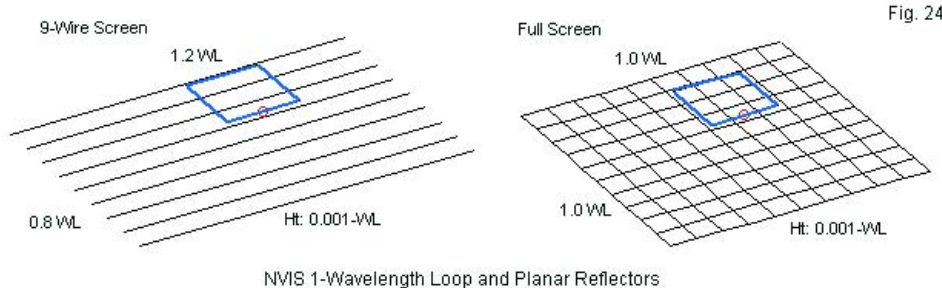
Fig. 23



One advantage of the planar reflector in either form is that it does not alter the impedance or the operating bandwidth of the driven element above it. **Fig. 23** provides the SWR curves for both types of reflector overlaid on the SWR curve for the dipole alone for both

75 and 40 meters. With or without the planar reflector, the curves are essentially identical.

We obtain similar properties if we place either type of planar reflector at ground level beneath a  $1-\lambda$  loop, as suggested by the sketches in **Fig. 24**. The same 9-wire and full screen reflectors used with the dipole also serve the loop very well. Like the dipole, the loops are at  $0.175\lambda$  above all ground types to ease the problem of performance comparison.



NVIS 1-Wavelength Loop and Planar Reflectors

Also like the dipole with a planar reflector, the loop-planar-reflector combination results in an operating bandwidth essentially identical to the bandwidth of a loop alone. **Fig. 25** provides SWR curves for loop-reflector combinations for 75-and 40 meters, with the loop-alone curve superimposed. Separating the curves visually is virtually impossible.

Fig. 25

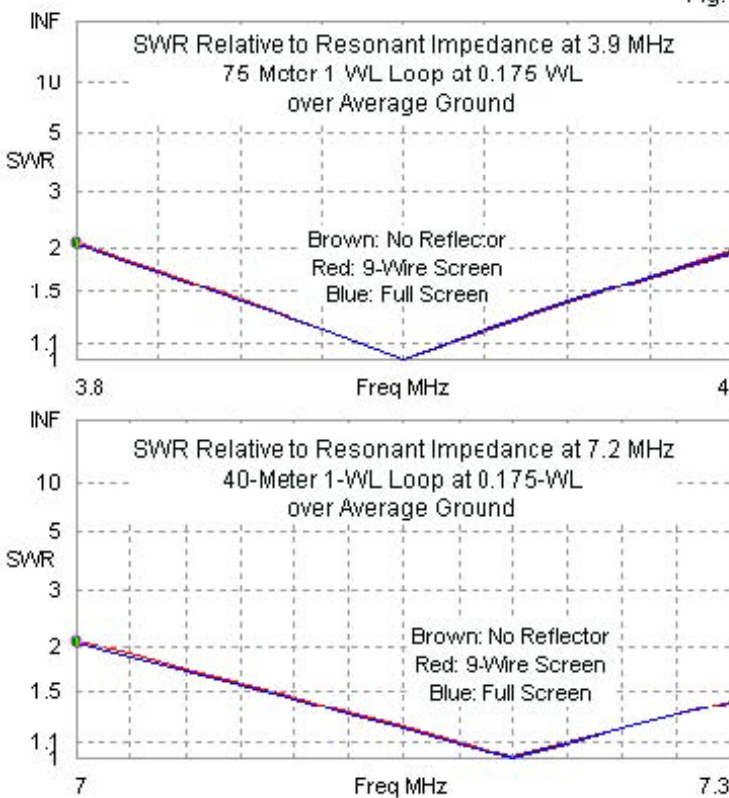


**Table 5** provides data on the planar reflectors for both dipoles (on the left) and loops (on the right). However, it also includes data for isolated NVIS antennas and for antenna-reflector combinations using the same set of limiting constraints. In all cases, the driven antenna is  $0.175\lambda$  above ground. The table indicates the antenna

dimensions and, where relevant, the reflector dimensions. For dipoles, the element dimensions are linear lengths, while for loops, they are circumference values. The arrays are sized for resonance over average ground, and the changes of impedance for very good and very poor soil are indicators of stability. For example, the arrays with parasitic reflectors show the least change with changes in soil quality, which is consistent with one role of a parasitic reflector, namely, to control the driver feedpoint impedance.

Summary Comparisons of Basic NVIS Antennas							Table 5				
75 Meters (3.9 MHz)							1-WL Loop: 1.0248-wl				
Ground	Dipole: 0.4804-wl	Max Gain	BS BW	EW BW	Feed R	Feed X	Max Gain	BS BW	EW BW	Feed R	Feed X
Vy Good	7.38	107.5	66.2	62.48	7.82	7.95	86.1	69.8	120.00	15.05	
Average	6.40	113.0	66.4	67.55	0.66	7.02	90.3	70.2	128.20	-0.64	
Vy Poor	5.05	122.4	67.2	71.66	-9.55	5.78	97.6	71.2	132.80	-23.87	
	Dipole + Reflector: 0.4794-wl + 0.5-wl @ 0.25-wl					Loop + Reflector: 1.0176-wl + 1.0248-wl @ 0.03-wl					
Vy Good	7.43	108.6	66.2	51.27	2.40	8.01	86.9	70.2	104.60	3.59	
Average	6.83	113.6	66.4	52.79	0.21	7.39	90.4	70.8	108.10	-0.54	
Vy Poor	6.11	120.8	66.8	52.62	-2.25	6.70	95.2	71.6	107.00	-0.39	
	Dipole + 9-Wires: 0.4798-wl + 1.2-wl BS x 0.8-wl EW					Loop + 9-Wires: 1.024-wl + 1.2-wl BS x 0.8-wl EW					
Vy Good	7.53	106.2	64.3	62.15	5.55	8.16	85.3	67.2	119.60	11.82	
Average	7.15	108.2	62.2	66.46	0.24	7.79	87.2	64.7	126.00	-0.38	
Vy Poor	6.74	111.0	60.6	72.41	-4.91	7.40	89.1	62.6	135.60	-13.26	
	Dipole + Screen: 0.4776 + 1.0-wl x 1.0-wl					Loop + Screen: 1.0192-wl + 1.0-wl x 1.0-wl					
Vy Good	7.73	104.8	65.8	59.78	-0.04	8.33	84.5	69.2	115.50	1.43	
Average	7.74	103.0	65.0	63.06	-0.20	8.26	83.5	68.2	121.70	0.28	
Vy Poor	7.83	98.8	63.4	65.51	0.42	8.38	80.7	65.9	126.60	0.60	
40 Meters (7.2 MHz)							1-WL Loop: 1.0248-wl				
Ground	Dipole: 0.4800-wl	Max Gain	BS BW	EW BW	Feed R	Feed X	Max Gain	BS BW	EW BW	Feed R	Feed X
Vy Good	7.15	108.8	66.2	63.86	8.98	7.74	87.0	69.8	123.10	19.63	
Average	6.03	114.8	66.0	67.28	0.26	6.71	91.4	69.6	127.30	0.84	
Vy Poor	4.71	123.3	66.8	69.99	-9.21	5.51	97.9	70.6	128.50	-20.72	
	Dipole + Reflector: 0.4786-wl + 0.5-wl @ 0.35-wl					Loop + Reflector: 1.0184-wl + 1.0296-wl @ 0.035-wl					
Vy Good	7.31	110.8	66.6	45.94	1.95	7.87	87.9	70.8	102.30	3.19	
Average	6.74	115.2	66.2	46.62	0.26	7.24	91.0	70.8	104.60	0.36	
Vy Poor	6.15	120.8	66.4	45.83	-1.38	6.75	94.0	71.4	101.80	-4.73	
	Dipole + 9-Wires: 0.4790-wl + 1.2-wl BS x 0.8-wl EW					Loop + 9-Wires: 1.0272-wl + 1.2-wl BS x 0.8-wl EW					
Vy Good	7.53	106.8	63.5	62.62	5.84	8.15	85.6	66.2	120.40	12.23	
Average	7.02	109.0	61.8	66.66	0.19	7.69	87.4	64.2	126.10	-0.47	
Vy Poor	6.74	109.6	59.8	72.40	-4.47	7.41	88.2	61.7	135.30	-12.45	
	Dipole + Screen: 0.4762 + 1.0-wl x 1.0-wl					Loop + Screen: 1.0212-wl + 1.0-wl x 1.0-wl					
Vy Good	7.73	104.6	65.6	60.21	-0.08	8.33	84.2	69.0	116.80	1.81	
Average	7.73	101.8	64.4	63.31	-0.36	8.32	82.4	67.4	122.70	0.37	
Vy Poor	7.93	96.6	62.7	65.34	0.34	8.48	79.6	65.0	126.90	0.90	
Notes:	All dipoles and 1-wl loops at 0.175-wl above ground										
	Dipole dimensions are linear lengths; loop dimensions are circumferences										
	Max. Gain = maximum zenith gain in dBi										
	BS BW, EW BW = broadside and endwise beamwidths in degrees										
	Feed R; Feed X = feedpoint resistance and reactance in Ohms										

Reading from left to right provides a guide to the gain advantage in all cases of the  $1\text{-}\lambda$  loop over the dipole, whether alone or in the surveyed arrays. Reading within an array type summarizes the gain change with soil quality. Reading from one group to the next provides a guide to the increasing gain advantage offered by successively more effective arrays. The table includes broadside and endwise beamwidth values to allow estimates of pattern circularity.

The entries for the full screen planar reflector may seem odd at first sight. For all preceding arrays, we find that very good soil yields the highest zenith gain. However, with a full screen, using either a dipole or a loop, the highest gain occurs over very poor soil. The difference is not operationally significant within each full screen group, but the phenomenon is interesting. Only the full screen provides sufficient coverage to isolate the antenna from the ground to the degree that very poor soil approaches the quality of free space. Even the 9-wire screen has ground losses between wires, losses that one can reduce by increasing the reflector wire diameter or by increasing the number of wires—or both.

Measured against the performance benefits of a  $1\text{-}\lambda$ -by- $1\text{-}\lambda$  full ground screen must be the site preparation difficulties, factors that lie beyond the scope of these notes. However, to focus more clearly on the potential gain benefits, **Table 6** provides a summary view. Even though the exercise does not place single-element reflectors at their optimum heights for very good and very poor soil, the maximum improvement in the gain values for those cases would be about 0.05 dB.

Gain Comparisons by Ground Quality and Supplements							Table 6
	Very Good		Average		Very Poor		
Dipoles	Zen Gain	Change	Zen Gain	Change	Zen Gain	Change	
Dp	7.38	----	6.40	----	5.06	----	
Dp+Ref	7.48	0.10	6.88	0.48	6.11	1.05	
Dp+9W	7.58	0.20	7.15	0.75	6.74	1.68	
Dp+Scr	7.79	0.41	7.74	1.34	7.88	2.82	
Loops	Zen Gain	Change	Zen Gain	Change	Zen Gain	Change	
Loop	7.95	----	7.02	----	5.78	----	
Lp+Ref	8.01	0.06	7.39	0.37	6.70	0.92	
Lp+9W	8.16	0.21	7.79	0.77	7.40	1.62	
Lp+Scr	8.33	0.38	8.26	1.24	8.38	2.60	
40-M	Very Good		Average		Very Poor		
Dipoles	Zen Gain	Change	Zen Gain	Change	Zen Gain	Change	
Dp	7.15	----	6.03	----	4.71	----	
Dp+Ref	7.31	0.16	6.74	0.71	6.16	1.45	
Dp+9W	7.53	0.38	7.02	0.99	6.74	2.03	
Dp+Scr	7.78	0.63	7.79	1.76	7.98	3.27	
Loops	Zen Gain	Change	Zen Gain	Change	Zen Gain	Change	
Loop	7.74	----	6.71	----	5.51	----	
Lp+Ref	7.87	0.13	7.24	0.53	6.77	1.26	
Lp+9W	8.15	0.41	7.69	0.98	7.41	1.90	
Lp+Scr	8.33	0.59	8.32	1.61	8.48	2.97	
Notes:	See Table 5 for source of values. Dp = Dipole; Lp = 1-wl loop +Ref = reflector element; +9W = 9-wire screen; +Scr = full screen Zen Gain = zenith gain Change = gain increase relative to dipole or loop						

The gain-table is not only useful in estimating the benefits of supplementing a basic level NVIS antennas in various ways, but it also sets in bold relief the overall range of gain values that we may expect from these antennas as a group. That data is useful in comparing basic antenna performance with the performance of more complex antenna types, such as variations on the lazy-H. More relevant to our discussion of basic antennas is the one that is missing so far: the inverted-V.

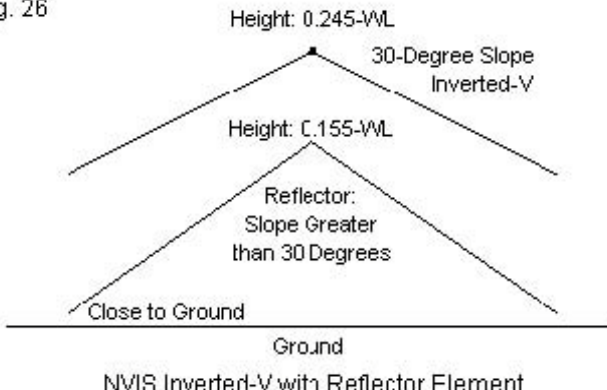
### *The Inverted-V with Parasitic and Planar Reflectors*

I have set aside the inverted-V from the discussion because it represents a special case when we consider adding a parasitic reflector to the antenna. Within the range of our survey, which has a maximum (center) height of  $0.255\lambda$ , an inverted-V obtains maximum gain over almost any ground quality only near the maximum height. In NVIS operation, the effective or virtual height of an inverted-V relative to its performance falls between half and  $2/3$  the physical center height. For most amateur installations,  $0.255\lambda$  is practical on 40 meters (about 35'), but less so on 75 meters (about 64'). However, we need to consider such heights if we wish relatively good performance from an inverted-V over the full range of soil qualities.

Inverted-V antennas with lower center heights will work, as shown in the preceding set of notes, but they do not permit the addition of a parasitic reflector. The reflector element must have at least some spacing from the driven element and still clear the ground at the reflector wire ends. In fact, ground effects upon a reflector for an

inverted-V impose interesting geometry requirements that oppose our natural desire to flatten the slope angle of the element. **Fig. 26** shows the general requirements for an effective inverted-V with a parasitic reflector.

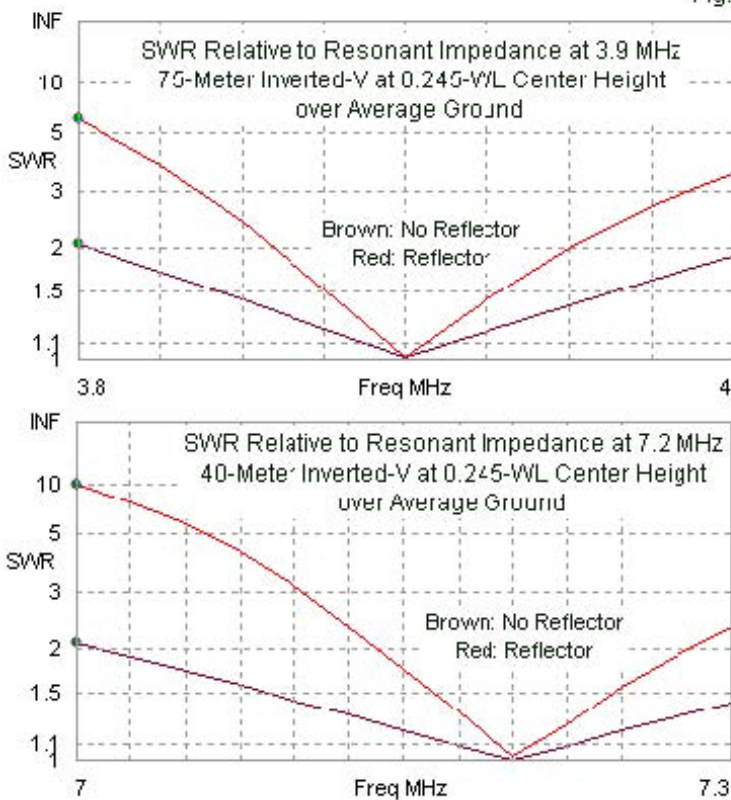
Fig. 26



For all soil qualities, the sketch shows the average optimal height for an inverted-V with a 30° slope (or a 120° included angle). The reflector, by virtue of its need for greater length than the driven element requires a center height of about 0.155- $\lambda$ , but the slope angle is greater than 30°. The precise angle is a function of the wire-end heights, which tend to be between 0.01- $\lambda$  and 0.015- $\lambda$  above ground. With respect to user safety, the reflector ends are too close to ground, but we shall bypass this legitimate concern in order to evaluate antenna performance.

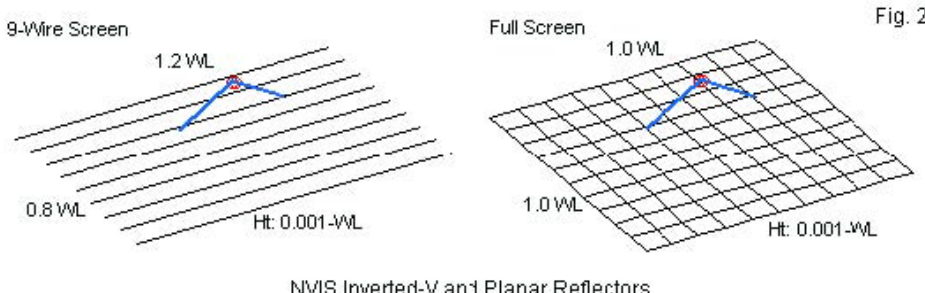
One facet of the inverted-V array's performance that we may readily compare to the performance of the level antennas is the operating bandwidth as measured by SWR curves referenced to the antenna resonant impedance. **Fig. 27** superimposes the curves for an inverted-V alone at the optimum height with the curve for the same antenna supplemented by a parasitic reflector. Both are over average ground, although the general shape of the curves would apply equally to all soil types. The figure records separate sweeps for 75 meters and for 40 meters. In the case of level antennas (dipoles and loops) using parasitic reflectors, we found moderate shrinkage of the 2:1 SWR bandwidth. See **Fig. 8**, **Fig. 12**, **Fig. 17**, and **Fig. 21** for samples. In contrast, the SWR bandwidth shrinkage for the inverted-V with a parasitic reflector is more radical, reducing the 2:1 SWR region by more than half relative to the inverted-V alone. One immediate consequence of this phenomenon for antenna builders is that field adjusting the antenna to a desired frequency will be a somewhat finicky task.

Fig. 27



There are means to obtain additional gain from the inverted-V while preserving the SWR bandwidth available with the V alone. We may place a ground-level planar reflector below the V using essentially the same techniques that we employed for the dipole and the loop antennas. Indeed, as shown in **Fig. 28**, the 9-wire and full-screen

reflectors may use the same dimensions as used with the level antennas. The same application rules also apply. We may improve the 9-wire reflector performance by adding either thicker wires or more wires. The full screen may use materials with opening no larger than  $0.05\lambda$ , although common materials will normally have much smaller openings relative to NVIS operating frequencies.



**Table 7** summarizes the performance values for all of the variations on supplementing an inverted-V, beginning with the V alone to form a reference data set for the three ground types. All driven inverted-V elements have a maximum center height of  $0.245\lambda$  and a  $30^\circ$  slope. Because the total element length varies from one design to the next, the end heights will vary slightly but fall within the range of  $0.123\lambda$  and  $0.125\lambda$ . The reflector ends are about  $0.01\lambda$  above ground.

Comparisons of NVIS Inverted-V Antennas					Table 7
<b>75 Meters (3.9 MHz)</b>					
	V: 0.4844-wl				
Ground	Max Gain	BS BW	EW BW	Feed R	Feed X
Vy Good	6.41	113.8	78.6	64.66	6.99
Average	5.52	119.4	77.4	67.15	-0.47
Vy Poor	4.30	128.6	76.2	67.32	-10.65
	V + Reflector: 0.4864-wl + 0.5114-wl @ 0.155-wl				
Vy Good	6.56	118.1	74.4	33.40	0.91
Average	5.98	123.0	73.6	33.51	-0.57
Vy Poor	5.19	129.6	72.4	32.80	-2.59
	V + 9-Wires: 0.4844-wl + 1.2-wl BS x 0.8-wl EW				
Vy Good	6.70	112.0	74.2	64.24	6.41
Average	6.42	114.8	69.6	65.32	0.75
Vy Poor	6.14	117.4	65.8	67.81	5.39
	V + Screen: 0.4822 + 1.0-wl x 1.0-wl				
Vy Good	6.84	110.6	77.6	62.95	1.30
Average	6.88	109.0	74.8	65.49	0.20
Vy Poor	7.14	104.4	71.0	67.55	-0.28
<b>40 Meters (7.2 MHz)</b>					
	V: 0.4844-wl				
Ground	Max Gain	BS BW	EW BW	Feed R	Feed X
Vy Good	6.19	115.4	78.4	65.57	8.56
Average	5.22	121.2	76.5	66.01	0.10
Vy Poor	4.06	129.2	75.4	64.95	-8.85
	V + Reflector: 0.4864-wl + 0.5062-wl @ 0.155-wl				
Vy Good	6.43	120.6	73.8	28.64	0.56
Average	5.87	124.8	72.4	28.23	-0.73
Vy Poor	5.28	129.6	71.2	26.95	-2.03
	V + 9-Wires: 0.4838-wl + 1.2-wl BS x 0.8-wl EW				
Vy Good	6.69	112.8	72.8	63.77	6.48
Average	6.31	115.4	69.6	64.69	0.85
Vy Poor	6.16	116.2	65.2	67.07	-4.88
	V + Screen: 0.4810 + 1.0-wl x 1.0-wl				
Vy Good	6.86	110.4	76.8	63.22	0.67
Average	6.96	107.6	73.8	65.48	-0.55
Vy Poor	7.24	103.0	70.3	67.21	-0.85
Notes:	All inverted-Vs have a 0.245-wl center height and a 30 degree slope. Dimensions are total element lengths. Wire-end heights vary with element lengths.				
Max. Gain = maximum zenith gain in dBi					
BS BW; EW BW = broadside, endwise beamwidths in degrees					
Feed R; Feed X = feedpoint resistance and reactance in Ohms					

The impedance columns for both 75 and 40 meters are instructive in accounting for the relatively narrow SWR bandwidth of the inverted-V with a parasitic reflector. On both bands, the

average feedpoint impedance for the V is about  $65 \Omega$ , a value preserved with either planar reflector. However, with a parasitic reflector, the resistive component of the impedance drops to about  $30 \Omega$ . At this impedance, small changes in the reactive component of the impedance have more notable effects upon the SWR.

For all of the entries, the inverted-V arrays have gain levels about a full dB below the levels achieved by the level dipole, despite the V's greater center height. (Loop arrays, of course, provide an additional gain increment.) Over very good ground, the gain benefits of any of the reflector systems are quite marginal, but over very poor soil, the gain increase can approach 3 dB. The gain of the full screen (using a model with twice the wire density shown in **Fig. 28**) over very poor ground parallels the value increases that we observed with the level antennas. To approach this level of performance with the 9-wire screen would require extensive revisions to cover the ground more thoroughly with conductive wires.

### *Conclusion*

The idea of adding a reflector element to a basic NVIS antenna to improve performance has lived in sound bites and mythology since the initial uses of the propagation mode. Therefore I decided to perform a more thorough modeling analysis of the idea to see what order of improvement might be possible and the conditions under

which we might optimize the improvement. This compendium of data is the result. For all three types of basic antennas—dipoles,  $1-\lambda$  loops, and inverted-Vs—the addition is questionable or marginal until we reach very poor soil qualities. In addition, the use of a parasitic reflector (which is not under any circumstances a counterpoise) requires attention to its height above ground and its separation from the driven antenna, although the gain curves are broad enough to allow for variation from the ideal. Over any soil, a single wire reflector close to the ground proves to be an unproductive expenditure of materials and energy. Variations in reflector size will require element pruning to reach a resonant impedance value. In all cases, the use of a parasitic reflector will lower the feedpoint impedance relative to the impedance of the basic antenna alone. As well, the reflector will narrow the operating bandwidth. Both consequences are more extreme for the inverted-V than for the level antennas.

An alternative to the parasitic reflector is a planar reflector. In theory, we might elevate a planar reflector to a position below the main antenna at which we may obtain very significant gain improvements. The required size of a planar reflector militates against the elevated version, so we confined our examination to near-ground versions. In general, a planar reflector needs to have dimensions that exceed the driven antenna dimensions by about  $0.4-\lambda$  to  $0.5-\lambda$  on all sides. The 9-wire and full-screen reflectors that we sampled showed that these guidelines are not absolutes. In fact, smaller planar reflectors will work, but they will seriously reduce the gain benefits. Both the parallel-wire and the full-screen reflectors significantly improved the gain performance of the basic

antennas, especially over lesser soil qualities. In addition, they preserved the impedance level and the SWR bandwidth of each individual basic NVIS antenna type.

The goal of these notes has been to provide as full and complete information as possible on reflectors for basic NVIS antennas. The notes make no recommendations about the selection of any reflector technique beyond the very general notes concerning the relative size of the gain benefits over the range of soil types in the survey. Such comments merely state the obvious. If blessed with very good soil, the antenna installation needs no supplementation, since reflectors in general only improve gain to the level of the antenna alone over very good soil. However, over lesser soils, including very poor soil, the use of a reflector can be beneficial, although one must measure the potential level of gain improvement against a host of other factors. Among these factors are the NVIS station mission, the difficulty of coverage, the available antenna site, and the investment of resources required for the improvements that might come from a reflector.

In general, parasitic reflectors require no additional supports or ground preparation. The investment comes in the field adjustments necessary to bring the antenna to best operation. In contrast, one may add a planar reflector to an existing antenna that is near an optimum height and incur very little need for subsequent adjustments. However, the work of installing either an extensive parallel-wire or full-screen reflector is very significant and requires access to a considerable area around the antenna. These factors

are only some of the mechanical considerations that go into the decision to add a reflector to a basic NVIS antenna.

## Chapter 67: NVIS Dipoles, Inverted-Vs, 1- $\lambda$ Loops & Doublets

The preceding Chapters have developed a data compendium on the performance of basic NVIS antennas, with special reference to the dipole, the inverted-V, and the 1- $\lambda$  loop. Our focus on these antennas has centered on fixed stations with well-prepared installation sites. Therefore, we sought to identify for each of the three soil types in our survey the antenna height for peak zenith gain, along with other trends that are relevant to performance. One collection worked with isolated or unsupplemented antenna elements, while the other collection featured both parasitic and planar reflector systems for the fed elements.

In the present exploration, we shall change our perspective. Instead of letting the antenna reach its peak zenith gain at whatever height might emerge, we shall work with some practical antenna heights that are typical of amateur installations. Fortunately, some of these heights happen to correspond closely with the natural heights for maximum zenith gain. For most level NVIS antennas, a height of 0.175- $\lambda$  is close to the center of the range of optimal heights for all soils. Very good soils need a slightly lower height, while very poor soils need a bit more height. However, we saw that gain changes fairly slowly in the region of maximum zenith gain, so our use of a single value to capture the best NVIS height for level antennas (such as linear dipoles and 1- $\lambda$  loops) will not be far from perfect. Two of the heights amateurs often use for wire antenna supports are 50' and 25'. The former comes close to the proper height on 75 meters, while the latter is about right for 40 meters. Along the way,

we shall look at some alternative heights for inverted-V antennas. As well, we shall look at 35' in two ways, first, as an alternative to the optimal height and second, as a compromise so that we may connect two antennas together with a common feedpoint.

We shall look at a number of antennas and combinations of antennas. Of course, the dipole, the inverted-V, and the  $1\lambda$  loop will undergo some close scrutiny within the confines of our height limitations. Then we shall begin pairing 75-and 40-meter antennas, initially stacking them both in-line and at  $90^\circ$  angles but keeping the feedpoints independent of each other. Next we shall look at the performance of crossed dipoles and inverted-Vs that use a common feedpoint. We can also create a 2-band array of nested  $1\lambda$  loops, one inside the other. Our next antenna will be both simpler and more complex than the others. It consists of a single center-fed 104' wire, but using it will require an antenna tuner at some point between the equipment and the antenna proper. Finally, we shall briefly look at a trap dipole and trap inverted-V for 75-and 40-meter NVIS use. All of the antennas will use AWG #14 copper wire.

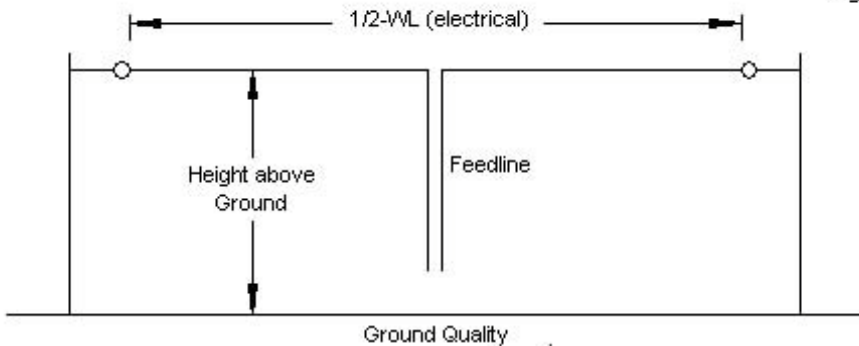
These selections do not exhaust our options for practical NVIS antennas. Still, they provide a broad selection of possibilities for performance comparisons. As well, they provide some broad outlines of the 3-dimensional space requirements required for a NVIS antenna installation. Their true function is not to guide actual antenna construction, but rather to form a background for antenna planning. To the antenna performance specifications, the antenna planner must bring detailed information on the antenna site, available resources, and mission specifications. Engineering—even

at an amateur level—an antenna installation is not as casual an affair as some beginners believe. Good electrical and mechanical design and construction become even more important if the NVIS station has emergency communications as part or the entirety of its mission. The data in this set of notes provides only one set of pieces in a relatively complex jigsaw puzzle.

### *The Practical NVIS Dipole for 75 and 40 Meters*

The standard linear or level dipole is so common a wire antenna on the lower HF bands that it seems to scarcely need mentioning. In fact, the most common backyard lower HF dipole installations are NVIS antennas, since amateurs rarely can achieve heights approaching  $\frac{1}{2}\lambda$  or more on 75 and 80 meters. Indeed, 40-meter dipoles rarely reach  $\frac{1}{2}\lambda$  (about 70').

Fig. 1



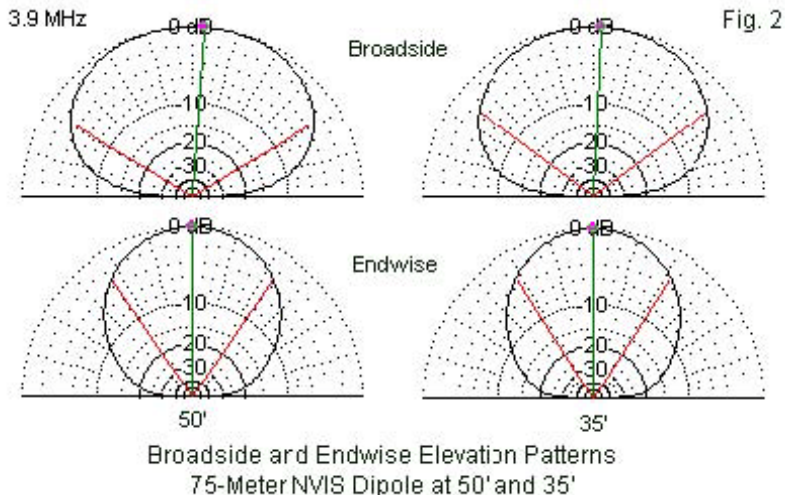
The NVIS (or Any) Dipole

**Fig. 1** shows the main components of a dipole installation, including two end supports, end insulators and ropes, a wire element fed at its center, and a feedline, normally coaxial cable. Most installation would also add a common-mode current attenuator at the feedpoint of the dipole and almost any other antenna. As a NVIS antenna within the constraints of these notes, the height above ground will be either 50' or 35' on 75 meters and either 35' or 25' on 40 meters. **Table 1** provides performance data for these options.

Dipoles		AWG #14 Copper Wire								Table 1	
Band M	Height ft	Length ft	Soil	Zen Gain	BS BW	EW BW	BW Ratio	Feed R	Feed X		
3.9 MHz	75	50	Vy Good	7.29	112.2	67.8	1.65	71.01	7.48		
			Average	6.40	117.8	67.8	1.74	73.76	0.14		
			Vy Poor	5.13	127.2	68.4	1.86	75.02	-9.74		
	40	35	Vy Good	7.30	101.6	64.4	1.58	48.73	6.71		
			Average	6.07	106.8	65.2	1.64	57.73	0.86		
			Vy Poor	4.59	115.8	66.8	1.73	66.82	-8.67		
7.2 MHz	40	35	Vy Good	6.48	127.2	74.4	1.71	87.62	6.00		
			Average	5.65	131.6	73.2	1.80	84.17	0.26		
			Vy Poor	4.58	137.2	72.2	1.90	79.78	-5.64		
	75	25	Vy Good	7.14	110.4	66.7	1.66	66.64	8.72		
			Average	6.07	116.4	66.4	1.75	69.16	0.08		
			Vy Poor	4.78	124.8	67.0	1.86	70.93	-9.27		
Notes:		Zen Gain = maximum zenith gain in dBi BS BW; EW BW = broadside and endwise beamwidths in degrees Feed R; Feed X = feedpoint resistance and reactance in Ohms									

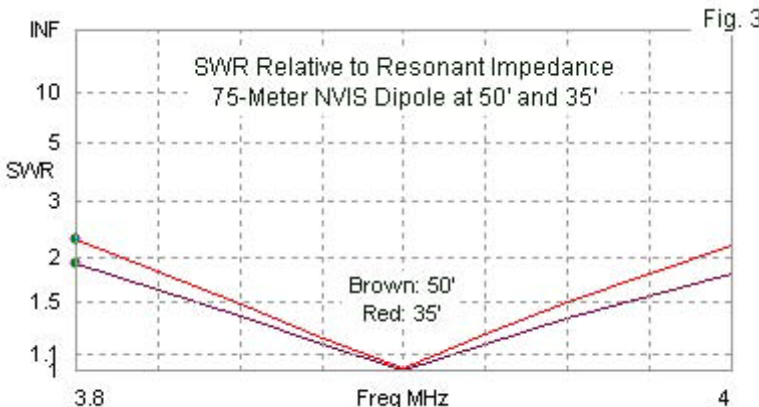
The table lists modeled dimensions for the dipole if composed of AWG #14 copper wire. On 75 meters, 121.2' will resonate at 3.9 MHz at either height over average soil. The dimensions must change very slightly for both better and worse ground qualities. As well, the dimensions might also change due to the proximity of objects within the installation site, since the model presumes flat, uncluttered terrain. Still, the numbers provide a starting point for field adjustments.

As the 75-meter entries show, the 50' height, if achievable, provides superior zenith gain performance, since the height is close to the generalized optimum height of  $0.175\lambda$ . The advantage shows up more clearly as we decrease the soil quality. In addition, the pattern becomes more oval and less circular for either height as we decrease ground quality. **Fig. 2** provides broadside and endwise elevation patterns for both heights. As we raise the height of a NVIS dipole, the oval becomes more elongated in the broadside direction. This fact may have a bearing upon the orientation of the antenna for some installations and missions.



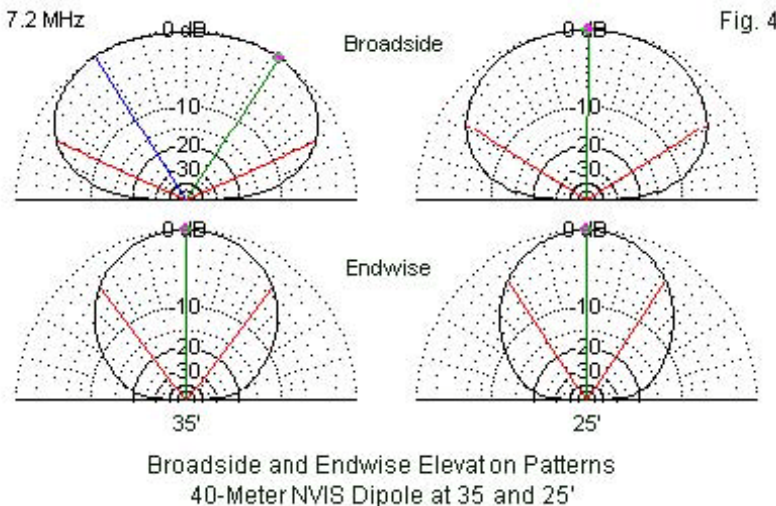
A wire dipole will not allow coverage of the entire 80-75-meter band, but it does suffice for the main part of the SSB portion at 75 meters. **Fig. 3** shows the SWR curves for both heights referenced

to the resonant feedpoint impedance over average ground. As the curves indicate, the 50' curve is flatter than the 35' curve. In addition, the tabular impedance data suggests that the lower height is a better match for a 50- $\Omega$  feedline, while the 50' heights better matches a 70 $\Omega$  coaxial cable.



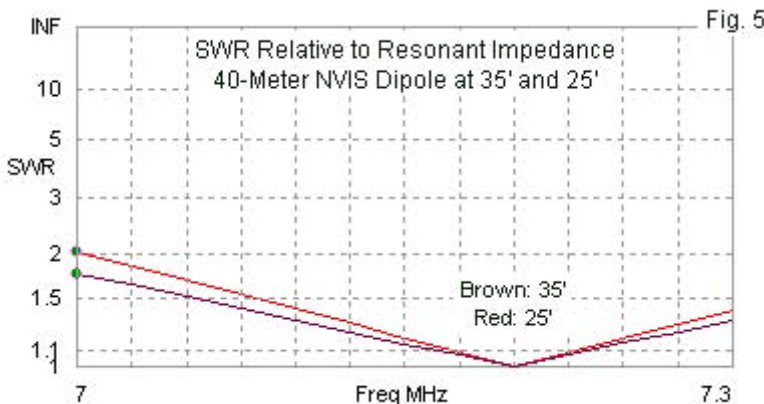
On 40 meters, the table offers a choice between heights of 35' and 25'. In this case, we obtain better zenith gain performance at the lower height, which is closer to  $0.175\lambda$  above ground. On 75 meters, our choices were a near-optimal height and a height below optimum. On 40 meters, we can select between a near-optimal height and another above the optimal level. If we examine the patterns in **Fig. 4**, we can see one effect of raising the antenna too high for best NVIS operation. At 35', the broadside pattern has already split into two maximum gain lobes offset from the zenith or straight-upward direction. The beamwidth ratio reflects the greater

ovalization of the pattern. For strict NVIS operation, a more circular pattern is desirable, but some missions may favor the pattern stretch broadside to the wire.



At either height, the wire dipole may cover the entire 40-meter band in terms of the SWR curves referenced to the resonant impedance over average soil. **Fig. 5** provides both curves. An actual installation might wish to lengthen the listed length values for the element to center the curves within the band. Note that on 40 meters, the two listed heights call for about a 5" difference in element length, with further adjustments needed as the soil quality changes. At 25', the feedpoint impedance favors a match with 70- $\Omega$  cable, while at 35', the impedance is a bit higher. In a practical installation at 35', the length of coaxial cable usually needed to

reach the equipment would introduce sufficient loss to reduce the equipment end SWR levels.

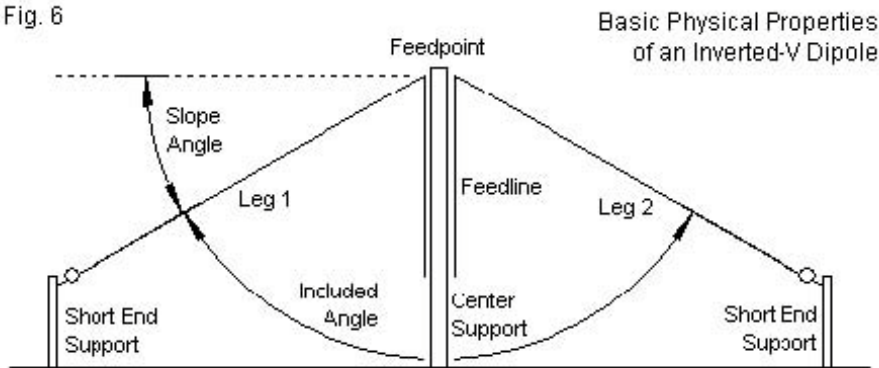


In principle, a NVIS dipole should use the height that yields best performance. However, as a practical matter, most installations may be forced to use other reasonable heights based on available supports and other site factors. The tabular data shows a modest degradation of performance at the alternative heights, but the overall level of performance is close enough to optimal that we can expect good performance from the alternative. The 75-and 40-meter NVIS dipoles provide a standard against which we can measure other basic NVIS antennas.

### The Practical NVIS Inverted-V for 75 and 40 Meters

As we found in earlier notes within this series, the inverted-V center-fed dipole requires a greater center height for maximum performance than a level dipole. Wire-end coupling to ground tends to reduce the effective height of the inverted-V relative to its effective height when placed well above ground for long-distance communications. **Fig. 6** outlines the inverted-V that we shall use: AWG #14 copper wire with a 30° slope from the horizontal (or a 120° included angle). Shallower slope angles will produce performance intermediate between the sample V and the linear dipole. Greater slope angles generally produce weaker zenith performance.

Fig. 6



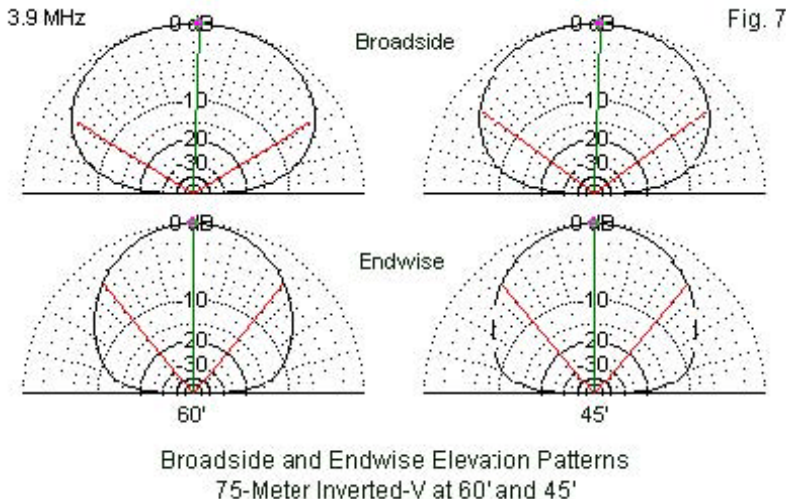
The 75-meter center height options are 60' and 45', while the 40-meter options are 35' and 25'. **Table 2** provides the modeled data

for all of these options over the standard three types of ground quality.

Inverted-Vs		AWG #14 Copper Wire							Table 2	
Band M	Height ft	Length ft	Soil	Zen Gain	BS BW	EW BW	BW Ratio	Feed R	Feed X	
3.9 MHz	75	122.10	Vy Good	6.42	112.2	78.6	1.43	62.09	7.37	
	End ht	29.48	Average	5.50	118.0	77.4	1.52	66.05	-0.19	
	End len	52.87	Vy Poor	4.26	127.2	76.2	1.67	66.96	-10.73	
	45	121.30	Vy Good	5.93	101.8	81.4	1.25	46.76	6.53	
	End ht	14.68	Average	4.59	107.2	80.4	1.33	57.05	-0.35	
	End len	52.52	Vy Poor	3.14	116.4	79.8	1.46	65.95	-13.10	
7.2 MHz	40	35	Vy Good	6.17	117.8	78.8	1.49	67.93	7.55	
	End ht	18.45	Average	5.24	123.8	76.8	1.61	67.41	-0.40	
	End len	28.67	Vy Poor	4.11	131.2	75.6	1.74	65.48	-8.70	
	25	65.76	Vy Good	5.67	104.0	80.8	1.29	50.85	9.87	
	End ht	8.50	Average	4.27	109.6	79.0	1.39	58.66	-0.20	
	End len	28.47	Vy Poor	2.94	118.4	78.8	1.50	63.93	-11.89	
Notes:										
End ht = height above ground in feet of each end of inverted-V										
End len = distance in feet from V center to wire end parallel to ground										
Zen Gain = maximum zenith gain in dBi										
BS BW; EW BW = broadside and endwise beamwidths in degrees										
Feed R; Feed X = feedpoint resistance and reactance in Ohms										

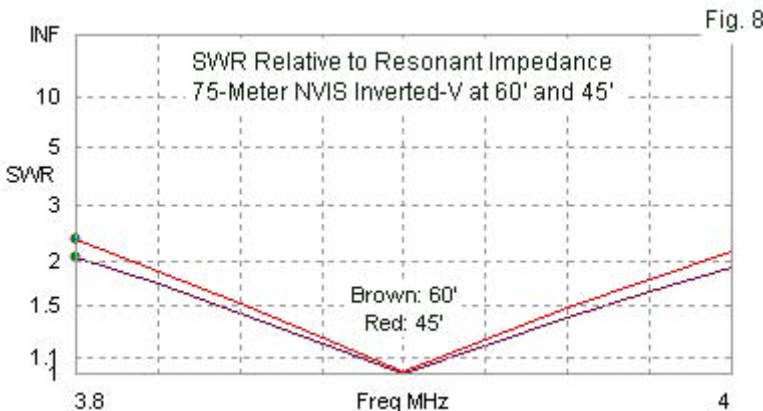
The table shows the total element length, but adds two other figures for each version of the inverted-V. The end height is the height of the wire tip (excluding end ropes and insulators) above ground. The end length is the horizontal distance parallel to the ground from the center of the antenna to the wire end. Double the end length to obtain the total horizontal distance needed for an inverted-V installation. One advantage of the V-configuration for some sites is the reduced linear space needed for the antenna, while the need for a single tall center support and two shorter end supports is often a second attraction.

On 75 meters, the available zenith gain, even at the 60' center height, does not match the gain of a level dipole at optimal height. However, the performance is quite adequate for many situations, and the pattern does show greater circularity relative to a dipole pattern. The V radiates more effectively in the endwise direction than the level dipole, contributing to the reduction in the ovalization. **Fig. 7** shows the broadside and endwise elevation patterns of the V at both center heights. You may wish to compare the shapes of the endwise patterns, especially at low elevation angles, to corresponding 75-meter dipole endwise patterns.



The inverted-V provides adequate SWR coverage of the SSB portion of the 75-meter band, as shown by the SWR curves in **Fig. 8**. The impedance data in the table show the 60' center height to

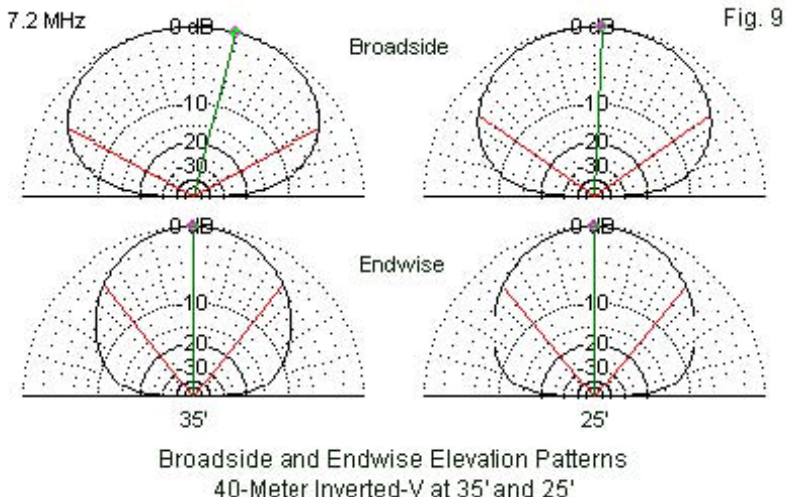
have a stable resistive component that favors a match to  $70\Omega$  cable. However, at 45' above ground, wire ends are sufficiently close to ground to create a wide swing (nearly  $20\Omega$ ) of the feedpoint resistance with changes in ground quality.



Some amateurs attempt to install 75-meter NVIS antennas using center heights below the shorter of our two options. The cost is a continued reduction in zenith gain, which tends to fall off very rapidly as we bring down the center height and tie off the ends very close to the ground.

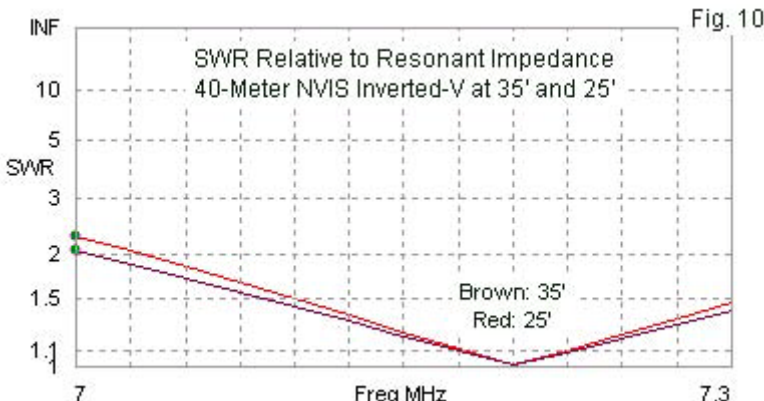
On 40 meters, the two alternative center heights are 35' and 25'. The lower height proved better for the level dipole, but for the inverted-V, the higher center support provides superior zenith gain. As well, the 25' height for the V results in wire ends only about 8.5' above ground, which may fall below the safety level for a fixed

installation. (A temporary field installation may need to use lower heights for wire ends—with suitable safety flagging for personnel—but with consequential further reductions in performance.) **Fig. 9** provides broadside and endwise elevation patterns for the 40-meter options. Unlike the dipole at 35', the V at that center height does not show the splitting of the broadside lobe, although the canted angle of the maximum gain indicator line suggests that the height is approaching the limit prior to splitting. In general, broadside beamwidth angles greater than  $130^\circ$  usually accompany the splitting of the maximum gain angles.



As the SWR curves in **Fig. 10** indicate, a wire V, even at the lower center height, is capable of covering all of 40 meters relative to the resonant impedance (over average ground). One may wish to

lengthen the listed element length to better center the SWR curve within the band. The 35' center height tends to favor 70- $\Omega$  feedlines, while the lower 25' height yields feedpoint impedance values closer to 50  $\Omega$ .



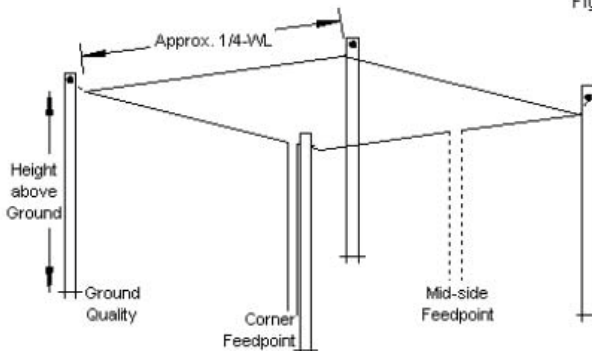
The inverted-V is often mechanically simpler as a NVIS antenna. However, even with an optimal center height, its performance, while adequate, does not match the performance of the standard dipole. The critical factor in inverted-V installations is not to install the antenna at optimal dipole heights, but to select a higher center height to best optimize the effective height of the antenna.

### *The Practical NVIS 1- $\lambda$ Loop for 75 and 40 Meters*

As a level antenna, the 1- $\lambda$  loop shows height properties similar to those of the level dipole. Therefore, we shall look at the 75-meter

version at 50' and at 35'. The 40-meter height options will be 35' and 25'. **Fig. 11** outlines some of the critical aspects of loop installation, including the need for four tall corner supports. (Although the number may seem problematical for a single antenna, it will become less so when we consider multi-band installations.) We may select either a mid-side feedpoint (used in the models) or a corner feedpoint. The latter allows feedline support along the support post with no change in the tabulated data in **Table 3**. The only differences are the physical axes for the broadside and endwise radiation patterns that move from a side-to-side orientation to a corner-to-corner perspective.

Fig. 11

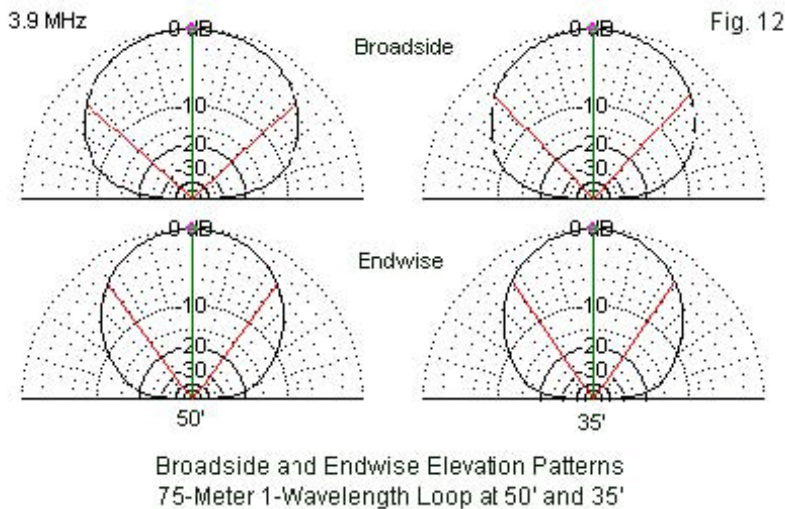


Key Properties of a Square 1-WL Closed NVIS Loop

1-WL Loops		AWG #14 Copper Wire							Table 3	
Band M	Height ft	Circum. ft	Soil	Zen Gain	BS BW	EW BW	BW Ratio	Feed R	Feed X	
3.9 MHz	75	259.04	Vy Good	7.87	89.8	71.6	1.25	136.40	15.72	
			Average	7.03	94.5	71.6	1.32	140.20	0.07	
			Vy Poor	5.86	102.4	72.2	1.42	139.50	-21.50	
	35	257.92	Vy Good	7.87	81.8	67.8	1.21	93.35	14.13	
			Average	6.70	85.3	68.6	1.24	109.00	0.15	
			Vy Poor	5.32	91.8	70.8	1.30	123.00	-24.01	
7.2 MHz	40	142.32	Vy Good	7.16	104.7	78.8	1.33	166.50	11.33	
			Average	6.39	110.1	77.4	1.42	158.00	-0.25	
			Vy Poor	5.41	117.2	76.6	1.53	146.60	-12.05	
	25	141.20	Vy Good	7.73	88.2	70.4	1.25	127.90	18.98	
			Average	6.74	92.6	70.0	1.32	130.60	0.43	
			Vy Poor	5.57	99.1	70.8	1.40	130.40	-20.54	
Notes:	Circum. ft = loop circumference in feet; divide by 4 for side length									
	Zen Gain = maximum zenith gain in dBi									
	BS BW; EW BW = broadside and endwise beamwidths in degrees									
	Feed R; Feed X = feedpoint resistance and reactance in Ohms									

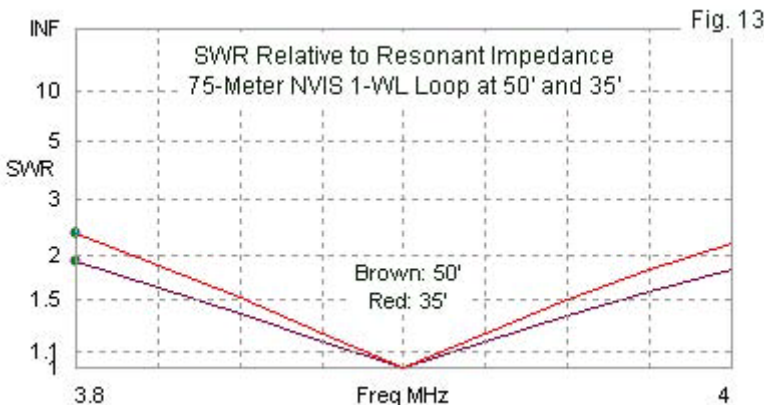
Although 50' is close to optimal over average ground on 75 meters, the best height for very good ground is slightly lower—in the 40' to 45' range. Hence, the zenith gain values for both heights over very good ground are the same. The advantage of a 50' height appears

as we reduce the ground quality, although the decline is slow. In all cases, the zenith gain of the loop is greater than the gain from a dipole at the same height and soil quality. In addition, the patterns for a loop are more circular than those for either a dipole or a V, as indicated by the lower values in the beamwidth-ratio column. The circularity of the loop patterns also appears in the broadside and endwise elevation patterns for both heights in **Fig. 12**. (It is possible to further circularize the NVIS pattern by shortening the fed wire and its opposite wire, and by lengthening the “side” wires—and to obtain a very small gain increase as well. However, this refinement is rarely practical in an amateur installation.)



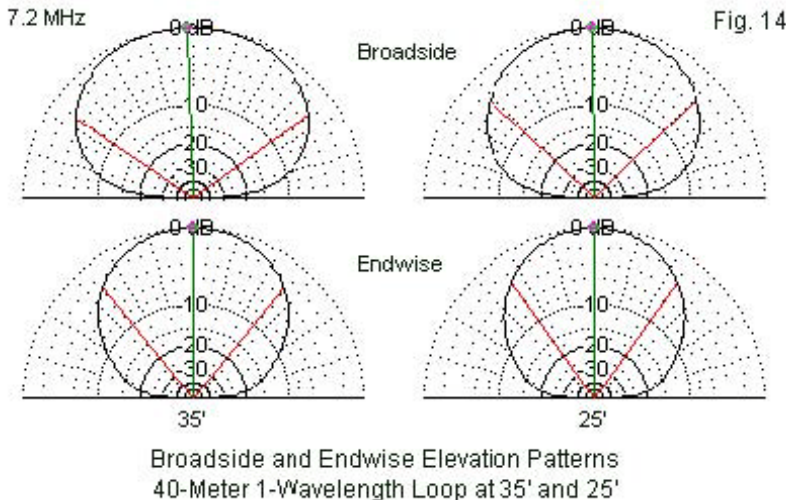
The impedance data shows wider swings of reactance as we change soil quality than we find with dipoles, but the effect of the

swings on the SWR relative to a resonant impedance value is proportional to the resistive component value. The 75-meter SWR curves in **Fig. 13** are very similar to those for the dipole, despite the higher loop impedance. For a match to a  $50\Omega$  coaxial cable, a  $\frac{1}{4}\lambda$  series section of  $70-75\Omega$  cable is usually satisfactory for impedance values up to about  $130\Omega$ . For higher feedpoint impedance values,  $93\Omega$  cable may prove more effective for the matching section.

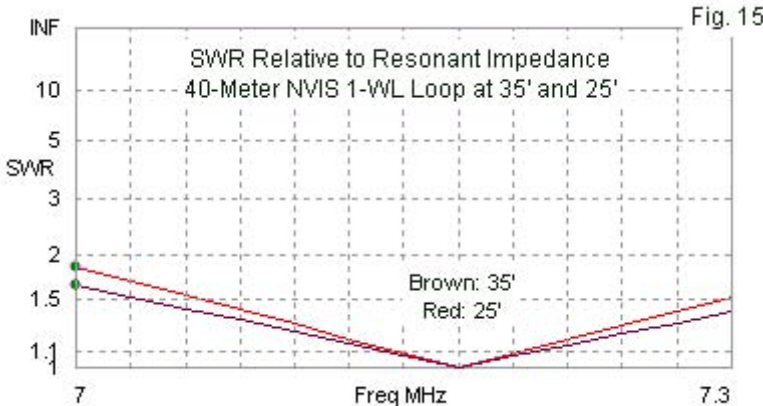


On 40 meters, the greater loop height shows its gain disadvantage over every soil type. Like the dipole, the loop at 25' is closer to an optimal height for NVIS operation and shares many of the properties of the 75-meter loop at 50' above ground. The broadside and endwise elevation patterns for 40 meters appear in **Fig. 14** to confirm the near circularity of the loop patterns when the antenna is

at its best height. As we raise the loop above its best height, the pattern becomes more oval.



The 35' loop, being above optimal height, shows higher feedpoint impedances that suggest the use of a 93- $\Omega$  matching section. At 25', the impedance values are on the borderline that allows testing of each matching section impedance value for the widest 50- $\Omega$  SWR curve. The curves in **Fig. 15** are relative to the resonant feedpoint impedance over average ground for each antenna height. They confirm the ability of the loop easily to cover the entire 40-meter band.

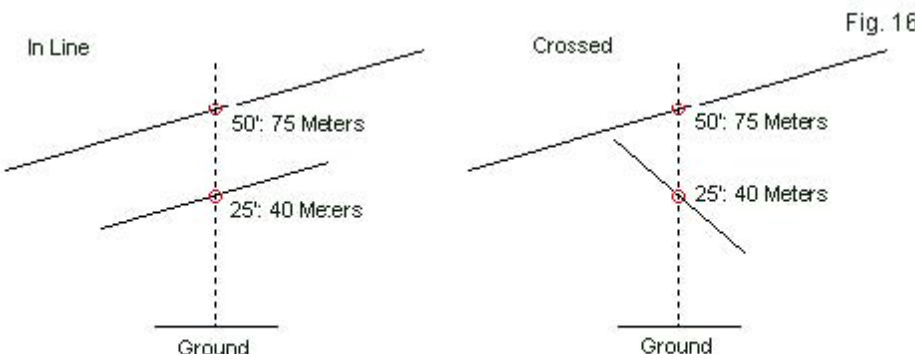


Despite the requirement for 4 tall corner supports, the 1- $\lambda$  loop is a highly usable antenna. The dimensional values show the circumference of the wires, with each side having  $\frac{1}{4}$  the value shown. The loop fits a square location that may not fully support a dipole's  $\frac{1}{2}\lambda$  total length. Moreover, the zenith gain level is somewhat higher for any height above any ground. A corner feedpoint permits full cable support, reducing strain on the element-to-cable junction. For some missions, the greater circularity of the patterns may also be an advantage.

### *Practical Multi-Band Antennas: Multiple Independent Dipoles*

So far, we have looked in detail at monoband antenna installations. There are a number of highly practical ways to create antenna systems for both 75 and 40 meters besides widely separating independent monoband antennas. Our first candidate is simply to

place two independent dipoles, each at its own best height, close to each other. **Fig. 16** outlines two options for us to consider. In each case, we shall place the 75-meter dipole at 50' above ground, with the 40-meter dipoles at 25'.



In-Line and Crossed Configurations for 75- and 40-Meter Dipoles

The in-line version of the dual independent antennas requires the fewest support structures. We only need to add two ropes to the 75-meter dipole support posts to hold up the 40-meter dipole element. In contrast, the crossed version demands 4 supports posts, a pair for each band.

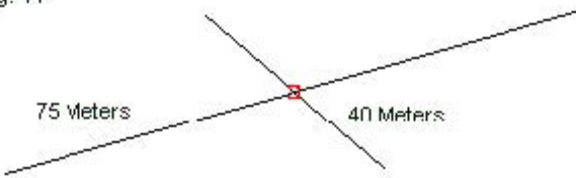
Paired Independent Dipoles				AWG #14 Copper Wire					Table 4	
Band M	Height ft	Length ft	Soil	Zen Gain	BS BW	EW BW	BW Ratio	Feed R	Feed X	
<b>In Line</b>										
75	50	121.20	Average	6.38	118.0	67.8	1.74	74.35	-0.61	
40	25	65.16	Average	5.70	117.0	65.8	1.78	65.85	0.65	
<b>Crossed</b>										
75	50	121.20	Average	6.40	117.8	67.8	1.74	73.76	0.14	
40	25	65.56	Average	6.07	116.4	66.4	1.75	69.16	0.08	
Notes:	Zen Gain = maximum zenith gain in dBi									
	BS BW; EW BW = broadside and endwise beamwidths in degrees									
	Feed R; Feed X = feedpoint resistance and reactance in Ohms									
	See Table 1 for approximate values over very good and very poor soil for crossed dipoles.									

**Table 4** provides the performance data on models of the two systems. In both cases, the 75-meter dipole performance is unaffected by the orientation of the 40-meter antenna. If we cross the two antennas, each performs almost identically to independent antennas over the same average ground at the same height. You may confirm the values by comparing the present table with the appropriate entries in **Table 1**. However, the lower band dipole does have some significant effects upon the upper band element when both are aligned with each other. The required length for resonance changes, and the zenith gain decreases. Whether the gain difference between the two systems is enough to offset the differential in mechanical requirements is a user judgment, taking into account site, resource, and mission factors. In either case, the system requires two feedlines running to either a switch at the equipment room or to a remote switch closer to the antennas.

## Practical Multi-Band Antennas: Crossed Dipoles and Vs with a Common Feedpoint

We may simplify the feeding system by using a dipole for each band, but at 90° to each other to minimize interactions. By using a common feedpoint, each dipole will resonate on its own band with minimal current on the element for the other band. **Fig. 17** shows the general outline of a pair of dipoles, although the system will also work with inverted-V elements. Like crossed independent dipoles, the common-feedpoint system requires at least 4 full-length support posts, one at the end of each element wire. As well, when we cross dipoles, the wider broadside beamwidth also changes by 90° as we switch bands. This aspect of the system may or may not be meaningful to a given installation or mission. In many cases, the site dimensions may override the desire to direct the broadside beam.

Fig. 17



Crossed 75- and 40-Meter Dipoles: Common Feedpoint

**Table 5** provides modeled data for the crossed dipoles at two heights over average soil. (Past tables will allow close estimates of performance over other soil types.) For the moment, we need only

examine the upper portion of the table for dipoles at 35' and at 25'. We find a disparity of gain at both heights between the values for 75 meters and for 40 meters. In addition, we find that the interactions between dipoles are minimal in terms of performance, but they do require adjustments to dipole lengths relative to the required lengths of independent dipoles at each height.

Crossed Dipoles with a Common Feedpoint					AWG #14 Copper Wire				Table 5	
Band M	Height ft	Length ft	Soil	Zen Gain	BS BW	EW BW	BW Ratio	Feed R	Feed X	
75	35	121.40	Average	6.08	106.6	65.2	1.63	58.21	0.21	
40	35	65.84	Average	5.66	131.4	74.4	1.77	82.60	-0.40	
75	25	121.60	Average	4.94	101.6	65.4	1.55	49.95	-0.56	
40	25	65.52	Average	6.09	115.8	66.8	1.73	68.42	-0.45	

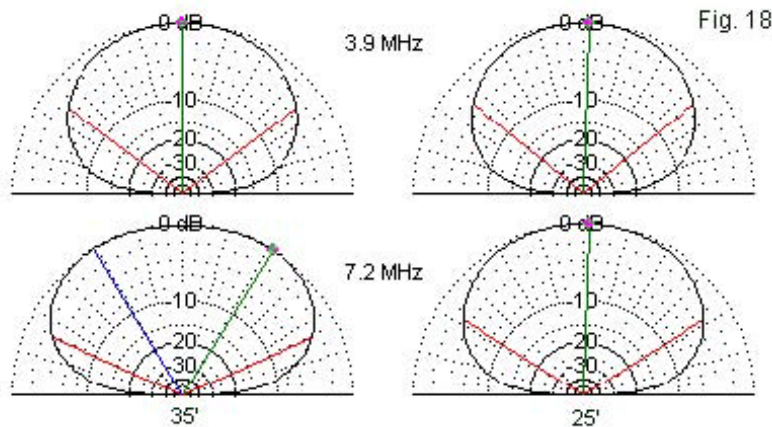
Crossed Inverted-Vs with a Common Feedpoint					AWG #14 Copper Wire					
Band M	Height ft	Length ft	Soil	Zen Gain	BS BW	EW BW	BW Ratio	Feed R	Feed X	
75	50	121.90	Average	5.06	110.2	87.6	1.26	60.38	0.11	
Wire End Height: 19.53'					Wire End Distance from Center: 52.78'					
40	50	66.94	Average	3.80	140.7	92.9	1.51	73.05	-0.05	
Wire End Height: 33.17'					Wire End Distance from Center: 28.99'					
75	35	120.10	Average	2.72	102.2	90.0	1.14	55.99	-0.17	
Wire End Height: 4.98'					Wire End Distance from Center: 52.00'					
40	35	66.20	Average	5.24	123.3	77.0	1.60	66.50	-0.45	
Wire End Height: 18.35'					Wire End Distance from Center: 28.67'					

Notes:

- Zen Gain = maximum zenith gain in dBi
- BS BW; EW BW = broadside and endwise beamwidths in degrees
- Feed R; Feed X = feedpoint resistance and reactance in Ohms
- See Tables 1 and 2 for approximate values over very good and very poor soil for crossed dipoles.

The lower height is close to ideal for 40 meters, but very low for 75 meters. 35' is somewhat low for 75-meters, but already high for 40 meter NVIS dipoles. Although 50' would provide better 75-meter performance, 40-meter zenith gain would drop, because the broadside pattern would be split into two lobes with a very noticeable zenith null between them. **Fig. 18** provides broadside patterns for both bands at both array heights. At the upper height

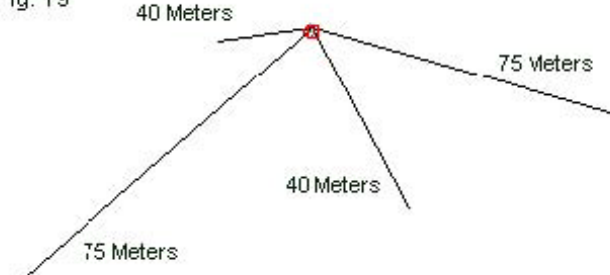
(35'), the 40-meter pattern already shows a split maximum-gain line pair with a tiny (operationally insignificant) gain decrease at the zenith angle. Further increases in height will rapidly increase the zenith null on 40 meters. The final selection of installation height for crossed dipoles will necessarily involve a compromise between the requirements of the two bands.



Broadside Elevation Patterns at 35' and 25'  
Crossed 75- and 40-Meter Dipoles: Common Feedpoint

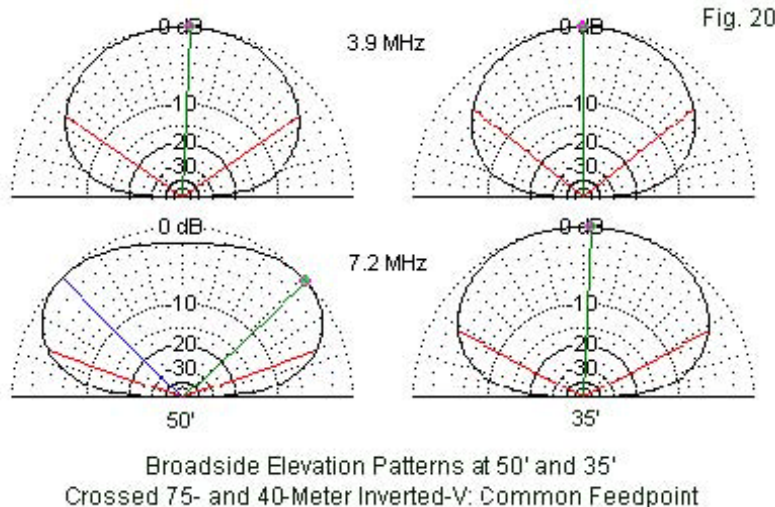
A mechanically attractive alternative to crossing level dipoles is to cross inverted-V elements. As suggested by the outline in **Fig. 19**, the system requires only a single tall center support, with shorter posts for the wire ends. For our sample, we shall use a 50' center support and a 35' center support to compare performance values on both bands.

Fig. 19



Crossed 75- and 40-Meter Inverted-V Dipoles  
with a Common Feedpoint

Crossed inverted-Vs have performance disadvantages relative to crossed dipoles. Despite using elevated center heights for both the higher and the lower arrays, the overall gain values are less than the values for the dipoles. In addition, we find a wider disparity between the zenith gain values for each band. Even if we find a “perfect” center height that yields nearly equal zenith gain values on each band, those values will fall well below the gain values that we can obtain from crossed dipoles.



Finding the ideal height for crossed inverted-Vs will involve more than just gain equalization. As shown in **Fig. 20**, the 40-meter broadside elevation pattern shows serious lobe splitting and a very wide broadside beamwidth. We may also examine the dimensions for the Vs in **Table 5** and uncover an additional installation temptation. At either height, the  $30^\circ$  sloping Vs place the 40-meter wire ends much higher above ground than required by the 75-meter V. The temptation would be to use a greater slope angle (that is, a smaller included angle) for the 40-meter V. The smaller angle also promises to lower the 40-meter impedance to a value that more closely matches the 75-meter value. However, as we decrease the included angle of an inverted-V (or any half-wavelength V-element), the gain decreases along the V-axis. The already low zenith gain of the  $30^\circ$  V element would drop to even less desirable levels.

The sequence of crossed-element arrays has shown a continuously growing number of performance compromises. With crossed independent dipoles, each at a nearly optimal height, we obtained full performance from each, although with wider broadside beamwidths 90° apart. When we simplified the feed system by using a common feedpoint for both dipoles, we encountered reductions in the maximum available zenith gain due to the need to find a common height for both antennas. Converting the linear dipoles to an inverted-V configuration further reduced available zenith gain. From the starting point to the final inverted-V array, we lost as much as 3 dB, depending upon the final selection of antenna height and the slope angle of the inverted-V elements. Such losses may be mandated by temporary field installations, but a fixed station antenna system should carefully weigh the performance penalties of simplified mechanical construction if the station mission includes more than casual operation.

### *Practical Multi-Band Antennas: Nested 1- $\lambda$ Loops*

Multi-band dipoles and inverted-Vs require four to five support posts. When we compared monoband dipoles to 1- $\lambda$  loops, we noted that the somewhat higher zenith gain of loops often fell prey to the desire for the simpler mechanical requirements of the dipole: 2 posts instead of

4. However, the mechanical advantage of dipoles and inverted-Vs becomes moot when we consider multi-band loop installations. We may nest 1- $\lambda$  loops for 75 and 40 meters within a single 4-post support system. Moreover, we may set each loop at a favorable

height. For our sample, outlined in **Fig. 21**, we can set the 40-meter loop at 25' above average ground, with the 75-meter loop 10' higher to obtain matched gain levels. One advantage of the nested loops is that we may also orient the broadside patterns in the same direction.

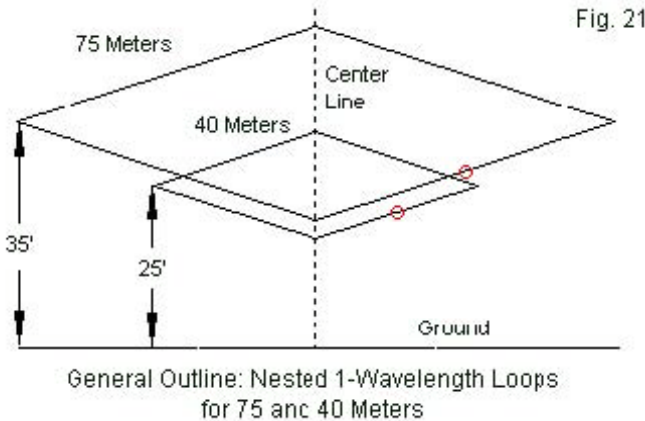
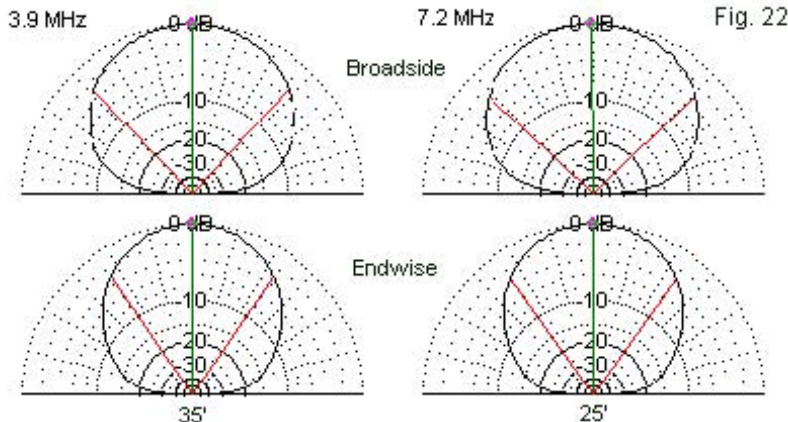


**Table 6** provides numerical data for the pair of loops. Not only do both loops share a nearly common zenith gain value, but as well, the beamwidth ratio is almost the same on both bands. Despite nesting, the performance data for the individual loops is nearly the same as for independent loops, such as those shown in **Table 3**. However, the proximity of the loops yields some revision of the loop dimensions relative to monoband versions. Since the 75-meter loop is nearly  $2\lambda$  in circumference on 40 meters, it shows a low but not wholly negligible level of activity when we drive the 40-meter loop.

Nested 75-40-Meter 1-WL Loops				AWG #14 Copper Wire			Feedpoint		Match	Table 6	
Band M	Height ft	Circum. ft	Soil	Zen Gain	BS BW	EW BW	BW Ratio	Feed R	Feed X	Feed R	Feed X
75	35	257.92	Average	6.71	85.2	68.6	1.24	105.50	1.09	46.52	-0.55
40	25	140.00	Average	6.66	92.4	70.0	1.32	135.30	-0.69	63.42	0.19

Notes: Circum. ft = loop circumference in feet; divide by 4 for side length  
BS BW; EW BW = broadside and endwise beamwidths in degrees  
Feed R; Feed X = feedpoint resistance and reactance in Ohms  
Match = 1/4-WL series matching section: 75-meter section = 70 Ohms; 40-meter section = 93 Ohms

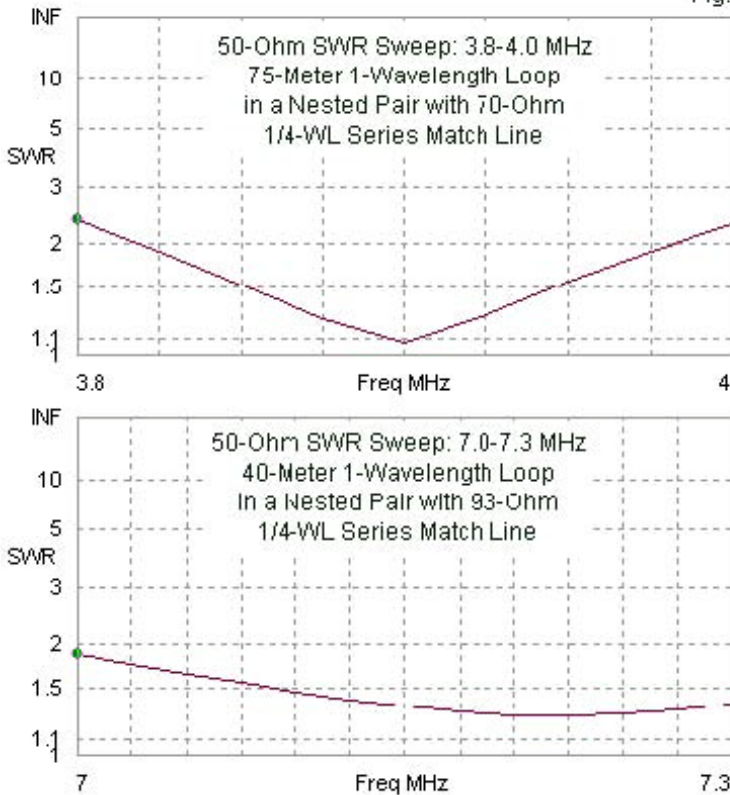


Broadside and Elevation Patterns  
Nested 1-Wavelength Loops for 75 and 40 Meters

The relationship between the two operating frequencies militates against trying to feed both loops from a common feedpoint. The two independent feedpoints have significantly different impedance values, and both require  $\frac{1}{4}\lambda$  series matching sections. The columns showing the alternative feedpoint impedance values employ a 70- $\Omega$  matching section on 75 meters and a 93- $\Omega$  section on 40 meters. **Fig. 23** shows the 50- $\Omega$  SWR curves on both bands with the prescribed matching sections. Of course, in an actual

installation, the builder would measure the resonant feedpoint impedance on each band before deciding upon the proper matching-section characteristic impedance.

Fig. 23



For multi-band service,  $1\text{-}\lambda$  loops become more attractive since they do not require more support structures than we would need for crossed dipoles or inverted-Vs. Their additional gain and the ease of matching them to a  $50\text{-}\Omega$  main feedline suggest that they deserve serious consideration, especially for installation sites that may strain to handle a full half-wavelength of linear space. Nested loops require a little over  $\frac{1}{4}\text{-}\lambda$  per side on the lowest band in the loop nest.

### *Practical Multi-Band Antennas: A Center-Fed Doublet*

Those who can manage only two supports may wish to consider a largely overlooked option for a NVIS antenna: a center-fed doublet.

**Fig. 24** shows the outline of one possibility. Although it looks like a common dipole, it is not. Rather, it will function as a center-fed element that ranges from about  $0.4\text{-}\lambda$  on 75 meters to about  $0.75\text{-}\lambda$  on 40-meters. In addition, we may operate the doublet on 60 meters, where it is just over  $0.55\text{-}\lambda$  long. For our sample, we shall use a height of 35', which is higher than ideal for a  $\frac{1}{2}\text{-}\lambda$  40-meter dipole, but nearly ideal for the longer length of the doublet.

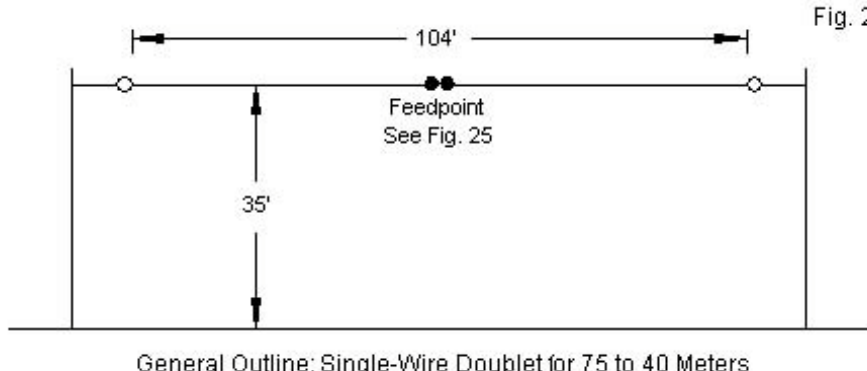


Fig. 24

General Outline: Single-Wire Doublet for 75 to 40 Meters

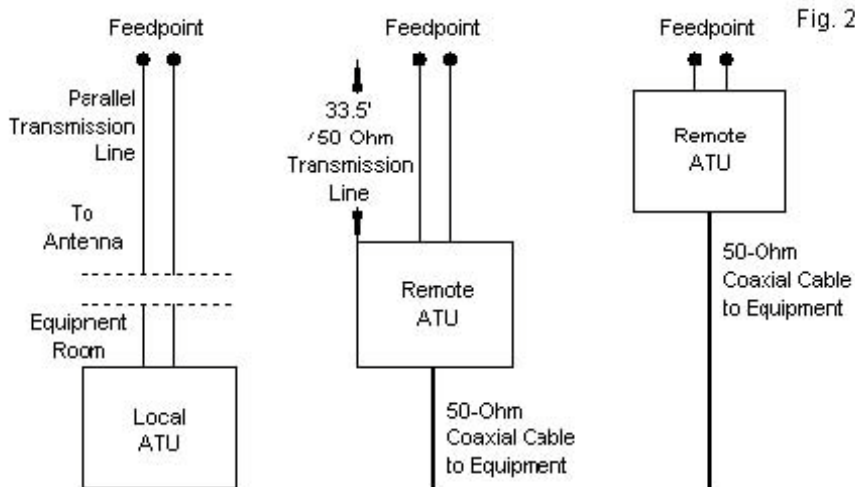
The length of the doublet resembles the length of a G5RV antenna/feed system. The resemblance is no accident, but has little to do with the reasoning behind the original system. It is possible to use a doublet that is a full half-wavelength long at the lowest operating frequency. However, as we nearly double that frequency (from 75 meters to 40 meters), the feedpoint impedance increases to values of resistance and reactance that are both over  $2000\ \Omega$ . To restrict the impedance excursions of the antenna, we cut the doublet short for 75 meters, but still within a reasonable impedance range for most antenna tuners (ATUs). As a consequence, we obtain impedance values on 40 meters that are also more amenable to normal ATU tuning ranges. The feedpoint impedance values in **Table 7** for each band over all three soil qualities give a good feel for the values that require matching.

104' Center-Fed Doublet				AWG #14 Copper Wire			Feedpoint		w/Line	Table 7	
Band M	Height ft	Length ft	Soil	Zen Gain	BS BW	EW BW	BW Ratio	Feed R	Feed X	Feed R	Feed X
75	35	104	Vy Good	7.16	101.5	66.2	1.53	31.60	-250.30	29.01	199.80
			Average	5.90	106.6	67.0	1.59	37.77	-253.90	34.20	195.80
			Vy Poor	4.40	115.8	68.8	1.68	44.04	-260.20	39.00	189.50
60			Vy Good	7.40	111.2	64.4	1.73	119.70	338.20	477.50	-946.60
			Average	6.43	117.2	64.2	1.83	123.10	324.00	537.10	-959.80
			Vy Poor	5.15	126.0	64.4	1.96	124.40	307.60	610.00	-981.50
40			Vy Good	7.14	127.2	61.0	2.09	682.60	1371.00	55.76	-53.43
			Average	6.34	131.6	60.2	2.19	638.90	1347.00	54.92	-57.52
			Vy Poor	5.30	137.2	59.8	2.29	590.60	1324.00	53.57	-62.07
Notes:	Zen Gain = maximum zenith gain in dBi BS BW; EW BW = broadside and endwise beamwidths in degrees Feed R; Feed X = feedpoint resistance and reactance in Ohms w/Line = at source end of 33.5' or 450-Ohm, VF 0.9 parallel transmission line										

Using a doublet requires an ATU somewhere along the line between the antenna feedpoint and the station equipment. As shown in **Fig. 25**, we may select among three main positions for the ATU. On the left is perhaps the most common system for feeding a doublet: the use of parallel transmission line (600- $\Omega$  ladder line or 450- $\Omega$  window line) from the antenna to the equipment room with a balanced ATU located indoors. A manual tuner with a record of settings for each band usually provides adequate speed when switching bands except where automatic link establishment (ALE) procedures may be in use.

The system shown at the center of **Fig. 25** uses a length of parallel feedline to effect an initial impedance transformation to reduce the impedance range required of an ATU. **Table 7** adds two columns to record the modeled impedance values that result from the insertion of the line. Although the range for 75 and 40 meters is small, the values are not direct matches for a standard coaxial cable. In addition, if one adds 60 meters to the set of operating bands, then the value range does not vary differently from the range of values at the feedpoint. The high impedance values simply occur at different

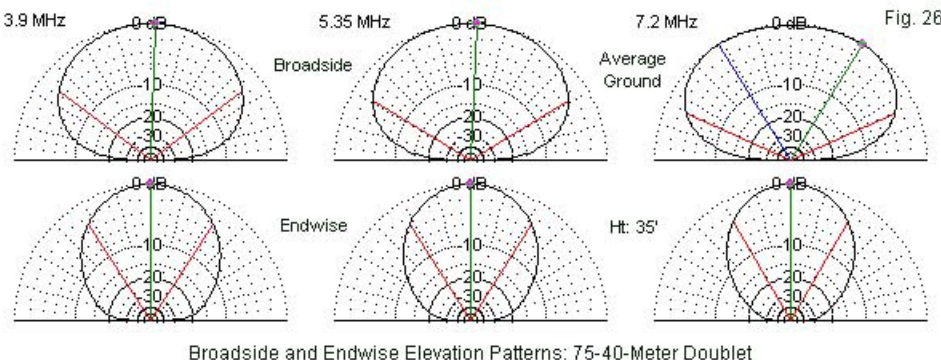
bands. With the added line, system requires a weatherproof remote tuner located below the feedpoint. The weight of such a unit would likely require a third support for the antenna. Nevertheless, the remote tuner, if equipped with memories, would permit rapid band switching.



Alternative Methods of Feeding the 75-40-Meter Doublet

We may also install the remote tuner directly at the antenna feedpoint, again with weatherproofing and a suitable support for the weight. Remote ATUs currently available have different matching ranges, running from quite small to very wide. Therefore, selection of the ATU for either remote system is a major installation decision.

A doublet at about 35' above ground provides relatively even band-to-band performance as a consequence of the increasing length of the element as we raise the operating frequency. The zenith gain numbers for comparable soil qualities confirm the near uniformity of performance. The broadside and endwise elevation patterns in **Fig. 26** confirm the impression left by the tabular data.



As we increase the length of a center-fed wire element (or raise the operating frequency, which amounts to the same thing), the zenith gain rises and the beamwidth narrows. However, with a fixed height above ground, increasing the operating frequency also increases the height in wavelengths above ground, which results in a wider beamwidth broadside to the antenna element with a lower zenith gain value. By judiciously selecting a physical height for the antenna, we may balance the conflicting trends—at least to a level that yields adequate performance over a wide range of frequencies. In general, the doublet at 35' above ground provides performance

that is similar to the performance of 3 independent half-wavelength dipoles, each near its optimum height for maximum zenith gain. The one deficiency in performance, relative to the independent monoband dipoles, is that the endwise beamwidth continues to diminish with rising operating frequencies.

Although the preceding set of notes has adequate information for estimating the benefits of a full screen at ground level for the major type of antennas that we have been reviewing, we have no data directly applicable to the doublet. Therefore, I created a near-ground screen below the doublet, as shown in **Fig. 27**. The screen is  $1-\lambda$  per side at 75 meters, making it larger than necessary for higher frequencies.

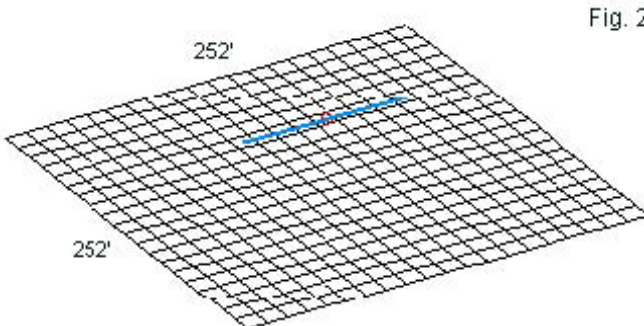


Fig. 27

104 Center-Fed Doublet with Near-Ground Screen

**Table 8** provides numerical data that parallel the values shown in **Table 7**, without the screen in place. (The new table omits the extra impedance columns.) Pattern shapes do not significantly change,

and the impedances values are not very far apart in the two tables, especially considering the application of an ATU to the feed system. As expected, the key benefit is to the zenith gain over lesser quality soils. Note that the gain values for 40 meters do not keep pace with those for the lower bands. The screen is simply oversized for that band.

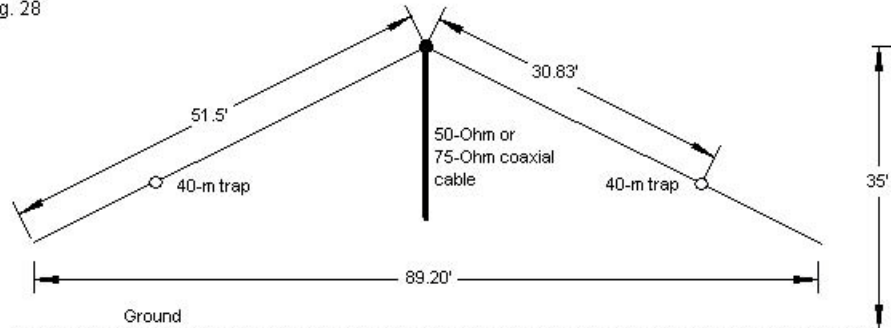
104' Center-Fed Doublet with 1-WLx1-WL Screen					AWG #14 Copper Wire			Feedpoint	Table 8	
Band M	Height ft	Length ft	Soil	Zen Gain	BS BW	EW BW	BW Ratio	Feed R	Feed X	
75	35	104	Vy Good	7.73	99.0	65.6	1.51	29.36	-248.80	
			Average	7.66	97.2	65.0	1.50	31.75	-247.90	
			Vy Poor	7.83	93.2	63.6	1.47	33.31	-246.90	
60			Vy Good	7.81	108.2	63.8	1.70	118.40	343.40	
			Average	7.67	108.0	63.5	1.70	123.90	340.30	
			Vy Poor	7.82	104.8	62.1	1.69	128.50	339.30	
40			Vy Good	7.38	125.2	61.6	2.03	699.00	1380.00	
			Average	6.92	126.8	63.6	1.99	690.40	1355.00	
			Vy Poor	6.58	127.0	66.0	1.92	691.60	1332.00	
Notes:	Screen is 1-WL by 1-WL at 39 MHz (252' by 252')									
	Zen Gain = maximum zenith gain in dBi									
	BS BW; EW BW = broadside and endwise beamwidths in degrees									
	Feed R; Feed X = feedpoint resistance and reactance in Ohms									

Additional engineering investigations might turn up a better compromise set of dimensions for the ground screen. Its use with the doublet will depend upon many factors, and so the information is not inherently a recommendation. Nevertheless, the basic doublet with any of the ATU systems shown is worthy of consideration, especially if land and support posts materials are limited.

## Practical Multi-Band Antennas: Trap Dipoles and Inverted-Vs

Trap dipoles and inverted-Vs represent an alternative means of providing multi-band performance with only two end supports—and, of course, a center support for the V-configuration. **Fig. 28** provides a general outline of a trap inverted-V. The trap dipole has the same dimensions using a level wire element.

Fig. 28



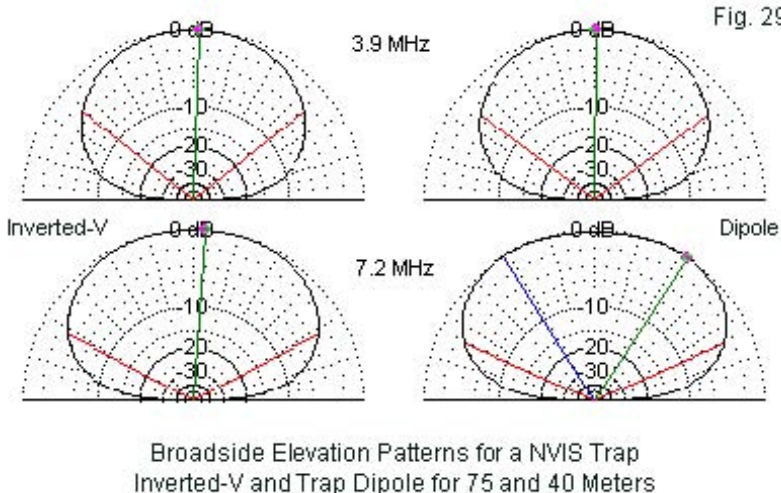
General Structural Outline: Trap NVIS Inverted-V for 75 and 40 Meters

Traps are parallel-tuned L-C circuits that we tune slightly lower in frequency than the lowest frequency used on the higher of the two bands. The traps used in the model require 60-pF capacitors and 8.7- $\mu$ H inductors. Most conventionally wound coils have Q-values of about 200 or so, although a careful builder might achieve a higher value. As a compromise between the bands, both the inverted-V and the dipole versions of the 75-40-meter antenna have peak heights of 35', a level that is high for 40 meters and low for 75 meters, if we use the ideal heights for dipoles as our reference

standard. In practice, the inverted-V peak height should be higher—perhaps 45' or so—but most amateurs who limit themselves to only two or three supports are unlikely to exceed the 35' height in the sample.

Trap Dipole and Inverted V									Table 9
Inverted V			AWG #14 Copper Wire						
Band M	Height ft	Length ft	Soil	Zen Gain	BS BW	EW BW	BW Ratio	Feed R	Feed X
75	35	103.00	Average	2.73	102.5	86.2	1.19	49.21	-14.35
40	35		Average	4.84	123.3	76.8	1.61	75.65	-28.11
Dipole									
75	35	103.00	Average	5.65	106.6	66.6	1.60	51.28	-25.10
40	35		Average	5.46	131.6	71.0	1.85	93.68	-20.26
Notes:	Inverted-V wire end is 9.25' above ground and 44.6' from element center.								
	Zen Gain = maximum zenith gain in dBi								
	BS BW; EW BW = broadside and endwise beamwidths in degrees								
	Feed R; Feed X = feedpoint resistance and reactance in Ohms								

The modeled data appear in **Table 9**. The zenith gain for the inverted-V is low by virtue of the V-configuration and the low height. The dipole model over average ground has more equal gain values, but the 75-meter performance shows a deficit relative to individual dipoles over the same ground. The 40-meter gain value for the portion of the antenna inside the traps is comparable to the value of the 40-meter dipole at the same height for crossed dipoles using a common feedpoint.



The use of traps imposes no revisions on the radiation patterns produced by the antenna. In **Fig. 29**, we find perfectly normal broadside elevation patterns for both versions of the antennas. The dipole version on 40 meters shows the split maximum-gain lines typical of dipoles above their optimum NVIS height.

One advantage of the trap multi-band NVIS antenna is the reduced linear space it requires. The level dipole version requires only 103' plus a small space required for end insulators and support ropes to the end posts. The inverted-V, with a 30° slope, needs less than 90' plus end-attachment space.

On 75-meters, the trap antenna exhibits impedance values that are compatible with 50- $\Omega$  coax. However, the 40-meter impedance

values are higher. Prior to building a trap antenna for NVIS work, one might experiment with trap components, including the trap resonant frequency, to arrive at a better match for the usual coaxial cable feedline. The dipole version of the antenna has a total length similar to the length of the doublet. Both antennas have complexities, in one case the traps, in the other the need for an ATU.

### *Conclusion*

Our survey of practical NVIS antennas has included many basic types and variations, but it is by no means exhaustive. Beginning with basic dipoles, inverted-Vs, and  $1-\lambda$  loops for monoband service, we progressed to various multi-band arrangements. Our goal has been to lay out the general structures of practical NVIS antennas and to compare performance level both at various normal amateur antenna heights and also among the antennas included. The overall goal of this set of notes has been to provide data that may be useful in planning and implementing a fixed-station NVIS antenna system for the two most commonly used amateur bands.

Unlike field antennas, which must employ simplified construction methods for rapid deployment, the fixed-station NVIS antenna system deserves careful attention to detail. Some NVIS stations engage almost solely in casual operation in order to sample the propagation mode. Such stations can take shortcuts with construction and live with the modest outcome. Many stations have more significant missions that include emergency communications work. Unfortunately, not all of them have the resources to

implement optimal antenna systems. Of the systems that we have surveyed, one of the best—in terms of pattern circularity and zenith gain—is a set of nested  $1\text{-}\lambda$  loops supplemented by a full ground screen for soil qualities less than very good. In amateur and local community terms, such a system is a relatively expensive proposition. As well, the antenna site often dictates antennas with different shapes and heights. Nevertheless, a fixed NVIS station with more than a casual mission would do well to engineer the best antenna system possible for the site and the operating goals. In many instances, the fixed station gain and radiation pattern properties must compensate for deficiencies in the field stations with which communications are essential.

For the fixed NVIS station with an important mission, casual design is not good enough, simply because we can do better. The notes in this collection provide some background data that I hope will contribute toward better NVIS antennas.

## Chapter 68: Fixed 3-Band NVIS Antennas

In the past, most amateur NVIS activity occurred on 75 and 40 meters. Recently, amateurs have begun expanding their coverage to include 60 meters. That has brought requests and suggestions for NVIS antennas that cover all three bands—without resorting to lossy terminated antenna configurations. An added requirement often cited is the need to switch bands rapidly without having to readjust an antenna tuner. Although it is possible to set up a single wire with a parallel feedline to a tuner and by careful selection of both the antenna height and length to achieve adequate pattern from 75 through 40 meters, this last requirement effectively precludes this option without the use of very fast automatic tuners with memories to eliminate tuner searching for settings while changing bands. Let's omit this option from our exercise.

The goal, then, is to develop wire antenna options for 3-band operation in the NVIS mode so that we may ideally switch bands without attention to the antenna. (We shall add a final option that requires only a single antenna switch.) Next, let's face reality. The ideal height for a linear or level antenna for maximum NVIS of upward gain falls in the  $0.15\lambda$  to  $0.22\lambda$  range. The upper end of the range places an 80/75-meteer antenna at about 60'. Higher antennas—up to  $0.25\lambda$  above ground—will work well for NVIS, but are physically prohibitive for most amateur installations. The upper limit of the NVIS height range also increases the radiation at lower elevation angles, a fact that favors an antenna that must do double duty by providing both NVIS and medium-range communications

duty. However, for pure NVIS work, such antennas tend only to increase atmospheric noise levels while receiving.

Therefore, let's restrict, for our exercise alone, the maximum height of our NVIS antennas to 35'. Some of our examples will also use a 25' height. As the data in **Table 1** show, these heights are very low on 75 meters, but approach optimal NVIS heights on 60 and may even exceed them on 40 meters. The main reason for using heights of 35' and 25' is that most amateur installations cannot usually exceed these heights without considerable difficulties.

Table 1. Heights of antennas in these notes in feet and wavelengths

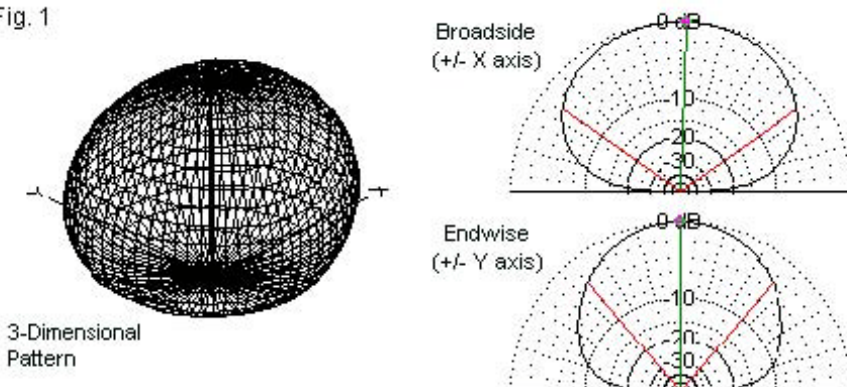
Height	Band	75 Meters	60 Meters	40 Meters
		Height in Wavelengths		
35'		0.14	0.19	0.25
25'		0.10	0.14	0.18

With very low antenna heights come a few very important cautions. The antennas in these notes will use either AWG #12 (0.0808" diameter) or AWG #14 (0.0641" diameter) copper wire. Dimensions will be in feet but may show up to 2 decimal places. These decimals result from the antenna modeling software used to generate the models. In fact, all dimensions are only starting points. Any replication of the antenna designs shown will require considerable field adjustment and dimensions may depart by a noticeable amount from the listed dimensions.

There are two major reasons for the potential variance between the model and reality. Antennas at very low heights vary their impedance values and their resonant lengths with only small changes in height. In addition, at very low heights, the resonant length and impedance of a basic antenna types vary with the quality of ground beneath the antenna. All of the models use average ground with a conductivity of 0.005 S/m and a permittivity (relative dielectric constant) of 13. Your ground quality may differ considerably from these numbers, ranging very likely from very good (0.0303 S/m, 20) down to very poor (0.001 S/m, 5). Ideally, you should plan your antenna by remodeling the samples in these notes for the most precise height values that you can obtain and for the best estimate of ground quality. Even so, expect significant field adjustment when you assemble the antenna.

Ideally, a perfect NVIS antenna in the abstract would have a circular azimuth pattern at any elevation angle with peak gain in the zenith or straight upward direction. Real antennas only approximate this condition. **Fig. 1** shows the 3-dimensional pattern of an inverted V. Beside the obviously imperfect pattern are two 2-dimensional elevation plots that we shall use to characterize the radiation patterns of the antennas we discuss. Broadside to the inverted V (and to all of the antennas in these notes) we find a pattern with a rather broad 3-dB beamwidth (as indicated by the red lines). Off the ends of the antenna, the pattern tends to have a somewhat narrower beamwidth. We shall use the dual elevation pattern system to characterize all of the antennas under discussion. High-angle azimuth patterns have systematic conical section errors.

Fig. 1



General Properties of a NVIS Radiation Pattern

From the two elevation patterns, you may infer the general departure from the ideal circular pattern. The inference may prove useful in orienting an actual antenna to provide a desired degree of coverage. As you continue to raise the height of a NVIS antenna, the broadside pattern tends to increase its beamwidth until the top flattens and the radiation pattern evolves into a pair of lobes, one in each broadside direction.

The reason that we may usefully spend some time looking at basic antennas for 3-band operation has to do with the properties of NVIS propagation. At night, the ionosphere lacks the absorbing D-layer and so 75 meters (and 160 meters) become very useful for refracting (reflecting) radiation from the nighttime F-layer, which may not be strong enough for usable return signals on 40 meters. In the daytime, the F-layer strengthens, but the D-layer reforms,

effectively closing 75 meters (and below) to NVIS propagation. However, the stronger F-layer allows good use of 40 meters. The attraction of 60 meters is for those transition time periods between the closing of one band and the opening of the other. Of course, like all HF communications making use of ionospheric refraction, there will not only be daily cycles of change, but as well both seasonal and sunspot-cycle variations, not to mention special conditions, such as solar flares.

Numerous web sites provide details of basic NVIS propagation phenomena as well as other basic data on the propagation mode and its use by radio amateurs. Essentially, NVIS propagation is most relevant to communications at distances from zero to about 200 to 300 miles, especially where intervening terrain may block ground wave communications or VHF/UHF line-of-sight activity.

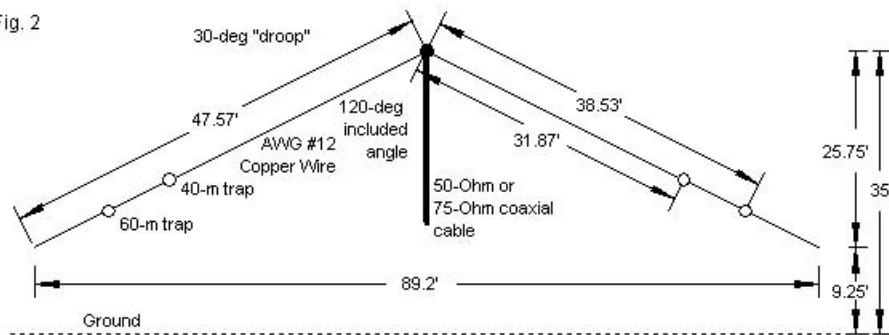
The following notes will examine three basic candidates for a 3-band NVIS antenna covering 75, 60, and 40 meters, with emphasis upon SSB operation. The first section evaluates the pros and cons of a 3-band trap inverted V antenna. The second looks at the potential for converting a common arrangement into a slightly more complex configuration. The use of crossed 75-40meter dipoles, laid out at 90° angles but with a single feedpoint, is common. We shall explore both level and inverted V versions of dipoles for the three bands, each separated by 60° from an adjacent element. Finally, we shall look at the advantages and disadvantages of nested 1- $\lambda$  loops for each band. Each arrangement has both physical and electrical properties that go into the evaluation process. Our goal is

not to make a final decision, but instead to organize some of the factors on each side of the ledger.

### A Trap Inverted V for 75-60-40-Meter NVIS Use

The design of a trap dipole is straightforward. Beginning with the highest band, we create a dipole or inverted V and place a trap at the end. The trap is tuned to a frequency just below the lowest frequency used on the highest band. When we wish to add the use of a lower band, we add wire to the assembly to extend its length. Since at the lower frequency, the trap acts like an inductive load for the lower frequency, the total element length is shorter than would be a full dipole or V for that frequency. We may continue the process indefinitely, but we need add only one more set of traps to achieve 3-band operation.

Fig. 2



General Structural Outline of a Representative Trap NVIS Inverted V for 75, 60, and 40 Meters

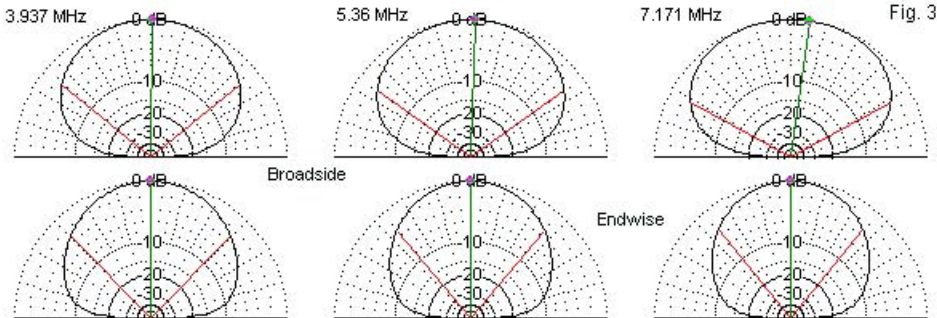
**Fig. 2** shows the dimensions for a trap inverted V for 75, 60, and 40 meters using AWG #12 wire, which is normally strong enough to support the weight of the traps. The dimensions are suited to a 35' center height above average ground with a 30° element slope (or a 120° included angle below the center point). The dimensions place the wire ends 9.25' above ground. The design aims for feedpoint impedance values that are compatible with either 50-Ω or 75-Ω coaxial cable. (I might note in passing that most cables, such as RG-59, have 70-Ω characteristic impedance values, but tradition allows a collective reference to 75-Ω cable.) The overall leg length for 75-meter operation is less than 48', although a simple inverted V for 75 meters might use leg lengths of about 60.5'. Hence, the trap 3-band V has the smallest footprint of all of our test designs. It requires less than 90' of horizontal length and only the wire or cable thickness for width. As well, it normally requires only one 35' support pole, while 10' poles can support the wire ends. Of course, the antenna design allows instant band changing with no required action upon the antenna itself once successfully installed. These are perhaps the major advantages of using a 3-band trap inverted V.

Table 2. Key properties of the 3-band trap inverted V 35' above average ground with traps designed for a Q of 200

Band Meters	Wire Length feet	Trap L μH	Trap C pF	Max. Gain dBi	B-S BW degrees	E-W BW degrees	Resonant Z R+/- jX Ω
75	47.57	--	--	2.13	102	87	52.5 – j0.6
60	38.53	8.5	60	3.24	110	81	73.6 + j0.5
40	31.87	11.3	80	4.80	123	78	73.3 – j0.0

**Table 2** supplies some of the major properties, both physical and electrical, for the antenna. Trap design is standard and almost any antenna handbook will provide guidance in construction. To the list of conditions that may require adjustment of the wire lengths for each band, we can add that small variation in trap values will also change the required length of the 60-meter and the 75-meter extensions. To reinforce the need to create a final design using height and ground quality values as close as possible to reality, we can compare the modeled resonant impedance values to free space values for the same assembly. On 75 meters, the free-space impedance is about  $50 - j50 \Omega$ . On 60, the value is  $69 - j29 \Omega$ , while on 40 meters, the resonant free-space impedance is  $63 - j19 \Omega$ . Note that the free-space values depart more radically from the values over ground—especially in the reactance column—as we place active parts of the antenna closer to ground.

In **Fig. 3**, we find pairs of elevation patterns for each band at the frequencies of resonance. Off-resonant patterns do not depart from the ones shown. As we increase the operating frequency, the antenna height increases as a fraction of a wavelength. The broadside patterns show an accompanying increase in beamwidth. In fact, the 40-meter pattern levels at the top, as indicated by the tilted line. The endwise patterns show a slight decrease in beamwidth with rising frequency.

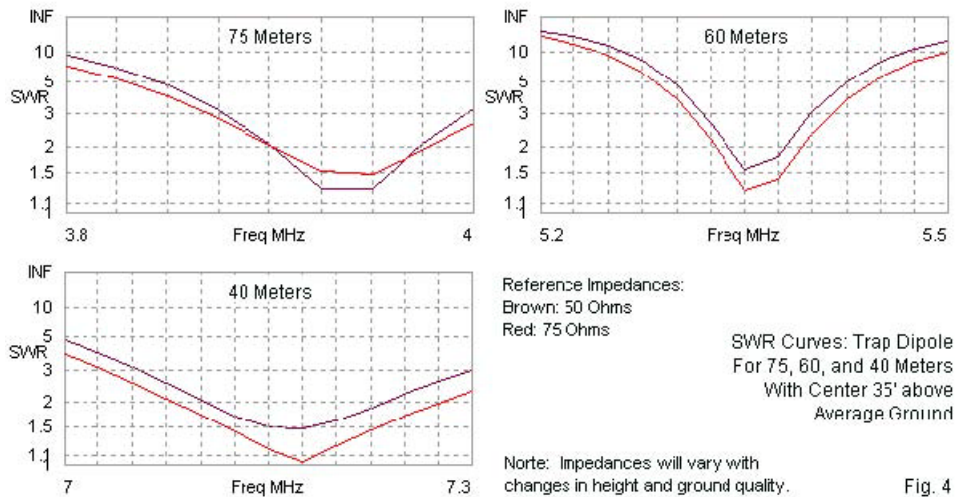


Sample Broadside and Endwise Elevation Patterns of a Trap Dipole for 75, 60, and 40 Meters

One deficiency of the trap inverted V is the relatively low possible gain. The tabular gain values show that the closer we place active parts of the antenna to the ground, the less gain that we can obtain from the antenna. As well, the inverted V structure inherently has less gain than a level trap dipole would have if at a 35' height. The combination of close ground spacing and inverted-V structure may provide mechanical simplicity to an installation, but it limits the antenna's possible performance. The gain at 40 meters (4.8 dBi) is typical of an inverted V at 0.25- $\lambda$  above ground, but the gain of a level dipole can be up to a full dB or more higher. Moreover, on the two lower bands, there are trap losses, about a half-dB per trap pair.

The design does not use a lower wire as what some call a "counterpoise" (in a total misuse of that term). Extensive modeling has shown that a single wire near ground below a NVIS element does not significantly change the antenna gain. The ground itself is

the primary reflective surface and it extends far beyond the limits of a low reflector wire. A way to improve performance is to lay out a series of 7-9 wires or a full (chicken-wire) screen that exceeds the active element dimensions by  $0.4 \lambda$  to  $0.5 \lambda$  in every dimensions. Then the local ground acts like a planar reflector, but only to a certain point. A full ground screen improves performance only to the level of very good ground. For a basic installation, the antenna element itself is all that one needs unless one creates ground screening or an elevated tuned reflector.



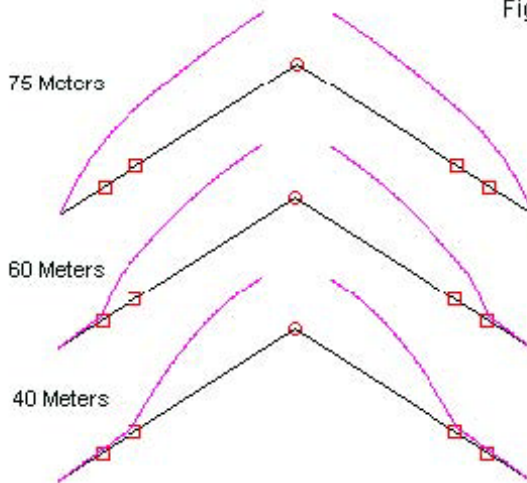
The SWR curves in **Fig. 4** show the relative sizes of the operating windows for each band. Since the antenna would require field adjustment as a matter of course, you can adjust the wire lengths to move the windows anywhere within the bands. Compared to other

antenna types, the SWR windows of the 3-band trap inverted V tend to be fairly narrow, calling for careful field adjustment. A final set of lengths for one installation may not prove satisfactory for another. One limitation of the trap inverted V is the fact that on bands with trap ends, the impedance tends to be higher than on the lowest band. As a result, 75- $\Omega$  coax provides wider SWR windows on 40 and 60 meters, while 50- $\Omega$  coax is best for 75 meters. If we add a significant length of coax between the antenna center point and the station equipment, line losses will broaden the SWR windows. However, the total energy available for radiation (and the receiving sensitivity) will undergo proportional reduction. These notes do not include a level version of the trap dipole at 35' for a significant reason. Leveling the antenna yields impedance values on 60 and 40 meters close to 90  $\Omega$ , while the 75-meter impedance remains close to 50  $\Omega$ . With even a 75- $\Omega$  feedline, the operating windows shrink on at least one band below a usable level. The inverted V configuration tends to lower all of the impedance levels to yield a usable antenna. However, obtaining usable feedpoint impedance values comes at a price: on all three bands, the maximum gain of a level 3-band trap dipole at 35' above ground falls between 5.3 and 5.7 dBi. Compare these gain values to those listed in **Table 2**.

For those unfamiliar with the action of traps, **Fig. 5** presents a set of current magnitude distribution curves along the inverted V on each of the three bands. The center gap is a function of the sloping element halves, since the magnitude is measured from the wire itself. On the two lower bands, note the increase in the slope of the curve as it passes a trap, which acts like a non-radiating load

inductance on the lower bands. Only on 40 meters do we find a normal current distribution up to the first pair of traps. Although we normally think of the current magnitude in wires beyond an operative trap as zero, the value is not quite that low. This fact adds to the somewhat finicky adjustments required of any multi-band trap antenna.

Fig. 5



Current Distribution on a NVIS Trap Inverted V Dipole  
on 75, 60, and 40 Meters

Assuming that trap construction is not a hindrance, the trap inverted V for 75, 60, and 40 meters in NVIS operation provides one of the simplest physical installations. Offsetting that advantage is the relatively low gain on the two lower bands and the relatively narrow

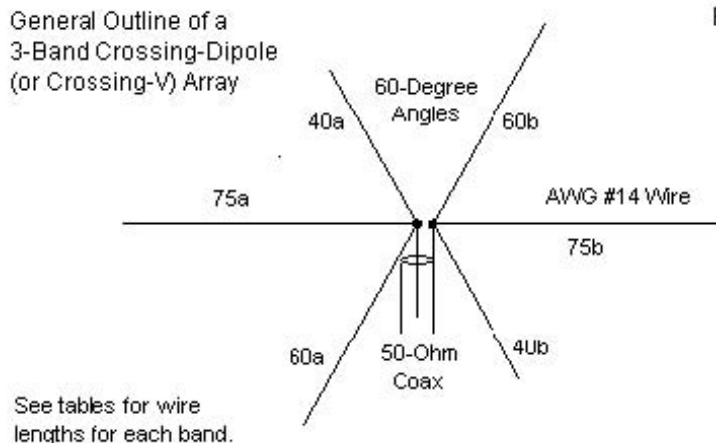
SWR windows for operation. In addition, the antenna requires careful adjustment to the conditions of the installation site.

### Crossing Dipoles for 3 Bands

One popular system for obtaining 75-and 40-meter operation with an antenna having only one feedline employs dipoles for each band in a cross, with each dipole oriented 90° from the other to minimize interaction. The system often uses the inverted V configuration so that a single center support with shorter wire-end supports simplifies the mechanical needs. We may expand the system to include 3 bands by separating the dipoles by 60°, as shown in outline form in **Fig. 6**. The legs may be level or slope to form Vs. The interactions among the dipoles are greater than we find in the 2-band version but are completely manageable.

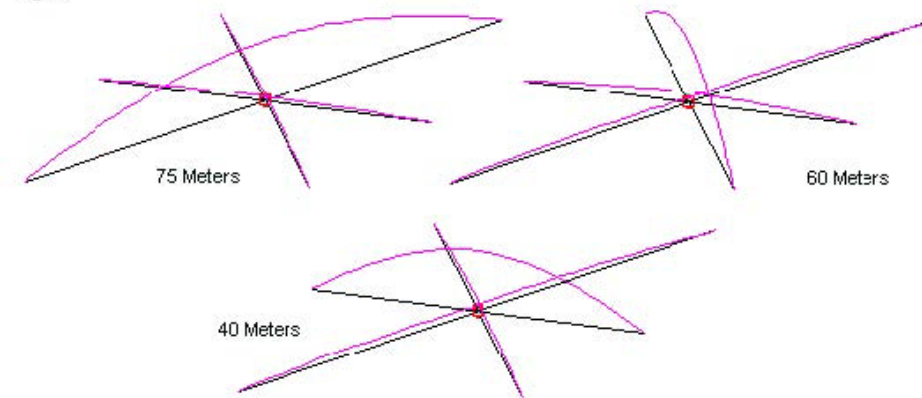
General Outline of a  
3-Band Crossing-Dipole  
(or Crossing-V) Array

Fig. 6



Feeding the antenna requires only a feedline, although adding a common-mode current attenuation device at the feedpoint is a useful precaution to take. **Fig. 7** shows the relative current magnitude distribution as we operate the array on each band. The distribution does not change with height or by using an inverted V configuration. Note that the unused elements are relatively quiescent, but not completely inactive. The chief effect of the low currents on the inactive elements is to require careful pruning of the dipoles for each band to place the low SWR passband to cover the operating frequencies on each band.

Fig. 7



Current Magnitude Distribution on a 3-Band Crossing Dipole Array for 75, 60, and 40 Meters

For NVIS operation, a level system of linear dipole would likely require seven full-length supports, one at the center and one at

each wire end. Although this system is probably more complex than most amateurs wish, let's examine it to see what level of performance we can obtain. We shall place the system at 35' above average ground and then drop it to 25' above ground. If you refer to **Table 1**, you can gauge the height of each dipole as a fraction of a wavelength and estimate the probable performance relative to performance at an optimal height (0.15- $\lambda$  to 0.22- $\lambda$  above ground). **Table 3** provides the modeled dimensions and performance data for both heights.

Table 3. Key properties of the 3-band cross-dipole arrays at 35' and 25' above average ground

Height: 35'

Band Meters	Dipole Length feet	Max. Gain dBi	B-S BW degrees	E-W BW degrees	Resonant Z
75	121.00	6.08	106	65	$54.1 - j0.5$
60	88.35	6.23	117	69	$88.0 + j0.6$
40	66.30	5.52	134	74	$60.9 - j0.8$

Height: 25'

Band Meters	Dipole Length feet	Max. Gain dBi	B-S BW degrees	E-W BW degrees	Resonant Z
75	121.00	5.04	101	66	$44.3 - j0.2$
60	88.35	5.30	107	67	$74.5 + j0.3$
40	66.30	6.10	121	66	$47.2 + j0.3$

A single set of dipole lengths is sufficient for both heights chiefly because the 50- $\Omega$  low SWR windows are considerably broader than those we encountered with the trap inverted-V 3-band antenna.

**Fig. 8** provides SWR curves for both heights with the level dipole system. The current magnitude curves showed higher off-band current activity on the 60-meter dipole than when using either 75 or 40 meters. This condition shows itself in the numerical impedance data and in the SWR curves in the form of a higher resonant

impedance value and a narrower SWR operating window. However, the 60-meter SWR window extends beyond the limits of the 60meter channel assignments.

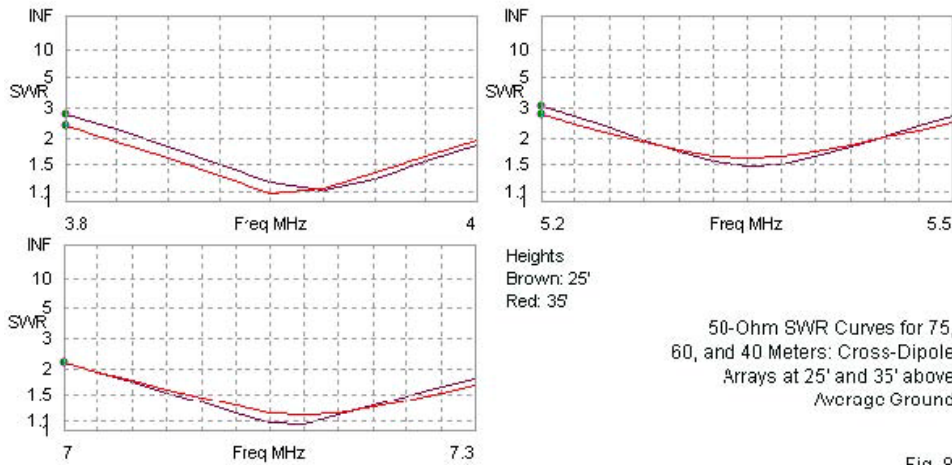
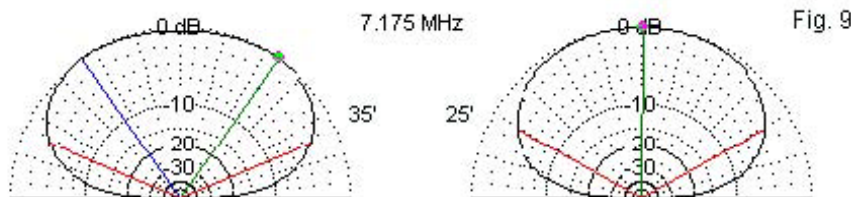


Fig. 8

The broadside and endwise beamwidth and the gain values in the table are worth noting. At a height of 25', only the 40-meter dipole is at optimal height for maximum gain straight up. The other dipoles fall increasing below the optimal height and therefore show lower gain, largely due to ground absorption. All patterns follow the model in **Fig. 1** with wider broadside beamwidth values than endwise values. When we move the antenna upward by 10', the 75-and 60-meter dipoles are closer to optimal NVIS height and show better gain than at 25'. However, the 40meter maximum gain value decreases relative to the value at 25'. As well, the beamwidth

significantly increases. **Fig. 9** compares the broadside elevation patterns of the 40-meter dipole at both heights. Above optimal NVIS height, the pattern begins its evolution into two separate broadside lobes. Note that there are two peak-gain lines equally spaced (in degrees) from the zenith angle. As well, the gain straight up is slightly less than maximum. The differences between the two patterns are not sufficiently great to disrecommend the higher installation level. In fact, if the station is also used for medium-range communications, the higher level provides more energy at lower elevation angles to enhance this operation. The increased beamwidth is the chief reason for finding a slightly lower maximum gain value at 35'. The exercise is useful as a caution against raising NVIS antennas too high. Eventually, the very slight reduction in zenith gain will develop into a very deep upward null.



Broadside 40-Meter Elevation Patterns at 35' and 25' above Average Ground:  
Cross-Dipole Array

Although the crossed-dipole array requires too many supports for most amateur installations, the exercise provides us with a reasonable perspective on dipole performance in NVIS service. It also shows us that 3 crossing dipoles separated by 60° angles is a

perfectly feasible multi-band array. Its final function will be to provide a baseline for comparing the performance of an inverted V form of the same array. The top-down outline would follow the pattern in **Fig. 6**, but the horizontal dimensions would shrink to about 0.866 of the dipole lengths as a result of sloping each dipole 30° below the level dipole line. **Table 4** provides the dimensions and performance data from the model.

Table 4. Key properties of the 3-band cross-V array at 35' (at center) above average ground

Band Meters	Element Length feet	Max. Gain dBi	B-S BW degrees	E-W BW degrees	Resonant Z $R+/- jX \Omega$
75	119.80	3.07	102	86	$51.6 + j0.1$
60	88.50	4.82	111	79	$74.6 + j0.9$
40	66.80	5.30	127	75	$49.7 + j0.9$

The V system uses a standard 30° angle for the wire slope. One result is a variation in the wire-end heights, which range from 5.8' on 75 meters up to 19.15' on 40 meters. A practical installation might wish to select a common height for all wire ends. For example, 10' end supports would place all wires above the potential for accidental contact but with reduced gain on the higher bands. However, to obtain a 30° slope angle, the center height needs to be about 35' to prevent the 75-meter V from touching ground.

Veeing a set of elements tends to lower the feedpoint impedance relative to level dipoles. However, in the crossed V configuration, interactions tend to limit the degree of feedpoint impedance decrease. Hence, the 50-Ω SWR windows shown in **Fig. 10** are about the same size as those for the level dipoles. To place the windows within approximately the same frequency limits on each

band requires a slightly different set of overall element lengths. Because the element ends are close to ground level, the actual lengths needed for the three bands will vary with small structural variations from the model and with changes in the ground quality below the antenna. The width of each SWR passband is great enough to keep the adjustment task from becoming too onerous.

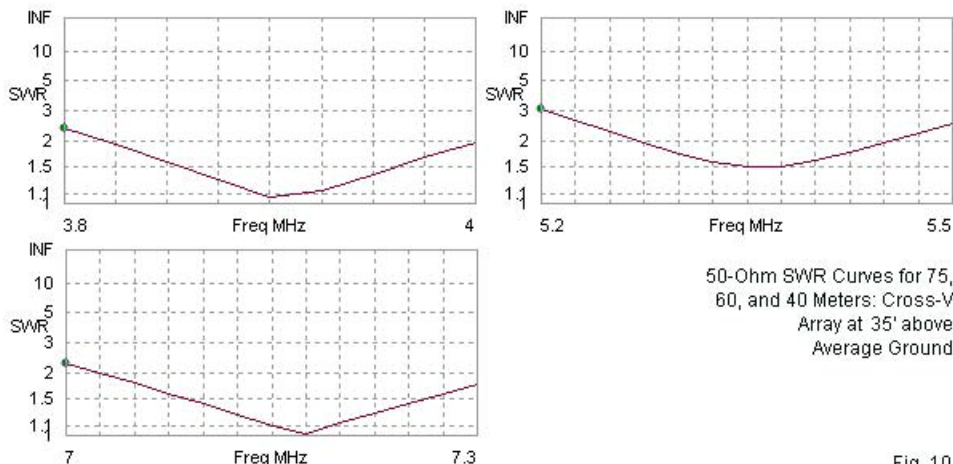
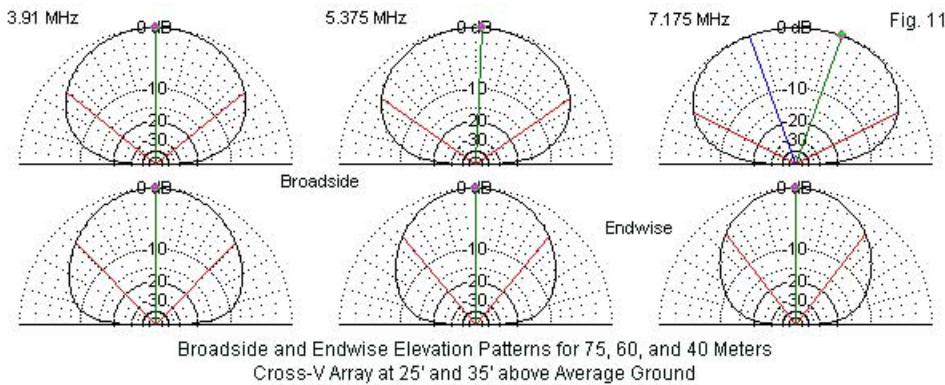


Fig. 10

We often hear a sound bite about inverted V antennas, namely, that their gain values are nearly as good as the gain of level dipoles. Unfortunately, this nugget of wisdom applies to inverted V antennas at significant heights above ground for use in long distance communication. Close to the ground and used for NVIS communications, the proximity of the antenna ends to ground creates a significant gain deficit straight up. Compare the gain

values to those for the level dipoles at 25' and 35'. Only the 40-meter V dipole, with its ends at over 19' above ground is clearly competitive with the level dipole versions. As the V ends more closely approach ground level, the gain decreases. The 75-meter maximum gain is nearly 3 dB lower than the gain of the dipole at 35'. Although the inverted V version of the cross dipole array is mechanically simpler than the level dipole version, there is a gain price for the convenience. (As a side note, compare the crossed V array gain values to those of the trap dipole in **Table 2** to obtain a rough estimate for the further losses due to trap construction.)



**Fig. 11** provides broadside and endwise elevation plots for the crossed V array for each of the three bands. All but one pattern follows the nearly ideal NVIS pattern form. The broadside 40-meter pattern, with a center height of 35' above ground, shows similarities to the 40-meter pattern for a level 35'-high dipole in **Fig. 9**. Because the V element ends droop, the effective height of the 40-meter V is

slightly lower than its center height, so the pattern is less distinctly split into separate broadside lobes.

A 3-band crossed dipole or V array can provide quite adequate NVIS service on a single feedline. However, there are trade-offs for each version. The dipole system provides better performance, but requires up to 7 tall supports. (A little ingenuity with ropes might reduce the required number of supports to 5.) The crossed V configuration reduces the required height of wire-end supports, but imposes a penalty on performance on at least two of the bands.

### *A Nest of Three 1- $\lambda$ Square Loops*

An alternative to the crossed dipole system can reduce the number of required supports to 4, one at each corner of the array. **Fig. 12** shows the very general outline of a set of three 1- $\lambda$  loops that are the core of this NVIS array.

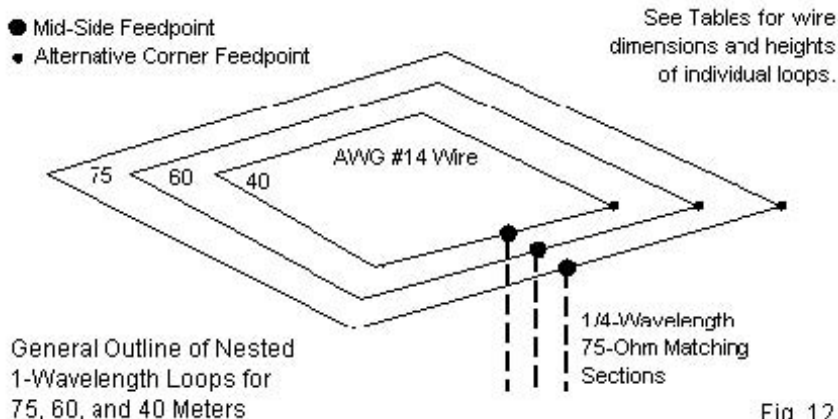


Fig. 12

Each loop is independent and assumes an antenna switching arrangement. Depending upon the installation and its distance from the operating equipment, the switch may be either at the station (with three lines) or at the antenna at the equipment end of the required  $\frac{1}{4}\lambda$  70-75- $\Omega$  matching sections. The feedpoint impedance of the loops themselves falls in the range of 90  $\Omega$  to 130  $\Omega$ . The series matching sections are a very simple way to yield impedance values compatible with 50- $\Omega$  coaxial cable. The sketch shows a mid-side feedpoint. However, the alternative feedpoint at the array corner is just as apt. As well it would allow cable support along the support post at that corner.

Although the basic sketch shows the loops on a level plane, the model for them places the 75-meter and the 60-meter loops at 35', heights closer to optimum for those frequencies. (In fact, a height of 45' to 50' would be best for the 75-meter loop, but we started this

exercise with a 35' height restriction.) In fact, even within our restriction, we might lower the 60-meter loop slightly so that ropes from the corner support posts would place each loop at a slightly lower height, with a 25' height minimum for the 40-meter loop. 60-meter performance would drop to about the 75-meter level. With the 35'/25' split, **Table 5** provides dimensions and performance data for the nested loops using both mid-side and corner feedpoints.

Table 5. Key properties of the 3 nested 1- $\lambda$  loops above average ground

Mid-side fed						
Band Meters	Side Length feet	Circumference feet	Max. Gain dBi	B-S BW degrees	E-W BW degrees	Resonant Z $R+/- jX \Omega$
75	64.4	257.6	6.71	85	69	62.3 – $j4.6$
60	47.0	188.0	6.83	94	71	49.2 – $j3.2$
40	23.5	139.2	6.43	94	70	45.6 – $j1.8$
Corner fed						
Band Meters	Side Length feet	Circumference feet	Max. Gain dBi	B-S BW degrees	E-W BW degrees	Resonant Z $R+/- jX \Omega$
75	64.4	257.6	6.71	86	68	62.4 – $j5.0$
60	47.0	188.0	6.83	97	70	49.2 – $j2.6$
40	23.5	139.2	6.43	97	69	45.7 – $j1.3$

Note: Impedance values assume a  $\frac{1}{4}\lambda$  75- $\Omega$  matching section at each feedpoint. 75- and 60-meter loops are at 35'; 40-meter loop is at 25'.

Note that we need not change any dimensions when we change the feedpoint position; indeed, all performance values show only undetectable differences in the modeled performance values. (Of course, like the dipoles, the loops may require dimension adjustments with small changes in height or significant changes in soil quality.) In the table, we determine the broadside pattern by drawing a line from the feedpoint to a point just opposite on the

loop. Endwise patterns are along a line at right angles to the original line. Broadside for a corner-fed system means a line from one corner to the opposite corner, while mid-side feeding defines broadside from wire center to wire center.

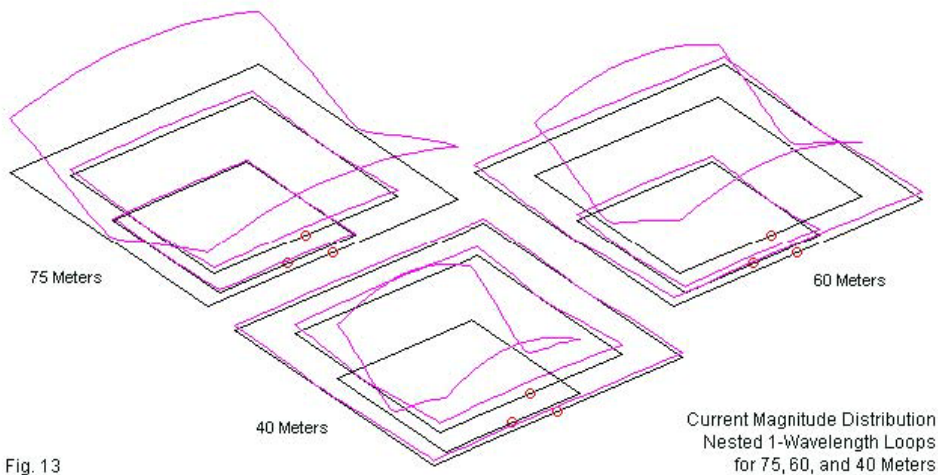
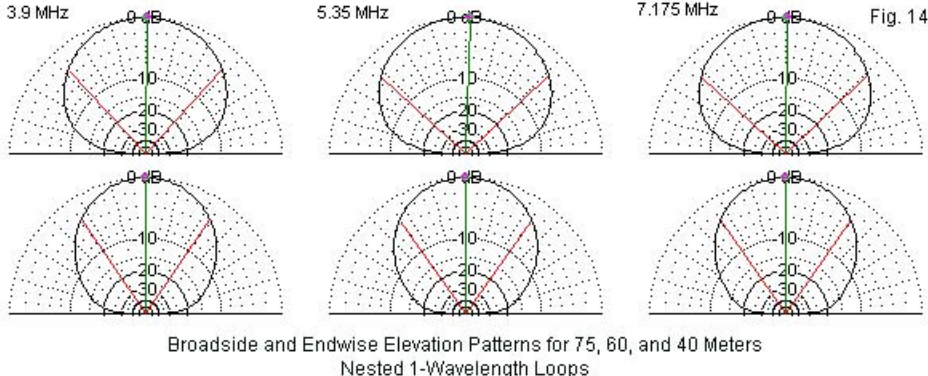
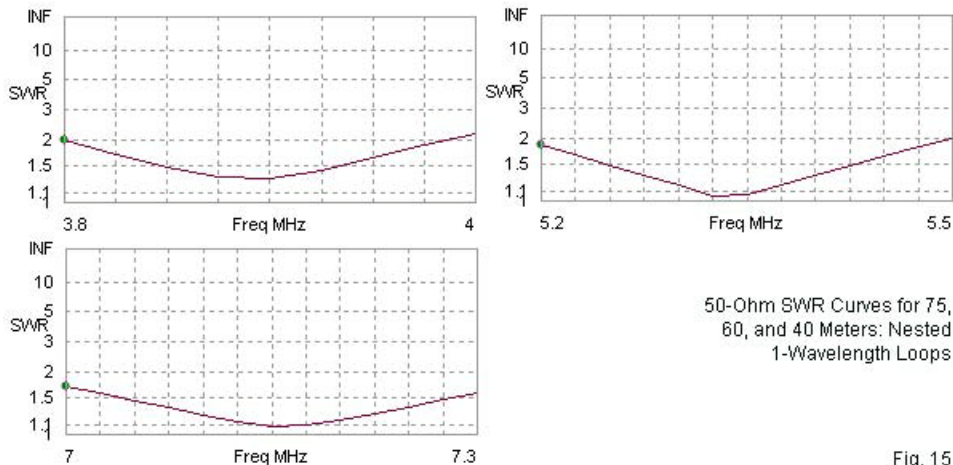


Fig. 13

Even with separate feedlines, the loops do show some interaction between the most active loop and the next adjacent loop. As shown in **Fig. 13** for mid-side feeding, the 60-meter loop shows activity on both the 75-and the 40-meter loops. These interactions have a bearing on the final loop dimensions, but are low enough to create no hindrance to the formation of typical NVIS patterns. A sampling of those patterns (with mid-side feeding) appears in **Fig. 14**.



The 75-meter loop is below its optimum height and shows a slightly narrower broadside beamwidth than the broadside patterns for 60 and 40 meters, both of which are at close to optimal heights. Loops tend to produce more circular patterns than dipoles, as suggested by the endwise patterns, which vary from the broadside beamwidths by only about 20°. As well, loops have slightly higher gain values than dipoles. For the nest shown, the gain varies between 6.4 and 6.8 dBi.



50-Ohm SWR Curves for 75,  
60, and 40 Meters: Nested  
1-Wavelength Loops

Fig. 15

**Fig. 15** provides another advantage inherent in the nested loop array. With series  $\frac{1}{4}\lambda$  75- $\Omega$  matching sections, all of the loops show the widest 50- $\Omega$  SWR bandwidths of any of the options under discussion. The worst case is 75 meters: the 90- $\Omega$  loop impedance under conversion by a standard  $\frac{1}{4}\lambda$  75- $\Omega$  cable only drops to about 62  $\Omega$ . However, the SWR passband changes values very slowly, allowing access to the entire top 200 kHz of the band.

The nested loops do have constraints. They require a square installation region about 70' per side, including support posts. As well, the system needs 4 full-height posts. Finally, the loops require independent feedlines with either a station or a remote switch.

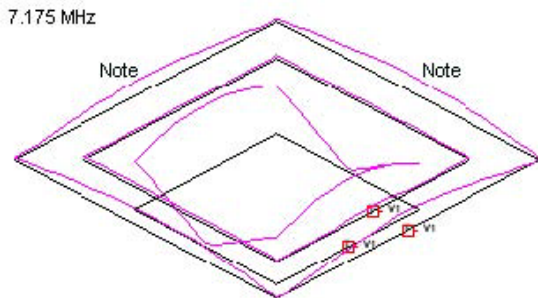
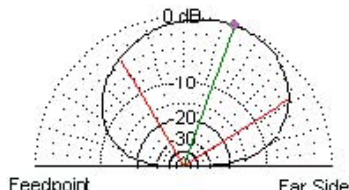


Fig. 16



40-Meter Current Distribution and Broadside Elevation Pattern of Nested Loops with a Common Feedpoint

Unlike quad beams, some of which use a common feedpoint, the nested NVIS loops should use separate feedlines and line switching. **Fig. 16** shows why. On 40 meters, with a common feedpoint for all loops (simulated but not shown in the model), we obtain significant activity on the 75-meter loop, which is close to  $2\lambda$  long. Each side of the 75-meter loop is about  $\frac{1}{2}\lambda$  long on 40 meters. One consequence appears in the offset broadside pattern, with the main lobe tilting away from the feedpoint. A second consequence follows from the fact that the impedance of the 75-meter loop, when excited on 40 meters, is about  $220\Omega$ . The parallel combination of impedances for the 40-and 75-meter loops yields a net impedance value that is more difficult to match. The impedance challenge is not insurmountable by careful adjustment of loop lengths. However, the pattern offset will remain.

If the 4-corner support system is feasible, the nested  $1\lambda$ -loop array provides the highest performance of any of the systems in these notes, all of which have observed a 35' maximum height restriction.

## Conclusion

Our goal has been to explore some basic 3-band antenna systems for NVIS operation on 75, 60, and 40 meters. We have tried to portray reasonably the advantages and disadvantages of each system. As well, we have used the occasion to address some basic issues in NVIS antennas, such as the ineffectiveness of so-called single-wire reflectors or “counterpoises,” and the effects of using the inverted V configuration in contrast to level dipoles. The trap inverted V uses the least real estate as measured by its area, but has overall the lowest performance level. Crossed dipoles improve performance significantly but require an extensive structure. Setting the dipoles into a V-configuration eases the support requirements but at the cost of severe performance reductions, especially on 75 meters. The nested 1- $\lambda$  loops require 4 full-height supports and separate, switched feedlines, but provide the highest level of performance of the group of candidates.

These notes have not covered all possibilities. For example, we did not discuss using a single antenna across the entire spectrum by employing either a lossy terminating resistor (or set of resistors) or by using high-speed matching systems. Our aim was to stick to basic antennas and basic installation techniques. These notes do not form in any way a complete menu of tri-band NVIS coverage. Indeed, they are at most appetizers, food for thought.

## Chapter 69: NVIS Antennas for Special Needs

**N**ot all NVIS missions are the same, and so not all antenna requirements are the same. In this set of notes, we shall examine a few of the special requirements that some missions might impose upon antennas and look at a few samples ways to fulfill the needs. Not all of the antennas that we shall explore fall in the category of basic NVIS antennas, but they are all buildable by experienced radio amateurs.

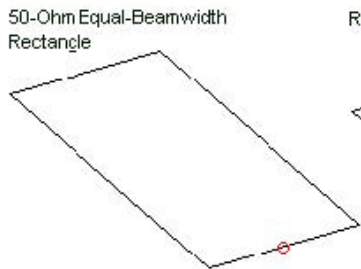
We shall, somewhat arbitrarily, divide the effort into three sections. The first part of our work will be to design a good NVIS antenna that has as circular a pattern as possible. In other words, the beamwidth ratio will be within the limits from 0.9:1 to 1.1:1. Our goal will also be to ensure that the zenith gain of the antenna matches or exceeds the gain of a dipole at the same height above ground. The second section will explore ways of maximizing zenith gain regardless of the beamwidth ratio. Ultimately, we shall aim for a gain of perhaps 12 dBi over average ground, compared to a dipole's maximum zenith gain of about 6.4 dBi over the same ground.

A perfectly vertical pattern is not always the best fit for a station's mission. In the third and final part of our work on special purposes NVIS antennas, we shall examine some ways in which we might reliably tip the pattern of a NVIS antenna in a desired direction while maintaining adequate zenith gain. In fact, we shall begin with a tempting proposal that simply does not work. Then we shall examine a few workable ideas, exploring along the way the

parameters of any antenna that we might use to do the job. As always, the final part of this set of notes is in no way the final word on the many possibilities for NVIS antennas.

### Nearly Perfectly Circular NVIS Pattern Production

Suppose that the NVIS mission includes a requirement for a perfectly circular pattern in which the broadside and endwise beamwidths are the same—or as close to the same as we may achieve. The lowest value of beamwidth ratio achieved by any of the basic antennas was about 1.25:1 for some of the square loops. Still, that value is far from the 1:1 goal of the present hypothetical requirement. We can do better. **Fig. 1** outlines a relatively basic way to attain the desired beamwidth ratio, increase zenith gain, and provide a direct match to the standard 50- $\Omega$  amateur feedline. We simply create a rectangle, fed on a narrow side, either alone or with a ground-level screen.



50-Ohm Equal-Beamwidth Rectangle

Rectangle with Planar Screen

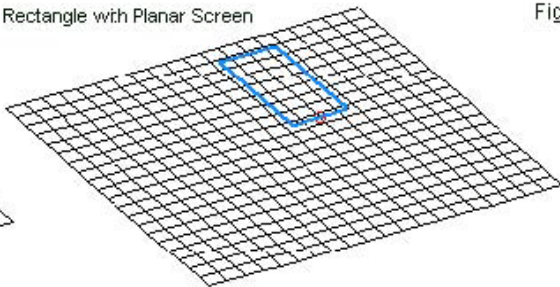
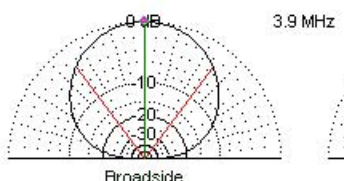


Fig. 1

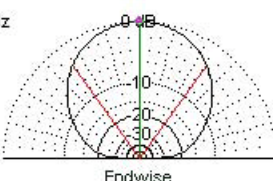
General Outline of a Special-Purpose Rectangular 1-Wavelength Loop

The development of vertically and horizontally polarized rectangular antenna shapes has a long history, and we may easily adapt those designs to NVIS service by laying out the wires parallel to the ground. If the ratio of long side wires to the fed wire (and its opposite) is about

2.29 to 2.30 to 1, several beneficial consequences emerge (along with one limitation as well). First and most relevant to our project, the radiation from the side wires increases, widening the beamwidth relative to the broadside beamwidth that we measure from the feedpoint through the center of the opposing wire. In fact, the suggested ratio (applicable to the AWG #14 wire antennas that we are modeling) produces a nearly perfect 1:1 ratio, depending upon the antenna height and the ground quality beneath the antenna. **Fig. 2** shows a set of typical patterns for a rectangle with the specified dimensions.



3.9 MHz



Broadside and Endwise Elevation Patterns: Representative  
50-Ohm Equal-Beamwidth NVIS Rectangle

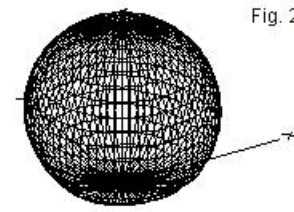


Fig. 2

The broadside and endwise elevation patterns are virtually indistinguishable. The 3dimensional version of the radiation pattern is about as close to a sphere as one may achieve with a ground-based antenna system. The second consequence of constructing a

rectangle of the suggested dimensions and fed at the center of one of the short wires is that the feedpoint impedance changes its value relative to the impedance value for a square loop. Instead of an impedance level greater than  $100\ \Omega$  at resonance, the impedance value decreases as we elongate the rectangle. At the proportions necessary for a circular pattern, the feedpoint impedance is approximately  $50\ \Omega$ , the value we need for our coaxial cable.

The third consequence of elongating a square loop into a rectangle is increased zenith gain for the  $1-\lambda$  loop. (Like square loops, the rectangle will actually have a circumference that is slightly greater than  $1-\lambda$  at resonance. The circumference values for our samples will be between  $1.03\ \lambda$  and  $1.033\ \lambda$ .) In NVIS service, the additional gain may not be enough to be truly decisive in deciding to install a rectangle. However, the combination of advantages may have more weight than the simple sum of the three individually.

An AWG #14 copper wire rectangle for 75 meters will require side wires about  $0.358\text{-}\lambda$  long, with end wires about  $0.157\text{-}\lambda$  long. For the numerical data in **Table 1**, I first resonated the loop at a height of  $0.175\text{-}\lambda$  above average ground and then sought the height of maximum zenith gain over our three standard soil varieties: very good, average, and very poor. (See the first set of notes for soil quality specifications in terms of conductivity and relative permittivity.) For each soil quality, I recorded the zenith gain, beamwidths, and feedpoint impedance between  $0.145\text{-}\lambda$  and  $0.235\text{-}\lambda$  above ground in  $0.01\text{-}\lambda$  increments. The table indicates by italics the heights of maximum zenith gain for each soil quality. For this class of antennas, there is no difference between zenith gain and

maximum gain, since the patterns are so circular. BS BW and EW BW indicate the broadside and endwise beamwidth values respectively, while the ratio is always broadside over endwise. Hence, where the endwise beamwidth is greater than the broadside value, it is possible to obtain ratios less than 1.00. The Feed R and Feed X columns show the feedpoint impedance based on the initial resonance of the sample model.

75-Meter 1-WL Rectangle							Table 1		
AWG #14 Copper Wire: Circumference = 1.030 WL							3.9 MHz		
Very Good Soil									
Height wl	Height ft	Zen Gain	BS BW	EW BW	BW Ratio	Feed R	Feed X		
0.145	36.57	8.13	68.6	69.8	0.98	39.89	10.60		
0.155	39.09	8.20	69.4	70.4	0.99	42.46	9.29		
0.165	41.61	8.25	70.2	70.8	0.99	45.04	7.91		
0.175	44.13	8.27	71.1	71.6	0.99	47.58	6.42		
0.185	46.66	8.27	72.1	72.4	1.00	50.03	4.82		
0.195	49.18	8.25	73.2	73.2	1.00	52.38	3.08		
0.205	51.70	8.21	74.5	74.2	1.00	54.60	1.20		
0.215	54.22	8.16	75.8	75.2	1.01	56.65	-0.81		
0.225	56.74	8.09	77.4	76.6	1.01	58.51	-2.95		
0.235	59.27	8.00	79.1	77.8	1.02	60.17	-5.20		
Average Soil									
Height wl	Height ft	Zen Gain	BS BW	EW BW	BW Ratio	Feed R	Feed X		
0.145	36.57	7.03	70.9	70.6	1.00	45.66	5.10		
0.155	39.09	7.18	71.7	71.0	1.01	47.32	3.50		
0.165	41.61	7.29	72.7	71.4	1.02	49.02	1.92		
0.175	44.13	7.36	73.6	72.0	1.02	50.73	0.32		
0.185	46.66	7.41	74.7	72.6	1.03	52.40	-1.33		
0.195	49.18	7.42	76.1	73.4	1.04	54.00	-3.04		
0.205	51.70	7.42	77.4	74.4	1.04	55.50	-4.82		
0.215	54.22	7.39	79.0	75.4	1.05	56.88	-6.68		
0.225	56.74	7.34	80.7	76.4	1.06	58.11	-8.60		
0.235	59.27	7.27	82.7	77.8	1.06	59.19	-10.59		
Very Poor Soil									
Height wl	Height ft	Zen Gain	BS BW	EW BW	BW Ratio	Feed R	Feed X		
0.145	36.57	5.77	74.8	72.8	1.03	49.94	-4.70		
0.155	39.09	5.95	75.8	72.8	1.04	50.54	-6.22		
0.165	41.61	6.09	76.8	73.0	1.05	51.23	-7.65		
0.175	44.13	6.20	78.0	73.2	1.07	51.97	-9.02		
0.185	46.66	6.27	79.2	73.6	1.08	52.72	-10.38		
0.195	49.18	6.31	80.8	74.2	1.09	53.45	-11.74		
0.205	51.70	6.33	82.3	74.8	1.10	54.14	-13.11		
0.215	54.22	6.33	84.0	75.6	1.11	54.77	-14.50		
0.225	56.74	6.30	85.9	76.6	1.12	55.31	-15.91		
0.235	59.27	6.24	88.1	77.6	1.14	55.77	-17.34		

**Fig. 3** provides a graphic view of the gain curves for the three soil qualities. They are quite shallow and selecting a mounting height that differs a bit from the optimum height would yield undetectable differences in performance. In fact, the optimum heights for maximum zenith gain for the rectangle are uniformly slightly higher (by about  $0.01\text{-}\lambda$ ) than those for the square loop. We may note in passing that the fed wire and the opposite wire are significantly farther apart in the rectangle than the corresponding wires are in the square loop. Although not very significant relative to building a loop, this fact will take on more importance when we examine other types of antennas in these notes. We should remember that we may analyze the square loop and the rectangle as two dipoles in phase, bent so that the ends join at the center of the side wires.

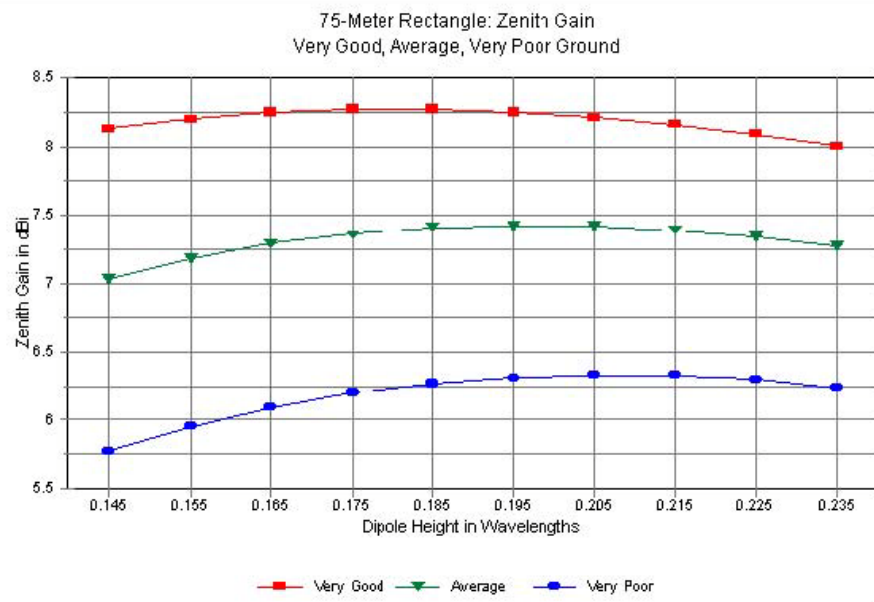
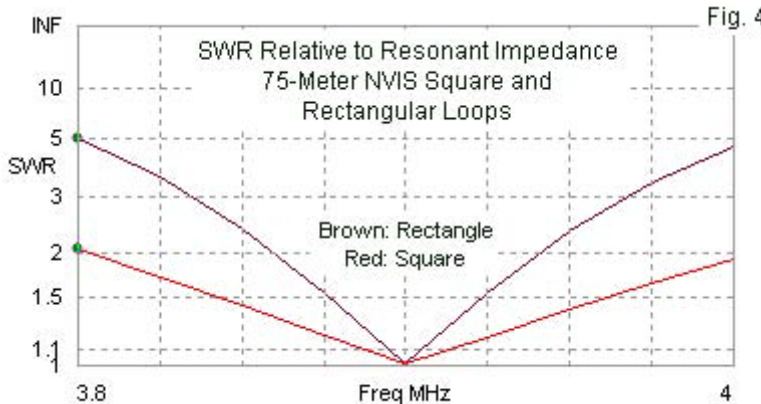


Fig. 3

Besides having circular patterns and  $50\Omega$  feedpoint impedance values, rectangles also show very good gain over each soil type. However, they have one limitation relative to a square loop. The SWR bandwidth is much narrower. **Fig. 4** shows overlaid SWR curves relative to the respective resonant impedance of a square loop and a rectangle. The 2:1 bandwidth is about 1/3 the width achieved by the square loop. As a consequence, the rectangle will likely require considerably more field adjustment effort than a dipole or square loop.



We may retrace our steps on 40 meters (7.2 MHz) to assure ourselves that the trends that apply to 75 meters are quite general. **Table 2** provides data over the same span of heights (in wavelengths) and the same soil types that we applied to 75 meters. Because ground losses at 40 meters are slightly higher than at 75 meters, we expect a slight reduction in gain values for comparable heights. The rectangle is  $0.36\text{-}\lambda$  by  $0.157\text{-}\lambda$  using AWG #14 copper wire.

40-Meter 1-WL Rectangle							Table 2	
AWG #14 Copper Wire: Circumference = 1.033 WL      7.2 MHz								
Very Good Soil								
Height wl	Height ft	Zen Gain	BS BW	EW BW	BW Ratio	Feed R	Feed X	
0.145	19.81	7.94	69.0	70.0	0.99	40.59	11.56	
0.155	21.17	8.03	69.9	70.6	0.99	42.91	10.13	
0.165	22.54	8.09	70.7	71.2	0.99	45.24	8.65	
0.175	23.91	8.13	71.5	71.6	1.00	47.54	7.10	
0.185	25.27	8.14	72.5	72.4	1.00	49.76	5.45	
0.195	26.64	8.12	73.8	73.4	1.01	51.89	3.68	
0.205	28.00	8.09	75.0	74.4	1.01	53.90	1.80	
0.215	29.37	8.04	76.4	75.4	1.01	55.74	-0.20	
0.225	30.74	7.98	78.0	76.6	1.02	57.41	-2.31	
0.235	32.10	7.89	79.7	78.0	1.02	58.89	-4.51	
Average Soil								
Height wl	Height ft	Zen Gain	BS BW	EW BW	BW Ratio	Feed R	Feed X	
0.145	19.81	6.72	71.5	70.4	1.02	44.90	4.26	
0.155	21.17	6.90	72.2	70.6	1.02	46.23	2.77	
0.165	22.54	7.03	73.2	71.0	1.03	47.63	1.33	
0.175	23.91	7.13	74.1	71.4	1.04	49.05	-0.12	
0.185	25.27	7.19	75.3	72.0	1.05	50.47	-1.60	
0.195	26.64	7.22	76.6	72.8	1.05	51.84	-3.13	
0.205	28.00	7.23	78.0	74.6	1.05	53.13	-4.72	
0.215	29.37	7.22	79.4	74.4	1.07	54.33	-6.38	
0.225	30.74	7.18	81.1	75.6	1.07	55.42	-8.09	
0.235	32.10	7.12	83.0	76.8	1.08	56.36	-9.86	
Very Poor Soil								
Height wl	Height ft	Zen Gain	BS BW	EW BW	BW Ratio	Feed R	Feed X	
0.145	19.81	5.56	74.9	72.6	1.03	46.91	-4.92	
0.155	21.17	5.76	75.8	72.4	1.05	47.44	-6.23	
0.165	22.54	5.91	76.8	72.4	1.06	48.04	-7.43	
0.175	23.91	6.03	77.8	72.6	1.07	48.71	-8.58	
0.185	25.27	6.12	79.0	72.8	1.09	49.39	-9.70	
0.195	26.64	6.18	80.3	73.2	1.10	50.07	-10.83	
0.205	28.00	6.21	81.8	73.8	1.11	50.73	-11.96	
0.215	29.37	6.22	83.4	74.6	1.12	51.33	-13.12	
0.225	30.74	6.21	85.1	75.4	1.13	51.88	-14.30	
0.235	32.10	6.17	87.1	76.4	1.14	52.35	-15.49	

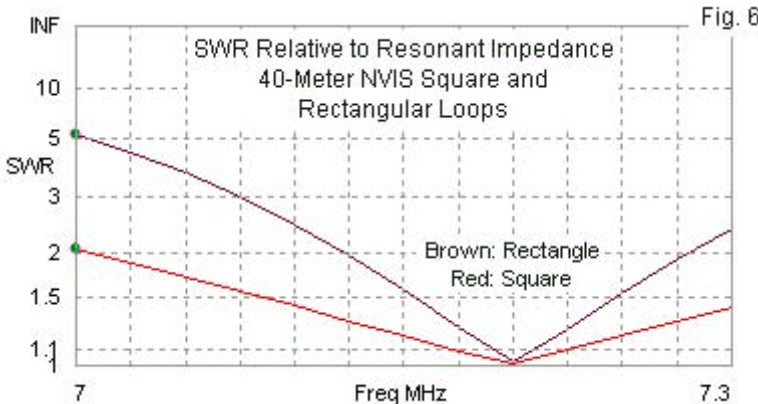
In general, the heights required for maximum zenith gain are about one step higher on 40 than on 75. In addition, they are equivalently higher than for the square loop on 40 meters. **Fig. 5** provides a graphic view of the gain curves for each soil type in the table. Like the curves for 75 meters, the 40-meter gain graphs show very slow changes in the zenith gain in the general height region of maximum gain, a fact that allows the user to vary the physical height of the antenna with no perceptible difference in operational performance.

The feedpoint impedance values remain tame in the sense that small changes of the rectangle's dimensions can easily yield a precise  $50\text{-}\Omega$  impedance. Since resonance is a function of the circumference, every modification to either the long or the short sides will require a comparable modification to the other sides. Elongating the long sides will reduce the resistive component value, while increasing the length of the short sides will raise the value. Since the amount of change for the side lengths will be small, the beamwidth ratio will not change much.



Fig. 5

Like the 75-meter rectangle, the 40-meter version also displays a narrower SWR bandwidth than a square loop, as measured relative to the resonant impedance of each type of antenna. **Fig. 6** displays the narrowing on 40 meters by superimposing loop and rectangle SWR curves. The rectangle's 2:1 SWR bandwidth is about 1/3 the value for a square loop.



The tables have shown zenith gain values that may seem high compared to those we developed in the second set of these notes for the dipole and the square loop. To confirm this impression, **Table 3** presents maximum zenith gain data for each type of antenna over each type of soil, along with the height above ground at which the maximum zenith gain occurs. The heights of maximum gain for both the dipole and the square loop are almost identical, but the rectangle requires about  $0.01\lambda$  greater height to reach maximum gain. As noted earlier, this is a fact worth remembering for the moment.

Summary of Maximum Zeith Gain Values and Heights						Table 3
Antenna	Very Good		Average		Very Poor	
	Max Gain	Height	Max Gain	Height	Max Gain	Height
	Zenith	WL	Zenith	WL	Zenith	WL
75 m						
Dipole	7.40	0.165	6.42	0.185	5.13	0.200
1-wl Loop	7.96	0.165	7.04	0.185	5.85	0.200
Rectangle	8.27	0.180	7.42	0.200	6.33	0.21
40 m						
Dipole	7.15	0.170	6.09	0.195	4.86	0.205
1-wl Loop	7.74	0.175	6.76	0.195	5.64	0.210
Rectangle	8.14	0.185	7.23	0.205	6.22	0.215
Notes:	Max Gain Zenith = maximum zenith gain in dBi					
	Height WL = maximum zenith gain height in wavelengths					

The rectangle provides an added increment of gain over the square loop with any soil type. The increment is not as great as the increment of the square loop over the dipole. However, the rectangle provides an average of about 1 dB higher gain than the dipole when both are at optimal heights above ground. The increase is highest over very poor soil and least over very good soil and slightly higher on 40 meters than on 75 meters. Whether the gain increase offsets the narrower SWR bandwidth of the rectangle is a complex judgment that requires consideration of all mission and resource information applicable to a given installation site.

**Fig. 1** provided the outlines of the rectangle in isolation, the case with which we have been working, and of the rectangle with a near-ground screen. The screen is  $0.001\lambda$  above ground to allow the modeled wires to avoid ground penetration. It uses openings that

are  $0.05\lambda$  per side to simulate better the sorts of screening that might actually find use at a site. For uniformity over the three soil types, the antenna is fixed at  $0.175\lambda$  above ground and uses the dimensions set for resonance without a screen. **Table 4** presents the results of the screen test.

1-Wavelength Rectangle + $1\lambda \times 1\lambda$ Screen						Table 4
Rectangle at $0.175\lambda$ -Wavelength; Screen at Near-Ground Level						
Ground	Zen Gain	BS BW	EW BW	BW Ratio	Feed R	Feed X
75 Meters						
Vy Good	8.64	70.1	71.0	0.99	46.42	8.69
Average	8.57	69.9	69.8	1.00	48.79	8.18
Vy Poor	8.67	69.0	67.4	1.02	50.63	8.14
40 Meters						
Vy Good	8.71	70.1	70.8	0.99	46.06	10.71
Average	8.69	69.3	68.8	1.01	48.25	10.08
Vy Poor	8.82	68.5	66.5	1.03	49.77	10.11
Notes:	Zen Gain = maximum zenith gain in dBi					
	BS BW; EW BW = broadside & endwise beamwidths in degrees					
	Feed R; Feed X = feedpoint resistance and reactance in Ohms					

Although the screen is  $1\lambda$  by  $1\lambda$ , making it a bit short for the broadside dimension of the loop, the supplement does improve gain, even over very good soil. More significant is the uniformity of both gain and feedpoint impedance values over all three soil types. The total variation in feedpoint impedance on either band is about  $4\Omega$  of resistance. As we saw with the dipole and the square loop in past notes, the gain value over very poor soil is (by an insignificant operational amount) the highest on both bands. Over very poor soil, installation of a ground screen may be a worthy investment, since

the gain improvement can be up to about 2.5 dB over the same antenna without the screen.

Our exercise has been largely hypothetical, since it rests on the assumption that for some given mission, a circular beamwidth pattern is required or desired. The rectangle proves to be one of the simplest means for achieving the goal—and for obtaining slightly more gain than the other basic antennas and for achieving a feedpoint impedance close to  $50\ \Omega$ . The cost, as we have seen, is a major narrowing of the SWR bandwidth of the resulting antenna.

### *Maximum Zenith Gain*

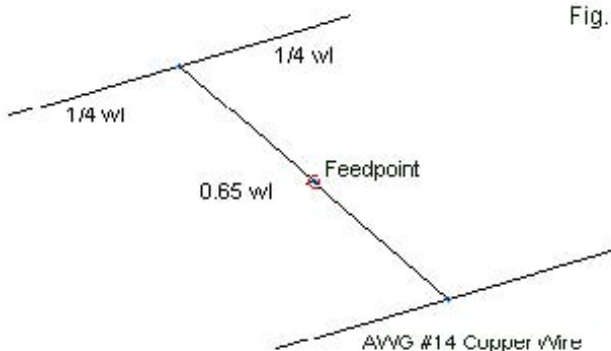
In theory, we may produce much higher gain than we obtained even with the rectangle. One very basic way to achieve this goal is to create a large array of parallel dipoles spaced  $\frac{1}{2}\lambda$  apart and fed in phase. The net gain will be a function of the number of dipoles in the array. The array achieves its increased gain by reducing the beamwidth of the zenith lobe. A very long collection on in-phase collinear sections can achieve similar ends by the same beamwidth narrowing means.

Within the realm of practical antennas for NVIS work, most suggested high-gain arrays have restricted themselves to 2 elements fed in phase. Past suggestions have acquired some odd names, but all of the 2-element arrays are variations on the lazy-H. In this section, we shall look at two of the past arrays and then create a third version of the lazy-H with superior gain. Along the way, we shall acquire a better understanding of the relationship of

an array's broadside dimension and the required height above ground for maximum zenith gain.

One of the earliest antennas in this group has carried the label "Shirley" array. As shown in **Fig. 7**, it is a form of lazy-H that uses relatively short ( $1/2\lambda$ ) elements with a wide spacing ( $0.65\lambda$ ) between them. The lines joining the elements are transmission line sections. To achieve in-phase feeding of the elements, we use equal length sections to a central feedpoint.

Fig. 7



General Outline: NVIS Shirley Array  
(Wide-Space, Short-Element Lazy-H)

In our notes, shall omit feedpoint impedance values. The feedpoint impedance depends upon the length of the elements, the characteristic impedance and velocity factor of the phasing lines, along with the length of the lines. Because the  $1/2\lambda$  elements are still within a range that permits mutual coupling, the impedance of

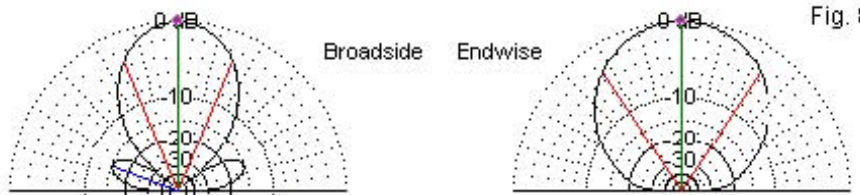
$\frac{1}{2}\lambda$  elements will not be identical to the impedance of each element in isolation. As well, different installations may opt for different feedpoint positions, some using an elevated feedpoint and others using longer lines for a feedpoint at or near the ground. With judicious element pruning, one might develop the array to use  $\frac{3}{4}\lambda$  (electrical length) sections of phasing line with a 70-75- $\Omega$  impedance to transform element 50- $\Omega$  impedance values to 100  $\Omega$ . In parallel, the array might then be fed with a 50- $\Omega$  coaxial cable.

The lazy-H configuration with two elements fed in phase increases the broadside gain relative to a single element. The particular configuration used in the Shirley array employs  $\frac{1}{2}\lambda$  elements with a spacing that approaches maximum gain for the element length.

**Table 5** summarizes the potential performance of the array over each ground type. We may omit the scanning of many heights with the understanding that for the height region around maximum zenith gain, the change per height increment is relatively small. The table lists only the heights of maximum gain and the zenith gain value for each soil on each of our two bands.

Shirley Array (Short-Element, Wide-Space Lazy-H)						Table 5
Ground	Height wl	Height ft	Zen Gain	BS BW	EW BW	BW Ratio
75 Meters						
Vy Good	0.180	45.40	10.70	43.0	65.8	0.65
Average	0.205	51.70	9.95	44.2	67.8	0.65
Vy Poor	0.210	52.96	8.95	45.4	68.4	0.66
40 Meters						
Vy Good	0.190	25.96	10.52	43.4	66.6	0.65
Average	0.210	28.69	9.71	44.6	67.4	0.66
Vy Poor	0.220	30.05	8.76	45.6	68.2	0.67
Notes:	75 Meters = 3.9 MHz; 40 Meters = 7.2 MHz					
	Zen Gain = maximum gain in dBi at zenith angle					
	BS BW, EW BW = broadside and endwise beamwidth in degrees					

The phased dipoles at wide spacing produce an average of about 3.5 dB over single dipoles. The required height for maximum zenith gain averages about  $0.02\lambda$  higher than for the single dipole. The height values are about  $0.01\lambda$  higher than for the rectangle. Note that the Shirley array uses a spacing between dipoles that is close to twice the spacing of the broadside wires in the rectangle. The increased height of maximum gain from the reflective surface—in this case, the ground—is also noticeable with planar reflector arrays. In fact, the required height increase of the array over a single dipole is less with very poor soil, a relatively poor reflector.



Typical Broadside and Endwise Elevation Patterns  
for a Shirley NVIS Array

**Fig. 8** in conjunction with the beamwidth ratios shows other interesting facts about the performance of two dipoles spaced more than  $\frac{1}{2}\lambda$  apart. First, the broadside beamwidth narrows considerably to yield the higher gain levels. However, the endwise beamwidth remains close to the value for individual dipole elements. As a consequence, the array has beamwidth ratios well under 1.00. Still, the motivation for employing a phased array to obtain higher gain is the gain itself. In most such cases, designers are not concerned with the beamwidth ratio. The higher-gain NVIS antennas tend to focus solely upon NVIS effectiveness, to the exclusion of almost all other missions. The second interesting fact about the present array is the development of secondary broadside lobes. Such lobes are typical of any phased array in which the element spacing exceeds  $\frac{1}{2}\lambda$ .

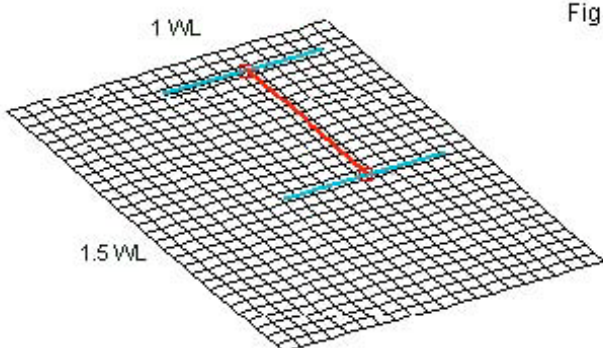


Fig. 9

Shirley Array with Ground-Level Screen

**Fig. 9** shows Shirley array over a ground-level screen. Because the spacing between elements is so wide, the modeled screen uses a broadside dimension of  $1.5 \lambda$ . The results of modeling the antenna at a height of  $0.2\lambda$  above ground with the screen beneath appear in **Table 6**.

Shirley Array above Near-Ground Screen				Table 6
Screen: 1.5 wl Broadside x 1.0 wl Endwise				
Ground	Zen Gain	BS BW	EW BW	BW Ratio
75 Meters				
Vy Good	10.95	43.4	67.0	0.65
Average	10.88	43.4	66.2	0.66
Vy Poor	10.95	43.0	64.4	0.67
40 Meters				
Vy Good	10.95	43.4	66.8	0.65
Average	10.92	43.2	65.4	0.66
Vy Poor	11.03	42.8	63.6	0.67
Notes:	See Table 5			

With a ground screen, the array provides only a very small gain improvement over very good ground, but about 2-dB of improvement over very poor soil. The reported gain values are insignificantly different as we change soil types once we add the screen. Indeed, the uniformity of operating characteristics tends to apply to all of the antenna parameters.

The second of our older antenna systems bears the label “Jamaica” array. In fact, as shown by the outline sketch in **Fig. 10**, the array is nothing more or less than a traditional lazy-H. The elements are  $1 \lambda$  long, which presents to the individual phase lines a very high impedance value. Normally, a lazy-H builder uses equal lengths of parallel transmission line to a central feedpoint. Again, the precise impedance at the feedpoint is the parallel combination of individual impedance values, as transformed by the lines. The transformation will depend upon the characteristic impedance, velocity factor, and length of the lines employed. In many cases, the net feedpoint impedance will consist of a relatively low resistive component and a high reactance. As a result, matching at the feedpoint generally results in lower losses than using a long run of parallel transmission line.

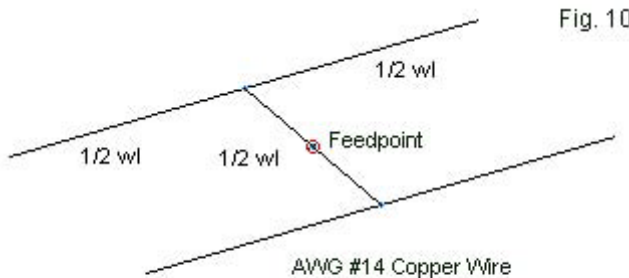


Fig. 10

General Outline: NVIS Jamaica Array  
(Standard/Traditional Lazy-H)

Because the Jamaica or standard lazy-H uses longer elements, its gain potential is higher than we can obtain from the Shirley array.

**Table 7** summarizes the heights and values of maximum zenith gain from the standard lazy-H configuration.

Jamaica Array (Standard/Traditional Lazy-H)						Table 7
Ground	Height wl	Height ft	Zen Gain	BS BW	EW BW	BW Ratio
75 Meters						
Vy Good	0.165	41.61	11.53	54.0	43.6	1.24
Average	0.185	46.66	10.88	56.2	44.2	1.27
Vy Poor	0.195	49.18	10.00	58.6	44.8	1.31
40 Meters						
Vy Good	0.170	23.22	11.38	54.6	43.8	1.25
Average	0.190	25.96	10.65	56.8	44.2	1.29
Vy Poor	0.200	27.32	9.80	59.0	44.6	1.32
Notes:	75 Meters = 3.9 MHz; 40 Meters = 7.2 MHz					
	Zen Gain = maximum gain in dBi at zenith angle					
	BS BW, EW BW = broadside and endwise beamwidth in degrees					

The Jamaica array provides about a dB higher gain than the Shirley. However, it is more notable for what it reveals about array performance in general. The longer elements result in a narrower endwise beamwidth, as shown in **Fig. 11**. The broadside beamwidth exceeds the endwise beamwidth, resulting in beamwidth ratio values greater than 1.00. Still, the values average only about 1.25:1, indicating a fairly circular NVIS pattern. In addition, because the spacing between the elements does not exceed  $1/2\lambda$ , the broadside pattern has no secondary lobes. Finally, the closer element spacing also produces maximum zenith gain heights that are very similar to those for a single dipole.

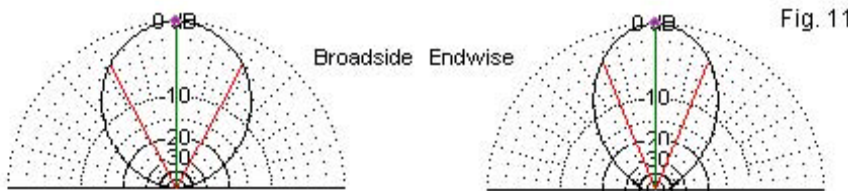


Fig. 11

Typical Broadside and Endwise Elevation Patterns  
for a Jamaica NVIS Array

As we did for the Shirley array, we may place a ground-level screen below the Jamaica array. The greater element length requires a screen enlargement. For this exercise, I used a screen that is  $1.5\lambda$  per side. All of the screens used in these notes use  $0.05\lambda$  openings. **Fig. 12** shows the general outline of the Jamaica array and its screen. The results of the modeling appear in **Table 8**.

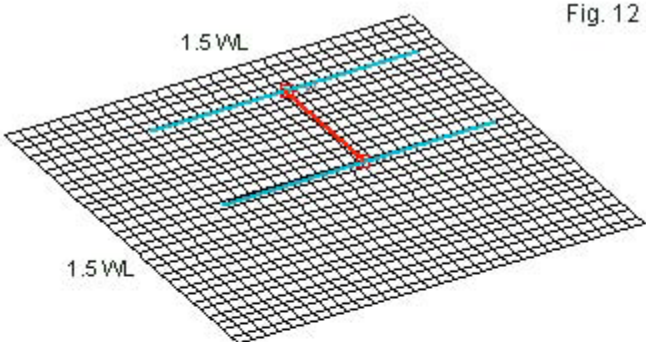


Fig. 12

Jamaica Array with Ground-Level Screen

Jamaica Array above Near-Ground Screen				Table 8
Screen: 1.5 wl Broadside x 1.5 wl Endwise	Zen Gain	BS BW	EW BW	BW Ratio
Ground				
75 Meters				
Vy Good	11.68	55.2	44.4	1.24
Average	11.63	55.0	44.2	1.24
Vy Poor	11.70	54.4	43.8	1.24
40 Meters				
Vy Good	11.67	55.2	44.4	1.24
Average	11.65	54.8	44.0	1.25
Vy Poor	11.75	54.0	43.4	1.24
Notes:	See Table 7			

The table provides no surprises. The screened array over very good soil provides very little added gain, but about 1.7 dB more gain over very poor soil. Across all soil types, the performance values are very consistent, with very poor soil showing again the highest numerical gain values. Indeed, for all implementations, the

standard lazy-H provides high-gain NVIS service compared to the basic antenna. The remaining question is whether we can further improve zenith gain without adding further elements to the lazy-H configuration.

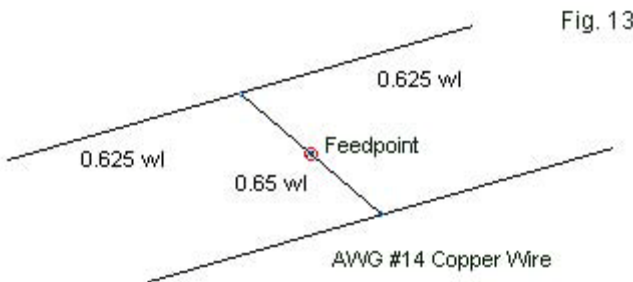


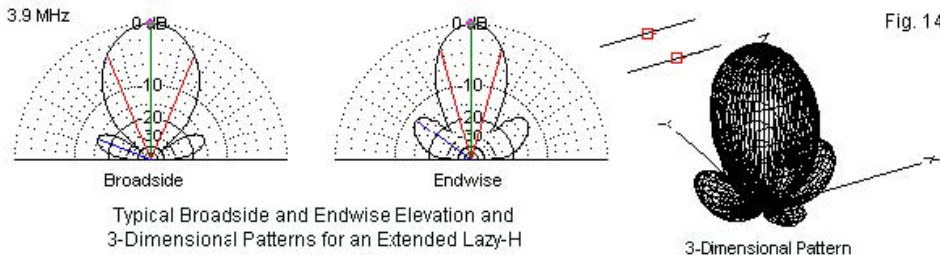
Fig. 13

General Outline: NVIS Extended Lazy-H

There is a version of the lazy-H, sometimes called the extended or expanded lazy-H, that uses  $1.25 \lambda$  elements with a spacing value of about  $0.65\lambda$  (sketched in **Fig. 13**). The individual elements are called extended double-Zepps, which provide about the maximum gain possible from a simple length extension before the pattern breaks into multiple lobes with a reduced broadside lobe. The elements are spaced as far apart as possible to yield maximum gain when fed in phase with each other. The combination produces the maximum possible broadside gain (measured from the plane of the element pair). **Table 9** provides a glimpse into the gain and other performance attributes of the extended lazy-H when pressed into NVIS service.

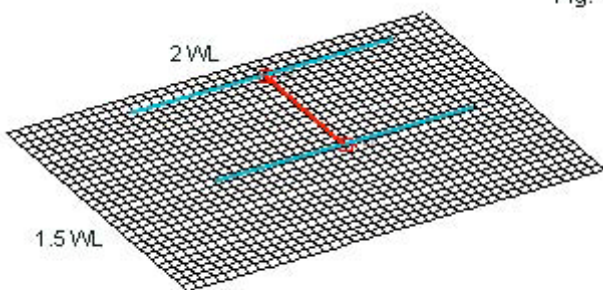
Extended Lazy-H Array							Table 9
Ground	Height wl	Height ft	Zen Gain	BS BW	EW BW	BW Ratio	
75 Meters							
Vy Good	0.210	52.96	13.45	43.8	31.3	1.40	
Average	0.225	56.74	12.68	45.0	31.6	1.42	
Vy Poor	0.230	58.01	11.66	46.2	31.8	1.45	
40 Meters							
Vy Good	0.215	29.37	13.27	44.2	31.4	1.41	
Average	0.230	31.42	12.44	45.4	31.6	1.44	
Vy Poor	0.240	32.79	11.50	46.2	31.8	1.45	
Notes:	75 Meters = 3.9 MHz; 40 Meters = 7.2 MHz						
	Zen Gain = maximum gain in dBi at zenith angle						
	BS BW, EW BW = broadside and endwise beamwidth in degrees						

The maximum zenith gain of the extended lazy-H array averages about 6 dB more than we can obtain from a single dipole. However, the antenna height at which the array reaches maximum gain averages about  $0.04\lambda$  higher than the maximum gain heights for the dipole. The increased spacing between elements explains only part of the required heights, for the extended lazy-H has the same spacing distance as the Shirley, which has lower maximum gain heights. The extended lazy-H shrinks both the broadside and endwise beamwidths to achieve its gain. As a result, it shows secondary lobes for both types of elevation patterns, as is evident in **Fig. 14**.



The patterns not only show secondary lobes along both axes, but as the 3-dimensional view of the pattern reveals, the secondary lobes are separate. An elevation pattern along an axis at  $45^\circ$  to the broadside and endwise directions would show virtually no secondary lobe structure. The strongest secondary lobe is about 12 dB lower in strength than the main lobe and would normally not constitute a problem for NVIS operation. However, strong atmospheric noise at medium elevation angles in certain (mostly endwise) directions may raise the overall background noise level. Perhaps a more interesting problem is the fact that, at the endwise half-power beamwidth angle, the communications radius is less than about 150 miles, rather than the 200-300 mile range we expect of more basic antennas. (Broadside, the radius is over 200 miles.) The situation reveals that, so long as NVIS gain comes at the expense of radiation pattern beamwidth, there are limits to the gain that we should expect from NVIS arrays.

Fig. 15



Extended Lazy-H with Ground-Level Screen

As shown in **Fig. 15**, we may place a ground level screen below the extended lazy-H. The increased element length and spacing distance of the array requires a screen that is  $2 \lambda$  endwise and  $1.5 \lambda$  broadside. As in all of the screen tests in this section, the antenna is  $0.2\lambda$  above ground. **Table 10** provides the test results.

Lazy-H Array above Near-Ground Screen				Table 10
Screen:	1.5 wl Broadside	x 2.0 wl Endwise		
Ground	Zen Gain	BS BW	EW BW	BW Ratio
75 Meters				
Vy Good	13.79	43.4	31.0	1.40
Average	13.73	43.4	30.6	1.42
Vy Poor	13.83	43.0	30.0	1.43
40 Meters				
Vy Good	13.80	43.4	30.8	1.41
Average	13.77	43.2	30.4	1.42
Vy Poor	13.90	43.0	29.8	1.44
Notes:	See Table 9			

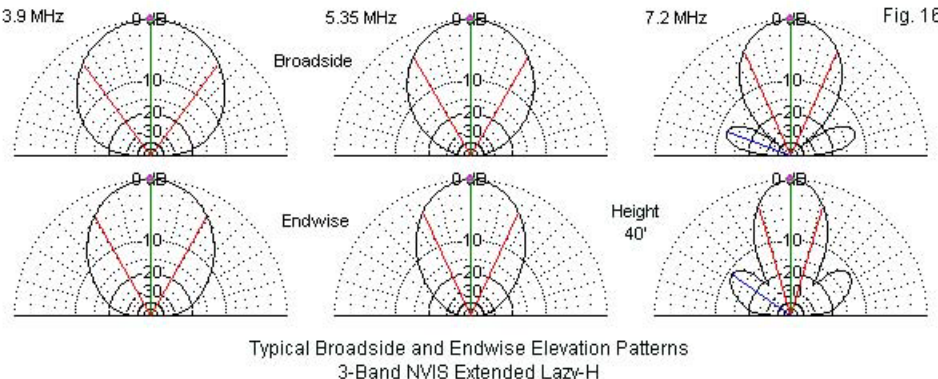
The consequences of adding an adequate ground screen below the lazy-H parallel previous results for the Shirley and Jamaica arrays. Gain improvement over very good ground is negligible, while over very poor ground, we improve gain by just over 2 dB. The gain figures are almost uniform over the range of soil qualities, with very poor soil showing its now typical numerical edge. The beamwidth values and the ratio between them show virtually no change.

The extended lazy-H has an additional potential. It provides usable gain over a 2:1 frequency ratio, counting downward from the frequency at which the elements are about  $1.25\lambda$  long. The gain, however, is not constant as we reduce the operating frequency. At lower frequencies, the elements are shorter as a fraction of a wavelength. On 60 meters, the 40-meter extended lazy-H elements are about  $0.9\lambda$  long, while on 75 meters, the length shrinks to about  $0.7\lambda$ . In addition, the space between the elements undergoes an equally proportional reduction. (For example, on 60 meters, the antenna is close to the Jamaica array proportions.) Both decreases in effective array size combine to reduce gain on the lower bands. The user question is whether the remaining gain is adequate to the mission assigned to the antenna.

**Table 11** provides data for all three bands over the surveyed soil types. As the best compromise among the bands, the antenna is set 40' above ground, which is somewhat high for 40 meters, somewhat low for 75 meters, and nearly optimal for 60 meters. However, element and spacing reductions yield lower gain on the 60-meter band than on the 40-meter band.

3-Band Lazy-H (Extended 40-Meter Lazy-H at 40°)						Table 11
Ground	Zen Gain	BS BW	EW BW	BW Ratio	Sample R	Sample X
75 Meters						
Vy Good	9.21	70.4	58.6	1.20		
Average	8.37	73.0	59.0	1.24	191	-468
Vy Poor	7.26	77.2	59.8	1.29		
60 Meters						
Vy Good	10.78	59.0	49.4	1.19		
Average	10.17	60.6	49.2	1.23	36	-35
Vy Poor	9.32	62.4	49.2	1.27		
40 Meters						
Vy Good	12.81	48.0	33.2	1.45		
Average	12.09	48.8	33.2	1.47	81	459
Vy Poor	11.24	49.0	32.8	1.49		
Notes:	75 M = 3.9 MHz; 60 M = 5.35 MHz; 40 M = 7.2 MHz					
	Zen Gain = maximum gain in dBi at zenith angle					
	BS BW, EW BW = broadside and endwise beamwidth in degrees					

As we lower the operating frequency, the broadside and endwise bandwidth values both increase, as suggested by the tabular entries. However, the rates of increase are not identical in both directions, as the beamwidth ratio values show. We may glean a further understanding of the changes by examining the broadside and endwise elevation patterns in **Fig. 16**. With the shortening of the elements and of the space between elements, the patterns for bands below 40 meters show no secondary lobes.



Of the bands covered, 75 meters shows the lowest gain. Before discounting the performance on this band, compare the values with those for a rectangle. The 40-meter extended lazy-H on 75 meters still provides an added full dB of gain.

A more significant problem perhaps is the range of feedpoint impedance values offered by the 3-band extended lazy-H. The numbers cited in the table only show the possible range and are not actual values. The actual values would depend upon the characteristic impedance, velocity factor, and length of the two phasing lines. In most cases, a 3-band extended lazy-H would employ lines running to near-ground level with a remote antenna tuner installed at that point. A parallel transmission line from the feedpoint to the equipment room may well suffer significant loss on one or more bands, especially where the reactance at the feedpoint is very high relative to the resistance.

Despite its limitations, the extended lazy-H—either as a monoband or a multi-band array—offers high gain for NVIS operations. It requires only 4 corner tall supports and possibly a short center support for the remote antenna tuner. The smaller versions of the lazy-H might also serve as monoband antennas with slightly lower gain but generally wider beamwidth values for a larger calculated communication radius. If we expect effective NVIS communications with a prescribed radius, the family of lazy-H configurations may approach the practical gain limits for NVIS work.

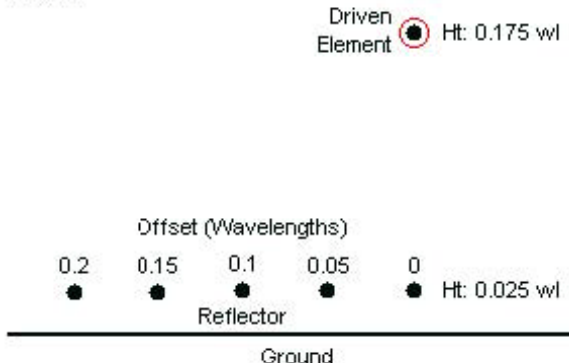
### *Tilting the NVIS Radiation Pattern*

Thus far, we have presumed that the zenith angle is best for virtually all missions. However, some stations have indicated a need for tilted NVIS patterns. The primary examples both come from near-shore locations. In one case, the goal was for maximum inland coverage; in the other instance, the aim was for over-water coverage. The design question that emerges is whether we can not only tilt the NVIS pattern, but also maintain gain directly upward at least at dipole levels.

One method that suggests itself to many is to use a dipole and reflector wire. In the third set of notes, we examined this arrangement in perfect vertical alignment to find the combination of antenna height and reflector height that provided the best performance. To tilt the radiation pattern, perhaps we need only displace the reflector wire to some position behind the driven dipole without materially altering the wire relationships relative to ground. **Fig. 17** shows the general outline of what we might do. The driver

remains fixed while we offset the reflector to various positions. Theoretically, the pattern should tilt to the right relative to the sketch.

Fig. 17

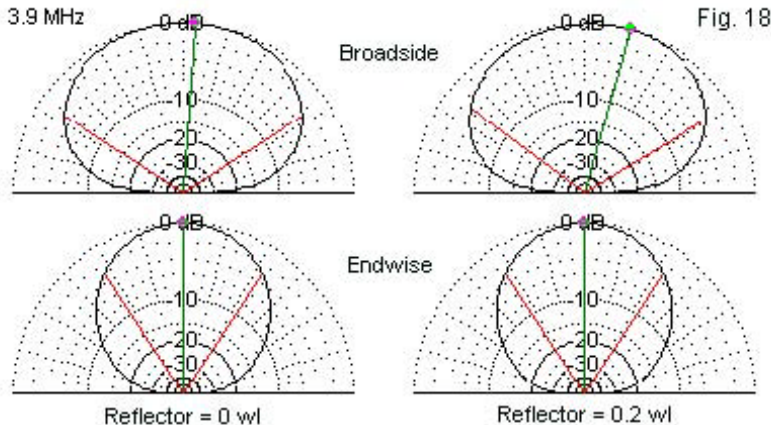


Moving the Reflector Wire to Tilt a NVIS Pattern

Unfortunately, the plan fails to account for an important fact about NVIS antennas with single element parasitic reflectors. The reflector element is only one of two major sources of radiation reflection. The ground itself is the other major reflective element, and in many ways, it can override the effects of a parasitic element. **Table 12** provides comparative results between a vertically aligned pair of elements and a driver with the reflector offset to the rear by  $0.2\lambda$ . (Intermediate positions for the reflector show intermediate results between the two parts of the table.)

Performance of Aligned and 0.2-WL Offset Dipole Plus Reflector									Table 12
Antenna at 0.175-WL			Reflector at 0.025-WL						
Ground	Max Gain	TO Angle	BS BW	Forward	Rearward	Zen Gain	EW BW	Feed R	Feed X
<i>75 Meters: Vertically Aligned</i>									
Vy Good	7.48	90	108.6	54.3	-54.3	7.48	66.2	51.27	2.40
Average	6.88	90	113.6	56.8	-56.8	6.88	66.4	52.79	0.21
Vy Poor	6.11	90	120.8	60.4	-60.4	6.11	66.8	52.62	-2.25
<i>75 Meters: Reflector 0.2-WL behind Dipole</i>									
Vy Good	7.39	80	108.2	56.1	52.1	7.34	66.4	59.32	6.09
Average	6.59	74	111.6	58.6	-53.0	6.49	66.8	65.05	1.73
Vy Poor	5.67	70	115.1	62.4	-52.7	5.42	67.6	71.21	-4.89
Notes:	Max Gain = maximum gain at TO (take-off) angle in dBi								
	BS BW = broadside beamwidth in degrees								
	Forward, Rearward = angle from zenith in degrees of forward (positive) and rearward (negative) half power (-3 dB) points								
	Zen Gain = maximum gain at the zenith (90 degree elevation) angle in dBi								
	EW BW = endwise beamwidth in degrees at the zenith angle								
	Feed R, Feed X = feedpoint impedance								

Although the offset reflector versions of the array show a take-off angle that is less than 90°, the amount of overall pattern offset is disappointingly small. Operationally, the difference would not be noticeable. **Fig. 18** compares patterns for the two cases over average ground. In effect, the reflector element cannot overcome the greater influence of the ground itself in reflecting signals straight upward.



Broadside and Endwise Elevation Patterns: Dipole + Reflector  
Vertically Aligned and Offset by 0.2-Wavelengths

The goal of having a tilted radiation pattern is significantly to reduce signal strength to a defined rearward area while preserving signal strength overhead and in the defined forward direction. One way to achieve this goal is reorient the 2-element array into a horizontal position and to place it in a relatively low position over the ground. We shall employ  $0.175\lambda$  as the beam height as a reasonable compromise height among the precisely optimum heights over each of the soil types.

Before we model a beam under these conditions, we may wish to consider which beam to use. The beam should be basic, perhaps limited to 2 elements. We might construct larger beams, but the net effect would be greater gain at lower angles, a feature that falls outside of the project specifications. We need only enough gain to

provide good signal reduction to the rear while maintaining the highest possible gain in the zenith and high-angle forward directions.

Fig. 19

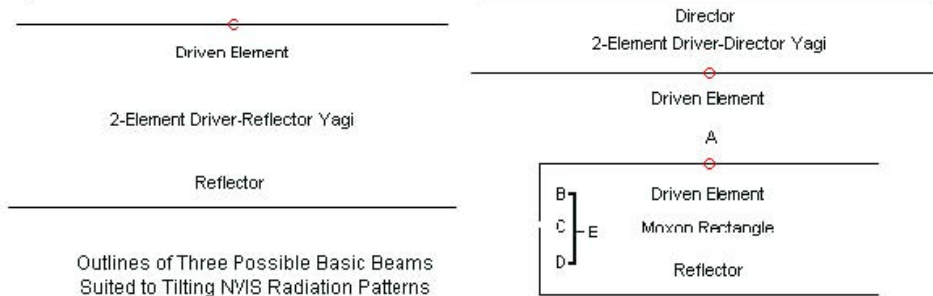


**Fig. 19** presents 3 candidate beams for the role. All happen to be parasitic beams, but one might as easily employ a 2-element phased horizontal array. The outlines are in proper proportions to each other. The driver-reflector array uses wide element spacing, while the driver-director version uses much closer spacing. The Moxon rectangle requires the least endwise space of the three beams. **Table 13** provides the 75-meter and 40-meter dimensions of each modeled beam in feet.

Table 13. Dimensions of sample beams for tilting NVIS radiation patterns

2-element driver-reflector Yagi: AWG #14 copper wire

	75 Meters	40 Meters
Reflector length	125.0'	67.48'
Driver length	120.2'	64.98'
Element spacing	50.4'	27.32'

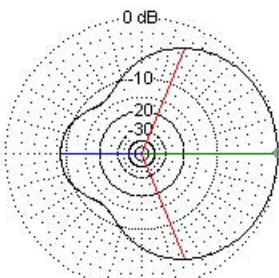
2-element driver-director Yagi: AWG #14 copper wire

	75 Meters	40 Meters
Driver length	126.1'	68.30'
Director length	121.1'	65.67'
Element spacing	20.2'	10.93'

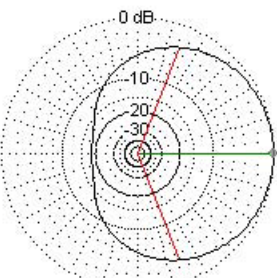
2-element Moxon rectangle: AWG #12 copper wire (see Fig. 19 for dimension designations)

	75 Meters	40 Meters
A (Endwise length)	90.86'	49.22'
B (Driver tail)	14.69'	7.95'
C (Gap)	2.44'	1.32'
D (Reflector tail)	17.66'	9.56'
E (Total broadside dimension)	34.79'	18.83'

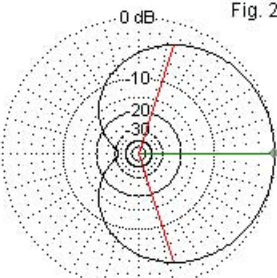
Prior to any practical modeling, we may estimate the relative probabilities among the candidates of fulfilling the radiation pattern specification. Free-space E-plane patterns, such as those shown in **Fig. 20**, provide excellent guidance in selecting a beam for the task. These patterns approximate—with the correct interpretation—the shape of the final pattern above ground, with adjustments for ground reflections.



2-Element Driver-Reflector Yagi



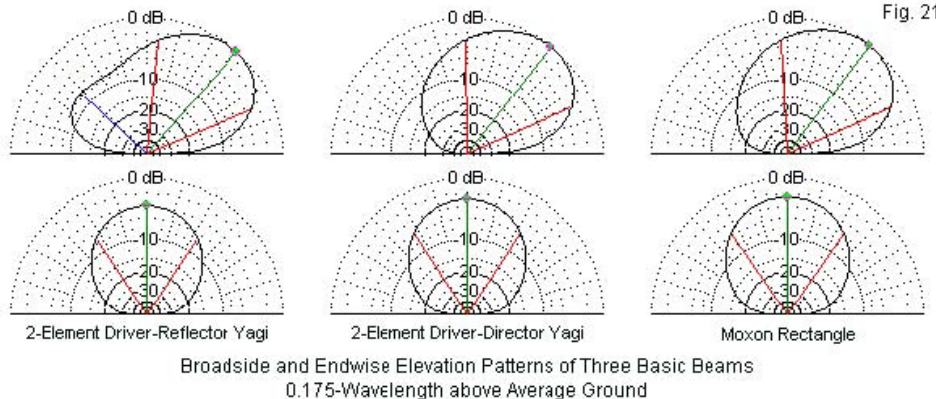
2-Element Driver-Director Yagi



Moxon Rectangle

Free-Space H-Plane Patterns of Three Basic Beams  
Suited to Tilting NVIS Radiation Patterns

The driver-reflector Yagi shows a narrower beamwidth than the other beams. As well, its shape shows less width along the plot's vertical axis. In contrast, the driver-director Yagi and the Moxon rectangle have wider beamwidths and more gain along the plot's vertical axis. These rapidly read comparisons will translate into distinctive features in patterns over real ground. **Fig. 21** presents samples of the broadside and endwise patterns of each beam at a height of  $0.175\lambda$  above average ground.



The upper row of patterns provides broadside views of the radiation patterns. The two more promising beam designs show less medium-angle gain to the defined rearward side of the antenna. In contrast, the driver-reflector Yagi has a considerable rearward elevation lobe. The lower row of patterns are the endwise plots at the zenith angle, with the limit of the plot scaled to the overall maximum gain of each beam. In all cases, the maximum gain is greater than the zenith gain. Of the three candidates, the driver-reflector Yagi has the weakest zenith gain compared to its maximum gain. The driver-director Yagi and the Moxon rectangle show only small differences in the relative strength of zenith gain.

The remaining step is to compare numerical data to determine if there is a clear winner among the three candidate beams. **Table 14** supplies the values for both 75 and 40 meters.

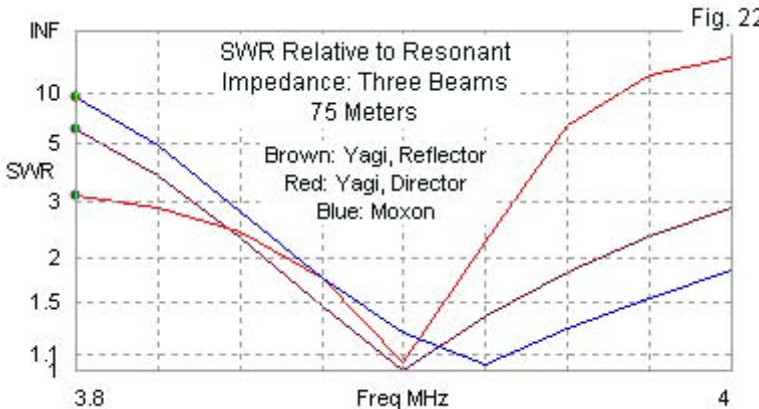
Performance of 2-Element Beams 0.175-WL above Ground								Table 14		
Driver-Reflector Yagi		Max Gain	TO Angle	BS BW	Forward	Rearward	Zen Gain	EW BW	Feed R	Feed X
<b>75 Meters: 3.9 MHz</b>										
Vy Good	8.81	51	61.7	65.5	3.8	5.22	66.4	34.40	1.80	
Average	8.01	49	61.3	66.9	5.6	4.10	66.8	39.99	0.14	
Vy Poor	7.04	46	61.0	69.1	8.1	3.69	67.6	46.94	-2.76	
<b>40 Meters: 7.2 MHz</b>										
Vy Good	8.72	49	60.4	66.2	5.8	4.73	66.6	43.20	2.82	
Average	7.74	48	60.3	67.6	7.3	3.49	66.4	39.63	-0.11	
Vy Poor	6.70	45	60.6	69.7	9.1	2.12	67.0	45.76	-2.98	
Driver-Director Yagi		Max Gain	TO Angle	BS BW	Forward	Rearward	Zen Gain	EW BW	Feed R	Feed X
<b>75 Meters: 3.9 MHz</b>										
Vy Good	8.49	55	68.7	64.6	-4.1	6.03	66.1	31.83	-4.31	
Average	7.76	52	67.5	66.4	-1.1	4.91	66.3	30.99	-1.31	
Vy Poor	6.80	48	66.2	68.9	2.7	3.43	66.8	29.93	1.78	
<b>40 Meters: 7.2 MHz</b>										
Vy Good	8.53	52	65.6	65.6	0.0	5.53	66.2	25.39	0.80	
Average	7.62	50	65.2	67.3	2.1	4.30	65.8	25.71	1.86	
Vy Poor	6.59	47	64.7	69.6	4.9	2.85	66.4	25.41	4.33	
Moxon Rectangle		Max Gain	TO Angle	BS BW	Forward	Rearward	Zen Gain	EW BW	Feed R	Feed X
<b>75 Meters: 3.9 MHz</b>										
Vy Good	8.62	56	70.5	63.8	-6.7	6.47	68.8	36.36	-9.54	
Average	7.87	53	69.1	65.7	-3.4	5.32	69.2	41.04	-8.40	
Vy Poor	6.90	49	67.5	68.4	0.9	3.78	70.4	47.31	-7.21	
<b>40 Meters: 7.2 MHz</b>										
Vy Good	8.49	55	70.1	64.3	-5.8	6.23	69.0	37.74	-3.19	
Average	7.58	52	69.1	66.2	-2.9	4.96	68.8	43.05	-2.91	
Vy Poor	6.55	49	68.3	68.8	0.5	3.48	69.8	49.12	-2.08	
Notes:	Max Gain = maximum gain at TO (take-off) angle in dBi									
	BS BW = broadside beamwidth in degrees									
	Forward, Rearward = angle from zenith in degrees of forward (positive) and rearward (negative)									
	half power (-3 dB) points									
	Zen Gain = maximum gain at the zenith (90 degree elevation) angle in dBi									
	EW BW = endwise beamwidth in degrees at the zenith angle									
	Feed R, Feed X = feedpoint impedance									

The maximum gain varies by only a small amount among the three beams for any given frequency and soil quality. Where we find more important differences is in the zenith gain columns, with the

Moxon providing the strongest values. (However, the margin is not so great as to rule out use of the driver-director Yagi.) As well, the wider free-space beamwidth of the Moxon translates into rearward half-power points that extend over most soils just to the rear of the zenith angle, thereby assuring adequate radiation in the immediate vicinity of the antenna location. (Negative values in the rearward column indicate radiation to the rear within 3 dB of maximum gain within the specified angular distance. A positive value in this column indicates that the –3-dB point occurs forward of the zenith angle.)

In fact, all three candidate beams (and many other basic arrays that we might select for the task) tilt the pattern in the defined forward direction. The driver-director Yagi and the Moxon rectangle provide better reduction of signal strength to the rearward areas. The numbers and the pattern shapes that we have so far observed do not quite complete the information that we need in order to make a decision.

The wide spacing of the elements in the driver-reflector Yagi assures a broad SWR bandwidth (relative to the resonant impedance). The Moxon rectangle also has a relatively wide SWR bandwidth. However, on 75 meters, as shown by the superimposed SWR curves in **Fig. 22**, the driver-director Yagi reveals its typically narrow operating bandwidth. Unlike 2-element arrays with reflectors, the presence of the director reverses the SWR trend so that it rises more steeply above the resonant frequency than below it. Nevertheless, the region with an SWR of less than 2:1 is scarcely 60 kHz wide.



On 40 meters, we find a similar situation, as revealed by **Fig. 23**. The wide-spaced driver-reflector Yagi and the Moxon rectangle have relatively wide operating bands. The values are not as great as would be the case for a single linear dipole, but they are wide enough to allow easy tuning of the arrays to the SSB portions of the band. On both bands, the Moxon bandwidth is slightly greater than the driver-reflector Yagi bandwidth. In contrast, the driver-director Yagi SWR bandwidth is not wholly adequate to cover the upper half of the 40-meter band. Adjusting the narrow-spaced Yagi for both the correct frequency and optimum performance might be a somewhat daunting task.

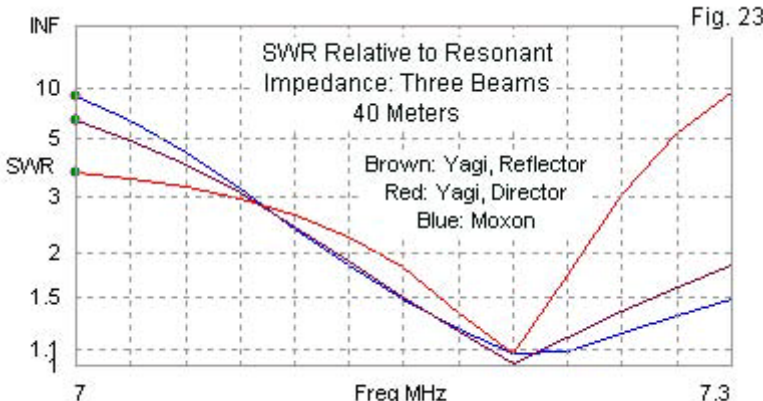


Fig. 23

If we add up the total information provided by the models, then the Moxon rectangle might be the best candidate for pattern tilting among the three candidates. However, our samples have covered only some of the possible directional antennas that we might consider in this regard. Nevertheless, the goals definitely rule out tilting vertically aligned arrays. Low horizontal directional arrays of the types considered hold the most promise of performing well in this specialized task.

Before we close the book on the Moxon rectangle, let's add one more test by placing a  $1\text{-}\lambda$ by $1\text{-}\lambda$  near-ground screen below it, similar to tests that we have performed with other antennas in this overall collection of notes. Since the dimensions of the Moxon rectangle are modest, when measured in terms of wavelengths, the smaller screen—outlined in **Fig. 24**—will suffice.

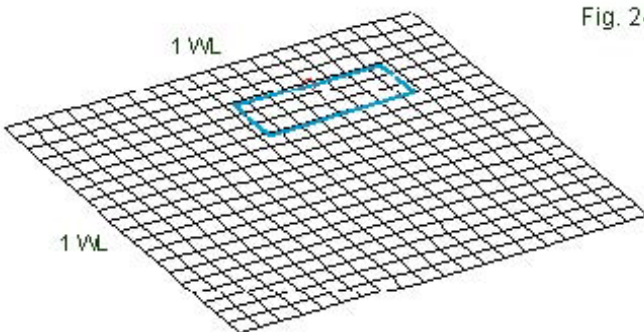


Fig. 24

Moxon Rectangle with a Ground-Level Screen

The results of our test appear in **Table 15**, which may hold a surprise for the unwary. In all other tests, we found that the gain over very poor soil exceeded the gain over other soils with the screen in place. While this trend holds true for the zenith gain values, it does not hold true for the maximum gain values.

Maximum gain at the take-off angle involves ground reflection not only in the immediate vicinity of the antenna, but also well beyond the screen limits in the forward direction. As a result, some major components of the reflected rays that combine with the incident rays are reflected from bare soil and hence show heavier losses. The amounts are not operationally significant, but are just enough to show up in the lack of parallelism between the progressions of maximum gain and zenith gain values.

Performance of a Moxon Rectangle with a 1-WL by 1-WL Ground-Level Screen								Table 15	
Ground	Max Gain	TO Angle	BS BW	Forward	Rearward	Zen Gain	EW BW	Feed R	Feed X
<b>75 Meters: 3.9 MHz</b>									
Vy Good	8.87	57	72.1	63.4	-8.7	6.94	68.2	34.57	-9.65
Average	8.70	57	73.0	64.1	-8.9	6.81	67.2	35.41	-8.08
Vy Poor	8.56	59	75.6	64.8	-10.8	6.92	65.2	35.60	-6.71
<b>40 Meters: 7.2 MHz</b>									
Vy Good	8.89	57	72.1	63.5	-8.6	6.96	68.0	34.96	-3.23
Average	8.71	58	73.5	64.1	-9.4	6.90	66.6	35.80	-1.72
Vy Poor	8.64	60	75.6	64.4	-11.2	7.06	54.4	35.82	-0.50
Notes:	Max Gain = maximum gain at TO (take-off) angle in dBi								
	BS BW = broadside beamwidth in degrees								
	Forward, Rearward = angle from zenith in degrees of forward (positive) and rearward (negative)								
	half power (-3 dB) points								
	Zen Gain = maximum gain at the zenith (90 degree elevation) angle in dBi								
	EW BW = endwise beamwidth in degrees at the zenith angle								
	Feed R, Feed X = feedpoint impedance								

Apart from the small surprise in numbers, the Moxon's performance over a sufficiently large ground screen is remarkably consistent across the entire span of soil qualities. As in virtually all other trials, the screen has negligible effect over very good soil, makes a marginal improvement over average soil, and improves performance noticeably over very poor soil. As always, its implementation depends not only upon soil quality, but as well upon the time, energy, and monetary resources available for the antenna installation.

### Conclusion

In our exploration of some special purpose NVIS antennas, we have had occasion to suggest the use of some antenna types not usually considered by radio amateurs (or many others): rectangles, extended lazy-Hs, and horizontal beams. The special needs that we have explored may not match the special needs of your

particular installation. However, they do illustrate that fact that the possible antennas for NVIS operations go well beyond the basic dipole, inverted-V, and square or diamond loop. For every need, there likely is an antenna type that we can adapt to the application.

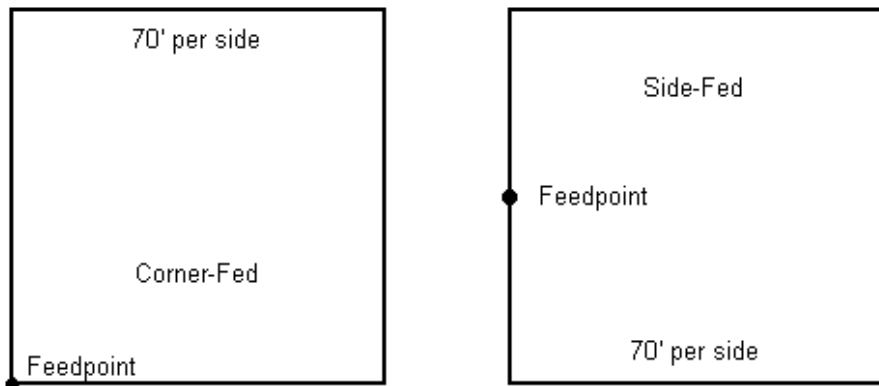
These notes have not covered all possible special needs. One fairly obvious omission is the need for rapid frequency changes, such as those demanded by automatic link establishment (ALE) techniques. Antennas to meet these needs, such as terminated antennas with relatively constant feedpoint impedance values over a very large frequency range, are the subject of extensive notes elsewhere at this site. The gain deficits that are inherent in these antennas have spurred investigation in two directions. One is the development of an antenna without the loss of gain but with the uniform feedpoint impedance. The other is the employment of high-speed antenna tuner switching to allow the use of common antennas with higher gain to do the job. In addition, for non-military, non-governmental applications, such as the wide range of type of emergency communications, the situation has raised the question of whether we need frequency change times in the microsecond range or whether we might ably use change times in milliseconds, of which many ATUs are capable.

Moreover, we have not addressed the special needs of mobile and field antennas. Many new commercial offerings are appearing in this arena, and a few of them actually offer some incremental improvements. Obviously then, these scant closing notes only function to say that the subject of NVIS antennas is far from

concluded with this set of observations on special purpose NVIS antennas.

## Chapter 70: All-Band Horizontal-Plane Loops

To set a contrast with the vertical-plane (VP) loops (covered in another note in this series on vertical-plane deltas), I made a couple of models of 80- meter 4-sided horizontal-plane (HP) loops, each 70' per side to bring them close to resonance in the 80-meter band. One I fed at a corner; the other a fed mid-side. The loops are at 35' up over medium earth and are #12 copper wire.



Top views of two ways to feed a horizontal-plane loop

The general summary is this: on 80, either loop is a cloud burner, but with pretty good gain at 45 degrees elevation. In general, except for 40 meters, the corner-fed loop shows more bi-directional patterns (with minor side lobes), mostly through the corners where

the feedpoint is the backside. On bands from 20 meters, there is up a slight (3-4 dB) front-to-back ratio.

Fed on one side (rather than at a corner), there is a tendency for the antenna to exhibit more lobes per band, with those to the far side from the feedpoint being slightly stronger--again by no more than 2-4 dB.

Both the corner-fed and the side-fed antennas, as the charts will show, represent easy work on an antenna tuner, with very reasonable values of R and X. Indeed, a 300- ohm line will likely show the smallest excursions of R and X along the line length, although 450-ohm line is perfectly good as well. From the values in the chart, line length should not be critical.

In the charts below, all maximum gain figures use the TO angle (elevation angle of maximum radiation) except for 80 meters, whether the gain is at a 45-degree TO angle.

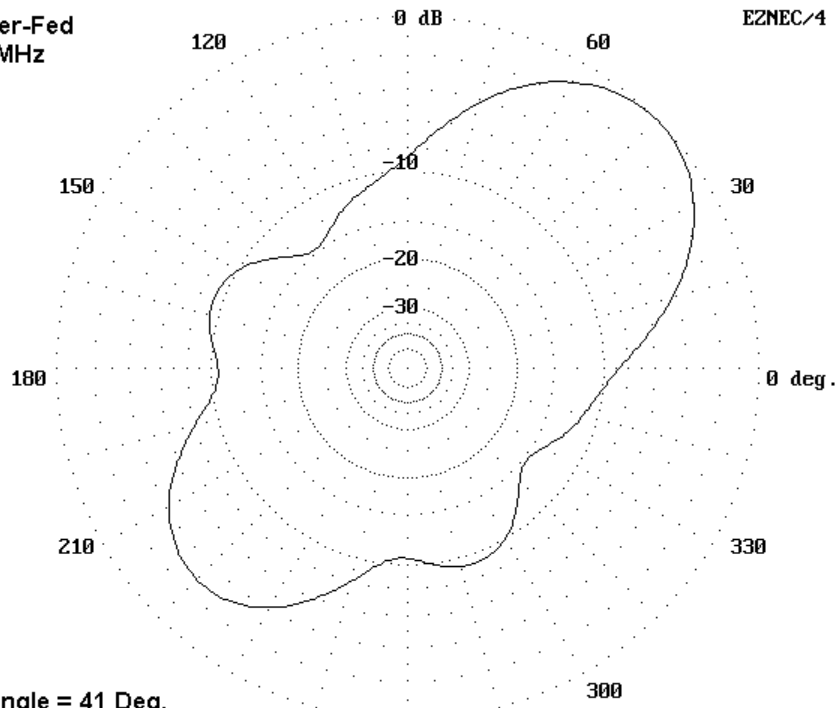
1 wl loop (70'/side), corner-fed: #12 copper 35' up over medium earth:				
Freq.	TO angle	Max Gain	Feed Z	Pattern notes
MHz	degrees	dBi	R+/-jX	
3.58	90	5.16@45	67 +j 4	oval thru corners
7.1	48	5.69	84 -j150	oval across corners
10.1	41	9.32	370 -j575	narrow oval thru corners
14.1	27	10.51	305 -j105	clover leaves thru corners
18.1	20	13.75	350 +j240	EDZ-like thru corners
21.1	17	13.63	245 -j105	clover
24.95	14	14.09	320 +j110	thru crnrs w/side lobes
28.1	12	12.92	225 -j145	12 lobes

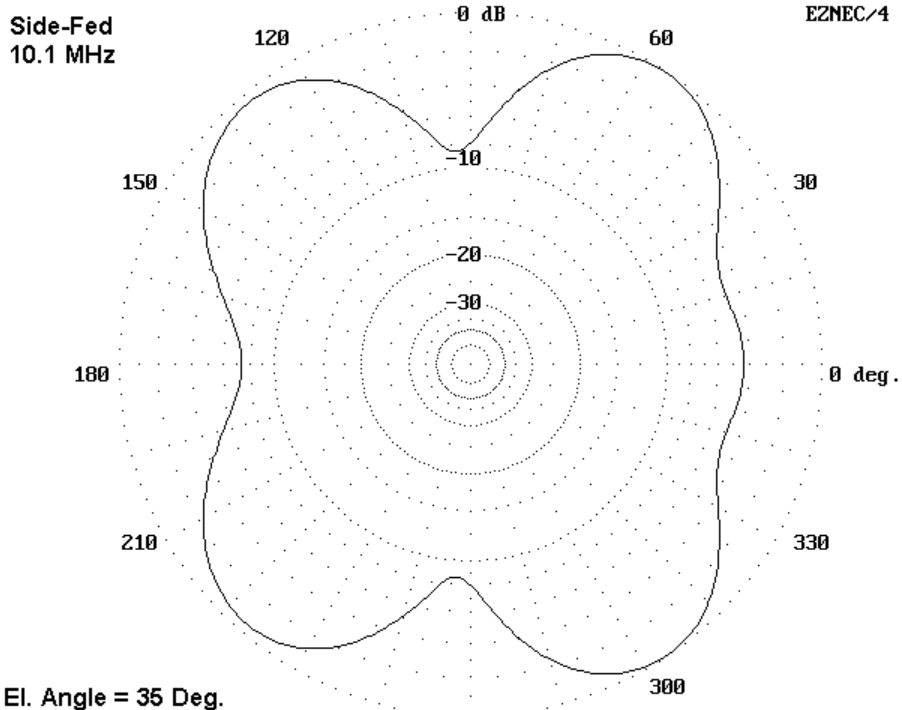
1 wl loop (70'/side, side-fed:) #12 copper 35' up over medium earth:				
Freq.	TO angle MHz	Max Gain degrees	Feed Z dBi	Pattern notes
3.58	90	5.09@45	65 +j 4	oval thru sides
7.1	44	6.73	275 +j130	oval thru sides
10.1	35	6.86	285 -j535	lobes at corners
14.1	27	9.69	265 -j165	4 lobes at corners
18.1	21	11.65	400 +j180	6 lobes, strng=far side
21.1	18	10.61	400 -j120	many lobes, strng=far side
24.95	15	11.08	370 +j 45	many lobes, strng=far side
28.1	11	11.83	250 -j180	many lobes, strng=far side

The side-fed shows slightly less max gain on the upper bands, but has more stronger lobes other than the corner-fed version. If the pattern notes can be deciphered, you can choose whichever suits your operating desires most.

To assist in interpreting the brief pattern notes, the following azimuth patterns of corner-fed and side-fed HP loops at 10.1, 21.1, and 28.1 MHz may be useful. For each pattern, the antenna is a square aligned with the graphic borders. The corner-fed model is fed at the lower left corner of the graphic. The side-fed model is fed at the middle of the left side.

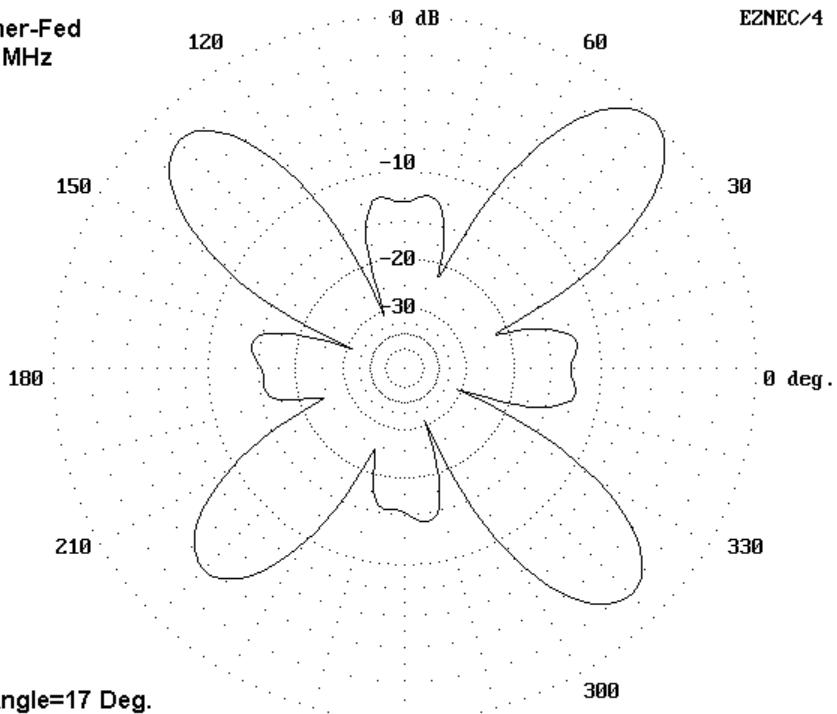
Corner-Fed  
10.1 MHz

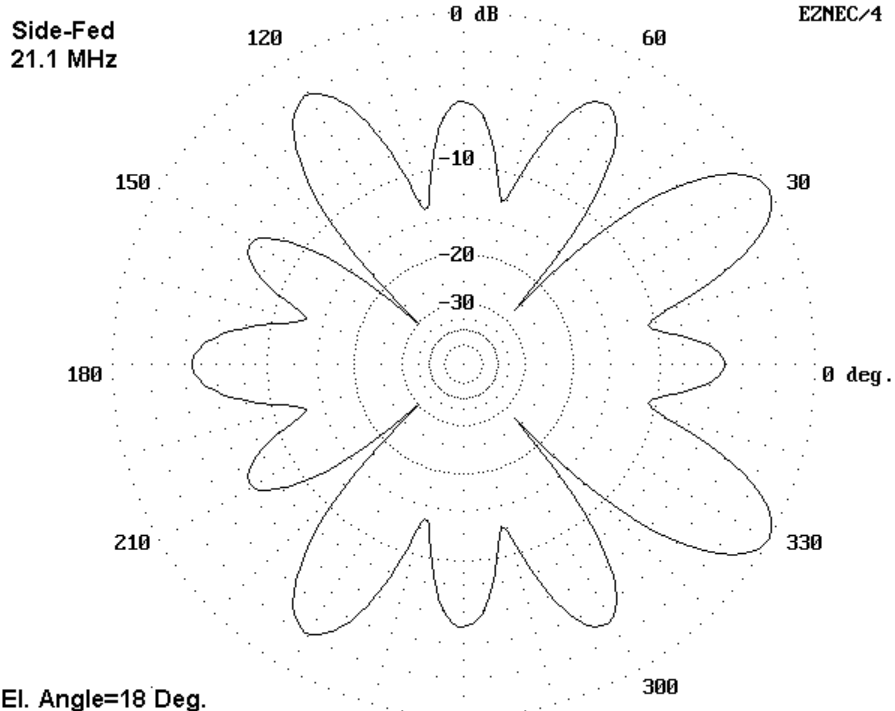




The 10.1 MHz patterns show the most unique differences, with the corner-fed model having a beam-like pattern, while the side-fed model pattern is somewhat non-descript but more omni-directional.

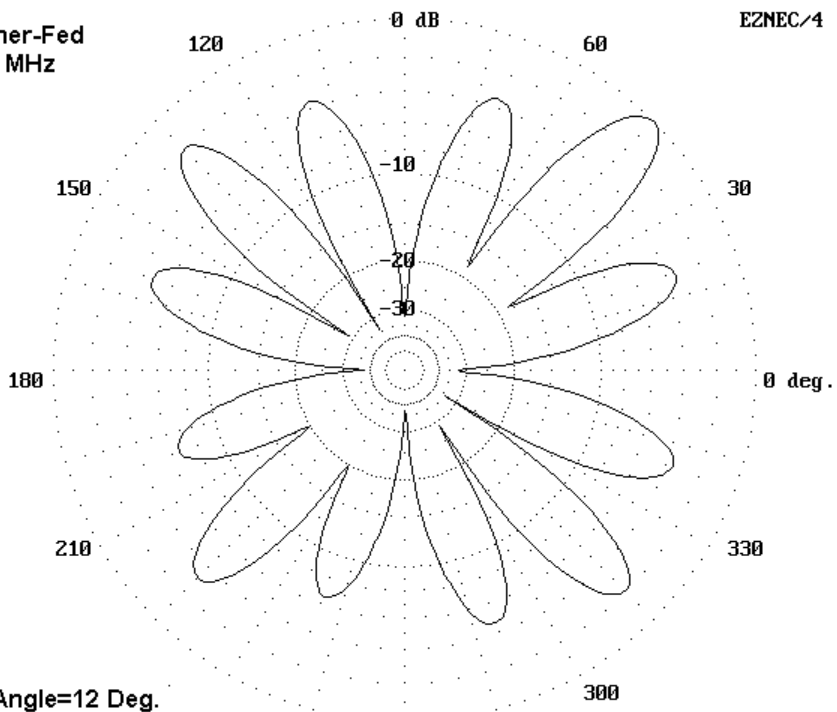
Corner-Fed  
21.1 MHz

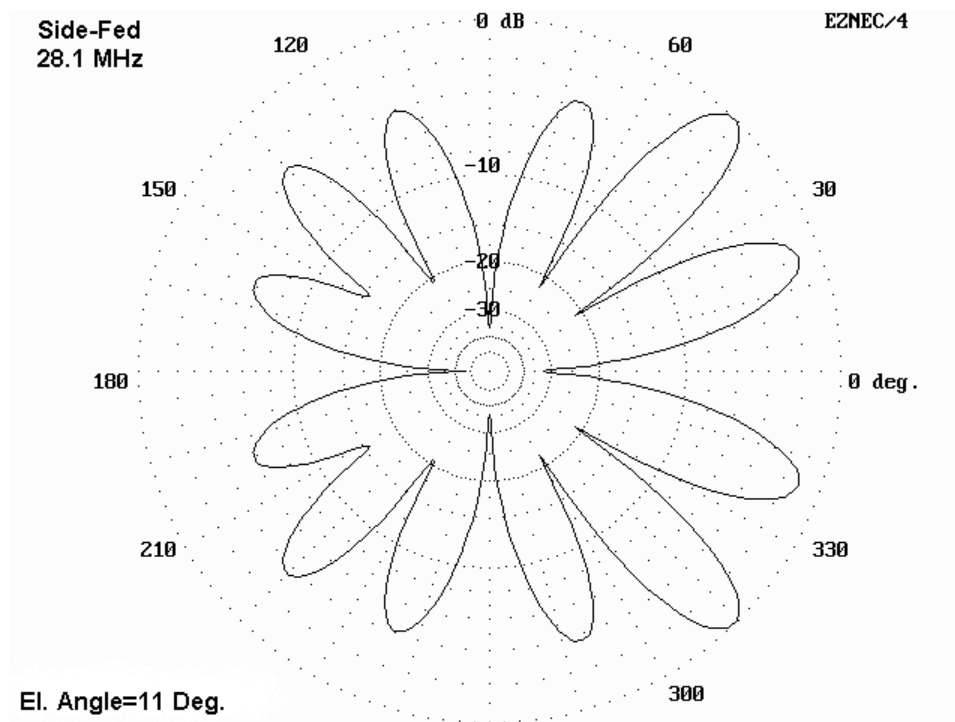




At 21.1 MHz, the side-fed model shows much broader lobes, while the energy from the corner-fed model is concentrated in 4 fairly narrow lobes.

Corner-Fed  
28.1 MHz





By the 10-meter band, there is little to choose from between the two antennas.

As a general rule, the horizontal loop offers more directions, especially in the side-fed version, than the single wire, which concentrates its energy more toward the ends as the frequency goes up. A compendium of patterns for 135' doublets and for 102' doublets appears in notes taken from the series done for *Low*

*Down.* The loop has fewer bands with problematical impedances than any of the doublets.

For all-band use, the HP loop seems to offer more than the VP loop. The HP loop elevation angles are close to those of a single wire doublet, which places them lower and stronger than those for a VP loop. In general, with either mode of feeding, expect strongest results in the quadrants across the way from the feedpoint.

## Chapter 71: A 40-Meter Star-Shape Loop

The horizontally oriented 1-wavelength square loop is a fairly standard low-HF amateur antenna. It lends itself to use with parallel feedline for multi-band application. However, a 1-wavelength loop tends to radiate broadside to the loop. Therefore, the antenna tends to provide better performance on bands above the lowest.

### The Standard Square and the 4-Pointed Star Loops

The need for a longer circumference is often at odds with amateurs who have only limited space for wire antennas on the lower HF bands. However, one way to increase the circumference of a loop without increasing its footprint is to draw in the 4 sides of the loop toward the center. The result is a 4-pointed star configuration. **Fig. 1** shows the difference between the standard and star loops, as viewed from above (or below, as the case may be).

**Comparison of a Standard 4-Sided Horizontal Loop  
and a 4-Pointed Star Alternative**

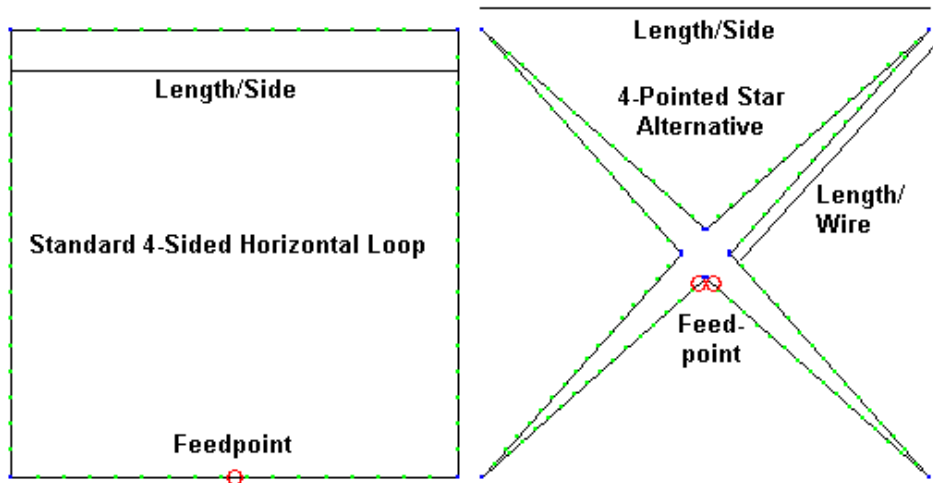


Fig. 1

**Fig. 1** also provides us with a key to the main dimensions of the loop and the star. The length of a side for a square horizontally oriented loop is also the length of one side of its footprint. For the 40-meter (7.15 MHz) test case, each side of the loop is about 36.2' long for a near resonant loop. This provides an antenna and a footprint circumference of 144.8' or about 1.05 wavelengths at 7.15 MHz for a near-resonant loop. On the right side of **Fig. 1** is the star. Here, we must distinguish between the wire length and the footprint. For a near resonant loop, we require a footprint side dimension of about 31.9', which results in a footprint circumference

of 127.6'. This dimension set is actually smaller than for the square loop. However, as shown in the sketch, each wire is stretched inward toward the center. We cannot make the wire touch at the center, but we can come in rather close. The most radically inset case that I have so far explored positions the apex of each angle formed from the side wires at 1.75' from the antenna center. This yields a distance of about 3.5' between opposing points. The resulting wire length for each side of each point in the star is about 21.35'. The total wire circumference thus becomes about 170.8' or close to 1.25 wavelengths.

We can compare the potential performance of the two configurations on 40 meters via the following table of modeled results.

.....  
Square and Star Loop Performance at 7.15 MHz

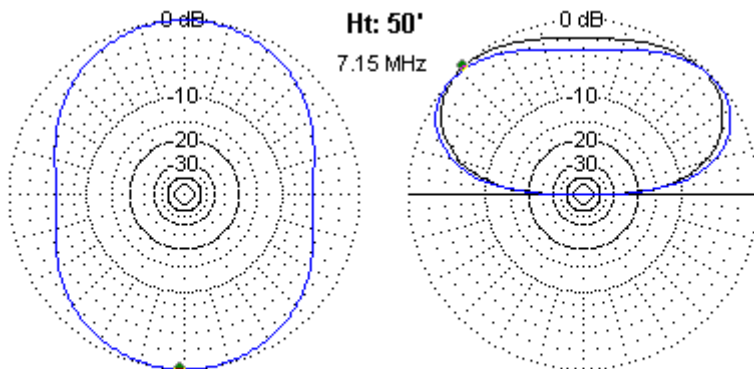
Antenna Height 50'. Antenna Wire AWG #12 copper. "Insets" refers to the distance of the limit of the star side inset point from the exact center of the array.

	Gain dBi	El. Angle Degrees	Feed Z R +/- jX Ohms
Square	5.54	47	157.5 - j 6.3
Star: 1.75' insets	5.50	39	65.7 + j 9.0
Star: 2.0' insets	5.50	39	66.8 + j12.0
Star: 3.0' insets	5.50	40	71.1 - j 0.6

.....

Several aspects of the tabular data are significant. First, the 40-meter gain of the two versions of the loop is virtually the same. However, the elevation angle of maximum radiation is considerably

lower in the star version. **Fig. 2** graphically illustrates these matters by showing the two azimuth patterns, each at its respective TO angle, to exactly overlay each other. However, the elevation pattern of the star along the axis of maximum radiation has a noticeably lower angle of maximum radiation (take-off or TO angle).



Az. & El. Patterns: 40-M Loop and Star

Black = Loop; Blue = Star

Fig. 2

Second, if operation is contemplated only on 40 meters, then the impedance of the star configuration is suitable for a coaxial cable as the feedline. Either 50-Ohm or 75-Ohm cable will do. For similar operation, the square configuration would require either the use of a parallel feedline or the use of a 4:1 balun with a 50-Ohm coaxial cable feedline.

Third, the star configuration is not especially sensitive to just how far toward the array center we push the insets. The distances from

center shown may be doubled to see how far apart we may place the inner points of the star. There is considerable room for variation before we lose our advantage over the square loop in terms of TO angle. However, note that the 3.0' inset has bumped the TO angle upward one notch. As we further move the inner start points away from center, the antenna slowly returns to the characteristics of a simple square loop.

The principle behind the star is an attempt to increase its wire circumference length without increasing its footprint. The 0.2-wavelength increase, while not giving us the almost pure edge-wise radiation of a 2-wavelength loop, does raise the entire wire length in the star loop to 1.25 wavelengths. That much length is sufficient to lower the 40-meter radiation angle by a noticeable amount.

## The Square Loop as a Multi-Band Wire Antenna

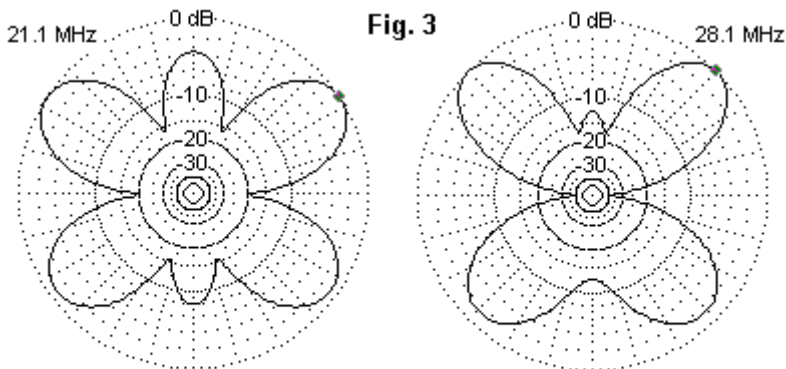
The square loop allows us to feed the antenna on higher bands, relative to the base-line 40-meter band to which we have cut it. We can summarize the performance with the following tabulated samples for the HF bands.

## 40-Meter Square Loop Performance

Antenna Height: 50'. Antenna Wire AWG #12 copper.

Freq. MHz	Gain dBi	TO angle Degrees	Feed Z R+/-jX Ohms	Pattern Shape
7.15	5.5	47	160 - j 6	Oval
10.125	4.8	32	3060 + j 3140*	Almost square
14.1	8.5	19	275 + j 120	4-leaf clover
18.1	7.2	16	1035 + j 1480*	wobbly oval
21.1	8.7	13	255 + j 55	4 main lobes, 60 degrees off axis
24.95	8.0	11	1230 - j 1380*	6 near-equal lobes
28.1	10.8	10	265 + j 115	4 lobes 45 degrees off axis

With exceptions, the patterns generally are strongest in a line through the feedpoint and the corresponding center point of the wire opposite. We may call this the main axis of the antenna. On two bands of high interest, however, the patterns depart from the noted tendency.



**40-Meter Standard Square Horizontal Loop:  
Two Bands with Irregular Azimuth Patterns**

**Fig. 3** shows the azimuth patterns of the square loop on 15 and 10 meters, with the axis presumed to run vertically on the page. The 15-meter pattern forms a sort of butterfly, with small lobes along the antenna axis. However, the strongest lobes are angled to the sides by about 60 degrees. The 10-meter pattern has only 4 notable lobes, each about 45 degrees off axis.

We may also note in passing the starred entries in the feedpoint impedance (Feed Z) column. Each of the non-harmonic bands presents an impedance where the resistance and the reactive components are both above 1000 Ohms. Without careful attention to the characteristic impedance and length of the parallel feedline used, the impedance at the antenna tuner terminals may fall outside the range of values that it can match.

## The 4-Pointed Star Loop as a Multi-Band Antenna

We may perform the same modeling experiment with the 4-pointed star loop to evaluate its potential as a multi-band antenna for 40-10 meters. The results appear in the following table.

40-Meter Star Loop Performance

Antenna Height: 50'. Antenna Wire AWG #12 copper.

Freq. MHz	Gain dBi	TO angle Degrees	Feed Z R+/-jX Ohms	Pattern Shape
7.15	5.5	39	65 + j 10	Oval
10.125	6.7	26	6820 - j 7650*	Diamond
14.1	9.3	19	540 + j 1850*	4-leaf clover
18.1	6.9	16	925 + j 75	Broad beam: F-B 5.2 dB
21.1	6.2	13	945 - j 1270*	Broad beam: F-B 1.3 dB
24.95	6.8	11	55 + j 340	Broad beam: F-B 2.5 dB
28.1	6.9	10	715 - j 670	Triple forward lobes

For the entries called "Broad beam," the direction of maximum gain is toward the side of the star containing the feedpoints. If we overlay the outline of the antenna on top of the azimuth patterns in **Fig. 4**, the feedpoint will be above the plot center line across the page.

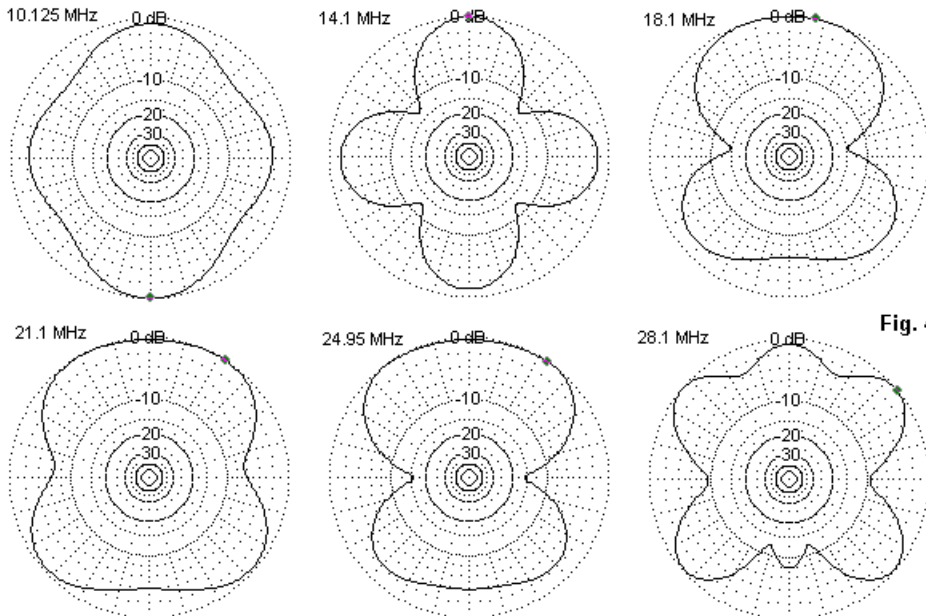


Fig. 4

**4-Pointed Star Loop: Representative Azimuth Patterns for Bands Above 40 Meters**

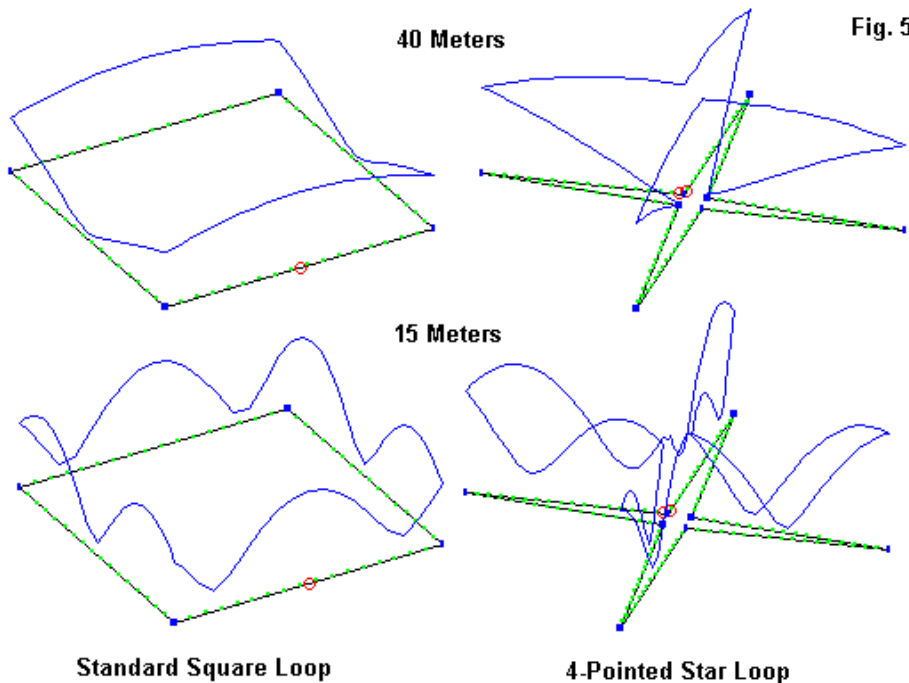
The patterns show one potential advantage of the star as a multi-band antenna. On all bands, there is a main lobe along the antenna axis through the feedpoint. Hence, the user is always aware of the direction of strongest signal. (30 meters is the one exception, but the main lobe to the reverse of the feedpoint side is only 0.7 dB stronger than on the feedpoint side, a difference that will not be detectable in operation.) Although the beam action--that is, having a small front-to-back ratio--is small, the reliability of having the main lobe along the same axis on every band used is a distinct plus.

There are three bands on which the reactance rises above 1000 Ohms. However, only on 30 meters are the values for both resistance and reactance so high as to create a very distinct problem for matching the feedline termination to the transceiver 50-Ohm system.

## Why?

The distinctness of the square loop and the star loop patterns should arouse some curiosity as to the reason for the differences.

**Fig 5** provides a partial answer.



**Two Representative Comparisons of Current Magnitude Distribution  
Along the Wires of the Two Types of Loops**

The upper diagrams compare the relative current magnitude distribution of the two loops on 40 meters. The current on the star remains higher further outward toward the array corners than on the square loop, and this phenomenon plays a role in lowering the elevation angle of maximum radiation (the take-off or TO angle).

Otherwise, the gain and pattern shape of the 2 versions of the loop are the same.

The 15-meter case is especially interesting. For the star loop, the current magnitude peaks and valleys appear in close proximity along the outward star-point wires. Hence, the currents (or, more properly, the fields that result) tend to simply add to or subtract from each other-- with due place given to the phase of each current magnitude sampled. However, in the square loop, we have current magnitude peaks more linearly separated from each other, with distinct peaks at the four corners of the array. The result is the 6-lobes pattern, with the largest lobes at a considerable angle from the axis of the antenna.

These brief notes suggest that for some users of square loops, modification to a star design may be useful. The array dimensions for 40 meters will easily scale to 80 and 160 meters, although most users will have difficulty in scaling the height as well as the wire length. Since we are only approximating resonance on the lowest band of use and presuming parallel feedline to an antenna tuner, fussiness with dimensions seems out of place. Since the wire of the antenna has a small diameter relative to a wave length, any 50-Ohm resonance on the lowest band of use is likely to be a very narrow-band phenomenon.

Nonetheless, for the loop-user who wishes a lower TO angle on the lowest band of use and a pattern that has a maximum along the axis of the antenna on every band used, the 4-point star is viable alternative to the standard square loop. The cost is less than 20%

more wire, which is likely to be the cheapest part of the antenna anyway. The star loop is not an answer to every loop problem. However, it does show that it pays to explore different wire geometries to see whether they have any potential for use.

## Chapter 72: Horizontally Oriented & Polarized Big Wire Loops

**L**arge wire antennas are deservedly popular among QRP operators who have room for them. They are cheap and effective: the two favorite words among hams.

Among the more usable of the large wire antennas is the loop that is at least 1 wl long at the lowest frequency of operation. However, large loops belong to three different families, each with distinct characteristics.

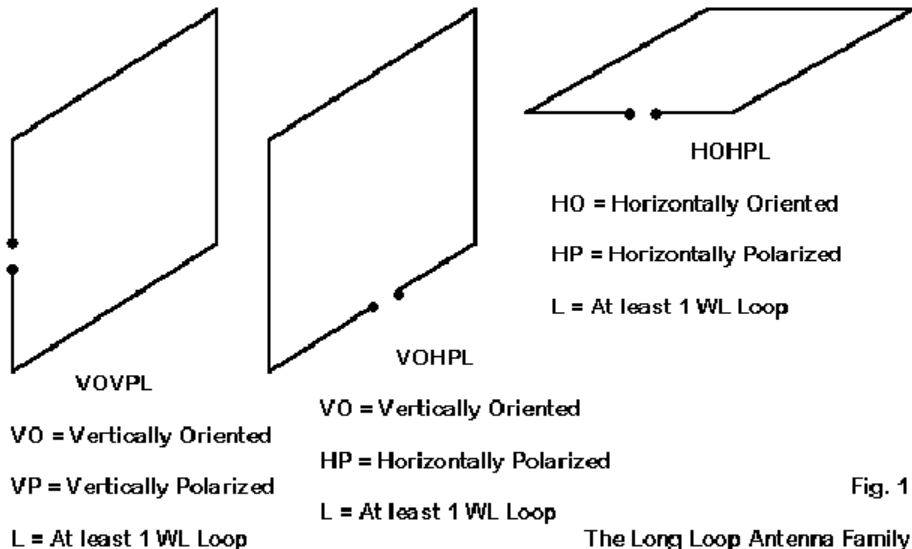


Fig. 1

The Long Loop Antenna Family

**Fig. 1** shows the three families of antennas. VOVPLs are vertically oriented, vertically polarized wire loops, such as the delta and the rectangle when we feed them along the side. They stand upright and vertically polarized radiation is broadside to the antenna plane. Ordinarily, VOVPLs are monoband antennas and perform less well than their relatives when pressed into service on other bands.

VOHPLs are vertically oriented, horizontally polarized wire loops. The quad loop fed along a horizontal wire is the most popular member of this group, although horizontally polarized triangular antennas are also common. VOHPLs show significant superiority over VOVPLs in all band use. However, they have two limitations. First, if we can place a wire doublet at the top height of the VOHPL, it will usually show a lower angle of maximum radiation, because the VOHPL's radiation is a combination of the upper and lower wires. Second, to be a truly large loop of 1 wl or greater, the VOHPL requires exceptionally tall supports.

For the ham with more area than height in his yard or field, a more frequent selection is the HOHPL: the horizontally oriented, horizontally polarized large wire loop antenna. The standard installation is to place the loop as high as one can, with only the placement of supports and the overall yard size as restrictions on the loop length. Loops up to several wavelengths long around their perimeter are in use on 80 meters--and on all of the bands above.

(We should note in passing that there is no known HOVPL, that is, a horizontally oriented, vertically polarized large loop antenna.)

HOHPLs can be strung around the edge of a yard, meaning that even a city lot whose perimeter is at least 280' long can support a 1 wl version at 80 meters. Such a lot is about 70' by 70' if square. If the yard width is only 50', then the yard need only extend 90' back to hold the antenna. With allowance for sidewalks, flower beds, trees, and the like, there is still room for a HOHPL in many more ham homesteads than we might think. Therefore, the entire class of HOHPLs deserves a longer look to discover their strengths and their weaknesses.

Let's develop a plan of attack for understanding HOHPLs. The first part of our work will include some answers to the most pressing questions about HOHPLs:

- 1. How big should we make HOHPLs?
- 2. What shape should we make them?
- 3. Where and how should we feed a HOHPL?
- 4. At what height should we place the antenna?
- 5. On what frequencies can we use the HOHPL?
- 6. How does the HOHPL compare to other all-band antennas?

The second part of our effort will be devoted to a compendium of modeled antenna patterns to give you some idea of what to expect from HOHPLs. Some of the answers we give to questions just outlined will become graphically clear when we peak at a number of antenna patterns.

## 1. How big should we make HOHPLs?

Ideally, a HOHPL should include at least 1 wl of wire at its lowest frequency of operation. For 80 meters, that means about 280' defines the antenna perimeter. In a pinch, we can make the antenna shorter and still effect a match using parallel feeders and an antenna tuner. However, let 3/4 wl be about the absolute minimum for the antenna.

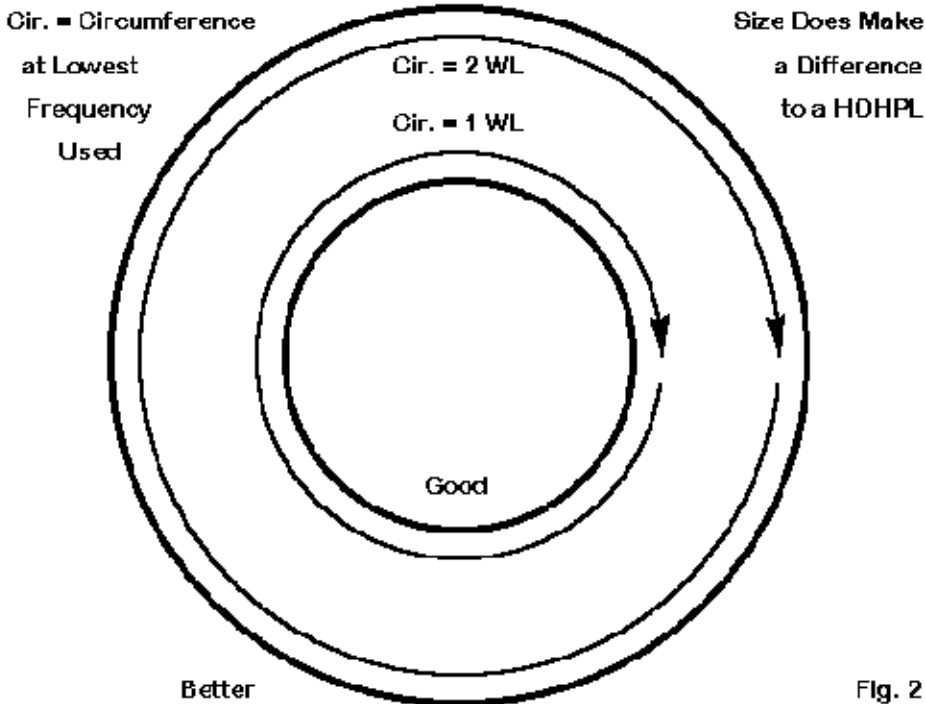


Fig. 2

The circular HOHPL outlines in **Fig. 2** show my best suggestion: make the loop larger than 1 wl. A 1 wl horizontal loop that is less than 1/2 wl above ground tends to be a cloud burner. NVIS (near vertical incidence skywave) antennas are certainly useful--and desirable to certain types of operation. But they have very poor DX potential.

By the time a loop is at least 2 wl long at its fundamental frequency of operation, it loses its ability to warm the clouds and becomes an antenna with some potential for longer distance communications. So, the general rule for HOHPLs is this: make them as long as you can support in your yard.

These notes apply to the use of a HOHPL at the lowest desired operating frequency. However, longer is not always better if our main interests are at the upper end of the HF spectrum. As we shall see, a desire to operate on both 80 and 10 meters with a HOHPL may provide us with a bit of a dilemma.

Although I shall be speaking in terms of 1 wl and 2 wl HOHPLs, there are no rules against making them even larger or against making them some non- integral multiple of a wavelength. In some respects, we can say with assurance that performance of a 1.5 wl HOHPL will be intermediate between a 1 wl and a 2 wl version. However, as we shall discover, there are enough variations in the performance of a 1 wl HOHPL to make my claim fall among the world's most vague statements.

## 2. What shape should we make a HOHPL?

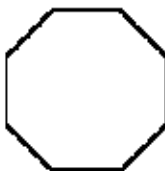
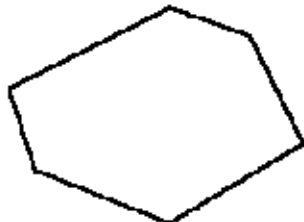
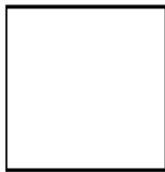
Ideally, a circular HOHPL would likely be best from a theoretical perspective. However, a circular at 80 or 160 meters is usually impractical for most ham installations. Therefore we must turn to polygons, that is, shapes with straight lines that compose the perimeter.

Before we speak in geometric terms, let's note a mechanical issue that will be involved in the shape decision. Besides the position of the supports for corners, we must also take into account the length of each side vs. the strength of the wire used to form the HOHPL. Assuming the availability of supports, we would normally place supports at distances to protect the antenna from undue stress, especially stress due to weather. Wind and ice are the major enemies of large loop antennas with long wire runs.

Copperweld is a good material for a long wire loop and may call for fewer supports than soft-drawn copper wire. Although heavier than pure copper, quality copperweld wire has many times the strength. However, another reality of HOHPL construction is that hams tend to use whatever bargain wire they can find at hamfests, close-outs, and other inexpensive sources. If you choose the economic route, be prepared to splice breaks during the life of the antenna.

Realities of ham antenna farms usually breed irregular shapes for HOHPLs. These shapes are not only usable, but as well they can be modeled and analyzed. However, we can only do this on a case-

by-case basis. For our work today we must confine ourselves to regular polygons. You may think of any regular polygon as a greater or lesser approximation of a circle: the more sides to the polygon, the closer the approximation to a perfect circle.



Typical Shapes for Modeling Studies

Typical Real Shapes

Some of the Many Possible HOHPL Shapes

Fig. 3

**Fig. 3** Illustrates some of the typical geometries used in constructing making HOHPLs of both regular and irregular shape. We shall from here on confine ourselves to the regular shapes. Our reason is a matter of both the general application of the ideas and the ease of making calculations.

Regular polygons have some dimensions that are especially useful in planning and calculating the various antenna dimensions. **Fig. 4** shows them in outline form for the triangle through the octagon. Note the Side (S), radial to a peak (A), and radial to a side (H).

Fig. 4

Figuring a HOHPL

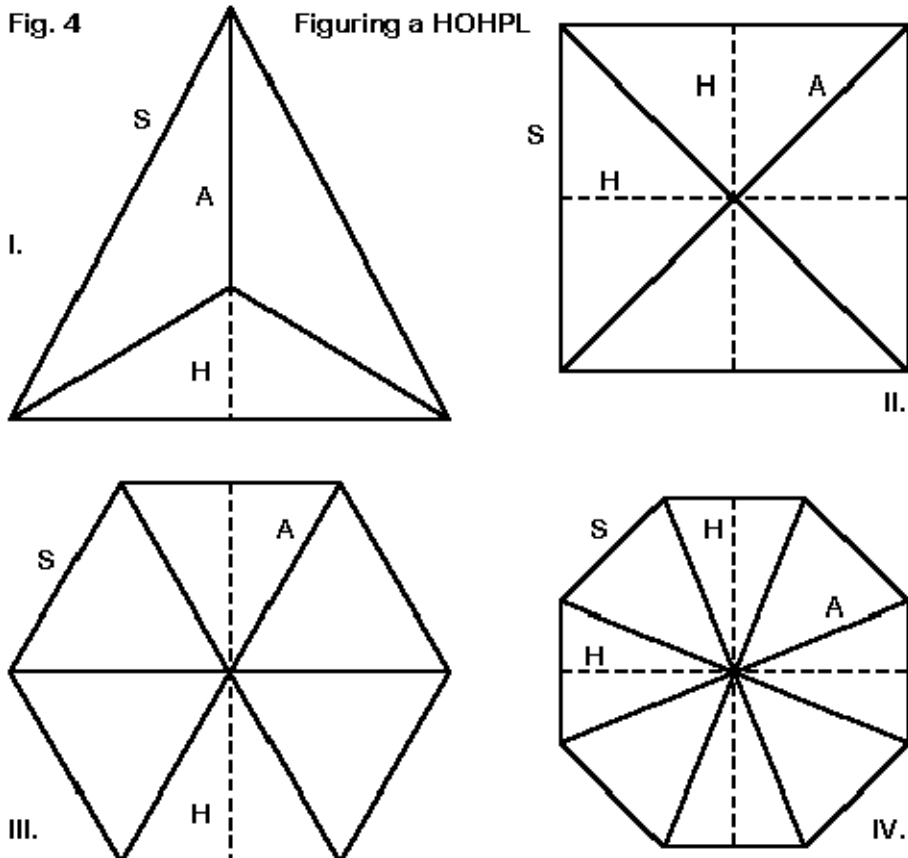


**Table 1** lists some of the relationships among S, A, H, and C (the overall circumference or total wire length of the loop. Note that the more numerous the sides, the closer the lengths of A and H to each other. A circle with an infinite number of sides from a geometric perspective finds A and H to be equal.

Table 1. Figuring a Regular HOHPL

## A. Deciding the Wire Length

$$L = \text{wire length} = 300 / F_1 \text{ (meters)} = 984 / F_1 \text{ (feet)}$$

$$L (1.8 \text{ MHz}) = 167 \text{ m} = 547'$$

$$F_1 = \text{lowest frequency used in MHz}$$

$$L (3.5 \text{ MHz}) = 86 \text{ m} = 281'$$

## B. Figuring the Layout (See fig. 4)

$$C = \text{length of circumference} \quad S = \text{length of side} \quad A = \text{length of radial from center}$$

$$H = \text{length of } X \text{ or } Y \text{ from center of loop}$$

## I. Triangle

$$S = C / 3$$

$$H = 0.29 S \quad (= 0.10 C)$$

$$A = 0.58 S \quad (= 0.19 C)$$

$$A + H = 0.87 S \quad (= 0.29 C)$$

## III. Hexagon

$$S = C / 6$$

$$H = 0.87 S \quad (= 0.14 C)$$

$$A = S \quad (= 0.17 C)$$

## II. Square

$$S = C / 4 \quad (= 0.25 C)$$

$$H = 0.5 S \quad (= 0.13 C)$$

$$A = 0.7 S \quad (= 0.18 C)$$

## IV. Octagon

$$S = C / 8$$

$$H = 1.2 S \quad (= 0.15 C)$$

$$A = 1.3 S \quad (= 0.16 C)$$

## V. Circle

$$A = H = 0.16 C$$

## VI. "Irregular"

String wire along ground and adjust

The table of relationships is especially handy when you begin the process of planning a HOHPL with a paper sketch of your yard space. They are also handy if you wish to calculate the wire end coordinates on an antenna modeling program. The main shapes that we shall focus on in generating patterns for possible HOHPLs will be the square, the hexagon, and the octagon--the last because it most closely approximates a circle.

### 3. Where and how should we feed a HOHPL?

Since the HOHPL is a multiband antenna, the feedpoint impedance will vary from band-to-band. Therefore, the only practical feed system is a parallel transmission line to an antenna tuner. The line can be anything from TV lead to commercial or home brew bare wires spaced every so often with almost any weather-resistant insulating rod. Even segments of plastic coat hangers will do for insulators, since the spacing will keep the rods from undergoing undue electrical stress.

You may locate the feedpoint of a HOHPL at any point along its length. Mechanically, this usually means intersecting the antenna at the position that allows the straightest line from the antenna to the shack entry point. For some installations, the feedpoint may be at a corner (or junction of sides); for others, the feedpoint may be centered on a side--or even off-center on a side.

One of the surprises that modeling the HOHPL produced is this: at what point you feed the antenna does make some difference in the resulting pattern on at least some of the bands in the HF region. As we shall see, when we explore the antenna over many ham bands with several geometric configurations, even the octagon fails to act like a circle on some of the upper HF bands. When we look at the patterns of the various antenna versions, keep in mind where you want the lobes and nulls to be relative to your own possible installation. A less direct feedline might yield a superior pattern relative to your operating desires.

At this point I shall make a brief pitch for every serious antenna buff to acquire at least one of the antenna modeling programs. There is no reason for us to simply accept what a roughly constructed antenna might give us. We can plan and tame the beast-- whether by relocating wires or relocating the feedpoint--to give us the best compromise of lobes going just where we want them.

#### **4. At what height should we place a HOHPL?**

Like all of the questions surrounding large loops, this question has two dimensions: the mechanical and the electrical. Therefore, the simple answer ("As high as possible") does not tell us everything we need to know or think about in constructing an antenna that consists of hundreds of feet of wire and a system of at least 3 and up to 8 support structures.

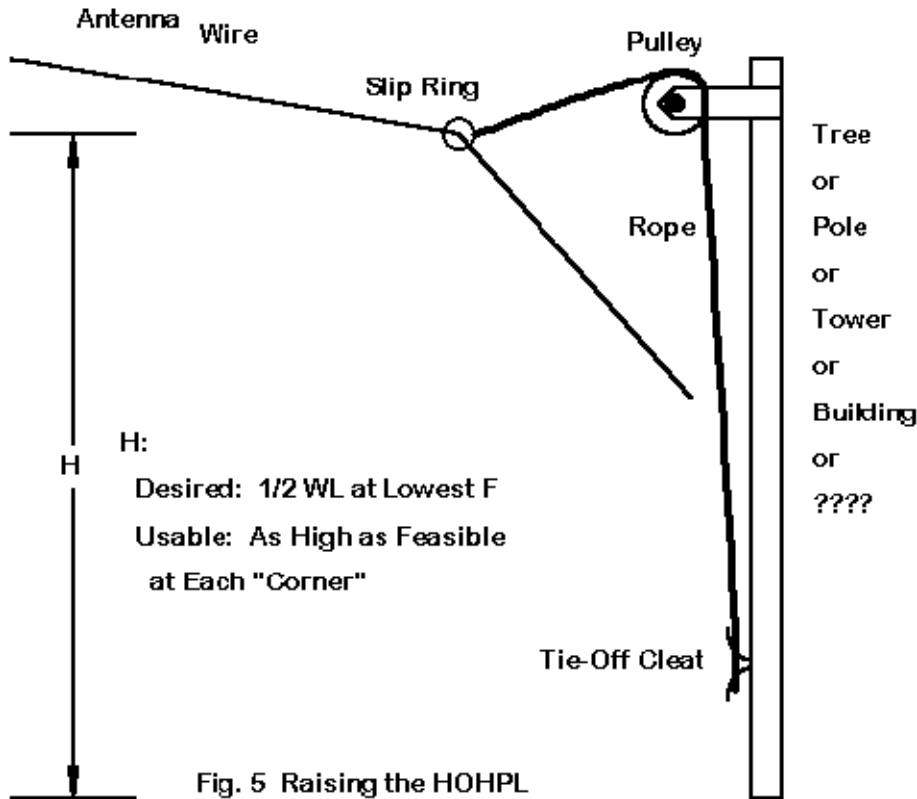


Fig. 5 Raising the HOHPL

The most ideal and yet practical arrangement for supporting a HOHPL corner appears in **Fig. 5**. Note that the system includes a pulley and rope for raising and lowering the wire. A cleat near the ground is useful for tying off the rope. I have also used rope loops and clip rings at the cleat level. I disconnect the extra rope used

only when lowering the antenna and store it out of the weather. I clip the upper rope to a hook instead of a cleat. When I need to lower the antenna, I add the extra section, which is long enough to reach but not pass through the pulley.

A slip ring can be made from almost any plastic, although I tend to prefer Schedule 40 PVC Tee fittings for their durability. Their smooth interiors also tend to minimize wire kinking and rubbing, thus prolonging the life of the antenna. I do not offer these mechanical notes as a final and best answer to every situation. Instead, I hope that they get you to think about the mechanical details of your antenna as being just as important to its successful performance as the electrical details.

Electrically, the question of HOHPL height is a matter of the elevation angle of the radiation. We can best picture what height means to use if we select an antenna design, a set of heights, and a few test frequencies. So let us take a square HOHPL that is 1 wl long at 80 meters and place it 35' up, 50' up, and 75' up--all typical ham installations. Now let's see, with the aid of computer modeling, what happens. But first, be sure to understand that antenna modeling presumes flat terrain with no ground clutter. Hence, the results will be very general.

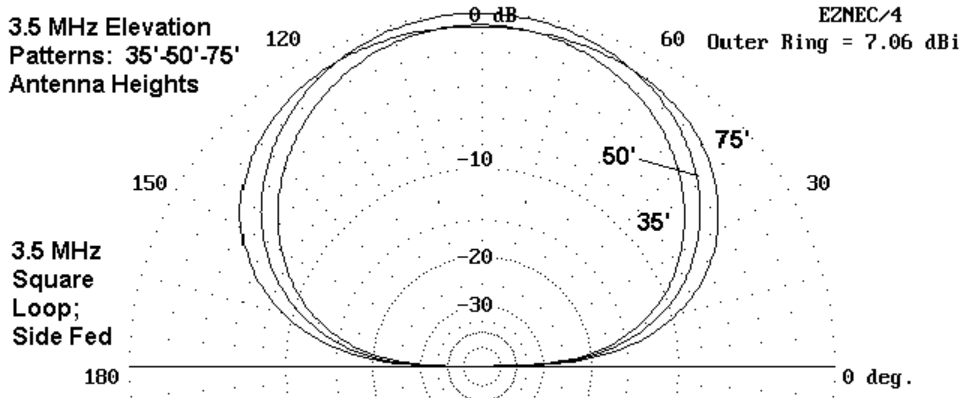
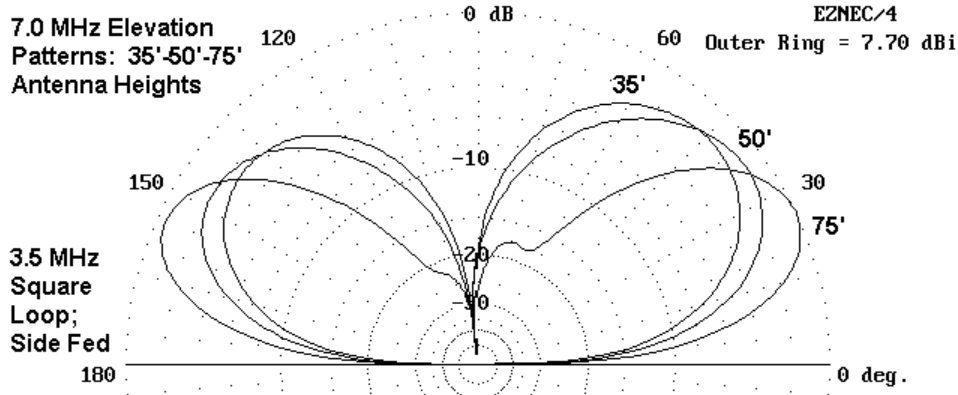
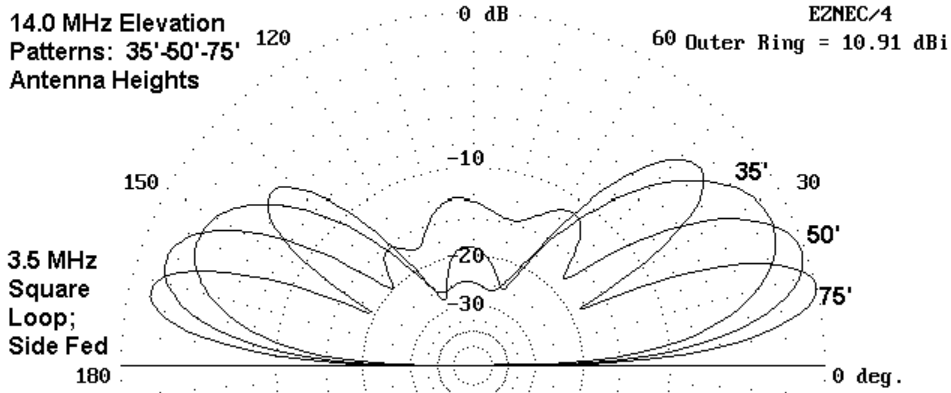


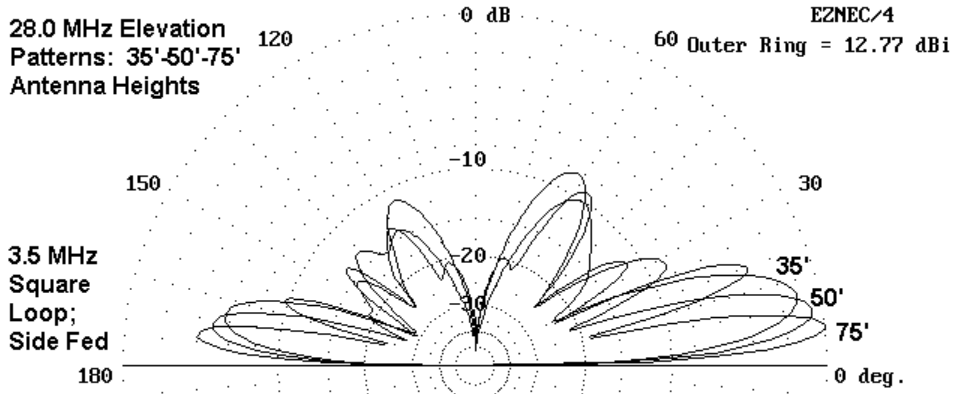
**Fig. 6** demonstrates the difficulty of using a HOHPL at its lowest frequency (where it is 1 wl long). The 1 wl loop radiates predominantly broadside to the plane of the wire, which is straight up and down. Even at 75' up, the antenna is a "cloud-burner," or a suitable candidate for NVIS (Near Vertical Incidence Skywave) service.



On 40 meters, as the patterns in Fig. 7 show, the antenna begins to form patterns that are suited to normal sky wave communications. However, the antenna is still a bit low when under 75' up, so the angles of maximum radiation are 37° at 50' up and 44° for 35' up. Longer distance effectiveness is enhanced by raising the antenna to 75' up, where the angle is about 26°.

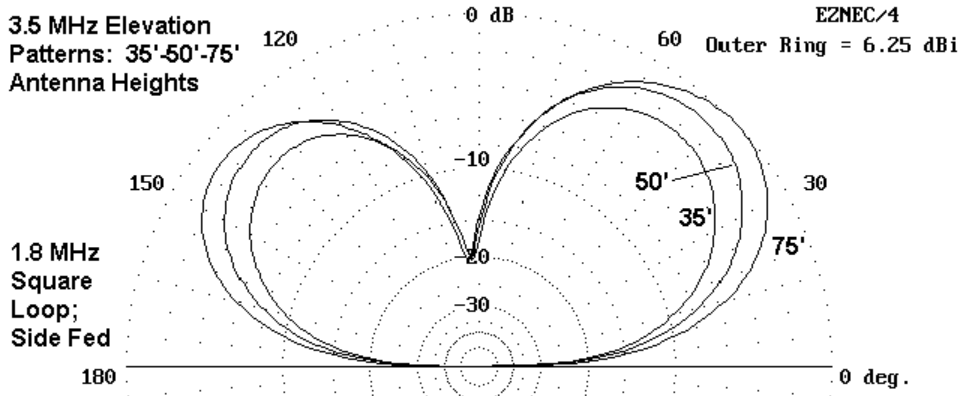


On 20 meters, as illustrated in **Fig. 8**, the same antenna begins to show excellent DX potential. At 35' up, the elevation angle of maximum radiation is  $26^\circ$ , with angles of  $19^\circ$  and  $14^\circ$  appearing at heights of 50' and 75', respectively. The emergence of higher angle secondary lobes becomes apparent, but these lobes are generally not as large as those that form with doublets at the same height.



On 10 meters, as revealed by the patterns in **Fig. 9**, the HOHPL become an excellent DX antenna, with very low elevation angles of radiation: 12°, 9°, and 6° for heights of 35', 50', and 75' respectively. (Remember that the lobes have a vertical beamwidth so that the angles cited represent the center points of reasonably broad angular spreads that can handle propagation angles somewhat distant from the center line.)

If the HOHPL has a significant weakness, it lies in the operation of the antenna at its fundamental frequency. To some extent, this weakness can be ameliorated by further elevating the antenna. A better solution, if land area is available, is to build a longer antenna, so that the fundamental frequency is lower. When the antenna is operated at its 2nd harmonic (when it is 2 wl long), the primary radiation is mostly in the same plane as the wire loop. Elevation angles at 80 meters will still be high, but not nearly as high.



Compare **Fig. 10** to **Fig. 6**. Although the elevation angle on 80 meters for the 2 wl loop is not ideal, it is considerably better than the elevation angle of the 1 wl version.

## **5. On what frequencies can we use the HOHPL?**

The answer to this question is simple: on any HF frequency. With parallel feedlines and an antenna tuner--hopefully a link-coupled tuner--we can load the antenna and produce useful signals on every band, whether traditional or WARC. What we get for radiation, however, depends on many factors, including the shape of the antenna, the length of the wire, and where we feed the antenna.

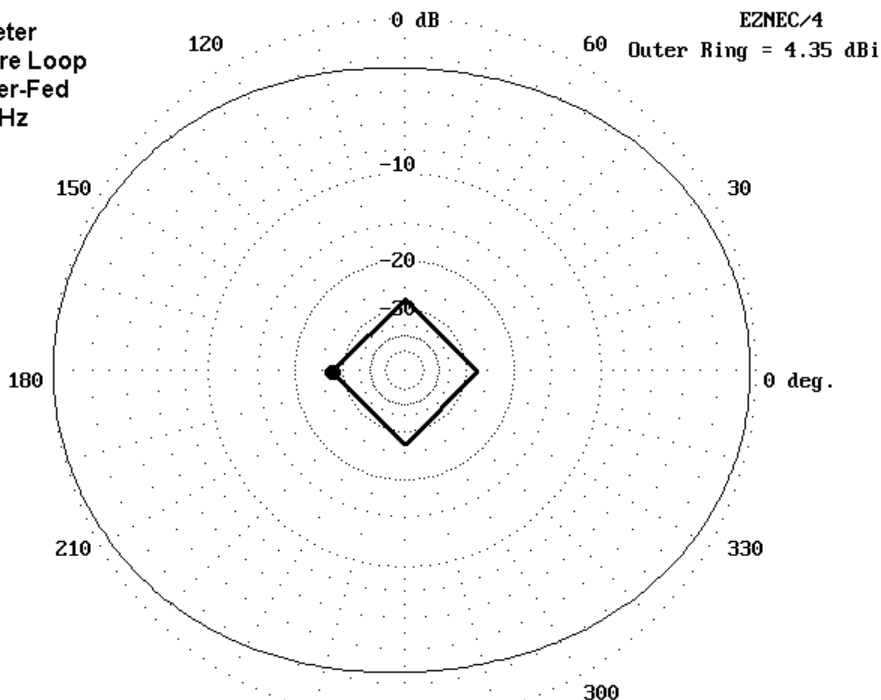
Therefore, let's look at a compendium of azimuth patterns for the HOHPL using a variety of configurations to sample the territory. (Remember that a full set of patterns would use up a book, so we

must restrict ourselves to a relevant sample.) We shall look at 1 wl antennas in the square and the octagon configurations, each fed at the center of a side and at a corner. Then we shall repeat the process with a 2 wl long hexagon as a sample of a longer HOHPL. From these examples, you can likely extrapolate what might happen with a large loop placed in your own yard.

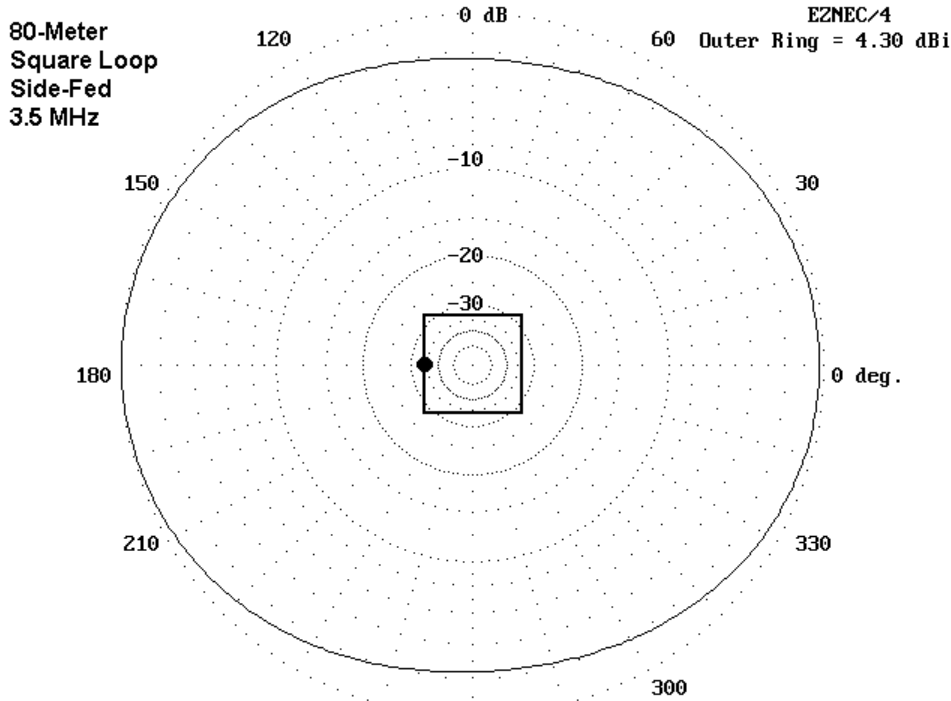
In all cases, the feedpoint of the antenna is placed at the left-most point on the antenna relative to the pattern shown. This procedures gives you a fair comparison, especially of patterns that are too complex to place in a single figure by laying one pattern on top of the other. In some cases, it would be impossible to keep track of which lobe belonged to which antenna. Therefore, we shall use separate figures and devote one page to each of the amateur bands for the 80-meter antennas--and a column to each band for the 160-meter model.

## 80 Meters

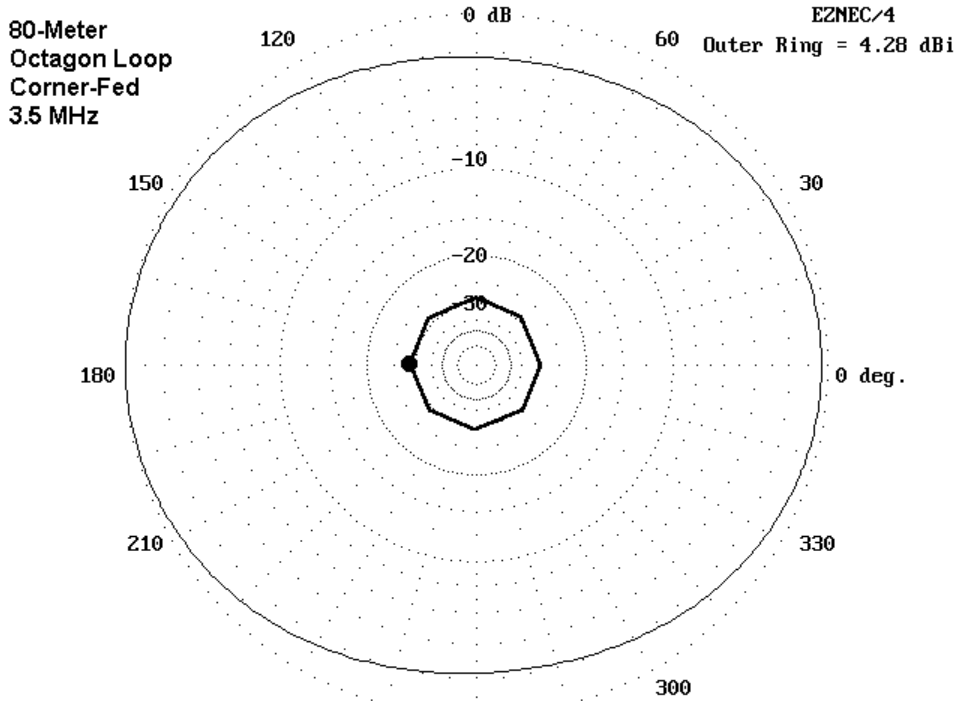
80-Meter  
Square Loop  
Corner-Fed  
3.5 MHz



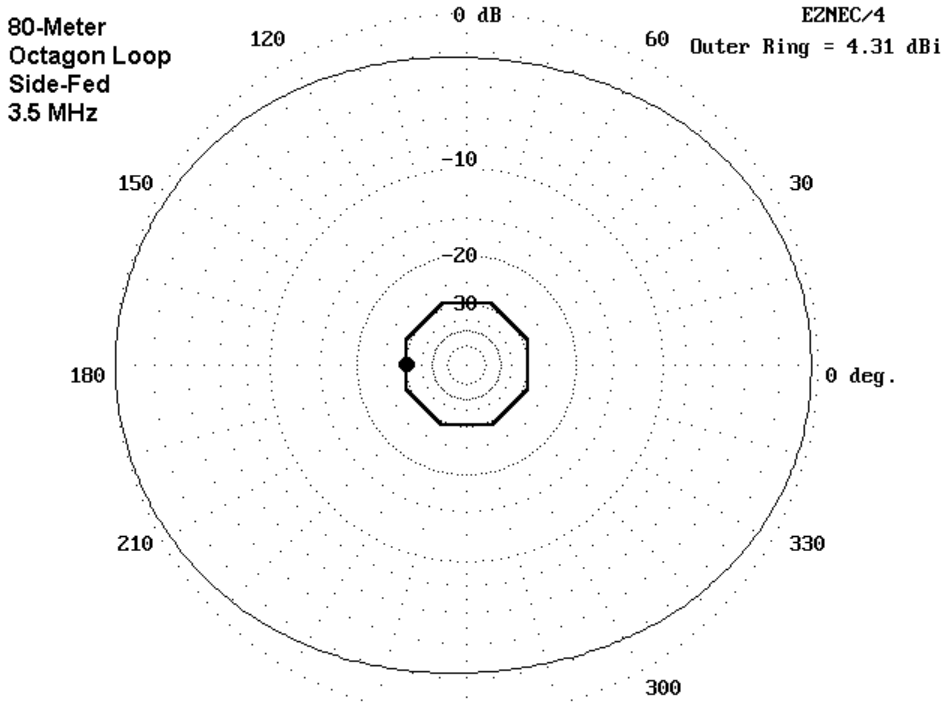
Any differences of performance among the loops shown here are too small to detect in operation, amounting to only 0.07 dB. The basic pattern of the loop at its fundamental frequency is a broad oval, stretched in the direction through an axis running from the feedpoint to a point on the opposite side of the loop. The loop "sides" are only a little over 2 dB down from the gain maxima.



All of the loops in this long sequence of azimuth patterns have been modeled so that the feedpoint is to the far right, whether that point is in the middle of a side or the point where the wire takes a new direction. The orientation of the loop is shown only for the 80-meter azimuth patterns. However, the loop and feedpoint positions do not change as the modeling runs increase in frequency on succeeding pages. You can draw your own North line on each pattern.



For all of the loops shown here, the 3.5 MHz azimuth patterns have been taken at an arbitrary  $45^\circ$  elevation angle. The actual elevation angle of maximum radiation on 80 meters is  $90^\circ$  or straight up for these loops, which are  $1\lambda$  long. If you compare these patterns with Fig. 6, you will see that there is very little low elevation angle radiation on 80 meters, since the basic radiation pattern is broadside to a  $1\lambda$  loop.



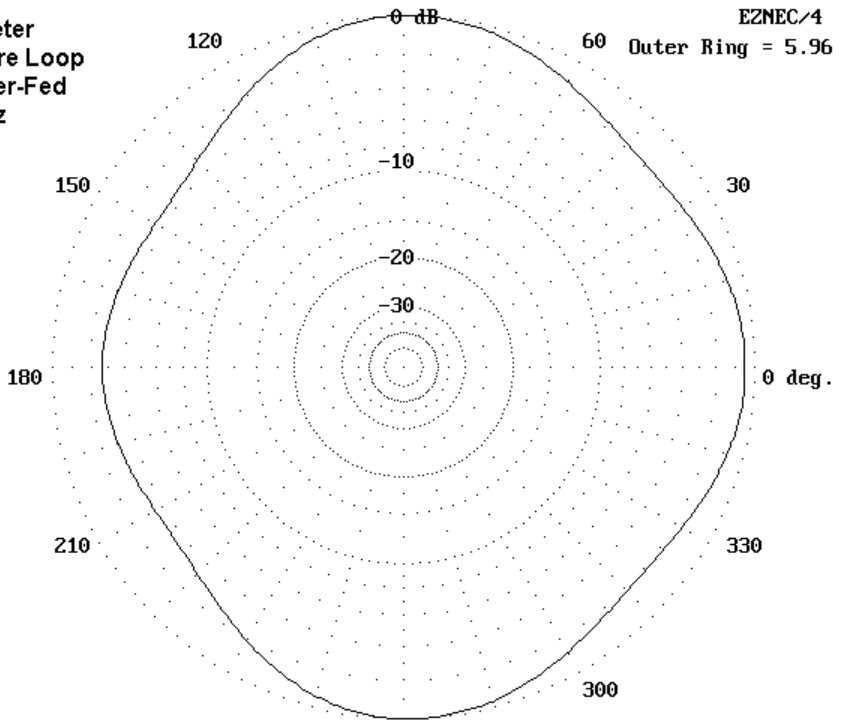
On 80 meters, an 80-meter loop arranged as a HOHPL makes a very good NVIS (near vertical incidence sky wave) or cloud burner antenna. Long-distance contacts will likely be rare on 80 meters, although contacts within a 300-500 mile radius may be stronger than with some other types of antennas, such as verticals and inverted Vees. See the 80-meter patterns of **Fig. 15** and **Fig. 16** for an alternative, composed of 2 wl loops at 80 meters.

## 40 Meters

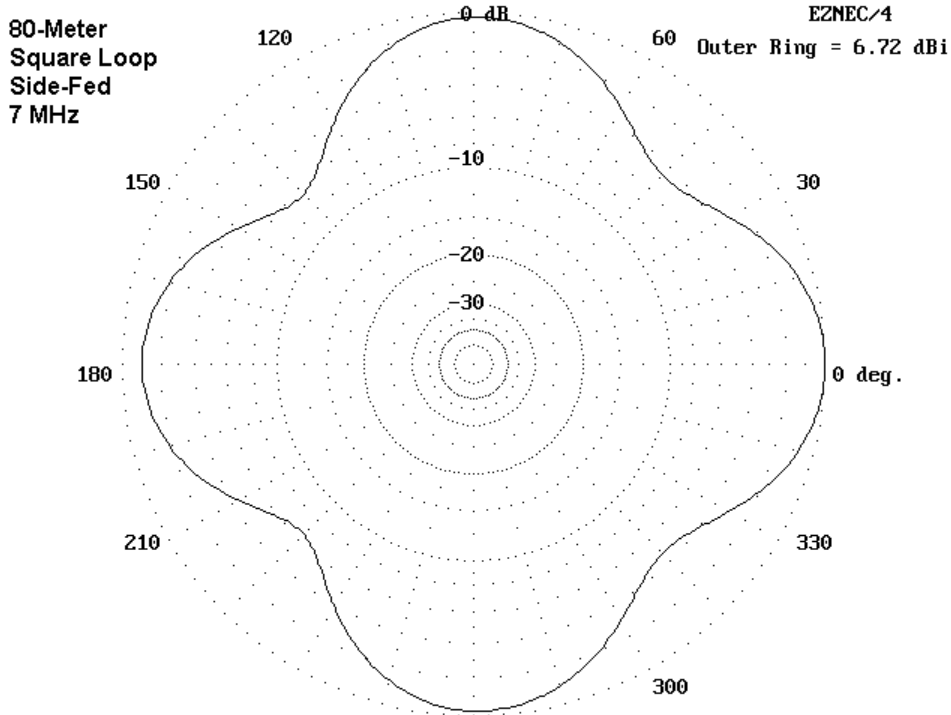
80-Meter  
Square Loop  
Corner-Fed  
7 MHz

EZNEC/4

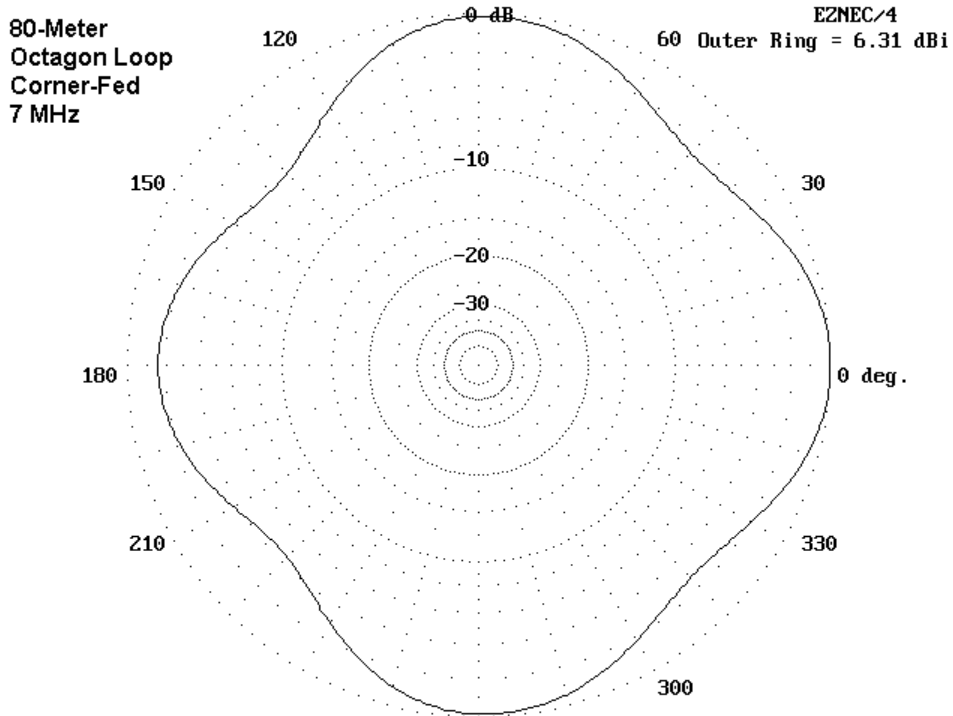
Outer Ring = 5.96 dBi



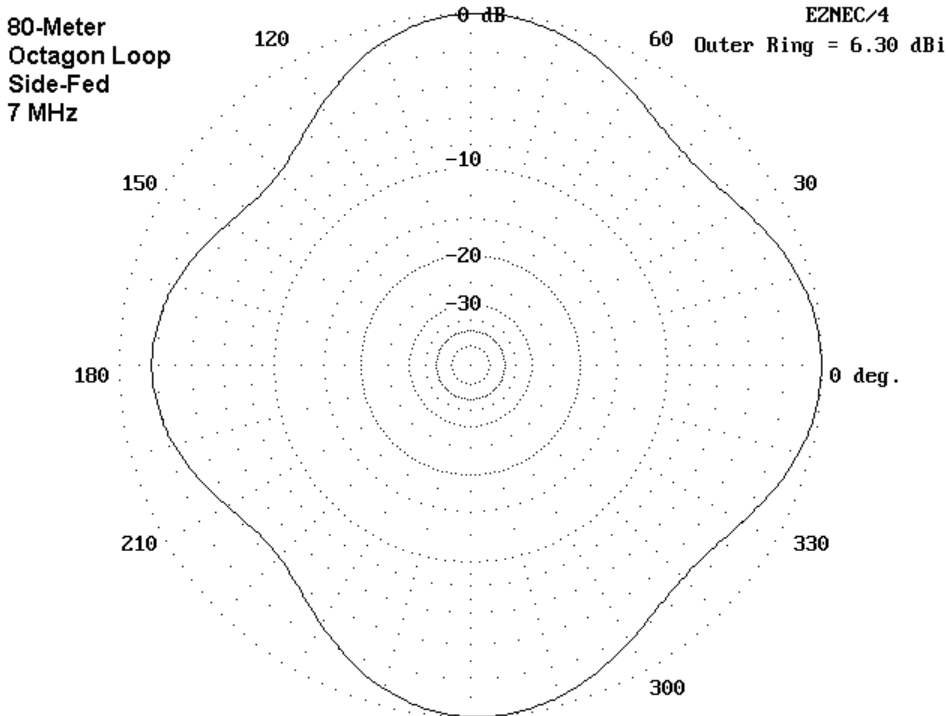
Both the loop shape and the feed position begin to make themselves evident on the 40-meter azimuth patterns. Elevation angles of maximum radiation run from 37° to 43° for these 1 wl loops at 7 MHz, which allows direct comparisons among the azimuth patterns. Beginning with the square loops, we can examine them a pair at a time.



The square loops show a very distinct difference in shape and gain that depends upon the feed point. The side-fed model shows stronger lobes (by almost 0.8 dB) and deeper nulls. In contrast, the corner-fed model is a round-cornered diamond, with a bit less gain in the direction of the feedpoint. Moreover, the points of maximum gain for the corner-fed model are to the sides; that is, at right angles to the axis passing through the antenna feedpoint and the point opposite it on the antenna loop.



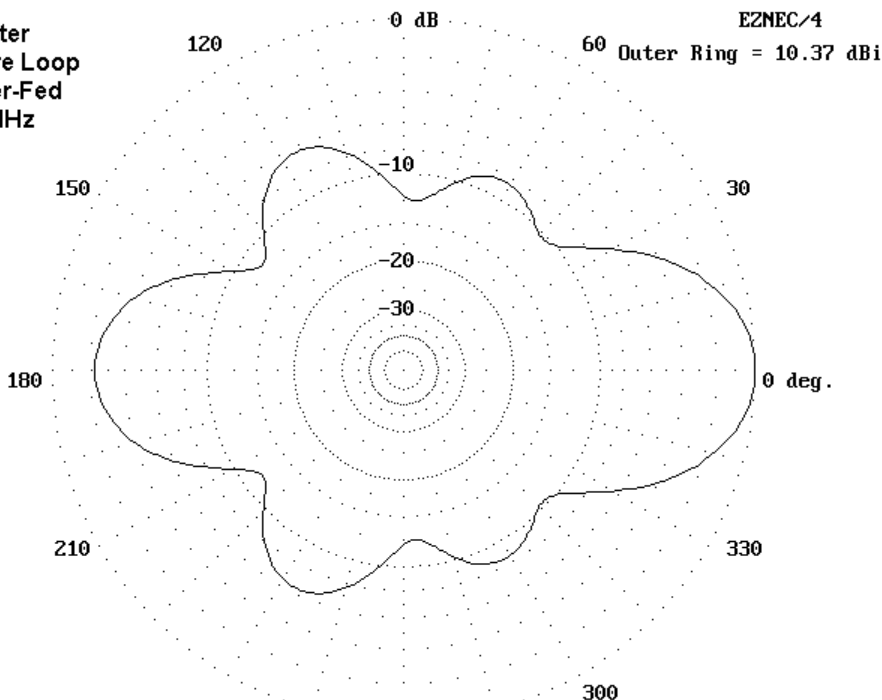
In contrast to the differences between patterns depending on the feedpoint for the square loops, the octagon loops show an almost insignificant difference in pattern, whether the antenna is fed at a corner or in the middle of one side. The smaller differences also show up in the feedpoint impedances, with the squares showing a large difference as the feedpoint is moved.



The simultaneous change in both pattern and feedpoint impedance in the square models indicates that the diamond and square configurations make a difference in the current distribution and interaction as they turned with the change in feedpoint. At 40 meters, the effect is much less for the octagon, since the difference in length between a radial to a corner and a radial to a side is much smaller. Whatever the differences, all four of these loops would make very good omni-directional antenna for 40 meters.

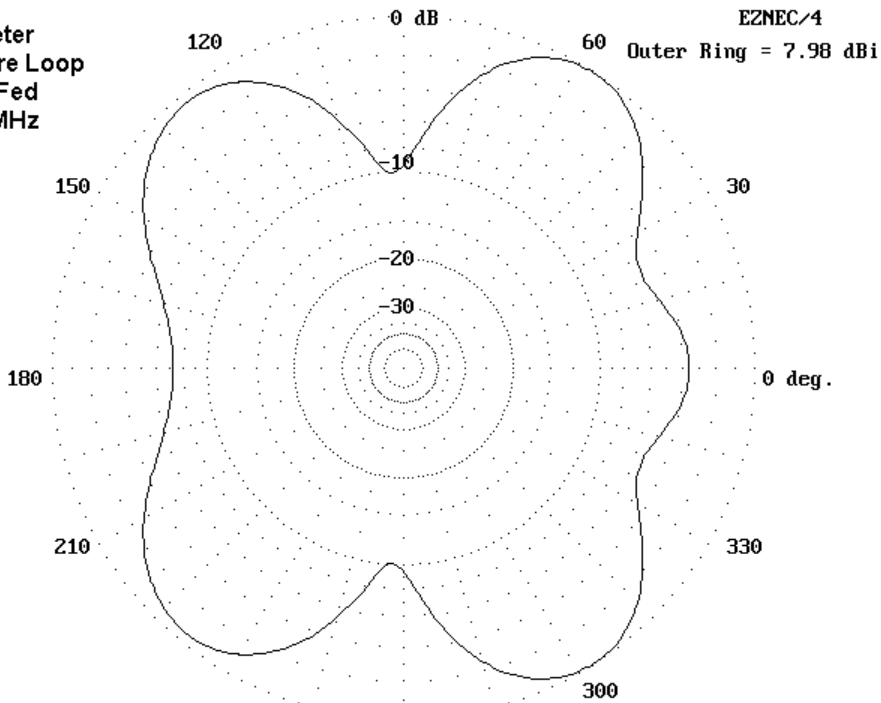
## 30 Meters

80-Meter  
Square Loop  
Corner-Fed  
10.1 MHz

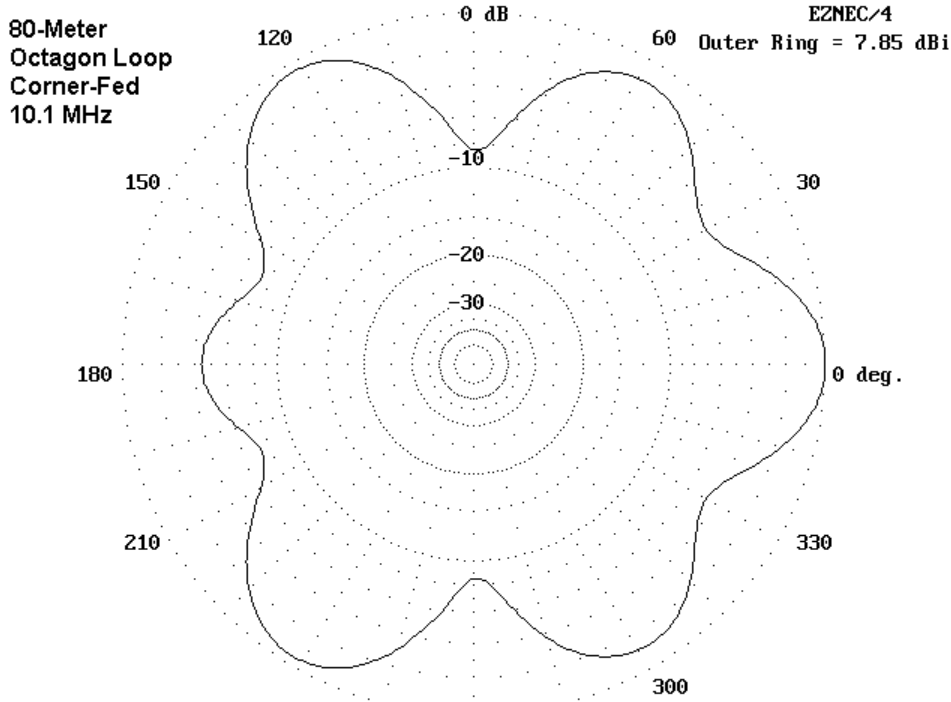


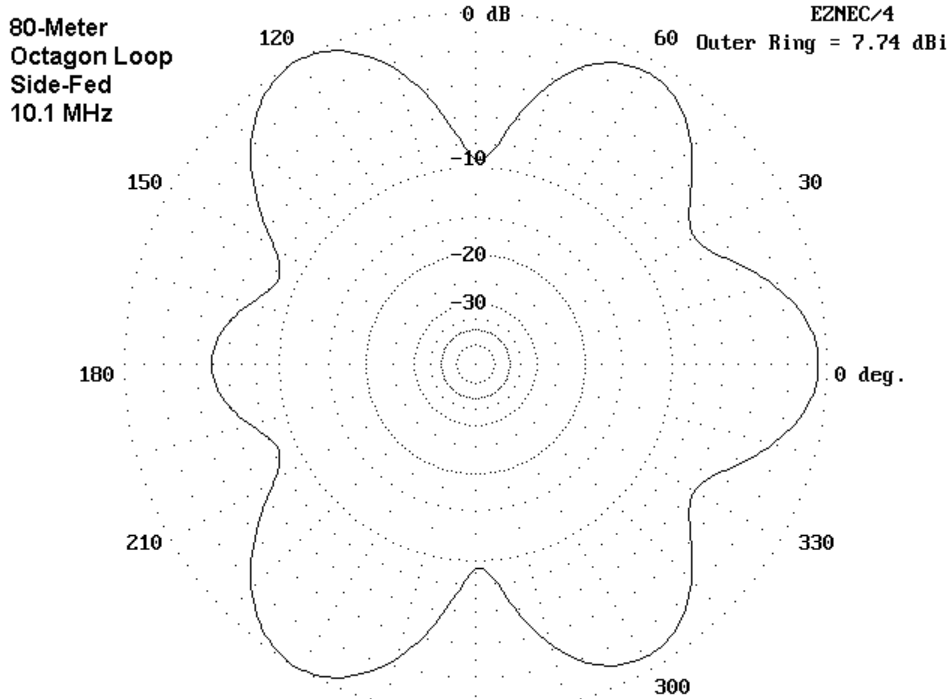
On 80 and 40 meters, the loops are close to resonance. Sometimes, differences show up most graphically when an antenna is operated at a frequency for which it is not resonant. For all of the loops, the feedpoint reactance is in the vicinity of 600 Ohms at 10.1 MHz. Once again, the squares show a stronger pattern difference that depends solely on the feedpoint selection.

80-Meter  
Square Loop  
Side-Fed  
10.1 MHz



When fed at the corner, the 30-meter square pattern becomes very bi-directional, with about a 2 dB front-to-back ratio and about 8 dB or more front-to-side ratio. The distance from the feedpoint to the opposite peak is about  $3/8$  wl. In contrast, the side-fed square feedpoint is only about  $1/4$  wl from the opposite point across the square. Radiation remains strongest off the corner peaks, and the gain along the feedpoint axis is nearly 7 dB down from the forward gain of the corner-fed model.





In addition, the nulls of the side-fed octagon are slightly deeper than those of the corner-fed model. This feature shows a kinship between the side-fed square and octagon models.

In all, three of the four arrangements make very respectable omnidirectional antennas. Only the corner-fed square arrangement is less suited to this service and better suited to bi-directional operation that requires careful antenna orientation for effective use.

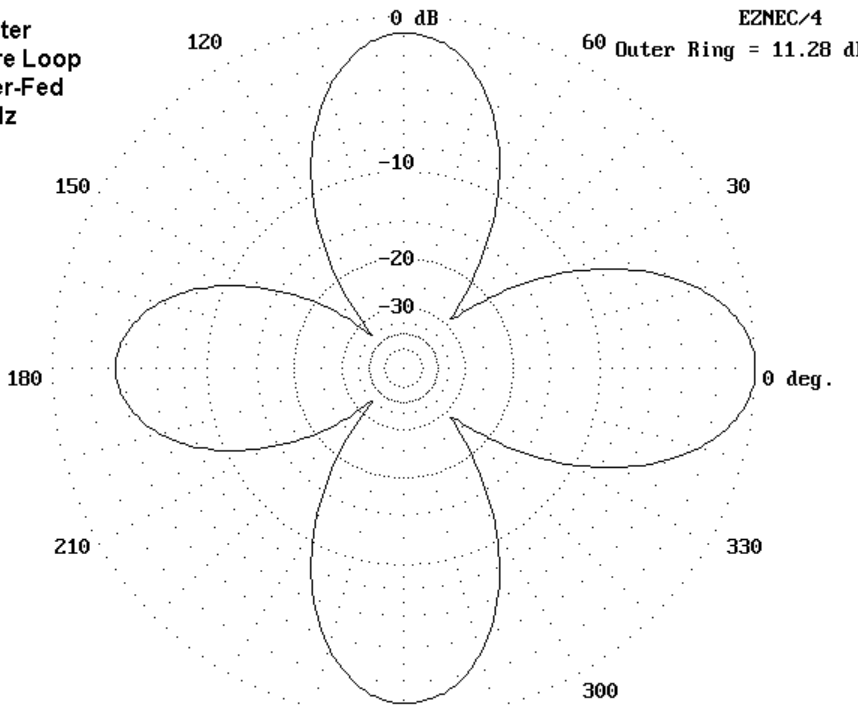
## 20 Meters

80-Meter  
Square Loop  
Corner-Fed  
14 MHz

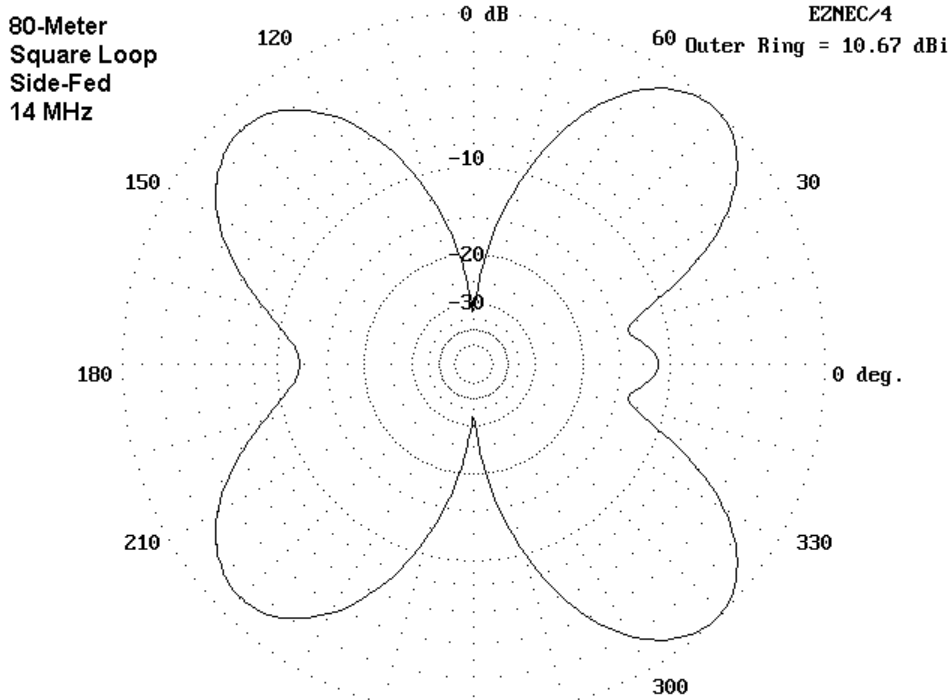
0 dB

EZNEC/4

60 Outer Ring = 11.28 dBi

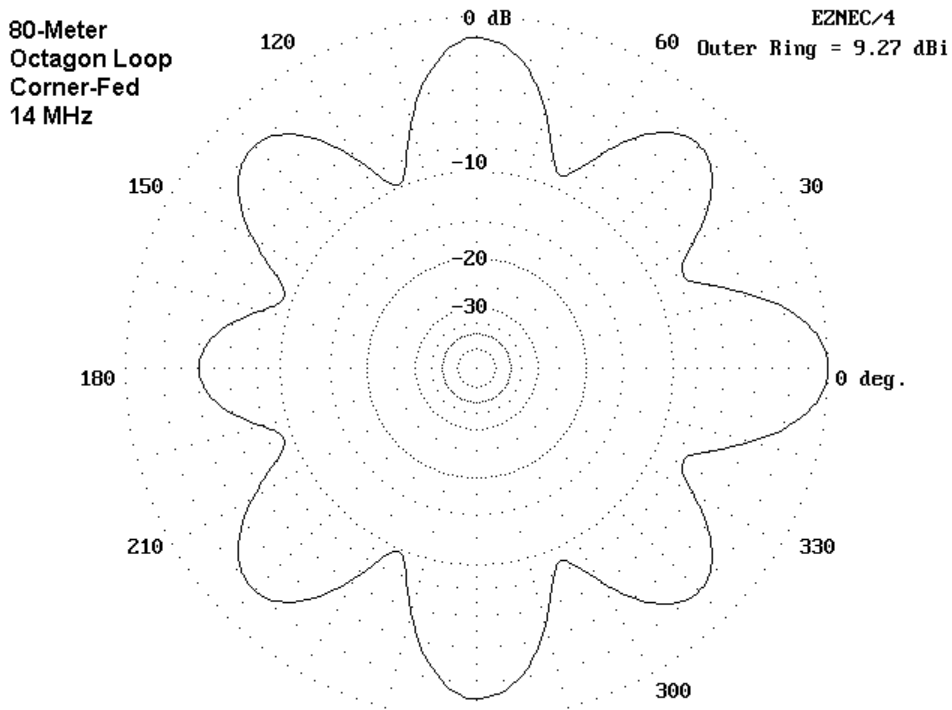


On 20 meters, the elevation angle for the loop, whatever its shape or feedpoint position, has decreased to about 20°. This angle (a product of the 50' height for all of the models) places the antenna radiation into the DX range, although signals would be stronger with the antenna even higher. On 20 meters, the antenna planner is faced with further decisions.



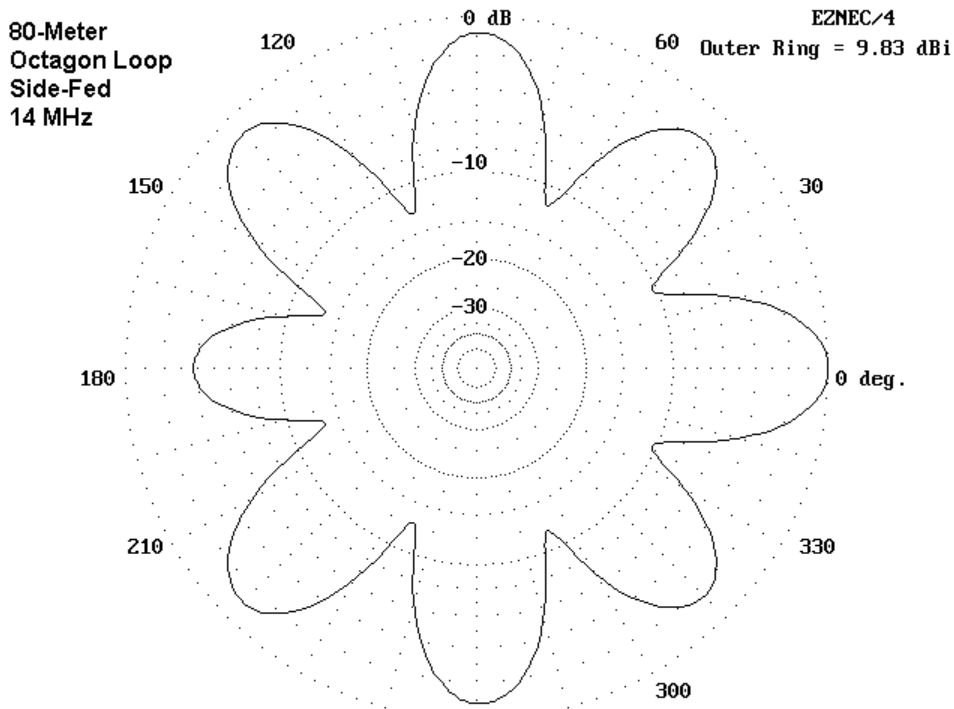
The square loop shows major lobes near or above 10 dBi off each of the four corners. The lobes of the side-fed model are broader, which would lessen the problem of orienting the antenna toward desired areas of the world. In contrast, the narrower but stronger lobes of the corner-fed square would provide a gain advantage, especially in three of the four directions that the antenna favors. The cost of the added gain is a collection of very wide and deep

nulls in the pattern, which would effectively limit communications in many directions.



In contrast, the octagons seem once more to have very similar patterns to each other, regardless of the feedpoint position. However, note the fact that the lobes are a function of feedpoint position and not of whether there is a side or a corner at the lobe

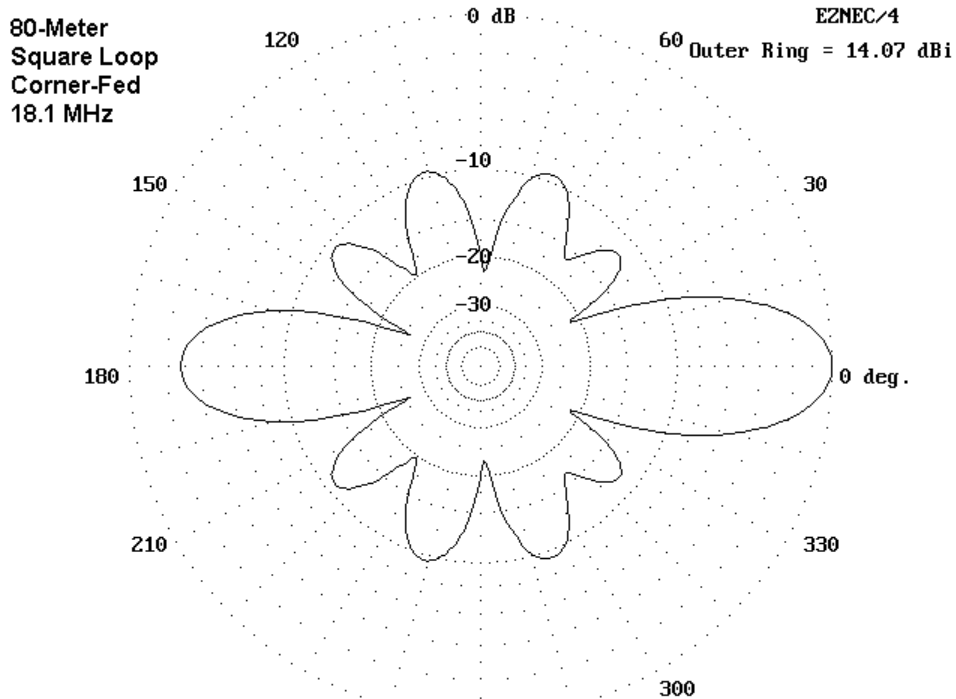
location. This factor shows up in the differential in the feedpoint impedances for the two octagon models.



What the octagons lack in maximum gain, they make up for in omni-directional potential. Although nulls can be as deep as 10 dB below the lobes, they cover less territory and are shallower than most of the nulls in the patterns for the square models. The lesson here is simple: if 20 meters is a desired band for operation of a

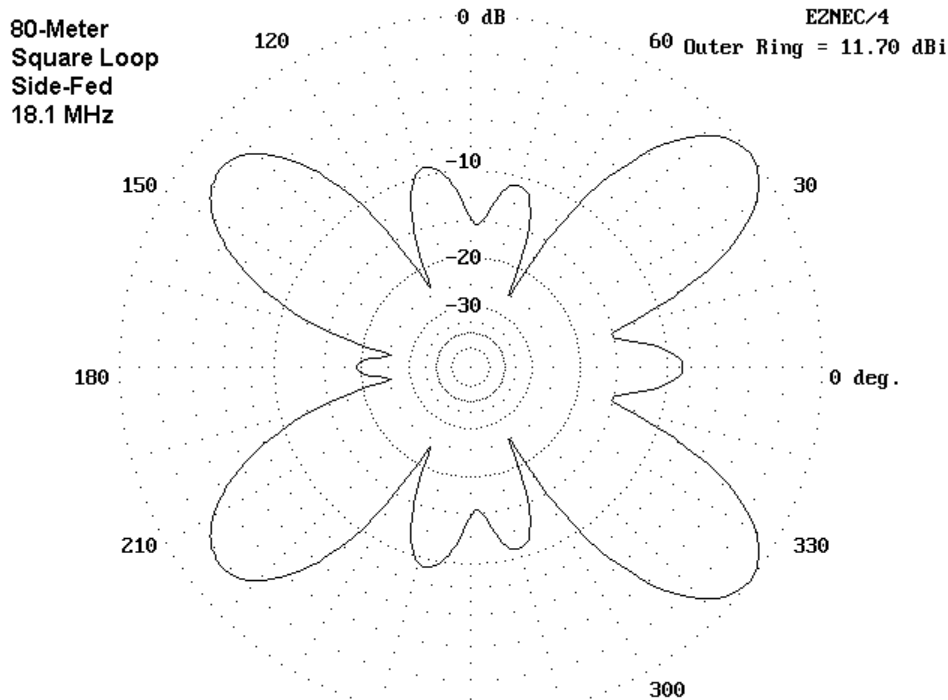
HOHPL and if one wishes to work in every possible direction, then the HOHPL should be as round as one's terrain permits. The squarer the shape, the larger and deeper the pattern nulls.

## 17 Meters



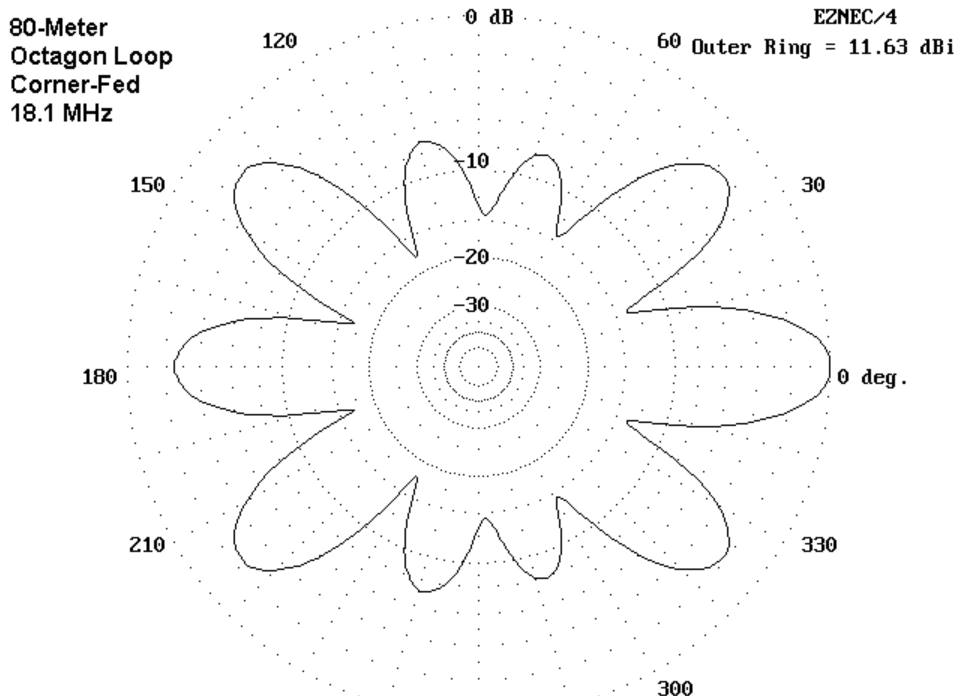
The patterns for 17 meters appear to have no rhyme or reason--indeed, they seem to suggest an error in modeling. However, they

are as correct as NEC-4 can make them. Once more, nonresonant operation of the loop permits the current distribution to change radically with small changes of configuration. The result is a diverse set of patterns.



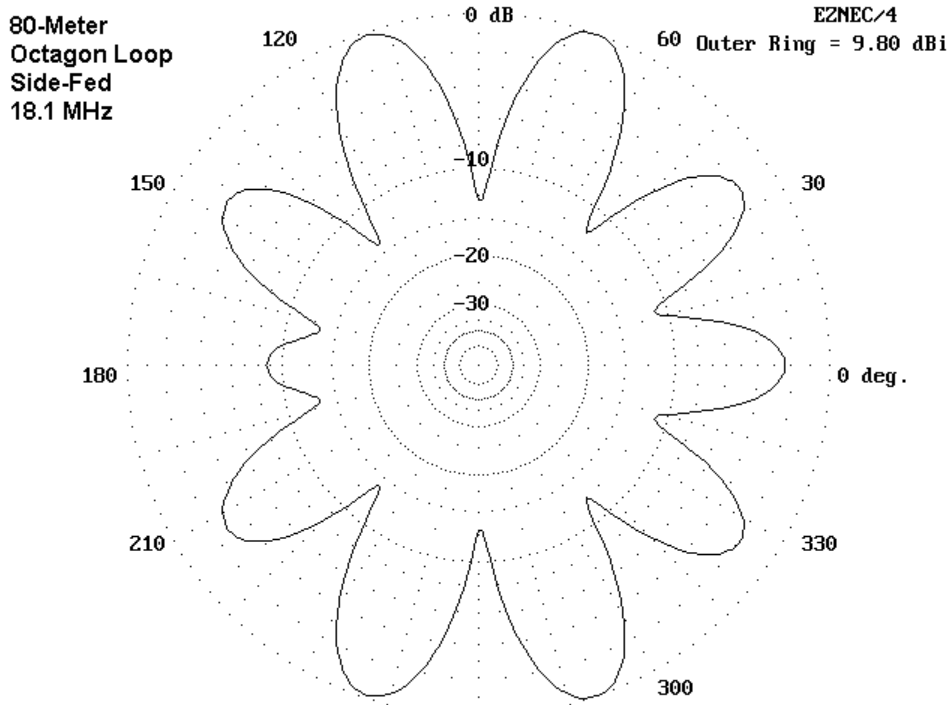
The corner-fed square shows a high-gain bi-directional pattern that is similar to and in line with the 30-meter pattern for the same model. Maximum gain is off the corners that are in line with the

feedpoint. The side-fed square also shows its maximum gain off the corners. However, since the feedpoint is between corners, the gain is more evenly distributed among all four corners. Hence, the apparent major difference in the operation of the loops turns out to be smaller than at first sight, but very significant for planning.



The corner-fed octagon pattern shows its affinity to the corner-fed square with a noticeable but less extreme bi-directional pattern.

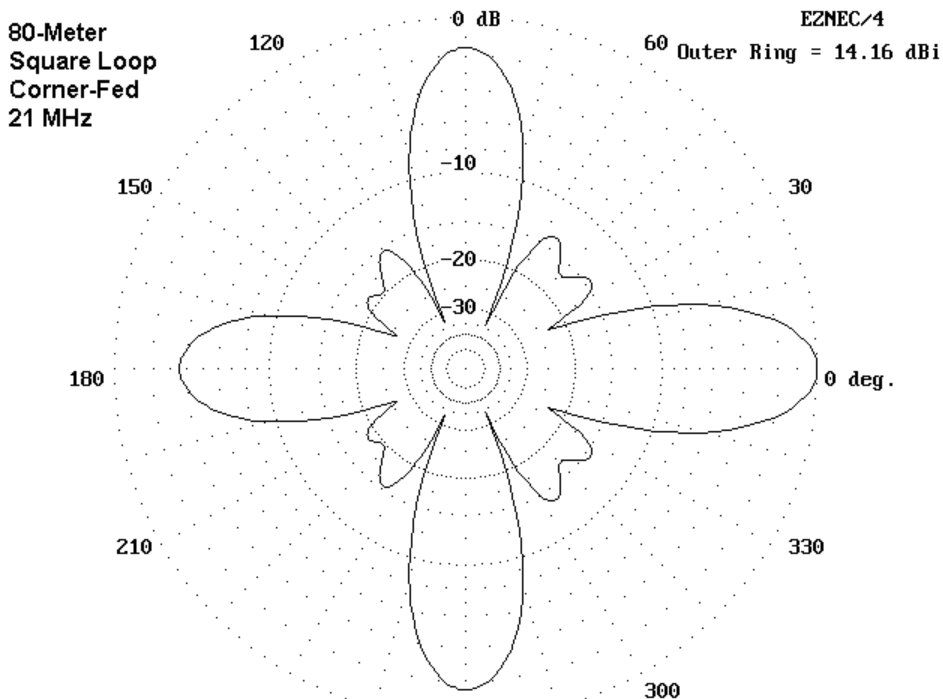
The greater "side" gain results in a lower gain along the major axis of the antenna, compared to the square. However, the "side" gain is not sufficient to qualify this arrangement as having good omnidirectional potential.



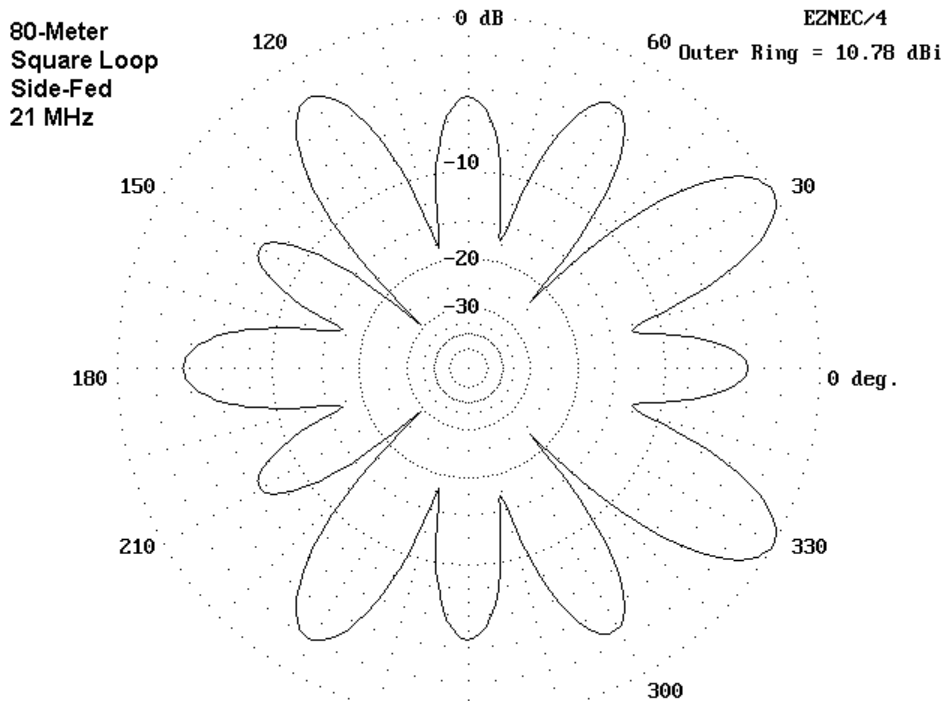
The pattern for the side-fed octagon may seem initially mysterious. Twisting the antenna and moving the feedpoint by only  $22.5^\circ$  alters the axis of highest gain by  $90^\circ$ . Part of the mystery begins to clear

up when we note that the antenna is attempting to produce 10 lobes from 8 sides and 8 corners. Since the antenna is over 5 wl long at 18.1 MHz, current distribution and resultant gain distribution can change rapidly with small changes in antenna configuration. Since 17 meters is less widely used, these difficulties are usually minor.

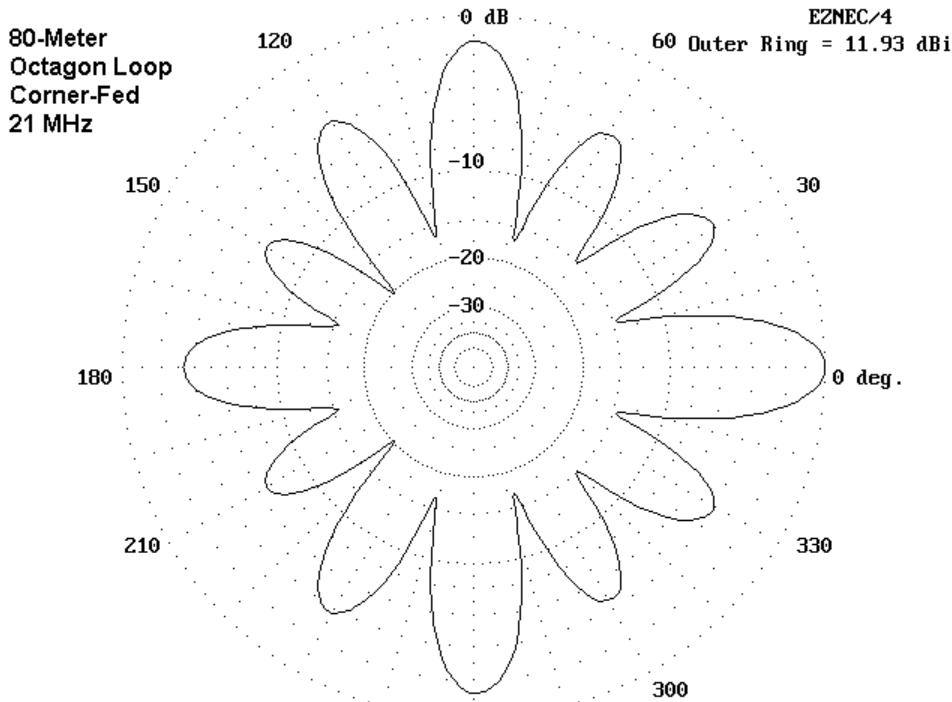
## 15 Meters



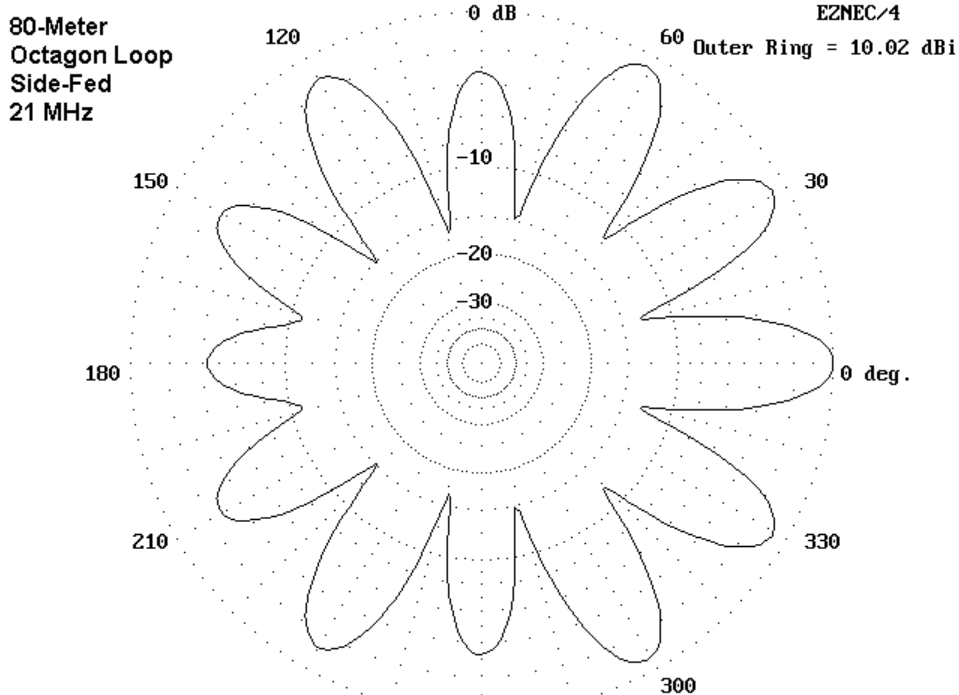
The tendency of a square loop to radiate with maximum gain from its corners continues on 15 meters. The elevation angle is in the 13-14° regions, which gives the antenna significant DX potential. The strongest lobe of the corner-fed square has a gain rivaling a 3-element Yagi, but over a much narrower beamwidth. (We should especially note this fact, because wire antenna makers often advertise their wares as equal to beams. The illusion only persists if we ignore beamwidth.)



With corner feed, current magnitude and phase combine to yield 4 strong, narrow lobes with corner feed. With side feed, the major lobes become many (12, to be exact), well spread around the horizon, but at loss of over 3 dB of maximum gain. (Note that the corner-fed version also has 12 lobes, but 8 are very minor.) The side-fed square becomes the configuration of choice if we desire maximum coverage on 15.



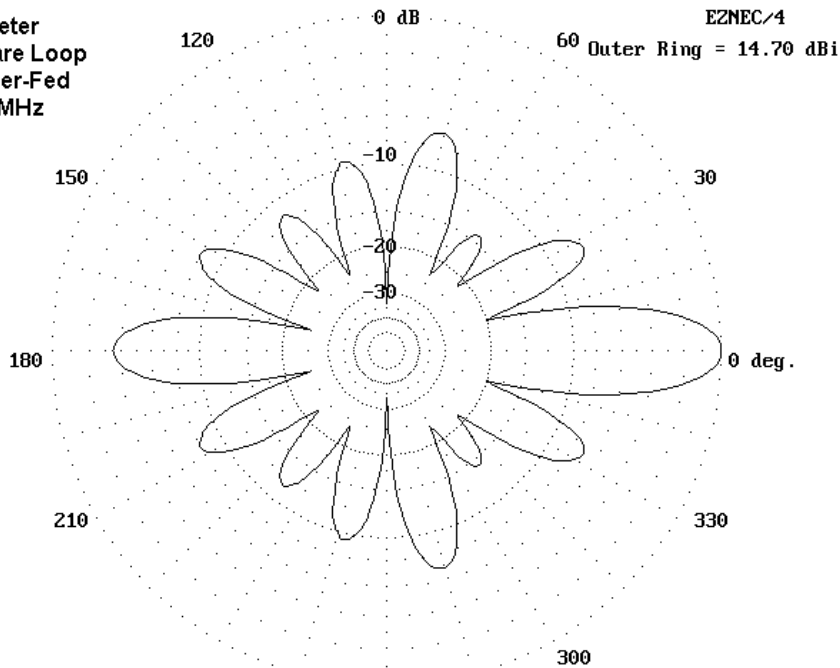
Like the 17-meter model, the 15-meter models of the octagon show far greater similarity than do the square models. The corner-fed version retains a bit of the 4-lobe dominance found in its square counterpart, but the minor lobes have grown into major ones, giving the antenna better potential for omni-directional contacts. However, the side-fed octagon has the most even pattern of all, with only a small tilt of the pattern away from the feedpoint.



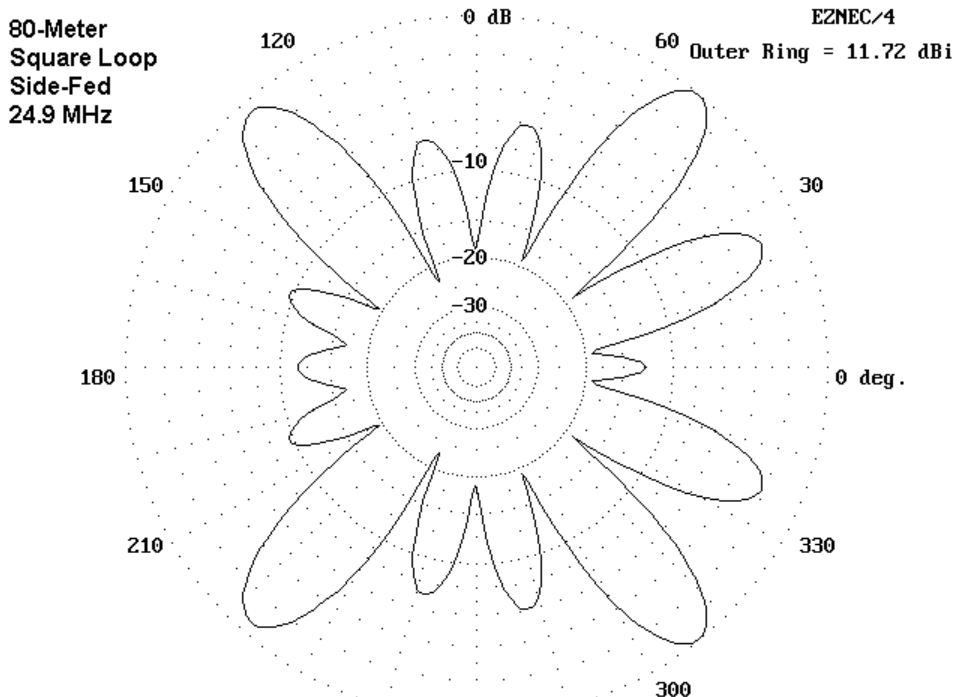
As has been the case on other bands, the feedpoint impedance differs most widely between the two square models, with considerably less difference between the two octagon models. The corner-fed square has a lobe with the highest gain of the four models. In contrast, the highest gain of the very even-lobed side-fed octagon is about 4 dB lower than the corner-fed square. Even lobes usually mean lower maximum gain.

## 12 Meters

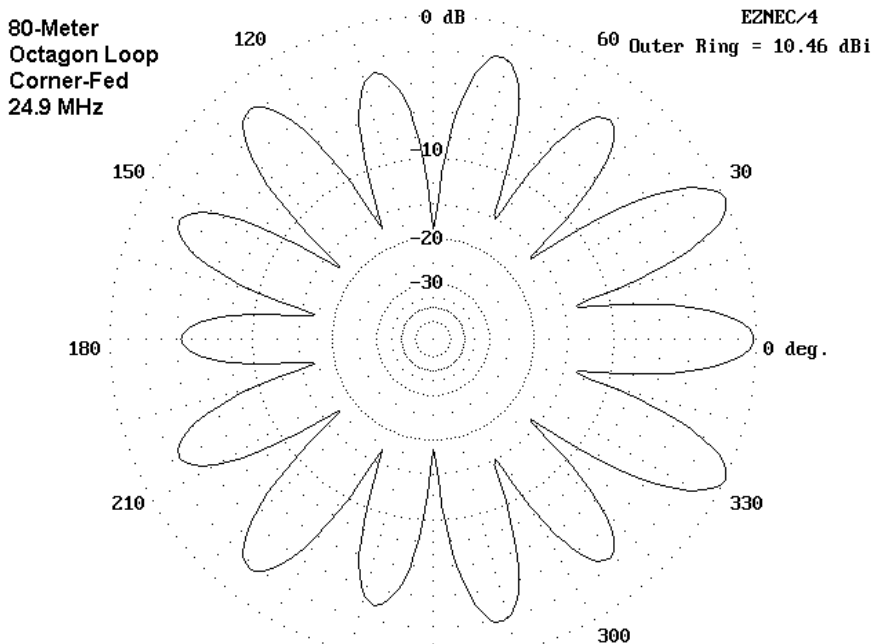
80-Meter  
Square Loop  
Corner-Fed  
24.9 MHz



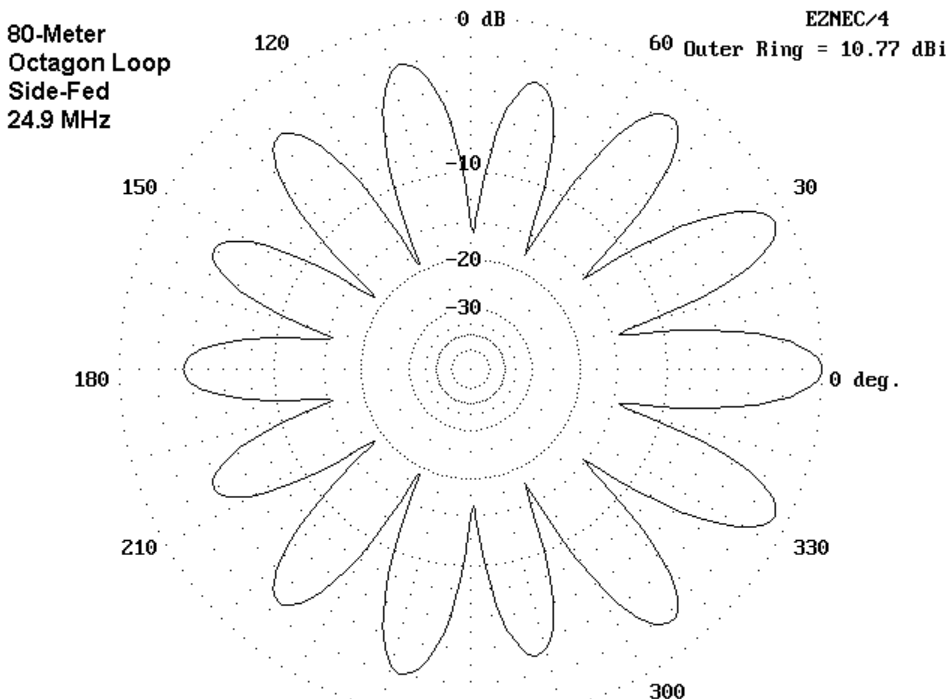
The 12-meter corner-fed square continues the pattern of bi-directionalness on this model on the non-harmonically related bands. As was the case with lower band models, the highest gain is along the axis from the corner feedpoint through the corner opposite. When side fed, the square once more shows maximum gain from the four corners of the loop.



The loop which is 1 wl long on 80 meters has 14 lobes, or 7 per half loop on 12 meters. This is no accident, since the length of the loop at 24.9 MHz is a little over 7 wl. (On 80 meters, the loop showed only two lobes in the oval pattern, 1 per half wavelength.) As the side-fed pattern shows, some lobes may be very small. In other cases, lobes may merge to become almost indistinguishable from a single lobe. However, you can always count on them being present as a function of the length of the wire at one lobe per half wavelength.

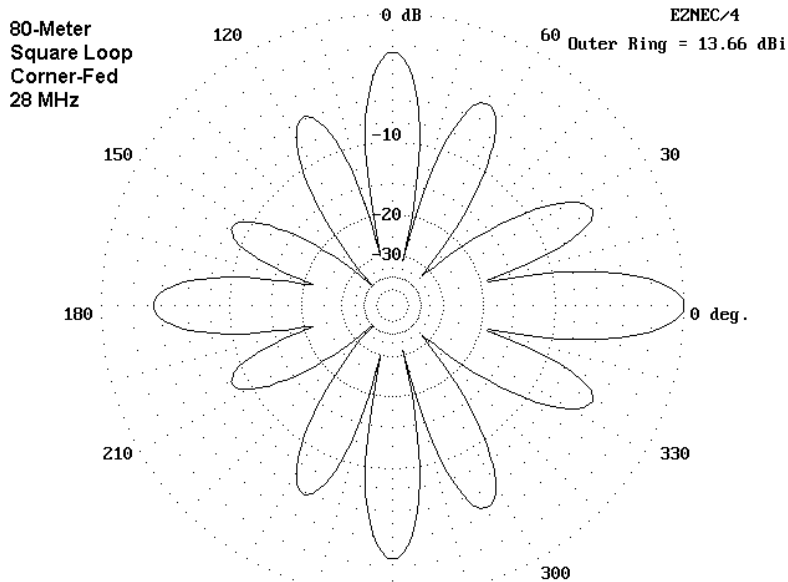


The 14 lobes of the 12-meter octagons are clear and distinct in both the corner and side fed versions of the antenna. In the octagons, the lobes are functions of the feedpoint in terms of direction. However, the difference between the two feed positions shows up in the minor differences in the relative strengths of the individual lobes, except for the one directly opposite the feedpoint.

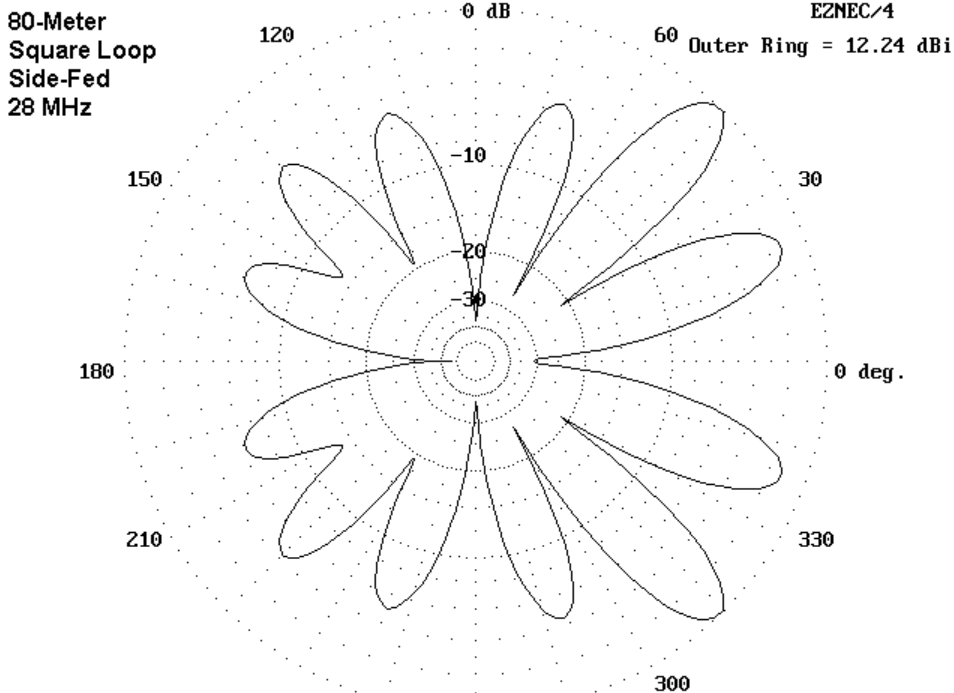


Interestingly, the 12-meter models are as a group closer to resonance than any other group. The bi-directional corner-fed square shows the highest reactance. The other models, with their more even collection of lobes, show between 20 and 75 Ohms reactance. You may track the feedpoint impedances in the reference table that immediately follows this compendium of azimuth patterns. You may find it useful to correlate the pattern descriptions, the maximum gains, and the feedpoint impedances of the models.

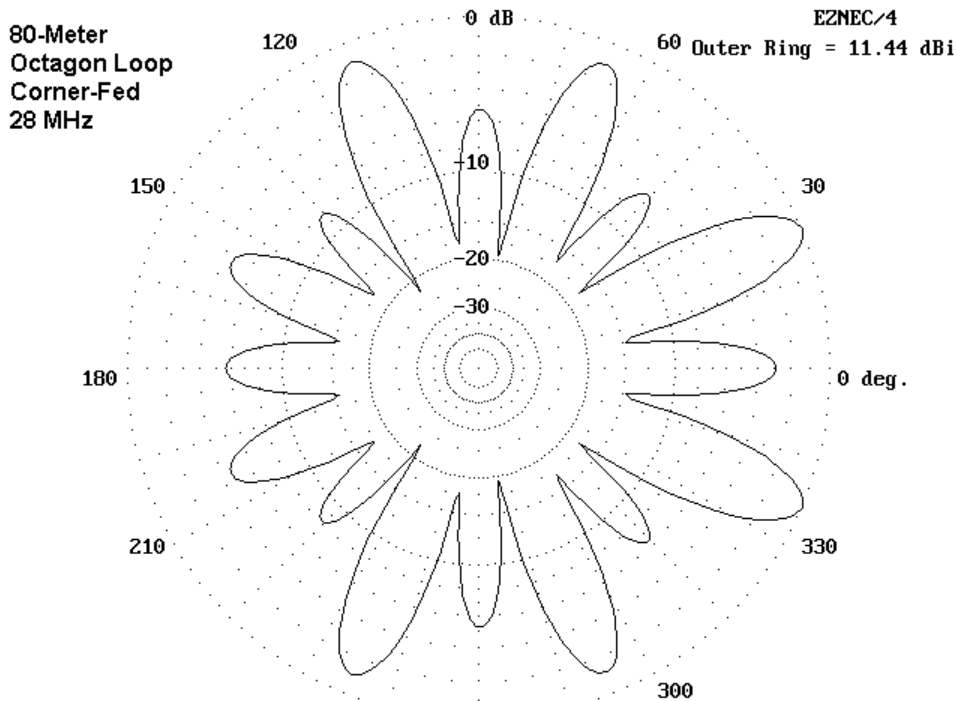
## 10 Meters



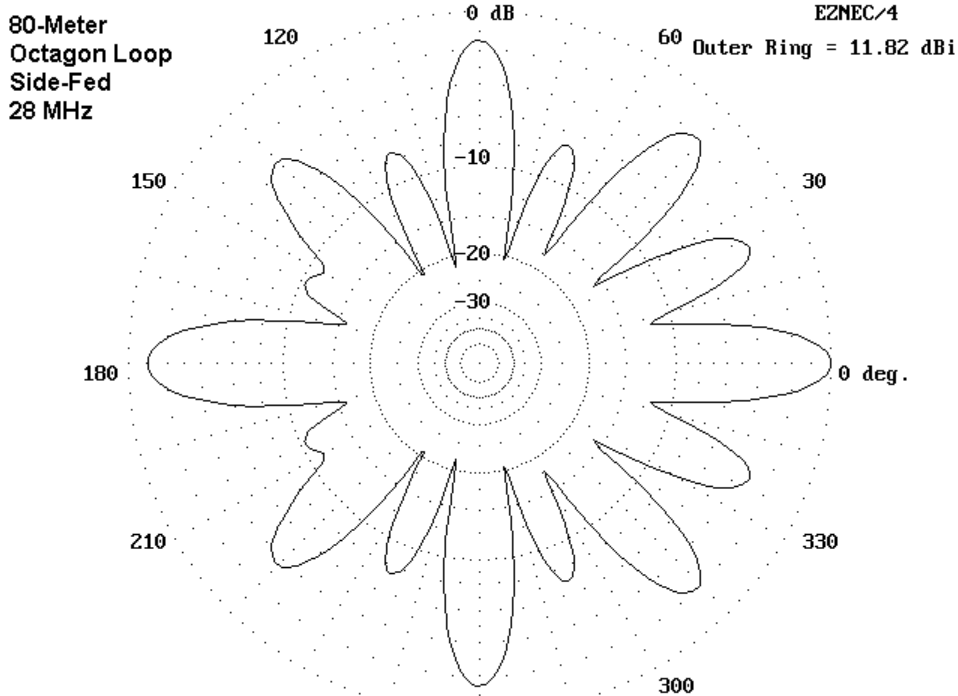
28 MHz is exactly 8 times 3.5 MHz. since the loops at 80 meters had two lobes, we should be able to count 16 lobes in the 10-meter models. In fact, the square models only show 12 lobes. What has happened to 4 lobes? In principle, two things can occur. One is that the lobes merge. In most instances, merges lobes show some aberration of the normal cigar shape of a lobe. No such odd shape appears in the square models.



The other possibility is that lobes cancel each other due to the presence of equal but opposite radiation from symmetrical points across a loop. In the corner-fed model, notice the wide and very deep nulls at the 45° angles, and in the side-fed model, notice similar nulls at the 90° points. Both sets of nulls correspond to the middle points along the sides of the squares. In effect, the lobes for these positions have cancelled each other out across the antenna loop.



The relative positions in the octagon that might correspond to those in the squares are not quite right for complete cancellation of any lobes. Hence, the full complement of 16 lobes appears in each of these models. The corner-fed octagon shows its strongest lobes on either side of the position where the corner-fed square has its strongest lobe. The side-fed octagon positions its strongest lobes like those of the corner-fed square.

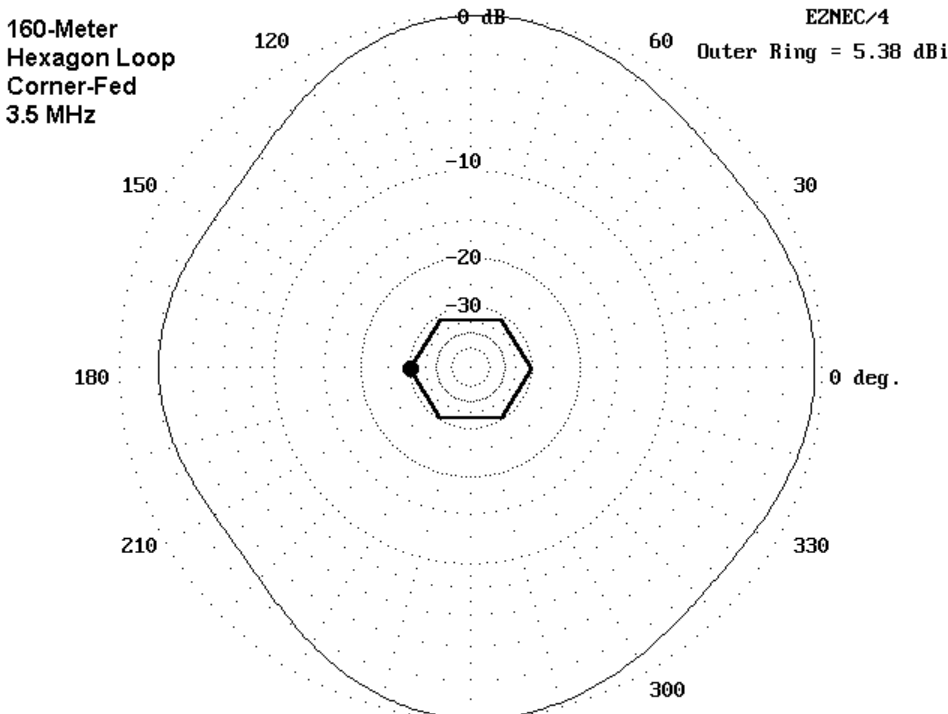


The side-fed octagon also illustrates lobe merging and the consequent distortion of lobe shape as two or more lobes come together. The "mittens" at 135° and 225° are good examples of merging lobes.

It is clear from this compendium that loop shape can make a difference in how the loop performs on various bands. If you plan to build an irregular loop, by all means, anticipate its performance through modeling.

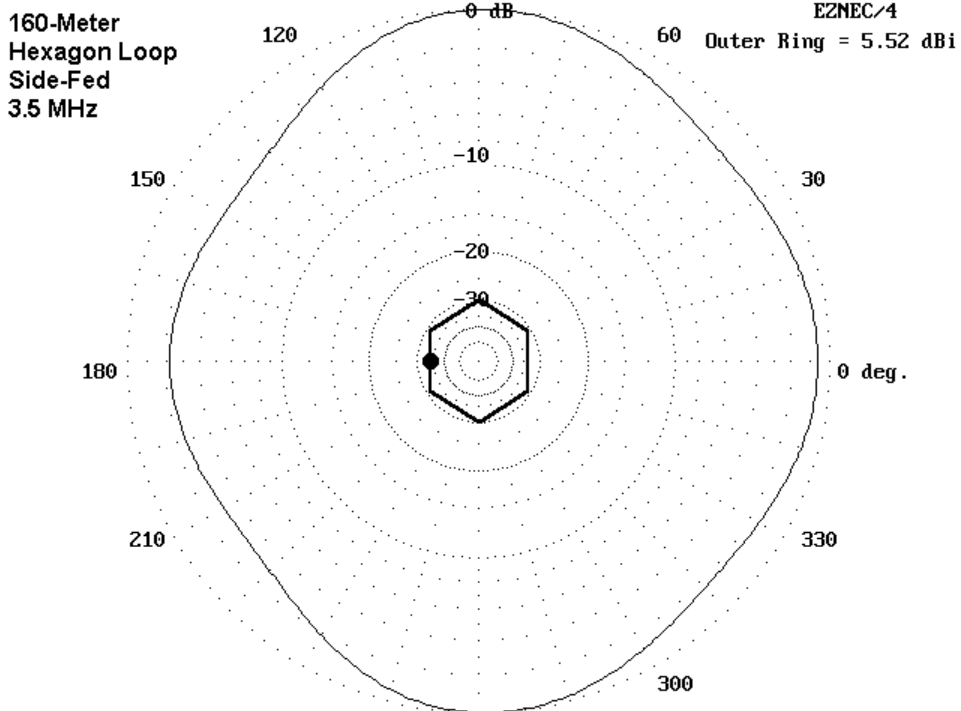
### Azimuth Patterns of Hexagon 160-Meter Loops, Corner and Side Fed

## 80 Meters

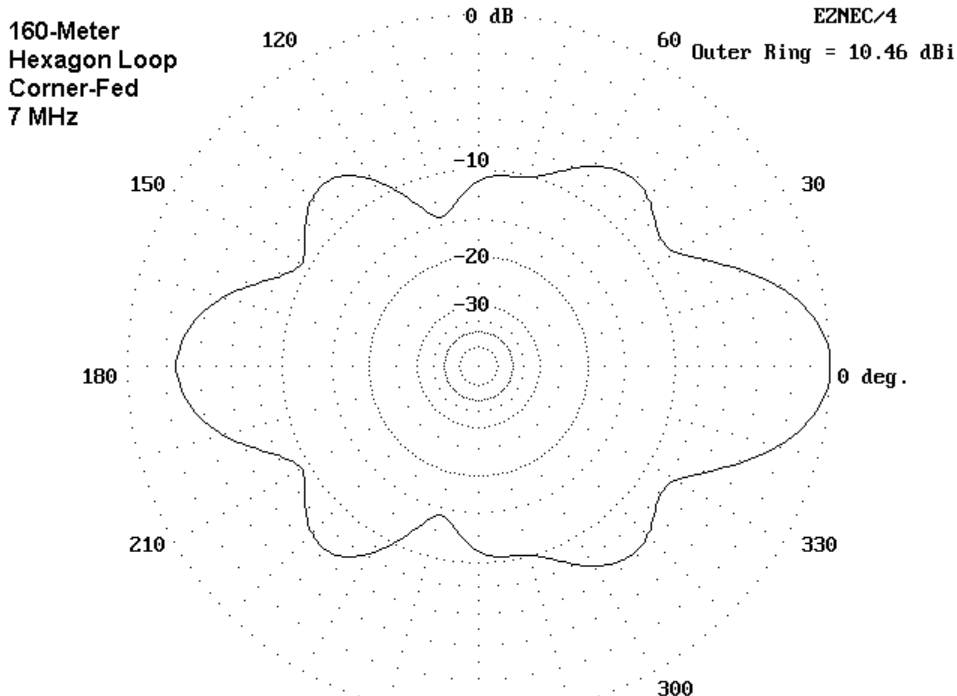


Because the 160-meter loop is about 2 wl long at 3.5 MHz, the pattern resembles that of the 80-meter loop when used on 40 meters. However, the antenna height is proportionately lower (about 0.18 wl for the 160-meter loop on 3.5 MHz vs. 0.35 wl for the 80-meter loop on 7 MHz), so the elevation angles of maximum radiation are higher: in the 48° to 49° range. Nevertheless, there is far more radiation at lower elevation angles than with the 1 wl loop

on 80 meters. The additional low angle gain holds the promise (but not the guarantee) of more regular longer distance contacts on 80 meters. Although the radiation pattern is fairly even all the way round the loop, it is slightly stronger at  $90^\circ$  to the feedpoint axis. There is virtually no difference between the patterns for the version using a corner feedpoint or for the one using a side feedpoint.

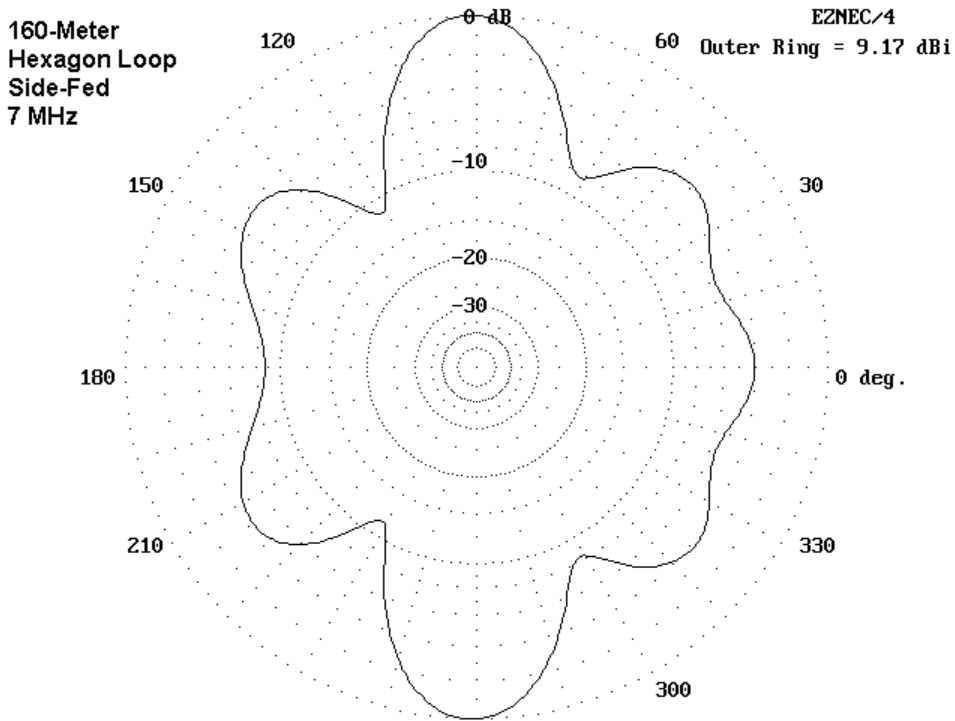


## 40 Meters

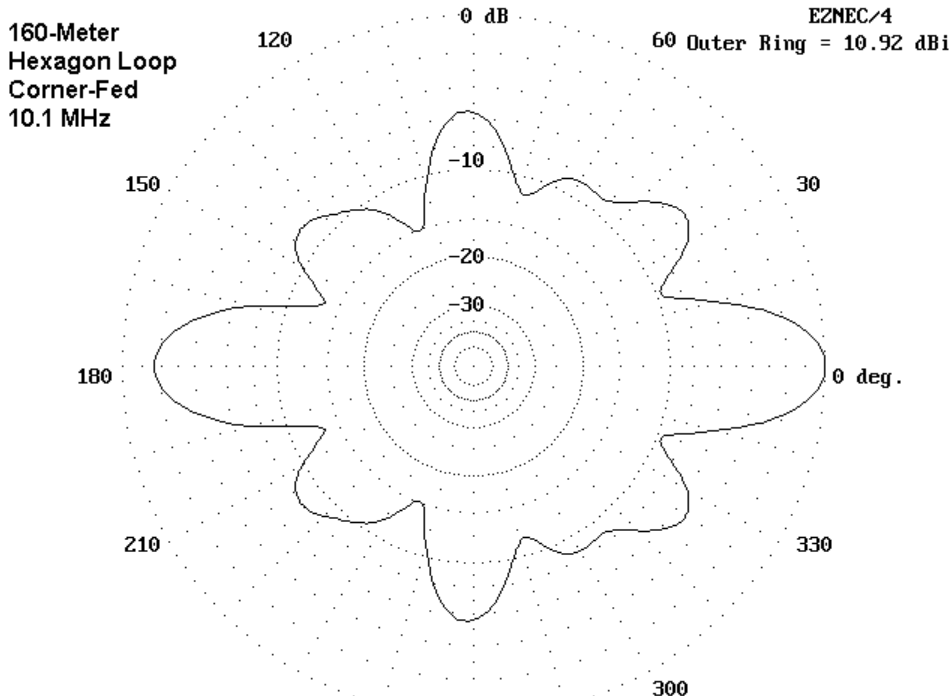


On 40 meters, the 160-meter loop becomes quite bi-directional with either corner or side feeding. Maximum gain occurs off opposite points of the hexagon. With corner feeding, the axis of maximum gain is through the feedpoint to the opposite corner. However, if we side-feed the hexagon, the axis of maximum gain is at right angles to the feedpoint-to-opposite side axis.

Both of the 40-meter patterns of the 160-meter loop are exercises in finding hidden lobes. We expect 8 lobes. In the corner-fed model, we can almost count them in terms of small bumps in the pattern. The side-fed model appears to be missing a lobe--the one to the rear of the feedpoint. In fact, this lobe is highly suppressed and would appear only if there were deeper nulls on each side of it.

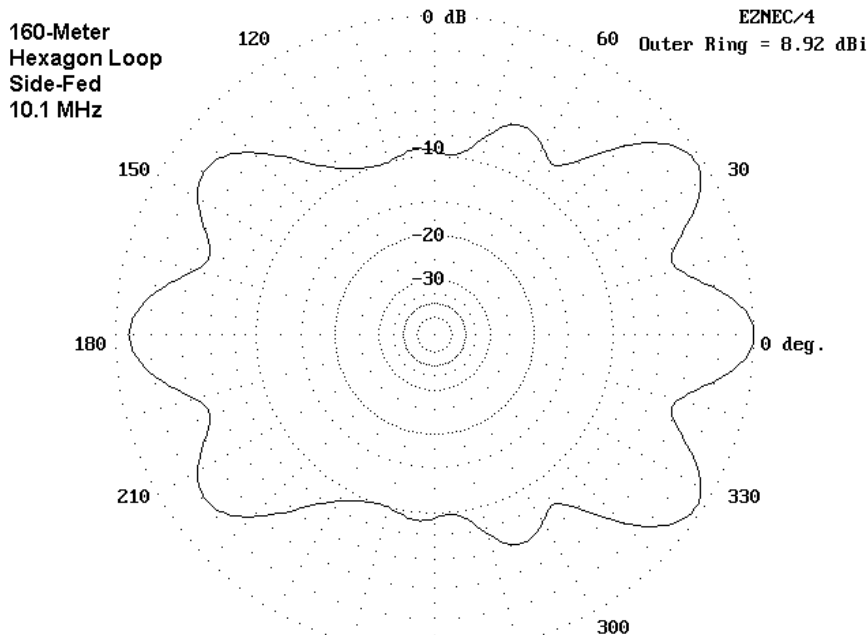


## 30 Meters

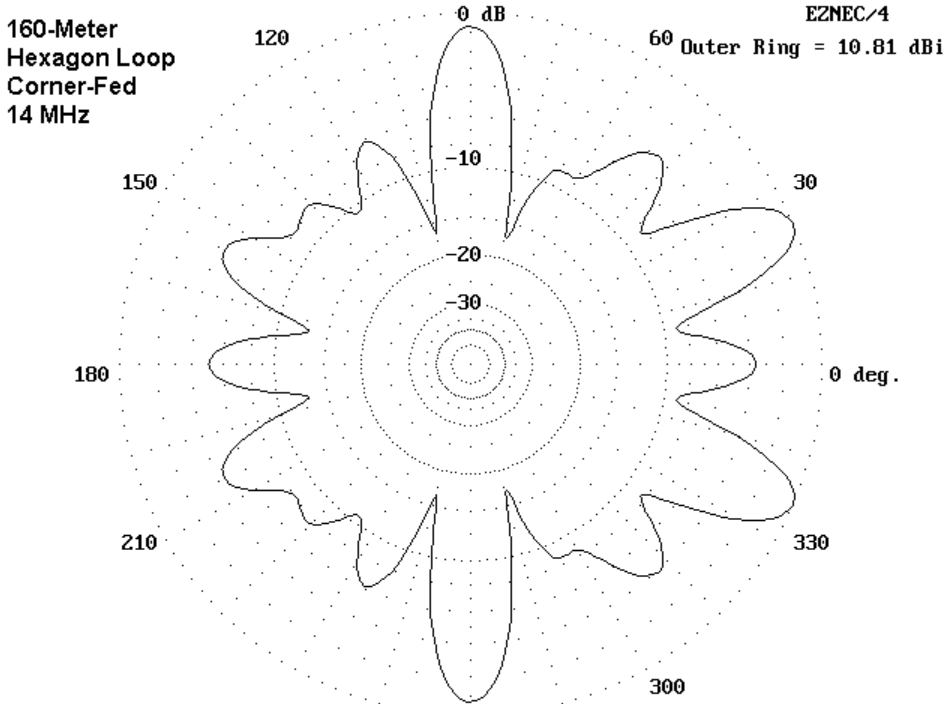


The patterns for the 160-meter hexagon at 10.1 MHz are roughly bi-directional along the axis from the feedpoint to the opposite position on the loop. However, the side-fed version achieves an almost rectangular pattern, which is somewhat of an oddity.

Of equal significance with the pattern shape are the high values of resistance and reactance at the feedpoint of either version of the 160-meter hex. The 80-meter loop showed only a few values of reactance above 500 Ohms, and no resistance values reached that level. In contrast, the 160-meter loop will show values in excess of that level for many bands. The length of the feedline used may require careful selection with the larger loop to ensure that the values presented to the antenna tuner are within the range of available adjustment. Some feedline length-switching may be required as one moves from one band to another.

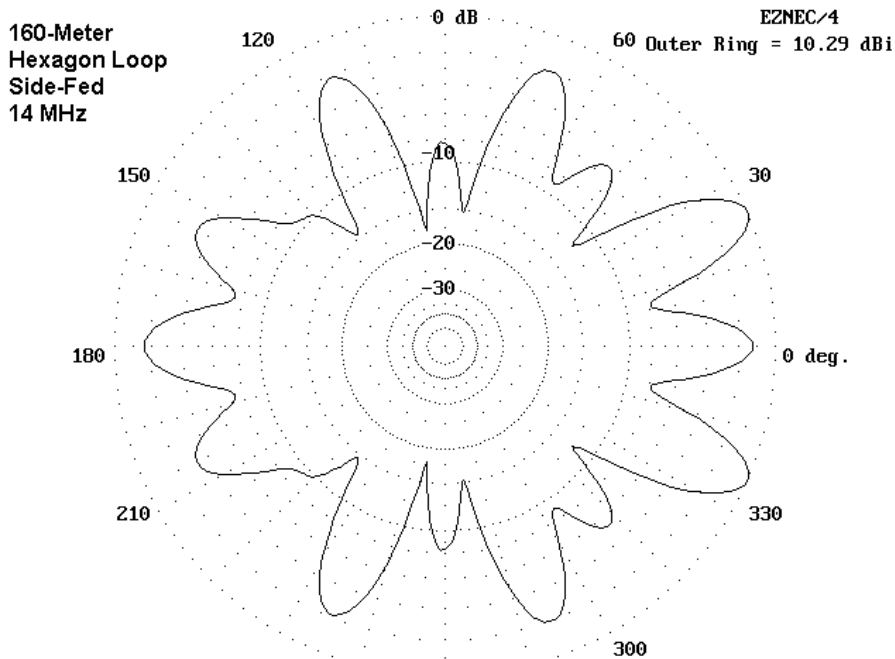


## 20 Meters



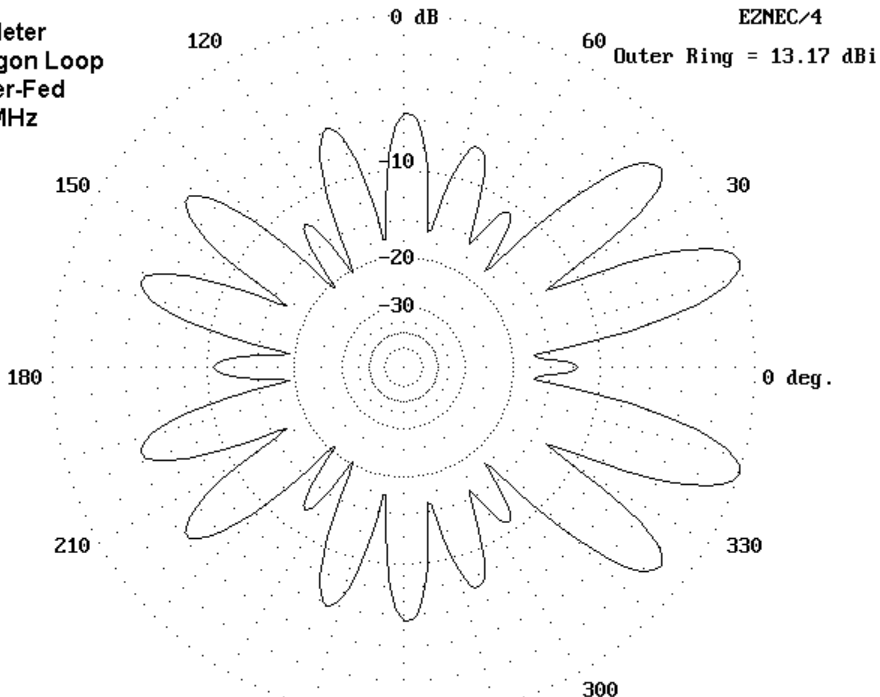
The 20-meter patterns for the larger loop show a combination of most of the pattern characteristics we have already seen: bi-directionalness, merged lobes, and a number of others. Primary radiation is off opposing sides, as with the 40-meter patterns, but with a greater complexity of lobe structure. As well, the feedpoint resistance and reactance values are fairly high.

Of interest is the fact that maximum gain values fall only in the middle of the span of those exhibited by the 80-meter loop when run at 14 MHz. On this band--and on others as well, the antenna offers little to justify the added complexity of running a wire twice as long as the 80-meter loop. One might well argue for some installations that the benefits derived on 80 meters from the larger loop are offset by the disadvantages on some of the higher bands. Indeed, the shorter loop and a separate 80-meter antenna might be easier to use.



## 17 Meters

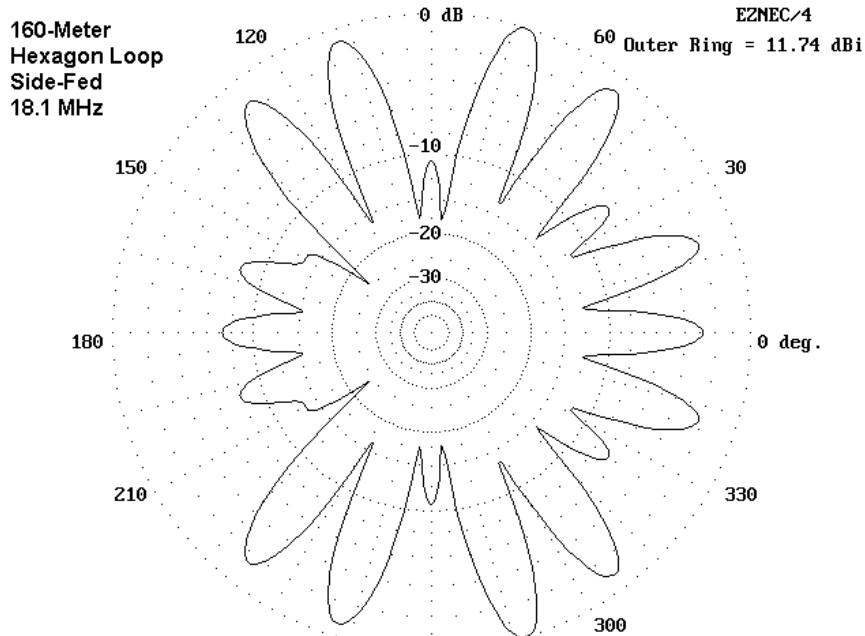
160-Meter  
Hexagon Loop  
Corner-Fed  
18.1 MHz



The 17-meter patterns for the 160-meter loop bear a striking resemblance to those for 40-meter operation if we do two things. First, we have to smooth the peaks of the narrower and more numerous 17 meter lobes. Second, we have to notice the movement of the peak gain regions a small angular distance away

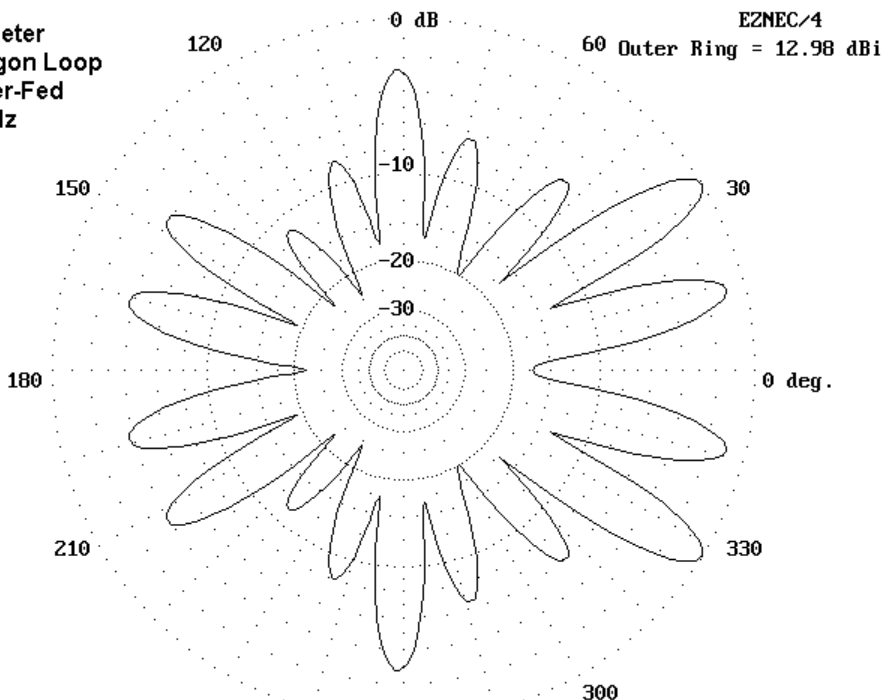
from their axes on 40 meters so that a narrow weak area develops along the precise axes of 40 meter peak gain.

As curious as the patterns are, the 17-meter impedance values are also interesting because they come closer to resonance than the values on any other band. However, there will still be considerable excursions of voltage and current on the feedline, because the high values of feedpoint impedance on other bands almost dictate the use of 600-Ohm open parallel feeders as the best compromise among all the impedance levels encountered.



## 15 Meters

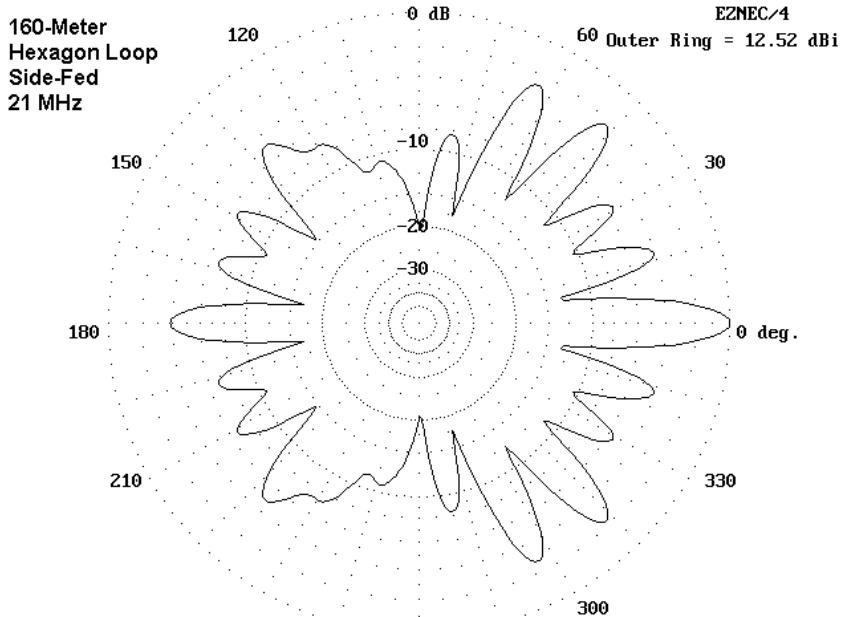
160-Meter  
Hexagon Loop  
Corner-Fed  
21 MHz



At a certain level of lobe multiplication, azimuth patterns tend to lose their identity as guides to antenna radiation and become more like Rorschach ink blot tests. With the 15-meter patterns of our large loop, we may have reached that stage. Local ground clutter, terrain irregularities, and simple blowing of the antenna wire in the

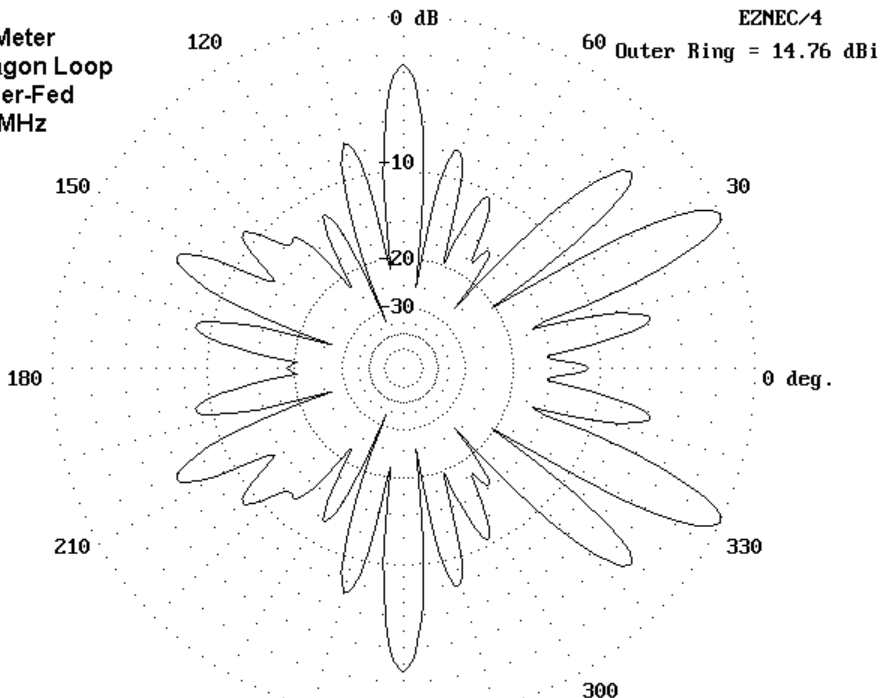
wind may lessen the utility of following out each pencil-thin lobe of the azimuth pattern.

Nonetheless, we can gain something from observing the azimuth patterns, if only by gaining a general impression of regions of strength and weakness. For example, between the corner-fed and the side-fed patterns, the former seems to have more lobes of higher strength in more directions, thus promising contacts in both the morning and the evening hours of the daily skip cycle (assuming that the antenna is set up on a rough East-West axis).



## 12 Meters

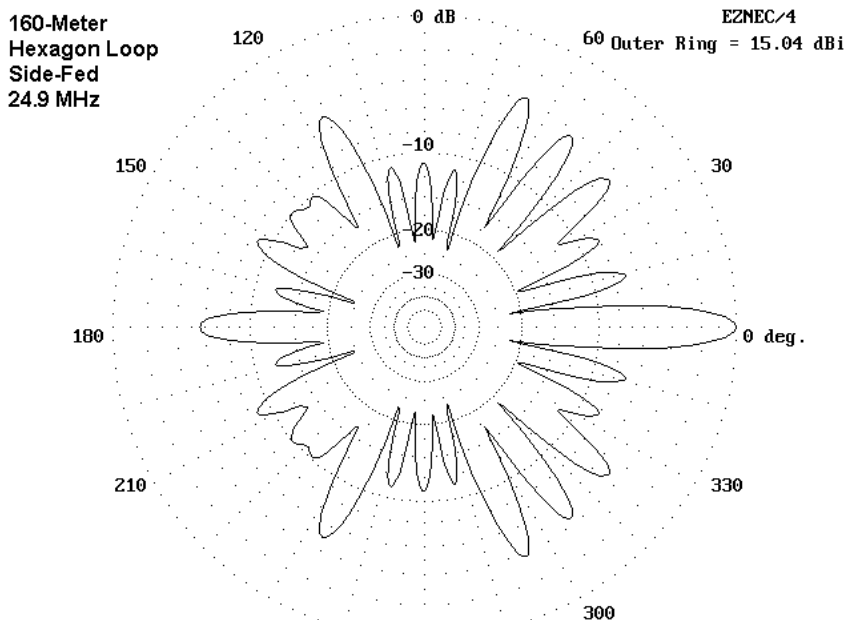
160-Meter  
Hexagon Loop  
Corner-Fed  
24.9 MHz



The patterns for both 12 meters and 10 meters share some interesting characteristics. Regardless of the feedpoint, there are very few lobes that are less than 8 to 10 dB down from the peak gain lobes, and almost all of them have very narrow beamwidths. Therefore, the effective gain of the antenna is not given by the maximum gain figures, which happen to range in the vicinity of 14

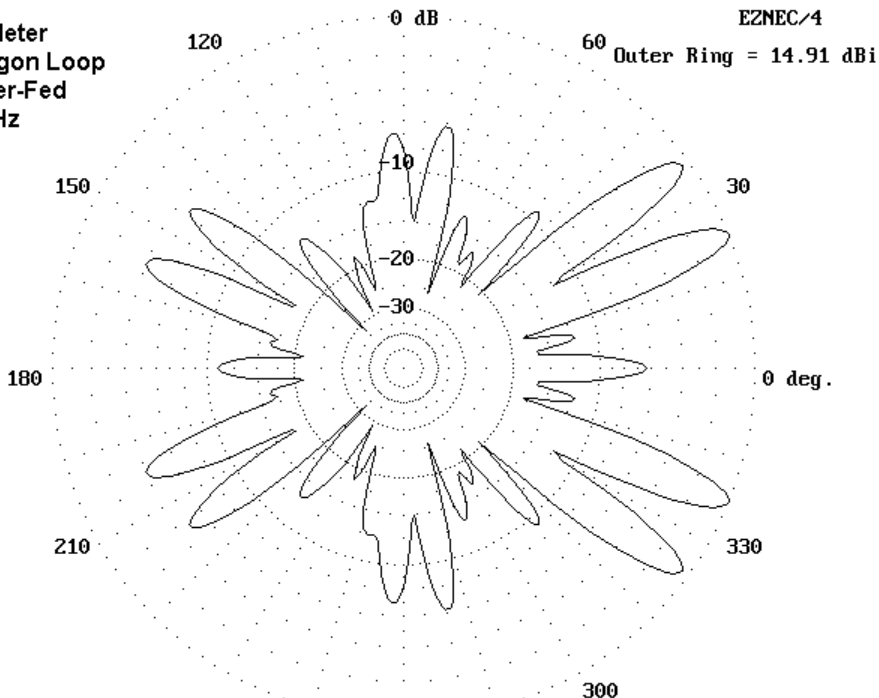
to 15 dBi. Rather, the average gain over the 360° horizon is more like 5 to 8 dBi. These are gain values more akin to a multiband quarter-wavelength vertical with a ground plane mounted on a roof top than they are to typical gain antennas.

There is a strong possibility that, if your interests are in upper HF operations, the large 160-meter loop will prove to be a disappointment. Its true virtue lies in the lower HF region, especially on 80 meters, with reasonable good performance through 20 meters.



## 10 Meters

160-Meter  
Hexagon Loop  
Corner-Fed  
28 MHz

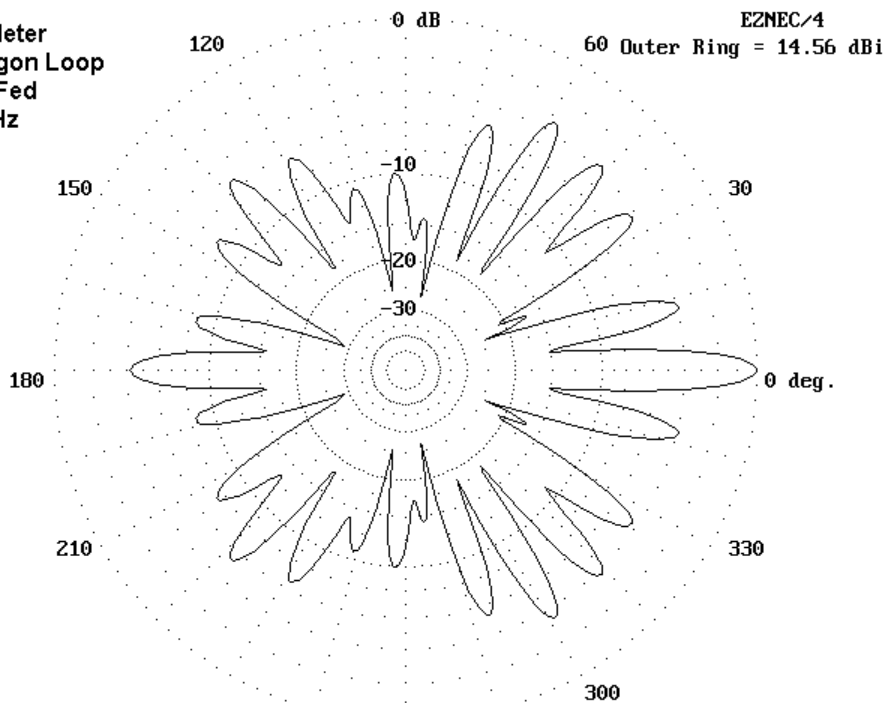


Although the 80-meter loop shows poor performance on 80 meters for every application other than NVIS, the smaller loop has distinct advantages over the larger loop on almost every other band. The patterns are smoother, with reasonable gain in most directions. The feedpoint impedances are moderate and amenable to the use of inexpensive and readily available 300-Ohm or 450-Ohm parallel

feedlines. The values of impedance presented to antenna tuners are more likely to be within the adjustment range of inexpensive units.

Size alone then, is not the sole determinant of HOHPL performance. Smaller size can be better for some operational purposes. As important as size is the antenna shape and the feedpoint position in the determination of the antenna patterns that will most benefit our operational needs. A HOHPL that best fits our needs is a blend of many factors.

160-Meter  
Hexagon Loop  
Side-Fed  
28 MHz



## Reference Tables of Modeled Antenna Performance for Antenna Azimuth Patterns Shown

80-Meter Square Loop, Corner-Fed: Fig. 11

Freq. MHz	Gain dBi	TO Deg	Feedpoint Z R +/- jX Ohms
3.5	4.4	45*	120 - j 100
7	6.0	43	95 - j 230
10.1	10.4	29	280 - j 650
14	11.3	20	245 - j 240
18.1	14.1	15	375 + j 245
21	14.2	13	250 - j 170
24.9	14.7	10	345 + j 125
28	13.7	9	260 - j 220

80-Meter Square Loop, Side-Fed: Fig. 12

Freq. MHz	Gain dBi	TO Deg	Feedpoint Z R +/- jX Ohms
3.5	4.3	45*	120 - j 100
7	6.7	37	290 - j 105
10.1	8.0	27	280 - j 610
14	10.7	19	215 - j 265
18.1	11.7	15	415 + j 210
21	10.8	13	410 - j 215
24.9	11.7	11	380 + j 20
28	12.2	9	280 - j 250

80-Meter Octagon Loop, Corner-Fed: Fig. 13

Freq. MHz	Gain Bi	TO Deg	Feedpoint Z R +/- jX Ohms
3.5	4.3	45*	135 - j 55
7	6.3	41	205 - j 150
10.1	7.9	29	250 - j 580
14	9.3	21	155 - j 250
18.1	11.6	15	310 + j 250
21	11.9	13	275 - j 230
24.9	10.5	11	300 + j 40
28	11.4	10	310 - j 310

## 80-Meter Octagon Loop, Side-Fed: Fig. 14

Freq. MHz	Gain dBi	TO Deg	Feedpoint Z R +/- jX Ohms
3.5	4.3	45*	135 - j 70
7	6.3	41	200 - j 180
10.1	7.7	25	250 - j 610
14	9.8	19	270 - j 230
18.1	9.8	16	295 + j 150
21	10.0	14	275 - j 335
24.9	10.8	11	265 - j 70
28	11.8	10	300 - j 415

## 160-Meter Hexagon Loop, Corner-Fed: Fig. 15

Freq. MHz	Gain dBi	TO Deg	Feedpoint Z R +/- jX Ohms
3.5	5.4	49	145 - j 265
7	10.5	36	350 - j 505
10.1	10.9	23	2810 - j 1140
14	10.8	21	815 - j 1010
18.1	13.2	15	415 - j 90
21	13.0	14	1830 - j 370
24.9	14.8	11	870 - j 540
28	14.9	10	1300 + j 635

## 160-Meter Hexagon Loop, Side-Fed: Fig. 16

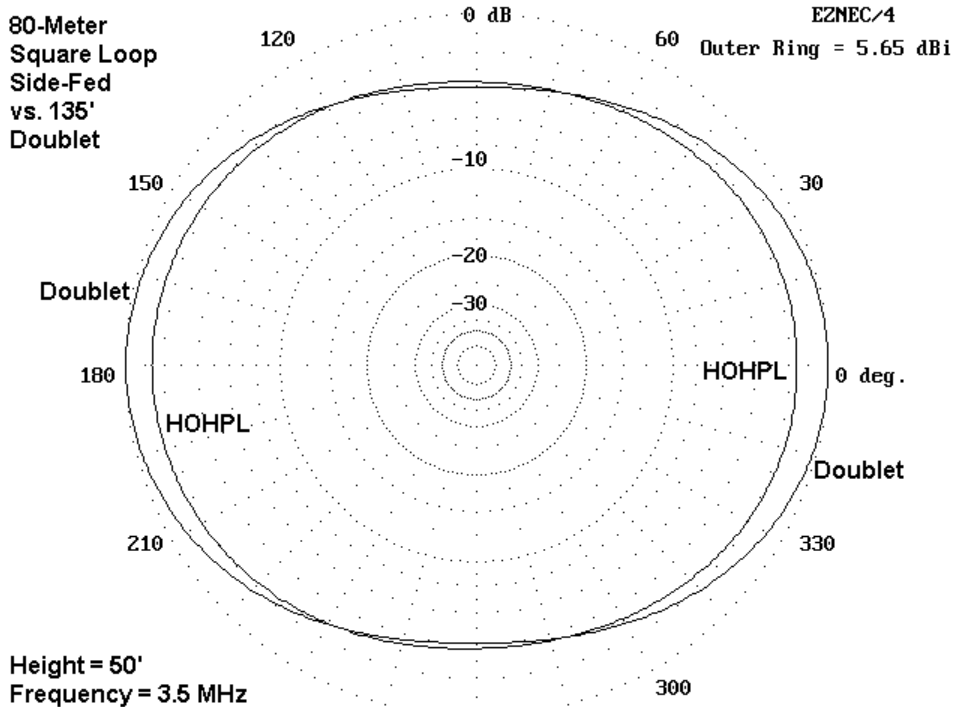
Freq. MHz	Gain dBi	TO Deg	Feedpoint Z R +/- jX Ohms
3.5	5.5	48	145 - j 260
7	9.2	33	285 - j 495
10.1	8.9	25	2205 - j 1105
14	10.3	18	655 - j 920
18.1	11.7	15	385 - j 130
21	12.5	14	1570 - j 687
24.9	15.0	11	735 - j 585
28	14.6	9	1455 + j 125

**Notes:**

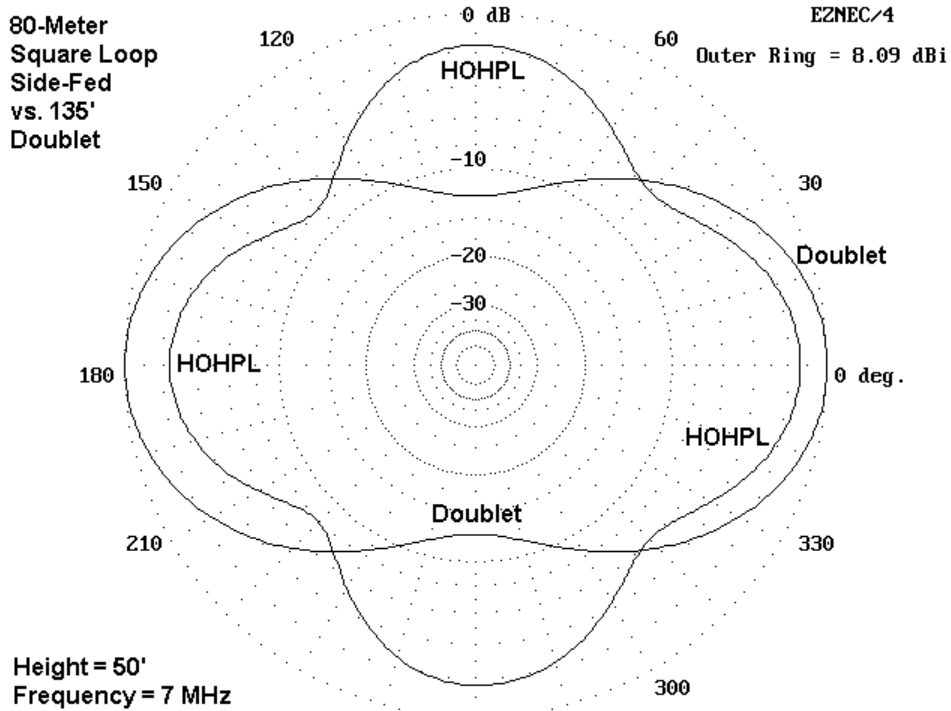
1. \* beside a TO entry means that the angle used is arbitrary. Maximum gain is straight up (elevation angle = 90°).
2. Feedpoint impedance figures are representative and will vary with the exact length and layout of the antenna loop. The impedance presented to the antenna tuner will also be a function of the exact length, characteristic impedance ( $Z_0$ ), and velocity factor (VF) of the transmission line used for each particular installation.
3. Gain figures represent the maximum gain of the strongest lobe in the azimuth pattern and should not be interpreted as the sole basis for deciding among HOHPL designs. Equally important are the distribution of the lobes, the depth of the nulls, access to all desired communications directions, and other factors.
4. TO angles are the elevation angles of maximum radiation from the strongest lobe. The vertical structure of lobes may vary.

## **6. How does the HOHPL compare to other all-band antennas?**

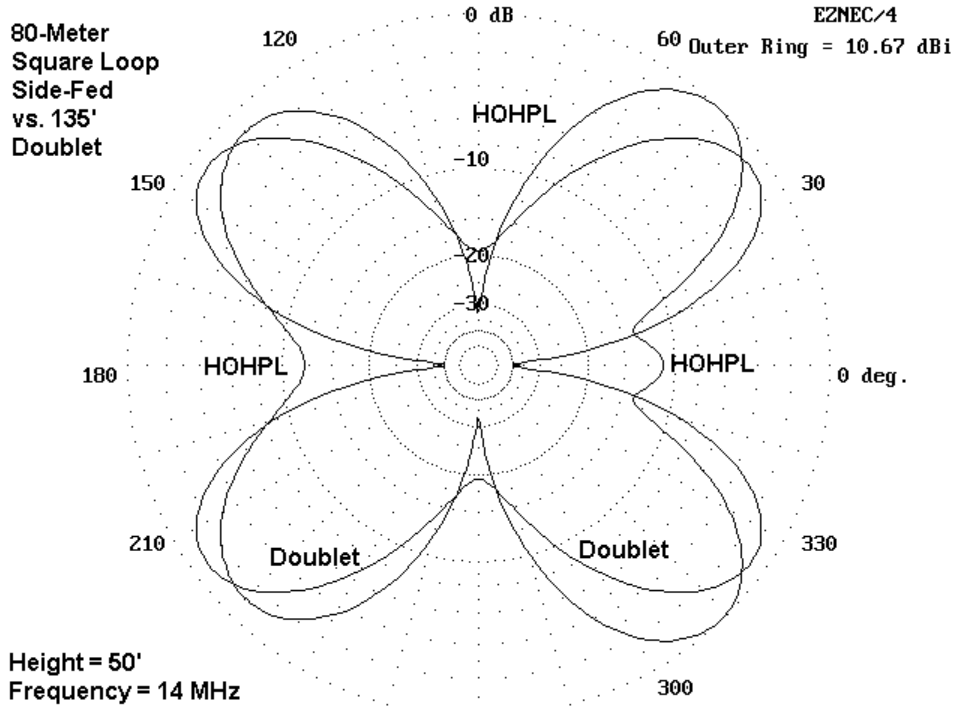
Although it would be impossible to do a detailed comparison with every possible contender against the HOHPL, we can sample one case: the standard 135' center-fed doublet. For fairness, we shall place both antennas at 50 feet and overlay azimuth patterns for 80, 40, 20, and 10 meters, as representative of a fuller comparison.



On 80 meters, there is no major difference between the doublet and the square HOHPL. *The HOHPL shows a higher radiation angle, giving the doublet about 1.2 dB more gain (5.6 vs. 4.3 dBi at the arbitrary 45° elevation angle).*

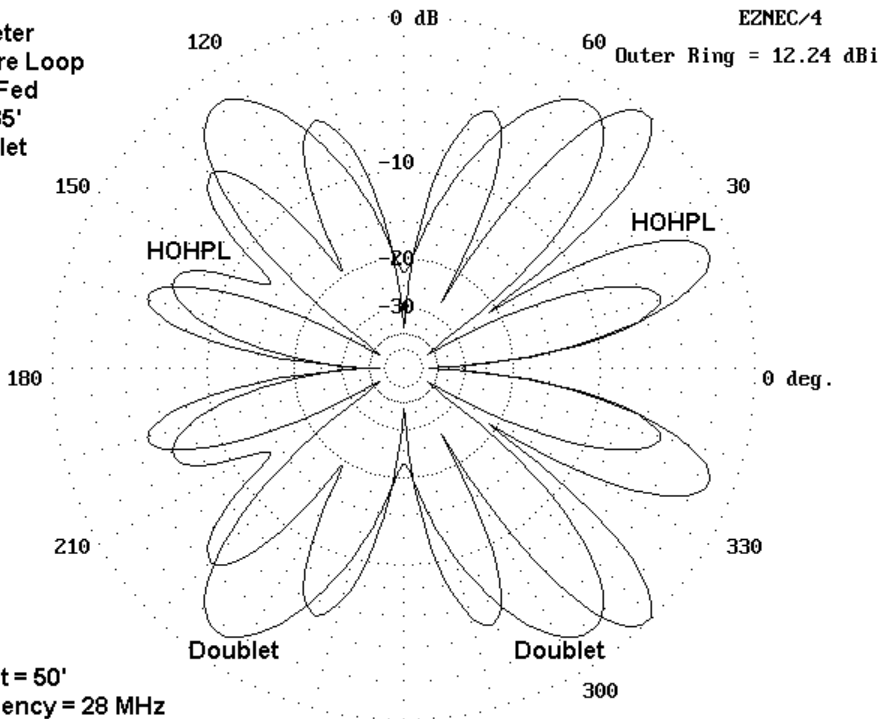


There is a distinct difference between the HOHPL and doublet 40-meter patterns. The doublet is 1 $\lambda$  long and shows a bi-directional pattern. The HOHPL loop is 2  $\lambda$  long and displays major lobes in four directions, although at lesser gain (8.1 vs. 6.7 dBi at about 36° elevation). Which antennas have the advantage depends on one's operating needs.



On 20 meters, the 1wl HOHPL shows enough tilt in the pattern away from the feedpoint to give it a small gain advantage at similar elevation angles. Although the patterns seem otherwise fairly similar, with only small offsets in the lobes, the doublet shows some deep nulls broadside to the antenna, nulls that can adversely affect communications in certain quadrants. Although the "side" nulls of the HOHPL are deep, they do not differ as much from the doublet wire-end nulls.

80-Meter  
Square Loop  
Side-Fed  
vs. 135°  
Doublet



The 10-meter patterns, while a bit confusing at first sight, also show that the HOHPL has somewhat fewer nulls of great depth than the doublet. Moreover, especially in the direction away from the feedpoint, the HOHPL lobes are stronger (by about 1.5 dB) and more even in gain. In contrast, the doublet is beginning to show greater strength in lobes that are further from the broadside direction and more towards the antenna ends.

## Conclusion

Summing up all of the patterns for the HOHPL shows it to be a somewhat better performer over a full azimuth circle than the 135' doublet. A 2 wl HOHPL would show an even greater evenness in the lobe structures, since its 80-meter pattern is already like the 4-lobe pattern we saw above for 40 meters. In this summary comparison, I have not stressed matters of raw gain, but instead, I have placed emphasis upon the nature and position of the lobes and nulls. For nation-wide and world-wide communications, evenness of pattern may often be more important than the gain of one or more individual lobes.

As a consequence of this behavior, the advantage of the HOHPL will not show itself in any one contact or in a short period. Satisfaction with the antenna grows with time and changes in the propagation paths, a successful communications almost everywhere shows up in the log.

Still, the HOHPL, even in its smaller 1 wl form, requires a considerable investment in real estate, supports, wire, and accessories compared to the simpler doublet. Only the potential user can decide if it is the right antenna for his or her installation.

## Chapter 73: Configuring Horizontal Wire Loops

In the previous Chapter 72, I provided some extensive notes on horizontally oriented, horizontally polarized wire loop antennas (HOHPLs). In those notes, the most common practice with horizontal loops was using a 1-wavelength circumference at the lowest operating frequency. Since writing that Chapter, I have changed the recommendation that I usually make, depending on the space available to the loop builder.

So let's begin again and work with a different plan. My plan of attack is based on the 3 most asked questions:

- How Big?
- How High?
- What Shape?

Since we shall defer the question of shape until last, we shall need a paradigm model with which to begin. Let's use a nearly perfectly circular loop as our starting point, as outlined in **Fig. 1**. The loop uses 40 wires to form the circle, so the approximation is quite good. For our first 2 questions, the feedpoint will be on the right, in the +X direction. (We shall alter that for our last question for reasons that will become apparent when we arrive at questions of shape.) Note the orientation of the X, Y, and Z axes in the outline drawing. These axes lines will be important to orienting ourselves to some of the patterns in upcoming figures.

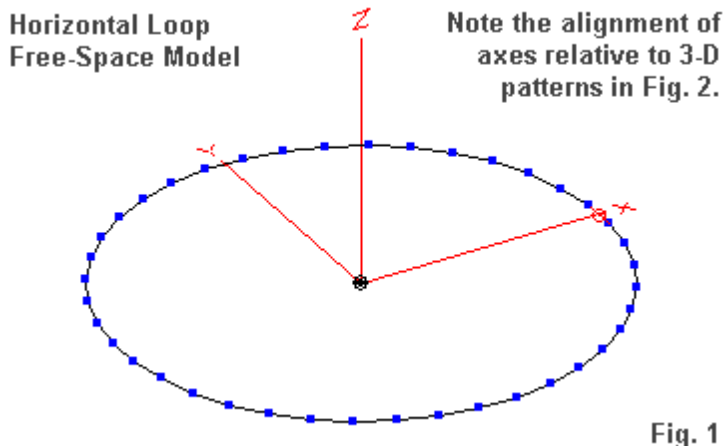


Fig. 1

A circular loop as a starting point has some advantages over beginning with other shapes. With both regular and irregular polygons, we tend to find performance differences depending on whether we feed the antenna at a corner or somewhere within a side. Since a circle has no sides (or infinitesimal ones, at best), we can avoid those differences until we reach our last question.

## How Big?

The question of how big to make a horizontal loop antenna is a function of frequency, specifically, the lowest frequency of intended use. Virtually any size will work to some degree, but some sizes are better than others. Remember that here we are speaking of relatively large loops, not mini- or micro-loops used as table-top antennas. Since I cannot know the lowest frequency of intended

use, let's express dimensions as a function of a wavelength at the lowest operating frequency. Since a horizontal loop is usually used as a multi-band antenna, we shall likely feed it with parallel transmission line and an antenna tuner. Hence, ultra precision of dimension is not necessary (as it might be for an antenna that must have some particular feedpoint impedance). So if I suggest a length, such as 3 wavelengths, for a loop size, anything relatively close to that size will do fine. "Relatively close" means about +/- 15% of the suggested size.

The basic dimension of loop size is normally its circumference, that is, the total length of wire making up the loop. Of course, being a loop implies that there is relative parity of cross dimensions, although distended rectangles, rhombics, etc. will work. However, we have to confine our work to what we can handle, so we shall stay with regular polygons throughout these notes.

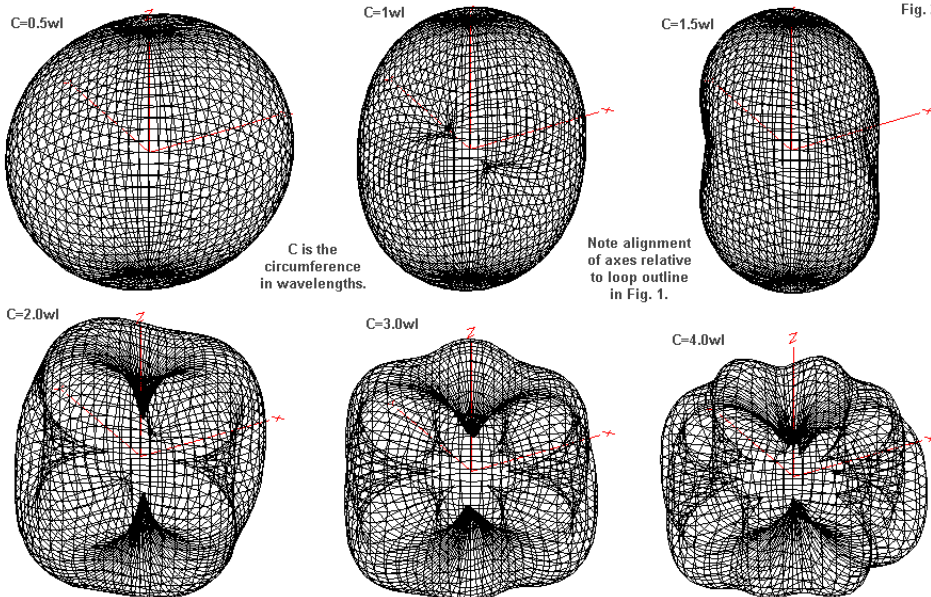
For our work, if you wish to translate a length in wavelengths into an English measure, you may use a very simple equation:  $L_{(\text{feet})} = (984 / F_{(\text{MHz})}) * n$ , where  $n$  is the number of wavelengths specified. If you wish to go metric, then use this equation:  $L_{(\text{meters})} = (300 / F_{(\text{MHz})}) * n$ . These equations are not precise, but they are within the limits that we need to convert a horizontal loop into a length of wire.

To see how big to make our loop at the lowest operating frequency, let's put the loop into free-space and examine some 3-dimensional radiation patterns. These patterns will tell us something about why I have changed my recommended length for a horizontal loop. The following table provides the key dimensions of the loops whose

patterns appear in **Fig. 2**. The basic loop size is the circumference, but the diameter gives you an idea of the backyard space needed to hold the loop.

**Some Possible Circular Loop Sizes**  
**(All dimensions in Wavelengths)**

Circumference	Diameter
0.5 WL	0.159 WL
1.0	0.318
1.5	0.476
2.0	0.636
3.0	0.955
4.0	1.273



Free-Space 3-D Patterns for A Horizontal Circular Loop With Various Circumferences

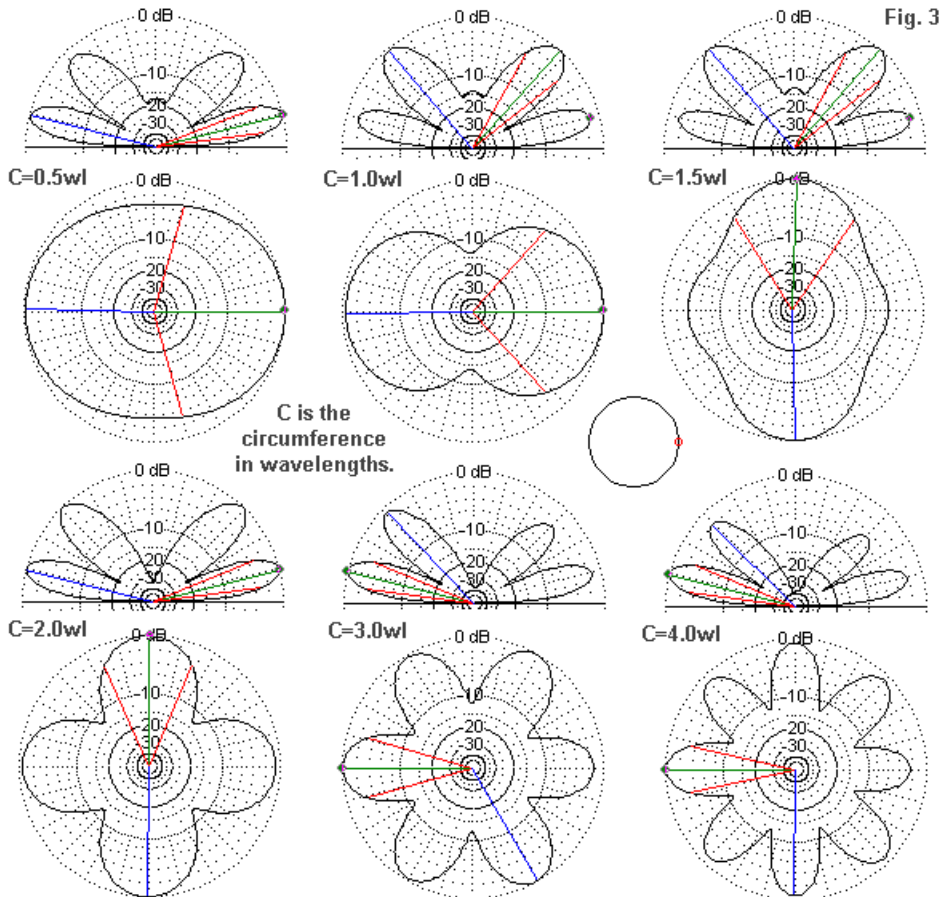
The 3-D patterns may seem a bit confusing, but let's align ourselves with **Fig. 1** and its axes lines. The X-axis and the Y-axis indicate horizontal directions relative to the orientation of the loop, presumed to be horizontal, even if we are working in free space with no real "ups" and "downs." The Z-axis is the vertical direction at right angles to the plane formed by the loop.

Since each 3-D pattern has about the same total volume, relative to the axis lines, we can see a few trends. First, the 1/2-wavelength loop forms an oval with slightly stronger radiation in the X direction than in the Z-direction. The next two loops (1.0-wavelength and 1.5-wavelength) have stronger radiation along the Z-axis than along either the X- or Y-axes. Not until we reach a circumference of 2 wavelengths does radiation strength occur predominantly in the X-Y plane. Another way of expressing this is to say that when a loop reaches a circumference of 2 wavelengths, it radiates more strongly off the loop edge than it does broadside to the loop.

This conclusion tallies well with our practice of using 1-wavelength loops in quad beams that rely on radiation broadside to the plane of the loop. If we want a 2-wavelength loop to radiate more strongly in the broadside direction, we must break the connection across from the feedpoint. However, our job is not to make a quad beam, but to see what a wire horizontal loop can do for our signals. So we may omit any consideration of broken loops.

The longer loops also show stronger radiation in the X-Y plane than in the +/-Z direction. However, their patterns are so convoluted that it is almost impossible to see exactly where the radiation is going.

To get a better handhold on the radiation of all of the loop sizes, let's return almost to earth. We shall place each loop 1 wavelength above average soil. (With horizontal antennas, the actual soil quality makes little difference to the signal, so using average soil will not distort the conclusions that we reach.) **Fig. 3** presents the modeled elevation and azimuth patterns for the loops sizes surveyed in **Fig. 2**. Each pattern indicates the strongest lobe, and the small inset of the loop shows how that lobe is oriented relative to the loop's feedpoint.



Elevation and Azimuth Patterns of Circular Loops of Various Sizes at 1 WL Above Ground

The primary feature to note is that for loops with a 1.0- or 1.5-wavelength circumference, the upper elevation lobes are stronger

that the lower lobe. Given the high elevation angle (about 35 degrees) of the upper lobe, the lower lobe is obviously that one that we rely upon for most communication (NVIS excepted, of course). When we reach a circumference of about 2 wavelengths, the lower lobe begins to dominate once more. Hence, for skip communications, the smallest advisable circumference for a horizontal loop is about 2 wavelengths at the lowest operating frequency. Smaller loops will work, but at reduced signal strengths.

The second notable feature is the fact that horizontal loops above a half-wavelength over ground answer to the standard lobe development angles that apply to virtually all horizontal antennas and arrays. All of the lower lobes, regardless of loop length, have a 14-degree elevation angle. The length of a loop does not change the elevation angle.

For a given power from the transmitter, all of the loops radiate the same power over the hemisphere above ground. Hence, they differ only in the maximum gain created by the formation of lobes and nulls in the pattern (both horizontal and vertical). The following table summarizes the gain of the strongest lower lobe and gives an indication of the impedance at the feedpoint. That impedance may vary considerably with variations in the actual wire length used to make a loop.

**General Performance Values for Circular Loops****Height:** 1 wavelength above Average Ground**Elevation Angle:** 14 degrees

Circumference wavelengths	Gain dBi	Impedance $R+/-jX$ Ohms
0.5	7.03	>100k - j85k
1.0	6.09	125 - j110
1.5	5.56	9200 + j6500
2.0	7.23	180 - j125
3.0	8.16	215 - j130
4.0	9.26	235 - j135

Loops that are integral multiples of 1-wavelength tend to have lower impedances, while those in the n.5-wavelength category tend to have very high impedances. Although the gain value for the 1/2-wavelength loop looks quite usable--when compared to the other values--the feedpoint impedance is not especially promising. As well, a 1/2-wavelength loop becomes a 1-wavelength loop on the next band upward in frequency, and we lose a lot of gain in the lower lobe on that band.

You may relate the improving signal strength maximum values that accompany longer loops with the width of the lobes for those larger loops in **Fig. 3**. Hence, as we make a loop longer, the beamwidth of the individual lobes grows narrower. As we increase the number of lobes, we also increase the number of nulls, where signal strength decreases to a level that may prevent communications.

Finally, for a circular loop (but not necessarily for other shapes), the number of lobes follows a regular pattern. The number of lobes is twice the loop circumference in wavelengths. Hence, a 4-

wavelength loop shows 8 distinct lobes. When we disturb the circular shape of the loop, the flat sides that we produce will alter this pattern of lobes and nulls, and we shall sample those alterations before we finish.

To obtain an estimate on how good a loop may be in our own backyard, let's pause to make a comparison. We shall place a 1/2-wavelength dipole at 1 wavelength above average ground. For that antenna, we obtain the following performance report.

**General Performance Values for 1/2-Wavelength Dipole**

**Height:** 1 wavelength above Average Ground

**Elevation Angle:** 14 degrees

Dipole Length wavelengths	Gain dBi	Impedance R+/-jX Ohms
0.5	7.98	72 + j2

**Fig. 4** shows the dipole, its 3-D free-space pattern, and its elevation and azimuth patterns at the specified height. The dipole has as many lobes as a 1-wavelength circular loop, but they are stronger at the prime 14-degree elevation angle.

Reference Graphics:  
Wire Dipole

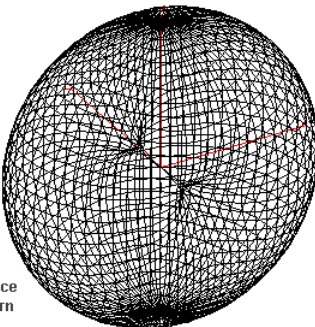
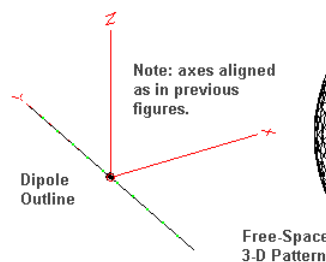
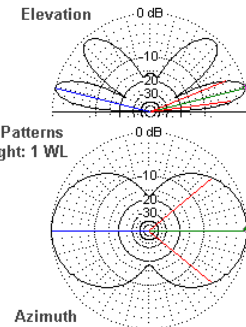


Fig. 4



The loop does not catch up to the dipole until we reach a circumference of 2 wavelengths, where we also have the loop's 4 lobes.

## How High?

Those who do not seem to have much luck with loops--even when at least 2 wavelengths long--very often have neglected the role of height in the performance of any horizontally polarized antenna. Most of these antennas are aimed at improving performance on the lower HF bands. However, the average height (from my e-mail reports) seems to be between 35' and 50' above ground. This height range covers about 0.06 to 0.11 wavelength on 160 and 0.12 to 0.18 wavelength on 80 meters (low end figures).

So far, we have looked at the circular loop when it is 1 wavelength above average ground. We do not know what the patterns might look like at other heights. Therefore, let's take a 2-wavelength

circumference loop and place it at a number of different heights, from a high and improbable 2 wavelengths up to a low value of 0.15-wavelength above ground. The shape of the azimuth pattern will not change significantly from the view at 1 wavelength. However, the elevation patterns will change considerably.

For contrast, let's also look at the numbers for a dipole at the same height. As always, we shall list the maximum gain of the strongest lobe or lobes. More important than gain will be the TO angle, that is, the elevation angle of maximum radiation. The following table summarizes the loop and dipole results. Since the data should be applicable to any lowest frequency of use, the heights are functions of a wavelength.

**Comparative Performance of a Circular 2-wavelength Loop and a Dipole at Various Heights**

Height wavelengths	Circular Loop		Dipole	
	Max. Gain dBi	TO Angle degrees	Max. Gain dBi	TO Angle degrees
2.0	7.36	7	8.05	7
1.0	7.27	14	7.98	14
0.75	7.75	19	7.57	19
0.5	7.43	29	7.91	28
0.25	5.94	47	6.33	60
0.15	4.76	52	6.59	90

Both types of antenna show the same or nearly the same TO angles down to 1/2-wavelength above ground. As well, they both show the same pattern of maximum gain levels. The slight depression of the maximum gain value that the dipole shows at a height of 0.75-wavelength appears in the loop at a height of 1 wavelength.

However, the loop shows a faster reduction in gain as it gets close to the ground, but it sustains a lower TO angle with height reductions. If you re-examine the patterns in **Fig. 4**, you can clearly understand why the dipole TO angle climbs rapidly as we reduce the height below 1/2 wavelength. The dipole in free space shows as much radiation vertically as it shows horizontally. Close to ground, the radiation directed upward dominates. At heights from about 0.15 to 0.25 wavelength, the dipole makes a quite good simple NVIS antenna.

In contrast, if you return to **Fig. 2**, you will see that the 2-wavelength circular loop has stronger radiation off its edges than it has perpendicular to the plane of the loop. As a result, the loop (at a closed circumference of 2 wavelengths) does not make a particularly good NVIS antenna. If you examine **Fig. 5**, you will see that the loop lacks radiation straight up. Hence, its TO angle is lower than that of the dipole when close to the ground.

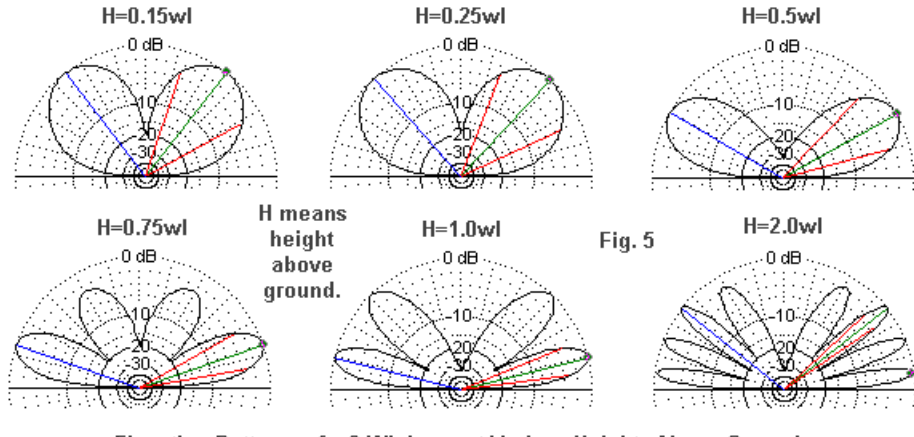


Fig. 5

Elevation Patterns of a 2-WL Loop at Various Heights Above Ground

The comparison between the dipole and the circular 2-wavelength loop does not mean that the loop is a stellar performer when close to the ground. For general propagation conditions, angles of 47 and 52 degrees are still too high for strong communications. However, if you look also at the half-power angles in the diagrams (the red line on either side of the main-lobe center line), you will see that the lower of these angles does tend to fall within the set of angles that provide relatively reliable communications in the lower HF region. (See a recent edition of *The ARRL Antenna Book* for further information on typical propagation angles on the various amateur bands.)

So the reputation of the loop for improved communications relative to a dipole at the same height has some truth to it for antenna heights below 1/2 wavelength. However, examine the gain values

for these heights and then subtract another 2-3 dB for working near the half-power angles. Raising the antenna higher not only yields a higher maximum gain value, but also places the TO angle nearer to--if not within--the range of angles providing stronger communications.

For any horizontal wire antenna, there is no substitution for height. This rule of thumb applies up to at least 1.25 wavelengths above ground, if not higher. On the lowest amateur bands (160 and 80 meters), there is always room for height improvement before reaching the limits of the rule of thumb. What we lack normally are the means to support the antenna at the most desirable height.

## What Shape?

We have so far confined our examination of loops to a circular shape--mostly to ensure that all comparative figures are fair. However, few of us have the means to set up a truly circular horizontal loop on the lowest amateur bands. In most cases, we are lucky to approximate a regular polygon. Hence, it is not possible here to cover all of the possible loop shapes that your circumstances might dictate. In fact, we shall confine ourselves to the circle, the triangle, and the square.

There are two reasons for the confinement. First, polygons with limited numbers of sides have two general feedpoint positions. One is at a corner, where the wire changes direction. The other is the midpoint of a side. Of course, we can feed a loop anywhere along a

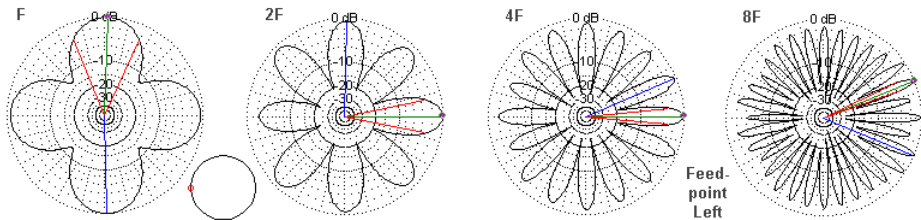
side, but, again, that would give us too many variables to cover. So we shall look at 1 circle, but 2 triangles and 2 squares.

Second, most horizontal loops are intended for multi-band use. So for each option, we need to look at several options. If a 2-wavelength loop is cut for 160 meters, then 80, 40, and 20 meters constitute a progression of frequencies ( $F$ ) that include  $2F$ ,  $4F$ , and  $8F$ . If we cut the original antenna to be 2 wavelengths at 80 meters, then the corresponding harmonically related bands are 40, 20, and 10 meters for the same  $F$ ,  $2F$ ,  $4F$ , and  $8F$  progression. Space does not permit us to include non-harmonically related bands in the progressions.

As we increase the operating frequency, the height of the antenna also changes when related to a wavelength. Hence, if we start 1 wavelength above ground, the upper bands will see the antenna at 2, 4, and 8 wavelengths above ground. The 14-degree TO angle at a 1-wavelength height becomes progressively 7, 4, and 2 degrees (with the angle confined to integer values).

Under these conditions, the 2-wavelength circular loop shows the azimuth patterns in **Fig. 6**. I have moved the feedpoint to the "left" on the antenna so that its position corresponds to the feedpoint position of the remaining shapes that we shall explore. Although the lobes increase in number as earlier noted, we might think of them as having equal strength. However, the  $8F$  pattern makes clear the fact that the lobes have slight variations in strength despite the fact that all of the models use lossless wire. The interaction among the

sections of the circle is sufficient to create the small differences. These differences will not be small with other shapes.

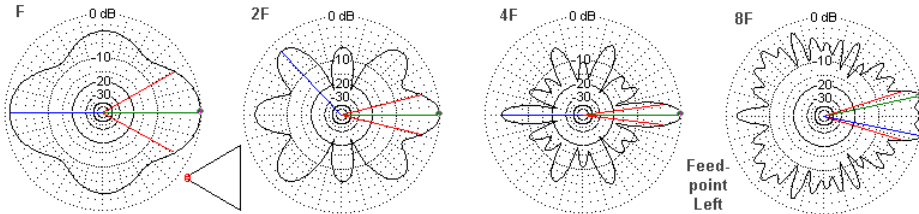


Azimuth Patterns of a 2-WL Loop, 1-WL Above Ground at Frequency F and Harmonics  
Circular Loop

Fig. 6

We might be tempted to mentally draw a line connecting the outermost tips of the lobes and think that the antenna has the resulting near circle as its pattern. However, every pair of lobes has an intervening null. The practical effect of having a large number of narrow lobes and nulls tends to be a rapid fluctuation in signal strength, especially on windy days, that can slightly alter the exact orientation of the wire antenna. At lower frequencies, where the lobes are broad, the antenna is nearly immune to this effect.

One popular arrangement for a 2-wavelength loop is a triangle, since that shape needs the fewest support posts or trees. We shall first look at a triangle fed at a corner, specifically, the left-most corner relative to the orientation of the patterns. Of course, we shall retain the 2-wavelength circumference and the 1-wavelength antenna height.

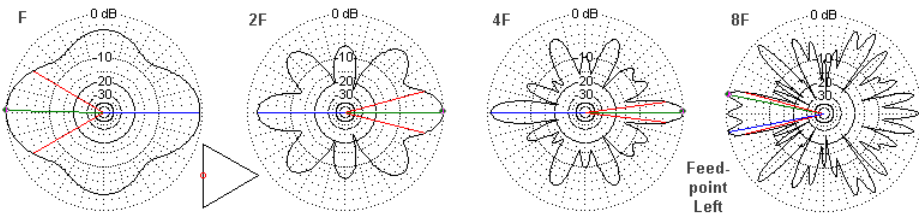


Azimuth Patterns of a 2-WL Loop, 1-WL Above Ground at Frequency F and Harmonics

Corner-Fed Triangular Loop

Fig. 7

**Fig. 7** shows the patterns that result for each frequency when using a corner-fed triangle. The nearly equal strength of the lobes disappears, even at the lowest frequency. The antenna has a slight beaming effect along a line that runs from the feedpoint to the middle of the side opposite the feedpoint. In all cases, the strongest radiation is in the direction of that far side of the triangle. Therefore, if you use an equilateral triangle for a loop, it pays to orient the antenna toward a primary communications target region.



Azimuth Patterns of a 2-WL Loop, 1-WL Above Ground at Frequency F and Harmonics

Side-Fed Triangular Loop

Fig. 8

If we feed a triangle in the middle of a side, as shown in **Fig. 8**, we obtain patterns that in general terms are not very different from the ones for a corner feedpoint. However, note that the patterns for 2F and 4F are strongest across the antenna and away from the feedpoint side, while the patterns for F and 8F are strongest to the side containing the feedpoint.

When we move to square shapes, a side-fed loop looks square, while a corner-fed square looks like a diamond in terms of the orientation to the patterns. We shall look at the side-fed square first. The patterns are in **Fig. 9**.

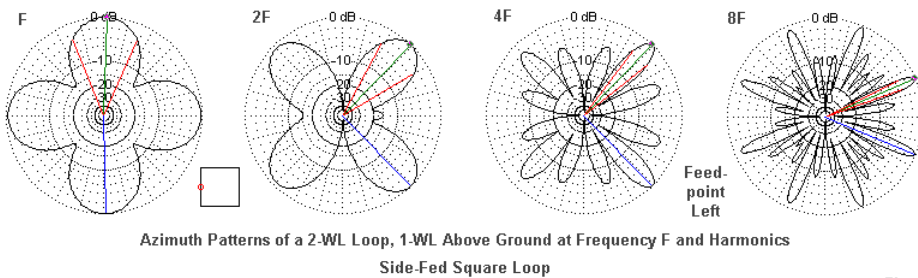
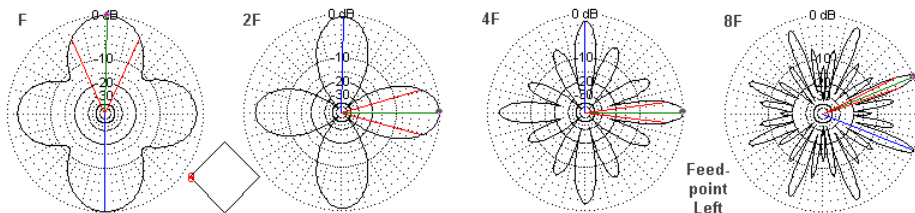


Fig. 9

The square has a pattern at F that is very similar to the one for the circle. However, from that frequency upward, everything changes. Each pattern has fewer lobes than the corresponding pattern for a triangle. As well, the strongest lobes are not aligned with the feedpoint and the opposite side of the square. Instead, the strongest lobes occur at oblique angles to the square for 2F through 4F. Since that angle changes with the operating frequency,

finding a good orientation for all intended frequencies may be difficult.



Azimuth Patterns of a 2-WL Loop, 1-WL Above Ground at Frequency  $F$  and Harmonics  
Corner-Fed Square Loop

Fig. 10

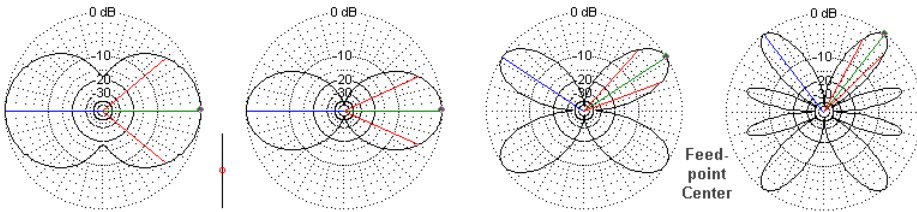
When we feed the square at a corner, we once more align the patterns along a line from the feedpoint corner to the opposite corner of the diamond, at least through 4F. **Fig. 10** provides the patterns. At 8F, the strongest lobes are at an angle to the array. The following table provides a summary of the modeled maximum gain values. However, above about 2F (a circumference of 4 wavelengths), the lobes become so narrow that a maximum gain value can be quite misleading as a guide to the general communications capabilities of each antenna.

## Maximum Gain Values for Each Antenna at Each Sampled Frequency

All loops are 2-wavelengths at F.

Antenna	Frequency TO angle (degrees)	F	2F	4F	8F
Circle		7.27	9.22	10.71	11.57
Triangle, corner-fed		8.34	9.95	14.38	8.41
Triangle, Side-fed		8.34	10.45	13.24	8.94
Square, side-fed		8.42	11.29	13.59	14.29
Square, corner-fed		6.95	11.51	14.28	14.92
Reference Dipole/Doublet		7.99	9.66	9.64	11.16

The gain data is only useful in comparing the outer rings of each pattern. Note the reduction in gain for the two triangles when operated at 8 times the lowest frequency. I have included the data for a 1/2-wavelength dipole at F to allow comparisons on the various harmonics when using that antenna as a multi-band doublet. The patterns for the doublet appear in **Fig. 11**. Only up to 2F (or 1-wavelength) does the doublet show its strongest lobes broadside to the wire. Above that frequency, the strongest lobes depart at oblique angles that change with frequency.



Azimuth Patterns of a 0.5-WL Center-Fed Doublet, 1-WL Above Ground at Frequency F and Harmonics

Fig. 11

These small demonstrations show that a loop's shape can make a great deal of difference to the azimuth patterns of radiation from it. I shall select no version as better than the others, since I cannot know the lay of the land for each installation. However, it does appear that operating a 2-wavelength loop much above twice the design frequency does yield narrow lobes that may or may not be useful to communications. The remaining body of radiation in the pattern is considerably weaker than the main lobes. For patterns associated with other loop shapes, see the article mentioned at the beginning of this one.

## Conclusions

Based on what we have explored in the realm of wire horizontal loops, we can draw a few conclusions. These recommendations are based on the idea of using the loop for more than one band.

1. *How Big?* The loop should be at least 2 wavelengths in circumference, regardless of the final shape. For most purposes, the antenna should be considered for use over a 2:1 frequency range, even though it will load on other bands well above the design frequency. The exception to this recommendation is the case in which the antenna is for NVIS use on the lower band and for normal skip communications above that band. In that case, a 1-wavelength loop at the lower frequency will provide the best compromise.
1. *How High?* Because the antenna is used mostly on the lower HF bands, it is safe to suggest that the antenna should be as high as

feasible. A height of 1 wavelength above ground is certainly not too high, although in most circumstances the antenna will be restricted to lower heights. The exception is the case in which the antenna serves for NVIS communications on the lower band. In that case, the 1-wavelength loop should be between 0.15 and 0.25 wavelength above ground for the strongest upward pattern. On the second harmonic, the antenna will be 2 wavelengths long and between 0.3 and 0.5 wavelength above ground for better, if not ideal, longer-range communications.

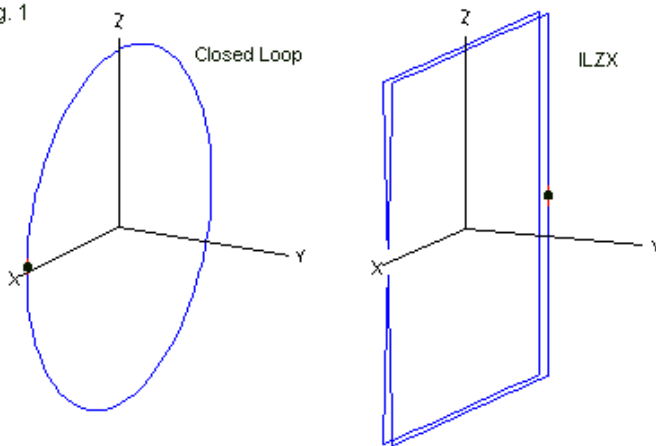
3. *What Shape?* Of the sampled shapes, the circular version produces the most even set of lobes on all frequencies. Hence, a polygon that approaches circularity is more likely to have fewer interactions among the sections of the antenna to produce a pattern with only a few spiky lobes. However, even a circular design will produce 4 main lobes when it is 2 wavelengths in circumference.

None of these recommendations is absolute, since the loop will work at many lengths, heights, and shapes. It is not possible to cover all eventualities in a single set of notes or even many sets of notes. Hence, the prospective loop builder should strongly consider obtaining at least a rudimentary antenna modeling software package to test any possible design. In that way, you can predict more accurately the performance of a loop designed to fit a given yard.

## Chapter 74: Closed & Interrupted Loops for 40 Meters

In the next Chapter 75 "The IL-ZX Antenna for 40 Meters", I present (or resurrect, depending upon one's point of view) a compact interrupted loop antenna for 40 meters. By using folded element wire construction, it provided a coax-compatible feedpoint impedance with no compensating or loading components. Since the overall circumference of the interrupted loop was about  $1/2$  wavelength, the antenna was very compact, fitting within a 20' wide by 20' High (plus ground clearance) footprint. **Fig. 1** on the right shows the essential outline of the ILZX when used vertically. Single wire horizontal versions of the antenna exist. Indeed, in Britain, you may obtain a multi-band version of the antenna.

Fig. 1



Basic Model Outlines: Closed Loop and ILZX

On the left in **Fig. 1** is an antenna that is similar in size and that also uses a vertical orientation. It is a closed loop with a diameter of about 0.127 wavelength, with a resulting 0.4-wavelength circumference. As we move from the region of very small loops with feedpoint resistive components in the 1-Ohm range up to the medium-loop range (circumferences between about 0.25 and 0.75 wavelength), we find some interesting properties. First, the resistive component of the feedpoint impedance climbs so that we no longer need worry as much about the losses of compensating and matching components or the losses of construction joints. Second, the reactance of the closed loop becomes increasingly inductive. When the loop is electrically about 1/2 wavelength in circumference (which for a closed loop is physically larger than 1/2 wavelength), the reactance reaches a peak inductive value only to suddenly reverse to a peak capacitive reactance value with only a slight further increase in circumference. (This phenomenon is familiar to those who have center-fed linear wire antennas that are about 1 wavelength long.) At the same time, the performance of the loop improves with increasing size. The result is a compromise. When the loop is about 0.4 wavelength in circumference, The feedpoint resistance approaches 100 Ohms while the inductive reactance has a high but manageable value for which we can compensate with a small (low-pF) series capacitor. By tradition--derived from very small loop construction more than from necessity--most closed loops in this arena use fat elements--often copper pipe.

Both antennas are interesting, if for no other reason than the similarity of their sizes. One can square the closed-loop circle or circularize the square shape of the ILZX. However the shapes have

little bearing on performance. The closed-loop's circle is convenient for the most commonly used materials, while the wire structure of the ILZX lends itself to the use of non-conductive side supports with rope ties to the corners of the square. Therefore, in the discussion to follow, I shall use the modeled construction shown in **Fig. 2**, which gives the dimensions for both subject antennas.

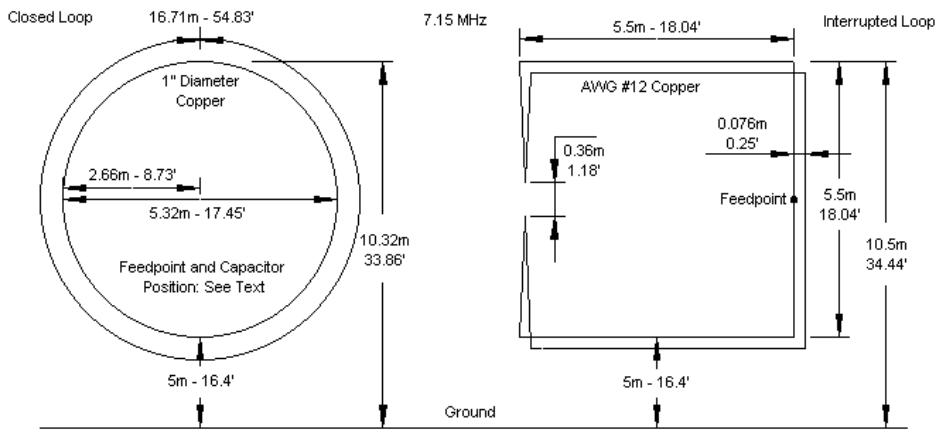


Fig. 2

Dimensions of the Modeled Antennas Used in Comparisons

In a situation calling for a very compact 40-meter antenna, the structure is likely to be close to the ground. I selected a 5-meter (16.4') bottom height to have a rounded number that accords reasonably well with amateur practice. In both cases, the top height of the antenna is less than 11 meters (or 35') above ground. The radius of the closed loop is 0.0635 wavelength at 7.15 MHz, the selected common test frequency for both antennas. The loop

material is 1" copper, a diameter that results in a 98.5% power efficiency according to NEC model reports. (The NEC report does not include losses incurred from the average ground over which I placed both antennas). For an important reason that we shall consider shortly, the dimensional outline of the closed loop does not show the position of the feedpoint or of the required series capacitor.

The ILZX has several notable features. It uses AWG #12 wire (0.0808" diameter). Although the wire is thin compared to the value used in the closed loop, the power efficiency is over 96%. Instead of viewing the antenna as an interrupted loop, let's think of it as a folded dipole with 3" spacing between wires and with the linear elements bent into a square that is 5.5 meters (18.04') on a side. Like a folded dipole, the equal-diameter elements create a 4:1 impedance transformation (regardless of spacing--within limits). Hence, a single wire version of the antenna might show a feedpoint impedance in the 12- to 16-Ohm range. The folded version shows an impedance in the 50- to 65-Ohm range, depending on orientation and height above ground. With the side feedpoint shown, the impedance is about 64 Ohms.

The difference between a linear folded dipole and the bent version in the ILZX is the proximity of the element ends, added to the parallel sections of the "top" and "bottom" sections. The element tips exhibit strong coupling. Therefore, the gap between them becomes an important means of setting the reactance at the operating frequency. Note that the tips come to a point on each side of the gap. If we leave the tips blunt--as we might in a regular

folded dipole--the gap dimension becomes very finicky. By bringing the tips to a point, we reduce the amount of reactance change with each unit of physical change in the size of the gap. Such antennas actually go back to the 1930s and sometimes used copper pipe construction (on unbelievably heavy wood frames) with gap extensions that consisted of small plates soldered to screw threads for fine tuning.

The sketches show the ILZX at a relatively low height, vertically oriented, with a side feedpoint and a side-gap position. This orientation yields the best low angle patterns that we can obtain from the antenna. In contrast, most common implementations of the closed loop have chosen a bottom position for the feedpoint and reactance-compensating capacitor. In fact, the closed loop has properties sufficiently like a very small loop to allow us to position the feedpoint and the required capacitor almost anywhere along the circumference, and not necessarily at the same place. Each selection has consequences that we may accept or reject according to our needs. For example, a very small loop has a current magnitude and phase that remain virtually constant along the length of the loop. In the 0.4-wavelength circumference loop, the current magnitude changes by no more than a 3:1 ratio of maximum to minimum. This change is small compared to the current levels that we find along a linear element. As well, it is small compared to the ratio of maximum to minimum current in a full 1-wavelength loop.

Let's assume that the terms "top," "bottom," and "side" have conventional meanings relative to the ground. We may place the

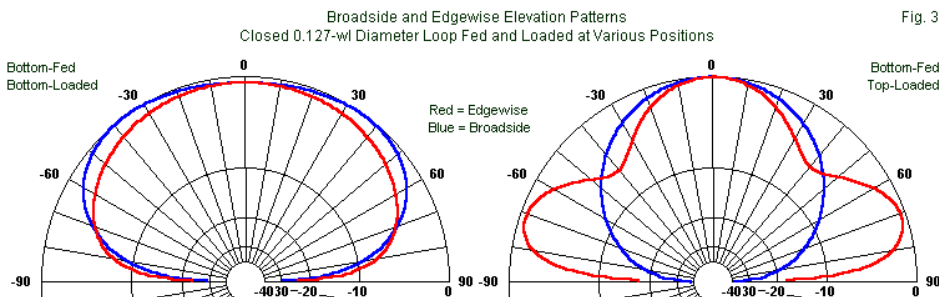
feedpoint at any one of these positions. Likewise, we may place the series capacitor at any one of these positions. The following table shows what happens to the maximum gain, the elevation angle of maximum radiation, and the feedpoint impedance for various combinations. In all cases, the compensating series capacitor value remains constant and represents a reactance of  $-j2417$  Ohms at 7.15 MHz. As well, the closed loop remains physically constant.

Consequences of Alternative Placements of a  $0.4\text{-}\lambda$  Closed-Loop's Source and Series Capacitor

Feedpoint	Placement	Gain (dBi) and TO Angle	Feedpoint Z	Capacitor	
	Feedpoint	Broadside Bottom	Edgewise $3.34/55^\circ$	$R +/- jX \Omega$ $120 + j1$	pF 9.21
Bottom	Bottom	0.99/90°	0.99/90°	3 - j1	9.21
Bottom	Top	-0.73/28°	0.70/25°	10 - j2	9.21
Bottom	Side	-0.71/28°	0.79/25°	99 - j25	9.21
Side	Side	-0.71/28°	0.79/25°	99 - j25	9.21
Side	Top	0.99/90°	0.99/90°	5 - j2	9.21
Side	Other Side	-0.71/28°	0.70/25°	7 - j1	9.21

With the feedpoint and capacitor both positioned at either the top or bottom, the pattern for the relatively low and vertically oriented loop is mostly straight up. The dominant polarization is horizontal. **Fig. 3** shows the broadside and edgewise elevation patterns for some of the cases. The left pair of elevation plots yield the most NVIS-like upward patterns at a reasonably good gain level. The right side of **Fig. 3** shows the elevation patterns for the use of a bottom feedpoint and a top-positioned capacitor. However, the patterns also apply to the case in which the feedpoint is on the side and the capacitor is at the top. The top-mounted series capacitor pattern has a significant lower angle component, but only edgewise to the

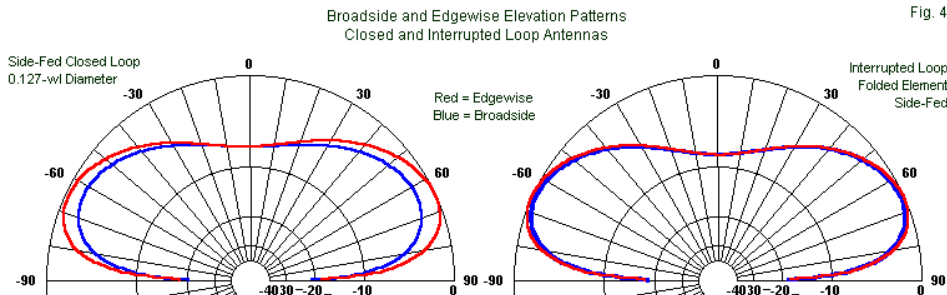
plane of the loop. These cases appear to illustrate the fact that the position of the series capacitor has a stronger bearing on the pattern shape than the feedpoint position. For example, the table suggests that the feedpoint at the bottom with the capacitor on a side yields patterns very much like those where both the source and the capacitor are positioned on a side.



Only two of the options present a highly workable feedpoint resistance: bottom-bottom and side-side. The side-side position combination does require adjustment to the capacitor value to 9.31 pF to null the remaining loop reactance. The very small amount of required change (0.1 pF) suggests that tuning the loop can be very finicky without either special components or excellent ingenuity.

**Fig. 4** compares the elevation plots of the side-side closed loop and the ILZX. In the configuration shown in **Fig. 2**, the ILZX shows a maximum edgewise gain of 0.05 dBi at 24 degrees. The maximum edgewise gain is -0.26 dBi at 25 degrees. The average gain of the two antennas is almost identical, while the ILZX exhibits a slightly

more circular azimuth pattern. (With the ILZX fed at the bottom and the gap at the top, the resulting patterns are similar to those for the closed loop in the bottom-bottom configuration.)



When oriented at relatively low heights, both the closed loop and the ILZX benefit from side feeding to yield low angle patterns that benefit HF communications. Indeed, their patterns are not sufficiently different to be detectable in ordinary operations. The remaining question is whether there is a more decisive factor to separate the two antennas for amateur operations. There might be, if we assume that most amateurs prefer wider operating bandwidths from their antennas.

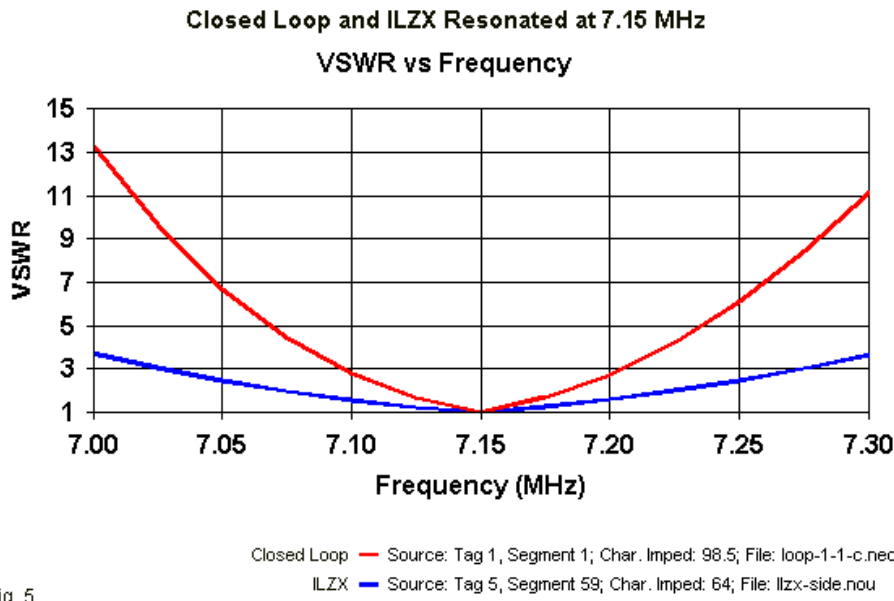


Fig. 5

**Fig. 5** presents the SWR sweeps for the closed-loop and the ILZX from 7.0 to 7.3 MHz. In each case, the curve is references to the resonant impedance of the individual antenna. For the ILZX, the reference impedance is 64 Ohms. The 98.5-Ohm reference impedance of the closed loop includes the use of a 9.31-pF series capacitor at the side feedpoint. The 2:1 SWR bandwidth of the closed loop is 60-70 kHz. In contrast, the 2:1 SWR bandwidth of the ILZX is about 150 kHz. As well, even without 50-Ohm matching at the feedpoint, the rate of SWR change for the ILZX is low enough that the internal tuners that come with many current transceivers

could easily handle the matching task. At 40 meters, the losses of coaxial cables larger than RG-58 would not be troublesome for most operations. Nevertheless, for maximum 40-meter QRN reduction, the narrower bandwidth of the closed loop may serve a useful purpose.

When we lay out the physical and the electrical properties of both antenna types, each has advantages and disadvantages. The point of these notes is not to recommend one over the other, but to make the relative properties of each more readily apparent. Perhaps the only general conclusion to these notes is the fact that if we construct either antenna in a vertical plane and at relative low heights, then side feeding is generally highly beneficial for long distance operations, although bottom feeding can create a compact NVIS antenna. Enjoy the interesting conundrum. . .

## Chapter 75: The IL-ZX Loop for 40 Meters

**E**very antenna design has a niche in the overall world of amateur radio antennas. The one described here has a quite small niche: it is for the individual who requires operation on 40 meters at low elevation angles, but who does not have the real estate to erect one of the SCV (self-contained vertically polarized 1 wavelength loop) antennas. The IL-ZX provides low-elevation angle radiation within a narrow operating bandwidth at low gain with a bi-directional pattern and reduced radiation at higher angles. It can be fed directly with 50-ohm coaxial cable, although a network antenna tuner will likely be useful for increasing the usable bandwidth.

IL-ZX is shorthand for Intermediate Loop-Impedance Transformation antenna. The design has some of the properties of a small loop, for example radiation off the edges of the loop rather than off the face. However, it does not require the level of mechanical care associated with small loops and replaces the capacitor with a simple capacitive gap, the spacing of which resonates the loop. The native feedpoint impedance of such a loop, about 1/2 wavelength in circumference, is around 10 ohms. By using a double-loop form of construction, the impedance is raised to about 40 ohms.

### Small Loops

The small loop is defined by some experimenters, such as W5QJR, as a loop whose circumference is between 0.1 and 0.3

wavelengths. **Figure 1** shows the elevation pattern of one such loop resonated at 7.2 MHz. The maximum gain for copper loops and lossless capacitors is relatively constant across the range of defined size at 0.4 to 0.45 dBi at low elevation angles. Feedpoint impedances range from 0.5 ohms for the smaller sizes to about 1.5 ohms for the larger sizes. Below 0.1 wavelength circumference, the loop gain drops rapidly, as does the feedpoint impedance.

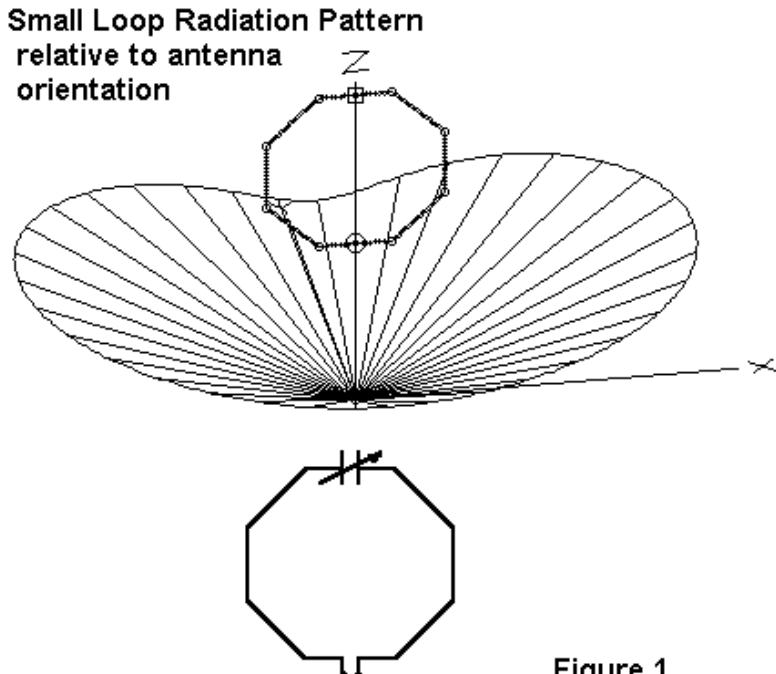


Figure 1

Small loops require extreme care in construction, since every fraction of an ohm connection loss results in large increases in power lost to heat. Hence, 3/4" diameter copper water pipe, soldered at every joint, is a common material. The required resonating capacitor demands special care of construction and attachment. If one has the skills to build one, a small loop can be a very effective antenna. With a stepper motor operating the capacitor, a 2:1 frequency range of operation is easily possible with good results.

## Large Loops

In contrast, a large loop is thought of as a full wavelength in circumference, such as the quad loop. This loop has a natural resonant feedpoint impedance of 125 to 130 ohms. Many users reduce this impedance with a 1/4 wavelength section of 75-ohm coax so that it presents a reasonable match to 50-ohm coax for the remainder of the run. The antenna offers a fairly wide operating bandwidth without further adjustment.

The full wavelength loop is capable of higher gain than a dipole placed at the center height of the loop. However, a large loop is about 1/4 wavelength on a side, about 35' horizontally and vertical on 40 meters. If fed at the bottom or top, the radiation pattern is largely horizontally polarized and subject to the same high-angle of maximum radiation as a dipole. Hence, low mounting heights reduce the effectiveness of this antenna.

Fed in the middle of one side, the antenna offers low angle radiation, largely vertically polarized. However, for maximum effectiveness, the antenna requires about 10' spacing above ground, raising its top height to about 45' or so. **Figure 2** shows the pattern of a vertically polarized 40-meter large loop.

**Large Loop Radiation Pattern  
relative to antenna orientation**

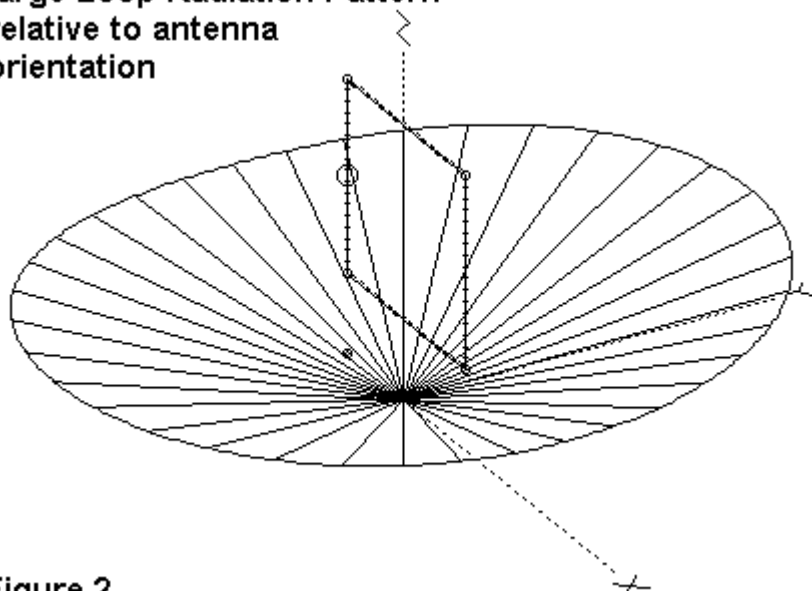


**Figure 2**

The full-size quad loop is but one of several SCV designs for achieving low angle vertically polarized radiation without need for a ground plane and without high angle radiation or reception of QRM

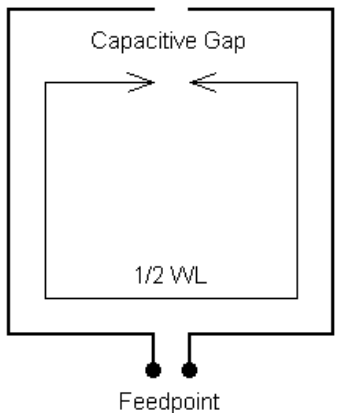
and QRN from those upper angles. They have come into increased use by those who have directly or indirectly read into materials researched by ON4UN and others. Another entry in this series of notes attempts to put into perspective the entire spectrum of SCV antennas.

SCVs require significant real estate, either or both horizontally and vertically. The modern city lot or rental property does not always offer sufficient space even for a 40-meter SCV.

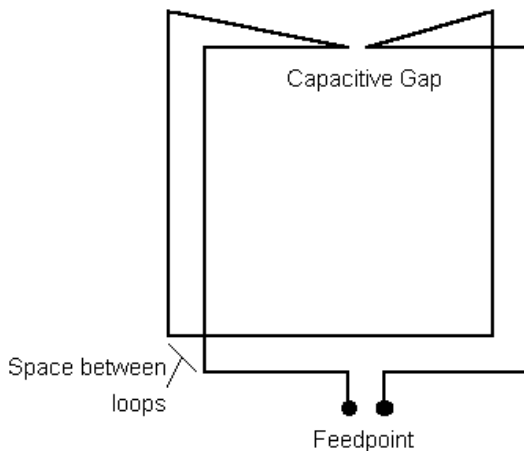
## The Intermediate Loop

The Intermediate Loop (IL) is a small loop enlarged to approach 1/2 wavelength in circumference. Because the antenna approaches a natural resonant point, its operating bandwidth enlarges, reducing its gain at any single frequency. However, the antenna offers lower construction losses because the resonance can be established simply by adjusting the width of the gap at the top of the antenna. Capacitance from one wire end to the other is sufficient for the task, but the low-C high L nature of this circuit also contributes to broader response and lower gain. **Figure 3A** shows the outline of the basic IL, which has a natural resonant feedpoint impedance of about 10 ohms. Relative to a small loop with an adjustable capacitor, the IL-ZX is a one-band antenna.

Figure 3



A. Intermediate Loop



B. IL-ZX

The feedpoint impedance can be raised to about 40 ohms by doubling the loop and feeding only one of the wires, as shown in **Figure 3B**. (Hence, ZX = Impedance Transformation.) This method is essentially the same impedance transforming technique used in the folded dipole. With wires of the same diameter at any spacing, the transformation is 4:1. This transformation applies to both radiation and heat components of the impedance, so no magical reduction in losses occurs--and likewise, no magical increase in gain occurs. However, the feedpoint impedance is now more manageable for use with 50-ohm coax.

A second benefit of the double loop is that it offers the builder standard techniques of wire antenna construction. The loops may

be spaced from 6" to 3' apart with corner CPVC spacers. Wire joints should be carefully constructed and soldered. The antenna benefits from the use of large wire sizes, with 1" wire showing an additional 0.5 dB gain over #12 wire. Therefore, one may wish to build the antenna from such materials as 450-ohm parallel line for each loop to simulate fatter wire. If such a method is selected, it is usually wise to solder a short across the parallel line periodically to ensure equal currents on each wire. (Do not short the two loops except at the top gap.)

Figure 4

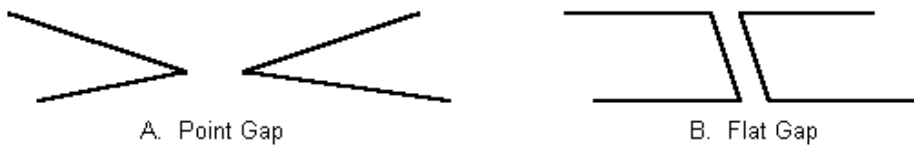


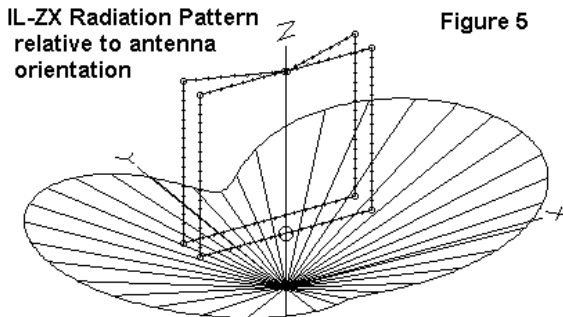
**Figure 4** shows two arrangements for the top gap. In one case, the loops are brought together as a point; in the other they approach each other as a bar across the loop ends. Since the gap is actually the dielectric space for a capacitor formed by the loop ends, the difference in construction can make a big difference in antenna size and adjustment. Models of the point-gap required about 18' per side for the antenna, with a gap between 0.2 and 1.0' wide, depending on spacing of the loops. The flat-gap antenna, for loops spaced at 2' and a gap of 0.8' required sides of only 17' each. The flat-gap construction will make side length a much more sensitive

function of the loop spacing, since the capacitance between ends will change more radically with loop spacing and the consequential lengthening or shortening of the wires facing each other. In all cases, the builder should be prepared to do considerable experimentation to achieve resonance.

## Performance

The IL-ZX offers the would-be 40 meter operator a relatively small antenna, no more than 18' per side. Its best low angle performance occurs with the center about 15' high and its bottom wire therefore about 6' off the ground. The high point becomes about 24' up.

The 2:1 VSWR operating bandwidth is about 100 kHz at 40 meters. However, a network ATU in the line should expand this without introducing significant losses on this lower HF band where a full wavelength of coax feedline is over 90' long (accounting for velocity factor).



The primary signal direction of the IL is like that of the small loop: off the edges of the loop, as shown in **Figure 5**. With a center height of 15' or so, the elevation angle of maximum gain is 21 to 22 degrees, similar to SCV angles. Front-to-side ratio is generally around 10 dB.

In the process of further experimenting with the IL-ZX design, I discovered that you can easily create a virtually circular low angle pattern--still of relatively low gain--by turning the IL-ZX "on its side." In this orientation, we need to raise the antenna to a base height of about 15' (for a top height of about 33') in order to eliminate excessive influence of the ground on one side of the antenna wire run more than on the other. At the 15' height, the impedance is about  $64 + j15$  Ohms, still an easy match for coax.

Circularized Radiation Pattern  
Resulting From Turning IL-ZX  
90 Degrees and Elevating to  
a Base Height of 15'

Figure 6

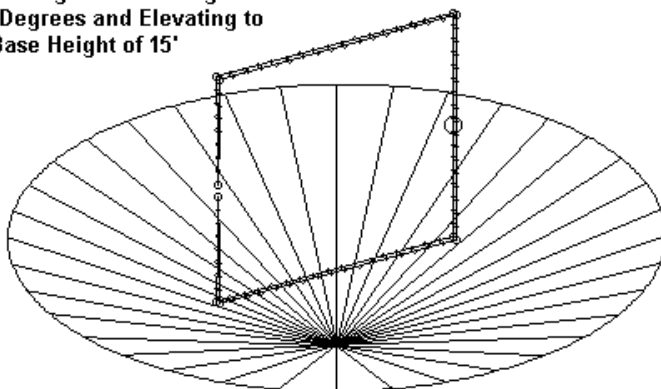


**Figure 6** shows the circularized pattern at about the same take-off angle as the "upright" IL-ZX. Gain is not significantly different from one version to the other. Hence, which orientation you choose to use is largely a matter of the pattern that you desire and the ease of feeding the antenna at the side vs. at the bottom.

The principle disadvantage to the IL-ZX antenna is low gain. The antenna gain at maximum is about 3 dB less than that of a full size quad loop and about 4.5 dB less than that of a half square, when each of these is at optimum height. The reduction is less than a full S-unit in signal strength.

However, the antenna offers two advantages that offset the reduction in gain. First, although not as narrow in reception bandwidth as a small loop, the sensitivity of the antenna to reception noise is considerably less than that of a resonant dipole or large loop. Second, the attenuation of signals at higher angles (in the 45-degree elevation angle range) reduces the reception strength of QRN and QRM. Hence, the signal-to-noise ratio of the antenna should be quite good for signals in the desired main lobes of the antenna. Since most receivers have excess gain at 40 meters, reception of desired distant signals should be a matter of increasing either pre-filtration or post-filtration gain.

Even if we become very conservative and estimate performance at 6 dB down (1 S-unit) from an optimized half square, the transmitting success ratio should only go down in contest and pile-up conditions. For QRP operation, raising power from an initial 1 watt to a final 4 watts would restore signal strength at the reception end.

The IL-ZX is not by any means a perfect antenna, designed to outperform anything else on the market. However, neither is any other antenna. Every set of performance figures carries with it a set of operating specifications within which performance is measured. We too often ignore this fact when evaluating antennas.

If vertical and horizontal space are at a premium and skills needed to build an effective small loop are somewhere in the future, the IL-ZX may serve as an effective low radiation angle antenna in the interim until a perfect antenna site can be purchased. If you decide that you do not like the antenna, you can likely put the materials to use on other projects.

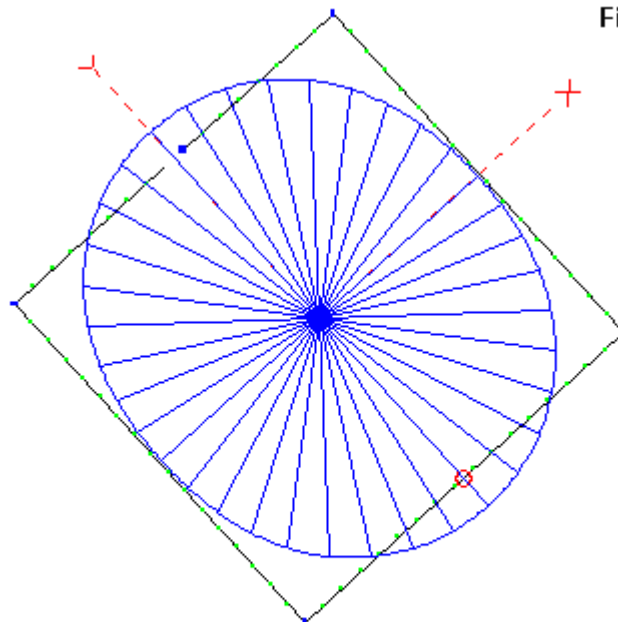
### **The ILZX Horizontally**

Considerable interest has grown up in the last few years relative to the intermediate or interrupted loop used in a horizontal position. One or more such antennas--strung together for multi-band use--have appeared on the market within the British Commonwealth; one is called the "Cobbweb." However, a single-wire intermediate loop shows a very low impedance and requires a matching system for the ubiquitous coaxial cable feedlines preferred by many amateurs.

The ILZX form of the interrupted loop is quite usable in a horizontal position. In fact, with almost no adjustments, the vertical ILZX for 40 meters can be used horizontally. In the following notes, we shall build the model ILZX in the same way for horizontal use that we

used for vertical applications. The #12 elements will be separated by 6" and form a square that is 18' on a side. The tips that approach each other will form a "spear tip" pair for ease of adjusting the gap to refine the source impedance. The tips will be 1' apart.

Fig. 7



The Horizontal ILZX at 50' Above Average Ground,  
Along with its Azimuth Pattern

If we place the antenna at 50' above ground, we find a pattern resembling the one in **Fig. 7**. Note that the pattern is stronger along the axis formed by the feedpoint and the gap. The feedpoint impedance under these conditions is about 53 Ohms, with about the same bandwidth as the vertical version: 100-150 kHz or about 1/2 of the 40-meter band. Since the antenna is set for mid-band, a user would have to adjust the dimensions to favor either the CW or the SSB portion of the band.

One myth surrounding interrupted loops is that they have a circular pattern. They do not. Due to the current distribution along the wire, radiation from the region on each side of the feedpoint yields a stronger pattern on the feedpoint-gap axis. In order to develop a circular pattern, one must readjust the shape of the ILZX into a long rectangle with shorter feed-region and gap-region dimensions. An example of such an antenna appears in the next Chapter 76 "Experimental Omni-Directional Antennas for 6-Meters." The general proportions would be a partial guide to developing a truly omni-directional interrupted loop for any other band. However, expect to make considerable adjustments for differences in the wire spacing, the wire size as a function of a wavelength, and the shape of the wire ends at the gap.

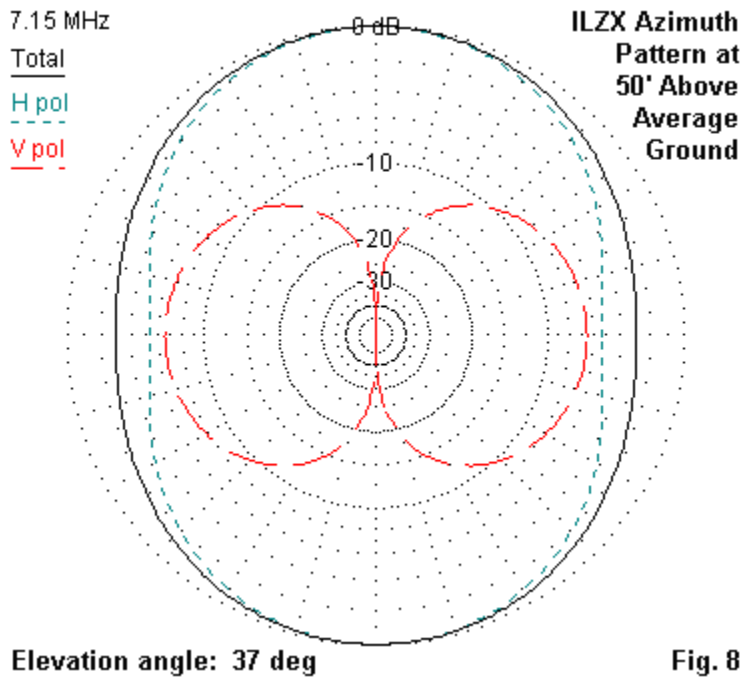


Fig. 8

The maximum gain of the horizontal ILZX is about 5.1 dBi at a 37-degree TO angle. The minimum or side gain is 3 dB less. Nevertheless, the pattern shows considerable side-pattern development, as displayed in **Fig. 8**. The graphic shows both the vertical and horizontal components of the total pattern. The vertical components are largely a function of ground reflections, but they still contribute to the overall useful radiation. Since 3 dB difference between the main and cross axes amounts to about half an S-unit,

the radiation might be considered to be adequate for omnidirectional operation.

Compared to a dipole, the horizontal ILZX holds its own quite well, as demonstrated in **Fig. 9**. I modeled a resonant dipole at 50' above average ground for comparison. The dipole's maximum gain is about 1.1-dB higher than the maximum for the ILXZ. However, the dipole shows about 7-dB difference between its maximum and minimum gain, where the minimum is off the ends of the antenna. Note that for dipoles well under 1-wavelength above ground, we do not obtain a true figure-8, but only a peanut. Brought closer to ground, the pattern becomes a broad oval.

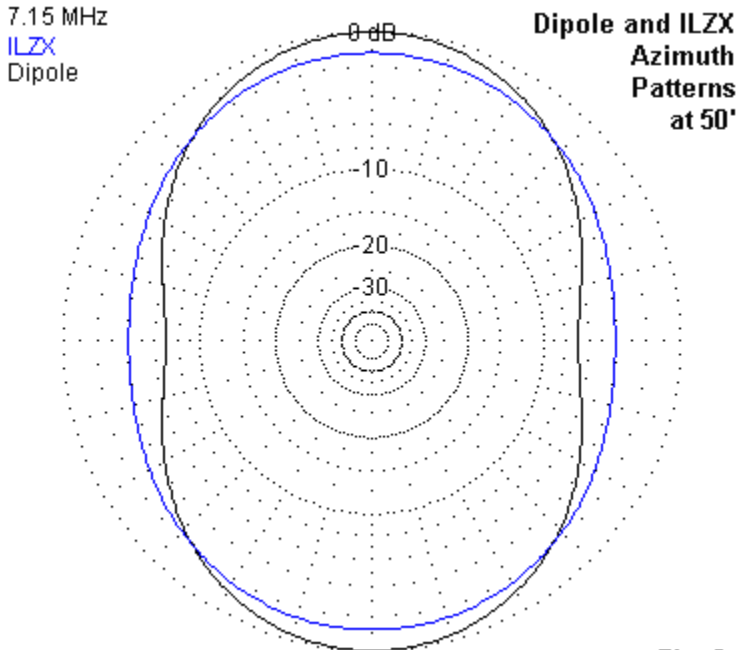


Fig. 9

Since the ILZX has a naturally oval pattern, it better approaches the omni-directional pattern favored by many hams who have only a single, fixed-position antenna. Erecting an ILZX requires only an 18' by 18' space, but does require 4 corner support posts for the 40-meter version. A version for 20 meters would require only a 9' by 9' space and might be supported on a single mast with fiberglass spreaders. The higher the frequency, the easier the ILZX will be to support. Because the antenna has a pattern that approaches the omnidirectional, it requires no rotator. However, it does call for

orienting the strongest axis in the direction(s) of the most favored communications targets.

Although the antenna looks something like a beam, it is not. Hence, it will not provide the QRM attenuation to the sides and/or rear of a beam. Indeed, the gain is less than that of a dipole (and hence considerably less than the gain of any well-designed beam). That is the price one pays for omnidirectional coverage. About the only way to obtain more gain from the ILZX is to extract it from the high-angle radiation. One (impractical) scheme for doing so is to stack and feed in-phase two ILZXs spaced 1/2-wavelength vertically. The result is about 3-dB more gain in every direction.

The horizontal ILZX is suited to an exceptionally wide variety of construction techniques, depending on the frequency of operation and the exact layout of the loop and gap structures. Nested multi-band version may use a fairly low impedance line to connect feedpoints. The system of closed sleeve coupling sometimes works best when the main feedpoint is the highest frequency loop. Wire interactions will require loop adjustments, especially for the inner loops. As well, expect significant current on the inactive band loops and consequential modifications of the overall pattern on some bands. Finally, if one or more bands seem hard to bring into line, try moving the composite feedpoint to a different element relative to the one initially used. Be certain to check the SWR bandwidth for each trial arrangement before finalizing the selection.

For a multi-band antenna, you may have better luck separating the bands. 20-15-10 provides less element-to-element interaction than

a 5-band version of the antenna, although the harmonic relationship of 20 and 10 meters may show some pattern deviations. Of course, a second smaller array for 17 and 12 meters makes a good antenna to stack on top of the tri-band model.

The ILZX principle of raising the feedpoint impedance simplifies the matching problem that faces single-wire interrupted loops.

However, it requires greater care in supporting the double-wire loops. The wire problem might be resolved by using TV twinlead or 450-Ohm window line. Such insulated transmission lines will likely require adjustment of the dimensions downward by 2 to 5 percent to account for the antenna velocity factor of the vinyl coatings.

Every variation of the horizontal ILZX will demand ingenuity and considerable experimentation. As well, remember that the horizontal ILZX resembles every horizontal antenna in the relationship of its elevation angle of maximum radiation to the height above ground. The original vertically polarized ILZX provided low-angle radiation, but suffered gain losses due to its proximity to ground. The horizontal ILZX provides more gain, but at higher elevation angles until the antenna is at least 1/2-wavelength above ground. The higher the operating frequency, the easier it is to meet the height requirement for long-distance communications.

Happy experimenting!

## Chapter 76: Experimental Omni-Directional Antennas for 6M

**A**lthough our subject matter refers to the 6-meter band--more specifically, 50.5 MHz as a design frequency--the ideas in the following notes are applicable to any other band on which we wish to use any of the antenna designs to obtain a horizontally polarized omni-directional pattern.

We shall do a brief review of turnstiles and their limitations, followed by the introduction of some different types of omni-directional antennas.

### Turnstiles

The basic idea of a turnstile is not dependent upon any one type of antenna. Any horizontally polarized antenna is a fit subject for turnstiling. The most common type of turnstile employs two dipoles, as sketched in **Fig. 1**.

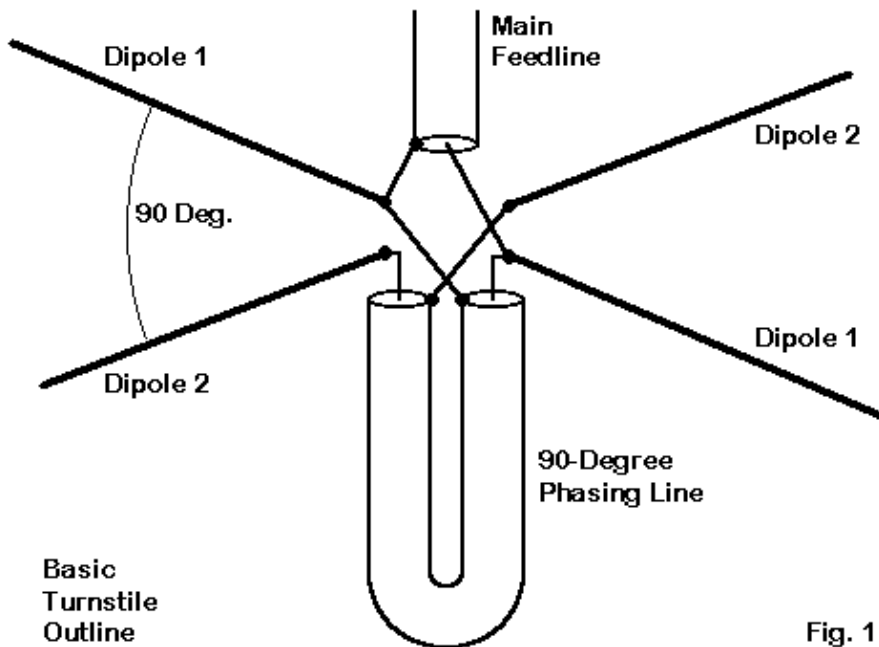
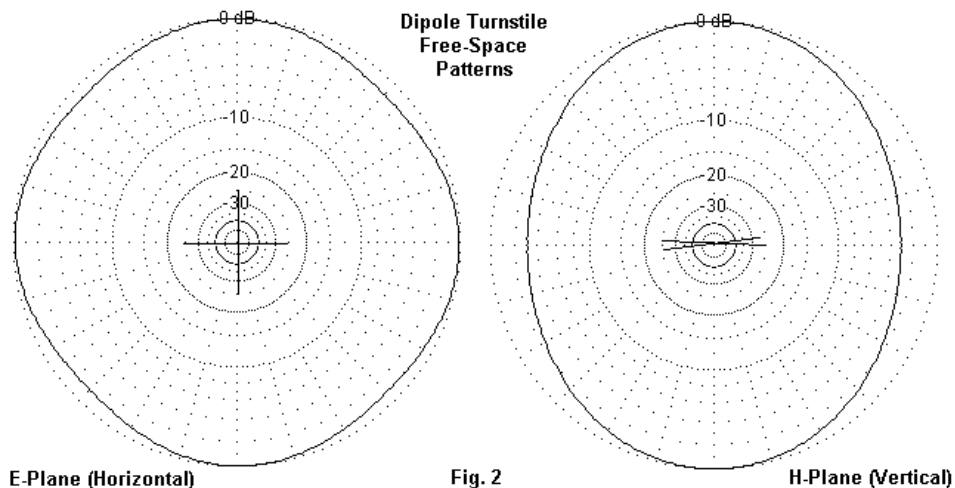


Fig. 1

The dipoles are set at right angles to each other. We then run a 90-degree long phasing line between the two to obtain quadrature, that is, 90-degree phasing. There are more complex systems of achieving the required phasing, but each is subject to the same limitations. The key requirement for the simple phasing system is that the characteristic impedance ( $Z_0$ ) of the phasing line must be very close to the natural resonant impedance of the individual dipoles. A 70-Ohm line is a good match for the dipole turnstile. The

net feedpoint impedance will be 1/2 of the impedance of the individual dipoles, or about 35 Ohms for the antenna sketched in **Fig. 1**.

A dipole has a limited -3 dB beamwidth. Therefore, the pattern that it produces in a turnstile antenna will be less than perfectly circular. The gain variation around the rim of the pattern is a little over 1 dB for an ideally constructed turnstile. **Fig. 2**--on the left--shows the squared but usable dipole turnstile azimuth pattern.

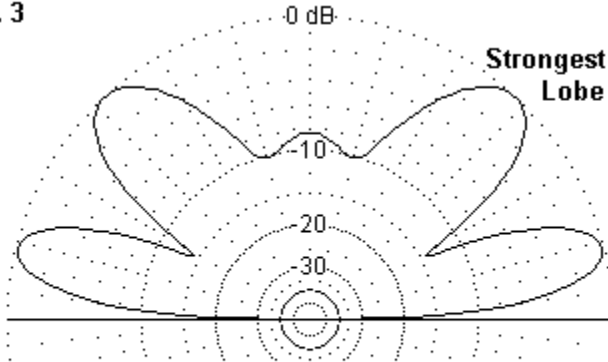


The azimuth pattern--whether a free-space E-plane pattern or an azimuth pattern over real ground--does not change except for the increase in signal strength created by ground reflects and the elevation angle of maximum radiation over ground. All of the

antennas that we shall discuss have take-off angles of 13 degrees when mounted 1 wavelength above ground.

The H-plane pattern in free space becomes the elevation pattern over ground. **Fig. 2**--to the right--shows the free space H-plane pattern for the dipole turnstile. From it, we should draw a clue as to one major limitation of the dipole turnstile: it radiates better broadside to the plane of the wires than off the edges--and it is the edge radiation which makes horizontally polarized communications possible from point-to-point.

**Fig. 3**



**Elevation Pattern: Dipole Turnstile  
1-Wavelength Above Average Ground (240'' = 20')  
50.5 MHz**

**Fig. 3** shows the resulting elevation pattern when we place the dipole turnstile 1 wavelength above ground. At 50.5 MHz, this is a height of about 20'. The strongest lobe is not the lowest lobe, but

the second lobe. The lowest lobe of the dipole turnstile has a gain of only about 4.8 dBi. While adequate for many purposes, designers have felt that we can do somewhat better. However, we must always remember that when we create a nearly or perfectly omni-directional pattern, we should always expect lower gain than from a dipole. The dipole achieve between 7.5 and 8.0 dBi gain at the same height because it has only two lobes, with deep nulls off the ends. The dipole turnstile uses that same power evenly in all directions, so there will be lower power in each direction than in the bi-directional main lobes of the solitary dipole.

Low gain is not the sole limitation of the dipole turnstile. As we vary the frequency, the turnstile gives us the illusion of being a simple antenna, because the SWR remains almost constant for a very wide frequency span. However, the pattern does not stand still. As we vary the frequency off the design frequency, the pattern grows increasingly less circular. **Fig. 4** shows the dipole turnstile patterns 1 MHz off the design frequency.

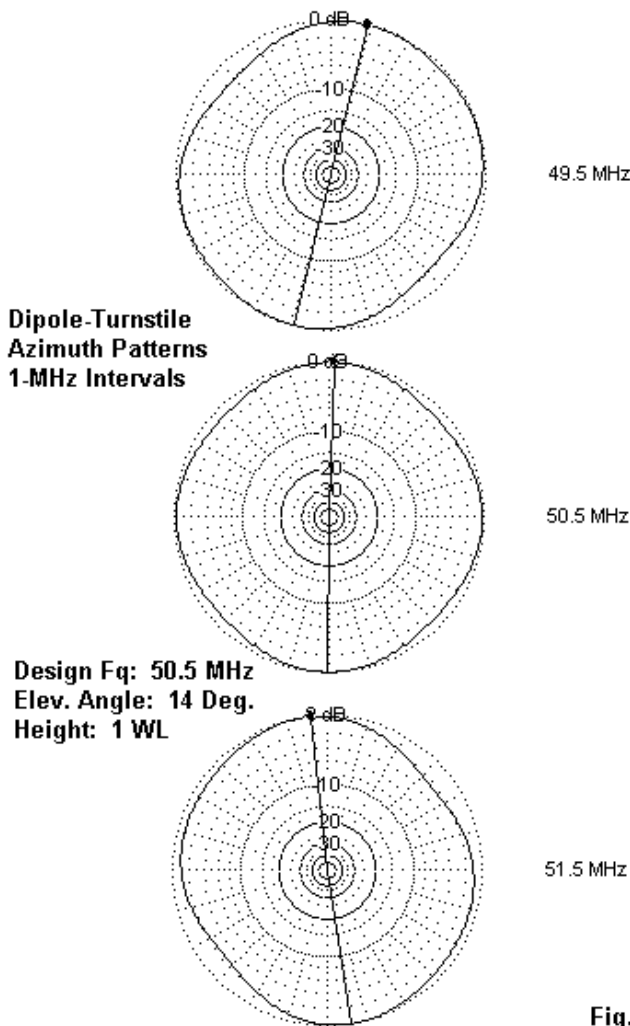


Fig. 4

The patterns in **Fig. 4** would also be good illustrations of other deviations from perfect construction. For example, if the phase line is too long or too short, we shall obtain non-circular patterns. If the line has a higher or lower  $Z_0$  than the individual antennas, we shall obtain non-circular patterns. There are a number of schemes for obtaining a 50-Ohm feedpoint impedance by using differential lengths of line to each dipole. However, it is not impedance that sets the pattern. Instead, it is the current at each dipole being equal in magnitude and different in phase angle by 90 degrees that yields a circular pattern. Virtually all of the matching schemes result in distorted patterns.

The dipole turnstile, then, is a somewhat precision instrument that is not amenable to casual construction unless we can live with a non-circular azimuth pattern. If we can achieve good precision in our element measurements and in the construction of the phase line, we can make some improvements over the dipole elevation pattern and achieve a bit more gain.

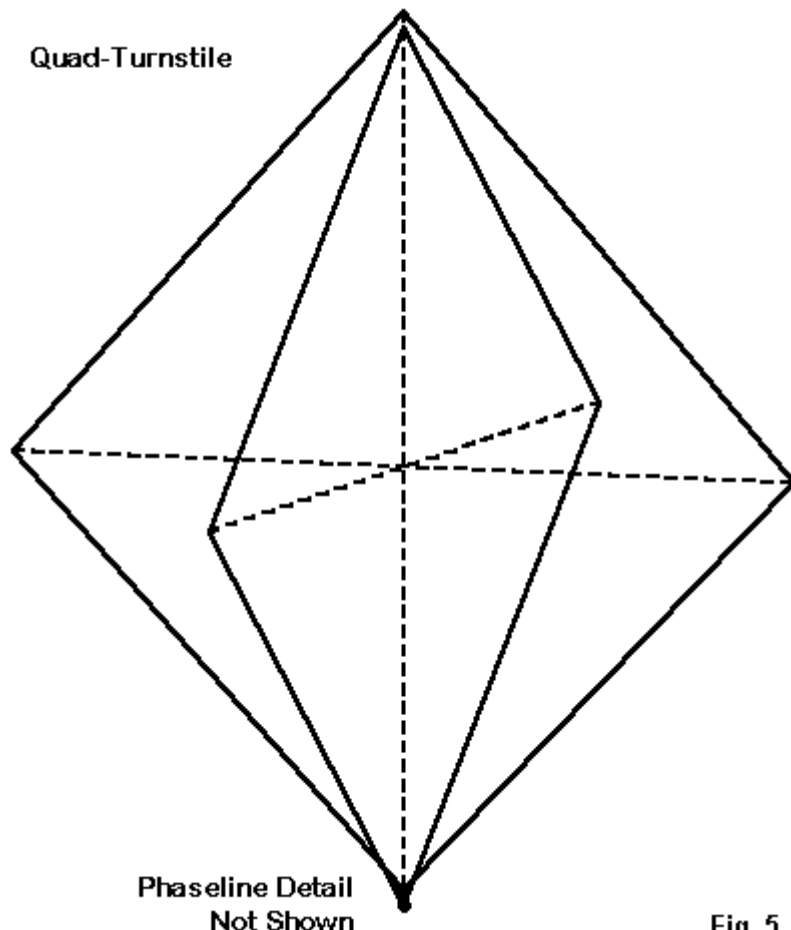


Fig. 5

**Fig. 5** shows one direction that we might go: the quad turnstile. Essentially, the quad turnstile is two quad loops--shown in diamond configuration--fed at the base just as we would feed two dipoles. However, the impedance of the resonant quad loop at 6 meters composed of #14 copper wire is about 125 Ohms. Hence, we must make our phasing line out of RG-63, about the only available 125-Ohm coax. The net impedance will be about 62 Ohms, which yields an adequate coax match, especially since the quad SWR curve will be as flat as the dipole curve. Indeed, SWR tells us almost nothing about the performance of a turnstile, with two exceptions. It may tell us that we have an open circuit or a short circuit somewhere along the line. As well, it may reveal the need for some means of suppressing common mode currents.

Because the lobes of an individual quad loop are somewhat wider than those of a dipole, the E-plane or azimuth pattern will be somewhat more rounded. **Fig. 6** shows the free space azimuth pattern (on the left) for the quad turnstile. The maximum-to-minimum gain variation is somewhat under 1 dB for the quad turnstile.

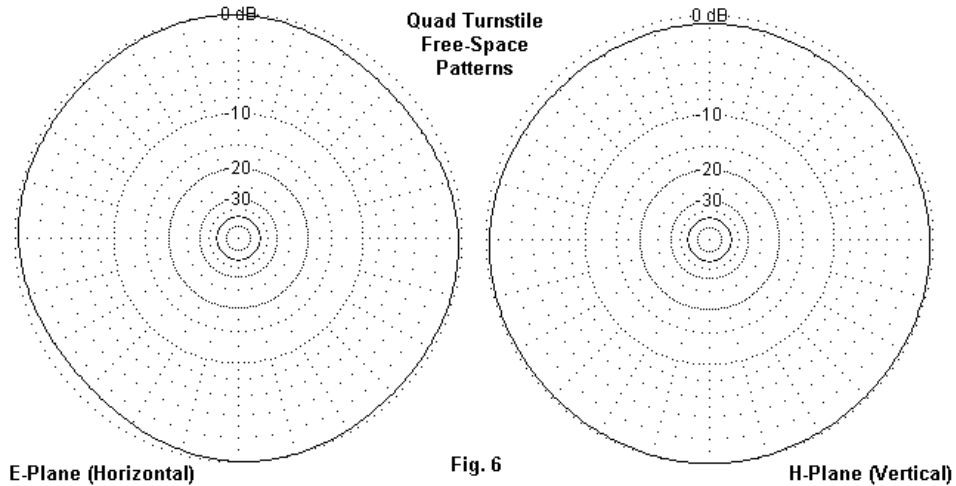
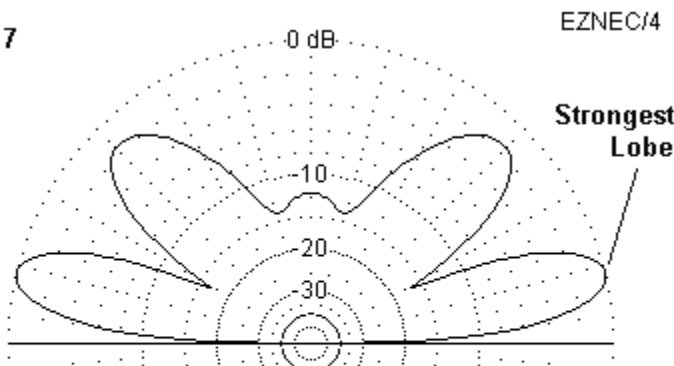


Fig. 6

The H-plane pattern on the right reveals the advantage of the quad over the dipole as an antenna to put into turnstile operation. The gain in the vertical direction does not exceed the gain in the horizontal direction. As a result, the elevation pattern of a quad turnstile with the center hub 1 wavelength above ground will exhibit a main lobe that is significantly stronger than the second lobe upward. As well, the radiation directly upward drops by about 5 dB. **Fig. 7** provides a sample elevation pattern.

Fig. 7



Elevation Pattern: Quad Turnstile  
1-Wavelength Above Average Ground (240" = 20')  
50.5 MHz

The quad turnstile shows a gain (over ground at 13-degrees elevation) of about 5.7 dB, almost a full dB stronger than the dipole turnstile. However, the quad turnstile is subject to all of the same sensitivities to imprecise construction and design as the dipole turnstile. QEX ran an article in Mar/Apr, 2002, covering those sensitivities in detail.

### Updating a Practical 6-Meter Turnstile Quad

In May, 2002, I published in *QST* some notes on a practical 6-meter turnstiled quad for omni-directional horizontally polarized communications ("A 6-Meter Quad Turnstile," pp. 42-46). The general outline and dimensions of the antenna appear in **Fig. QT-1**. You will find details and background in the article.

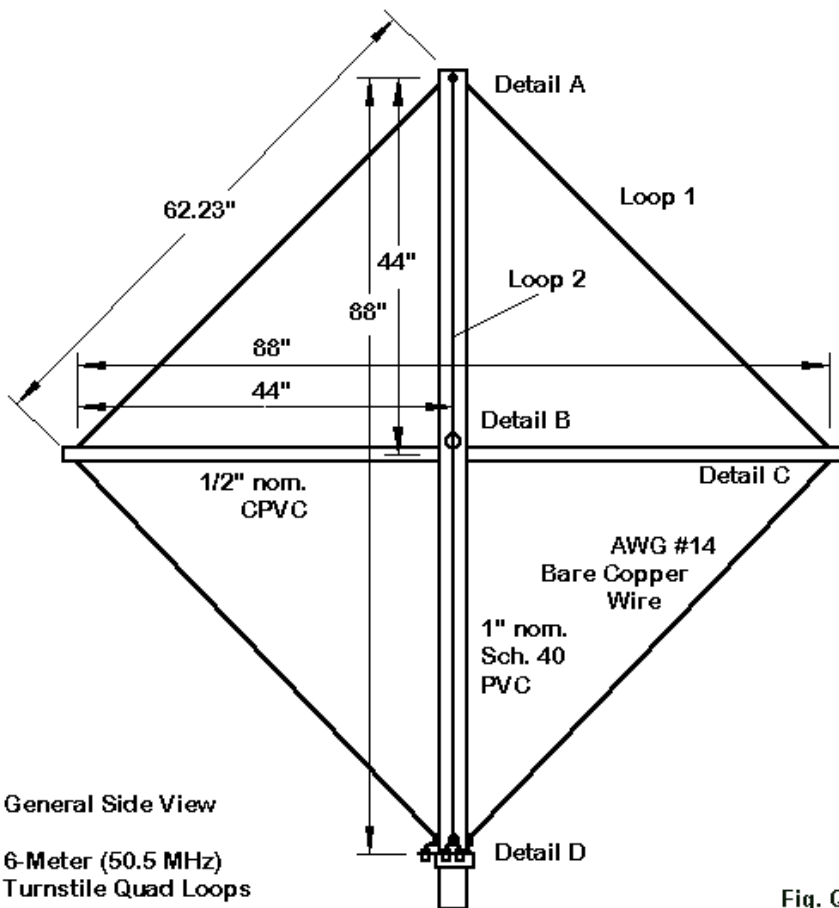


Fig. QT-1

The key elements for these update notes are the particular construction methods that I used, with crossed CPVC arms to

spread the wires. **Fig. QT-2** shows some of the details. Note especially the use of holes in the main mast and bolts to secure the cross arms.

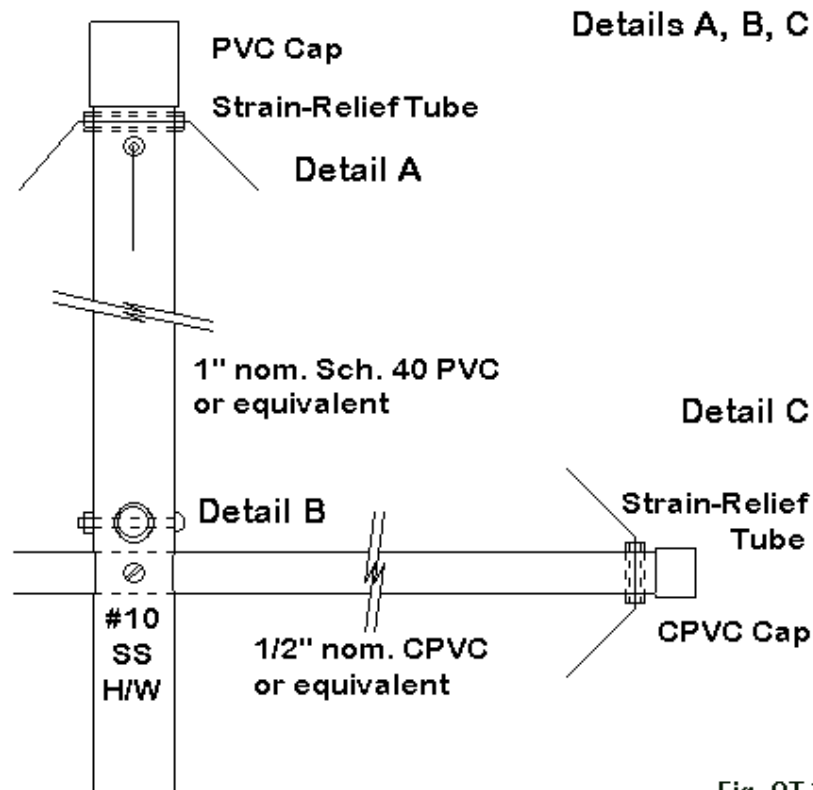
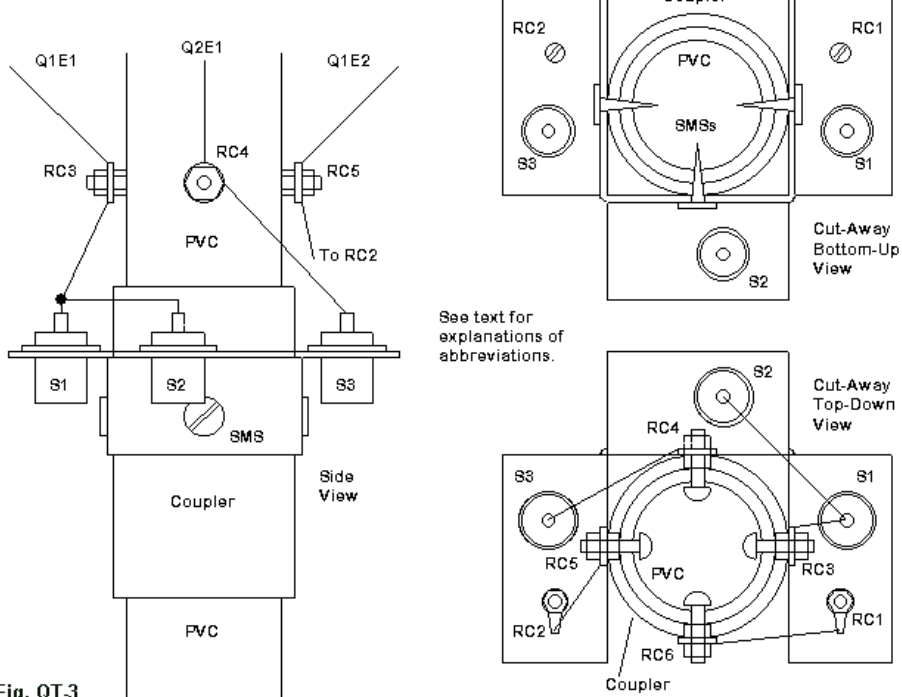


Fig. QT-2

**Fig. QT-3** shows the method that I used to join the phase-line and main feedline, with a plate that surrounds the mast at the bottom of the loops. The original article provides explanations for all of the abbreviations in the sketch.

**Detail D: Quad Loop Base and Phaseline Feedline Connections**



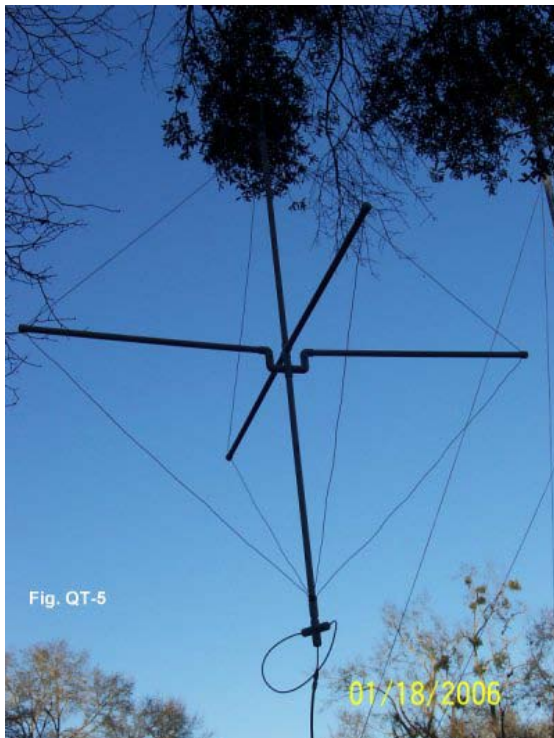
**Fig. QT-3**

Ivan Cook, K4SRB, has built an interesting variation on the turnstile quad for 6. His version uses some ingenious twists on PVC--literally. **Fig. QT-4** shows Ivan explaining his antenna to a local club. In terms of construction, perhaps the most notable feature is the absence of nuts and bolts at the center junction of the support arms with the mast. Instead, Ivan uses a set of elbows and short PVC links to put the arms at the same level. He cements most joints, but leaves a few using only a friction fit.

Fig. QT-4



The reason for the friction fit is that Ivan uses his turnstile quad in the field. To transport it, he can twist the elements into a flat plane. In addition, he has used soldered connections--covered by the PVC--for the phase-line and the main feedline connections. These moves effectively eliminate the need for a mast extending from the ground to the base of the antenna. In lieu of a mast, Ivan has put a hook at the top of the central arm and hangs the antenna from a tree limb. **Fig. qt-5** provides a general idea of the antenna in use.



Ivan's variations show two things of importance to antenna experimenters. The first item is the versatility of PVC as a general support structure that is RF invisible at least through 2 meters and for many purposes through 70 cm. The second item is the ingenuity of the individual experimenter in adapting an antenna design to a specific set of needs and goals. Ivan has converted a somewhat ungainly structure into one that is field-friendly both in use and in transport.

The quad turnstile is not necessarily an ideal antenna. It does have a disadvantage. Its loop construction essentially places two dipoles an average distance apart of 1/4 wavelength. It is the double or phased dipoles that account for the stronger lower elevation lobe of the antenna, relative to the dipole turnstile. However, it is not usually practical to place two quad turnstiles in a vertical stack. The practice is common with dipole turnstiles, but with a degree of usual carelessness that results in relatively poor performance. The pair of dipole turnstiles will interact with each other. If the stack is to have a nearly ideal circular pattern, the individual dipoles must be re-resonated in the stack. Only under this condition will they provide a circular pattern.

For better control of the feedpoint impedance, some quad-turnstile builders have turned to the vertical rectangle as the base antenna. If we increase the vertical dimension of a square and decrease the horizontal dimension, we can change the feedpoint impedance from the square's 125-Ohm value to something closer to what we need. In fact, we can arrive at 50 Ohms, but that is not our goal here. Instead, we want an impedance of between 95 and 100 Ohms so

that the turnstile phaseline will give us a direct 50-Ohm feedpoint impedance. **Fig. R1** provides an outline of such a turnstile using AWG #14 copper wire and set for 50.5 MHz.

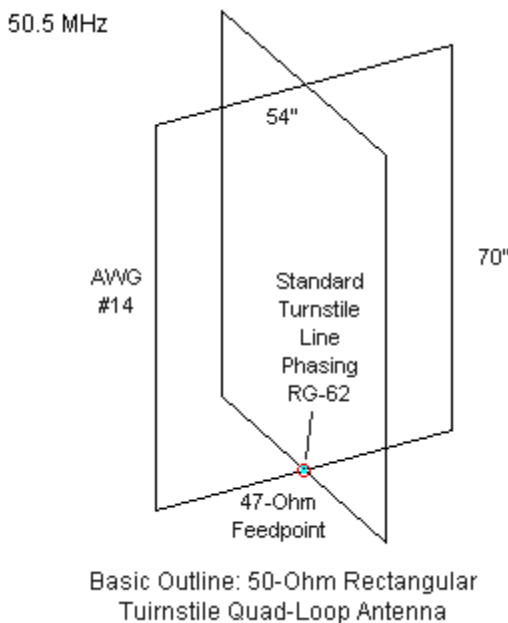


Fig. R1

The vertical sides are about 1.3 times the length of the horizontal wires. The phaseline is 49" of RG-62, which has a velocity factor of 0.84 (for a 58.33" electrical length). The feedpoint impedance is so close to 50 Ohms that the SWR does not rise above 1.1:1 across the first MHz of 6 meters. However, SWR is never a problem with turnstiled elements. The SWR remain nearly constant over a

bandwidth that is much wider than the bandwidth over which the pattern holds its omni-directional shape.

Azimuth Pattern  
Elevation Angle:  
14 Deg.

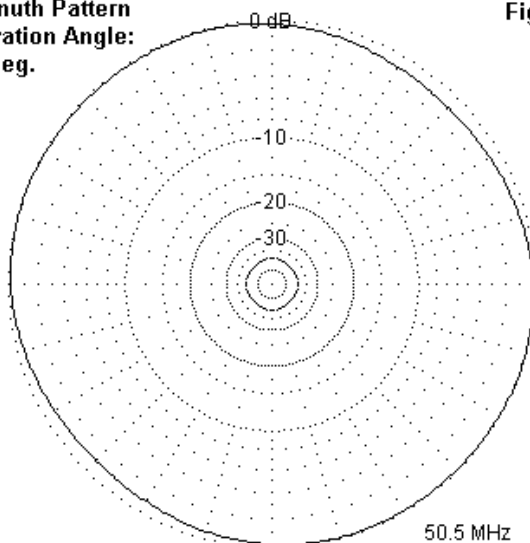
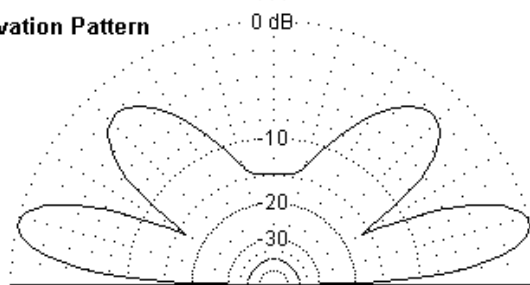


Fig. R2

Elevation Pattern



Rectangular Quad Turnstile Patterns  
1-Wavelength above Average Ground

**Fig. R2** shows the elevation and azimuth patterns of the rectangular quad turnstile. The pattern is virtually identical to the pattern for the diamond quad-turnstile version. Because the rectangles are so little out of square to arrive at individual loop impedances near 100 Ohms, the gain does not increase significantly. In this case, the average gain is about 5.5 dBi with a 1-dB variation between maximum and minimum points.

The finickiness of turnstile antennas--as well as their relatively large size at 6 meters and below--has led designers to look for other options in producing a horizontally polarized omni-directional antenna.

## Unclosed Loops

It is possible to create an omni-directional horizontally polarized antenna by employing a interrupted loop less than 1 wavelength in total wire length. There are two sorts of these loops--which resemble triangles or rectangles: larger loops with a total wire length that is about 3/4 wavelength and smaller loops with a wire length in the vicinity of 1/2 wavelength. There are interesting differences between the larger and smaller loops, so we shall look at them separately.

### *Larger Loops*

In any of the open-loop designs, one key to success is to find the right shape so that the radiation from the center-portion and the

radiation from the legs balances into a circular pattern overall. For this reason, only certain relationships between the center portion and the end pieces will work. The current on the center and end portions is not equal. Therefore, in general, the shaping of the larger loops will be triangular. Bending the end portions towards each other is one way to fine tune the balance of currents and the resulting pattern.

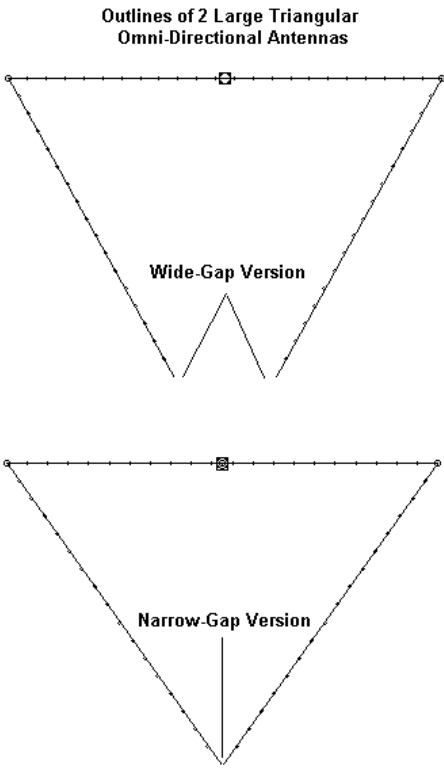


Fig. 8

**Fig. 8** shows two examples of larger loops: the wide-gap and the narrow gap versions. The versions result from giving precedence to one of the other goals of the exercise in addition to pattern shape. The other two goals are the feedpoint impedance and the distance between the tips of the loop ends. In general, with larger loops, the two goals are not compatible.

The top wide-gap triangle in **Fig. 8** sacrifices the convenience of closely spaced tips for a 50-Ohm feedpoint impedance. In fact, like all of the loops that we shall examine, there is a high inductive reactance at the feedpoint. However, we may compensate for this with series capacitance at the feedpoint, using methods that we shall describe further on. The wide-gap model shows a 50-Ohm impedance after compensation, with a 1 MHz 2:1 SWR bandwidth.

The antenna material for the initial design is 1/4" aluminum. Dimensions will vary with the diameter of the element. The center portion is 68" long, with 53.7" ends. The bending of the ends to make a near triangle results in a 47" dimension from the center section to the element tips. The tips are 16" apart. The pattern shows a maximum azimuth pattern gain variation of well under 0.1 dB. With the antenna 1 wavelength up, the gain over average ground at a 13-degree take-off angle is 6.0 dBi, about 0.3 dB higher than the quad turnstile.

Elevation Patterns:  
Large Triangles

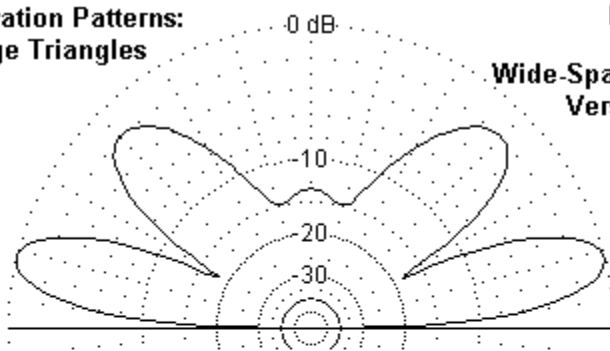
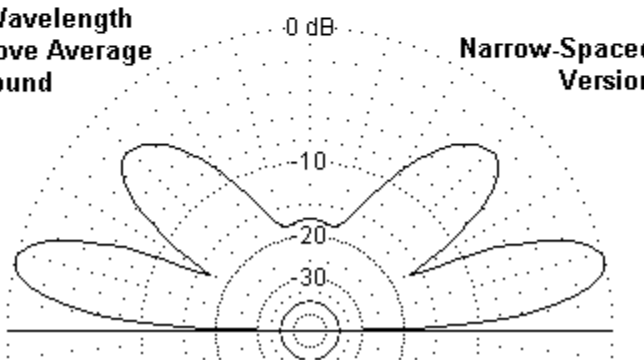


Fig. 9

Wide-Spaced  
Version

1-Wavelength  
Above Average  
Ground



The top of **Fig. 9** shows the elevation pattern of the antenna at the 1-wavelength height. The vertical radiation (straight up) is several dB lower than for the quad loop.

Let's return to **Fig. 8** and examine the lower loop. Here the gap is narrowed to 0.5" so that aligning the ends becomes a much simpler mechanical process. To sustain a circular pattern, the 1/4" diameter

element is 62" long in the center portion. The ends are 52.9" long, resulting in a 43" distance between the center element section and the tips.

The azimuth pattern for this version of the interrupted loop is circular within 0.6 dB around the horizon. As the lower half of **Fig. 9** shows, the secondary lobes are further reduced, with vertical radiation running nearly 18 dB below the strength of the main lobes. The gain--again at a 13-degree take-off angle with the antenna 1 wavelength up--averages about 6.3 dBi, a further increase over the wide-space loop.

Like the wide-spaced loop, the feedpoint of the narrow-gap version of the antenna has a high inductive reactance, calling for compensation. The resistive component of the impedance is about 23.3 Ohms. Therefore, we require a further method of matching this antenna--even with the reactance compensated--to a 50-Ohm coaxial cable. The simplest method is to use a 35-Ohm 1/4 wavelength section of cable. We can construct the section from 38.5" of RG-83 (with a velocity factor of 0.66, for an electrical length of 58.4") or from parallel sections of 70-Ohm cables (which come in various velocity factors, depending upon the use of solid or foam dielectrics).

The result at the design frequency is a very close match to 50-Ohm coax. However, the 2:1 SWR bandwidth is only about 540 kHz at the antenna terminals. Due to cable losses, SWR measured at the transmitter end of the line would likely show a wider bandwidth.

Both loops require that we place series capacitors in the line at the feedpoint terminals. The total capacitance for the wide-gap version is 4.98 pF, while the total for the narrow-gap version is 5.48 pF. These numbers are unduly precise, because construction variables will create considerable differences in the feedpoint inductive reactance.

Perhaps the best way to arrive at the required capacitance with maximum trimming control is to install capacitors in each side of the line, using double the required total capacitance for this series set-up. We can experiment with small fixed capacitors or trim the antenna with variables and replace them with fixed values when tune-up is complete. However, for maximum control, we might consider running insulated wire or thin tubing snugly against the split fed element on each side of the line. The capacitance of the wire and the element depend upon several variables: the facing areas of conductor, the distance between conductors, and the dielectric constant of the insulation on the wire or thin tube. Since a builder will likely use materials on hand, it is impossible to provide detailed guidance. It likely pays to start with wire lengths that are too long and to prune them--evenly on each side--until the reactance disappears at the design frequency.

### ***Smaller Loops***

The larger loops just described will have a center-section length between 5 and 6 feet. This size is a considerable saving over a dipole or quad turnstile antenna. However, it is still considerable for

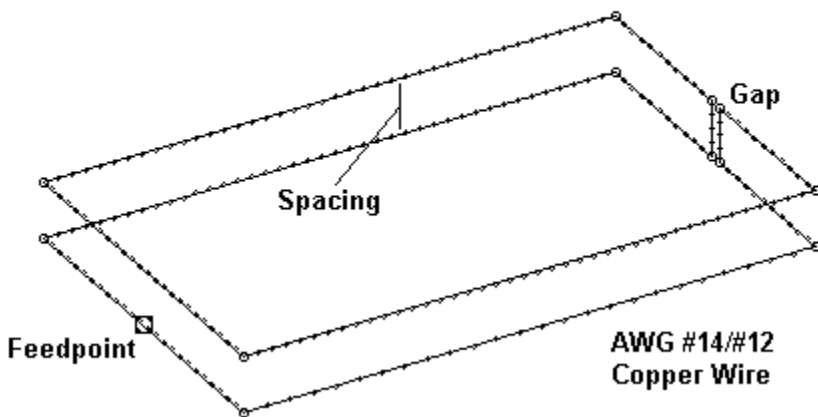
many installations. Therefore, one may wish to explore interrupted loops in the 1/2-wavelength total wire region.

There are on the commercial market single element broken loops of the smaller sort. They measure about 41" at the center, with 49" legs--approximately and use a narrow gap between ends. I do not have all of the physical specifications of these antennas--made by Par Electronics in North Carolina. Therefore, the following notes do not necessarily apply to these antennas.

Most intermediate-size interrupted loops using single elements tend to have very low resistive components to the feedpoint impedance, while sustaining considerable inductive reactance. By compensating for the reactance first, one can use a balun or a broad-band toroidal transformer to raise the impedance to coaxial cable levels. However, at the feedpoint itself, the low impedance raises the potential of resistive losses for the home builder without a well equipped shop. Every fraction of an Ohm in a connection converts a higher percentage of supplied power into heat than with a higher impedance at the feedpoint. Therefore, one might leave such assemblies to the pros and for home construction take a cheaper and easier-to-build approach.

In Chapter 75 I introduced as a limited-space 40-meter antenna the IL-ZX, the intermediate or interrupted loop impedance transforming antenna. We can apply the same approach to a 6-meter version of the IL-ZX.

Fig. 10

**Outline Sketch of the ILZX (Interrupted Loop Impedance Transforming Antenna)**

**Fig. 10** shows the general outline of the rectangle forming the IL-ZX. The short portions are 25" long per side, while the longer sections are 41". There is a gap, which is set at 1". Note that the loop resembles a mutilated folded dipole. Only one wire of the over-under pair is fed. The gap consists of parallel wires, each 4" long, the spacing between the upper and lower wires.

In several design models, the spacing between wires was varied from 1" to 4" with only minor changes in the remnant inductive reactance at the feedpoint. As well, changing the wire from AWG #14 to AWG #12 resulted in similar minor variations in feedpoint reactance. In fact, one might well control the reactance by making

the wires at the gap into arrow points, thus reducing the rate of change of capacitance between ends as the gap spacing is changed. However, changing the gap spacing with the present arrangement also creates only slow changes in feedpoint reactance.

The key to the design--and the reason why it is a rectangle rather than a square--lies in the need to have a circular azimuth pattern and a feedpoint impedance with a resistive component near 50 Ohms. The dimensions noted above result in a pattern with about 0.1 dB variation. The top portion of **Fig. 11** shows how nearly circular the pattern is with the antenna 1 wavelength over average ground. The elevation pattern is equally well-controlled.

Azimuth Pattern  
Elevation Angle:  
13 Deg.

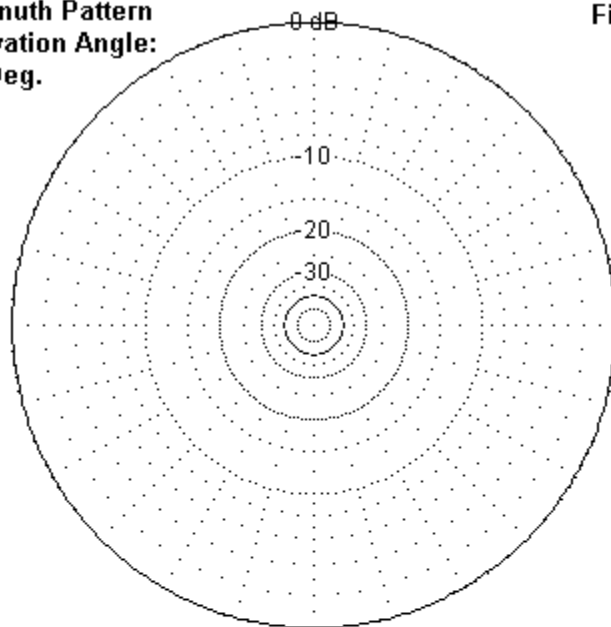
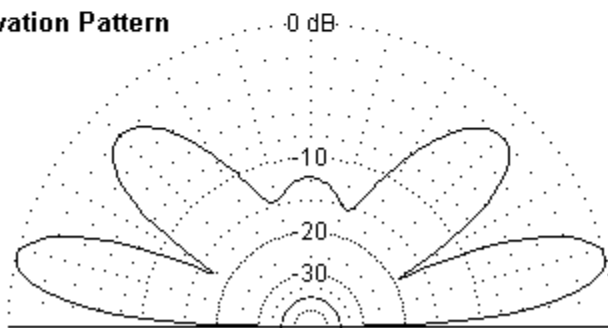


Fig. 11

Elevation Pattern



ILZX Patterns: 1-Wavelength  
Above Average Ground

Since the antenna is smaller than the larger loops that we discussed, the average gain of 5.8 dBi may seem surprising. The resistive portion of the feedpoint impedance is about 58 Ohms, and the 2:1 SWR bandwidth is about 500 kHz. Thus, the operating bandwidth matches the narrow-gap large loop, but not the wide-gap larger loop. The gain levels of all three are comparable.

The IL-ZX loop has a considerable inductive reactance, and required about 4.32 pF of total capacitance--or 8.64 pF per feedpoint terminal. The notes given earlier on methods of providing the required series capacitance for the larger loops are equally applicable for the IL-ZX.

One of the advantages of the loops that we have been discussing is the ease with which we may stack them. Unfortunately, many folks still labor under the mistaken rule of thumb that a stack nets the user 3 dB of gain. In fact, the gain advantage that we get from a stack depends on the spacing between antennas. For dipoles, 5/8 wavelength yields about the highest gain advantage over a single antenna, and with practical materials, this amounts to a little over 2.5 dB.

The goal in stacking a pair of IL-ZX antennas might initially be to further suppress vertical radiation, since that is the most useless part of the elevation radiation pattern. A spacing of 1/2 wavelength yields maximum vertical radiation suppression, but the gain advantage over a single array drops to under 2.4 dB. Although this is highly usable gain, it is simply not the theoretical 3.0 dB bandied about by so many.

Equally important is the fact that a stack will lower the overall take-off angle of the array. If the lower antenna is at 1 wavelength height and the upper is at 1.5 wavelengths, then the take off angle will drop from 13 degrees to 10 degrees. For a stack of 2 IL-ZXs, the gain will be about 8.2 dBi.

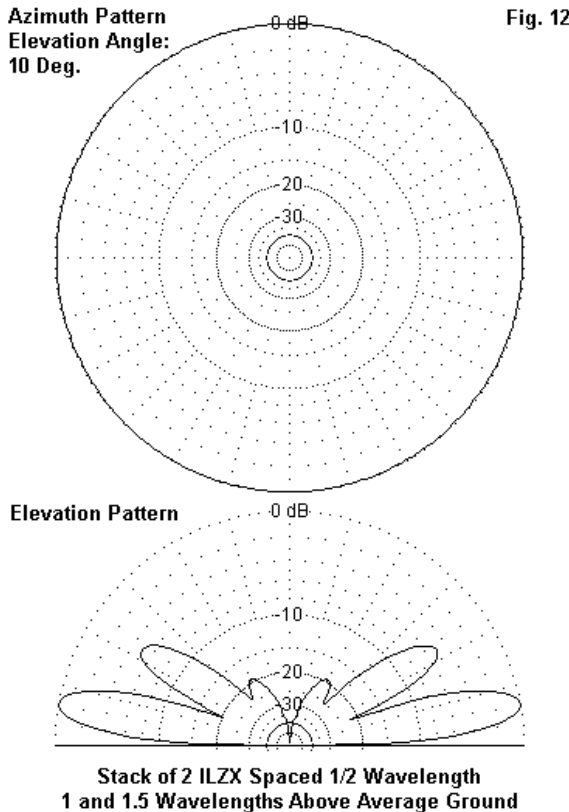


**Fig. 12** shows the azimuth and elevation patterns for a stack of two IL-ZX antennas. The circular azimuth pattern appears solely to confirm that we may stack these types of loops without redesign, as is required by stacked dipole turnstiles.

The elevation pattern shows the results of using the 1/2-wavelength spacing between antennas. All lobes except the lowest have reduced strength, a desirable effect for omni-directional horizontally polarized local and regional communications.

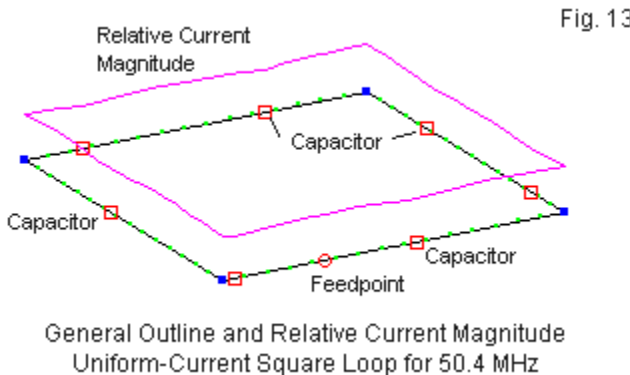
The stacking harness requires careful construction. Two lengths of 70-75-Ohm coax, each electrically 3/4 wavelength long (because 1/4-wavelength sections would not meet) will transform each pre-compensated 50-Ohm impedance to 100 Ohms. A Tee fitting parallels the two impedances to result in a 50-Ohm match to the main feedline.

## Uniform-Current Loops

An overlooked design emerged in 1944 (Donald Foster, "Loop Antennas with Uniform Current, *IRE*, Oct, 1944). Recently, Robert Zimmerman resurrected the idea in "Uniform Current Dipoles and Loops," in *antenneX* for April, 2006. The principle is to divide the circumference of a loop into sections such that the inductance of each wire length is offset by a periodic capacitor and so that the loop exhibits a 50-Ohm impedance--without need for any form of matching. Let's divide a square of wire into 7 sections. Each section will be 0.12-wavelength long, for a total circumference of 0.84

wavelength. At each wire junction, we shall insert a capacitor. The capacitor size will vary with the wire diameter. AWG #14 calls for 9.63-pF units, whereas AWG #10 needs 10.31 pF capacitors. The design comes closest to an even 10 pF with AWG #12 wire.

In real terms for 50.4 MHz, each AWG #12 wire section is 28.1" long. The square is 49.2" on a side for a circumference of 196.7". Note that the sections (7) do not correspond to the sides (4), which is no hindrance to effective antenna operation. One model of the antenna looks like the outline in **Fig. 13**.



Note that it does not matter if the feedpoint is placed mid-side or offset, so long as the feedpoint is in the middle of a wire section. The figure also shows the relative current magnitude along the circumference of the loop. The level changes by under 4% all along the perimeter. (Initially, this phenomenon appears to have been the

goal of the open-ended CCD long doublet, but the open ends preclude obtaining that result.).

The uniform current square loop provides horizontally polarized radiation. Although only a little larger than the triangles, the results are equal in omni-directionality and superior in gain. At 1 wavelength above average ground, the antenna gain averages about 6.8 dBi, with a total variation in gain of about 0.6 dB. The gain is almost a dB better than the best triangle. **Fig. 14** shows the elevation and azimuth patterns and also reveals one significant reason for the improved gain from the loop.

Azimuth Pattern  
Elevation Angle:  
14 Deg.

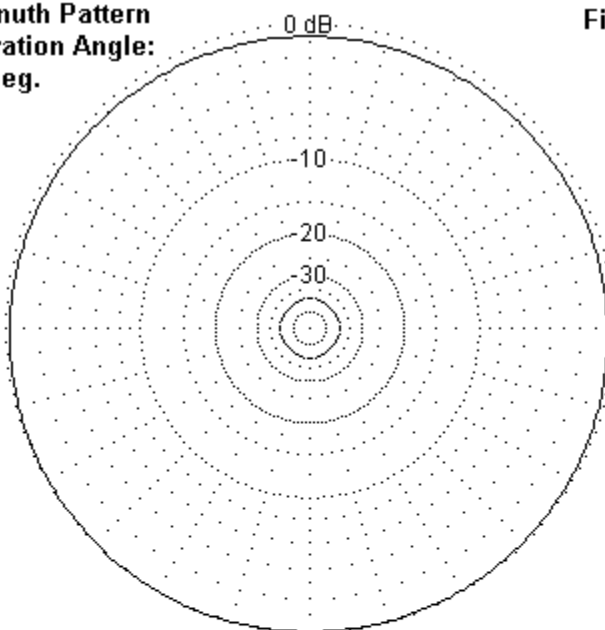
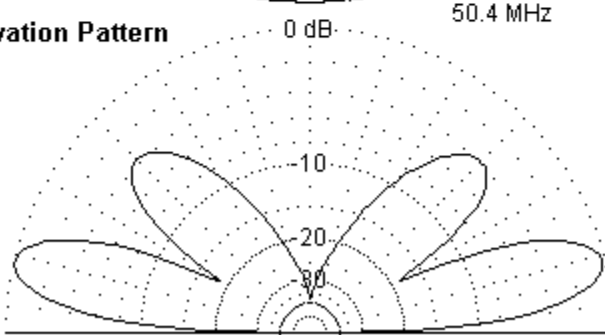


Fig. 14

Elevation Pattern



Uniform-Current Square Loop  
1 Wavelength above Average Ground

If you compare the elevation patterns with the one shown for the triangle, you will see that the loop produces virtually no radiation straight upward, leaving more energy for the lower lobes. Since the antenna does not need to compensate for rapidly changing reactance values, it shows a reasonable SWR bandwidth. As shown in **Fig. 15**, the 2:1 50-Ohm SWR range is 50 to 50.85 MHz. Once you arrive at a usable wire section length and employ the most precise and well-matched set of capacitors that will handle the anticipated power level, you can change the exact center frequency by altering the wire length, since the same capacitance within about 0.1 pF will hold good for nearly a 400-kHz change in center frequency.

Among the experimental designs shown, the uniform-current square loop is perhaps the "best in show."

## Conclusion

The interrupted-loop and the uniform-current square-loop designs shown here are experimental. Any builder should expect to spend considerable time adapting local materials to the needs of the design of choice. As well, field adjustment will also require considerable care and effort. In the end, the goal is to produce a truly circular horizontally polarized pattern with a feedpoint impedance compatible with the main feedline. Hence, much work will be devoted to proportioning the antenna for pattern shape, and an equal amount of work will go into compensating for the reactance and arriving at a usable resistive impedance.

In the end, it is doubtful whether the loop designs are any less finicky than the turnstiles. Instead, they simply change the places in construction and design that require close attention to detail. Producing a circular pattern that is horizontally polarized is no mean feat, whatever the design direction we take.

For frequencies above 400 MHz, the design concepts can be applied to circuit-board construction techniques, since the elements and capacitors are easily fabricated with these methods. The antenna would be only a few inches per side. However, detailed design would require FDTD or comparable techniques that are not at my disposal.

## Chapter 77: Modeling the T2FD

The "terminated, tilted folded dipole" (T2FD) antenna has been subject to much recent conversation, some of which has come my way in the form of questions about modeling the antenna. So I decided to take a systematic look at models of the T2FD. The original T2FD was intended for use as a vertical or a sloping antenna, often as an appendage to the tall tower. Later (WWII), the antenna found use as a horizontal "all-band" wire antenna used in either flat or inverted-V configurations. These notes will deal largely with the vertical and sloping versions. For further and deeper looks into the horizontal versions, see Chapter 28 in Volume 2 of this series on Wire Antennas.

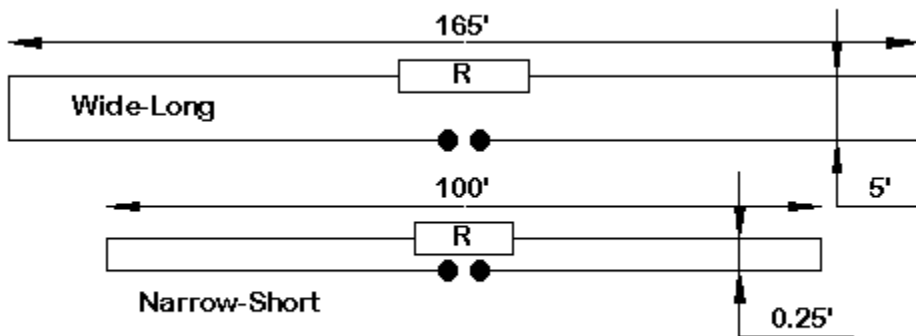


Fig. 1

Two Versions of the T2FD-Type Antenna

The two models I investigated are sketched in **Fig. 1** (shown horizontally to save space). Both are similar in that they are indeed

folded and dipoles, although not folded dipoles in the normal sense of that term. The resistor placed opposite the feedpoint limits the impedance excursions at the feedpoint relative to an unterminated folded dipole. At the same time, the resistor also introduces losses into the antenna in the form of converting some of the RF energy into heat.

Both antennas are designed for use from 2 MHz through 30 MHz as initial design criteria. We shall explore limitations in that frequency spread along the way. The "Wide-Long" version coincides with standard construction formulations, since the antenna is about  $300/F(\text{MHz})$  long and  $10/F(\text{MHz})$  wide. (Excessively fussy cutting formulas for this antenna are largely superfluous, since strict resonance is not in question.) The "Narrow-Short" version generally approximates or approaches the dimensions of commercial versions of the T2FD, even if that name is not used for the antenna. Both antennas use #12 copper wire.

Modeling the T2FD involves nothing that in any way presses the limitations of NEC (either -2 or -4), so long as the segment length in the long wires is not out of balance with the segment length in the short wires and as long as sufficient segments are used per wavelength for all frequencies to be investigated. In short, nothing in the antenna design suggests that NEC should not give accurate predictions of performance.

We shall look at several questions that seem to perpetually arise in connection with the T2FD. The first involves the antenna's feedpoint impedance across the frequency range of intended use,

relative to the selected value of terminating resistor. The second will involve antenna patterns when the antenna is oriented vertically. Related to this second question is the matter of tilting the antenna, as our third inquiry. Finally, we shall look at the question of losses relative to uses to which one might put the T2FD.

Since these are notes on two models of the T2FD, they do not yield more than suggestive results. Hence, nothing in these notes should be construed as fixed, final, or necessarily in rebuttal of existing claims, many of which may be based on different version of the antenna type.

## **Impedance, SWR, and the Terminating Resistor**

All modeling runs for the T2FD (both versions) were made with the antenna lower end 20' above average ground and with the antenna **vertical**. Check runs with the antenna tilted 45 degrees produced no significant differences in the impedance results.

One common recommendation for the T2FD is to use a 390-Ohm resistor for the termination and to employ 300-Ohm feedline. (The general recommendation is to use a terminating resistor that is about 5% to 10% higher in value than the feedline characteristic impedance.) I performed frequency sweeps with this configuration using both models. The technique is to obtain an SWR curve from 2 to 30 MHz using as a standard the characteristic impedance of the desire line, with a resistive load in the model matching the desired terminating resistor.

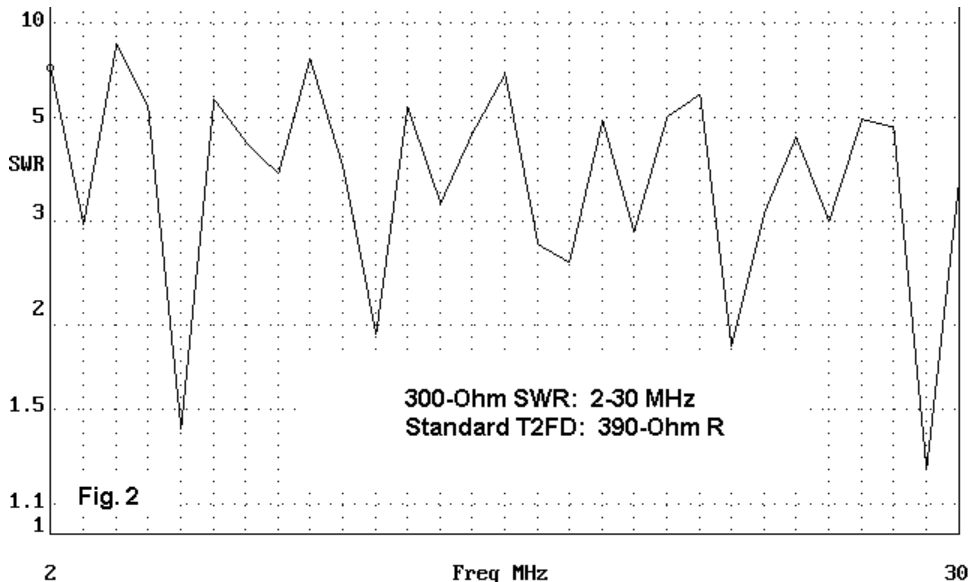
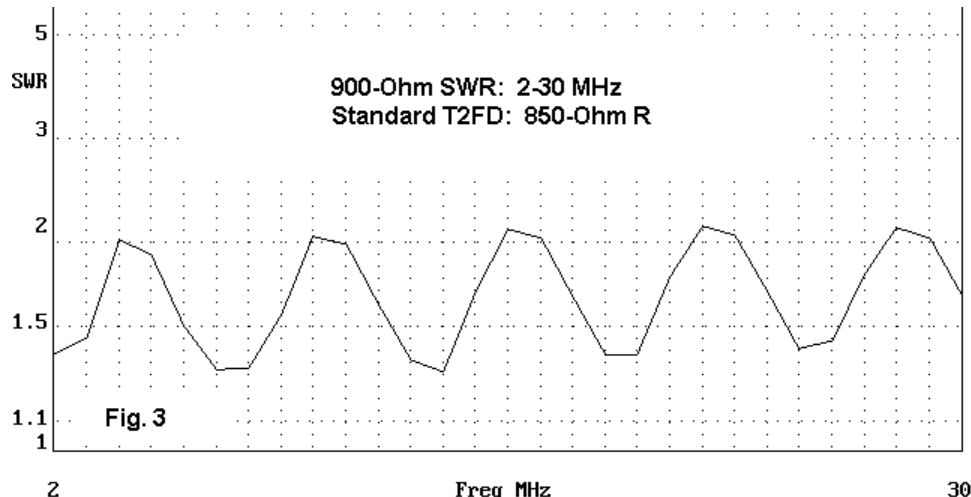


**Fig. 2** shows the results of the 390-300 Ohm combination for the standard T2FD configuration cut for 2 MHz. (The model used is the 165' long wide version from **Fig. 1**. Although called a 2-MHz antenna, the antenna is about 1.2-wavelength long at 3 MHz.) The SWR excursions are very wide, ranging from about 1.2:1 to nearly 9:1.

I could provide a mass of similar graphics representing my search for a combination of terminating resistor and feedpoint impedance standard that would yield the shallowest SWR excursions. Instead, I shall drop to the bottom line. For the standard "wide" T2FD configuration cut for a lowest frequency of use of 2 MHz, a loading

resistor of 850 Ohms combined with a feedpoint impedance standard of 900 Ohms yields the following "best" SWR curve.

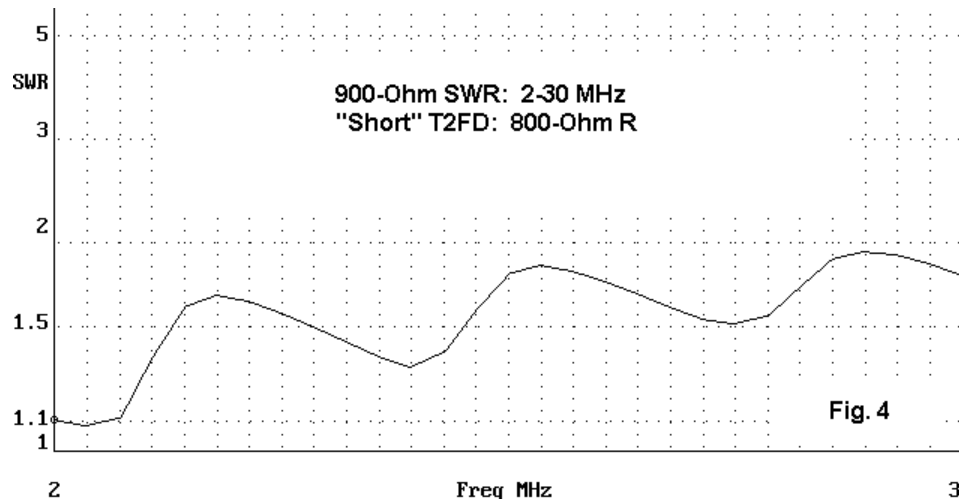


In **Fig. 3**, the highest value of SWR relative to 900 Ohms is about 2.1:1, with peaks in this vicinity occurring every 6 MHz from 4 to 28 MHz. This value does not coincide with any one particular feedpoint impedance, as the following table shows.

Freq.	R +/- jX
4	1435 - j 615
10	1085 - j 700
16	855 - j 665
22	690 - j 575
28	590 - j 466

Although the reactive component is consistently negative at these frequencies, the resistive component ranges from well above to well below the 900-Ohm standard. The resistive component of the source impedance ranged from 450 to over 1400 Ohms, while the reactive component ranged from  $+j250$  to  $-j700$  Ohms across the frequency span. These ranges must be considered tentative, since the check points are 1 MHz apart.

Interestingly, the narrow version of the T2FD with its shorter length (100') also required an SWR standard of 900 Ohms, with a terminating resistor only 50 Ohms less (that is, 800 Ohms) than that used for the optimized wide T2FD version.



30

With these conditions, as shown in **Fig. 4**, one can obtain an SWR curve between 2 and 30 MHz of under 2:1 relative to 900 Ohms. The peak values occur at 10 MHz intervals: 7, 17, and 27 MHz. The wire is about 1.2-wavelength long at 5.5 MHz. However, the extreme resistive and reactive component values are not very different from those of the standard configuration.

In principle, it would seem that some scheme to transform the standard impedance value for both versions of the antenna (900 Ohms) down to a desired feedline value (perhaps a 50-Ohm coaxial cable) might be necessary. For a 50-Ohm result, an 18:1 transformation would be in order, perhaps done in two steps: 9:1 followed by 2:1. However, due to the high values of reactance present at the feedpoint at numerous frequencies within the overall antenna design range, one would need to use great care in selecting the means of impedance transformation. Some methods and materials may combine to yield losses which might then show artificially low values of SWR on the final feedline. These losses would be in addition to those incurred via the terminating resistor. Whether these additional losses would be acceptable might well depend upon the application proposed for the antenna.

## Patterns and Frequency Limitations of the T2FD

Although a properly designed T2FD-type antenna is capable of providing (with suitable matching devices or networks) a low SWR over a very wide frequency range, the utility of the antenna displays other limitations, as some simple elevation patterns can illustrate.

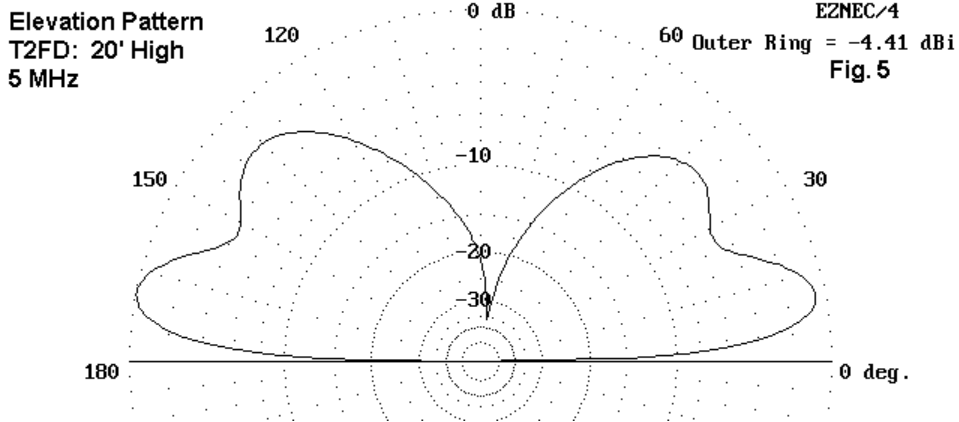
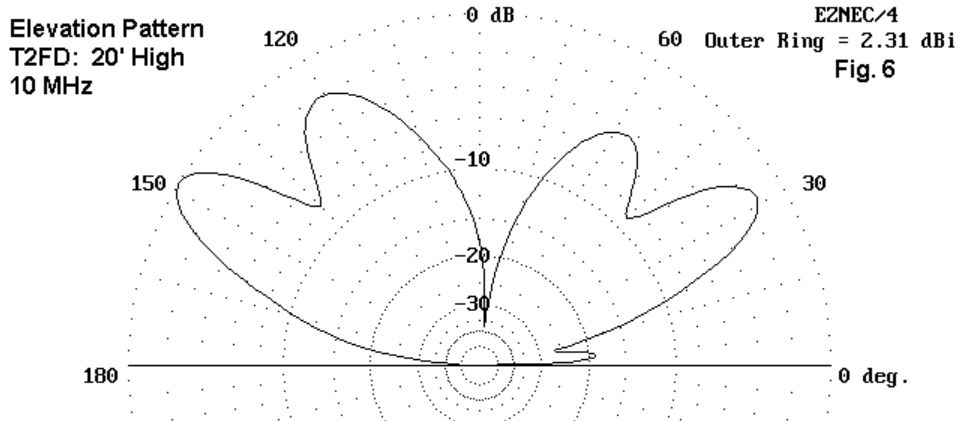


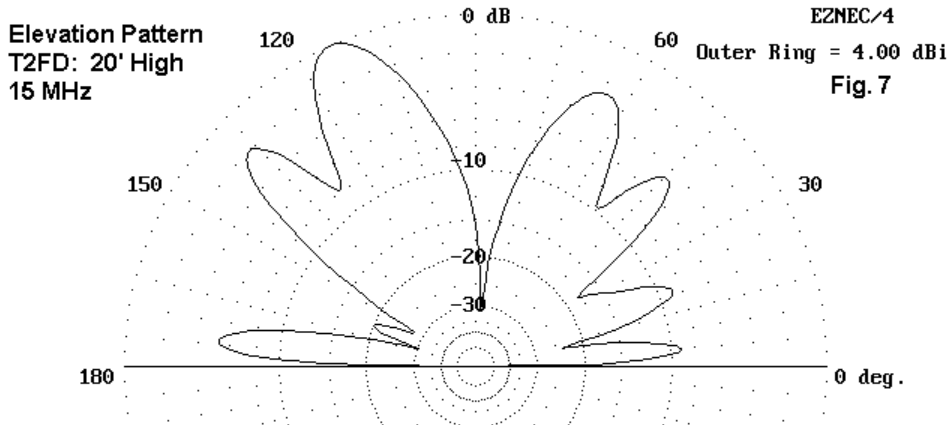
**Fig. 5** shows the elevation pattern of the standard vertical configuration T2FD (as cut for a 2 MHz lower limit or a length of 165') at 5 MHz. The low angle of radiation is one of the features of the T2FD that make it appealing in certain applications. The antenna remains 20' above average earth at the lower end. Note that the pattern is not symmetrical when taken across the plane of the wires (with a 5' separation), with slightly less gain in the direction of the loaded wire. In general, the closer the wire spacing the less the gain differential. Broadside to the plane of the wires, the elevation pattern would be symmetrical with a gain intermediate to the high and low values shown in this edgewise view.



In **Fig. 6**, we find the elevation pattern for the same vertical antenna at 10 MHz. (Note that the wider standard configuration tends to show some pattern displacement to one side or the other, due to the spacing of the wires. The more dominant side depends on the frequency of operation. The narrow version shows an almost perfectly circular pattern.)

The most noteworthy aspect of **Fig. 6** is the absence of low angle radiation, with the first main lobe peaking at greater than 30 degrees above the horizon. The high-angle of the main radiation lobes results from the fact that at 10 MHz, the antenna is well over 1.5-wavelengths long. A linear vertical doublet would show a low radiation angle to a length of about 1.25-wavelengths. As the antenna becomes longer, the main lobes are no longer broadside to the wire, but at angles to the wire. This shows up in the vertical configuration as high-angle radiation rather than low-angle radiation

that would correspond to a broadside pattern in free space (or when used horizontally)



To establish that **Fig. 6** is no fluke, **Fig. 7** is the elevation pattern for the antenna at 15 MHz.

The explanation for these less than optimal patterns is the nature of the antenna. Although terminated, the antenna is still a folded doublet and shows in free space all of the pattern tendencies of any dipole. So long as the antenna is 1.25 wl long or less, then there is in free space a single main lobe broadside to the antenna wire. (In the range of 1.1 to 1.35 wl long, the antenna shows the side lobes typical of the extended double Zepp.) The main lobe, when the antenna is vertically oriented over ground, results in a low-angle lobe of radiation or reception sensitivity.

As the antenna length approaches  $1.5 \text{ wl}$ , the broadside lobes give way to dominant angular lobes relative to the plane of the wire. When the antenna is vertically oriented, these lobes combine to form high angle radiation maxima, with low angle radiation either much reduced or wholly absent.

The standard T2FD at 165' long reaches the  $1.25 \text{ wl}$  limit at about 7.5 MHz, while the shorter 100' version reaches the same limit at about 12.3 MHz. Beyond 8 MHz for one and 13 MHz for the other, high angle patterns become standard. When any version of a T2FD reaches a length relative to the operating frequency of more than 1.25 MHz, its utility for low angle radiation may become less than desired.

The solution to this problem is fairly simple: the construction of a second T2FD. A T2FD (this time in the narrow configuration) of 40' overall length and 0.25' width, using the same loading resistor and feedpoint standard impedance was modeled. The SWR graph is a single curve that does not reach 2:1 from 7 through 30 MHz when the antenna bottom is 20' above average earth. In fact, the peak value of SWR relative to a 900-Ohm standard is 1.72, which occurs between 19 and 20 MHz. This new antenna is already over  $0.5 \text{ wl}$  long at 14 MHz and does not reach a length of  $1.25 \text{ wl}$  until nearly 31 MHz.

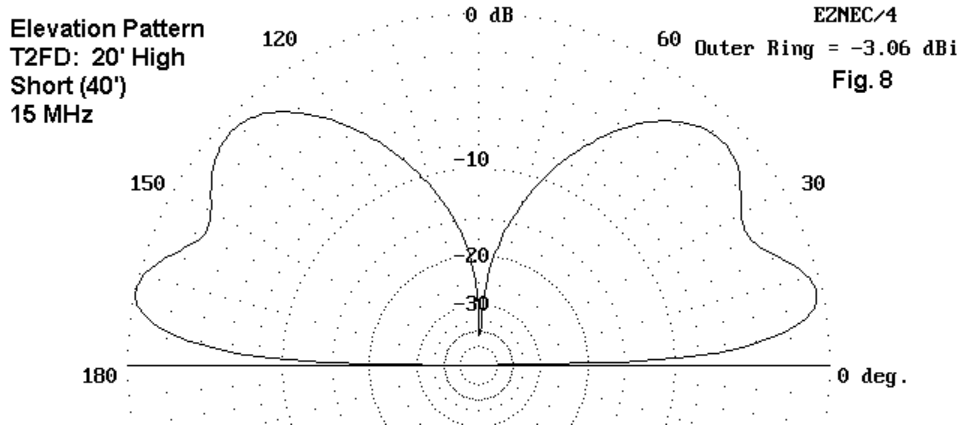


**Fig. 8** shows the elevation pattern of the second T2FD at 15 MHz, for comparison with the pattern for the long T2FD in **Fig. 7**. Although the peak gain value is lower with the shorter antenna, the radiation is at an angle of greater utility in most applications.

## To Tilt or Not to Tilt: That is the Question

All of the patterns shown so far use a vertical T2FD. Tilting the T2FD alters its pattern considerably. Modeling does not confirm reports of omni-directional performance from a tilted T2FD. We may illustrate this fact with a simple comparison at 5 MHz using the standard version of the T2FD. In one pattern, the antenna is vertical; in the other, it is tilted 45 degrees.

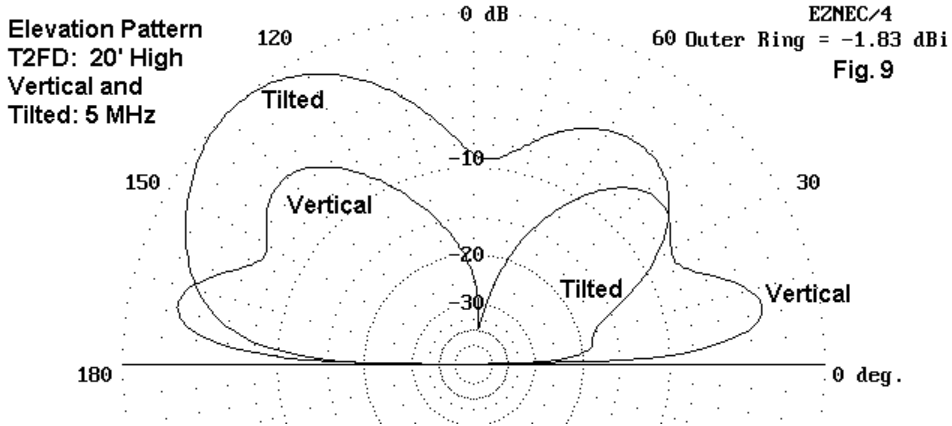


**Fig. 9** shows the two patterns. The vertically oriented T2FD shows minimal pattern displacement from one direction to the other. However, the tilted version shows a heavy pattern displacement, but in neither direction is the radiation field as strong as at the peak of the lowest lobe of the vertical version.

Elevation Pattern  
and Tilted Antenna  
T2FD: 5 MHz

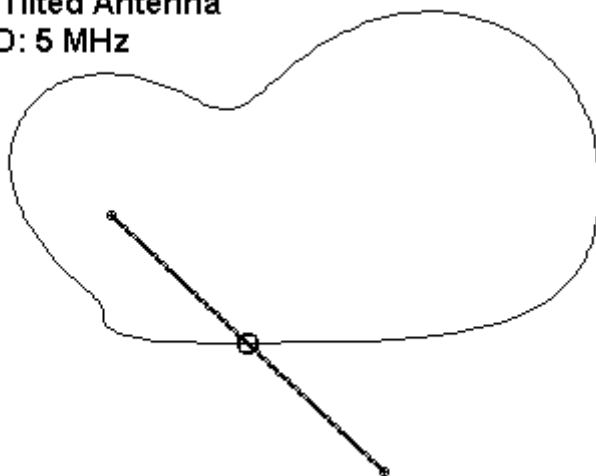


Fig. 10

**Fig. 10** shows the orientation of the pattern displacement to the tilt of the antenna. The patterns off the sides of the antenna are equal and approach those of the vertically oriented antenna. Nothing in the models shows any advantage to tilting the antenna with respect to skip communications or reception. Perhaps the only advantage may be mechanical, for those lacking a suitable high support from which to hang the antenna vertically.

## Terminator Resistor Losses

Although transmitting uses have been made of the T2FD, its chief use appears to be as a short wave reception antenna. In this application, the excess available receiver gain can largely make up for losses incurred in the terminating resistor.

The losses in the terminating resistor are considerable, ranging from nearly half power to amounts in excess of 90% of the available RF power. The pattern of losses is not a simple smooth curve, but varies throughout the operating range of the antenna. The following graph plots the losses in terms of dB. For reference, a 3 dB power loss represents half the power being dissipated in the resistor. Higher values indicate more of the power being dissipated rather than being radiated (or transferred to the receiver).

## Resistive Load Losses T2FD-Type Antenna

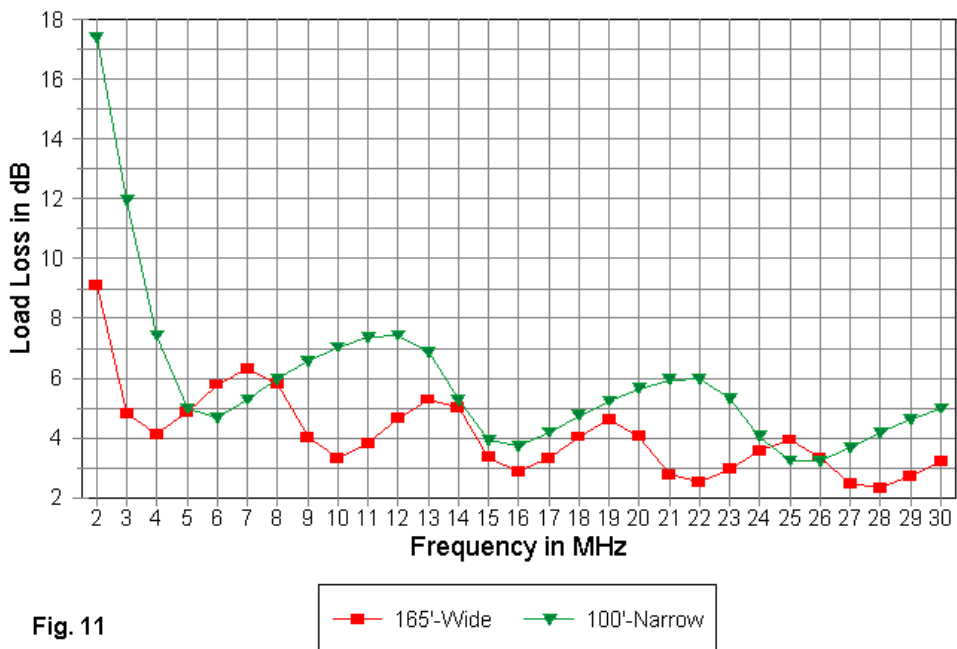


Fig. 11

**Fig. 11** is notable because it tracks the SWR curves for the two versions of the T2FD in quite interesting ways. The lowest losses in the wide or standard version of the T2FD (165' long) occur at the same frequencies as the peaks in SWR. For the shorter (100') version, the lowest loss points show a slight displacement (1 MHz) but occur at the same intervals. The actual loss within the resistor is

a function of the current on that segment of the antenna. Other lengths and load resistors will show different levels and patterns of loss from the terminating resistor.

It should not be surprising that the shorter T2FD shows much higher losses at the lowest frequencies of operation, since the antenna is about  $0.2 \text{ wl}$  long at 2 MHz. Basic antenna efficiency increases rapidly as the antenna length passes the  $0.3 \text{ wl}$  mark, which is well above 3 MHz for the shorter antenna. Indeed, we may call the frequency at which the antenna is about  $1/2$ -wavelength long the "knee" frequency. Below the knee, gain drops rapidly and losses (as well as dissipation in the terminating resistor) increase with equal rapidity.

The losses incurred in the terminating resistor occur in the form of heat. For reception-only applications, simple low-wattage non-inductive resistors may be used. For transmitting purposes, heat dissipation for the terminating resistor assembly becomes a major factor in antenna design.

## Conclusion

The purpose of these notes is not to recommend or disrecommend the vertical or sloping T2FD. Instead, the purpose has been to explore what modeling might tell us about the basic performance characteristics of the T2FD. Actual use decisions must measure the antenna performance characteristics (refined for the actual proposed design) against the application.

There are a number of questions that modeling cannot answer, even if precise design and installation data are supplied. For example, the standard version of the T2FD is said to be quieter than random wires and doublets in receiving applications. The closed loop construction with wider spacing between wires may well account for this report, but modeling cannot itself show the phenomenon.

Nonetheless, the models used here were constructed with sufficient care to warrant reasonable trust in the analytical results. These notes may provide a basis for prospective users to check out their proposed designs prior to installation to ensure that the resulting antenna has a good chance of meeting expectations.

## Chapter 78: Wire Linear-Resonator Dipoles

I have written elsewhere about dual-band linear-resonator dipoles for the upper HF region that used elements having a substantial diameter. 20-meter main elements used 7/8" tubing, while 15-meter main elements used 3/4" tubing. One major consequence of the material selection was our ability to use a fairly wide separation between the main element and the 1/4"-diameter linear-resonator rod. We centered our focus on 6", but explored some narrower and wider spacing values between 4" and 8".

In this look into the land of linear resonators, we shall reduce the main element diameter to wire size. One consequence of the reduction is that we shall be able to use the same diameter material for both the main element and the linear resonator. Since all wires in the NEC-4 models will have the same diameter, the modeling accuracy, as indicated by the average gain test (AGT) scores, should improve. However, there will be a second consequence for the models (and for any physical implementation of a wire-based linear-resonator dipole). The ability to find acceptable dimensions to achieve a set of resonant points on 2 bands with a 50-Ohm SWR of less than 2:1 depends in large measure on the mutual coupling between the parallel wires within the linear-resonator section of the antenna. Since we are wholly dependent on the wires as linear inductors for the mutual coupling, the degree of coupling depends upon the wire diameters and the spacing between them. As we reduce the diameter of the wires, we must bring them closer together to achieve the same level of coupling.

Suppose that we reduce the wire size by a factor of 7:1. That is, suppose that we reduce the diameter from 7/8" to about 1/8". The required spacing between the wires is roughly proportional to the element diameter. Hence, the spacing between the main element and the linear-resonator rod will decrease from about 6" to the vicinity of 1". As we shall see, the narrow spacing will be quite critical in dual-band dipoles with small ratios between the upper and lower frequencies, but will be less critical with higher frequency ratios.

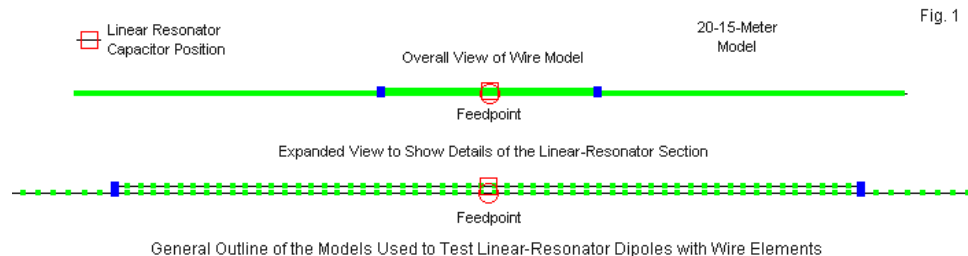
To sample both possibilities, let's explore two different wire-based linear-resonator dipoles. The first will cover 20 and 15 meters. The 3:2 frequency ratio falls at the lower end of the scale. As well, the combination allows us to compare the results with the model used in Part 1 of this series. Later, we shall examine a 20-10-meter combination. The larger 2:1 frequency ratio will show us both the advantages and the disadvantages of the alternate design.

## A 20-15-Meter Wire Linear-Resonator Dipole

The 20-15-meter combination dipole that we explored in Part 1 proved that the linear-resonator technique can be successful if we observe its limitations. The large-diameter (0.875" diameter) model allowed us a wide SWR bandwidth on 15 meters. However, the 20-meter impedance dropped to the vicinity of about 35 Ohms. Obtaining coverage of 20 meters required careful attention to the overall length of the antenna. The 1/4"-diameter linear-resonator rod--spaced 6" from the main element--was a little under 100" long

and required a capacitor value of about 16 pF for 15-meter resonance.

Translating that "fat-element" model to wire size requires that we reduce both the element diameter and the rod-to-element spacing. For reasons that will become evident a little later, I did not start with the usual amateur AWG #12 wire 0.0808" or 2.05 mm diameter). Instead, I used the less common AWG #8 wire (0.1285" or 3.26 mm diameter). As well, I reduce the rod-to-element spacing down to 1". Since the end wires of the resonator section are so short, I had to increase the overall segmentation density of the model to preserve some semblance of segment-length equality. **Fig. 1** shows both an overall outline of the model and an expanded view of the linear-resonator section.



Quite likely, any implementation of a wire-based linear-resonator dipole will require the use of parallel sections of rod to effect the resonating capacitance. The development of a homemade concentric capacitor that is thin enough to avoid touching the main element is difficult at best. For our initial model, all wires are AWG

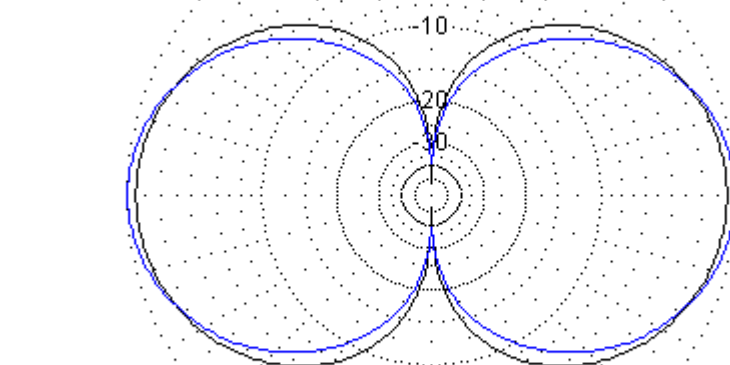
#8. The proximity of the wires does not yield perfect AGT scores. However, the values (0.985-0.988) are significantly improved relative to earlier models that had junctions of wires with different diameters.

The close spacing between the wires does not affect the general radiation pattern of the dipole. As shown in **Fig. 2**, the 15-meter performance includes slightly high gain and a slightly narrower beamwidth than we obtain on 20 meters. The free-space patterns show a 0.5-dB difference in gain. In the plane formed by the main element and the resonator rod, the close spacing does make a difference. In this plane, the front-to-back ratio is down to 0.1 dB, a reduction from the 0.5-dB value we obtained from the fatter model. As a consequence, the 15-meter pattern shows deeper side nulls than we obtained using fatter elements: about 25 dB below the level of maximum gain.

20-15-Meter Wire Dipole  
with a Linear Resonator  
Overlaid Free-Space  
E-Plane Patterns

0 dB

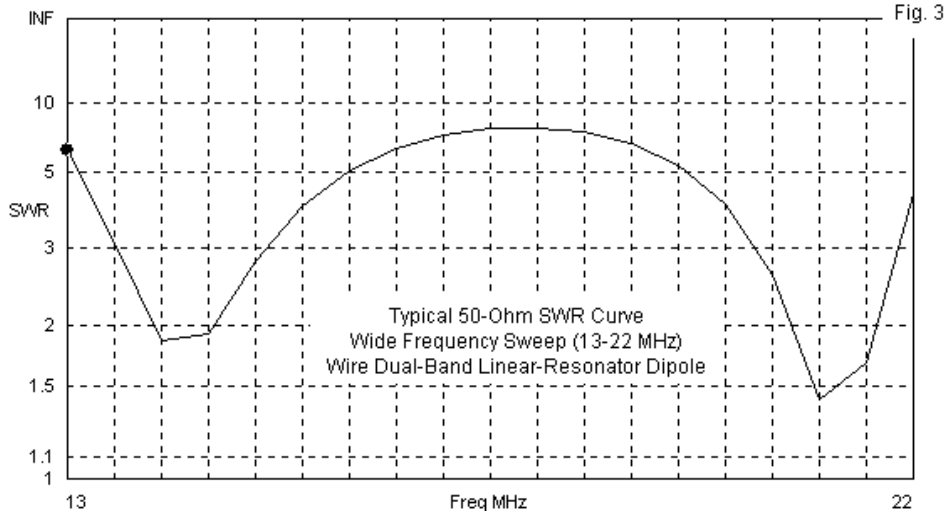
Fig. 2



Blue = 21.225 MHz

Black = 14.175 MHz

Smaller diameter elements do produce other effects that are noteworthy. For a linear element, a smaller diameter element generally produces an antenna with a narrower SWR bandwidth. We can observe this effect in a general way by looking at a typical wide-band SWR sweep. **Fig. 3** shows a 50-Ohm sweep from 13 to 22 MHz to include the bands of interest.



The peak 50-Ohm SWR value between bands was between 5:1 and 6:1 for the fatter models of Part 1. For our wire versions, the peak value will climb to the 8:1 or higher region. The actual value is not important in operation, but it does provide a caution to experimenters. Finding the precise values for all dimensions, including the capacitor setting, will likely be somewhat more finicky for a wire-base dipole than for a tube-based dipole.

By the terms of our project, we are looking for dimensions that will produce 50-Ohm coverage on both 20 and 15 meters with less than a 2:1 SWR. (Indeed, if we forget this project specification, we might as well use a simple wire with a parallel feedline and an antenna

tuner.) As we did for the fat-element models, we shall freeze some dimensions and vary others to obtain a sense of the trends at work.

### *Varying the Resonator Rod Length*

The first set of tests will use AWG #8 wire throughout. A simple dipole for 14.175 MHz would normally require a length of about 403". One feature that we shall look for is the amount of reduction that the use of a linear resonator forces on the overall element length. With the tubular models, we found a usable constant main-element length that was about 14" or 3.5% shorter than a self-resonant 20-meter dipole. Shifting to wire does not change the level of reduction, but it does introduce a new factor into the building equation. Changing the length of the resonator also requires a change in the length of the main element. For every 4" decrease in resonator rod length, we find a 2" increase in the main element length.

As shown by the data in **Table 1**, the survey covers rod lengths from 92" to 108". At the same time, the main element changes from 390" to 382". The range of resonating capacitance for the entire spread is about 3 pF--from 18 to 21 pF. The average value is itself about 3-pF higher than the average value needed for the tubular models of Part 1.

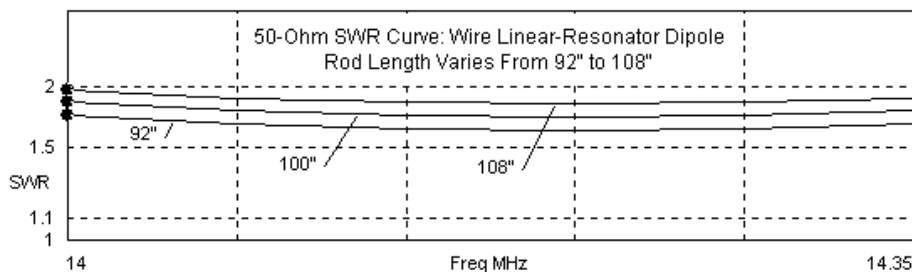
Table 1. Varying rod length with AWG #8 with 1" rod-to-element spacing: 20-15-meter dipole  
Note: Both element and resonator rod are AWG #8 (0.1285" = 3.26 mm diameter).

El. Length Inches	Rod Length Inches	14.175 MHz $R +/- jX \Omega$	21.225 MHz $R +/- jX \Omega$	Cap. pF
382	108	$27.4 + j3.6$	$61.7 + j3.9$	18.1
384	104	$28.1 + j5.1$	$50.9 + j4.6$	18.9
386	100	$29.2 + j4.8$	$45.1 - j1.7$	19.5
388	96	$30.2 + j4.8$	$39.4 - j5.6$	20.2
390	92	$31.3 + j5.1$	$34.0 - j8.0$	21.0

We have already viewed a wide-band SWR sweep for a typical dipole from the group. In fact, that sweep used the version with a 100" rod and a 386" main element. We may therefore confine our examination of 50-Ohm SWR values to the specific operating bands. The impedance values at 14.175 MHz give us an additional reason for taking a close look at the in-band SWR values. As we reduced the element sizes in Part 1, we saw a decrease in the 20-meter resistive impedance. We also wondered at what rate the impedance would continue to decrease as we reduced the element size further. At some diameter, the impedance might slip below 25 Ohms, removing all hope of obtaining 20-meter performance with less than a 2:1 50-Ohm SWR. As the mid-band impedance values show, we are getting close.

20 Meters

Fig. 4

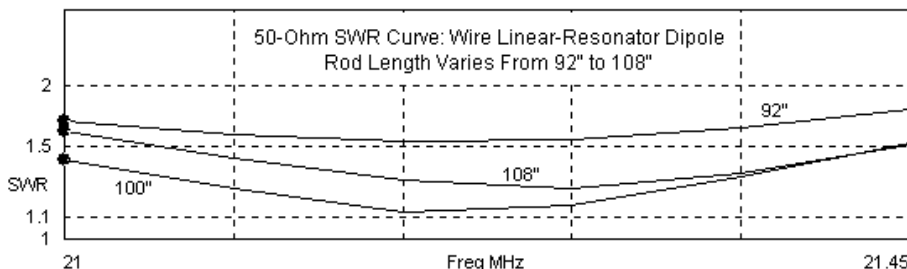


Using AWG #8 wire allows us to obtain a barely usable SWR curve across 20 meters. The shorter the resonator rod (and the longer the main element), the better SWR curve that we obtain. Unlike the tubular elements, the wire elements required that we adjust both the main element and the rod lengths to arrive at this result.

The corresponding SWR curves for 15 meters appear in **Fig. 5**. On this band we face a different challenge created by the increasingly narrow-banded performance of thinner elements. Between rod-length increment changes, the mid-band impedance on 15 meters changes more rapidly, and this factor limits our ability to obtain a satisfactory SWR curve.

15 Meters

Fig. 5



The 92" resonator rod that gave us the best 20-meter SWR curve produces the least satisfactory SWR curve on 15 meters--although the performance is usable. As the rod length increases, the SWR curve tends to improve, at least through the 100" length. Further increases in rod length degrade the SWR curve. Nevertheless, all of the 15-meter curves within the set are usable. In general, 15-meter performance is less problematical than 20-meter performance with a wire-based dual-band dipole.

### *Varying the Rod-to-Element Spacing*

For further tests, I selected the model that used a 100" rod and a 386" main-element length as perhaps (but not absolutely) the best compromise in performance on both bands. The next test involves seeing what happens as we increase the spacing in small increments from the 1" initial value. (I judged that a smaller spacing is probably not feasible in most practical applications.) In these tests, the wire diameter remains constant (AWG #8). However, all

other dimensions of the antenna are allowed to change. **Table 2** shows the results of these modeling tests.

Table 2. Spacing vs. other dimensions with AWG #8 20-15-meter dipole  
Note: Both element and resonator rod are AWG #8 (0.1285" = 3.26 mm diameter).

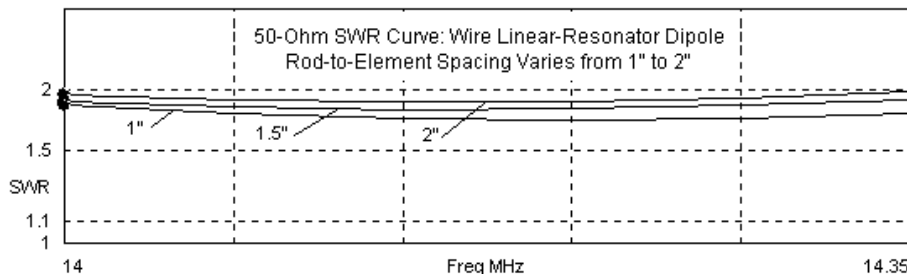
Rod-Element Space Inches	El. Length Inches	Rod Length Inches	14.175 MHz R +/- jX Ω	21.225 MHz R +/- jX Ω	Cap. pF
1	386	100	29.2 + j4.8	45.1 - j1.7	19.5
1.5	384	98	28.3 + j7.1	59.5 + j5.6	17.7
2	382	96	27.3 + j7.2	69.4 + j13.8	16.8

As we increase spacing between the main element and the resonator rod, the required lengths of the main element and of the resonator rod decrease. So too does the required capacitance for the resonator capacitor. (Otherwise expressed, the capacitive reactance increases.) These numbers show the physical demands of increasing the spacing.

The spacing increase also has consequences for the impedances on each band and the resulting SWR performance. **Fig. 6** provides SWR curves for 20 meters.

20 Meters

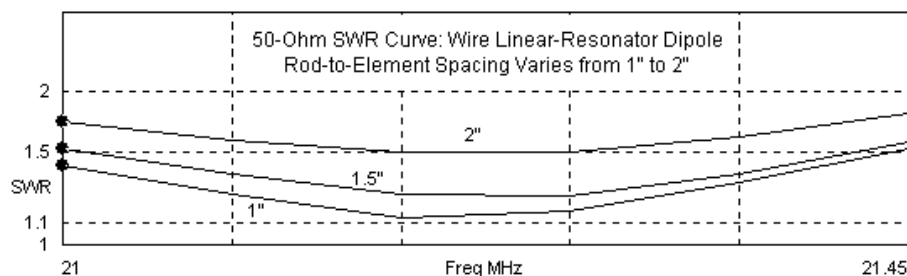
Fig. 6



The mid-band impedance values for 20 meters suggest that the 50-Ohm SWR curve may grow less satisfactory as we increase the spacing between wires. **Fig. 6** confirms the suspicion. Indeed, although the curve for 2" spacing appears barely to meet the standard, it might not be so easy a matter to place that curve precisely when pruning an actual antenna. In general, 20-meter performance depends upon using the narrowest feasible spacing between the resonator and the main element wires.

15 Meters

Fig. 7



The 15-meter 50-Ohm SWR curves in **Fig. 7** tell much the same story. As the spacing increases, the SWR curves grow less satisfactory. On 15 meters, the problem is not a decreasing feedpoint impedance. Rather, the problem arises from an increasing resonant impedance. The bottom line for the spacing tests is that a wire-based linear-resonator dipole does not offer the flexibility of fatter elements. Narrow spacing is a requisite on both bands when the frequency ratio is fairly low.

### *Varying the Wire Size*

Admittedly, AWG #8 wire is somewhat impractical for end-supported antennas. In copper, its weight is excessive, and in aluminum, the wire junctions become difficult. I selected #8 because it permitted me to find all of the dimensions required in the model for a successful design using a 1" spacing between wires in the assembly. Whether AWG #8 represents a limit for a practical antenna depends on what we find if we vary the wire size. For this test, I held the spacing constant at 1". As well, I held the rod length to a constant 100" length. I used standard AWG wire gauges from #6 through #12, letting the remaining physical dimensions settle at the most optimal values. **Table 3** shows the results of this test set.

Table 3. Wire size vs. other dimensions of a 20-15-meter wire dipole

Note: Rod-to-element space is constant at 1".

Wire Size	El. Length	Rod Length	14.175 MHz	21.225 MHz	Cap.
AWG	Inches mm	Inches	Inches	R +/- jX Ω	pF
#6	0.1620 4.11	388	100	30.5 + j5.4	37.7 - j3.6
#8	0.1285 3.26	386	100	29.2 + j4.8	45.1 - j1.7
#10	0.1019 2.59	386	100	28.9 + j7.1	51.1 + j1.4
#12	0.0808 2.05	386	100	28.7 + j9.4	56.9 + j5.6

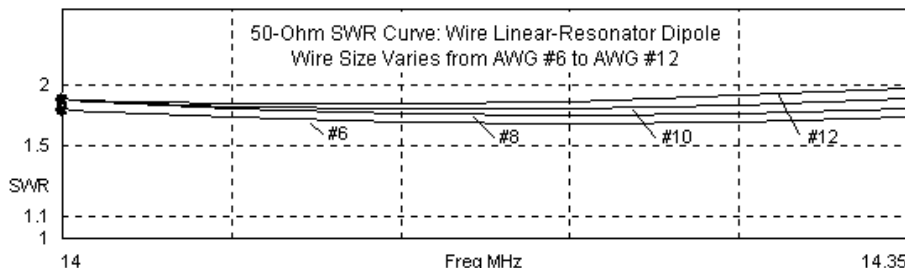
Note: AWG #6 dual-band dipole optimizes with the following values at 1" spacing:

Wire Size	El. Length	Rod Length	14.175 MHz	21.225 MHz	Cap.
AWG	Inches mm	Inches	Inches	R +/- jX Ω	pF
#6	0.1620 4.11	388	108	31.1 + j10.1	49.6 - j4.2

The table has a special section noting the most optimal settings for the AWG #6 sample. By increasing the length of the resonator rod 8", we obtain a marginally higher 20-meter impedance. We also obtain a superior 15-meter impedance and a capacitor value that approximates the value used with AWG #8 wire at its optimal resonator rod length. I did not include in the table models for AWG #10 and #12 wire with similar adjustments to the resonator lengths. Each of those models would have required significant resonator-rod shortening to obtain the desired 15-meter results. However, those rod lengths would have produced lower impedances on 20 meters, disallowing the use of the antenna on that band within the project terms of a maximum 2:1 SWR value.

20 Meters

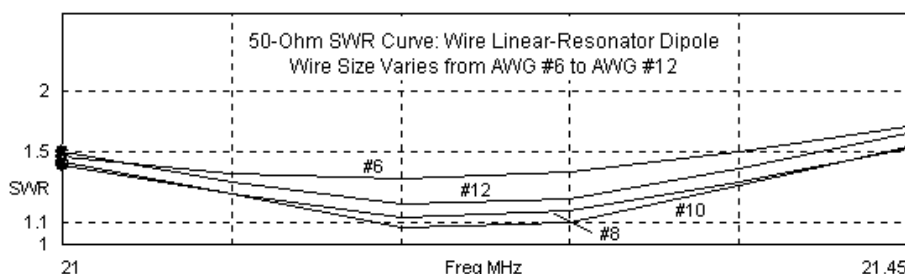
Fig. 8



With the values shown in the table, the 20-meter SWR curves become increasingly marginal as we reduce the wire size, as revealed by **Fig. 8**. The major problem of trying to optimize the resonator rod lengths with thinner wire is not so much the mid-band impedance. We likely can find a satisfactory impedance with less than a 2:1 50-Ohm SWR. The major difficulty lies at the band edges, where every reduction in resistance provides the reactance with a proportionately higher influence on the SWR level.

15 Meters

Fig. 9



The difficulty does not extend to 15 meters. The SWR curves in **Fig. 9** all fall within the highly acceptable range. The curve for AWG #6 wire is for the model using a 100" resonator rod. With a 108" rod, the curve largely overlaps the curve for AWG #8 wire.

### *Some Summary Thought for the 20-15-Meter Wire Dipole*

Increasing the diameter of the wires in a linear-resonator dipole with a frequency ratio of 1.5:1 between bands is always advisable. The increased diameter of the elements raises the flexibility of the antenna to accept wider spacing. Although I have not modeled such an antenna, one might consider using wire pairs for the main element and the resonator rod to simulate fatter conductors in a wire structure.

The essential difficulty faced by anyone experimenting with a wire version of the 20-15-meter dipole is the impedance on 20 meters. As the wire grows thinner, we require narrower spacing between rod and element wires to prevent the 20-meter impedance from dropping below the critical 25-Ohm value. Thinner wires also reduce the capacitance-per-inch of the rod wires that form a capacitor at the center. Finally, the narrow-band nature of thin wires increases the finickiness of adjustments--and their ability to hold during extremes of weather.

Nevertheless, the intrepid experimenter may wish to see what is possible with wire in a 20-15-meter linear-resonator dipole. To this end, the modeling experiments may serve as a guide. As with all of the modeling experiments, these are not design plans. Rather, they

illustrate some of the trends in operation for a linear-resonator dipole with a small frequency ratio.

## A 20-10-Meter Wire Linear-Resonator Dipole

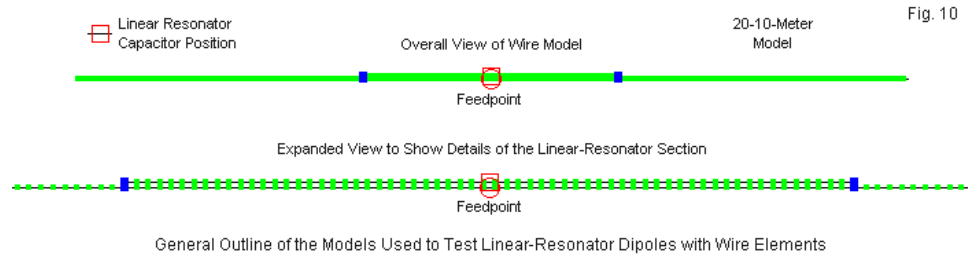
In Part 2, we examined a fat-element linear-resonator dipole for 20 and 10 meters. Using a 0.875"-diameter 20-meter dipole and a 0.25"-diameter resonator rod, with a spacing of 6", we obtain some results that reversed the difficulties for the antenna. On 20 meters, the antenna showed a near 50-Ohm impedance that easily yielded excellent SWR curves. However, 10-meters proved more problematical, since we barely obtained full-band coverage, even reducing the band to the first MHz.

When we reduce the elements to wire size, two major questions confront us. First, will the 20-meter operation continue to show near 50-Ohm impedance values? Second, will the narrow-band properties of thinner wires result in reduced 10-meter coverage?

Interestingly, some of the difficulties that we experienced with the 20-15 combination do not reappear with the 20-10-meter version. For example, as subsequent tables will show, an AWG #8 wire settles in at 392" long for all cases. The presence of the linear resonator section does result in a shorter 20-meter antenna than we find with a simple 20-meter dipole (392" vs. 403"). However, variations in the resonator rod length and the spacing have very little affect on the overall element length, since the second frequency is so far removed from the first. As well, the 20-10

version is an average of about 3" longer than the 20-15 combination.

Like the 20-15 antenna, the 20-10 dipole requires increased segmentation to handle the 1" spacing between the element and the resonator rod. **Fig. 10** shows both the overall structure and an expanded view of the linear resonator area of the model used. The segmentation detail differs slightly from the earlier model, since the 10-meter linear resonator sections are longer than those used to cover 15 meters. Nevertheless, the AGT scores of the antennas for both bands are very similar.



Just because we have reduced the element diameter and the spacing between wires, we do not lose the radical difference between the patterns for 20 and 10 meters. **Fig. 11** shows overlaid free-space E-plane patterns for 14.175 MHz and 28.5 MHz using a typical AWG #8 wire antenna. The 10-meter pattern has a 1.6-dB gain advantage over the 20-meter pattern, with a corresponding reduction in beamwidth.

20-10-Meter Wire Dipole  
with a Linear Resonator  
Overlaid Free-Space  
E-Plane Patterns

0 dB

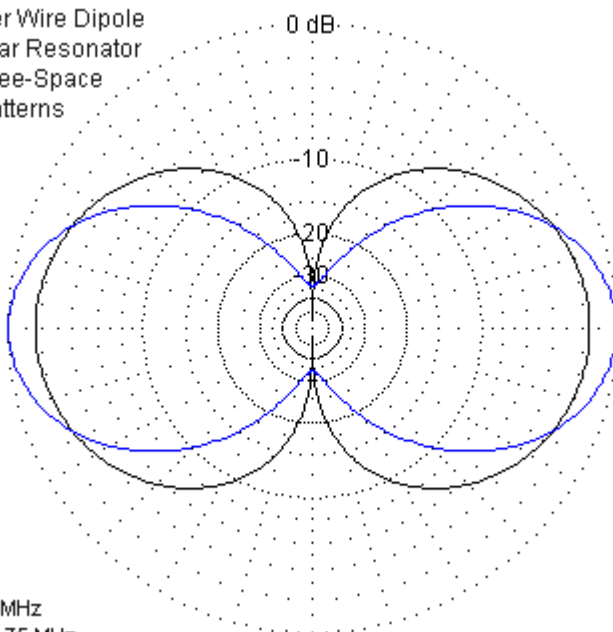
-10

-20

-30

Blue = 28.5 MHz  
Black = 14.175 MHz

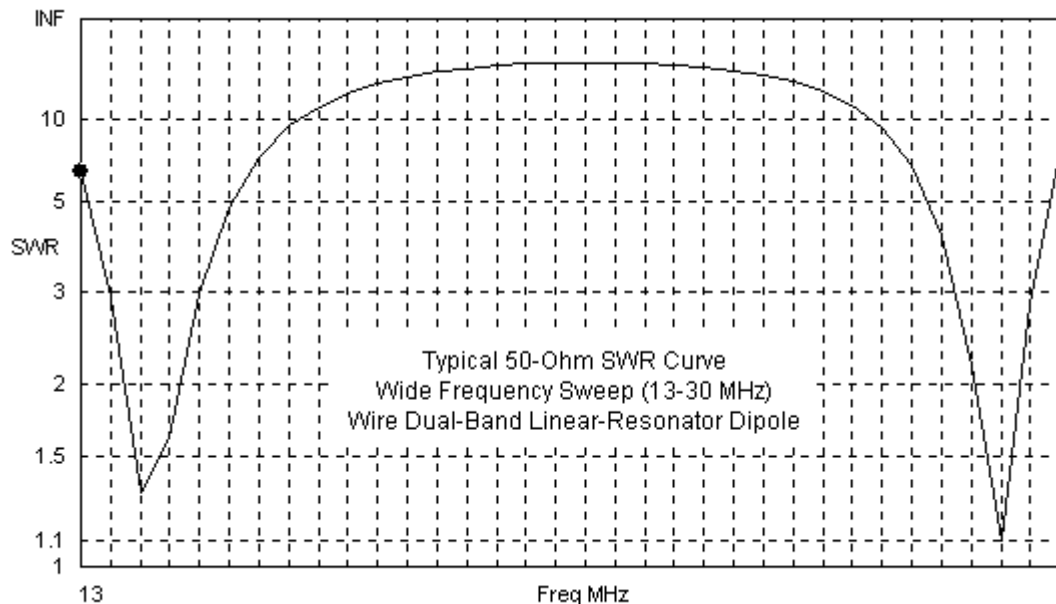
Fig. 11



Like the 20-15-meter antenna, the reduced spacing between wires yields a much smaller differential in gain in the plane of the resonator on the higher band. The difference is only 0.1 dB. As well, the 10-meter front-to-side ratio is nearly 34 dB, a considerable improvement over the models using fatter elements.

In concert with the 20-15-meter wire antenna, the 20-10 wire model shows a much higher 50-Ohm SWR peak value between operating frequencies than did the fat-element antenna for the same

coverage. **Fig. 12** provides a wide-frequency sweep (13-30 MHz) to show the overall performance tendency.



The peak 50-Ohm SWR value approaches 25:1 in the middle region of the plot, nearly twice as high as the peak value for the antenna with a 7/8"-diameter element. The increased peak 50-Ohm SWR value suggests that the operating bandwidth as defined by a 2:1 SWR maximum value may be reduced relative to either the wire 20-15 model or the fat-element 20-10 model.

Even though some dimensions of the wire 20-10-meter dipole may remain stable, the data to follow will have the same form as used with the 20-15 antenna. Except for the spacing test, the models will use a 1" uniform spacing between the main element and the resonator rod. I shall allow all other dimensions to settle to their near-optimum values.

### *Varying the Resonator Rod Length*

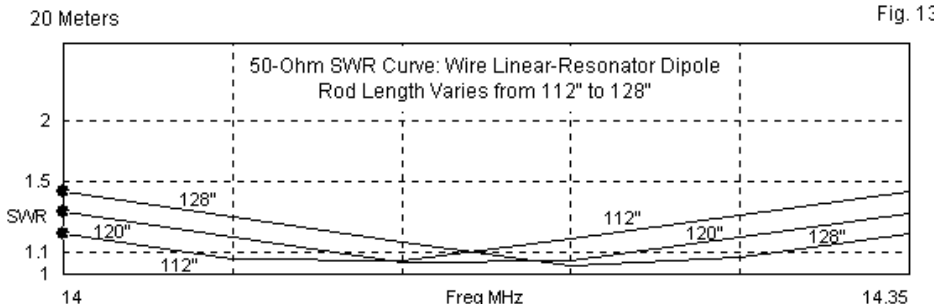
The initial test involves finding the resonator rod length and the corresponding capacitor value that most closely approaches perfection on both bands, as determined by the SWR curves. In fact, I found no significant reason to vary the main element from 392" in the entire set of test runs. The 10-meter resonator rods average about 20" longer than the rods required by the 20-15 wire model. **Table 4** shows the results for varying the rod length from 112" up to 124".

Table 4. Varying rod length with AWG #8 with 1" rod-to-element spacing: 20-10-meter dipole  
Note: Both element and resonator rod are AWG #8 (0.1285" = 3.26 mm diameter).

El. Length Inches	Rod Length Inches	14.175 MHz $R +/- jX \Omega$	28.5 MHz $R +/- jX \Omega$	Cap. pF
392	112	$48.5 + j3.6$	$64.9 + j15.0$	5.2
392	116	$48.7 + j5.1$	$56.1 + j16.1$	5.6
392	120	$49.0 + j0.4$	$51.7 + j4.4$	5.9
392	124	$49.1 - j1.8$	$45.7 + j2.6$	6.3
392	128	$49.4 - j4.1$	$40.8 - j0.8$	6.7

The table shows mid-band impedances for 20 meters that are very close to those found in fat-element models. For the larger

frequency ratio in this antenna, we may obtain a nearly ideal impedance at the middle of 20 meters. As the band-specific SWR curve in **Fig. 13** reveals, 20-meter SWR is not a significant concern, despite the use of thin elements. The lowest SWR shifts position as we change the length of the resonator rod, but never enough to elevate the SWR to 1.5:1 at the band edges.

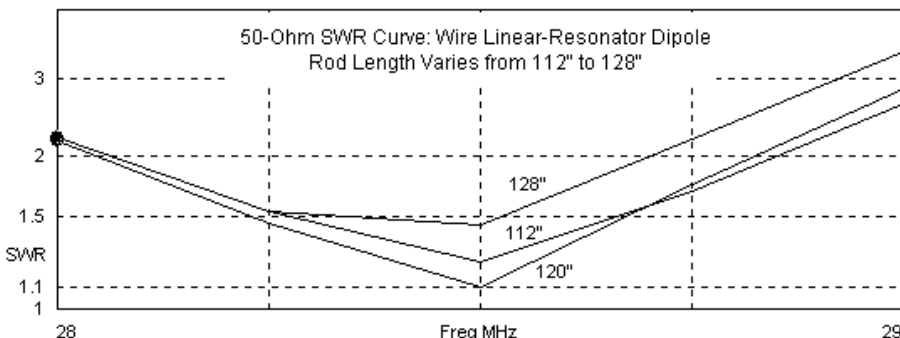


As we change the length of the resonator rod, the required capacitance varies over a narrow range from 5.6 to 6.7 pF. This range is very comparable to the range for the fatter model in Part 2 (4.9-6.0 pF). However, the resonator rod ranges differ: 100"-112" for the earlier model and 112" to 124" for the current wire model. Some of that difference results from the longer main element length of the wire model (392") over the 7/8"-diameter model (385").

As we suspected, the use of thinner wire elements results in narrower coverage on 10 meters. **Fig. 14** shows the 50-Ohm SWR curves for several of the rod lengths sampled.

10 Meters

Fig. 14



All of the curves show just above a 2:1 SWR at 28 MHz. However, only the shorter rod lengths provide coverage as high as 28.7 MHz with a 2:1 SWR. The mid-band impedance values in **Table 4** do not themselves reveal the more rapid change of impedance for each small frequency increment, relative to the fat-element models that allowed coverage of a full MHz of the band. One of the limitations of the 20-10 thin-wire model, then, is reduced upper-band coverage.

#### *Varying the Rod-to-Element Spacing*

In concert with the 20-15-meter wire model, I varied the spacing between the main element and the resonator rod in half-inch increments between 1" and 2". The baseline model used a 120" resonator rod with 1" spacing. I allowed the dimensions to settle at the most desirable values for each spacing increment. **Table 5** shows the results of this small experiment.

Table 5. Spacing vs. other dimensions with AWG #8 20-10-meter dipole

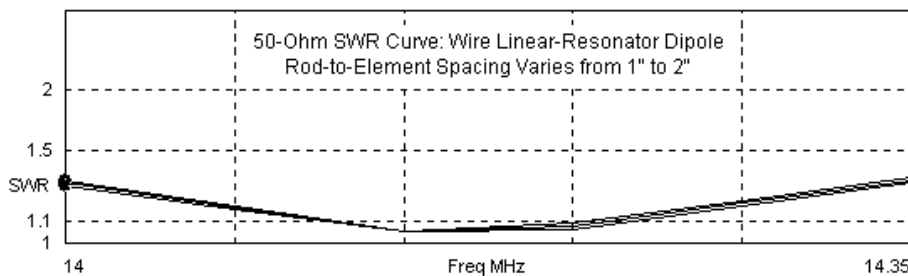
Note: Both element and resonator rod are AWG #8 (0.1285" = 3.26 mm diameter).

Rod-Element Space Inches	El. Length Inches	Rod Length Inches	14.175 MHz	28.5 MHz	Cap. pF
1	392	120	$49.0 + j0.4$	$51.7 + j4.4$	5.9
1.5	392	112	$48.6 + j0.9$	$52.2 + j2.8$	5.7
2	392	108	$48.3 + j1.5$	$52.5 + j9.4$	5.5

In all cases, the main element held its length. The 20-meter mid-band impedance does show a small decline as we increase the spacing. However, the decrease is in no way fatal to the SWR curves, which appear in **Fig. 15**. In fact, I have not identified the curves individually, since they form too tight a group to distinguish individual lines.

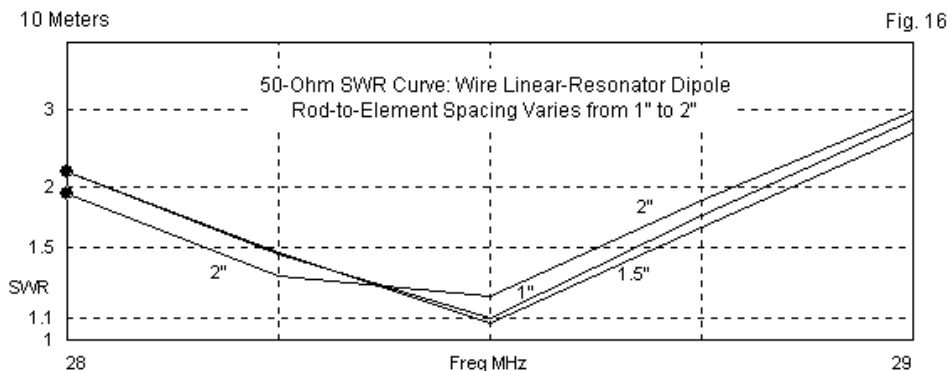
20 Meters

Fig. 15



The data show that as we increase the spacing, we must reduce the length of the resonator rod in order end up with a near-50-Ohm impedance at 28.5 MHz. The required capacitance also goes down

with increased spacing (indicating an increase in capacitive reactance). The effects of these changes on the SWR curves for 10 meters appear in **Fig. 16**.



The curves do not show any significant difference of bandwidth, although increased spacing does appear to have a small advantage over narrow spacing. However, increased spacing does require a lower capacitance value and may prove harder to adjust to perfection. The displacement of the curve for a 2" space results from my restriction of capacitance increments to 0.1 pF. Linear adjustment of parallel or side-by-side rods used to implement the resonator capacitor might make finer adjustment feasible, but difficult to hold as the weather changes from summer to winter and back again.

Due to the ever-lower value of required capacitance, I limited the test range to a maximum spacing of 2". In terms of raw impedance

values, we might in theory continue the progression, since the 20-meter impedance changes very slowly and increased spacing may yield wider 10-meter operating bandwidths. At a rate of about 0.4-pF-per-inch of spacing, it is doubtful that the spacing could reasonably approach the 6" value used for the fat-element models.

### *Varying the Wire Size*

Despite the narrower coverage of 10 meters, the use of thinner wire may be feasible for frequency ratios in the 2:1 range. The chief obstacle to using thinner wire for the wire 20-15 combination was the reduced 20-meter impedance as the wire grew thinner. The models that we have surveyed so far for 20 and 10 meters suggest that this problem will not occur. Therefore, I surveyed wires sizes from AWG #6 to AWG #12 using the 1" spacing and letting all other values settle to their optimal levels. The results appear in **Table 6**. We may initially note that by letting each resonator rod settle at its most perfect length, we obtain tuning capacitance values that vary over a very small range.

Table 6. Wire size vs. other dimensions of a 20-10-meter wire dipole

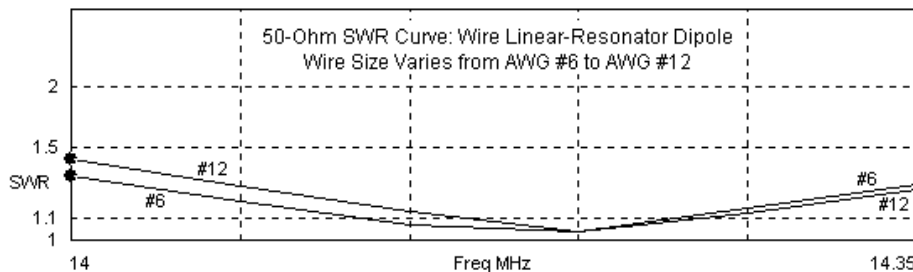
Note: Rod-to-element space is constant at 1".

Wire Size	El. Length	Rod Length	14.175 MHz	28.5 MHz	Cap.
AWG	Inches mm	Inches	Inches	R +/- jX Ω	R +/- jX Ω pF
#6	0.1620 4.11	392	120	49.4 - j0.6	47.4 - j1.9 6.4
#8	0.1285 3.26	392	120	49.0 + j0.4	51.7 + j4.4 5.9
#10	0.1019 2.59	392	116	48.5 - j1.1	50.6 + j3.4 5.8
#12	0.0808 2.05	392	112	47.9 - j2.6	47.3 + j10.7 5.8

All models in the set required no alteration in overall length. With the 392" main element length and resonator rods suited to the 10-meter requirements, the mid-band 20-meter impedance decreases quite slowly as we thin the wire to AWG #12. **Fig. 17** shows the resulting 20-meter 50-Ohm SWR curves for AWG #6 and AWG #12 wire. Although these curves are distinguishable, adding the other two wire sizes would have created a fat blurry line. As the curves make clear, the 50-Ohm SWR is always less than 1.5:1 across the 20-meter band with any of the wire sizes.

20 Meters

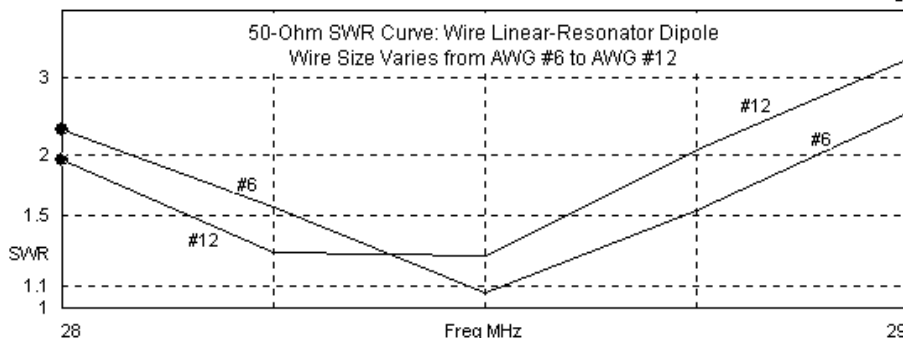
Fig. 17



The situation differs a bit on 10 meters. Due to the use of a 0.1-pF increment in the tuning capacitance, the SWR curves for 10-meters do not overlay each other as neatly as they do in 20 meters. Hence, the curves in **Fig. 18** require a bit of interpretation. Essentially, at the 2:1 SWR crossing points, the AWG #12 curve is only about 93% of the width of the curve for AWG #6 wire, despite the 2:1 ratio of wire diameters. The difference amounts to about 50 kHz (750 kHz vs. 800 kHz--approximately).

10 Meters

Fig. 18



Although the use of AWG #12 wire is not fatal to the construction of a 20-10 combination with 1" element-to-rod spacing, the narrower operating bandwidth will make antenna adjustment more difficult. As well, as we increase the diameter of the element, we also gain some flexibility in selecting the rod-to-element spacing. Nevertheless, for any size element, the most difficult adjustment to master and to make endure through all kinds of weather will be the capacitance.

## Conclusion

In this final section of our work, we have established that wire-based dual-band linear-resonator dipoles are feasible if we are willing to observe some restrictions. Foremost among the limitations is the need for close spacing of the resonator rod and the main element. Especially for antennas with a lower frequency ratio, such as 1.5:1, the close spacing is necessary to achieve even

a usable impedance on the lower band--using 50 Ohms as the standard. Close spacing is not quite as necessary where the frequency ratio is higher, such as 2:1, but wider spacing does reduce the required capacitance to a level at which stability may become a problem.

The second restriction requires that we use the largest diameter wire feasible. For lower frequency ratios, thin wire may reduce the low-band impedance below the acceptable level. Again, high frequency ratios are less of a problem on the lower band, but thinner wire tends to reduce the upper band operating bandwidth.

Wire versions of linear-resonator dual-band antennas also suffer from some finickiness of tuning, since virtually no dimension is fixed. Hence, adjustments to the resonator-rod length may affect the overall main element length. This potential difficulty is especially apparent with lower frequency ratios.

Perhaps the most difficult challenge for linear-resonator antennas using a higher frequency ratio involves the high capacitive reactance and low capacitor value required for precise tuning. Concentric and parallel capacitors formed by the resonator rods and associated materials are subject to linear expansion and contraction as the temperature changes. Replacing a test set-up with a wide-temperature-range fixed capacitor may prove useful in some cases. However, the experimenter must gauge this move against the knowledge that the linear resonator rod itself will change length with frequency.

As we close our look at linear-resonator dipoles, I should again remind you that all of the numbers fall far short of design plans. Rather, they reliably indicate only the trends in values. In an assembly as tricky as a linear-resonator dipole, field experimentation and adjustment must take precedence over NEC modeling results.

Nevertheless, linear resonators are a feasible means of producing a double 50-Ohm resonance from essentially a single element. It may be the case that frequency ratios of 1.7:1 or 1.8:1 produce the most desirable results. The low-band impedance would be less marginal and the high-band operating bandwidth would be more adequate and less finicky to establish. As well, the required tuning capacitance would likely fall around 9-10 pF, a value that might be usable in practice. Combinations for 30 and 17 meters or for 20 and 12 meters fall in this range. In both cases, the upper band is quite narrow, so tuning in one season would not yield an unusable SWR 6 months later.

Whether the linear resonator has applications in multi-element arrays remains in the category of work to be done. The wider we make the frequency ratio, the more that the radiation pattern changes from the lower to the higher frequency. How that change might affect the required dimensions for a multiband array remains to be discovered. For the moment, we may be doing all that we can by digesting the basic properties, potentials, and limitations of linear-resonator dial-band dipoles.

## **Other Publications**

We hope you've enjoyed 3-Volume series of books of the **Antennas Made from Wires**. You'll find many other very fine books and publications by the author L.B. Cebik, W4RNL and others in the ***antenneX Online Magazine Bookshelf*** at the web site shown below.

---

*A Publication by*  
***antenneX Online Magazine***  
**<http://www.antennex.com/>**

**POB 271229  
Corpus Christi, Texas 78427-1229  
USA**

---

Copyright © 2010 by ***antenneX Online Magazine***. All rights reserved. No part of this book may be reproduced or transmitted in any form, by any means (electronic, photocopying, recording, or otherwise) without the prior written permission of the publisher.

ISBN: 1-877992-87-9